

MATHEMATICAL MODELLING OF SEDIMENT TRANSPORT DYNAMICS IN THE BERG RIVER CONSIDERING CURRENT AND FUTURE WATER RESOURCES DEVELOPMENT SCENARIOS

By Sarel C. van der Walt

**Thesis presented in partial fulfillment of the
Requirements for the degree of Master of Engineering
At the University of Stellenbosch**



Study Leader: Prof G.R. Basson

December 2005

Declaration

I, the undersigned, hereby declare that the work contained in this thesis is my own original work and I have not previously in its entirety or in part submitted it at any university for a degree.

S.C. van der Walt

Summary

The environmental impacts of manmade changes to rivers are, in modern days, extremely important. The impact needs to be quantified in order to predict future happenings and to assist in determining preventative measures. Dam construction forms an essential part of modern life to provide the necessary water demand for the ever increasing population.

One manmade change that has a major impact on rivers is large dam developments in the upper reaches of rivers. These developments normally have the following effects on the lower reaches of the river due to the change in flow regime:

- Narrower main channel,
- Deeper main channel,
- Reduced sediment transport,
- Changes in sediment erosion and deposition patterns,
- Less frequent flood plain inundation,
- Overgrown flood plains,
- Changes in ecological and biological parameters.

All the above mentioned factors play an important part in the stability of the ecological and biological parameters. Prior to construction of a dam, however, the baseline ecological, physical /chemical, hydrological, hydraulic and social conditions of the river system, including its associated groundwater, estuarine and floodplain components, would need to be established, to allow clear identification of future changes as a result of implementation of the instream flow requirements (IFR), as well as to guide the post-construction monitoring programme itself.

The discharge and sediment transport changes that might occur as a result of the Berg River Dam development was thoroughly investigated in this research. The physical processes and mathematical modelling that formed part of this investigation are discussed in this thesis. The mathematical modelling was carried out using MIKE11, software developed by the Danish

Hydraulic Institute for Water and Environment. This program was developed especially for one dimensional modelling of hydrodynamics and sediment transport within a river system. The results obtained from the simulations were used to calculate a hydrodynamic and sediment mass balance for both the pre and post dam scenarios in the Berg River, Western Cape. The influence of artificial flood releases from the Berg River Dam which is currently under construction was also investigated.

Most of the data needed for the calibration and verification of the mathematical model was obtained from field work. Suspended and bed load sediment samples were taken in order to aid in the calibration of the sediment transport model. The bed roughness coefficients of the various sections of the river were calibrated against actual recorded water levels measured during flood events that occurred in 2003 and 2004.

An intensive study of the incipient motion of cobbles and boulders in the upper reaches of the Berg River was carried out. Unfortunately it has to be stated that the transport of cobbles and boulders cannot be simulated by most computer programs as almost all the transport models available are only defined up to a maximum diameter of 20mm. The lack of consistent sediment load data as well as the low rainfall during 2003 and 2004 presented problems during the calibration of the sediment transport model; it is therefore recommended that sediment load sampling is continued for at least two years in order to verify the calculated sediment yield for the various catchments.

From this study it can be concluded that the Berg River Dam will have a significant effect on the downstream river morphology of the first 70 kilometres of the river. Thereafter the effect will decrease to a minimum. The proposed artificial flood releases are effective in reinstating the river to its present state. This study also showed that a fully hydrodynamic model of a large river system such as the Berg River can be calibrated and validated.

Opsomming

Die omgewingsimpak van mensgemaakte veranderinge in natuurlike riviere raak meer en meer belangrik. Hierdie impak moet gekwantifiseer word om sodoende toekomstige gebeurtenisse te verstaan en om die nodige voorkomingsmaatreëls in werking te stel. Om aan die waterbehoefte te voldoen vorm damkonstruksie 'n belangrike deel van die hedendaagse samelewing.

Damme is moontlik een van die veranderinge aan die ewewig van riviere wat die grootste impak op die stroomaf dele van die rivier het. Die volgende veranderinge ten opsigte van die hoofkanaal word meestal opgemerk na die konstruksie van 'n dam in die hoërliggende dele van riviere:

- Nouer hoofkanaal,
- Dieper hoofkanaal,
- Afname in die volume sediment wat vervoer word,
- Veranderinge ten opsigte van die erosiepatrone,
- Vloedvlaktes word minder oorstrom,
- Toegegroeide vloedvlaktes,
- Veranderinge aan die ekologiese en biologiese parameters.

Die bogenoemde faktore speel 'n belangrike rol ten opsigte van die stabiliteit van die ekologiese en biologiese veranderlikes. Alvorens die konstruksie begin moet die natuurlike ewewigstoestand van die rivier ten opsigte van die ekologiese, fisiese, chemiese, hidrologiese, hidrouliese, en sosiale faktore gemeet word. Dit moet gedoen word om sodoende toekomstige veranderinge wat moontlik mag plaasvind as gevolg van die damkonstruksie en die omgewingsloslatings te kwantifiseer. Hierdie metings word ook gebruik om die na – konstruksie monitering te evalueer.

Die veranderinge ten opsigte van vloei en sedimentvervoer wat moontlik mag plaasvind as gevolg van die Berg Rivier Dam konstruksie is noukeuring ondersoek. Die fisiese prosesse as ook die wiskundige modelle wat gedurende hierdie studie aangewend is word in hierdie tesis

bespreek. Al die wiskundige modellering is met MIKE11 wat deur die Deense Instituut vir Water en Omgewing ontwikkel is, uitgevoer. Hierdie sagteware is spesifiek vir die een dimensionele simulatie van hidrodinamika en sediment vervoer van riviere ontwikkel. Die resultate wat verkry is, is gebruik om 'n hidrodinamiese en sedimentvervoer massabalans vir beide die voor – en na – dam toestande op te stel. Die effek van beheerde, kunsmatige vloede is ook ondersoek.

Die meeste van die data wat benodig word om die wiskundige model te kalibreer is verkry deur fisiese veldwerk te doen. Sediment monsters is geneem gedurende die winter seisoen van 2003 en 2004. Hierdie data is gebruik om die sediment vervoer model te kalibreer. Die bodemruheid van die verskillende dele van die rivier is gekalibreer teen gemete vloedhoogtes tydens 2003 en 2004.

'n Deeglik studie van die begin van beweging van die groter partikels wat in die bolope van die Berg rivier aangetref word is uitgevoer. Ongelukkig moet dit genoem word dat hierdie een van die groot tekortkominge is van die model aangesien dit nie in die sedimentvervoer model ingekorporeer kan word nie omdat die meeste van die sedimentteorieë wat tans beskikbaar is net gedefinieer is tot 'n partikel groote van 20 mm. Die tekort aan deurlopende sediment lading data as ook die lae reënval gedurende 2003 en 2004 het probleme veroorsaak tydens die kalibrasie van die sedimentvervoer model. As gevolg hiervan word daar aanbeveel dat die insameling van sedimentdata vir ten minste nog twee jaar volgehou word ten einde die beskikbaarheid van sediment in die verskeie opvanggebiede deeglik na te gaan.

Uit hierdie studie kan afgelei word dat die Berg rivier dam 'n beduidende effek op die morfologie van die eerste 70 kilometer van die Berg Rivier sal hê. Verder stoomaf sal die effek minder sigbaar wees. The beheerde kunsmatige vloedloslatings speel 'n beduidende rol in die normalisering van die sedimentvervoer van die Berg rivier. Hierdie studie toon dat 'n volledige hidrodinamiese model van 'n groot rivierstelsel gekalibreer kan word.

Acknowledgements

First I would like to express my gratitude towards the Lord, my Creator for providing me with the necessary patience, diligence and talent to conclude this study.

I would like to thank Professor Gerrit Basson, my study leader, for all the guidance and explaining that he had to do in order to assist me in achieving the goals that had been set out at the beginning of this long and interesting journey through the sophisticated physics of hydraulics and sediment transport in particular.

Many thanks to Ms. Julia Beck for all the assistance she offered me in understanding MIKE11 and for all her patience and guidance.

I would like to thank the laboratory staff at the University of Stellenbosch for their assistance with the field work that had to be carried out to gather the necessary information for the calibration of the mathematical model. Also for their assistance with the many surveys that had to be done, mostly in harsh weather conditions.

Many thanks to all who were involved in taking sediment samples during the winter months of 2003 and 2004.

Many thanks to my family and friends for their support and belief in me when the occasional problem did arise, especially Schalk Visser with all his assistance with the many computer bugs that had to be sorted out.

Table of Contents

Declaration	i
Summary	ii
Opsomming	iv
Acknowledgements	vi
List of Figures	x
List of Tables	xviii
List of Symbols	xxi
CHAPTER 1 INTRODUCTION	1-1
1.1 BACKGROUND	1-1
CHAPTER 2 MOTIVATION	2-1
CHAPTER 3 OBJECTIVES	3-1
CHAPTER 4 METHODOLOGY	4-1
CHAPTER 5 REVIEW OF RESEARCH ON SEDIMENT TRANSPORT DYNAMICS FROM CATCHMENT TO COAST	5-1
5.1 SEDIMENT TRANSPORT DYNAMICS AND SEDIMENT TRANSPORT EQUATIONS	5-1
5.2 SEDIMENT YIELD	5-3
5.2.1 <i>Sediment load – Discharge rating curves</i>	5-3
5.2.2 <i>Reservoir basin surveys</i>	5-5
5.2.3 <i>Regional sediment yield maps and statistical approach</i>	5-5
5.2.4 <i>Regression type models</i>	5-6
5.2.5 <i>Discussion</i>	5-6
5.3 IMPACTS OF DAM DEVELOPMENTS	5-7
5.3.1 <i>Discharge</i>	5-7
5.3.2 <i>Sediment transport</i>	5-8
5.3.3 <i>Channel depth and width</i>	5-8
5.3.4 <i>Bed material</i>	5-10
CHAPTER 6 GENERAL DESCRIPTION OF THE BERG RIVER CATCHMENT	6-1
6.1 LOCATION	6-1
6.2 TOPOGRAPHY	6-3
6.3 CLIMATE	6-3
6.3.1 <i>Rainfall</i>	6-3
6.3.2 <i>Temperature</i>	6-4
6.4 GEOLOGY	6-4
6.5 EXISTING WATER RESOURCES INFRASTRUCTURE WITHIN THE CATCHMENT	6-6
CHAPTER 7 REVIEW OF THE BERG RIVER FLUVIAL MORPHOLOGY	7-1
7.1 FLUVIAL MORPHOLOGICAL ASSESSMENT AND RIVER CLASSIFICATION	7-1
7.1.1 <i>Previous Fluvial morphological assessment</i>	7-1
7.2 AERIAL PHOTOGRAPH ANALYSIS – HISTORICAL CHANGES	7-4
7.3 CHANGES ON THE FLOODPLAINS	7-18
CHAPTER 8 MATHEMATICAL MODEL OF THE BERG RIVER	8-1

8.1	GENERAL DESCRIPTION OF THE ONE DIMENSIONAL MODEL – MIKE11	8-1
8.1.1	<i>Hydrodynamic Module</i>	8-1
8.1.2	<i>Non-Cohesive Sediment Transport Module (NST)</i>	8-4
8.1.2.1	The van Rijn sediment transport model:	8-5
8.1.2.1.1	Bed load	8-5
8.1.2.1.2	Suspended load	8-8
8.1.2.1.3	Non – uniform sediment transport	8-10
8.1.2.2	Cross – section deformation	8-12
8.2	ASSEMBLING OF MODEL PARAMETER DATA	8-13
8.2.1	<i>River Cross Sections and Coordinates</i>	8-16
8.2.1.1	Natural scenario cross sections	8-16
8.2.1.2	Post dam development cross-sections	8-16
8.2.1.3	Level of divide	8-17
8.2.1.4	Additional low flow channel	8-19
8.2.2	<i>Flow Boundaries</i>	8-20
8.2.3	<i>Downstream Boundary Conditions</i>	8-31
8.2.4	<i>Sediment Transport Boundaries</i>	8-32
8.2.4.1	Sediment Inflow via the Tributaries	8-32
8.2.4.2	Sediment particle size distribution	8-50
8.2.5	<i>Bed roughness coefficients</i>	8-52
8.2.6	<i>Incipient motion of coarse materials</i>	8-59
8.2.6.1	Basic Theory	8-59
8.2.6.2	Shields Diagram	8-61
8.2.6.3	The Liu Diagram	8-62
8.2.6.4	Hiding and Exposure	8-66
8.2.6.5	Comparison between Field Data, Laboratory tests and the Theory	8-69
CHAPTER 9	MATHEMATICAL MODEL CALIBRATION AND VERIFICATION	9-1
9.1	HYDRODYNAMIC MODEL	9-1
9.1.1	<i>Calibration</i>	9-1
9.1.2	<i>Verification</i>	9-6
9.2	SEDIMENT TRANSPORT MODEL	9-8
9.2.1	<i>Calibration</i>	9-8
9.2.2	<i>Verification</i>	9-11
CHAPTER 10	SIMULATION OF SCENARIOS	10-1
10.1	HYDRODYNAMIC MODEL SIMULATION RESULTS	10-1
10.1.1	<i>Return Period Floods</i>	10-1
10.1.2	<i>Flood Attenuation</i>	10-2
10.1.3	<i>Hydraulic Parameters</i>	10-7
10.1.3.1	Site BRM 2	10-8
10.1.3.2	Site BRM3	10-15
10.1.3.3	Site BRM4	10-23
10.1.3.4	Site BRM5	10-31
10.1.3.5	Site BRM6	10-39
10.1.4	<i>Hydrodynamic Mass Balance</i>	10-47
10.2	SEDIMENT TRANSPORT MODEL RESULTS	10-55
10.2.1	<i>Upper Berg River (Dam site to just upstream of Hermon): Effective Discharge and Sediment Mass Balance</i>	10-58
10.2.1.1	Site BRM2	10-58
10.2.1.2	Site BRM3	10-60
10.2.2	<i>Lower Berg River (Site 4 to Head of Estuary): Effective Discharge and Sediment Mass Balance</i>	10-66
10.2.2.1	Site BRM4	10-66
10.2.2.2	Site BRM5	10-67
10.2.2.3	Site BRM6	10-69
10.2.3	<i>Cumulative Sediment Loads</i>	10-74
10.2.4	<i>Sediment Rating Curves</i>	10-77
10.3	DISCUSSION	10-81

CHAPTER 11	CONCLUSIONS	11-1
CHAPTER 12	RECOMMENDATIONS	12-1
CHAPTER 13	REFERENCES	13-1
APPENDIX A	MIKE 11 CROSS SECTIONS	i
APPENDIX B	CROSS SECTION COORDINATES	i
APPENDIX C	WEIR CALIBRATION	i
C.1.	SURVEYED CROSS SECTIONS	I
C.2	DISCHARGE TABLE	II
APPENDIX D	SEDIMENT SAMPLES	i
D.1	PORTAL (G1H004 – A02)	I
D.2	DRIEFONTEIN WEIR (G1H004)	II
D.3	FRANSCHHOEK RIVER (G1H003)	III
D.4	PAARL WEIR (G1H020)	VI
D.5	HERMON WEIR (G1H036)	VIII
D.6	DRIEHEUWELS WEIR (G1H013)	XIII
APPENDIX E	INCIPIENT MOTION FIELD DATA	i

List of Figures

FIGURE 5-1	SHORT-TERM EFFECTIVE SEDIMENT CONCENTRATION COMPARED WITH LONG-TERM CONCENTRATION ON THE ORANGE RIVER (BASSON, 2004)	5-4
FIGURE 6-1	BERG RIVER CATCHMENT (ADAPTED FROM NITSCHKE, 2000)	6-2
FIGURE 6-2	GEOLOGY OF THE BERG RIVER CATCHMENT (ADAPTED FROM NITSCHKE, 2000)	6-5
FIGURE 6-3	TUNNEL RELEASES (G1H044M01/M02) DURING 1985 (DWAF, 2004)	6-7
FIGURE 6-4	TUNNEL RELEASES (G1H044M01/M02) DURING 1998 (DWAF, 2004)	6-7
FIGURE 7-1	LONGITUDINAL BED PROFILE OF THE UPPER REACH OF THE BERG RIVER (TRIBUTARIES INDICATED)	7-5
FIGURE 7-2	LONGITUDINAL BED PROFILE OF THE LOWER REACH OF THE BERG RIVER (TRIBUTARIES INDICATED)	7-5
FIGURE 7-3	BRAIDED RIVER SYSTEM UPSTREAM OF FRANSCHHOEK RIVER CONFLUENCE (1938)	7-6
FIGURE 7-4	TOPOGRAPHICAL MAP (3318 DD STELLENBOSCH)	7-7
FIGURE 7-5	BRAIDED RIVER SYSTEM UPSTREAM OF PAARL (1938) BETWEEN CH 13KM AND 16.5KM (BIENNE DONNE AND WATERVLIET)	7-8
FIGURE 7-6	BRAIDED RIVER SYSTEM UPSTREAM OF PAARL (1938) BETWEEN CH 16.5KM AND 18.5KM (BETWEEN WATERVLIET AND KUILENHOF)	7-8
FIGURE 7-7	BRAIDED RIVER SYSTEM UPSTREAM OF PAARL (1938) BETWEEN CH 19.5KM AND 20.5KM (KUILENHOF AND DRAAIHOOGTE UPSTREAM OF BRM3)	7-9
FIGURE 7-8	BRAIDED RIVER SYSTEM UPSTREAM OF FRANSCHHOEK CONFLUENCE (1953)	7-10
FIGURE 7-9	BERG RIVER BEFORE MISVERSTAND DAM	7-11
FIGURE 7-10	BERG RIVER AFTER MISVERSTAND DAM	7-11
FIGURE 7-11	BERG RIVER AROUND DEW DALE (1990), WITH MAIN CHANNEL (—) AND SECONDARY DIVERSION CHANNEL (- - -) INDICATED	7-13
FIGURE 7-12	TOPOGRAPHICAL MAP (3319CC FRANSCHHOEK)	7-14
FIGURE 7-13	SURVEY 2003 (BRC AND TCTA, 2003), WITH BLUE LINES INDICATING EXISTING CHANNELS	7-15
FIGURE 7-14	SURVEY 2003 (BRC AND TCTA, 2003), WITH BLUE LINES INDICATING EXISTING CHANNELS	7-16
FIGURE 7-15	FLOODPLAIN CHANGES (BRM SITE 1)	7-18
FIGURE 7-16	FLOODPLAIN CHANGES (BRM SITE 1)	7-19
FIGURE 8-1	ACTIVE AND PASSIVE LAYERS FOR THE SIMULATION OF GRADED SEDIMENTS	8-10
FIGURE 8-2	BERG RIVER SYSTEM (ADAPTED FROM NITSCHKE, 2000).	8-15
FIGURE 8-3	MISVERSTAND CROSS SECTIONS	8-16

FIGURE 8-4	LEVEL OF DIVIDE DEFINED AT A SECTION	8-18
FIGURE 8-5	ADDED CHANNEL AT SECTIONS OBTAINED FROM ORTHOPHOTOS	8-19
FIGURE 8-6	STORAGE – ELEVATION RELATIONSHIP FOR THE BERG RIVER DAM	8-22
FIGURE 8-7	DISCHARGE – WATER LEVEL RATING CURVE FOR THE BERG RIVER DAM SPILLWAY	8-23
FIGURE 8-8	RESERVOIR WATER LEVELS FOR THE POST-DAM SCENARIO	8-24
FIGURE 8-9	FLOOD RELEASE HYDROGRAPHS	8-27
FIGURE 8-10	OBSERVED FLOW SEQUENCE, G1H004 (INSTANTANEOUS PEAK DATA)	8-27
FIGURE 8-11	POST-DAM DAM OUTFLOW SEQUENCE WITH IFR LOW FLOWS (INSTANTANEOUS PEAK DATA)	8-28
FIGURE 8-12	POST-DAM DAM OUTFLOW SEQUENCE WITH IFR LOW FLOWS AND ARTIFICIAL FLOOD RELEASES (INSTANTANEOUS PEAK DATA)	8-28
FIGURE 8-13	ACTUAL IRRIGATION FLOW PATTERN ALONG THE BERG RIVER	8-30
FIGURE 8-14	SIMULATED IRRIGATION FLOW PATTERN ALONG THE BERG RIVER FOR THE PRESENT CONDITIONS	8-30
FIGURE 8-15	SIMULATED IRRIGATION FLOW PATTERN ALONG THE BERG RIVER FOR THE POST-DAM CONDITIONS	8-31
FIGURE 8-16	SUSPENDED SEDIMENT SAMPLING APPARATUS	8-34
FIGURE 8-17	SEDIMENT LOAD – DISCHARGE RELATIONSHIP AT G1H004 – A2 (DOWNSTREAM OF BRM SITE1)	8-35
FIGURE 8-18	SEDIMENT LOAD – DISCHARGE RELATIONSHIP AT G1H004	8-36
FIGURE 8-19	SEDIMENT LOAD – DISCHARGE RELATIONSHIP AT G1H003	8-36
FIGURE 8-20	SEDIMENT LOAD – DISCHARGE RELATIONSHIP AT G1H020	8-37
FIGURE 8-21	SEDIMENT LOAD – DISCHARGE RELATIONSHIP AT G1H036	8-37
FIGURE 8-22	SEDIMENT LOAD – DISCHARGE RELATIONSHIP AT G1H013	8-38
FIGURE 8-23	SEDIMENT LOAD – DISCHARGE RELATIONSHIP AT DRIEFONTEIN (G1H004) FOR 2003 AND 2004	8-39
FIGURE 8-24	SEDIMENT LOAD – DISCHARGE RATING CURVE AT FRANSCHHOEK RIVER (G1H003) FOR 2003 AND 2004	8-40
FIGURE 8-25	SEDIMENT LOAD – DISCHARGE RATING CURVE AT PAARL (G1H020) FOR 2003 AND 2004	8-40
FIGURE 8-26	SEDIMENT LOAD – DISCHARGE RATING CURVE AT HERMON (G1H036) FOR 2003 AND 2004	8-41
FIGURE 8-27	SEDIMENT LOAD – DISCHARGE RATING CURVE AT DRIEHEUWELS (G1H013) FOR 2003 AND 2004	8-41
FIGURE 8-28	DIFFERENCE IN SEDIMENT LOADS ON THE RISING AND FALLING LEG OF THE HYDROGRAPH – G1H004	8-42

FIGURE 8-29	DIFFERENCE IN SEDIMENT LOADS ON THE RISING AND FALLING LEG OF THE HYDROGRAPH – G1H003	8-43
FIGURE 8-30	DIFFERENCE IN SEDIMENT LOADS ON THE RISING AND FALLING LEG OF THE HYDROGRAPH – G1H020	8-43
FIGURE 8-31	DIFFERENCE IN SEDIMENT LOADS ON THE RISING AND FALLING LEG OF THE HYDROGRAPH – G1H036	8-44
FIGURE 8-32	DIFFERENCE IN SEDIMENT LOADS ON THE RISING AND FALLING LEG OF THE HYDROGRAPH – G1H013	8-44
FIGURE 8-33	SEDIMENT YIELDS FOR THE VARIOUS CATCHMENTS ALONG THE BERG RIVER SYSTEM	8-47
FIGURE 8-34	BED LOAD SAMPLING UPSTREAM OF WEST – PORTAL TUNNEL OUTLET	8-49
FIGURE 8-35	US – BLH 84 BEDLOAD SAMPLER	8-49
FIGURE 8-36	SCHEMATIC REPRESENTATION OF THE PERSPEX PIPES	8-53
FIGURE 8-37	PERSPEX PIPES INSTALLED TO REGISTER WATER LEVELS DURING FLOODS	8-53
FIGURE 8-38	PLAN VIEW OF PERSPEX PIPE LAYOUT AT EACH SITE	8-54
FIGURE 8-39	LOOP EFFECT AS A HYDROGRAPH PASSES A SPECIFIC LOCATION	8-55
FIGURE 8-40	HYDROGRAPH THAT WAS USED TO VERIFY LOOP EFFECT	8-55
FIGURE 8-41	HEIGHT – DISCHARGE RELATIONSHIP AT BRM SITE 1	8-56
FIGURE 8-42	LONGITUDINAL PROFILE OF THE CFP SETUP FOR A SITE	8-57
FIGURE 8-43	FACTORS INFLUENCING INITIATION OF MOVEMENT	8-59
FIGURE 8-44	FORCES ACTING ON AN EXPOSED PARTICLE	8-60
FIGURE 8-45	THRESHOLD OF MOVEMENT (SHIELDS, 1936)	8-62
FIGURE 8-46	THRESHOLD OF MOVEMENT (LIU, 1986)	8-66
FIGURE 8-47	DEFINITION OF EXPOSURE HEIGHT OF BED MATERIAL	8-68
FIGURE 8-48	MARKED PARTICLE AT BRM SITE 1 (MARITZ, 2003)	8-70
FIGURE 8-49	FIELD DATA PLOTTED ON THE SHIELDS DIAGRAM	8-71
FIGURE 8-50	FIELD DATA PLOTTED ON THE LIU DIAGRAM	8-72
FIGURE 8-51	COMPARISON BETWEEN SHIELDS THEORY AND EXPERIMENTAL DATA (DEY AND RAJU, 2002)	8-73
FIGURE 8-52	MULTIPLE LINEAR REGRESSION FOR GRAVEL BEDS (DEY AND RAJU, 2002)	8-76
FIGURE 8-53	MULTIPLE REGRESSION FOR COAL BEDS (DEY AND RAJU, 2002)	8-77
FIGURE 8-54	COMPARISON BETWEEN MEASURED AND CALCULATED CRITICAL SHEAR STRESS VALUES	8-78
FIGURE 8-55	CONTRIBUTING PARAMETERS PLOTTED AGAINST THE CRITICAL BED SHEAR STRESS	8-80
FIGURE 8-56	RECALIBRATION OF EMPIRICAL FORMULA	8-81
FIGURE 8-57	RELATIVE ROUGHNESS OF PROTECTED PARITCLES	8-82

FIGURE 8-58	PARTICLE DIAMETER VS STREAM POWER	8-83
FIGURE 8-59	THE RELATIONSHIP BETWEEN THE RELATIVE ROUGHNESS AND THE PARTICLE REYNOLDS NUMBER	8-84
FIGURE 8-60	LUI DIAGRAM K_s/D CONTOURS AGAINST BRM SITE 1 DATA	8-85
FIGURE 8-61	LUI DIAGRAM K_s/D CONTOURS COMPARED TO PARTICLE MOVEMENT	8-85
FIGURE 8-62	K_s/D TRENDLINE COMPARED TO PARTICLE MOVEMENT	8-86
FIGURE 9-1	CALIBRATION OF FLOW AT HERMON (G1H036) FOR 1999	9-4
FIGURE 9-2	CALIBRATION OF FLOW AT HERMON (G1H036) FOR 1999 (LOG SCALE)	9-4
FIGURE 9-3	CALIBRATION OF FLOW AT DRIEHEUWELS (G1H013) FOR 1999	9-5
FIGURE 9-4	CALIBRATION OF FLOW AT DRIEHEUWELS (G1H013) FOR 1999 (LOG SCALE)	9-5
FIGURE 9-5	FLOW RECORD AT DRIEFONTEIN (G1H004)	9-6
FIGURE 9-6	VERIFICATION OF THE CALIBRATION AT HERMON (G1H036) FOR 1995 TO 2001	9-7
FIGURE 9-7	VERIFICATION OF THE CALIBRATION AT DRIEHEUWELS (G1H013) FOR 1995 TO 2001	9-7
FIGURE 9-8	SEDIMENT LOAD RATING CURVE AT HERMON (G1H036)	9-9
FIGURE 9-9	SEDIMENT LOAD RATING CURVE AT DRIEHEUWELS (G1H013)	9-10
FIGURE 9-10	SEDIMENT LOAD VERIFICATION AT HERMON (G1H036)	9-12
FIGURE 9-11	SEDIMENT LOAD RATING CURVE VERIFICATION AT DRIEHEUWELS (G1H013)	9-12
FIGURE 10-1	ATTENUATION OF 100 M ³ /S FLOOD PEAK WITH DIFFERENT INITIAL FLOWS AT BRM4 AND HEAD OF ESTUARY FOR PRESENT SCENARIO	10-4
FIGURE 10-2	ATTENUATION OF 160 M ³ /S FLOOD PEAK WITH DIFFERENT INITIAL FLOWS AT BRM4 AND HEAD OF ESTUARY FOR PRESENT SCENARIO	10-5
FIGURE 10-3	ATTENUATION OF 220 M ³ /S FLOOD PEAK WITH DIFFERENT INITIAL FLOWS AT BRM4 AND HEAD OF ESTUARY FOR PRESENT SCENARIO	10-5
FIGURE 10-4	ATTENUATION OF 100 M ³ /S FLOOD PEAK WITH DIFFERENT INITIAL FLOWS AT BRM4 AND HEAD OF ESTUARY FOR THE POST-DAM SCENARIO	10-6
FIGURE 10-5	ATTENUATION OF 160 M ³ /S FLOOD PEAK WITH DIFFERENT INITIAL FLOWS AT BRM4 AND HEAD OF ESTUARY FOR THE POST-DAM SCENARIO	10-6
FIGURE 10-6	ATTENUATION OF 220 M ³ /S FLOOD PEAK WITH DIFFERENT INITIAL FLOWS AT BRM4 AND HEAD OF ESTUARY FOR THE POST-DAM SCENARIO	10-7
FIGURE 10-7	SIMULATED FLOW SERIES (9-YEARS) AT BRM2 – PRESENT SCENARIO (INSTANTANEOUS PEAK DATA) – LOG SCALE	10-9
FIGURE 10-8	SIMULATED FLOW SERIES (9-YEARS) AT BRM2 – PRESENT SCENARIO (INSTANTANEOUS PEAK DATA) – NORMAL SCALE	10-10
FIGURE 10-9	SIMULATED FLOW SERIES (9-YEARS) AT BRM2 – POST-DAM SCENARIO (INSTANTANEOUS PEAK DATA) – LOG SCALE	10-10

FIGURE 10-10	SIMULATED FLOW SERIES (9-YEARS) AT BRM2 – POST-DAM SCENARIO (INSTANTANEOUS PEAK DATA) – NORMAL SCALE	10-11
FIGURE 10-11	SIMULATED FLOW SERIES (9-YEARS) AT BRM2 – POST-DAM WITH FLOOD RELEASES SCENARIO (INSTANTANEOUS PEAK DATA) – LOG SCALE	10-11
FIGURE 10-12	SIMULATED FLOW SERIES (9-YEARS) AT BRM2 – POST-DAM WITH FLOOD RELEASES SCENARIO (INSTANTANEOUS PEAK DATA) – NORMAL SCALE	10-12
FIGURE 10-13	DISCHARGE - FREQUENCY GRAPH FOR BRM2	10-12
FIGURE 10-14	FLOW DEPTH - FREQUENCY GRAPH FOR BRM2 – TRANSECT A	10-13
FIGURE 10-15	FLOW DEPTH - FREQUENCY GRAPH FOR BRM2 – TRANSECT B	10-13
FIGURE 10-16	FLOW DEPTH - FREQUENCY GRAPH FOR BRM2 – TRANSECT C	10-14
FIGURE 10-17	FLOW VELOCITY - FREQUENCY GRAPH FOR BRM2 – TRANSECT A	10-14
FIGURE 10-18	FLOW VELOCITY - FREQUENCY GRAPH FOR BRM2 – TRANSECT B	10-15
FIGURE 10-19	FLOW VELOCITY - FREQUENCY GRAPH FOR BRM2 – TRANSECT C	10-15
FIGURE 10-20	SIMULATED FLOW SERIES (9 YEARS) FOR BRM3 – PRESENT DAY SCENARIO (INSTANTANEOUS PEAK DATA) – LOG SCALE	10-17
FIGURE 10-21	SIMULATED FLOW SERIES (9 YEARS) FOR BRM3 – PRESENT DAY SCENARIO (INSTANTANEOUS PEAK DATA) – NORMAL SCALE	10-18
FIGURE 10-22	SIMULATED FLOW SERIES (9 YEARS) FOR BRM3 – POST-DAM SCENARIO (INSTANTANEOUS PEAK DATA) – LOG SCALE	10-18
FIGURE 10-23	SIMULATED FLOW SERIES (9 YEARS) FOR BRM3 – POST-DAM SCENARIO (INSTANTANEOUS PEAK DATA) – NORMAL SCALE	10-19
FIGURE 10-24	SIMULATED FLOW SERIES (9 YEARS) FOR BRM3 – POST-DAM WITH FLOOD RELEASES SCENARIO (INSTANTANEOUS PEAK DATA) – NORMAL SCALE	10-19
FIGURE 10-25	SIMULATED FLOW SERIES (9 YEARS) FOR BRM3 – POST-DAM WITH FLOOD RELEASES SCENARIO (INSTANTANEOUS PEAK DATA) – NORMAL SCALE	10-20
FIGURE 10-26	DISCHARGE - FREQUENCY GRAPH FOR BRM3	10-20
FIGURE 10-27	FLOW DEPTH - FREQUENCY GRAPH FOR BRM3 – TRANSECT A	10-21
FIGURE 10-28	FLOW DEPTH - FREQUENCY GRAPH FOR BRM3 – TRANSECT B	10-21
FIGURE 10-29	FLOW DEPTH - FREQUENCY GRAPH FOR BRM3 – TRANSECT C	10-22
FIGURE 10-30	FLOW VELOCITY - FREQUENCY GRAPH FOR BRM3 – TRANSECT A	10-22
FIGURE 10-31	FLOW VELOCITY - FREQUENCY GRAPH FOR BRM3 – TRANSECT B	10-23
FIGURE 10-32	FLOW VELOCITY - FREQUENCY GRAPH FOR BRM3 – TRANSECT C	10-23
FIGURE 10-33	SIMULATED FLOW SERIES (9 YEARS) FOR BRM4 – PRESENT DAY SCENARIO (INSTANTANEOUS PEAK DATA) – LOG SCALE	10-25
FIGURE 10-34	SIMULATED FLOW SERIES (9 YEARS) FOR BRM4 – PRESENT DAY SCENARIO (INSTANTANEOUS PEAK DATA) – NORMAL SCALE	10-26

FIGURE 10-35	SIMULATED FLOW SERIES (9 YEARS) FOR BRM4 – POST-DAM SCENARIO (INSTANTANEOUS PEAK DATA) – LOG SCALE	10-26
FIGURE 10-36	SIMULATED FLOW SERIES (9 YEARS) FOR BRM4 – POST-DAM SCENARIO (INSTANTANEOUS PEAK DATA) – NORMAL SCALE	10-27
FIGURE 10-37	SIMULATED FLOW SERIES (9 YEARS) FOR BRM4 – POST-DAM WITH FLOOD RELEASES SCENARIO (INSTANTANEOUS PEAK DATA) – LOG SCALE	10-27
FIGURE 10-38	SIMULATED FLOW SERIES (9 YEARS) FOR BRM4 – POST-DAM WITH FLOOD RELEASES SCENARIO (INSTANTANEOUS PEAK DATA) – NORMAL SCALE	10-28
FIGURE 10-39	DISCHARGE - FREQUENCY GRAPH FOR BRM4	10-28
FIGURE 10-40	FLOW DEPTH - FREQUENCY GRAPH FOR BRM4 – TRANSECT A	10-29
FIGURE 10-41	FLOW DEPTH - FREQUENCY GRAPH FOR BRM4 - TRANSECT B	10-29
FIGURE 10-42	FLOW DEPTH - FREQUENCY GRAPH FOR BRM4 – TRANSECT C	10-30
FIGURE 10-43	FLOW VELOCITY - FREQUENCY GRAPH FOR BRM4 – TRANSECT A	10-30
FIGURE 10-44	FLOW VELOCITY - FREQUENCY GRAPH FOR BRM4 – TRANSECT B	10-31
FIGURE 10-45	FLOW VELOCITY - FREQUENCY GRAPH FOR BRM4 – TRANSECT C	10-31
FIGURE 10-46	SIMULATED FLOW SERIES (9 YEARS) FOR BRM5 – PRESENT DAY SCENARIO (INSTANTANEOUS PEAK DATA) – LOG SCALE	10-33
FIGURE 10-47	SIMULATED FLOW SERIES (9 YEARS) FOR BRM5 – PRESENT DAY SCENARIO (INSTANTANEOUS PEAK DATA) – NORMAL SCALE	10-34
FIGURE 10-48	SIMULATED FLOW SERIES (9 YEARS) FOR BRM5 – POST-DAM SCENARIO (INSTANTANEOUS PEAK DATA) – LOG SCALE	10-34
FIGURE 10-49	SIMULATED FLOW SERIES (9 YEARS) FOR BRM5 – POST-DAM SCENARIO (INSTANTANEOUS PEAK DATA) – NORMAL SCALE	10-35
FIGURE 10-50	SIMULATED FLOW SERIES (9 YEARS) FOR BRM5 – POST-DAM WITH FLOOD RELEASES SCENARIO (INSTANTANEOUS PEAK DATA) – LOG SCALE	10-35
FIGURE 10-51	SIMULATED FLOW SERIES (9 YEARS) FOR BRM5 – POST-DAM WITH FLOOD RELEASES SCENARIO (INSTANTANEOUS PEAK DATA) – NORMAL SCALE	10-36
FIGURE 10-52	DISCHARGE - FREQUENCY GRAPH FOR BRM5	10-36
FIGURE 10-53	FLOW DEPTH - FREQUENCY GRAPH FOR BRM5 – TRANSECT A	10-37
FIGURE 10-54	FLOW DEPTH - FREQUENCY GRAPH FOR BRM5 – TRANSECT B	10-37
FIGURE 10-55	FLOW DEPTH - FREQUENCY GRAPH FOR BRM5 – TRANSECT C	10-38
FIGURE 10-56	FLOW VELOCITY - FREQUENCY GRAPH FOR BRM5 – TRANSECT A	10-38
FIGURE 10-57	FLOW VELOCITY - FREQUENCY GRAPH FOR BRM5 – TRANSECT B	10-39
FIGURE 10-58	FLOW VELOCITY - FREQUENCY GRAPH FOR BRM5 – TRANSECT C	10-39
FIGURE 10-59	SIMULATED FLOW SERIES (9 YEARS) FOR BRM6 – PRESENT DAY SCENARIO (INSTANTANEOUS PEAK DATA) – LOG SCALE	10-41

FIGURE 10-60	SIMULATED FLOW SERIES (9 YEARS) FOR BRM6 – PRESENT DAY SCENARIO (INSTANTANEOUS PEAK DATA) – NORMAL SCALE	10-42
FIGURE 10-61	SIMULATED FLOW SERIES (9 YEARS) FOR BRM6 – POST-DAM SCENARIO (INSTANTANEOUS PEAK DATA) – LOG SCALE	10-42
FIGURE 10-62	SIMULATED FLOW SERIES (9 YEARS) FOR BRM6 – POST-DAM SCENARIO (INSTANTANEOUS PEAK DATA) – NORMAL SCALE	10-43
FIGURE 10-63	SIMULATED FLOW SERIES (9 YEARS) FOR BRM6 – POST-DAM WITH FLOOD RELEASES SCENARIO (INSTANTANEOUS PEAK DATA) – LOG SCALE	10-43
FIGURE 10-64	SIMULATED FLOW SERIES (9 YEARS) FOR BRM6 – POST-DAM WITH FLOOD RELEASES SCENARIO (INSTANTANEOUS PEAK DATA) – NORMAL SCALE	10-44
FIGURE 10-65	DISCHARGE - FREQUENCY GRAPH FOR BRM6	10-44
FIGURE 10-66	FLOW DEPTH - FREQUENCY GRAPH FOR BRM6 – TRANSECT A	10-45
FIGURE 10-67	FLOW DEPTH - FREQUENCY GRAPH FOR BRM6 – TRANSECT B	10-45
FIGURE 10-68	FLOW DEPTH - FREQUENCY GRAPH FOR BRM6 – TRANSECT C	10-46
FIGURE 10-69	FLOW VELOCITY - FREQUENCY GRAPH FOR BRM6 – TRANSECT A	10-46
FIGURE 10-70	FLOW VELOCITY - FREQUENCY GRAPH FOR BRM6 – TRANSECT B	10-47
FIGURE 10-71	FLOW VELOCITY - FREQUENCY GRAPH FOR BRM6 – TRANSECT C	10-47
FIGURE 10-72	UPPER BERG RIVER MASS BALANCE – PRESENT SITUATION (MILLION M ³ /A)	10-49
FIGURE 10-73	UPPER BERG RIVER MASS BALANCE – POST-DAM SCENARIO (MILLION M ³ /A)	10-50
FIGURE 10-74	UPPER BERG RIVER MASS BALANCE – POST-DAM WITH FLOOD RELEASES (MILLION M ³ /A)	10-51
FIGURE 10-75	LOWER BERG RIVER HYDRODYNAMIC MASS BALANCE - PRESENT SITUATION (MILLION M ³ /A)	10-52
FIGURE 10-76	LOWER BERG RIVER HYDRODYNAMIC MASS BALANCE – POST DAM SITUATION (MILLION M ³ /A)	10-53
FIGURE 10-77	LOWER BERG RIVER HYDRODYNAMIC MASS BALANCE - POST-DAM WITH FLOOD RELEASES (MILLION M ³ /A)	10-54
FIGURE 10-78	CUMULATIVE SEDIMENT DISCHARGE AT BRM2	10-55
FIGURE 10-79	CUMULATIVE SEDIMENT DISCHARGE AT BRM3	10-56
FIGURE 10-80	CUMULATIVE SEDIMENT DISCHARGE AT BRM4	10-56
FIGURE 10-81	CUMULATIVE SEDIMENT DISCHARGE AT BRM5	10-57
FIGURE 10-82	CUMULATIVE SEDIMENT DISCHARGE AT BRM6	10-57
FIGURE 10-83	PERCENTAGE OF TOTAL SEDIMENT LOAD VERSUS MEAN DISCHARGE AT SITE 2	10-60
FIGURE 10-84	PERCENTAGE OF TOTAL SEDIMENT LOAD VERSUS MEAN DISCHARGE AT SITE 3	10-61
FIGURE 10-85	UPPER BERG RIVER MASS BALANCE – PRESENT SITUATION	10-62
FIGURE 10-86	UPPER BERG RIVER MASS BALANCE – POST-DAM SCENARIO	10-63
FIGURE 10-87	UPPER BERG RIVER MASS BALANCE – POST-DAM WITH FLOOD RELEASES	10-64

FIGURE 10-88	PERCENTAGE OF TOTAL SEDIMENT LOAD VERSUS MEAN DISCHARGE AT SITE 410-67	
FIGURE 10-89	PERCENTAGE OF TOTAL SEDIMENT LOAD VERSUS MEAN DISCHARGE AT SITE 510-68	
FIGURE 10-90	PERCENTAGE OF TOTAL SEDIMENT LOAD VERSUS MEAN DISCHARGE AT SITE 610-69	
FIGURE 10-91	LOWER BERG RIVER MASS BALANCE – PRESENT SITUATION	10-71
FIGURE 10-92	LOWER BERG RIVER MASS BALANCE – POST-DAM SCENARIO	10-72
FIGURE 10-93	LOWER BERG RIVER MASS BALANCE – POST-DAM WITH FLOOD RELEASES	10-73
FIGURE 10-94	CUMULATIVE SEDIMENT LOAD AND WATER DISCHARGE AT BRM2(97 – 03)	10-75
FIGURE 10-95	CUMULATIVE SEDIMENT LOAD AND WATER DISCHARGE AT BRM3(97 - 03)	10-75
FIGURE 10-96	CUMULATIVE SEDIMENT LOAD AND WATER DISCHARGE AT BRM4 (97 – 03)	10-76
FIGURE 10-97	CUMULATIVE SEDIMENT LOAD AND WATER DISCHARGE AT BRM5 (97 - 03)	10-76
FIGURE 10-98	CUMULATIVE SEDIMENT LOAD AND WATER DISCHARGE AT BRM6 (97 - 03)	10-77
FIGURE 10-99	SEDIMENT RATING CURVES AT BRM2	10-79
FIGURE 10-100	SEDIMENT RATING CURVES AT BRM3	10-79
FIGURE 10-101	SEDIMENT RATING CURVES AT BRM4	10-80
FIGURE 10-102	SEDIMENT RATING CURVES AT BRM5	10-80
FIGURE 10-103	SEDIMENT RATING CURVES AT BRM6	10-81

List of Tables

TABLE 5-1	NON-COHESIVE SEDIMENT TRANSPORT EQUATION ACCURACY.....	5-2
TABLE 5-2	WIDTH CHANGES IN SOUTH AFRICAN RIVERS (BECK ET AL, 2003)	5-10
TABLE 6-1	BERG RIVER TRIBUTARIES AND CATCHMENT AREAS UP TO THE GAUGING STATIONS	6-1
TABLE 6-2	TEMPERATURE DATA FOR THE BERG RIVER CATCHMENT (WESTERN CAPE SYSTEM ANALYSIS,1994).	6-4
TABLE 7-1	SEGMENT CHARACTERISTICS OF THE BERG RIVER (ROWNTREE AND MCGREGOR, 1996).....	7-2
TABLE 7-2	REACHES ALONG THE BERG RIVER (ROWNTREE AND MCGREGOR, 1996)	7-2
TABLE 7-3	BRM SITE LOCATION	7-4
TABLE 8-1	DIVIDED SECTIONS.....	8-18
TABLE 8-2	INITIAL ADJUSTMENT FACTORS TO ACCOUNT FOR UNGAUGED AREAS AT TRIBUTARIES	8-20
TABLE 8-3	MONTHLY DISTRIBUTION OF AGRICULTURAL RELEASES.....	8-22
TABLE 8-4	PROPOSED (DWAF, 2003) AND SIMULATED IFR FLOWS AT THE DAM SITE	8-25
TABLE 8-5	TIMING AND MAGNITUDE OF SIMULATED ARTIFICIAL FLOOD RELEASES BASED ON HISTORICAL RECORDS	8-26
TABLE 8-6	IFR ESTIMATE LOW FLOW FOR THE QUATERNARY CATCHMENT AREA G10A AT IFR SITE 1 (DWAF, 2003)	8-29
TABLE 8-7	LOCATION OF SEDIMENT SAMPLES AND CALCULATED SEDIMENT YIELDS	8-45
TABLE 8-8	BED LOAD SAMPLING IN 2003	8-50
TABLE 8-9	BED LOAD SAMPLING IN 2004.....	8-50
TABLE 8-10	THE D_{50} OF THE BED SAMPLES THAT WAS TAKEN IN THE BERG RIVER.....	8-51
TABLE 8-11	PARTICLE SIZE DISTRIBUTION	8-51
TABLE 8-12	COMPOSITION OF ACTIVE AND PASSIVE LAYERS	8-52
TABLE 8-13	BRM SITE LOCATION	8-52
TABLE 8-14	MANNING'S N – VALUES FOR THE BRM SITES.....	8-57
TABLE 8-15	INITIAL ROUGHNESS COEFFICIENTS USED IN THE ONE DIMENSIONAL MODEL	8-58
TABLE 8-16	HYDRAULIC PARAMETERS FOR 2003 FLOODS	8-71
TABLE 8-17	INCIPIENT MOTION AT BRM SITE 1	8-87
TABLE 8-18	DURATION OF FLOOD FLOW EXCEEDENCE.....	8-87
TABLE 9-1	REVISED CALIBRATED ADJUSTMENT FACTORS TO ACCOUNT FOR UNGAUGED AREAS AT TRIBUTARIES	9-2

TABLE 9-2	OBSERVED AND CALIBRATED MAR AT HERMON (G1H036) AND DRIEHEUWELS (G1H013).....	9-3
TABLE 9-3	TIME ADJUSTMENTS MADE TO THE FLOW RECORD AT THE TRIBUTARIES.....	9-3
TABLE 9-4	REVISED ROUGHNESS COEFFICIENTS USED IN THE ONE DIMENSIONAL MODEL	9-3
TABLE 9-5	FACTORS USED TO CALIBRATE THE SEDIMENT TRANSPORT	9-10
TABLE 10-1	RETURN PERIOD FLOODS FOR TWO SCENARIOS AT BRM2, BRM3 BRM4, BRM5 AND BRM6 (BASED ON 9-YEAR RECORD).....	10-2
TABLE 10-2	RETURN PERIOD FLOODS BASED ON TOTAL FLOW RECORD AT DRIEFONTEIN (G1H004), HERMON (G1H036) AND DRIEHEUWELS (G1H013).....	10-2
TABLE 10-3	FLOOD PEAKS AND RETURN PERIODS AT BRM 2, WITH CORRESPONDING RECURRENCE INTERVAL FLOOD PEAKS AT BRM4 AND BRM6	10-3
TABLE 10-4	SIMULATED ATTENUATED FLOOD PEAKS AT BRM4 (HERMON) AND HEAD OF ESTUARY WITH DIFFERENT INITIAL FLOWS FOR THE PRESENT DAY SCENARIO....	10-3
TABLE 10-5	SIMULATED ATTENUATED FLOOD PEAKS AT BRM4 (HERMON) AND HEAD OF ESTUARY WITH DIFFERENT INITIAL FLOWS FOR THE POST-DAM SCENARIO	10-4
TABLE 10-6	CONTRIBUTION OF WITHIN YEAR FLOODS TO TOTAL FLOW FOR THREE SCENARIOS AT BRM2	10-8
TABLE 10-7	FLOODPLAIN INUNDATION AT BRM2	10-8
TABLE 10-8	NUMBER OF FLOODS ABOVE 100 m ³ /s FOR THE 9-YEAR PERIOD AT BRM2	10-9
TABLE 10-9	CONTRIBUTION OF WITHIN YEAR FLOODS TO TOTAL FLOW FOR THREE SCENARIOS AT BRM3	10-16
TABLE 10-10	FLOODPLAIN INUNDATION AT BRM3	10-16
TABLE 10-11	NUMBER OF FLOODS ABOVE 100 m ³ /s FOR THE 9-YEAR PERIOD AT BRM3	10-17
TABLE 10-12	CONTRIBUTION OF WITHIN YEAR FLOODS TO TOTAL FLOW FOR THREE SCENARIOS AT BRM4	10-24
TABLE 10-13	FLOODPLAIN INUNDATION AT BRM4	10-24
TABLE 10-14	NUMBER OF FLOODS ABOVE 100 m ³ /s FOR THE 9-YEAR PERIOD AT BRM4	10-25
TABLE 10-15	CONTRIBUTION OF WITHIN YEAR FLOODS TO TOTAL FLOW FOR THREE SCENARIOS AT BRM5	10-32
TABLE 10-16	FLOODPLAIN INUNDATION FOR BRM5	10-32
TABLE 10-17	NUMBER OF FLOODS ABOVE 200 m ³ /s FOR THE 9-YEAR PERIOD AT BRM5	10-33
TABLE 10-18	CONTRIBUTION OF WITHIN YEAR FLOODS TO TOTAL FLOW FOR THREE SCENARIOS AT BRM6	10-40
TABLE 10-19	FLOODPLAIN INUNDATION AT BRM6	10-40
TABLE 10-20	NUMBER OF FLOODS ABOVE 200 m ³ /s FOR THE 9-YEAR PERIOD AT BRM6	10-40
TABLE 10-21	SITE 2 - FLOW CLASSES AND ASSOCIATED SEDIMENT TRANSPORT	10-59
TABLE 10-22	SITE 3 - FLOW CLASSES AND ASSOCIATED SEDIMENT TRANSPORT	10-60

TABLE 10-23 SITE 4 - FLOW CLASSES AND ASSOCIATED SEDIMENT TRANSPORT 10-66

TABLE 10-24 FLOOD RELEASE ATTENUATION ALONG THE BERG RIVER 10-67

TABLE 10-25 SITE 5 - FLOW CLASSES AND ASSOCIATED SEDIMENT TRANSPORT 10-68

TABLE 10-26 SITE 6 - FLOW CLASSES AND ASSOCIATED SEDIMENT TRANSPORT 10-69

List of Symbols

a, b, c	=	Various axial lengths of the particle under consideration (m).
A	=	Flow Area (m ²).
A_m	=	Measured Catchment Area (km ²)
A_p	=	Area of exposed particle (m ²).
A_s	=	Surface Area (m ²).
A_u	=	Ungauged Catchment Area (km ²).
α'	=	Vertical Velocity Distribution coefficient.
B, W	=	Channel Width (m).
B_p	=	Post Dam Sectional Width (m).
c_b	=	Bed Load Concentration.
D, d	=	Particle diameter (m).
d_e	=	Effective Diameter (m).
d_i	=	Diameter of the i^{th} Fraction (m).
d_m	=	Diameter of the Arithmetic Mean of the Bed Material (m).
D_m	=	Hydraulic mean depth (m).
D_p	=	Post Dam Sectional Depth (m).
D_w	=	Water Depth (m).
d_{50}	=	Mean Particle Diameter (m).
C_d	=	Drag Coefficient.
C_l	=	Lift Coefficient.
F_d	=	Particle Froude Number.
ϕ	=	Angle of Repose.
g	=	Acceleration due to Gravity (m/s ²).
H, h	=	Water Depth (m).
I_b	=	Channel Bottom Slope (m/m).
k_s	=	Surface Roughness (m).
κ	=	von Karman Constant.
μ	=	Coulomb's Friction Coefficient.

μ	=	Absolute Viscosity (kg/m.s).
n	=	Manning's n Value to Describe Bed Roughness.
q	=	Unit Discharge (m ³ /s.m).
q_b	=	Unit Bed Load Transport (m ³ /s.m).
q_s	=	Unit Suspended Load Transport (m ³ /s.m).
Q	=	discharge (m ³ /s).
Q_{10}	=	1 : 10 Year Discharge (m ³ /s).
Q_{pl}	=	Highest Flood Peak for the Pre – Dam period (m ³ /s).
R_e	=	Reynolds Number.
R	=	Hydraulic Radius (m).
ρ	=	Water Density (kg/m ³).
ρ_s	=	Sediment Density (kg/m ³).
S_o	=	Local Bed Slope (m/m).
S_f	=	Energy Slope (m/m).
τ_o	=	Bed Shear Stress.
τ_{cr}	=	Critical Bed Shear Stress as Defined by Shields (1936).
u_*	=	Friction Velocity (m/s).
\bar{u}	=	Average Flow Velocity (m/s).
u_{bs}	=	Particle velocity (m/s).
u_p	=	Bed Shear Velocity (m/s).
ν	=	Dynamic Viscosity (kg/m.s).
V	=	Mean velocity (m/s).
V_{50}	=	50 Year Sediment Volume (m ³).
V_*	=	Shear Velocity (m/s).
w, v_{ss}	=	Particle Settling Velocity in Water (m/s).

CHAPTER 1 INTRODUCTION

1.1 Background

The Berg River is one of the largest rivers in the winter rainfall area of the Western Cape and is one of the most important water supply sources of the area. The river starts in the Groot Drakenstein Mountain range and from there it runs to the sea at Velddrif.

As the Cape Town Metropolitan continues to grow so does the water demand. Future schemes proposed to supply the demands are: the Berg River Dam, the Berg River supplement scheme downstream of Franschhoek, Wemmershoek and Dwars Rivers, and the Lorelei Diversion to an enlarged Voëlvlei Dam in the middle Berg River region (Nitsche, 2001). Concerns have been raised about possible changes in the sediment balance of the Berg River System, water quality as well as salinity problems should the above mentioned schemes be implemented.

In 2002 the Department of Water Affairs and Forestry initiated a project, the Berg River Baseline Monitoring Programme, to monitor some of the above mentioned changes. In short the overall objective of the Baseline Monitoring Programme (BRM) is to describe the natural and present state, including the natural variability, of those chemical, physical and biological characteristics of the river and its hydraulically linked systems (i.e. estuary, floodplains and groundwater) that are most likely to be affected by changes imposed after the construction of the Berg River Dam. Some of the variables that are being measured are:

- Biannual bed level surveys of the 6 BRM sites, together with water depths, flow velocities, cobble size and embeddedness in the upper reach,
- Habitat mapping,
- And various other biological measurements.

The sediment balance of the Berg River forms an integral part of the Berg River Baseline Monitoring Programme. Many of the hydraulic and fluvial morphological changes in the river can be quantified by looking at the changes in the sediment balance. A one dimensional

mathematical model was used to describe the hydrodynamics and sediment transport of the Berg River. This model was used to investigate various scenarios both without a dam development and with a new dam development.

Various studies have been carried with the main objective to quantify the sediment balance in a river system. For example Birkhead, Heritage, James, Rogers and van Niekerk (1998) did a study on the Sabie River, South Africa, in order to further the understanding of the sediment balance in the Sabie River Basin. A semi – quantitative sediment flux and storage model was developed for predicting change at the channel type scale on an annual basis. The Sabie River SEDiment FLux and stOrage model (SEDFLO) consists of two integral components. The first component deals with sediment production across the catchment and the delivery of this eroded source material to the study length of the Sabie River (Sediment Yield). Sediment Yield maps and various models like the Agricultural Catchments Research Unit (ACRU) model was used to estimate the sediment Yield. The second component of SEDFLO is the prediction of the total sediment load transported along the river. The theory developed by Ackers and White (1973) was used to calculate the sediment discharge of the study length of the Sabie River. Aerial photographs were utilized to calibrate SEDFLO against geomorphological change along the river.

CHAPTER 2 MOTIVATION

Kariba Reservoir on the Zambezi River, Zambia/Zimbabwe, has a surface area of 5 500 km² at full supply level and a full supply capacity of 180 billion m³. Gariep Reservoir on the Orange River, South Africa, had an original full supply capacity of 5.95 billion m³ (Beck and Basson, 2003). Considering the size of these reservoirs and of the other dams built over the past 100 years, it is not surprising to assume that these structures will have a major influence on the downstream river morphology as well as the sediment mass balance from catchment to coast.

With water resources development such as dam construction, floods are attenuated and dams trap most of the sediment load entering the reservoir. The relatively clear water that is released during floods from the dam therefore typically leads to bed degradation near the dam, but aggradation of the bed is also possible further downstream of tributaries due to the flood attenuation effect caused by the dam.

Regime theory can be used to describe the generally expected fluvial morphological changes in the river, but does not provide information on the sediment mass balance, and it was therefore decided to use hydrodynamic mathematical modelling linked to a sediment transport module to describe sediment transport through the Berg River system, considering bed roughness, floodplain flow, erosion, deposition, observed sediment loads and long-term equilibrium.

Furthermore, the fluvial morphological changes in the river, like any changes in channel width and/or depth as well as changes in the discharge and vegetation on the flood plains will have a significant effect on the ecological and biological parameters also being measured by the Berg River Baseline Monitoring Programme. The people responsible for these measurements need the sediment transport data as well as any other hydraulic changes that might occur due to the dam development in the upper reaches of the river in order to quantify the effect on the ecological and biological parameters.

CHAPTER 3 OBJECTIVES

The overall objective of this thesis is to quantify the sediment transport in the Berg River and investigate the sediment balance from catchment to coast (in this case up to the head of the Berg River Estuary) in the Berg River, by:

- Developing an understanding of the process of sediment transport in a natural stream.
- Utilization of physical processes and hydraulics to do the setup and calibration of a one dimensional mathematical model, Mike 11.
- Developing an understanding of the effects dam developments will have on the sediment balance in a river system.
- Quantify the influence of the Berg River Dam on the sediment balance in the Berg River System by utilizing the mathematical model to simulate and investigate the following scenarios:
 - Present day situation.
 - Dam development.
 - Dam development with addition artificial/managed flood releases.

CHAPTER 4 METHODOLOGY

The methodology followed in this research is as follows,

- An overview of literature on sediment transport dynamics, sediment yield estimation methods and impacts of dam developments on the downstream river morphology is given in **CHAPTER 5**.
- In **CHAPTER 6** a general description of the Berg River Basin is given. In this chapter special reference is made to factors that have an influence on either the sediment transport capacity of the river or on the sediment availability in the Berg River catchment.
- The geomorphological assessment of the Berg River as well as some historical changes that occurred over the years is presented in **CHAPTER 7** as part of the review of the Berg River fluvial morphology. Artificial changes on the floodplains are discussed.
- A one dimensional hydrodynamic and morphological numerical model (MIKE11) is utilized to investigate the sediment balance from catchment to coast. The various required input data is described in **CHAPTER 8**.
- The hydrodynamic and the sediment load calibration of the one dimensional model were done against measured field data. The calibration method is given in **CHAPTER 9**.
- The one dimensional model is utilized to quantified changes that will prevail in the sediment balance of the Berg River Basin due to the construction and operation of the Berg River Dam (**CHAPTER 10**). This was achieved by simulation of the following scenarios:
 - Present day scenario,
 - Post dam development scenario,
 - Post dam development scenario with additional artificial environmental flood releases.
- Various conclusions and recommendations with regards to the effect of the environmental flood releases and the sediment balance prior to the Berg River Dam as well as after the dam are made and discussed in **CHAPTER 11** and **CHAPTER 12**.

Both bed load and suspended sediment load samples were taken in order to calibrate the sediment transport model. Water levels were registered during the flood season to obtain initial bed roughness coefficients. All the field work, both the methods and results, are presented and discussed in the various chapters (mainly **CHAPTER 8 & CHAPTER 9**) as it was used to assist in obtaining input data or calibration/verification data for the one dimensional model.

Some consideration was given to the incipient motion of coarser (cobbles and boulders) bed materials as this is definitely an area that presents problems (**CHAPTER 8**). Most sediment transport theories are only valid for diameters smaller than 20 mm therefore these models are not applicable to particles larger than 20 mm. Literature was used to obtain an overview of the basic theory on incipient motion. This theory was applied and compared to field data in order to obtain a clearer understanding of the incipient motion of the coarser sediment in the upper reaches of the Berg River (upstream of Paarl).

CHAPTER 5 REVIEW OF RESEARCH ON SEDIMENT TRANSPORT DYNAMICS FROM CATCHMENT TO COAST

5.1 Sediment Transport Dynamics and Sediment Transport Equations

The basis of sediment routing in a river is the sediment transport equation used. When dealing with non-cohesive sediments where the sediment diameter > 0.03 mm, several sediment transport capacity equations are widely used. Most of these equations are based on the stream power principle, and are calibrated against field and/or laboratory tests. The sediment that is transported during flood events is of particular importance during the calibration as they are responsible for the bulk of the sediment volumes that are transported by the river. The range of applicability of the transport equations vary from 0.07 mm to about 2 mm in diameter and in some cases the equations were calibrated to a diameter of 30 mm. Due to the variation in the shape and size of the various sediments that are carried by rivers, the calibration of these equations in such a fashion that they are applicable to all scenarios, is extremely difficult. In the case of non – uniform sediments a multi – fraction approach is followed. The transport capacity of each fraction is calculated and possible entrainment from the bed is considered. This approach assumes that different fractions in the bed react independently with no interrelationship. In reality, however, the coarser particles will be more exposed, while the finer particles are hidden (shielded for the flow) by the coarser particles. Although several theories have been developed to describe sediment hiding, armouring and exposure in non-uniform beds, it is seldom used in sediment transport simulations.

Table 5-1 shows a comparison carried out by White et al.,(1973), Van Rijn (1984) and Yang and Molinas (1982) between formulae. In general a 50% prediction accuracy is considered to be good. The inaccuracies in predicting sediment transport cannot be blamed on the theory alone but also on the data reliability, availability and variability.

Table 5-1 Non-cohesive sediment transport equation accuracy

White et al., (1973) compared eight formulae using 1000 flume and 260 field measurements. The discrepancy ratio X_{calc}/X_{obs} was plotted against the dimensionless grain size ($\rho_{sq}/\rho q$) and the percentages within the 0.5 to 2 range were as follows:													
Formula					% in $0.5 \leq X_{calc}/X_{obs} \leq 2$ ranges								
Ackers and White (1973)					68								
Engelund and Hansen (1967)					63								
Einstein (1950) (total load)					46								
Bishop et al., (1965)					39								
Toffaletti (1968)					37								
Bagnold (1966) (total load)					22								
Meyer-Peter and Müller (1948)					10								
The laboratory data include particle sizes from 0.04 to 4.94 mm and field data from 0.095 to 68 mm.													
The comparison of formulae by Yang and Molinas (1982) also used laboratory and river data encompassing mean grain sizes from 0.15 to 1.71 mm, channel widths 0.134 to 532 m, flow depths 0.01 to 15.2 m, temperature 0° to 34.3°C, average velocity 0.23 to 1.97 m/s and slopes from 4.3×10^{-5} to 2.79×10^{-2} . The range of data is the same as given by Yang (1973) for the data from which the formula was derived. The discrepancy ratio, defined as the ratio between computed and measured values, is given as follows:													
Formula		Data											
		Lab.				River				All data			
Colby (1964)		0.31				0.61				0.34			
Yang (1973)		1.01				1.31				1.03			
Yang (1979)		1.02				1.12				1.03			
Engelund and Hansen (1973)		0.88				1.51				0.96			
Ackers and White (1973)		1.28				1.50				1.31			
Maddock (1976)		0.99				0.49				0.92			
A different picture is painted by the comparative study carried out by Van Rijn (1984), also using field and laboratory data. The discrepancy ratio, r, defined as the ratio of predicted to observed transport rates in percent were as follows:													
Data		$0.75 \leq r \leq 1.5$				$0.5 \leq r \leq 2$				$0.33 \leq r \leq 3$			
		1	2	3	4	1	2	3	4	1	2	3	4
US Rivers Corps Engrs		53	39	32	6	79	67	61	24	94	87	78	44
Middle Loop River		39	13	37	63	78	37	74	94	96	80	98	100
Indian Canals		30	15	27	3	60	45	48	6	90	73	70	24
Pakistan Canals		23	37	34	13	56	71	71	29	91	94	91	48
Niobrara River Canals		55	13	29	86	95	67	58	98	98	95	98	98
Average of field data		45	32	32	22	76	64	63	39	94	88	84	55
Flumes													
Guy et al., (1966)		40	67	56	68	70	89	85	90	91	98	99	98
Oxford		37	20	31	45	84	38	59	89	96	70	81	96
Stein (1973)		54	73	81	56	70	95	97	97	97	97	100	100
Southampton A		64	49	46	49	85	73	79	82	97	91	94	94
Southampton B		18	12	82	91	81	82	96	97	94	97	100	100
Average of laboratory data		41	46	52	59	77	74	77	89	95	89	94	98
Average of all data		43	37	40	36	76	68	68	58	94	88	88	71
In the above table, column 1 lists values obtained by the method of Van Rijn (1984); 2 by the Engelund-Hansen formula (1967); 3 by the Ackers-White (1973) formula and 4 by the Yang (1973) formula. The result is poor accuracy by the Yang formula for canals in India and Pakistan, which have the deepest flows of the above data. Since the other formulae produce reasonable results Van Rijn concludes that “the method of Yang must have serious systematic errors at large flow depth. On the average the predicted values are much too small”.													

5.2 Sediment Yield

Methods of obtaining the sediment yield from a catchment are well defined. These methods varies from a method as simple as reading a value from a sediment yield map to complicated mathematical formulae describing the loss of soil in a catchment. In these sections the various methods are discussed.

5.2.1 Sediment load – Discharge rating curves

The most reliable method of obtaining data to determine the sediment yield is river sampling, which should include both bed load and suspended sediment sampling. The frequency of sampling should be at least daily, but more frequently during floods. Discharge measurement should also be carried out to determine the total load (ton/s).

Sediment sampling is problematic in the remote areas in Africa and often dangerous due to crocodiles and hippos. In the semi-arid regions field research have indicated that due to the fine sediment in suspension, the vertical and lateral suspended sediment distribution is quite uniform and therefore a grab sample by hand from the river bank taken 0.3 m below the surface was found to represent the river sediment (fine) concentration quite well. Bed sediment loads are also difficult to obtain, especially due to high flow velocities and large bed dunes and field tests indicated that a factor of 1.25 applied to a single suspended sediment grab sample which takes into account the bed load and non-uniformity in suspended load across the river, gives a realistic total loads at relatively low cost. The bed load component can also be calculated, but a stable section is required and bed roughness is often difficult to obtain without a detailed hydraulic investigation (Basson, 2004).

The correlation between observed discharge and sediment loads in semi-arid areas is usually poor, but can be improved by considering beginning and end of the wet season, rising and falling stages of the hydrograph and time of the day of sampling for example in thunderstorm regions where storms usually occur in the late afternoon. The role of wind erosion should also be considered in more detail in future research (Basson, 2004).

The minimum record length required in semi-arid conditions is 5 years when data were found to converge to the long term mean sediment yield (**Figure 5-1**). Wet and dry climatic cycles often has 7 to 11 year durations each and should be accounted for in the sampling record period. It is important to include large infrequent floods in the record since observations have indicated that floods with recurrence intervals in the order of 1:50 years produce between 8 to 13 times the mean annual sediment yield in a single storm.

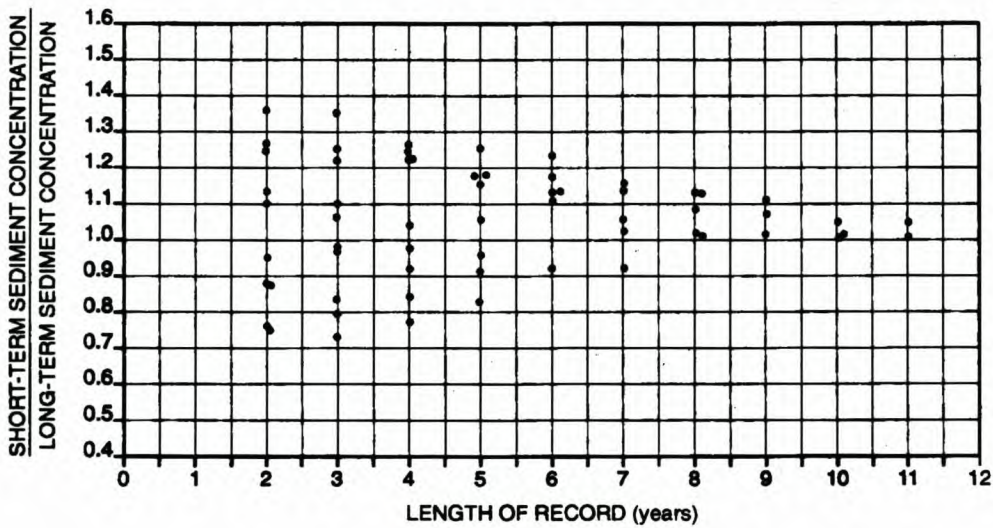


Figure 5-1 Short-term effective sediment concentration compared with long-term concentration on the Orange River (Basson, 2004)

The sediment yield is usually expressed in $t/km^2 \cdot year$ which is obtained by integrating the discharge – sediment load relationship over a long term flow record of say 40 years. The catchment area (A) is the effective area contributing to the runoff and sediment yield (downstream of large dam).

Turbidity meters can also be used in order to obtain long term sediment concentrations. The disadvantages of these meters are that they can only measure up to 4000 NTU and they require a constant power supply. One also needs to calibrate the meter against sediment grab samples. Further disadvantages are that the meters tend to clog up easily and that they are relatively expensive. In the upper reaches of rivers where the bed mainly consists of cobbles and boulders damage to the equipment can be expected as the cobbles and boulders collide with it during big flood events.

5.2.2 Reservoir basin surveys

In semi – arid regions the storage capacity of dams are normally in the region of the mean annual runoff. Therefore the reservoir traps about 97% of the sediment yield. By doing regular (10 to 15 year intervals) reservoir basin surveys it is possible to determine the sediment volume that is trapped in the dam. According to Rooseboom (1992) the volume must be converted to a 50 year volume, V_{50} , at a standardized sediment density of about 1.35 t/m^3 before the sediment yield can be determined. The yield is given by the following equation,

$$\text{Sed. Yield} = \frac{V_{50}}{50(1.35)A_s} \quad \text{Equation 5-1}$$

According to Basson (2004) the following aspects should be considered when a reservoir survey is carried out:

- Records longer than 20 years are preferable due to consolidation.
- Basin surveys should not be too frequent due to a vertical accuracy of 50 mm.
- Ultrasonic or echo sounding equipment to determine the bed level should be calibrated in the field for different sediment types and stages of consolidation.
- Above – water surveys by helicopter/fixed wing aircraft could be done by laser but should include the backwater area during floods above full supply level (FSL) since as much a 10 % of the sediment could be above FSL.
- The period between surveys should be based on the flood peaks and recurrence intervals.
- A survey carried out on fixed transects is preferred so that the triangulation is carried out in the same way for all surveys when the DTM is created.

5.2.3 Regional sediment yield maps and statistical approach

Regional sediment yield maps are mainly used to determine the sediment yield for large ungauged catchments. The first of these maps were plotted by extrapolation from observed catchment sediment yield data, in some cases also considering catchment and hydrological

characteristics such as catchment area and rainfall. A statistical regional approach was also proposed by Rooseboom (1992), in which a standardized yield was determined for each region which could be multiplied by a factor which accounts for probability of exceedance (median = 1) for the region, as well as low, median and high sediment catchment areas based on a soil erosivity index considering soil, rainfall, slope, land use, etc. The sediment yield was found inversely related to catchment area.

The above method describing direct measurements or empirical regional approaches using GIS are far from process based modelling, but probably yields the best answers for predicting long term sediment yields in large catchments ($> 2000 \text{ km}^2$) due to the variability in field data and the many unknowns when it comes to physically based models.

5.2.4 Regression type models

According to Basson (2004) the Universal Soil Loss Equation is the most widely used regression model for predicting soil erosion. It is an empirical formula for predicting soil loss due to sheet and rill erosion. The equation was developed from over 10000 plot-years of runoff and soil-loss data, collected on experimental plots of agricultural land in 23 states of the USA since 1930.

It was recognised that application of the USLE is limited to soil loss therefore another procedure for computing the sediment yield from a catchment was developed. The method determines a sediment yield based on single storm events. If the sediment yield from the land surface on an annual basis rather than on a single storm event is desired, MUSLE can also be used (Basson, 2004). The MUSLE sediment yield module uses factors that characterise physical conditions on the surface of a catchment as input information.

5.2.5 Discussion

During this study it was decided that the sediment load – discharge rating curves should be compiled through the utilization of the grab samples along the Berg River as well as on some of the tributaries in order to obtain a sediment yield for the various catchments. Unfortunately it was only possible to obtain data for the winter periods of 2003 and 2004. The sediment

transport in the upper reach of the Berg River is extremely low under low flow conditions and therefore the samples were only taken during the winter months. The dry winter that was experienced during 2003 as well as the short period of time over which data was collected has a negative effect on the investigation of differences between wet and dry periods.

5.3 Impacts of Dam Developments

Any hydraulic structure or manmade change to a natural river, irrespective of its size, can disturb an otherwise stable river. Therefore it is logical to assume that reservoirs will have a significant effect on the downstream morphology of any river. A river compensates for the imposed changes due to a dam by adjusting to a new quasi – stable form.

Numerous studies (e.g. Williams and Wolman (1984), Chien (1985), Hadley and Emmett (1998)) have been carried out in order to understand the impacts of dam developments and their causes. Only a short summary of the impacts relevant to this study are given below.

5.3.1 Discharge

The different purposes for which dams are built determine the effect the reservoir will have on the discharge. The lack of an abundance of water in South Africa causes most dams to be built with the purpose of water storage and supply. Most of the reservoirs that were built recently are of significant size and because as much water as possible is stored, most floods are either absorbed or at least attenuated so that only the very large floods move through the reservoir. According to Chien (1985) the Guanting Reservoir on the Yellow River, China, has reduced average peaks by 78% from 3700 m³/s to 800 m³/s.

The result is a decrease in the natural variability of streamflow (Beck and Basson, 2003). This can clearly be seen on the Orange River downstream of Gariep Dam (capacity of roughly 6 billion m³) (WCD, 2000). This is also the case on the Wemmershoek River downstream of the Wemmershoek Dam (capacity of roughly 60 million m³) (Beck and Basson, 2003).

5.3.2 Sediment transport

Together with the reduction in flood peaks a drastic decrease in the sediment volume released from the reservoir is experienced unless the dam is equipped to sluice or flush sediment through the reservoir (Beck et al, 2003). The well known Three Gorges Project in China was designed with 23 bottom outlets (7m by 9m) especially for sediment discharge during the flood season. During this season from June to September the Yangtze River carries 84% of its annual sediment load, which creates a favourable condition for sediment sluicing through the bottom outlets (Technical training course on dam safety management, China 2004). Williams and Wolman (1984) reported that the trap efficiency of large reservoirs, without bottom outlets, is greater than 99% in the USA.

Not only are the sediments trapped in the reservoir, but due to the attenuation of flood peaks and the reduction in frequency of occurrence of some of the floods, the transport capacity of the river downstream also decreases. For example downstream of the Danjankou Dam on the Han River, China, the sediment concentration at flows of 3000 m³/s was reduced by more than 60% (Chien, 1985).

5.3.3 Channel depth and width

The changes in flow regime and sediment load have a drastic effect on the channel morphology. Therefore any dam development will cause the width and depth of a channel to change.

A study by Beck and Basson (2003) on South African rivers led to a mathematical equation by which the change in width and depth due to dam developments can be determined. These equations were calibrated on observed South African river changes. The equation for change in channel width:

$$B_p = 4.034 Q_{10}^{0.365} S^{-0.228} d_{50}^{0.053} \quad (R^2 = 0.99) \quad \text{Equation 5-2}$$

And for changes in depth:

$$D_p = 0.071 Q_{10}^{0.374} S^{-0.154} d_{50}^{-0.02} \quad (R^2 = 0.99) \quad \text{Equation 5-3}$$

Where:

$$\begin{aligned} Q_{10} &= \text{the 1:10 year discharge (m}^3\text{/s)} \\ S &= \text{the energy slope (m/m)} \\ d_{50} &= \text{median particle diameter (m).} \end{aligned}$$

a) Change in Depth

Due to the clear, sediment free water released from most reservoirs the most common response of the river channel downstream of the reservoir is degradation. In most cases the maximum degradation will occur below or near the dam, the effect will decrease as the distance from the reservoir increases (Beck et al, 2003). Williams and Wolman (1984) reported a maximum degradation of 7.5 m below the Hoover Dam on the Colorado River, USA, 13 years after completion of the dam. The severity of this degradation depends on the local controls such as bedrock or development of an armour layer. Armouring occurs when fine materials in the bed are eroded, leaving coarser fractions behind. These create a protective layer that limits erosion of underlying material. Rutherford (2000) reported that some armouring limited erosion downstream of the Glenbawn Dam on the Hunter River, Australia.

b) Change in width

Two other factors that have a significant influence on changes in width after dam developments are bank material and vegetation. Cohesive banks offer some degree of resistance to erosion and an increase in vegetation adds to the stability of the banks as well as trapping of sediment. On the other hand, according to Williams and Wolman (1984), a lower sediment load resulted in widening of the channel, especially when accompanied by an increase in depth, which promotes bank undercutting and subsequent bank collapse. Channel contraction usually occurs on rivers where the flows are low or completely cut off for most of the time. This seems to be the case in most South African Rivers, as the main reason for dam construction is water supply (**Table 5-2**).

Both widening and contraction have been observed in South Africa. **Table 5-2** lists some changes in South African rivers that were affected by dam developments.

Table 5-2 Width changes in South African Rivers (Beck et al, 2003)

Dam	River	Pre – dam Width (m)	Post – dam width (m)	% change
Erfenis	Groot Vet	24	26	+ 8.3
Roodeplaat	Pienaars	26	15	- 42
Bloemhof	Vaal	92	82	- 11
Allemanskraal	Sand	49	21	- 57
Krugersdrift	Modder	32	24	- 25
Spioenkop	Tugela	53	36	- 32
Albertfalls	Mgeni	32	28	- 13
Theewaterskloof	Riviersonderend	37	33	- 11
Glen Alpine	Mogalakwena	36	24	- 33
Gamkapoort	Gamka	67	55	- 18
Gariep	Orange	269	255	- 5

Note : river reach widths measured from aerial photos downstream of dam / dam site.

5.3.4 Bed material

Due to the decrease in magnitude and frequency of high flows caused by the reservoir, the released flows are unable to transport the same load and size of particles as before the dam was built. On the other hand the clear water released can also be responsible for the entrainment of most of the fine material from the river bed, while the coarser fractions are left behind. Complete layers from the river bed can be removed by the clear water if they consist of finer materials and thereby expose coarser layers. Williams and Wolman (1984) found that the median bed particle diameter increased from 0.2 mm to 80 mm within 7 years after closure of the Hoover Dam on the Colorado River, USA.

These changes in bed material start taking place immediately after completion of a dam, but will decrease with time because the river will at some point reach a new state of equilibrium and the availability of fine materials decreases. It will also reduce with an increase in distance from the dam due to the tributaries that add both flow and finer sediment to the system (Beck et al, 2003).

CHAPTER 6 GENERAL DESCRIPTION OF THE BERG RIVER CATCHMENT

6.1 Location

The Berg River lies in the Western Cape and its catchment is located between latitude 23°45' and 33°50' south and longitude 18°15' and 18°55' east. The Berg River rises in the Jonkershoek and Franschhoek mountains and flows in a north westerly direction where it eventually discharges into the sea at Laaiplek. The major tributaries and their various catchment areas at the tributary gauging stations are shown in **Table 6-1**. **Figure 6-1** shows the Berg River Catchment.

Table 6-1 Berg River tributaries and catchment areas up to the gauging stations

Station Number	Tributary	Catchment Area at gauging station [km ²]
G1H003	Franschhoek	46
G1H019	Dwars	25
G1H037	Krom	52
G1H039	Doring	43
G1H041	Kompanjies	121
G1H040	Vis	75
G1H008	Klein Berg	370
G1H028	Twenty-fours River / 24 Riviere	185
G1H043	Sandspruit	260
G1H035	Matjies	615
G1H034	Mooreesburgspruit	175

The length of the Berg River is approximately 270 km, and its catchment covers an area of about 9000 km² (DWAF, 1993).



Figure 6-1 Berg River Catchment (Adapted from Nitsche, 2000)

6.2 Topography

The catchment is delimited in the south by the Franschhoek and Jonkershoek mountains and in the east by the Wemmershoek, Limiet, Elandskloof, Witzenberg, Twenty four and Olifants River mountains.

The upper reaches of the Berg River are hydraulically very steep with a bedslope of 0.67%. The river bed of this steep reach consists mainly of boulders and cobbles. From Paarl, the river profile flattens, with a bedslope of 0.045%. The river bed of this part of the river consists mainly of finer materials such as sands, silts and clayey materials. According to Bath (1989) this rapid fall in profile from the headwaters, the meandering of the main channel and the multiple channels separated by low lying islands in the lower reaches are an indication that the Berg River is geologically an old river system.

6.3 Climate

6.3.1 Rainfall

The Berg River has a Mediterranean climate and falls within the winter rainfall region of the Western Cape. The rainfall is mainly of a frontal nature caused by atmospheric turbulences drawing in air masses from different regions: warm air is drawn in from regions over the Atlantic Ocean, colder air from the sea south of the mainland and dry air from the southern parts of the country (Kersandt and Marais, 1973).

Frontal rains are caused by air masses with different moisture contents, temperature and densities. The mountain ranges cause the air to be forced upward resulting in reliable mountain rainfall compared with the frontal plains (Bath, 1989). As a result of the orographical influence of the mountains, a large spatial variability in the mean annual precipitation (MAP) is experienced. In the high lying areas of the mountains the mean annual precipitation can be as high as 3 200 mm, reducing to less than 500 mm in the lower areas in the north – east (DWAF, 1994).

6.3.2 Temperature

The mean annual temperature ranges between 16°C in the east central to about 18°C towards the west coast, with a average of 16°C for the Berg River Catchment as a whole. Maximum temperatures are experienced in January and minimum temperatures usually occur in July (DWAf,1994). **Table 6-2** below summarises temperature data for the Berg River Catchment.

Table 6-2 Temperature data for the Berg River Catchment (Western Cape System Analysis,1994).

Month	Description	Average Temperature (°C)
January	Mean Temperature	21.8
	Maximum Temperature	29.4
	Minimum Temperature	14.1
July	Mean Temperature	10.8
	Maximum Temperature	17.1
	Minimum Temperature	4.5

6.4 Geology

The geology of the Berg River Basin is shown in **Figure 6-2**. The catchment consists of semi – perennial streams arising in the mountains composed of Table Mountain Sandstone. Further north, in the Paarl area, several tributaries rise in the granite hills and flow through clay soils derived from weathered granite.

Below Paarl the overlying Table Mountain Sandstone has been progressively eroded exposing bedrock of Malmesbury shale. Malmesbury shale remains the main underlying rock formation down to the mouth of the river. In the middle reaches of the Berg River, Twenty Four Rivers and Klein Berg River are two semi perennial tributaries that arise in the Table Mountain Sandstone group.

From the suspended sediment samples that were taken during the winter months of 2003 it was clear that the Franschhoek River carried higher concentrations of suspended sediment than the tributaries that join the Berg River from the western side. From **Figure 6-2** it can be seen that these two tributaries arise in the more eroded Table Mountain Sandstone. The higher sediment availability in these catchments has to be the reason for the higher sediment transport by these two tributaries. Unfortunately sediment sampling was not done on the

Klein Berg and Twenty Four Rivers to confirm this theory, as they also arise from the same Table Mountain Sandstone.

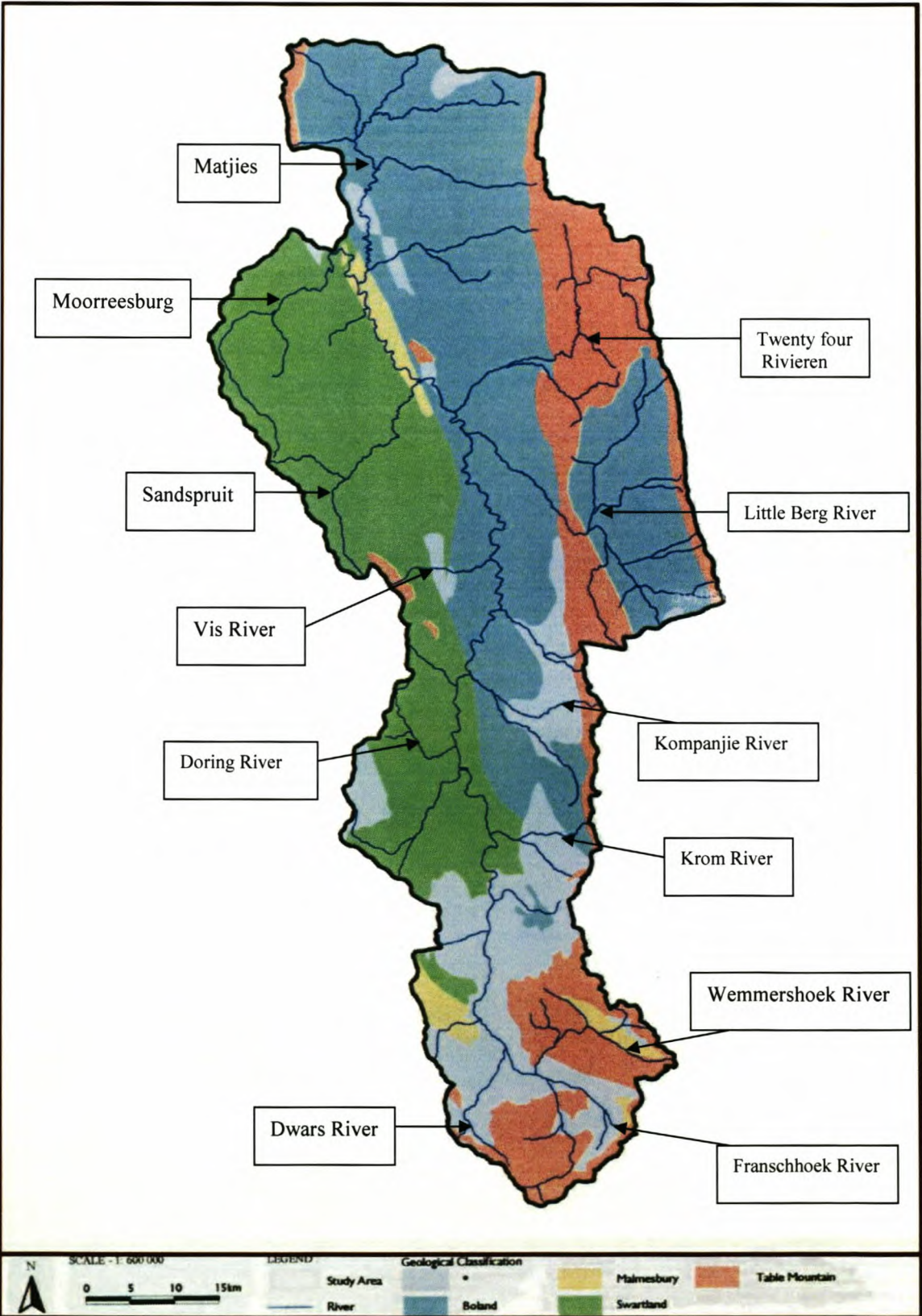


Figure 6-2 Geology of the Berg River Catchment (Adapted from Nitsche, 2000)

6.5 Existing Water Resources Infrastructure within the Catchment

In the upper Berg River, water is transferred as part of the Riviersonderend-Berg River Scheme to the Berg River via a tunnel, which releases water from Theewaterskloof Dam at West Portal, upstream of the proposed Berg River Dam site. Maximum releases from the tunnel have been around $5 \text{ m}^3/\text{s}$ in recent years (DWAF, 2004). The releases have caused a change in the seasonality of flow with higher flow during summer than low flows in winter since 1985. As can be seen from **Figure 6-3**, water was also released during the winter in the beginning which has now changed (**Figure 6-4**).

A recent BEng thesis (Greyling, 2001) at the University of Stellenbosch has shown that irrigation abstractions have increased by 0.75 million m^3 per year between 1998 and 2001. The thesis has also shown that around 3.6 million m^3 per year could be saved in the upper Berg River if the releases were optimized. Currently there is no irrigation over weekends (DWAF, 2004), which means that tunnel releases have to stop by about Wednesday, a very difficult way of managing the releases. The control over water releases could be done with the aid of a mathematical hydrodynamic model of the river, to simulate the discharge along the river, in order to reduce unnecessary irrigation tunnel releases in time. This could mean that the differences between summer and winter base flows would not be as pronounced as they are now.

Wemmershoek Dam on the Wemmershoek River was built in 1957. The original full supply capacity (FSC) was 59.9 Million m^3 , but during 1984 the dam had lost 1.8 % of its capacity due to sedimentation. This means that about 40 000 m^3/a sediment was trapped in the dam. The trap efficiency, based on the ratio of reservoir capacity to mean annual runoff (MAR), is around 90% according to Churchill (1948). This gives a catchment sediment yield of around 270 $\text{ton}/\text{km}^2.\text{a}$. The Wemmershoek River downstream of the dam narrowed considerably as a result of the flood attenuation caused by the dam.

On the lower Berg River, Misverstand Dam was built in 1977 and has a full supply capacity of 7.9 million m^3 . By 1988 the dam had lost 2% of its capacity due to sedimentation. This means that about 14 000 m^3/a was trapped in the dam. The dam has a trap efficiency of 45%, based on the Churchill empirical rule. The effect of Misverstand Dam on the river

downstream has not been as pronounced as downstream of Wemmershoek Dam because of the smaller storage capacity and sediment trap efficiency.

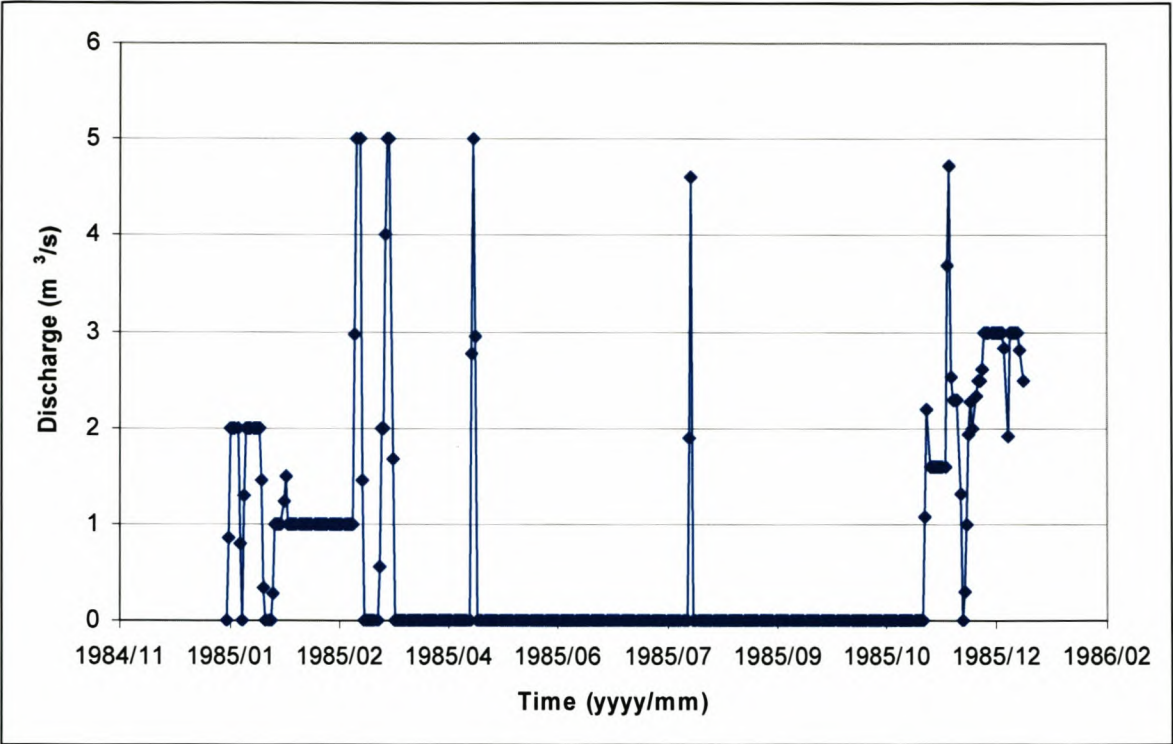


Figure 6-3 Tunnel releases (G1H044M01/M02) during 1985 (DWAF, 2004)

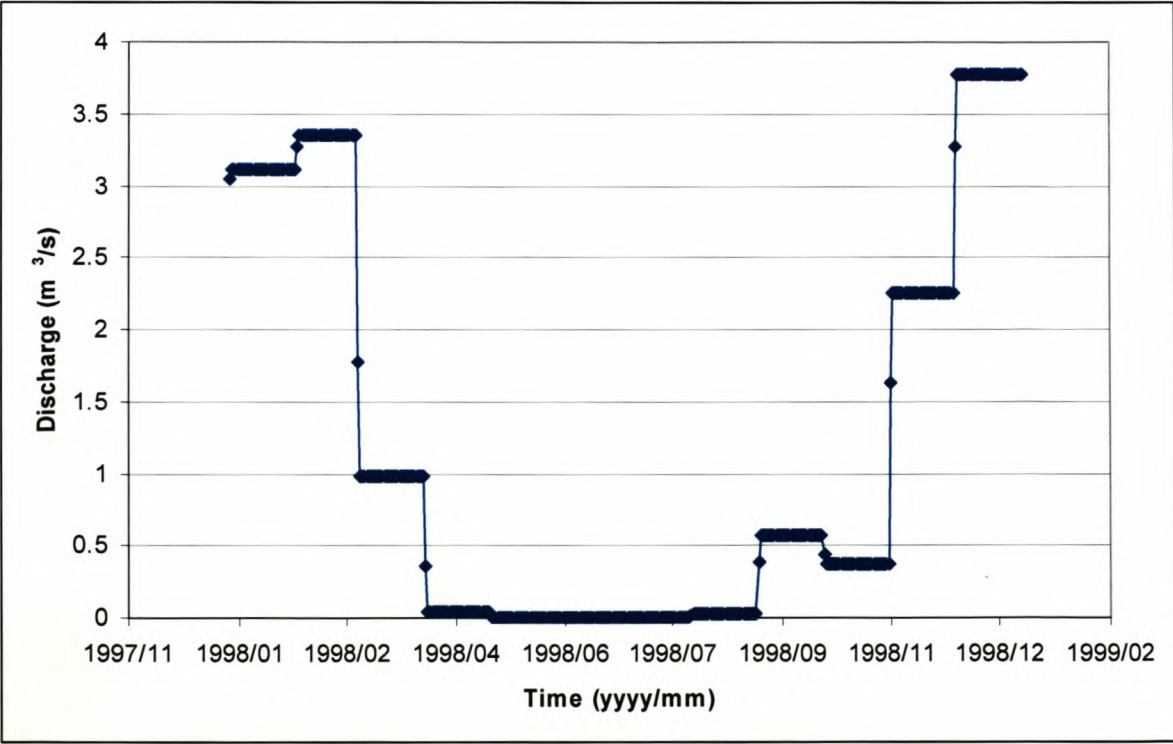


Figure 6-4 Tunnel releases (G1H044M01/M02) during 1998 (DWAF, 2004)

Further developments include Voëlvlei Dam with canals from vier- en- twintig Rivieren and the little Berg River supplying the dam. River diversion from Wolwekloof as well as Banghoek rivers through tunnels to Theewaterskloof Dam also form part of the current water developments.

CHAPTER 7 REVIEW OF THE BERG RIVER FLUVIAL MORPHOLOGY

7.1 Fluvial Morphological Assessment and River Classification

The fluvial morphology of the river channel provides the physical framework within which the stream biota lives. Fluvial morphology is therefore an important component of many river management initiatives. Geomorphology is one of several components used to assess the overall condition of a site.

7.1.1 Previous Fluvial morphological assessment

Rowntree and McGregor (1996) compiled a fluvial morphological assessment of the Berg River as part of the 1996 IFR study. A short summary of their findings is presented here. The river can be divided into different zones according to the incremental mean annual runoff (MAR) and sediment yields. The incremental MAR of the Franschoek and Berg River catchments above the confluence is in the order of 600 million m³ per year, and the annual sediment yields are low due to the resistant nature of the Table Mountain Sandstones and thin soils. Downstream of the confluence the incremental MAR decreases rapidly and is only in the order of 100 million m³ per year between Paarl and Wellington. The sediment yields increase in this zone as the river flows through a wide alluvial plain of sand sized material and the tributaries drain the Malmesbury series. Further downstream the incremental MAR decreases to around 30 million m³ per year.

According to Rowntree and McGregor (1996) the main channel of the Berg River can be subdivided into four segments (**Table 7-1**), based on the spatial distribution of runoff and sediment yield in the catchment. Reaches along the Berg River are discussed in **Table 7-2**.

Table 7-1 Segment characteristics of the Berg River (Rowntree and McGregor, 1996)

Segment	Topography	Geology	MAP (mm)	Vegetation	Soils	Erodibility	Sediment/discharge index
1 Mountain	Steep valley side slopes, narrow valley floor	Table Mountain Group and Cape Granite suite	1500 to 2500	Mesic mountain fynbos and coniferous plantations	Rock	Low	Very Low
2 Foothill	Moderate valley side slopes, wider valley floor	Table Mountain Group to east, Cape Granite suite and Malmesbury Group to west, valley floor alluvium	600 to 1000	Vineyards	Swart-land	Moderately high	Low to Moderate
3 Lowland	Rolling topography	Malmesbury Group	400 to 500	Wheat lands	Swart-land	Moderately high	Moderate
4 Coastal	Flat to gently undulating	Wind blown sands and alluvium	250 to 400	Wheat lands	Fern-wood	Low	Moderate

Table 7-2 Reaches along the Berg River (Rowntree and McGregor, 1996)

Reach	Extent	Length (km)	Gradient	Features
1 – 3	1400 – 600 m contours	2.3	0.33	Very steep head wall streams, Fynbos.
4 – 7	600 – 220 m contours	10.52	0.071	Confined valley, colluvial foot slopes, incised channel, and steep gradient mountain stream.
8	Above new Berg River dam site	5.21	0.0077	Steep valley side slopes, open valley floor, braided channel with shallow pools, rapids and plane bed morphology, Pine and black wattle in riparian zone, medium to sparse in-channel vegetation.
8	Immediately downstream of dam site	2.72	0.0074	Fan type feature with divergent drainage plus main channel, pool – riffle morphology, dense riparian vegetation.
9	160 to above 100 m contour	19.06 (to 100m contour)	0.0036	Open topography with gentle cultivated slopes, sinuous channel, sharp reduction in gradient, increased channel width, cobble bed with lateral cobble bars and pool riffle morphology.

Reach	Extent	Length (km)	Gradient	Features
10	Water Vliet to 80m contour	22.46	0.0009	Similar valley topography, increased channel sinuosity, further reduction in gradient, infrequent islands, variable channel width, mixed bed, long pools with cobble riffle and lateral bars, possible aggradation in pools, highly disturbed channel, middle section urbanized: channelisation, bank stabilisation, straightening etc. Below Paarl good riparian vegetation as far as Voëlgesang.
11	60 – 80m contour	18.74	0.00011	Similar valley topography, fairly significant direct contributing area for storm runoff and sediment, irregular meanders, wider divided channel, sand bed channel, pool with rapid morphology. Riparian woodland, woody debris in channel.
12	60m contour to confluence with Klein Berg	33.8	0.00042	Irregular meanders, single thread channel, highly variable channel width, some channel division where shrubby vegetation survived in riparian zone, sand bed channel, pool morphology with infrequent lateral bars and rapids.
13	Confluence with Klein Berg to confluence with Twenty-fours River (approx 40m contour)	5.2	0.00042	Short reach with tortuous meanders, sand bars and shallow pools.
14	Confluence with Twenty-fours River to confluence with Matjies Riviere	25.35	0.00055	Significant direct contributing area for storm runoff and sediment from cultivated lands, reduced gradient, irregular meanders with lateral bars, often associated with tributary slystreams' wider channel but variable width.
15	Confluence with Matjies Riviere to Moravia Station, below 20m contour	11.00	0.00055	Moderately confined valley, irregular wandering channel, narrow lateral bars with occasional islands, variable channel width, narrower channel
16	Moravia station to Estuary	48.00	0.00033	Less confined valley, irregular meanders, narrow lateral bars, continued narrow channel

7.2 Aerial Photograph Analysis – Historical Changes

The Berg River Baseline Monitoring study (DWAF, 2004) has identified six sites along the Berg River at which the monitoring of various parameters such as sediment concentration, biannual bed level surveys and habitat mapping occurred. The location of these sites in the numerical model is illustrated in **Table 7-3**.

Table 7-3 BRM site location	
BRM site	Chainage [m]
1	Not included in the model, just upstream of G1H004
2	4 000
3	23 500
4	72 500
5	121 800
6	141 000

The longitudinal profile of the Berg River is shown in **Figure 7-1** and **Figure 7-2** for orientation in terms of chainage along the river. Chainage 2.2 km is at the gauging station G1H004. The locations of major tributaries are also indicated in the figure.

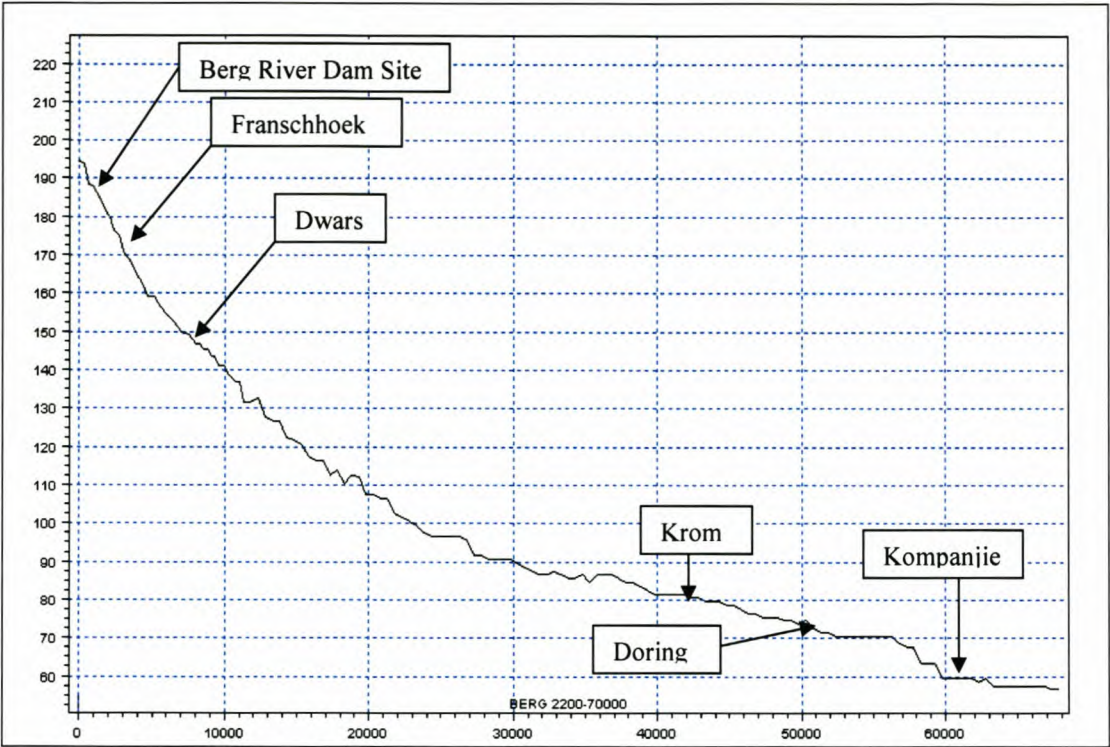


Figure 7-1 Longitudinal bed profile of the upper reach of the Berg River (tributaries indicated)

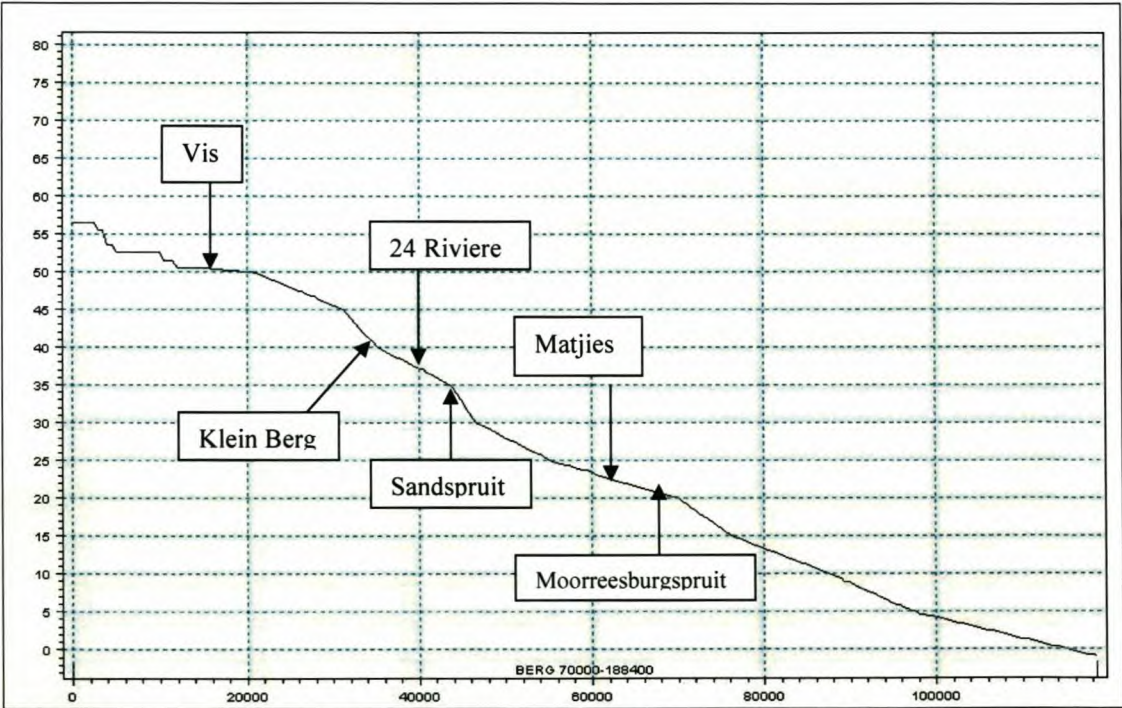


Figure 7-2 Longitudinal bed profile of the lower reach of the Berg River (tributaries indicated)

1930's: The Berg River had a braided channel system, which converged at chainage 2.6km. It remained in one main channel along its course through the farm Dew Dale, with a width of 60m at the proposed Berg River Dam site.

From **Figure 7-3** it can be seen that the Berg River had a visibly braided system for about 2km upstream of the confluence of the Franschhoek River. A similar wide braided system was characteristic of the reach between chainage 12.5 and 20.7km (between Bienne Donne and Draaihoogte just upstream of BRM3, see **Figure 7-4**). Wide floodplains with visible sandbanks existed along these parts of the river.

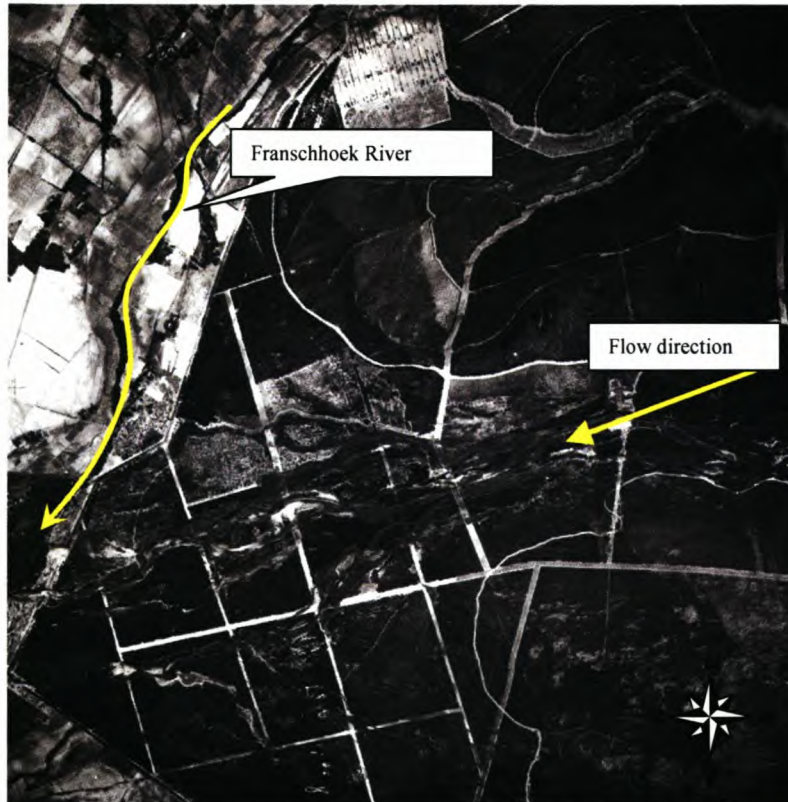


Figure 7-3 Braided river system upstream of Franschhoek River confluence (1938)

The Dwars River looked much wider than at present, similar in size to the Berg River. The braided river system downstream of the N1 Road Bridge with its smaller braided channels through Paarl was almost 750 m wide, compared to the 100 m wide single channel today.

The channel was also braided upstream of Paarl (N1) with many smaller side channels and tributaries. It was also apparent that the river was much straighter than at present, which is characteristic of a braided system. See the 1:50 000 topographical map in **Figure 7-4** for the present state of the river, with **Figure 7-5** to **Figure 7-7** depicting the state of the Berg River in 1938.

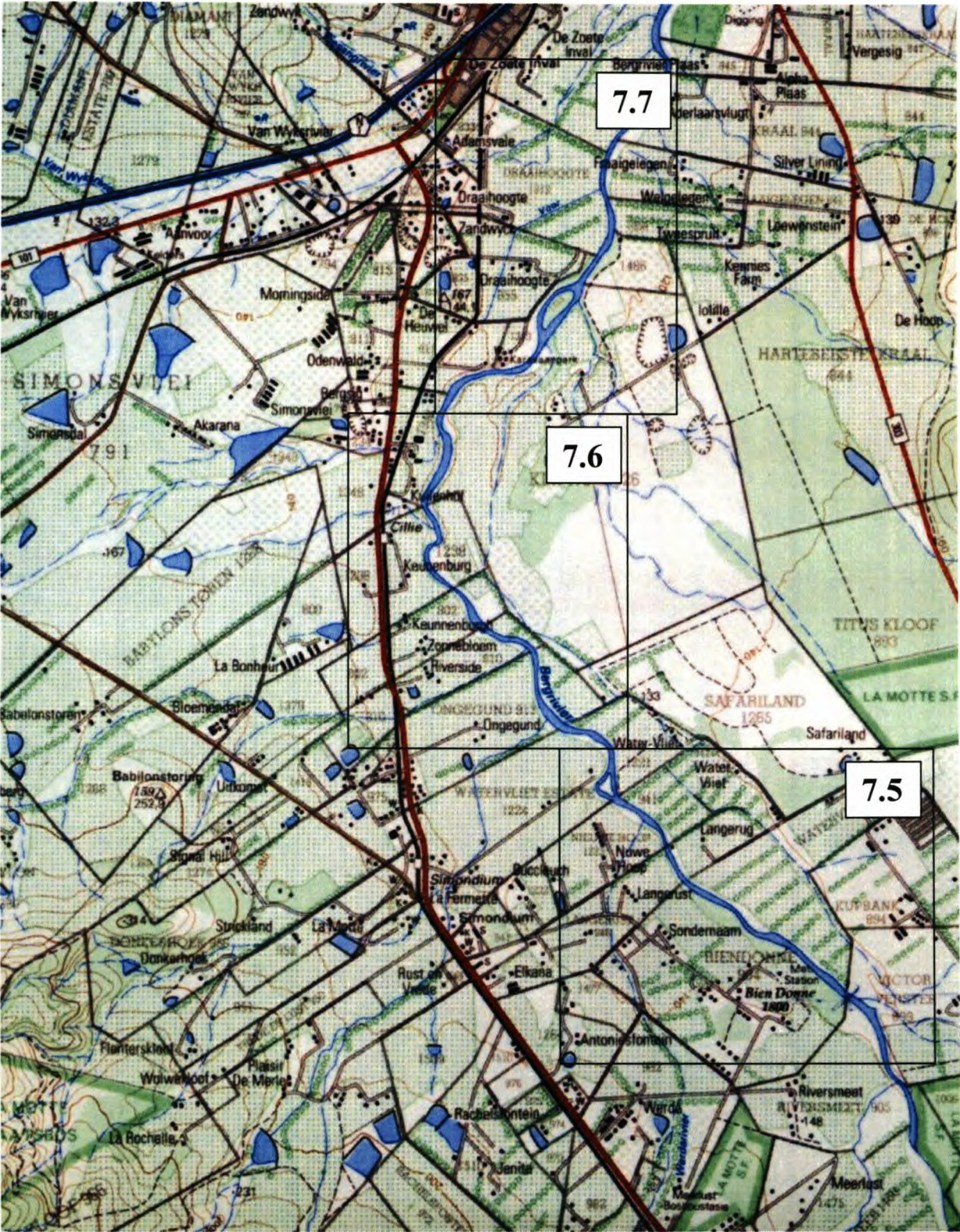


Figure 7-4 Topographical map (3318 DD Stellenbosch)

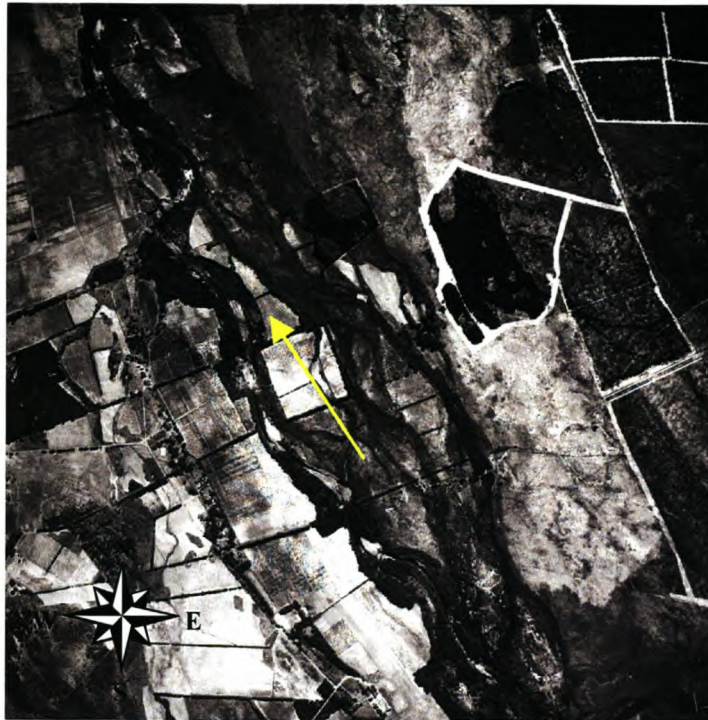


Figure 7-5 Braided river system upstream of Paarl (1938) between Ch 13km and 16.5km (Bienne Donne and Watervliet)



Figure 7-6 Braided river system upstream of Paarl (1938) between Ch 16.5km and 18.5km (between Watervliet and Kuilenhof)



Figure 7-7 Braided river system upstream of Paarl (1938) between Ch 19.5km and 20.5km (Kuilenhof and Draaihoogte upstream of BRM3)

No bridge existed at the Oosbosch Street crossing at chainage 30.5km in Paarl. The gauging station G1H020 did not exist and a clearly braided system downstream of chainage 30.5km could be observed from the 1938 photographs. Several large sandbanks could be spotted, for example at chainages 30.5, 33.5 (present location of sewage works) and 35.5km (at Riviera). A large braided system extended for 7km upstream of the Krom River confluence at chainage 43.5km.

At chainage 37.5km (Noord Agter-Paarl irrigation dam) an extremely wide braided system existed. At chainage 117.3km (1km downstream of the Sandspruit confluence) the river was more meandering compared to the present situation. A braided system existed at chainage 136km (2.5km downstream of the Matjies River confluence). Two channels and an island could be seen at the bridge at chainage 144km (4.5km upstream of the N7 road bridge at Die Brug). A similarly wide braided system existed, starting from the N7 Bridge up to chainage 150km (2km downstream of the N7 road bridge).

1940's: The floodplain upstream of the Franschhoek River (chainage 3.5 km) confluence was overgrown with trees, with very little bush. Trees had not yet been planted on the river banks. The section between Paarl and Wellington consisted of one main channel, except at Fleur de Lys, where a number of smaller channels could be seen. Upstream of the R44 at Nooitgedacht farm the braided river system was 400 m wide, where it is now only a 50 m wide single channel. At Nuwedrif downstream of the Paarl gauging weir the braided river system was 700 m wide, where the two channel system is now only 300 m wide.

1950's: Upstream of the Franschhoek River no major changes within the main channel were observable from the photographs compared with the 1930 conditions, and the braided nature of much of the channel was still evident (**Figure 7-8**).

The N1 road bridge has caused slight damming upstream. The river was about 150 m wide compared to a width of 100 m in the 1930's.

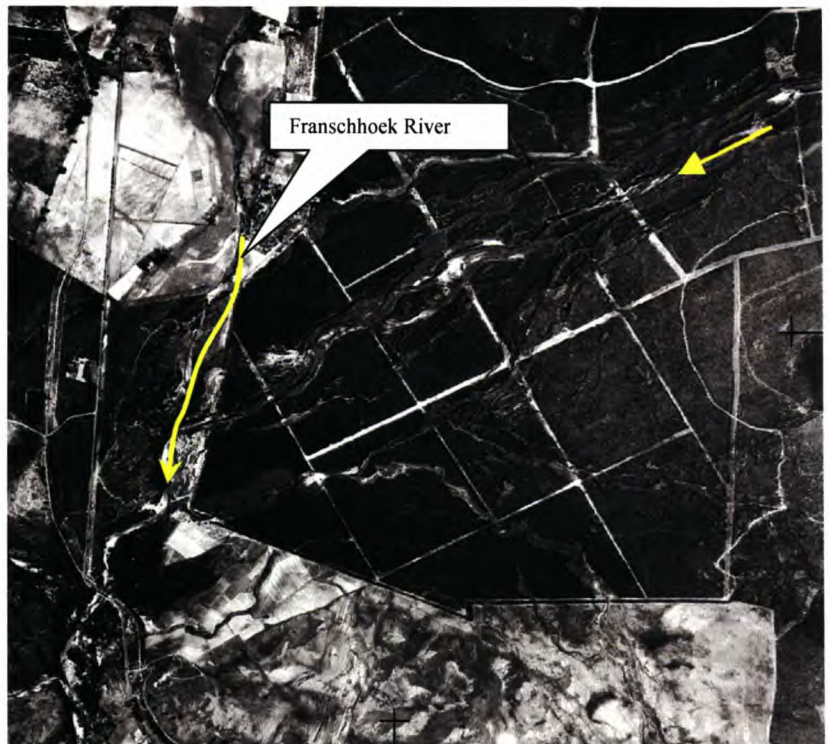


Figure 7-8 Braided river system upstream of Franschhoek confluence (1953)

The section of the river that was to be flooded by Misverstand Dam had a high degree of sinuosity with a number of sandbanks along the river bends (see **Figure 7-9**). The river was approximately 75 m wide. The river section between the Sandspruit and Matjies River confluences was approximately 200 m wide.

1960's: The river section downstream of the Platkloof and Boesmans River confluences had a number of islands and sandbanks. The river at Moravia was about 75 m wide, whereas in the

1970's the river was only 40 m wide. The river at the N7 road bridge was approximately 75 m wide, compared to only 25 m in the 1970's.



Figure 7-9 **Berg River before Misverstand dam**

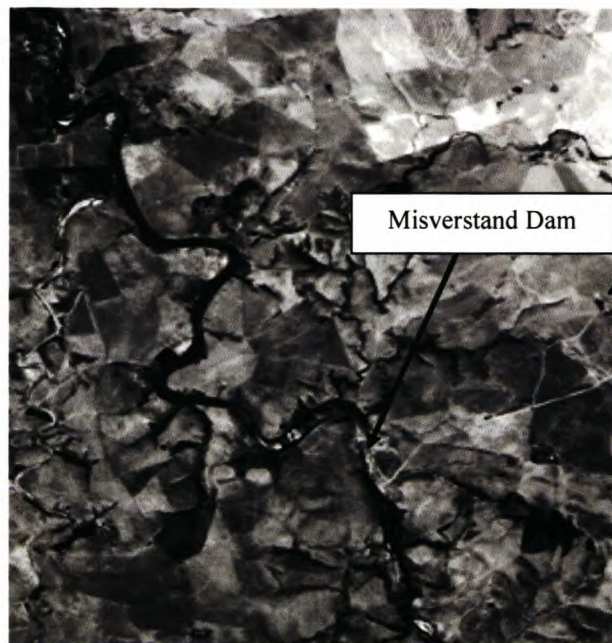


Figure 7-10 **Berg River after Misverstand dam**

1970's: As Paarl developed, the braided system that existed between chainage 13 and 19km disappeared (between Bienne Donne and Kuilenhof). Only one main channel can be observed, which is much the same as the present channel system. Trees had been planted along the river banks from Brandwag in Paarl up to the R44 intersection in an attempt to

stabilize the river. Lands on the right hand side of the river consisted mainly of cultivated areas, which were later to be occupied by industrial developments.

Misverstand Dam could clearly be seen on the aerial photographs. The effect of the dam was clearly visible (**Figure 7-9**) in the upstream reaches, where the damming of water had resulted in a considerably wider channel. The damming effect was visible up to Volstruisdrif just upstream of the Matjies River confluence.

1980's: The braided system that existed in the early 1930's as the river ran through Dew Dale disappeared. The trout dams at Dew Dale had been built, and the secondary channel had been closed as a result (see **Figure 7-11**). Only one main channel could be seen up to the Franschhoek River confluence. The Wolwekloof River entered the Berg River as one main stream, whereas previously two channels entered the Berg River.

The section of the river to be flooded by Misverstand Dam was narrower than during the 1950's. The river was approximately 50 m wide. The river section between the Sandspruit and Matjies River confluences was approximately 50 m wide. The Klein Berg River was around 40 m wide, compared to a width of between 50 and 100 m during the 1950's.

1990's: Trees had been planted on the floodplains downstream of the Dwars River confluence. Trees had also been planted on the riverbanks upstream of the Franschhoek River confluence. The river had a higher degree of sinuosity between Paarl and Franschhoek with a greater number of sandbanks(1930's). The braided system that previously existed between chainage 12.5 and 20.7km (Bienne Donne and N1 road bridge) disappeared. Only one main channel exists at chainage 122.5km (1.5km downstream of Drieheuwels) and through the years the bend at chainage 124km (2.5km downstream of Drieheuwels) moved to the left.

The river section between the Sandspruit and Matjies River confluences was between 50 and 100 m wide.

Remnants of some of the older channels are still indicated on the 1:50 000 topographical maps (see **Figure 7-12**). A recent survey of the area also shows that many of the older channels still exist and that some have been or will be closed as part of the Berg River Dam design to prevent flooding of certain areas (**Figure 7-13; Figure 7-14**).



Figure 7-11 Berg River around Dew Dale (1990), with main channel (—) and secondary diversion channel (- -) indicated

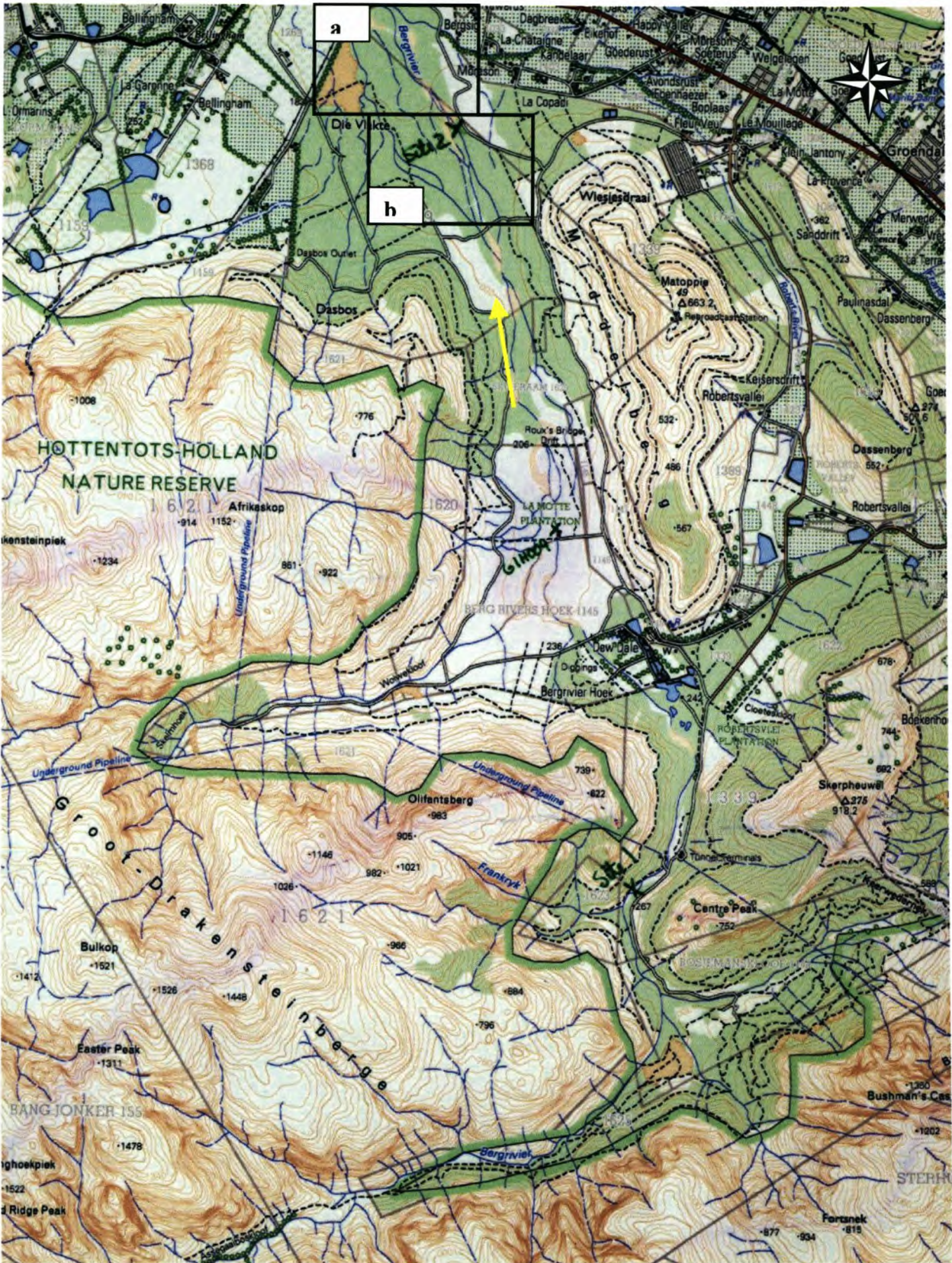


Figure 7-12 Topographical map (3319CC Franschhoek)

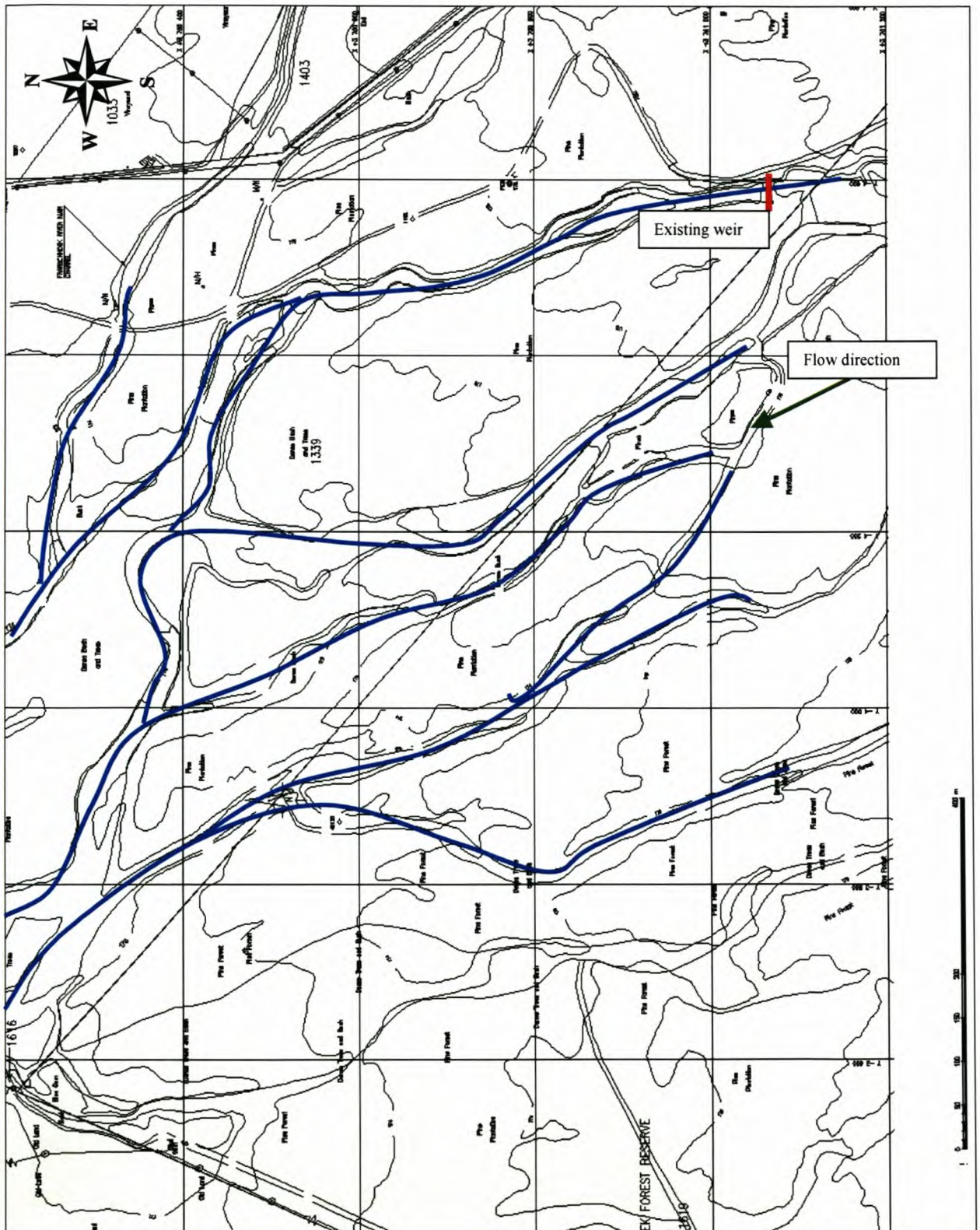


Figure 7-13 Survey 2003 (BRC and TCTA, 2003), with blue lines indicating existing channels

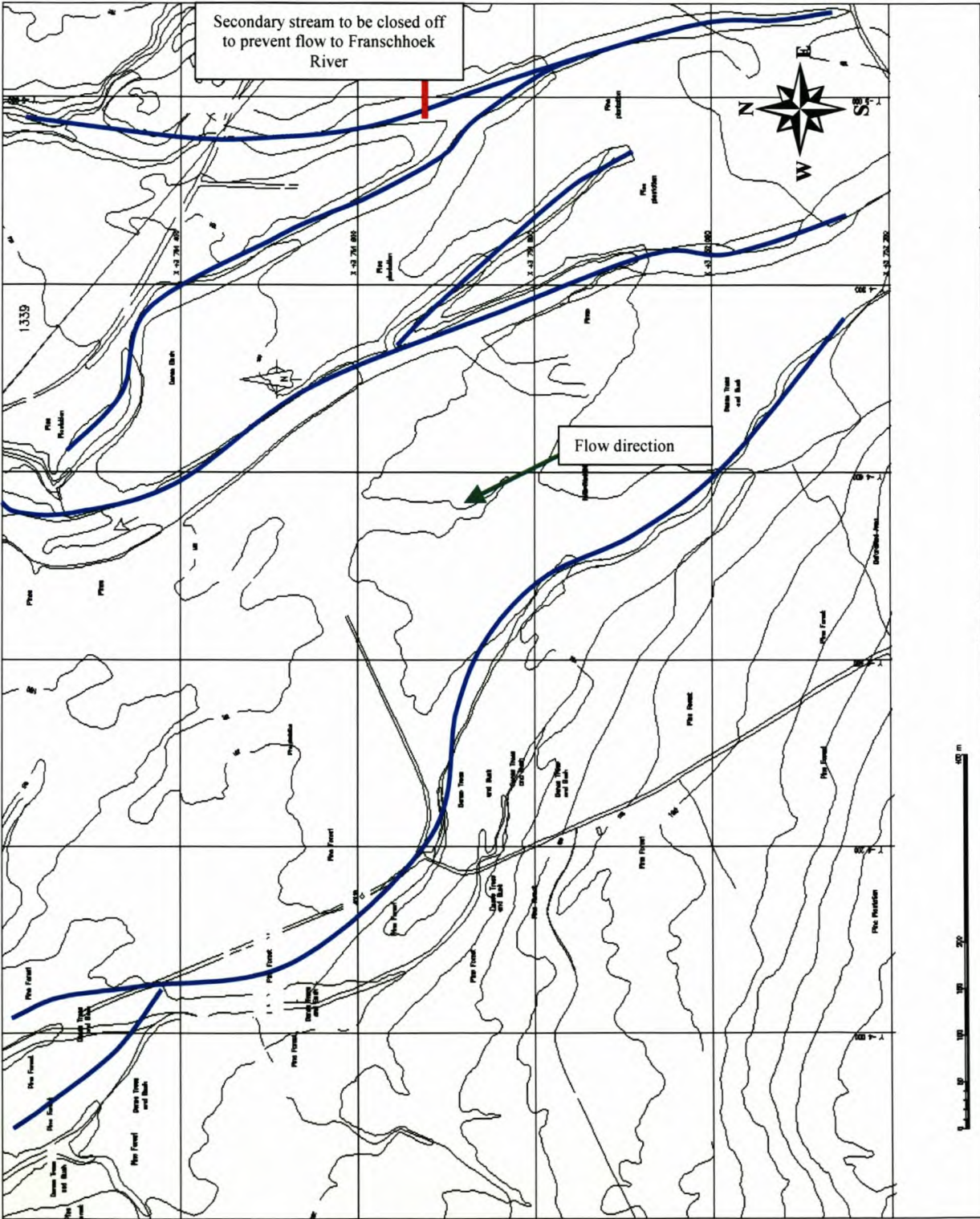


Figure 7-14 Survey 2003 (BRC and TCTA, 2003), with blue lines indicating existing channels

Summary

The river has been narrowed over the years by development of the floodplain such as afforestation and levees. This did result in higher flow velocities as the flow is confined to a smaller area, and thus scouring did occur in some areas.

In the upper reaches some of the channels of the braided system were cut off by weirs and afforestation, confining the river to a single channel during low flow conditions. This means that the river flows across the whole floodplain less frequently. This could mean that the sediment deposited on the floodplain during floods will remain there for longer periods. The infrequent inundation of the floodplain could also lead to the vegetation establishing a stronger hold and encroachment on the main channel. This would lead to higher floodplain resistances.

The afforestation also caused higher flow resistances on the floodplain. In general higher floodplain resistance leads to higher water levels during flood conditions, and a smaller sediment transport capacity.

Downstream of the Wemmershoek River floodplain flows became much more confined to a narrower single main channel due to flood levees constructed by farmers.

The only structures on the Berg River that had noticeable impacts, based on the photos and maps on the Berg River are the N1, N7 and Carinus road bridges, as well as Misverstand Dam. The road bridges have caused noticeable local confinement of the flow, while Misverstand and Wemmershoek Dam have trapped some of the sediment in the system. Many of the other structures and modifications on the river, such as the bridges and gauging weirs, will of course also have had some local effects, which could not be picked up from the photos and maps. It should also be borne in mind that farm dams reduce the mean annual runoff. This had a significant effect on the Berg River system.

The biggest changes that occurred on the Berg River between the 1930's and today are that the braided system in the upper reaches near Franschoek and the Paarl area have disappeared at least partially. The river now consists mainly of a single channel with a high degree of sinuosity. This is probably due to the fact that many of the smaller side channels have been

closed off to prevent flooding of the areas away from the main channel, which are now being used for agricultural purposes. Overall it seems that the river goes through minor natural periodic changes such as migrating sandbars.

7.3 Changes on the Floodplains

Various changes on the floodplains occur which has a major influence on the hydraulic characteristics of the river. Some of these changes occur due to natural disaster such as fires caused by lightning or by vandalism. These fires destroy the natural vegetation on the floodplains which has an influence on the roughness coefficient of the floodplains.

Some of the manmade changes that occur on the floodplains are afforestation activities by SAFCOL and Work for Water. From **Figure 7-15** and **Figure 7-16** it can be seen that all of the bigger trees on the floodplain were sawn down and piled into heaps for burning. This will definitely lower the flow resistance on the floodplains. These changes are very difficult to foresee, therefore it is difficult to do hydrodynamic simulations over an extended period of time with realistic floodplain flow resistance values, as these may change on a yearly basis.



Figure 7-15 Floodplain changes (BRM site 1)



Figure 7-16 Floodplain changes (BRM site 1)

CHAPTER 8 MATHEMATICAL MODEL OF THE BERG RIVER

8.1 General Description of the One Dimensional Model – Mike11

Mike 11, developed by the Danish Hydraulic Institute for Water and Environment (DHI) for the simulation of flows, sediment transport and water quality in rivers, estuaries and similar water bodies, was chosen to do the simulations for flow and sediment transport in the Berg River. The model comprises of the following modules:

- Hydrodynamic.
- Non-cohesive sediment transport.
- Advection-dispersion.
- Water Quality.
- Eutrophication.
- Rainfall-runoff.
- Flood forecast.

The overview given here is a summary of the MIKE 11 Reference Manual (DHI, 2002) describing aspects of the modules of the MIKE 11 modelling system used in this study.

8.1.1 Hydrodynamic Module

The MIKE 11 hydrodynamic (HD) module is an implicit, finite difference model for the computation of unsteady flows in rivers and reservoirs, based on the Saint Venant equations representing conservation of mass and momentum, which are derived on the basis of the following assumptions:

- The water is incompressible and homogeneous.
- The bottom slope is small.
- The surface wave lengths are large in comparison to the water depth. This ensures that the flow everywhere can be regarded as having a direction parallel to the bottom.

For a rectangular cross-section with horizontal bottom and constant width, the conservation of mass and momentum can be expressed as follows:

Conservation of mass:

$$\frac{\partial(\rho Hb)}{\partial t} = \frac{\partial(\rho Hb\bar{u})}{\partial x} \quad \text{Equation 8-1}$$

Conservation of momentum

$$\frac{\partial(\rho Hb\bar{u})}{\partial t} = - \frac{\partial \left[\alpha' \rho Hb\bar{u}^2 + \frac{1}{2} \rho gbH \right]}{\partial x} \quad \text{Equation 8-2}$$

Where, ρ is the density, H water depth, b the width, \bar{u} the average velocity along the vertical and α' the vertical velocity distribution coefficient.

If one allows variation in channel width and by introducing the bottom slope, I_b , the momentum equation is modified by adding two terms. Therefore the hydrostatic pressure acts on the side walls and bottom. These terms describe the projections in the flow direction of the reactions of the bottom and side walls to the hydrostatic pressure.

The momentum equation now becomes:

$$\begin{aligned} \frac{\partial(\rho Hb\bar{u})}{\partial t} &= - \frac{\partial \left[\alpha' \rho Hb\bar{u}^2 + \frac{1}{2} \rho gbH \right]}{\partial x} + \frac{\partial b}{\partial x} \frac{\rho g H^2}{2} - \rho g HbI_b \\ &= - \frac{\partial(\alpha' \rho Hb\bar{u}^2)}{\partial x} - b \frac{\partial \left[-\frac{1}{2} \rho g H \right]}{\partial x} - \rho g HbI_b \end{aligned} \quad \text{Equation 8-3}$$

The relationship between water level and water depth can be described as follows:

$$\frac{\partial h}{\partial x} = I_b + \frac{\partial H}{\partial x} \quad \text{Equation 8-4}$$

When this relationship is introduced into equation 8 – 3 and the equations are divided by ρ , the conservation laws of mass and momentum become:

$$\frac{\partial(Hb)}{\partial t} = -\frac{\partial(Hbu)}{\partial x} \quad \text{Equation 8-5}$$

$$\frac{\partial(Hbu)}{\partial t} = -\frac{\partial(\alpha Hbu^2)}{\partial x} - Hbg \frac{\partial h}{\partial x} \quad \text{Equation 8-6}$$

These equations can now be integrated to describe the flow through a cross section of any shape by dividing the cross sections into a series of rectangular cross sections. It has to be borne in mind that from the previous assumptions it is evident that $\partial h/\partial x$ is constant across the channel and no exchange in momentum occurs between subchannels. If the area after integration is called A and the discharge after integration is called Q and if B is the full width of the channel, then:

$$A = \int_0^B H \, db \quad \text{Equation 8-7}$$

$$Q = \int_0^B Hu \, db \quad \text{Equation 8-8}$$

By integrating the mass and momentum conservation equations and by introducing the above two equations the following are obtained:

$$\frac{\partial Q}{\partial x} + \frac{\partial A}{\partial t} = 0 \quad \text{Equation 8-9}$$

$$\frac{\partial Q}{\partial t} + \frac{\partial \left[\alpha \frac{Q^2}{A} \right]}{\partial x} + gA \frac{\partial h}{\partial x} = 0 \quad \text{Equation 8-10}$$

If lateral inflow, q, is introduced, the mass conservation equation becomes:

$$\frac{\partial Q}{\partial x} + \frac{\partial A}{\partial t} = q \quad \text{Equation 8-11}$$

By using the Chezy description for bed roughness, the momentum conservation equation becomes:

$$\frac{\partial Q}{\partial t} + \frac{\partial \left[\alpha \frac{Q}{A} \right]^2}{\partial x} + gA \frac{\partial h}{\partial x} + \frac{gQ|Q|}{C^2 AR} = 0 \quad \text{Equation 8-12}$$

Where:

$$C = 18 \log \left(\frac{12R}{k_s} \right)$$

R = Hydraulic radius (m).

k_s = Surface roughness (m).

With the above mentioned basic equations that are used by MIKE11 the model can describe both subcritical as well as supercritical flow conditions. Modules are also incorporated to describe flow past hydraulic structures. The model can be applied to looped networks and quasi two-dimensional flow simulation on flood plains. The hydrodynamic module provides three different flow descriptions:

- The dynamic wave approach, which uses the full momentum equation.
- The diffuse wave approach, which only models the bed friction, gravity forces and the hydrostatic gradient terms of the momentum equation.
- The kinematic wave approach, where flow is calculated on assumption of a balance between the friction and gravity forces. Backwater effects cannot be simulated by using this description.

8.1.2 Non-Cohesive Sediment Transport Module (NST)

The non-cohesive sediment transport (NST) module can be run in two modes: explicit and morphological. In the explicit mode output is required from the HD module, but no feedback occurs from the NST module to the HD module. In the morphological mode sediment transport is calculated together with the HD module and feedback is given from the NST module to the HD module. The results are in the form of bed level changes, sediment

transport rates and bed resistance. The morphological model updates either the whole cross-section or only a part of it (generally the part representing the river channel or the part below the water surface).

Traditional sediment transport equations are incorporated in the MIKE 11 model for non-cohesive sediment transport. Sediment transport models derived from these equations are:

- Engelund-Hansen
- Ackers and White
- Engelund-Fredsøe
- Smart and Jaeggi
- Meyer, Peter and Muller
- Sato, Kikkawa and Ashida
- Ashida and Michiue
- Van Rijn

All of these can be setup to simulate a single representative particle size or a particle distribution. As Van Rijn's model was used for all sediment transport calculations, only this model will be discussed in more detail.

8.1.2.1 The van Rijn sediment transport model:

This model is based on calculating both the bed load and suspended load. By summation the total load is calculated.

8.1.2.1.1 Bed load

The bed load transport rate is calculated from the product of particle velocity, u_{bs} , saltation height, δb , and the bed load concentration, c_b :

$$q_b = u_{bs} \delta b c_b$$

Equation 8-13

Expressions for the particle velocity and saltation height are obtained by numerically solving the equations of motion applied to a solitary particle. These expressions are given in terms of two dimensionless parameters which are considered to adequately describe bed load transport; a dimensionless particle diameter, D_* , and a transport stage parameter, T as defined below (Ackers and White, 1973):

$$D_* = d_{50} \left[\frac{s-1}{v^2} g \right]^{1/3} \quad \text{Equation 8-14}$$

and

$$T = \frac{(u'_g)^2 - (u'_{f,cr})^2}{(u'_{f,cr})^2} \quad \text{Equation 8-15}$$

u'_g is the bed shear velocity, related to grains, and $u'_{f,cr}$ is the Shields critical bed shear velocity. Since form drag does not contribute to bed load transport u_g is defined so that the influence of bed forms is eliminated.

$$u'_g = \frac{\sqrt{g}}{C'} u \quad \text{Equation 8-16}$$

where,

u is the mean flow velocity

C' is Chezy's coefficient related to skin friction (van Rijn, 1984)

$$C' = 18 \log \left[\frac{R}{3d_{90}} \right] \quad \text{Equation 8-17}$$

where,

R is the hydraulic radius related to the bed

$3d_{90}$ is considered as the effective roughness height of the plane bed.

The following expressions are determined for particle velocity and saltation height by applying the equations of motion to a solitary particle (Van Rijn, 1984):

$$\left(\frac{u_{bs}}{u_f} \right) = 9 + 2.6 \log(D_*) - 8 \left[\frac{\theta_c}{\theta} \right]^{0.5} \quad \text{Equation 8-18}$$

This expression was determined by expressing the computed particle velocity as a function of flow conditions and sediment size (D_*). A particle mobility, u_{bs} , was then defined as:

$$\frac{u_{bs}}{[(s-1)gd]^{0.5}} = 1.5T^{0.6} \quad \text{Equation 8-19}$$

Saltation height, δb , is given by van Rijn (1981) as:

$$\frac{\delta b}{d} = 0.3D_*^{0.7}T^{0.5} \quad \text{Equation 8-20}$$

From rearranging (8 – 13);

$$c_b = \frac{q_b}{u_{bs}\delta b} \quad \text{Equation 8-21}$$

From flume measurements of bed load transport the following expression was obtained for the bed load concentration (van Rijn, 1981):

$$\frac{c_b}{c_o} = 0.18 \frac{T}{D_*} \quad \text{Equation 8-22}$$

where,

c_o is the maximum bed concentration(=0.65)

Combining Equations (8 – 19), (8 – 20) and (8 – 22) gives the following expression that is used by the van Rijn model to calculate the bed load transport:

$$\frac{q_b}{\sqrt{(s-1)gd_{50}^3}} = \frac{0.053T^{2.1}}{D_*^{0.3}} \quad \text{Equation 8-23}$$

8.1.2.1.2 *Suspended load*

The suspended load is calculated using a reference concentration determined from the bed load transport. The reference concentration, c_a , is defined for a reference level 'a' below which all sediment is considered to be transported as bed load. This level is approximated by:

$$a = 0.5H \quad \text{Equation 8-24}$$

where,

H is the bed form height

The reference concentration is defined from Equation (8 – 13) as:

$$q_b = u_{bs} \delta b c_b = u_a a c_a \quad \text{Equation 8-25}$$

Where u_a is the effective particle velocity at reference level a. It is expressed as:

$$u_a = \alpha u_{bs} \quad \text{Equation 8-26}$$

By using the above equations and Equations (8 – 14) and (8 – 15) which describe the dimensionless parameters the following expression for the reference concentration, c_a , is obtained:

$$c_a = 0.015 \frac{d_{50}}{a} \frac{T^{1.5}}{D_*^{0.3}} \quad \text{Equation 8-27}$$

In describing the suspended load transport, van Rijn defines a suspension parameter Z which makes provision for the upward turbulent fluid forces and the downward gravitational forces. Z is defined as:

$$Z = \frac{w}{\beta \kappa u_f'} \quad \text{Equation 8-28}$$

where,

u_f' is the bed shear velocity

κ is the von Karman constant

w is the sediment particle's fall velocity in water

β is a coefficient related to the diffusion of sediment particles, defined as:

$$\beta = 1 + 2 \left[\frac{w}{u_f} \right]^2 \quad \text{Equation 8-29}$$

Many factors affect the suspension parameter Z , e.g. volume occupied by the particles, reduction in fall velocity and damping of turbulence. These factors are grouped into one correction factor ψ , which is used to calculate a modified suspension number.

$$Z' = Z + \psi \quad \text{Equation 8-30}$$

where ψ was found to be dependent on the main hydraulic parameters:

$$\psi = 2.5 \left[\frac{w}{u_f} \right]^{0.8} \left[\frac{c_a}{c_o} \right]^{0.4} \quad \text{Equation 8-31}$$

and c_o is the maximum bed concentration as defined in the previous section ($=0.65$).

From the above equations the following expression is derived for suspended load transport:

$$q_s = FuDc_a \quad \text{Equation 8-32}$$

where c_a is defined by equation (8 – 27), D is the total flow depth, u is the mean flow velocity and F is given by:

$$F = \frac{\left[\frac{a}{D} \right]^{Z'} - \left[\frac{a}{D} \right]^{1.2}}{\left[1 - \frac{a}{D} \right]^{Z'} [1.2 - Z']} \quad \text{Equation 8-33}$$

Equations (8 – 32) and (8 – 23) are used by MIKE11 to calculate the suspended and bed load transport when choosing the van Rijn Model.

8.1.2.1.3 Non – uniform sediment transport

A module is available for model applications in non-uniform sediments in which the sediment transport can be calculated by fraction and the variation in time and space of the particle size distribution determined.

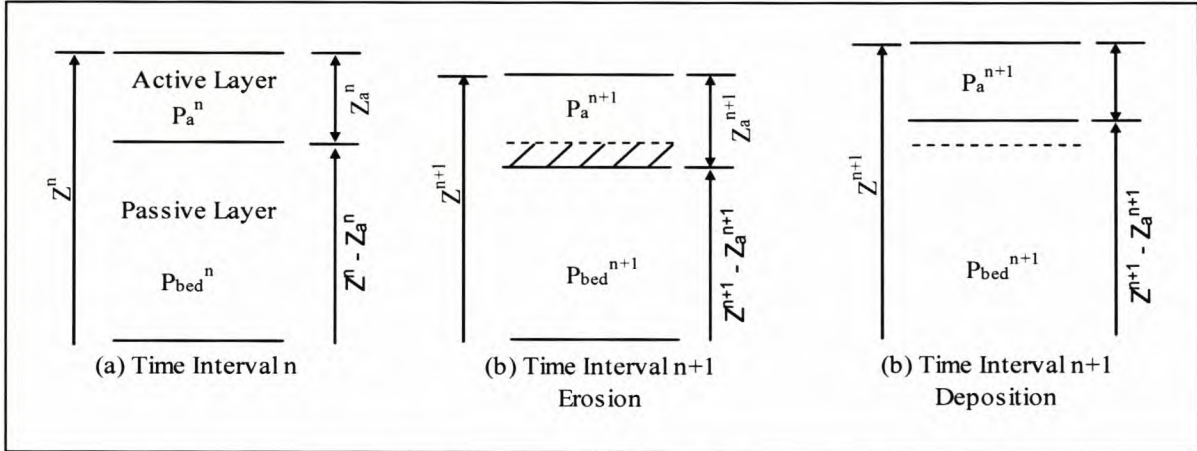


Figure 8-1 Active and passive layers for the simulation of graded sediments

For the simulation of graded sediments the bed is considered to comprise two layers; an active layer overlaying the passive layer (**Figure 8-1**).

The active layer is the layer within which the bed load transport takes place. The depth (Z_a) of the active layer is defined as one half of the dune height, which is predicted according to the selected transport model. For a decreasing dune height (i.e. decreasing bed shear stress) the minimum dune height is specified by the user.

If erosion of the bed material occurs, the composition of the material in the passive layer ($Z - Z_a$ in **Figure 8-1**) stays the same. However, if deposition of the bed material occurs, the active bed material is instantaneously mixed with the material in the passive layer and the composition is modified accordingly.

The additional input data required to simulate the transport of graded sediment are the initial percentage size distributions of the active (P_a) and passive (P_{bed}) layer. The data are specified as a number of fractions, which remain fixed, and the corresponding percentage and mean grain size for the fraction. This percentage varies as the sediment is transported selectively and mixed between the layers.

The transport and mixing of graded sediments is simulated in the following manner. The sediment transport is calculated for each specified class size separately. The calculation is modified in two ways to account for the non-uniformity in the composition of the bed material.

The criterion for the threshold of movement (θ_c) is modified to allow for the armouring of finer material and the greater exposure of larger particles as well as the mutual interference between particles of different size. The threshold of movement is modified by applying Egiazaroff's (1965) correction factor as follows:

$$\theta_{c_i} = \theta_c \left[\frac{\ln(19)}{\ln \left[\frac{19d_i}{d_{med}} \right]} \right]^2 \quad \text{Equation 8-34}$$

where,

- θ_{c_i} is the dimensionless critical bed shear stress for class i.
- θ_c is the dimensionless critical bed shear stress for a uniform sediment.
- d_{med} is the median grain size of the total sediment population.

The second modification is to multiply each class sediment transport, qt_i , by its percentage contribution, p_i . After the sediment transport rate in each class has been calculated, the total transport, qt , is determined by summation over all classes, N:

$$qt = \sum_{i=1}^N qt_i p_i \quad \text{Equation 8-35}$$

The sediment continuity equation is then solved in the same manner as for uniform sediment using the total transport obtained to calculate the change in bed level.

8.1.2.2 Cross – section deformation

The mathematical model that was used to do the sediment transport simulations makes provision for five different ways of updating cross – section information after each time step. Only the model that was selected for this study will be discussed in short.

This model makes the assumption that sediment deposition or erosion occurs over the whole cross – sectional area unless a level of divide is specified. In the latter case the deposition or erosion occurs up to the level of divide, no deposition or erosion will occur above this level. The level of divide is an indication of where the floodplain starts, therefore erosion and deposition only occurs in the main channel.

Assuming that the friction slope is constant across the free water surface width the discharge in the river channel can be expressed as follows:

$$Q_c = Q_t \left[\frac{M_c R_c^{2/3} A_c}{M_t R_t^{2/3} A_t} \right] \quad \text{Equation 8-36}$$

Where:

- M is Manning's roughness coefficient
- R_t is the composite hydraulic radius
- M_t is the composite Manning's roughness coefficient

And:

$$R_t = \left[\frac{\sqrt{R_c} A_c + \sqrt{R_f} A_f}{A_t} \right]^2 \quad \text{Equation 8-37}$$

$$M_t = \frac{M_c \sqrt{R_c} A_c + M_f \sqrt{R_f} A_f}{\sqrt{R_t} A_t} \quad \text{Equation 8-38}$$

The subscript t refers to the entire cross – section, f refers to the floodplains part and c refers to the main channel part.

The change in bottom level is obtained by solving the following the following equation at h-points using the Preissmann Scheme (MIKE 11 Reference Manual DHI, 2002).

$$(1 - \varepsilon) \left[(1 - \psi) \frac{W \Delta z_j^{n+1}}{\Delta t} + \psi \frac{W \Delta z_{j+1}^{n+1}}{\Delta t} \right] + \theta \frac{Qt_{j+1}^{n+1} - Qt_j^{n+1}}{\Delta x} + (1 - \theta) \frac{Qt_{j+1}^n - Qt_j^n}{\Delta x} = 0$$

Equation 8-39

where:

- W is the width of river channel
- Qt_j^n is the sediment transport rate
- Δz^{n+1} is the change in bottom level
- ε is the sediment porosity (specified as 0.35 – the default value)
- ψ is the space centring coefficient (specified as 0.9 – the default value)
- θ is the time centring coefficient (specified as 0.9 – the default value)

The above mentioned equations and the chosen assumptions for sediment erosion and deposition are used to determine the change in the bottom level at each cross – section between the time steps.

8.2 Assembling of Model Parameter Data

A hydrodynamic and sediment transport model of the first 188 km downstream of the proposed Berg River Dam down to the estuary was set up in MIKE 11 (See **Figure 8-2**). For simplicity and simulation duration the model was broken down into two segments, the first starting at the proposed Berg River Dam (designated as chainage 2.2 km) down to Hermon at chainage 70 km and the second from Hermon to the estuary. It is easier to find mistake if the model is broken up in smaller segments.

The upper reaches (segment 1) are steep while downstream of Wellington the slope decreases and the riverbed material consists of sand. The lower reaches (segment 2) are flatter and the riverbed material consists mainly of sand and some cohesive bed sediment.

Scenarios

The following scenarios were investigated for the period 1995 - 2003:

- Present day: based on the observed flows.
- Post- Berg River Dam.
- Post- Berg River Dam with environmentally required flood releases.



Figure 8-2 Berg River system (adapted from Nitsche, 2000).

8.2.1 River Cross Sections and Coordinates

8.2.1.1 Natural scenario cross sections

Surveyed river cross-sections of the upper 14 km immediately downstream of the proposed Berg River Dam were obtained from a recent survey for flood line calculations in the upper Berg River (BRC & TCTA, 2003).

The remainder of the cross-sections used for the upper segment were obtained from data in a report by Beck and Basson (2003). All the cross-sections used for the lower segment were obtained from orthophotos, except that for the cross-sections at Misverstand Dam, which were obtained from the Department of Water and Forestry from a survey of the reservoir (**Figure 8-3**). The intervals between cross-sections typically vary from 300 to 700 m.

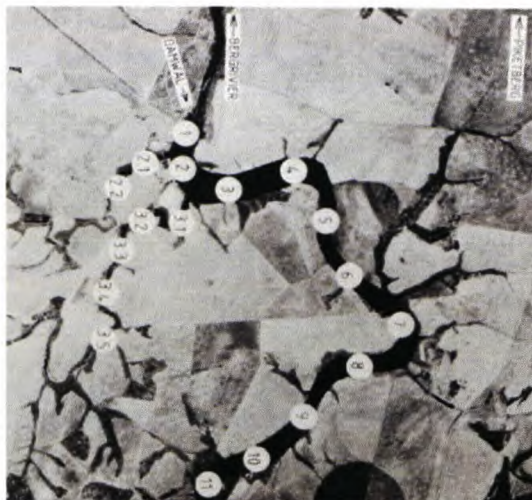


Figure 8-3 Misverstand Cross Sections

The coordinates for the cross – sections of the upper segment were obtained from the report by Beck and Basson (2003). All the other coordinates were obtained from the orthophotos.

8.2.1.2 Post dam development cross-sections

As was observed in the Wemmershoek River, the river cross-sections with the Berg River Dam in place are expected to become narrower because of the reduced flood frequency and peak discharges. For the post-dam scenarios the cross-sections were thus narrowed according to a formula developed by Beck and Basson (2003). The formula was calibrated on South African River data:

$$W_2 = -3.40 + 0.856 \cdot W_1 + 0.142 \cdot MAR_2 - 0.0013 \cdot Q_{p1} \quad \text{Equation 8-40}$$

where: W_1 and W_2 = Pre- and post-dam river widths, respectively (m).

MAR_2 = Post-dam mean annual runoff (m^3/s).

Q_{p1} = Highest flood peaks for the pre-dam periods (m^3/s).

The reduction in the cross-section widths of the main channel over the first 70 km down to Hermon varied by between 25% just downstream of the dam and 15% near Hermon. The cross-sections further downstream were not reduced because the adjustments are negligible.

From the above information it is clear that the same coordinates that were obtained from the orthophotos were used for all the scenarios.

8.2.1.3 Level of divide

The floodplains are overgrown with trees and smaller bushes; it is therefore natural to assume that the roughness of the floodplains should be higher than that of the main channel due to the higher flow resistance given by the trees and other vegetation on the floodplains. One of the ways to incorporate this into this mathematical model is to define a level of divide (**Figure 8-4**) at each cross – section. A different (higher) coefficient of roughness can be defined for the part of the section that falls above the level of divide. By visual inspection a level of divide was therefore introduced at most of the cross – sections. **Figure 8-4** shows one of the sections and the level that was defined as the level of divide.

Table 8-1 show the sections at which a level of divide was defined, the numerical stability of the model determined which sections could be divided. From **Table 8-1** it can be seen that no level of divide was specified for the first 37 km of the upper segment. This is due to the relatively steep bed slope. It should also be noted that the sediment deposition in this region could occur over the whole width of the cross – section. This will cause higher sediment transport rates than anticipated due to the fact that sediment can also be entrained on the flood plains if no level of divide is specified.

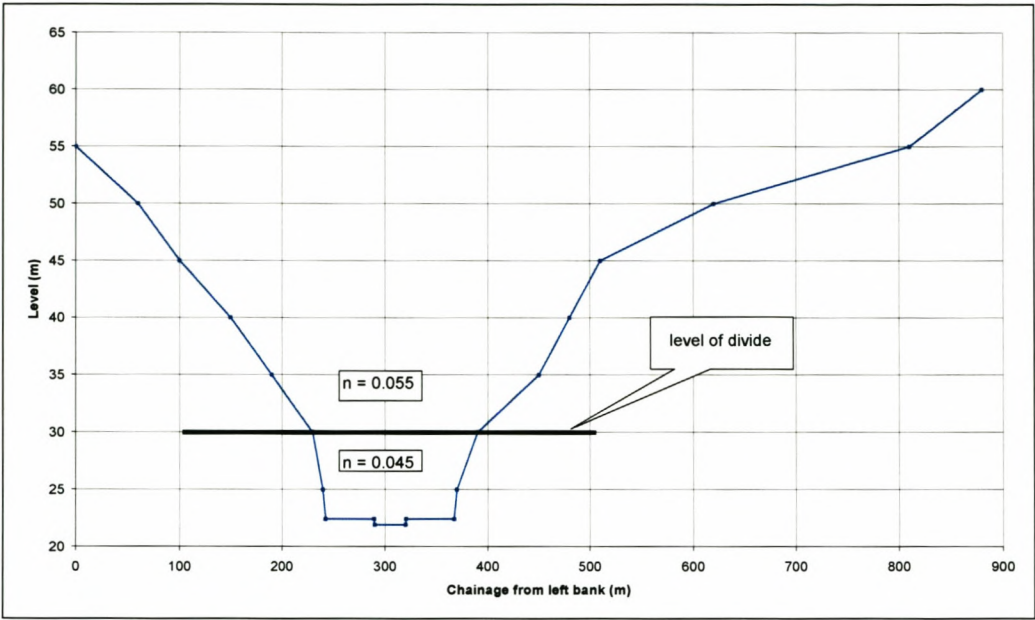


Figure 8-4 Level of divide defined at a section

Table 8-1 Divided sections	
	Chainage (Km)
Upper Section	37 – 37.5
	39 – 39.5
	40.5 – 41
	43
	44 – 44.5
	49
	51 – 52
	53.5
	54.5
	56
	57.5
	59-70
Lower Section	75 – 83.5
	87.5 – 130.9
	140.5 – 166.4
	178.4
	180.4 – 187.9

8.2.1.4 Additional low flow channel

The Orthophotos that were used to obtain the majority of the cross – sections had no contours in the main channel, except for those that cross the river. It was therefore decided to add an additional smaller channel between the two lowest contours of all the cross – sections that were obtained from the Orthophotos. This was done to ensure that the low flow conditions were simulated realistically and that the sediment transport simulation under low flow conditions is more accurate. Without this additional channel the water depth will be lower, and the width of flow wider which will cause inaccuracies in the simulated sediment transport rate in comparison to the actual situation. **Figure 8-5** shows a cross – section with the additional channel added.

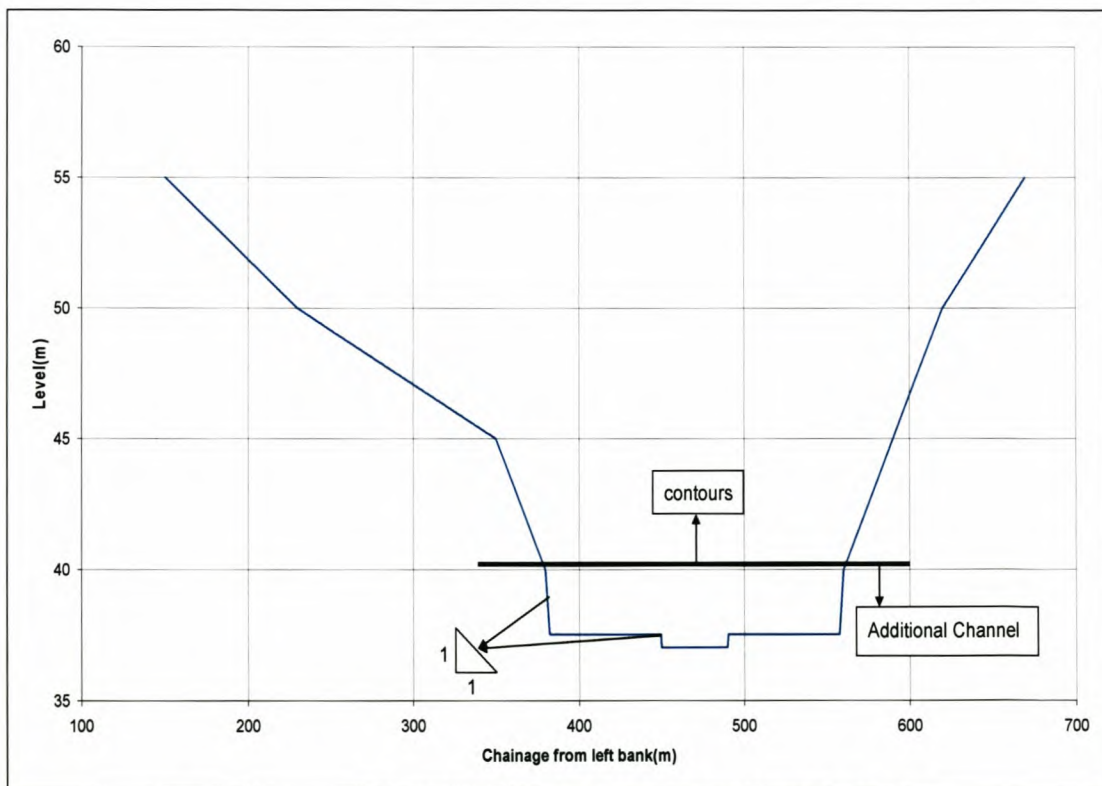


Figure 8-5 Added channel at sections obtained from Orthophotos

The bed level of each cross – section was obtained through interpolation between the positions where the contours cross the main channel of the Berg River.

8.2.2 Flow Boundaries

Discharge boundaries were specified at the upstream boundary of the model, as well as at all major tributaries. All the ungauged subcatchments were incorporated by scaling of the measured flows on the major tributaries.

Observed flow records are available at four DWAF gauging stations along the Berg River: G1H004 just upstream of the Berg River Dam site, G1H020 at Paarl, G1H036 at the Hermon road bridge and G1H013 at Drieheuwels.

The tributaries with flow measurement stations that were used in this study are: Franschhoek (G1H003), Dwars (G1H019), Krom (G1H037), Doring (G1H039) and Kompanjies (G1H041) for the upper segment and Vis (G1H040), Klein Berg (G1H008), Twenty-fours River (G1H028), Sandspruit (G1H043), Matjies (G1H035) and Mooresburgspruit (G1H034) for the lower segment. The measured tributary flows had to be scaled to allow for unmeasured catchment areas. The following relationship was used as an initial value to scale the tributary flows at each station:

$$Factor = \sqrt{\frac{A_u + A_m}{A_m}}$$

Equation 8-41

Table 8-2 Initial adjustment factors to account for ungauged areas at tributaries

Tributary	Flow gauging station catchment area (km ²)	Ungauged catchment area (km ²)	Initial Flow Factor
Franschhoek (G1H003)	46	262 (incl. Wemmershoek)	2.59
Dwars (G1H019)	25	206	3.04
Krom (G1H037)	52	18	1.16
Doring (G1H039)	43	256	2.64
Kompanjies (G1H041)	121	204	1.64
Vis (G1H040)	75	210	1.95
Klein Berg (G1H008)	370	205	1.25
Twenty-fours River (G1H028)	185	285	1.59
Sandspruit (G1H043)	260	7	1.01
Matjies (G1H035)	615	75	1.06
Mooresburgspruit (G1H034)	175	60	1.16

with A_u the ungauged catchment area and A_m the gauged catchment area. These values were changed during the calibration of the hydrodynamic model to ensure that the simulated flood peaks were accurate compared to the measured peaks that occurred at the measuring stations along the Berg River. The initial factors for the various tributaries are listed in **Table 8-2**. Note that the Wemmershoek catchment was included under Franschhoek River.

No flow records after 1992 are available for the measuring stations on the Krom River, Vis River and Twenty-fours River. The following records (adjusted) of adjacent rivers were used for the above mentioned rivers:

- Kompanjies River for Krom River.
- Sandspruit River for Vis River.
- Klein Berg River for Twenty-fours River.

These rivers have similar catchment areas to the ones they replaced, thus an assumption is made that flow will not vary dramatically between the adjacent rivers. The error that occurred by this replacement was corrected during the hydrodynamic model calibration, as the factors in **Table 8-2** were changed.

It should be noted that the model uses instantaneous flows, or “breakpoint” data (also known as primary data) as recorded by DWAF as input with a time step during simulation of less than 1 minute. Average daily or hourly flows are not used at all.

Flow data obtained from the Department of Water Affairs and Forestry for the gauging station, G1H004, was used as input at the proposed dam for the upper segment. This gauging station is situated 2.2km upstream of the proposed dam. It is therefore a reasonable assumption that the flow will not change to such an extent that it will have a drastic effect on the accuracy of the simulations in 2.2 km. The output of the last section of the upper segment (chainage 70 km) was used as input to the lower segment.

The proposed Berg River Dam will cause flood attenuation and this effect had to be determined to create the upstream flow boundary for the computational model. Level pool

routing was carried out with the following Berg River Dam characteristics (see **Figure 8-6** and **Figure 8-7**) as obtained from Ninham Shand (2001/2004):

- Full supply capacity (FSC): 126.4 million m³
- Full supply level (FSL): 250 m
- Spillway length: 40 m
- Agricultural demand: 55.5 million m³/a (including approximately 16.5 million m³/a of summer inflows which will be released above the basic agricultural demand), see **Table 8-3**.

Table 8-3 Monthly distribution of agricultural releases

Month	Oct	Nov	Dec	Jan	Feb	Mar	Apr	May	Jun	Jul	Aug	Sep
Flow (m ³ /s)	0	0.6	2.8	6.0	6.2	5.0	0.7	0	0	0	0	0

- Environmental releases (low flow IFR and flood releases): 34.5 million m³/a, of which 27.4 million m³/a is for the low flows
- Pumping to Theewaterskloof Dam: 76.2 million m³/a with flood releases, and 80.5 million³/a without flood releases
- Drakenstein supplement: 21.8 million m³/a

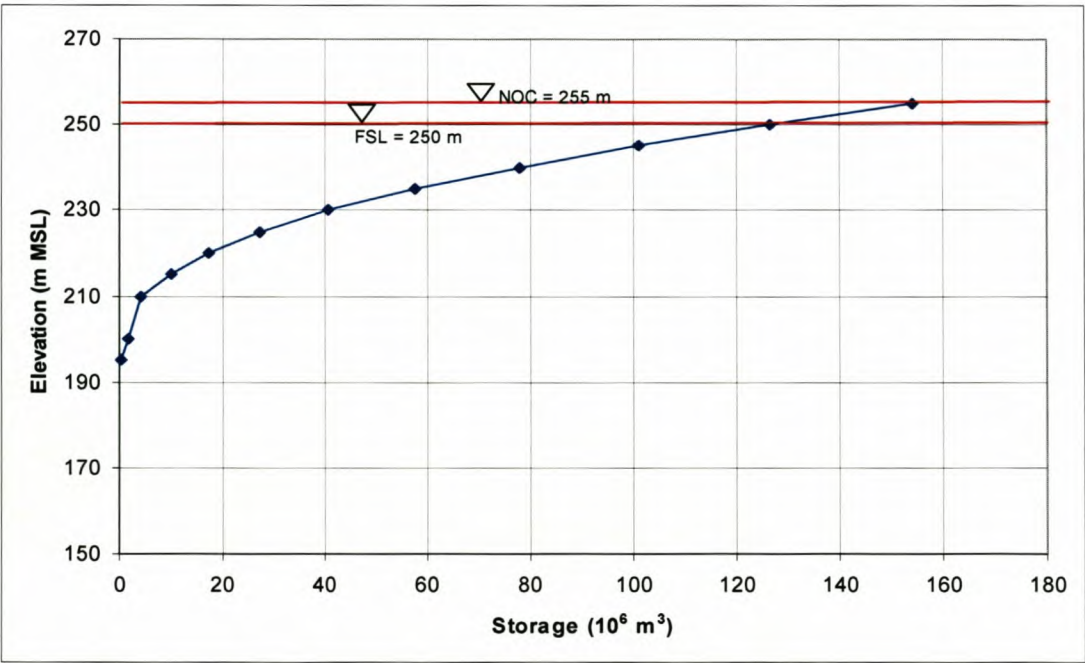


Figure 8-6 Storage – elevation relationship for the Berg River Dam

The volume of water pumped to Theewaterskloof was determined based on the following operating procedure:

- The dam will be operated so that spills will only occur once every four years (pers com Dr M Shand, Ninham Shand, 2004).
- Pumping to Theewaterskloof will occur at $6 \text{ m}^3/\text{s}$, as long as the water level in the reservoir is above 240.9 m (96 million m^3). This level was obtained through an iterative process by placing the total demand on the dam, as listed above (including flood releases), together with the supplement, with the aim that spills do not occur in more than two years during the nine year period (see **Figure 8-8**). In the total system analysis done by Ninham Shand for DWAF, spills occur once every two years on average, but there are a few periods where the dam does not spill in at least four consecutive years.

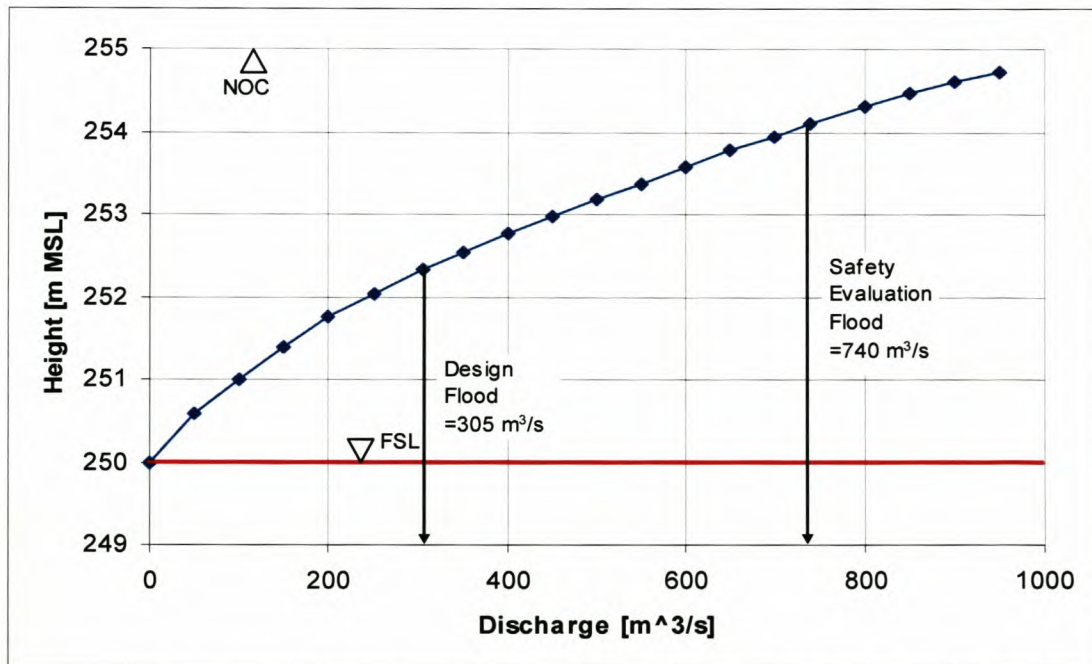


Figure 8-7 Discharge – water level rating curve for the Berg River Dam spillway

The supply from the supplement was based on an analysis of the abstraction works by taking the following components into consideration (BRC, 2004):

- River flow
- In-stream flow requirements

- Diversion capacity to the balancing dam ($6 \text{ m}^3/\text{s}$)
- Size of the balancing dam ($48\,000 \text{ m}^3$)
- Pumping capacity to the Berg River Dam from the balancing ($5 \text{ m}^3/\text{s}$)

While the Berg River Dam FSL is at 250 m (MSL), additional storage in the order of 28 million m^3 is available above that level up to the non-overflow crest of just below 255 m, as can be seen from **Figure 8-6**. The relatively narrow spillway (40 m) will constrict the flow and cause flood attenuation.

The 9-year measured flow record at G1H004 from 1995 – 2003 was routed through the reservoir, using 1.5-hourly time steps (**Figure 8-8** shows the water level in the reservoir over the 9-year period, without the flood releases). The routing was also repeated for the artificial flood release scenario. A time steps of 1.5 hours were only used in the reservoir routing exercise and not in the river simulation. NB: All the flow data discussed and presented in this section are instantaneous peak data, and not daily average values, unless stated otherwise.

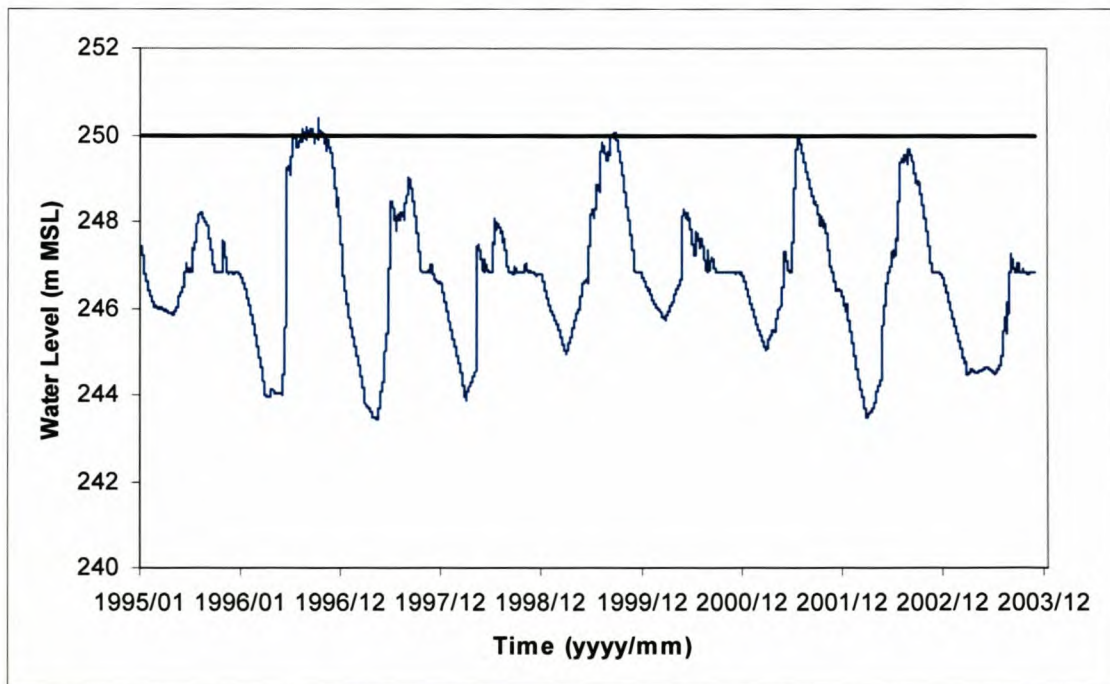


Figure 8-8 Reservoir water levels for the post-dam scenario

As part of the IFR (DWAF, 1996) study recommendation two large floods and one small flood should be released annually (see **Table 8-4**) from the dam in phase with a naturally occurring flood event of the same magnitude in order to be in phase with floods from the

subcatchments, which can, however, not be guaranteed. A rainfall-runoff model will be required during dam operation to forecast when managed floods should be released. If there should, however, not be a natural flood of the same magnitude, the flood should be scaled down (DWAF, 2003). The following operating rules were used for the flood releases in this thesis (the dates, actual flood peaks and released floods are listed in **Table 8-5**):

Table 8-4 Proposed (DWAF, 2003) and simulated IFR flows at the dam site

Month	High flows (proposed DWAF, 2003)		Simulated flood peak (this study)	
	Daily average peak (m ³ /s)	Volume (10 ⁶ m ³)	Instantaneous peak (m ³ /s)	Volume (10 ⁶ m ³) ^b
April	5	0.778	15	0.176
June	30 (65 ^a)	4.666	70 - 100	2.647 - 3.350
July	65 (160 ^a)	10.109	100 - 220	5.075 - 9.463

^a: Approximate instantaneous peak (DWAF, 2003) ^b: Range, depending on actual flood release peak

5 m³/s (daily average) flood: If there is a naturally occurring event of 15 m³/s or more during the first half of April a flood with a 15 m³/s peak should be released. Otherwise together with the first flow higher than baseflow. This flood was not scaled down according to the inflow, as this would result in very small floods that serve no purpose.

30 m³/s (daily average) flood: This flood was included to coincide with a naturally occurring flood in June to July of each year. The operating rule was as follows:

- Should an event of 70 m³/s or more occur during June or July the artificial flood will be released and the magnitude would depend on the size of the incoming flood, but with a maximum of 100 m³/s, otherwise no flood will be released. The 70 m³/s lower limit was chosen based on the proposed instantaneous flood peak in the IFR report. The upper limit of 100 m³/s is based on the maximum volume allocated for this flood release.

65 m³/s (daily average) flood: The third flood was incorporated between July and September according to the following operating rule:

- The flood will be released with the first naturally occurring flood with a magnitude of greater than 160 m³/s in July or August and the magnitude would depend on the size of the incoming flood, but with a maximum of 220 m³/s. Should these requirements

not be met the flood will be released with the first naturally occurring flood with a magnitude of greater than $100 \text{ m}^3/\text{s}$ in September. Should none of these requirements be met, no flood will be released. The $160 \text{ m}^3/\text{s}$ lower limit in July/August was chosen based on the proposed instantaneous flood peak in the IFR report. The upper limit of $220 \text{ m}^3/\text{s}$ is based on the maximum volume allocated for this flood release.

Table 8-5 **Timing and magnitude of simulated artificial flood releases based on historical records**

Dates of 1 st flood release	Incoming Peak (m^3/s)	Released Peak Flow (m^3/s)	Dates of 2 nd flood release	Actual Peak (m^3/s)	Released Peak Flow (m^3/s)	Dates of 3 rd flood release	Actual Peak (m^3/s)	Released Peak Flow (m^3/s)
20/04/1995	2.4	15	No floods released					
18/04/1996	28.8	15	07/06/1996	191.2	100	24/09/1996	136.8	136
27/04/1997	0.8	15	08/06/1997	79.6	79	No flood released		
05/04/1998	25.8	15	06/06/1998	82.9	82	15/07/1998	290.5	220
20/04/1999	6.1	15	18/06/1999	108.1	100	No flood released		
23/04/2000	2.9	15	18/07/2000	109.9	100	02/09/2000	125.9	125
13/04/2001	10.4	15	03/07/2001	81.3	81	No flood released		
16/04/2002	4.9	15	09/07/2002	87.6	87	28/07/2002	225.2	220
22/04/2003	1.8	15	No flood released			18/08/2003	184.5	184

A typical hydrograph, based on natural flood events, was used to determine the flood release pattern (see **Figure 8-9**). The blue hydrograph represents the $220 \text{ m}^3/\text{s}$ flood release while the red hydrograph represents the $100 \text{ m}^3/\text{s}$ flood release. The pre-dam flows at the dam site and the post-dam flows with and without artificial flood releases are indicated in **Figure 8-11** to **Figure 8-12** respectively. **Figure 8-10** shows the Observed flow sequence as it was registered by the Department of Water Affairs for gauging station GIH004 at Driefontein. By comparing **Figure 8-10** and **Figure 8-11** the effect of the proposed Berg River dam on the volume of water that will pass through any given main – stem location can clearly be seen.

As can be seen from **Table 8-5**, the 1st winter flood was released every year, however, 1995 was a very dry year and no other floods could be released. In 2003 the floods only occurred late in winter and therefore only the 3rd flood could be released. In 1997, 1999 and 2001 only the 2nd flood could be released. From **Figure 8-12** it can be seen that with the flood releases the smaller, more frequent floods are still missing, however, the adopted operating rule for the flood releases ensures that there is variability in the flood magnitude that are released.

The required flood releases and operating rules were refined based on the sediment mass balance findings in the river.

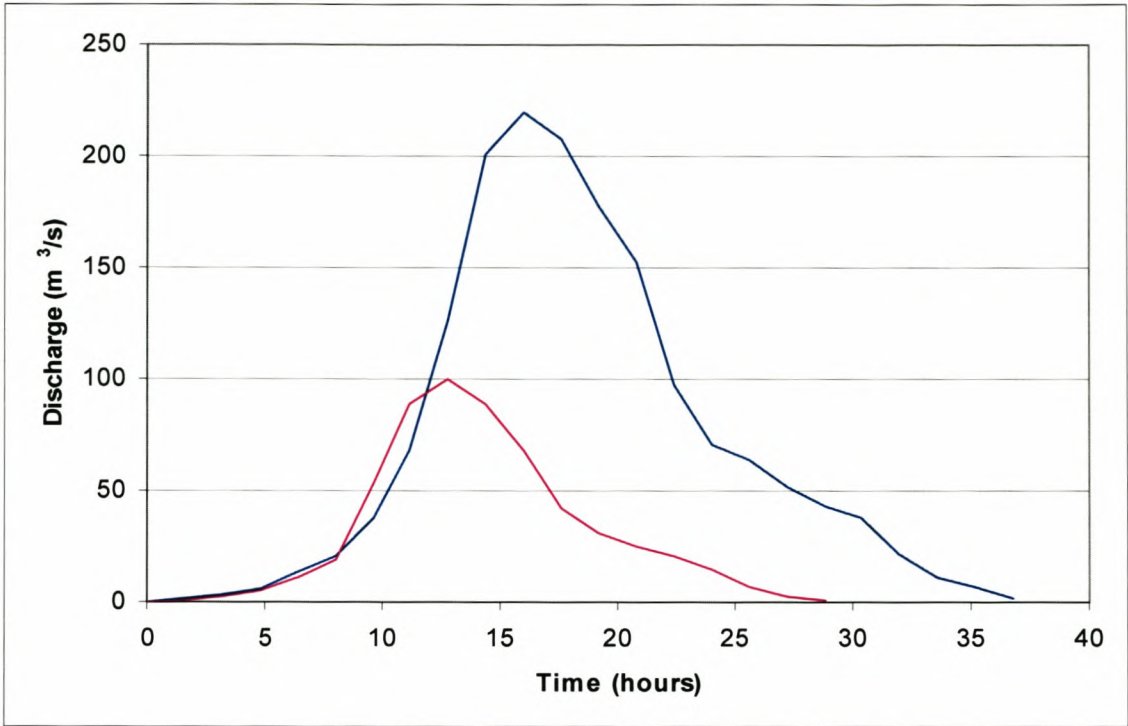


Figure 8-9 Flood release hydrographs

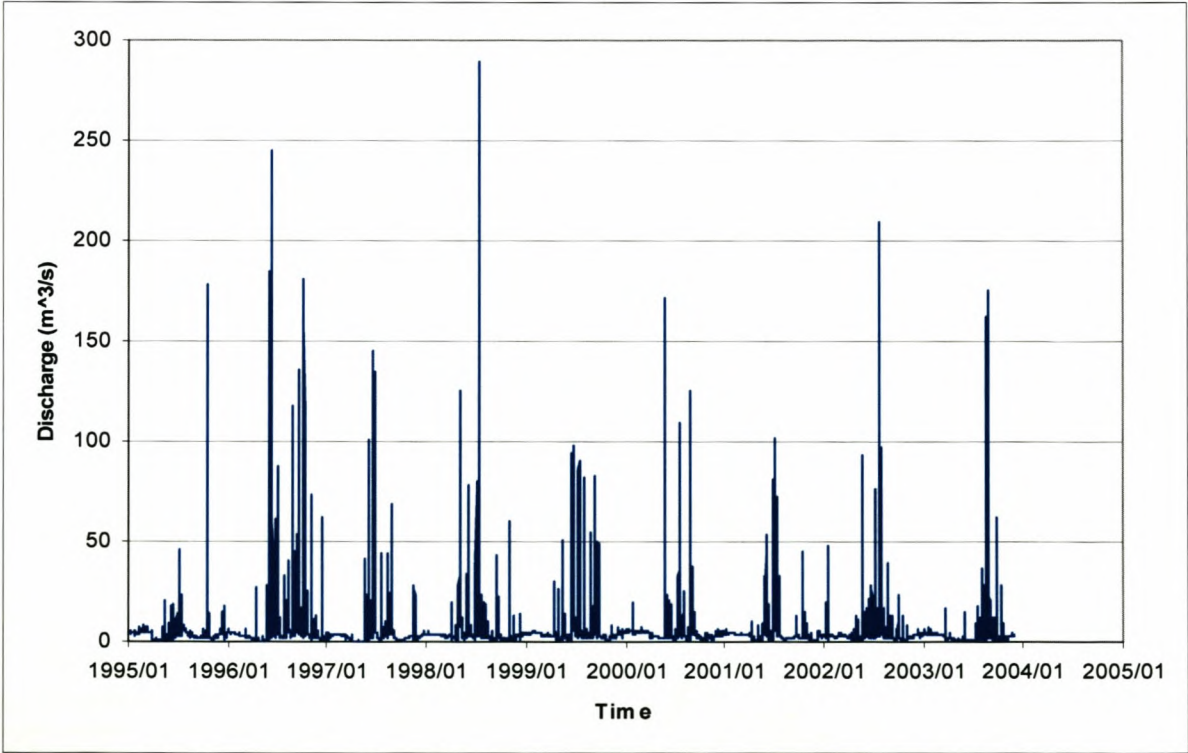


Figure 8-10 Observed flow sequence, G1H004 (instantaneous peak data)

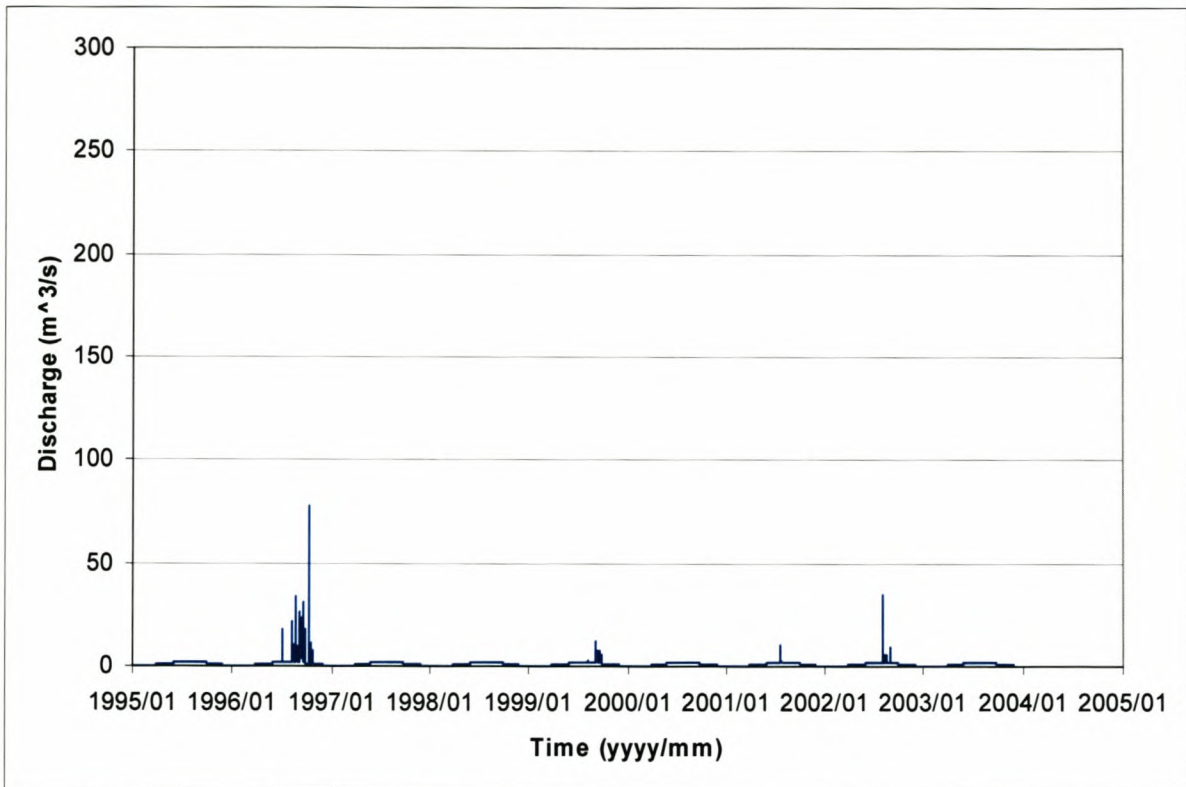


Figure 8-11 Post-dam dam outflow sequence with IFR low flows (instantaneous peak data)

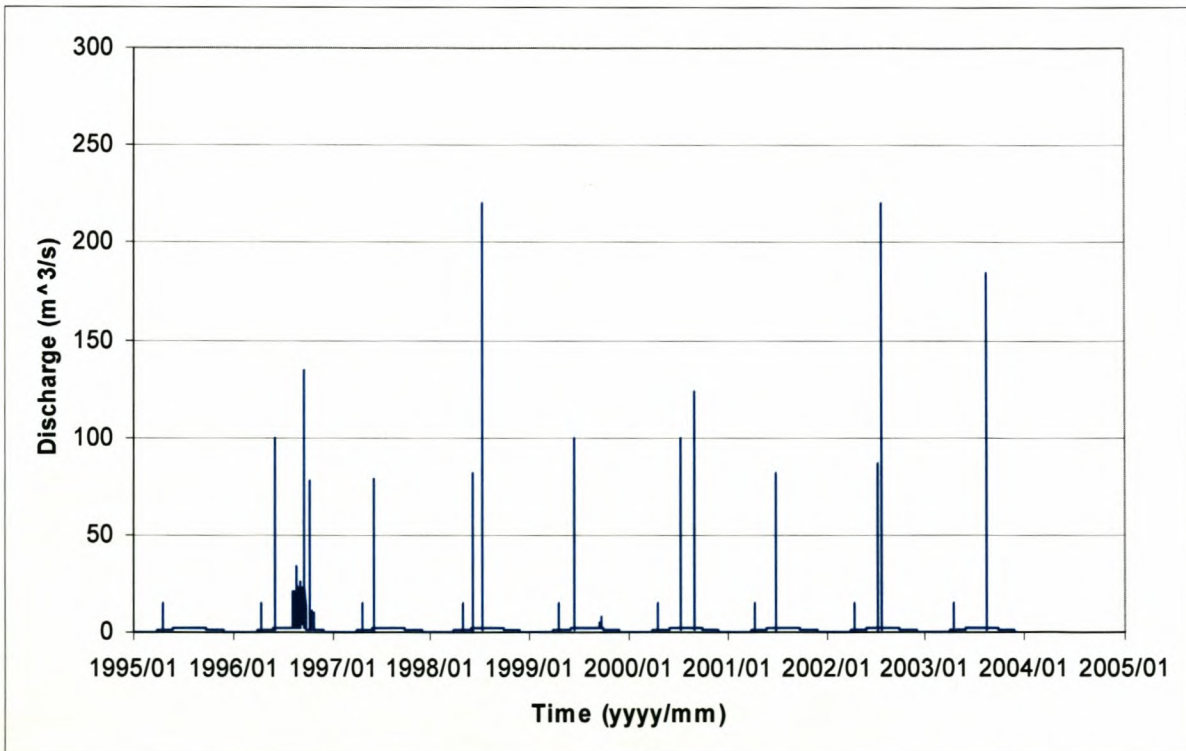


Figure 8-12 Post-dam dam outflow sequence with IFR low flows and artificial flood releases (instantaneous peak data)

From **Figure 8-8** it can be seen that without flood releases the dam would actually spill in four of the nine years but the highest flood peak would be about $77 \text{ m}^3/\text{s}$ compared to an

incoming flood of around 240 m³/s. During the summer months only the IFR and agricultural releases will ensure that there is water in the river. The proposed IFR low flows are listed in **Table 8-6**.

Table 8-6 IFR estimate low flow for the Quaternary catchment area G10A at IFR Site 1 (DWAF, 2003)

Month	Discharge [m ³ /s]	Volume [10 ⁶ m ³]
October	0.8	2.1
November	0.5	1.3
December	0.4	1.1
January	0.3	0.8
February	0.3	0.7
March	0.3	0.8
April	0.8	1.3
May	1.0	2.7
June	1.6	4.1
July	1.6	4.3
August	1.6	4.3
September	1.5	3.9

The flood attenuation occurs because, as the flood enters the reservoir upstream, it is slowed down because of the larger area of the reservoir basin. It will then take some time for the water level in the reservoir to rise to such an extent as to cause spillage over the spillway. If the reservoir is empty, the whole flood may be absorbed, depending on the volume, whereas when the dam is full, the flood may be attenuated only to a small degree. Also smaller floods are usually attenuated to a much larger degree than larger floods, or even absorbed completely. The flood releases allows for larger floods to be released downstream, but the smaller, more frequent floods which are responsible for a significant part of the sediment transport in the upper reaches, are completely removed.

Irrigation releases up to 5 m³/s are made upstream of the Berg River Dam site from the Theewaterskloof Dam. The water is abstracted along the river mainly between Paarl and Hermon. Downstream of Hermon releases are again made for irrigation from Voëlvlei Dam, which are abstracted along the river. The pattern of current irrigation flows along the river is therefore as illustrated in **Figure 8-13**. However, the current hydrodynamic model does not make provision for irrigation abstraction along the river since no detailed data were available, nor does it take into account water losses due to evaporation or infiltration, but could be incorporated in a future setup when the aim is on low flow calibration. It has to be borne in

mind that the low flows have a limited effect on the sediment transport. For this reason it was decided to simulate the irrigation releases at present as illustrated in **Figure 8-14**. Once the dam is in place the irrigation releases will be made at or downstream of the Wemmershoek River, and therefore the irrigation releases were simulated as shown in **Figure 8-15**. This means that the present and post-dam scenarios are directly comparable.

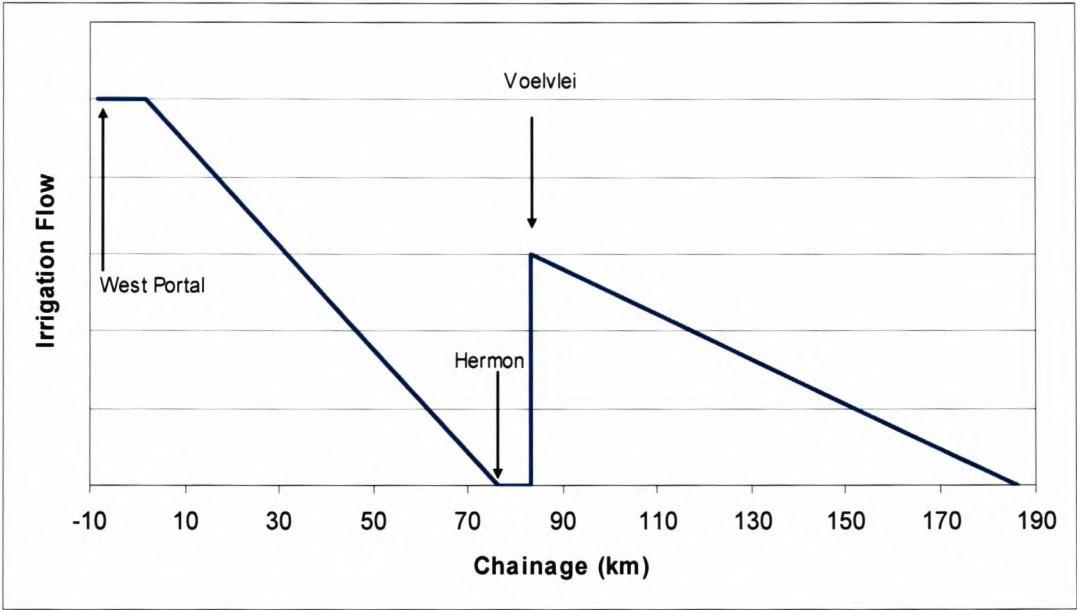


Figure 8-13 Actual irrigation flow pattern along the Berg River

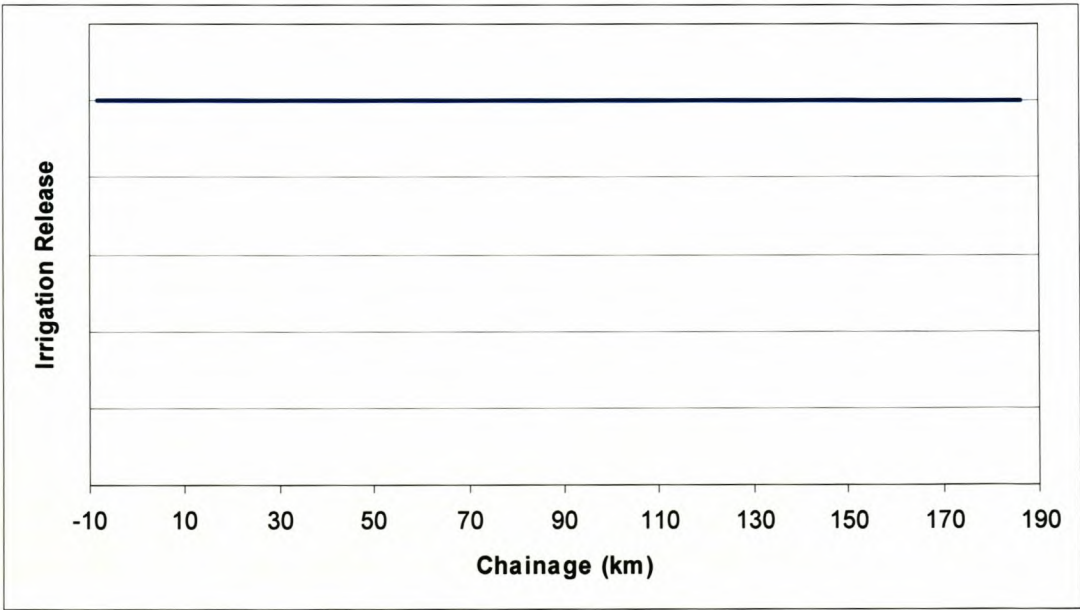


Figure 8-14 Simulated irrigation flow pattern along the Berg River for the present conditions

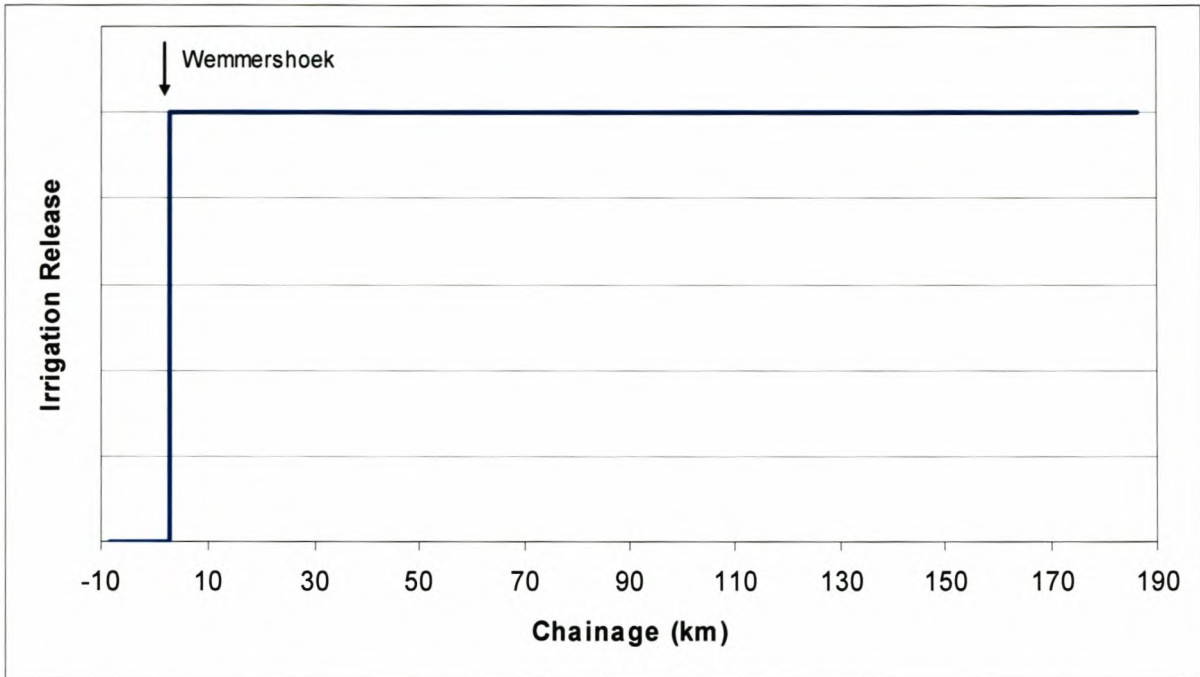


Figure 8-15 Simulated irrigation flow pattern along the Berg River for the post-dam conditions

8.2.3 Downstream Boundary Conditions

At the downstream end of both reaches under consideration a $Q - h$ boundary was set up relating the elevation above mean sea level to the discharge. The characteristics of the cross - sections of km 70 and km 188.4 were used to set up the $Q - h$ boundary for the upper and lower segments respectively. The discharge was calculated by using Manning's equation:

$$Q = A \frac{R^{\frac{1}{3}}}{n} \sqrt{S_o} \quad \text{Equation 8-42}$$

With:

- A the cross – section area at the specific height.
- R the hydraulic radius at the specific height.
- S_o the local bed slope.
- n Manning's n value to describe the bed roughness.

The local bed slope was determined by using the orthophotos at both Hermon bridge for the upper section and at the start of the estuary for the lower section.

8.2.4 Sediment Transport Boundaries

The sediment input into the Berg River system is important in quantifying the sediment balance in the river.

8.2.4.1 Sediment Inflow via the Tributaries

It is important to establish a sediment load – discharge relationship at each inflow into the Berg River. Normally such a relationship should be obtained from observed suspended sediment sampling over at least 3 – 5 years (**CHAPTER 5**). In this study no such data are available. It was found by Beck and Basson (2003) that the sediment transport capacity could be used if suspended sediment data are not available if calibration is carried out against the sediment yield in the catchment. The sediment transport capacity and sediment load are therefore calculated and integrated over the study period (in this case 9 years) for each inflow into the Berg River system via the tributaries.

The sediment transport capacity was calculated by using the orthophotos to obtain cross – sections on the tributaries just upstream of the confluence with the Berg River, and to obtain the local bed slope at each confluence. The Ackers and White (Chadwick and Morfett, 1998) sediment transport formula was used to determine the sediment transport capacity of each tributary. The equations are as follows:

$$G_{gr} = \frac{q_s D_m}{qD} \left[\frac{u_*}{V} \right]^n = C \left[\frac{F_{gr}}{A_{gr}} - 1 \right]^m \quad \text{Equation 8-43}$$

$$F_{gr} = \frac{u_*^n}{\sqrt{gD \left[\frac{\rho_s}{\rho} - 1 \right]}} \left(\frac{V}{\sqrt{32} \log \left(\frac{10D_m}{D} \right)} \right)^{1-n} \quad \text{Equation 8-44}$$

$$D_{gr} = D \left(\frac{g \left[\left(\frac{\rho_s}{\rho} \right) - 1 \right]}{v^2} \right) \quad \text{Equation 8-45}$$

Where,

$$q_s = \text{Sediment load per m. (m}^3\text{/s/m).}$$

q	=	Discharge per m. ($\text{m}^3/\text{s}/\text{m}$).
D_m	=	Hydraulic mean depth (m).
D	=	Particle diameter (m).
u_*	=	Friction velocity (m/s).
V	=	Mean velocity (m/s).
g	=	Acceleration due to gravity (m/s^2)
ρ	=	Water density (kg/m^3).
ρ_s	=	Sediment density (kg/m^3).

The index n does not have a physical significance, since its magnitude is related to D_{gr} . For fine grains $n = 1$ and for coarse gains $n = 0$. The values for n , m , A_{gr} and C are as follows:

For $D_{gr} > 60$ (coarse sediment with $D_{50} > 2$ mm):

$$\begin{aligned} n &= 0, \\ m &= 1.78, \\ A_{gr} &= 0.17, \\ C &= 0.025. \end{aligned}$$

For $1 < D_{gr} < 60$ (D_{50} in the range 0.06 – 2 mm):

$$n = 1 - 0.56 \log D_{gr} \quad \text{Equation 8-46}$$

$$m = 1.67 + \frac{6.83}{D_{gr}} \quad \text{Equation 8-47}$$

$$A_{gr} = 0.14 + \frac{0.23}{\sqrt{D_{gr}}} \quad \text{Equation 8-48}$$

$$\log(C) = 2.79 \log D_{gr} - 0.98(\log(D_{gr})) - 3.46 \quad \text{Equation 8-49}$$

The sediment transport capacity time series for the primary flow data received from DWAF was calculated by using the Equations 8 – 46 to 8 – 49 in conjunction with Equations 8 – 43 to 8 – 45.

Each time series of sediment transport calculated as described above had to be scaled due to the sediment availability that is usually much less than the sediment transport capacity in the various catchments.

The sediment yield can be determined from observed sedimentation volumes in reservoirs or from sediment sampling on the river. Rooseboom (1992) developed regional sediment yield maps for South Africa based on reservoir basin surveys. These methods are discussed in more detail in **CHAPTER 5**. In this study, however, it was decided to take suspended sediment samples at various locations on the Berg River in order to determine the sediment yield for different subcatchments along the Berg River System.

The sediment sampling was only done during the winter of 2003 and the winter of 2004. The data acquired during 2003 was used to determine the sediment yield. It should be stressed that one year of sediment sampling is insufficient to determine an accurate sediment yield for any catchment. Continuous data over at least 3 to 5 years should be used in order to determine a reliable sediment yield. Mainly due to time constraints but also due to a lack of financial resources, it was not possible to carry out sediment sampling over such an extended period. Therefore it was decided that suspended sediment sampling should also be done during the winter of 2004 to obtain verification data.



Figure 8-16 **Suspended sediment sampling apparatus**

The sampling was done using a standard 0.5 litre plastic bottle (see **Figure 8-16**). The samples were taken downstream of a gauging weir to assure that the suspended sediment and the bed load was well mixed. A holder was made from steel that was used to hold the plastic

bottle; this caused the plastic bottle to sink in order for it to be filled with water. A rope that was tied to the holder was used to throw the holder towards the main stream from the riverbank. This was done where it was not possible to lower it from a bridge or other structure directly from above the stream.

In order to determine the sediment yield at the various sampling locations (**Table 8-7**), a sediment load – (instantaneous) discharge rating curve had to be used to determine a sediment load time series over an extended period. From this time series and the catchment area the sediment yield was determined for each sampling location. **Figure 8-17** to **Figure 8-22** shows the sample scatter for the various locations as well as the regression formula that was obtained from the sampling during the 2003 winter season. When these figures were plotted all the samples with a sediment load less the 1 g/s were neglected. The floods are responsible for most of the sediment transport; therefore the regression should represent the higher sediment loads more accurately than that of the lower flows.

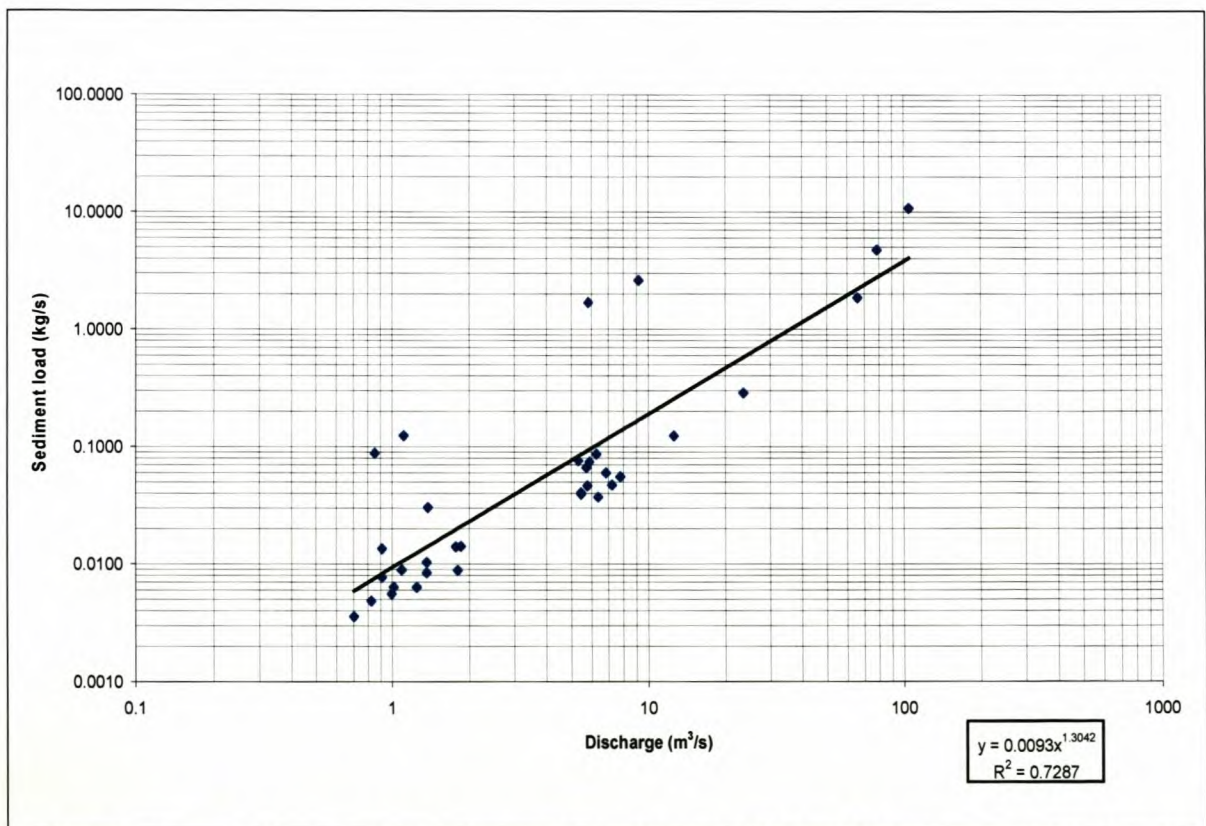


Figure 8-17 Sediment load – Discharge relationship at G1H004 – A2 (downstream of BRM site1)

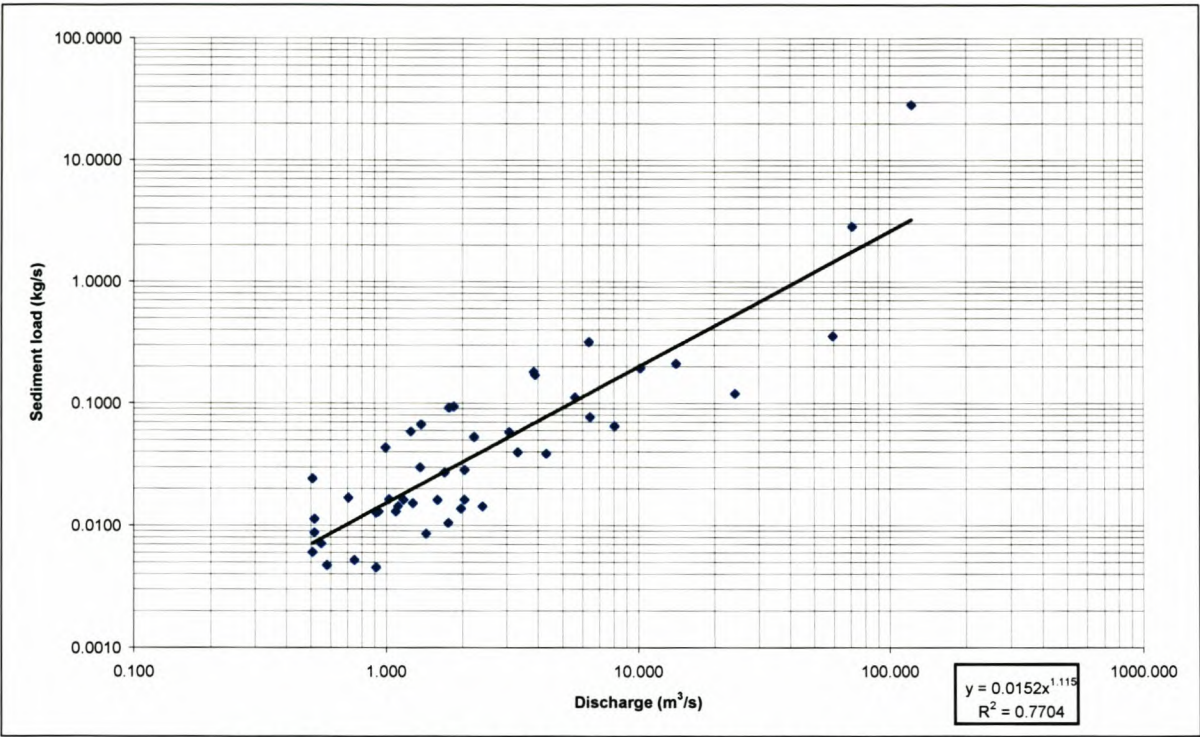


Figure 8-18 Sediment load – Discharge relationship at G1H004

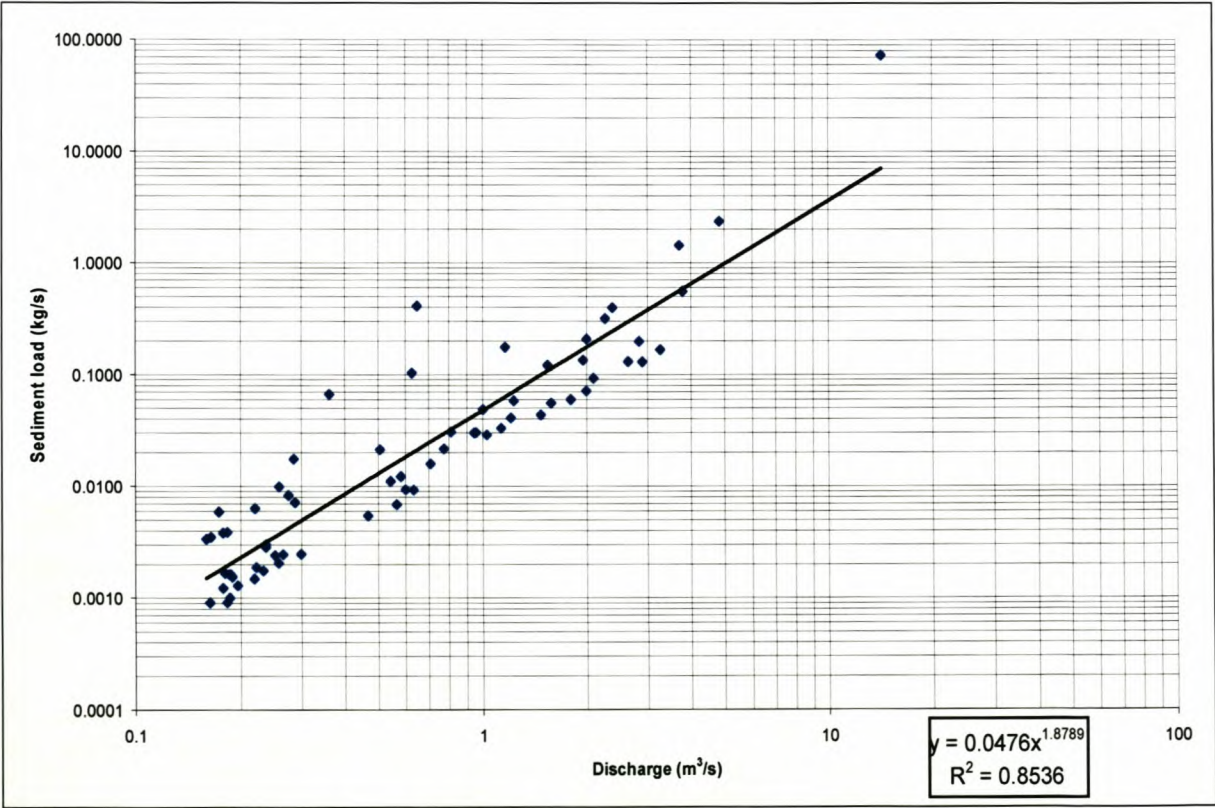


Figure 8-19 Sediment load – Discharge relationship at G1H003

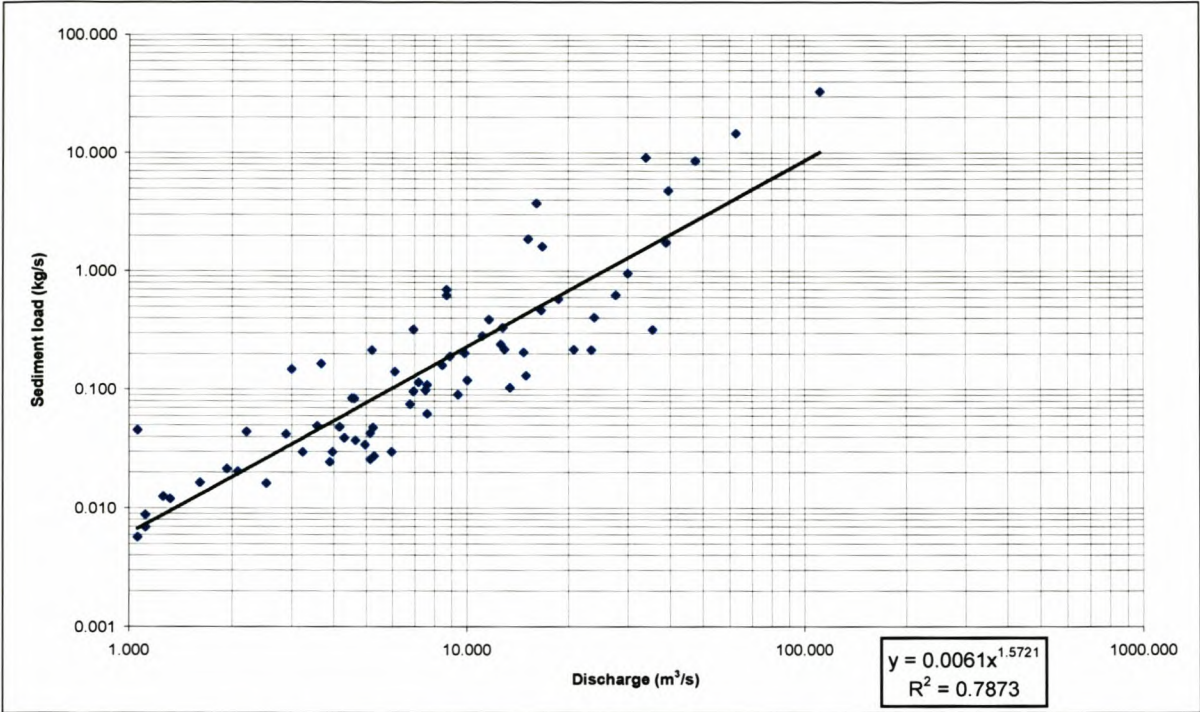


Figure 8-20 Sediment load – Discharge relationship at G1H020

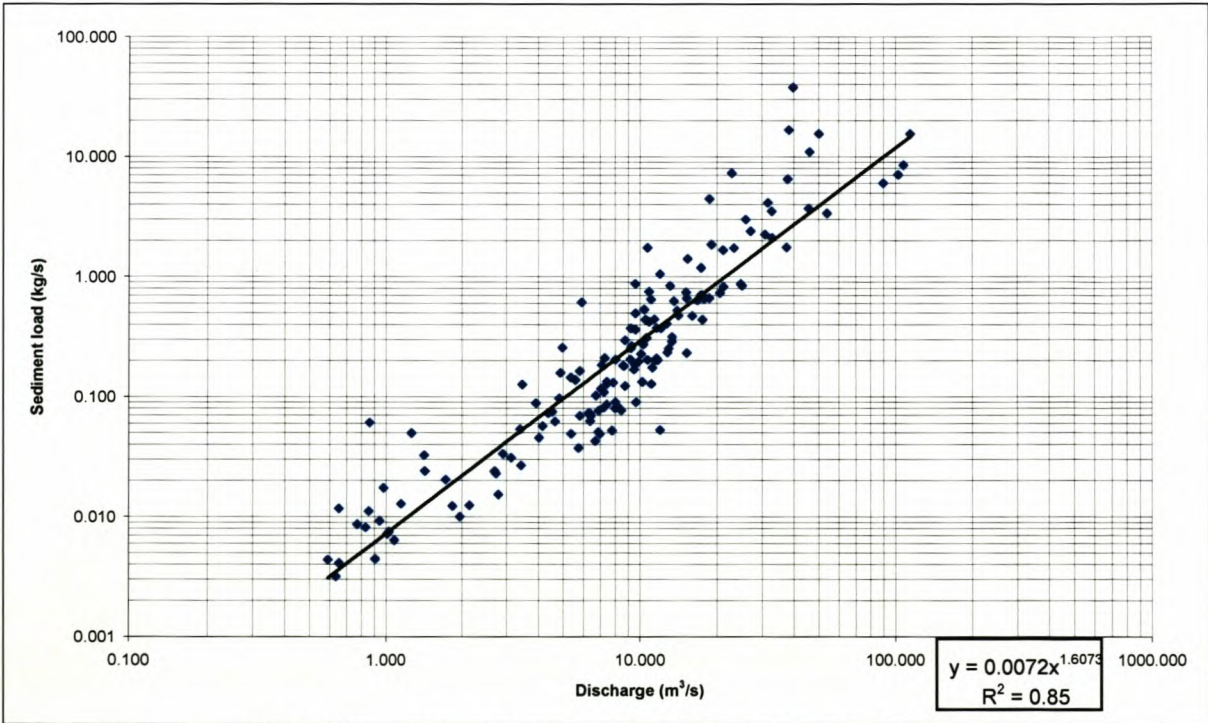


Figure 8-21 Sediment load – Discharge relationship at G1H036

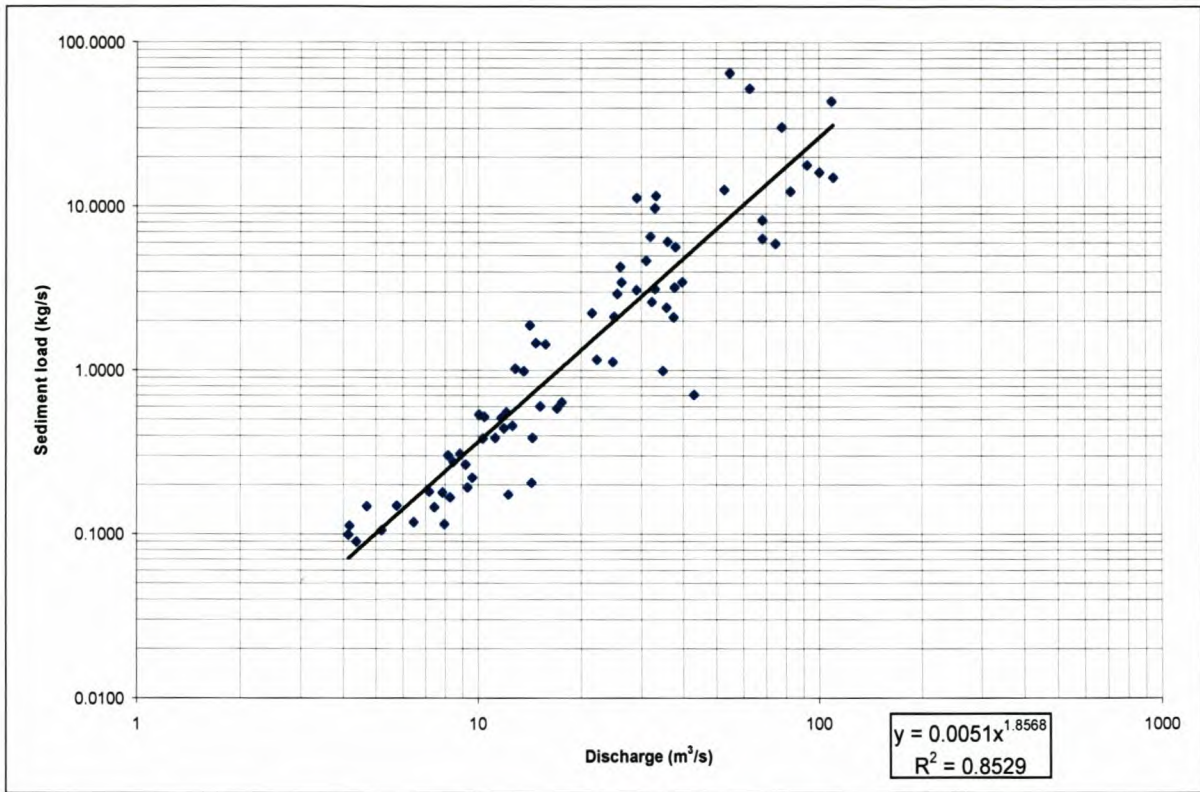


Figure 8-22 Sediment load – Discharge relationship at G1H013

As can be seen from **Figure 8-17** and **Figure 8-18** the sediment load of the upper steep river reach (West – Portal and Driefontein gauging weir (G1H004)) is relatively low and most of the samples had to be neglected because of a sediment load less than 1 g/s. This may be due to the fact that this river reach has a cobble bed; therefore sediment cannot be entrained from the riverbed. Precipitation that occurred in the 2003 wet season was insufficient to cause floods that are capable to entrain the larger particles that form part of the cobble bed in the upper reach. This also contributed to the lack of samples that could be used to obtain a representative regression formula for the sample site in the upper reach (Portal and Driefontein gauging weir (G1H004)). The relatively steep bed slope of the upper reach causes flood peaks to be short in duration. Since the samples were only taken twice a day, during the morning and late afternoon, many of these floods were missed. An ideal scenario would be to take sediment samples in short intervals, say 15 minutes, during a couple of large flood covering the entire hydrograph. These samples could have also assisted in determining whether significant differences exist between the sediment transport rate of the rising and falling leg of the hydrograph (**Figure 8-28** to **Figure 8-32**). **Figure 8-17** to **Figure 8-22** were also used to aid in the sediment calibration of the mathematical model (**CHAPTER 9**).

Figure 8-23 to Figure 8-27 show the sediment load – discharge rating curves with the data for both 2003 and 2004. From **Figure 8-23** it is clear that a wide spread exists between the data from the different years. This is due to variations in precipitation and sediment availability in the subcatchments. Therefore Rooseboom (1992) suggested that sediment samples be taken over a period of at least 3 years in order to get a proper, reliable sediment yield. At the rest of the sample stations the differences are visibly less. At G1H036 (**Figure 8-26**) and G1H013 (**Figure 8-27**), virtually no difference can be observed. From these figures it can be concluded that the sediment yields that were calculated using only the data from 2003 are representative of the mean sediment yield over time at the various locations along the river. It has to be borne in mind that no samples were taken during larger floods. The larger floods are responsible for the bulk of the sediment transport, therefore the calculated sediment yields might be lower than actual values.

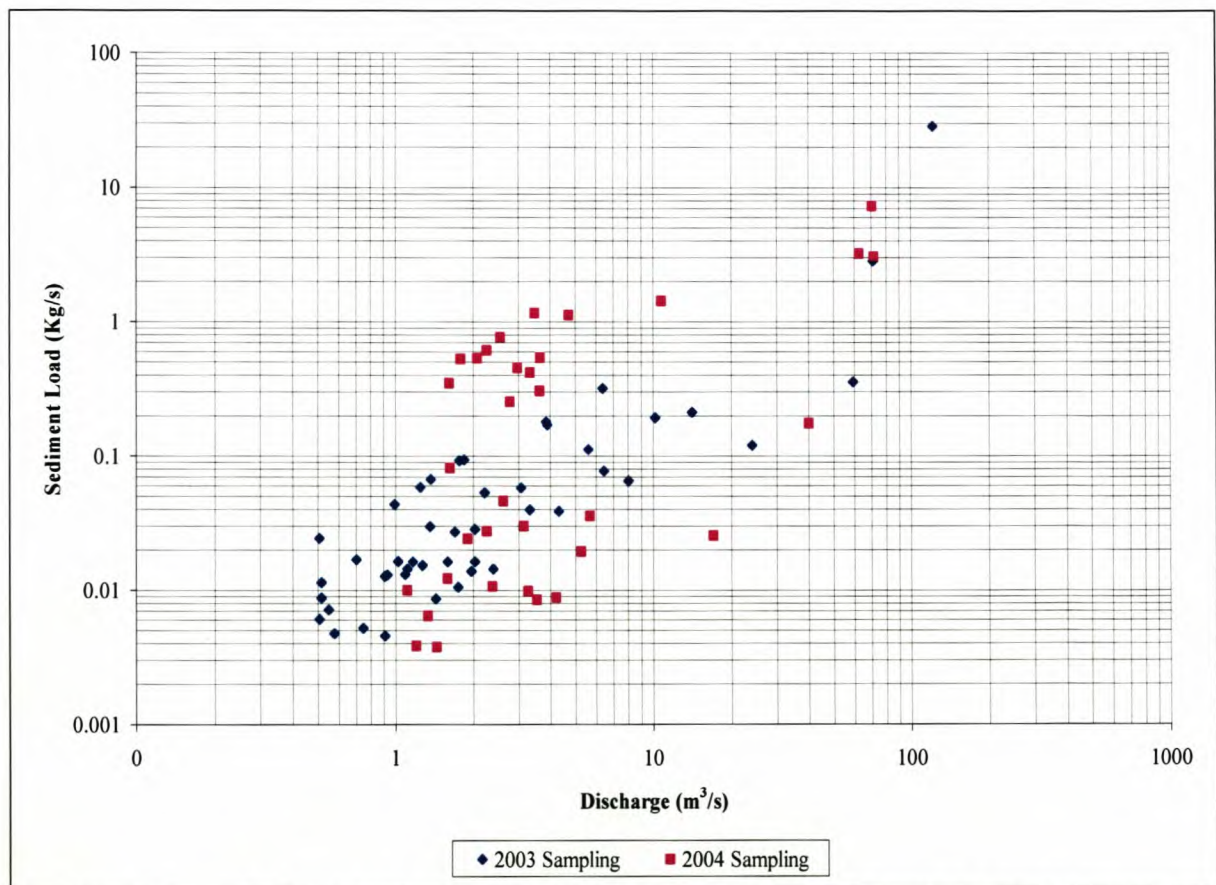


Figure 8-23 Sediment load – discharge relationship at Driefontein (G1H004) for 2003 and 2004

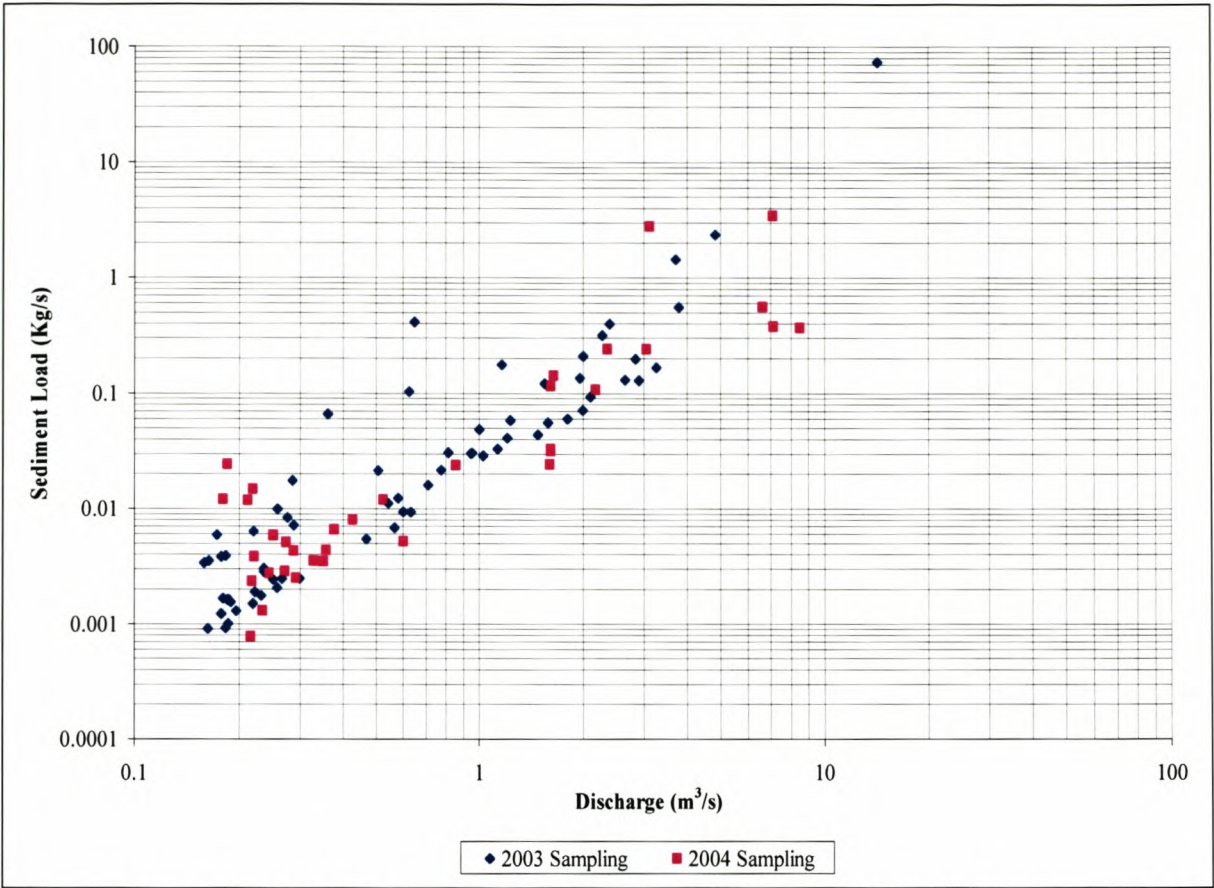


Figure 8-24 Sediment load – discharge rating curve at Franschhoek River (G1H003) for 2003 and 2004

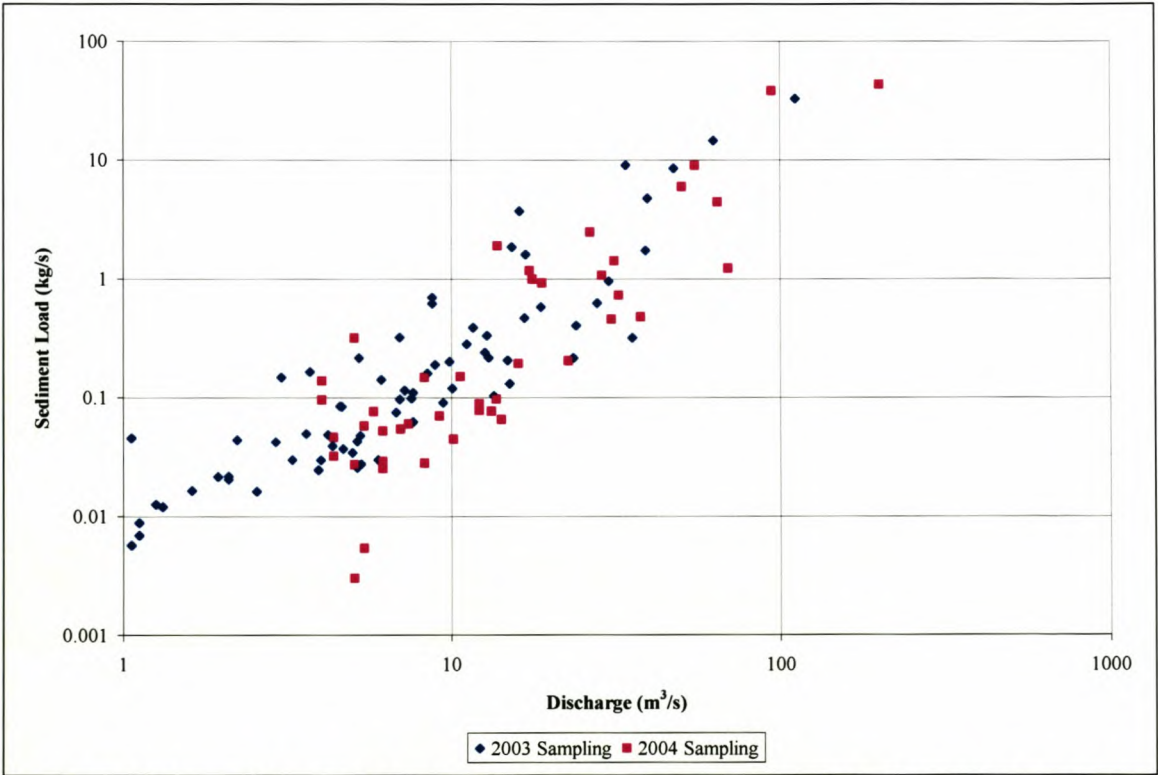


Figure 8-25 Sediment load – discharge rating curve at Paarl (G1H020) for 2003 and 2004

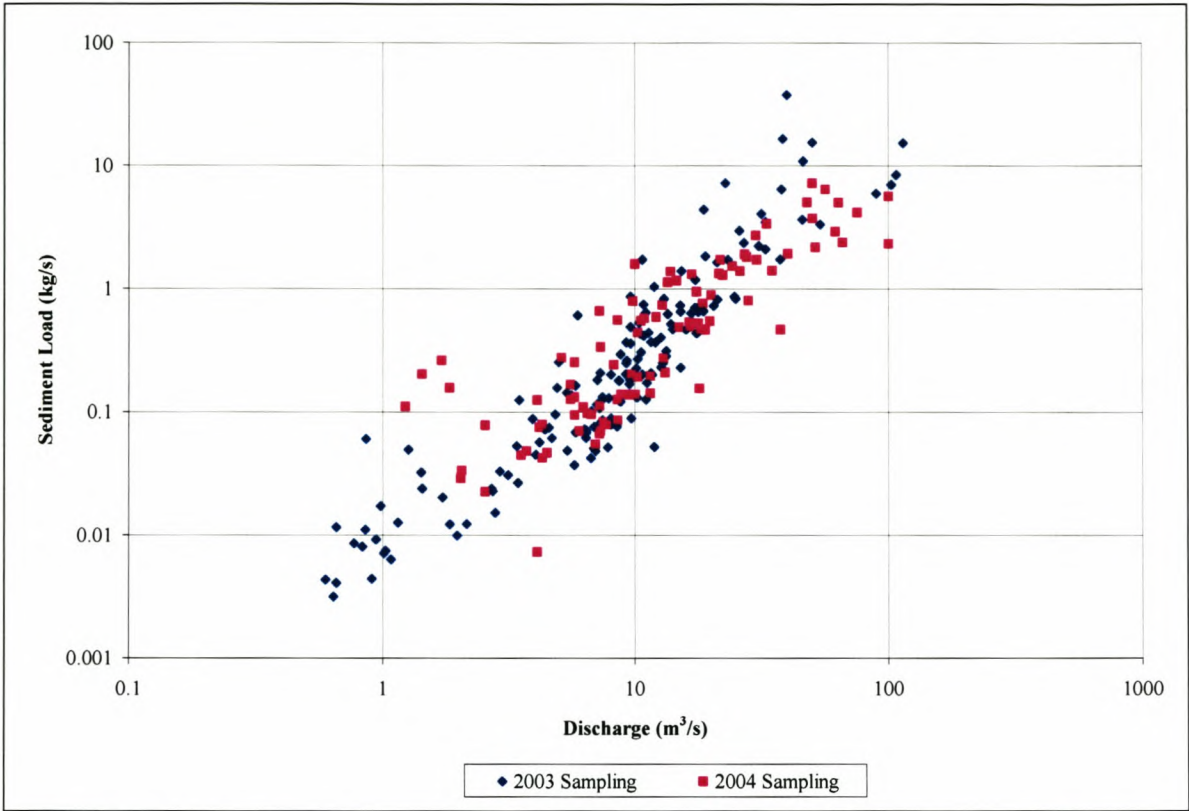


Figure 8-26 Sediment load – discharge rating curve at Hermon (G1H036) for 2003 and 2004

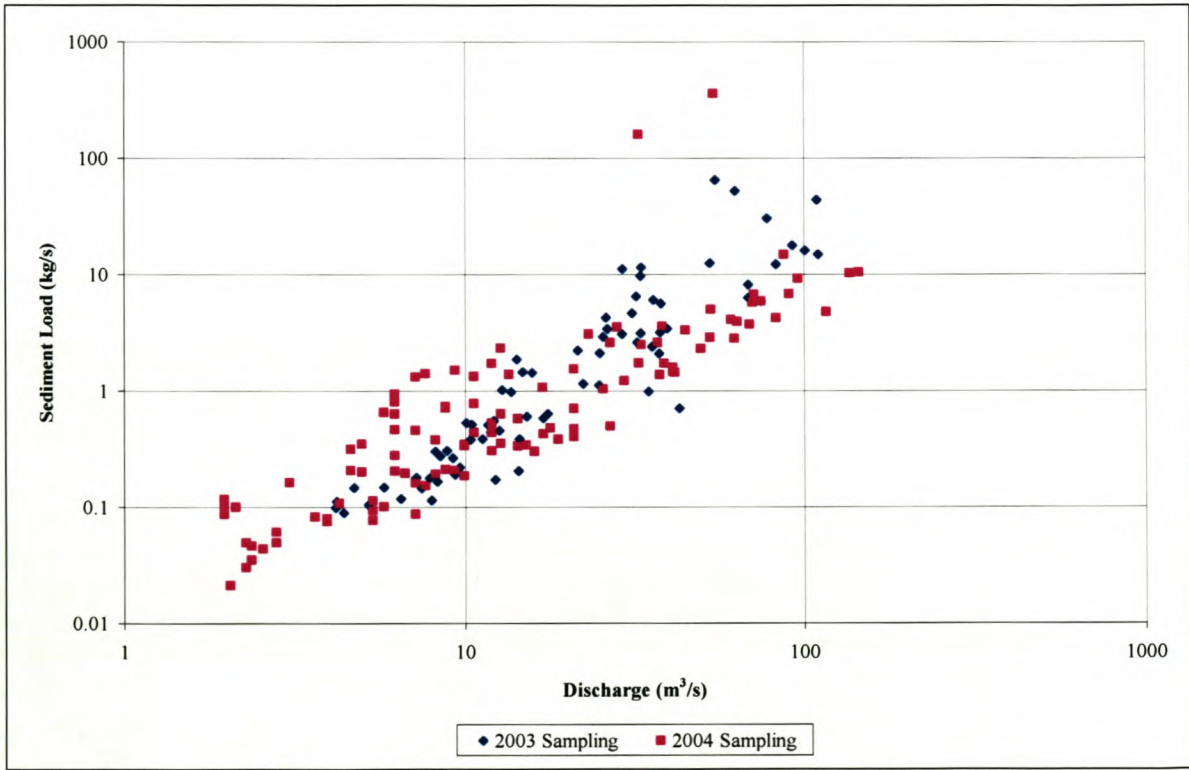


Figure 8-27 Sediment load – discharge rating curve at Drieheuwels (G1H013) for 2003 and 2004

Figure 8-28 to **Figure 8-32** show the difference in the sediment loads between the rising and falling leg of the hydrograph as it progresses down the river. It is evident from these figures that no real difference in sediment load can be observed between the rising and falling leg. This may be due to a lack of continuous long term data. Again continuous data of at least 3 to 5 years should be used in order to determine the influence of the rising and falling effect on the sediment load in the river. This data should also include summer and winter sediment loads.

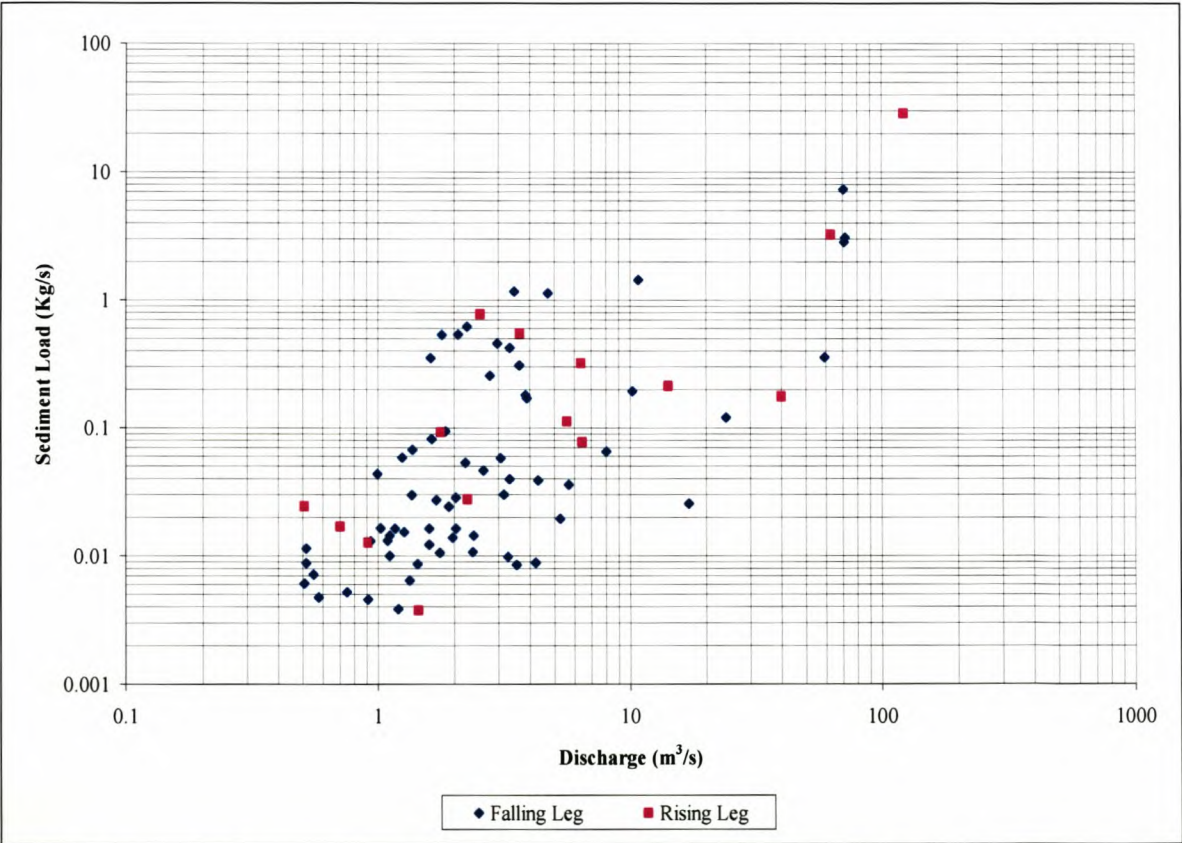


Figure 8-28 **Difference in sediment loads on the rising and falling leg of the Hydrograph – G1H004**

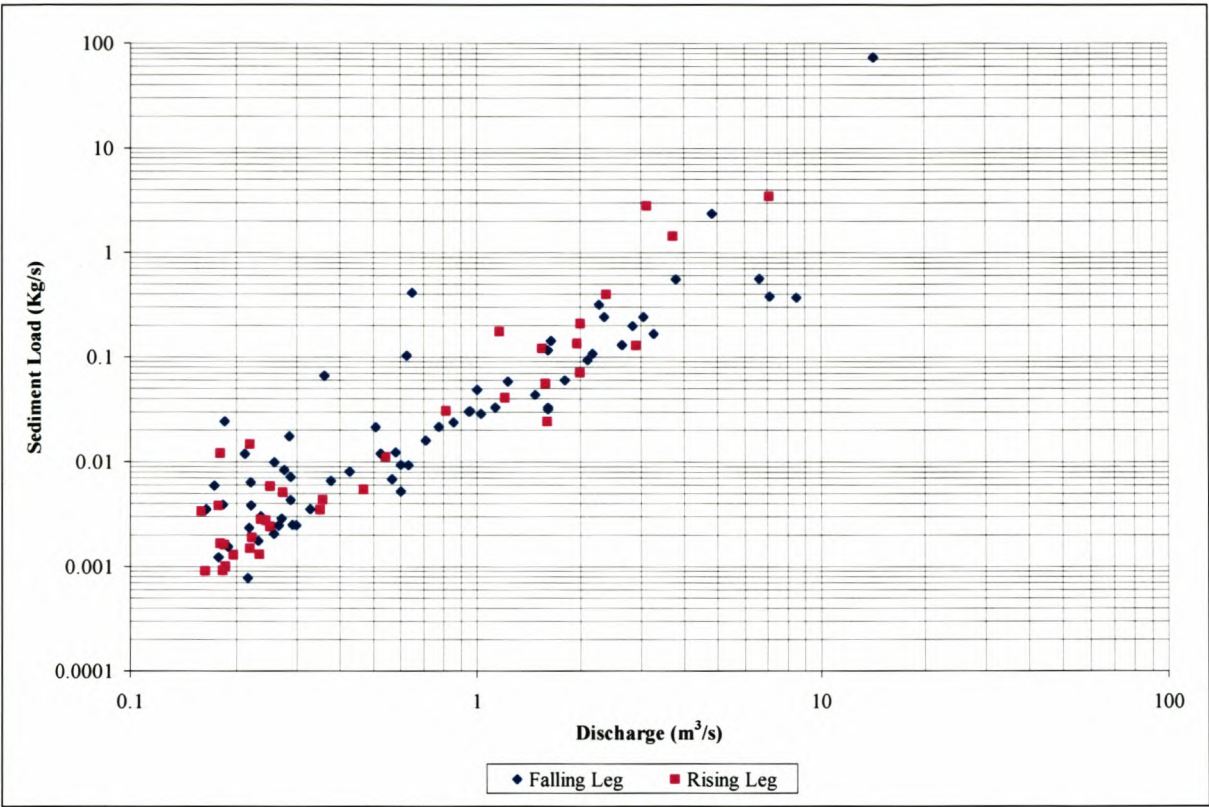


Figure 8-29 Difference in sediment loads on the rising and falling leg of the Hydrograph – G1H003

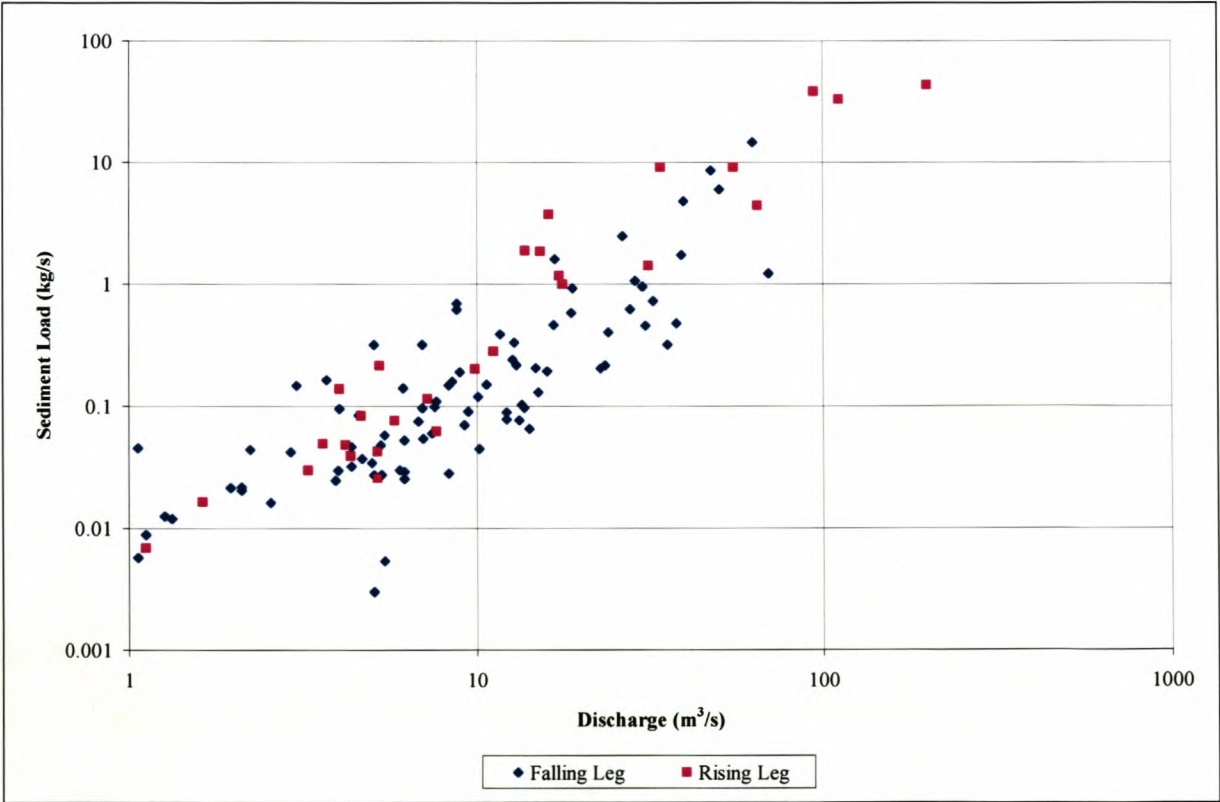


Figure 8-30 Difference in sediment loads on the rising and falling leg of the Hydrograph – G1H020

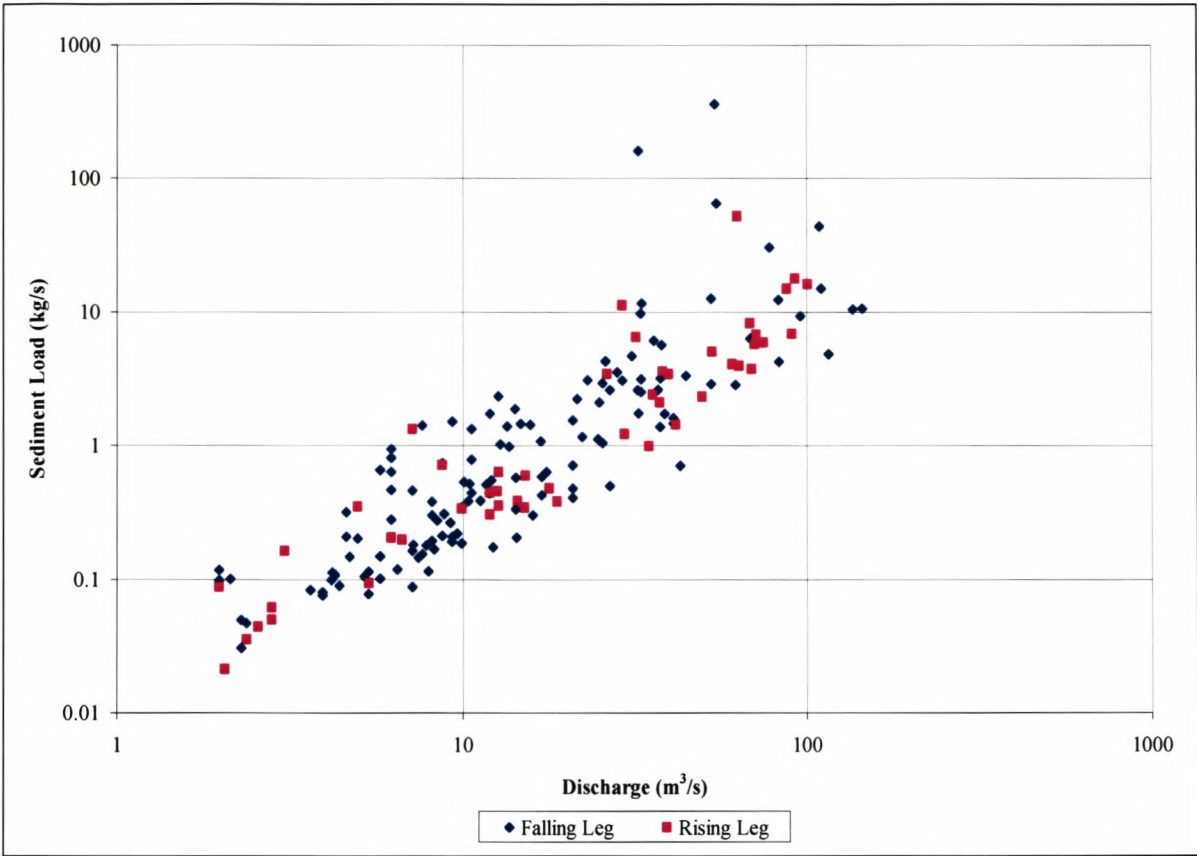


Figure 8-31 **Difference in sediment loads on the rising and falling leg of the Hydrograph – G1H036**

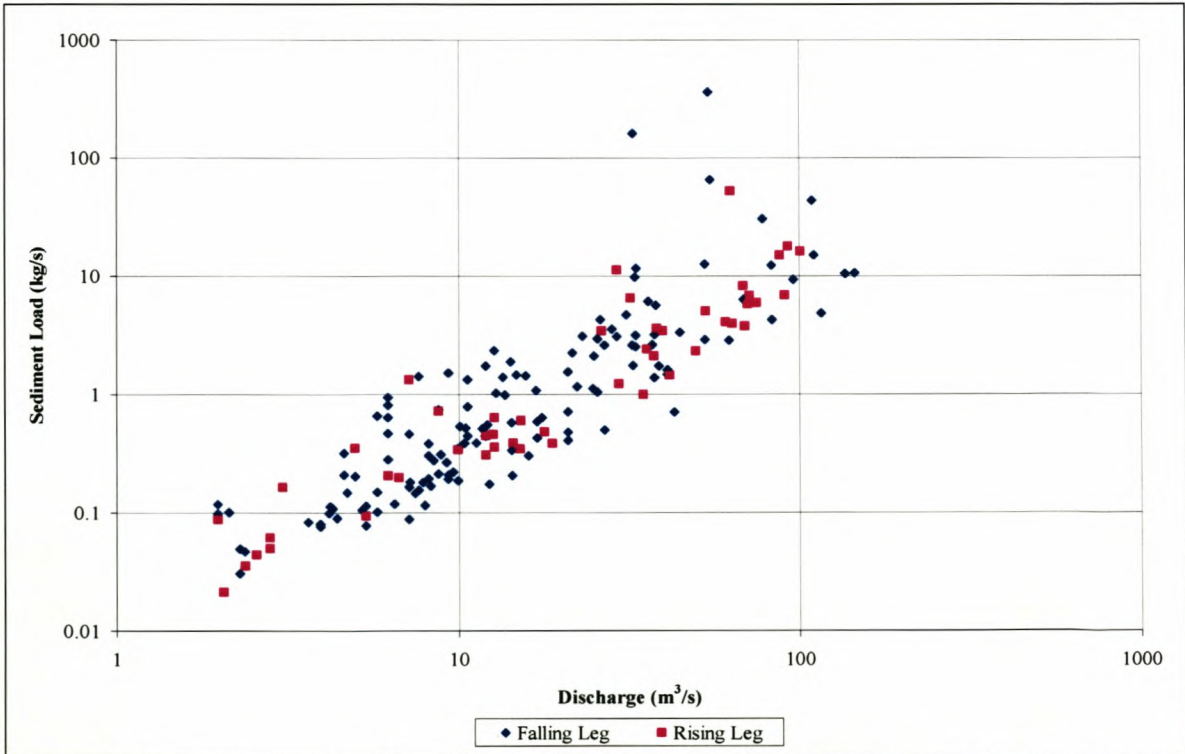


Figure 8-32 **Difference in sediment loads on the rising and falling leg of the Hydrograph – G1H013**

From **Figure 8-30** it is evident that the sediment load at G1H020 of the discharge on the rising leg of the hydrograph seems to be somewhat higher compared to the same discharge on the falling leg. It has to be borne in mind that the gauging weir at Paarl (G1H020) gives unreliable data due to damming caused by a bridge just downstream of the weir. Furthermore, not enough samples were taken to draw reliable conclusions with regards to differences between the sediment loads of the rising and falling leg of a hydrograph. Therefore it is believed that there is insufficient evidence to support a significant difference between the sediment loads of the rising and falling leg of the hydrograph.

Suspended sediment sampling was done at the locations depicted in **Table 8-7** along the Berg River System; the sediment yield is also shown as calculated from the sediment rating curves.

The time series of the sediment inflow at each tributary had to be scaled to account for sediment availability in the various catchments, **Figure 8-33** shows how the scaling was done. Each time series was scaled so that the sediment yield for a specific tributary equalled the mean of the sediment yields that was determined by using the sediment sampling in that area. For example all the tributaries between G1H004 and G1H020 was scaled to 30 ton/km².a, this is the mean value of the calculated sediment yields for G1H004, G1H003 and G1H020.

Table 8-7 **Location of sediment samples and calculated sediment yields**

Location	River	Sediment Yield [ton/km ² .a]	
		Calculated for 1989 - 2002	Calculated for 2003*
Wes Portal, downstream of the tunnel outlet	Berg	No Discharge data	38
Gauging station G1H004	Berg	38	21
Gauging station G1H003	Franschhoek	99	59
Gauging station G1H020	Berg	49	9
Gauging station G1H036	Berg	28	5
Gauging station G1H013	Berg	62	6

* Discharge data only available from April 2003 to October 2003

As the Berg River flows past Paarl it flattens out to a much milder bed slope. The steepness of the riverbed influences the river’s ability to entrain sediment particles; therefore the reduction that can be observed in **Table 8-7** in the sediment yield could partly be explained by

that. During the 2003 rain season the Swartland (Malmesbury, Moorreesburg and Piketberg) area had very little precipitation which caused most of the tributaries to experience a reduction in flow which in turn caused a reduction in the sediment volumes that are transported to the Berg River via the tributaries. This may explain the sudden reduction in the sediment yield that was calculated for G1H020, G1H036 and G1H013 from the sediment samples for 2003(**Table 8-7**).

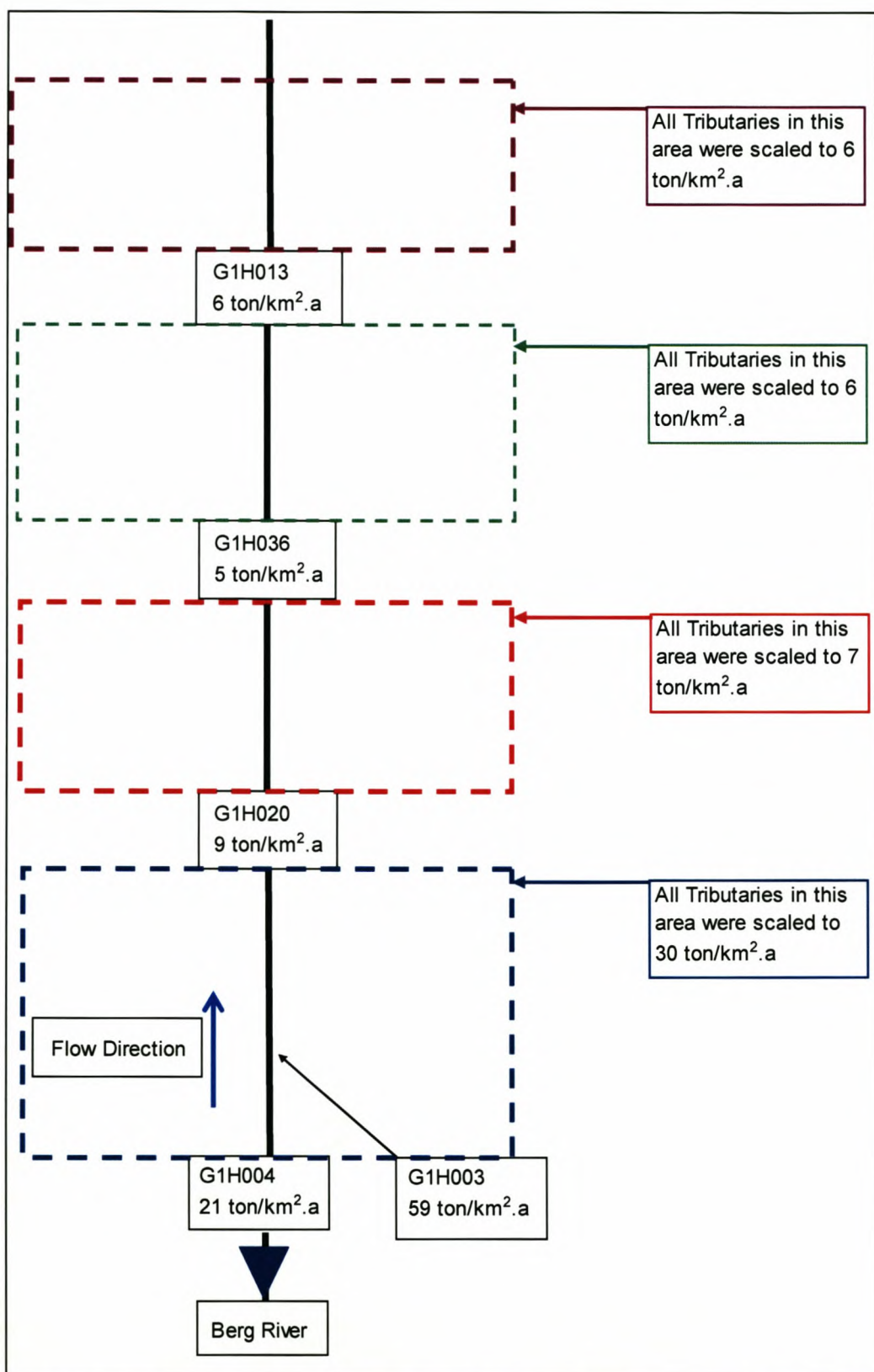


Figure 8-33 Sediment yields for the various catchments along the Berg River System

In order to obtain the total sediment load Rooseboom (1992) proposed that a further 25% should be added to the suspended sediment samples to account for bed load transport in South

African rivers. Therefore 25% was added to the time series that was determined as described above.

Measuring bedload transport in coarse – grained channels can be particularly difficult because flows necessary for transporting larger particles are usually deep, turbid and turbulent, making it difficult to directly measure particle movement. A limited amount of bedload sampling was carried out to try and verify the 25% that was added to account for the bed load transport. The sampling was done under flood conditions, once in 2003 at the gauging station (G1H003) on the Franschhoek River and on the Berg River sampling was done upstream of west – portal tunnel outlet. Samples were also taken at the gauging station (G1H003) on the Franschhoek River in 2004 to serve as verification data. The sampling was done in conjunction with suspended sediment sampling in order to determine the ratio of bed load vs. total load.

Bed - load movement can be highly variable in coarse – grained systems, both spatially and temporally. Spatially, transport often occurs in zones, the position of which is unpredictable and does not always correspond with the highest velocity or shear stress (Ryan & Troendle, 1997). Temporally, transport has been associated with the movement of bedforms, clusters, sheets, or pulses, which are often independent of variations in discharge (Ryan & Troendle, 1997). Quantification of the mean transport rates require procedures that account for the erratic nature of bed - load movement. Sufficient samples from different positions in the channel are needed for a representative spatial measure. The total sample period must be long enough to measure a suitable temporal average.

Bed load sampling was carried out with a US-BLH 84 sampler (**Figure 8-35**), developed by the Federal Interagency Sedimentation Project, at regular intervals across the river (**Figure 8-34**). Ryan and Troendle (1997) suggested a bag with mesh opening of 0.25mm be used to catch the samples. Bags with finer mesh restrict flow and clog faster, reducing the trapping efficiency of the sampler, those with larger openings clog less but finer particles may be lost through the openings. The sampling duration was 10min and the samples were later dried and weighed to obtain a sediment load.



Figure 8-34 **Bed load Sampling upstream of West – portal tunnel outlet**



Figure 8-35 **US – BLH 84 bedload sampler**

Table 8-8 Bed load sampling in 2003

Location	Discharge (m ³ /s)	Distance from left Bank[m]	Suspended load [g/s]	Bed load [g/s]	Ratio ⁽¹⁾
Berg	14.56	5	67	0.0002	0.0025
	14.66	11	111	0.0004	0.0035
	14.72	14.2	222	0.0005	0.0023
	14.96	17.5	152	0.0001	0.0008
	14.93	19.5	113	0.0008	0.0069
Franschhoek	2.596	1	160	0.0373	0.0233
	2.590	3	144	0.0332	0.0230
	2.587	5	139	0.0648	0.0466
	2.584	7	287	0.2177	0.0758
	2.584	9	181	0.0162	0.0089
	2.567	11	155	0.0062	0.0041

(1) The ratio of Bedload to Suspended load expressed as a percentage.

Table 8-9 Bed load sampling in 2004

Location	Discharge (m ³ /s)	Distance from left Bank[m]	Suspended load [g/s]	Bed load [g/s]	Ratio
Franschhoek	0.686	Centre	66	0.0021	0.0032
	0.686	Centre	61	0.0015	0.0024
	0.741	Centre	68	0.0043	0.0064
	0.741	Centre	70	0.0044	0.0062
	0.799	Centre	68	0.0054	0.0079
	0.92	Centre	134	0.0032	0.0023
	0.92	Centre	117	0.0083	0.0071
	0.92	Centre	155	0.0101	0.0065

From **Table 8-8** and **Table 8-9** it is evident that the 25% that was added according to Rooseboom (1992) to account for the bed load transport may be higher than the actual values. However it was decided not to lower the percentage of bed load transport due to the fact that the two sets of samples that were taken in relatively small floods (smaller than 20 m³/s) are insufficient to base such a change on. It should also be borne in mind that this factor also accounts for the non – uniformity in the suspended sediment transport across the river.

8.2.4.2 Sediment particle size distribution

Bed samples were taken during Jan 2003 at the Berg River Monitoring sites (**Table 8-13**) and a sieve analysis was performed on each sample to determine the grading of the bed material along the Berg River. Samples were only taken to represent the sand fraction in the bed. This was done in order to be able to determine a sediment distribution that will be transported. **Table 8-10** shows the d₅₀ that was obtained from the sieve analysis on the sand samples.

Table 8-10 The d_{50} of the bed samples that was taken in the Berg River

Site 1 d_{50} [mm]	Site 2 d_{50} [mm]	Site 3 d_{50} [mm]	Site 4 d_{50} [mm]	Site 5 d_{50} [mm]	Site 6 d_{50} [mm]
1	0.51	0.70	0.58	0.38	0.31
0.38	0.29	0.43	0.75	0.60	0.39
0.49	0.49	0.45	0.22	0.36	0.44
0.40	0.39	0.49	0.38	0.51	0.39

It can be seen from **Table 8-10** that most of the d_{50} 's are in the order of 0.5mm in magnitude. It was therefore decided that the sediment particle size that represents the sand fraction in the bed should be specified as 0.5 mm (**Table 8-11**). The finer particles such as the clay and silt particles will be transported through the system with a small degree of deposition in flat areas. In order to account for these particles a smaller fraction has to be specified. It was decided that 0.03 mm be used. An ideal way to determine exactly what diameter will be representative of the finer fraction is to do a sieve analysis on the suspended sediment loads. If all the sediment from the suspended load for a particular sample area is put together a sieve analysis can be preformed to obtain a better indication in regards to the size of the smaller fraction. The samples that were taken during 2003 were however insufficient in weight to do such an analysis.

Table 8-11 Particle size distribution

Fraction 1 = 0.5mm	Fraction 2 = 0.03mm
40%	60%

The distribution that was chosen makes provision for both the bigger size particles and for the smaller particles that will be transported in higher quantities, due to the fact that they are easier to entrain (lower settling velocity).

The sediment transport model also requires that the composition of the active and passive layers (see **Figure 8-1**) be given (**Table 8-12**). These percentages are only initial values and will be altered by the program as the simulation continues. They can be specified to serve as global values that are applicable to the whole river or as local values which only apply to a specific river section. The values in **Table 8-12** are the global values, no local values were specified.

Table 8-12 Composition of active and passive layers

Fraction	Percentage in active layer	Percentage in passive layer
1 = 0.5 mm	95	95
2 = 0.03 mm	5	5

The smaller fraction will be in transportation most of the time due to the small shear stress required to entrain these particles, therefore only limited amounts will form part of the bed composition. If any deposition occurs in flat areas it will be entrained during the next significant discharge. It was therefore decided that as an initial value the smaller fraction represents only 5% of the bed material. This percentage determines the amount of initial scouring that can take place. Thus if a bigger percentage is specified more material, that can be easily entrained, are available to be transported and vice versa.

8.2.5 Bed roughness coefficients

The Berg River Baseline Monitoring study has identified six sites along the Berg River at which the monitoring of various parameters such as sediment concentration, biannual bed level surveys and habitat mapping occurred. The location of these sites in the numerical model is illustrated in **Table 8-13**.

Table 8-13 BRM site location

BRM site	Chainage [m]
1	Not included in the model, just upstream of G1H004
2	4 000
3	23 500
4	72 500
5	121 800
6	141 000

Water levels during flood events in 2003 and 2004 were also registered at these sites specifically to aid in the determination of the bed roughness coefficients along the river.

Three sets of Perspex pipes (two pipes in each set) were installed over roughly 100 m at each site, as illustrated in **Figure 8-38**.

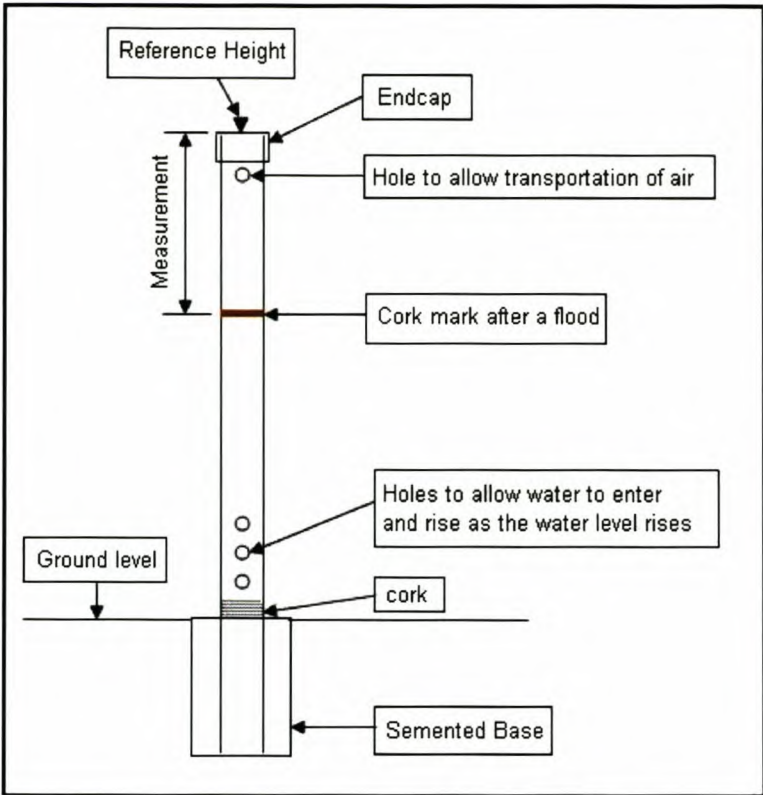


Figure 8-36 Schematic representation of the Perspex pipes



Figure 8-37 Perspex pipes installed to register water levels during floods

Figure 8-36 shows a schematic representation of the Perspex pipes that was installed at each site. As the water level in the river changes water will either enter or exit through the holes in the bottom of the pipe. During a flood the graded cork will rise with the water level inside the pipe and leave a mark at the maximum water level for that particular flood (**Figure 8-36**). The end – caps of the pipes were surveyed to obtain a reference height in global coordinates. The measurement that was taken after each flood was subtracted from the reference height to obtain the maximum water level in global coordinates. The cork mark was flushed down after the measurement to avoid confusion between different flood marks.

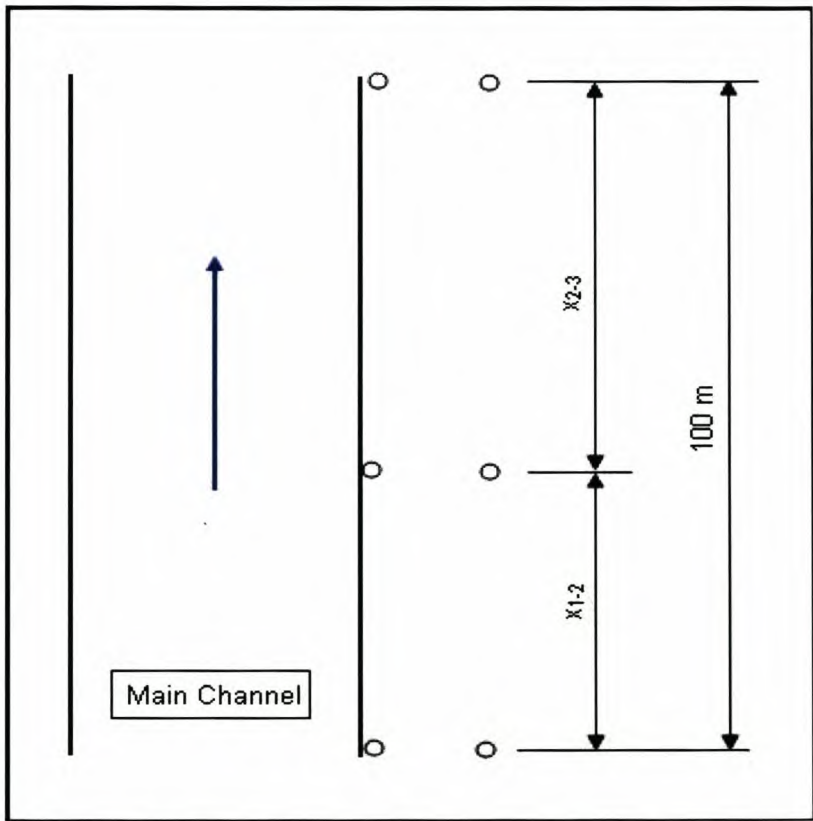


Figure 8-38 Plan view of Perspex pipe layout at each site

The wave action as a flood progresses down the river may cause water depths to differ for the same discharge on the rising and falling leg of a hydrograph (**Figure 8-39**). A simulation was carried out using MIKE 11 to ascertain whether this is the case at BRM site 1. The cross – sections that were surveyed during the biannual bed level survey by the Berg River Monitoring Study were used as input into MIKE 11. Heights that were measured, during a flood event in August 2003, at the gauging weir (G1H004 – A02) just downstream of BRM Site 1 were used as an upstream boundary condition for the purpose of the simulation.

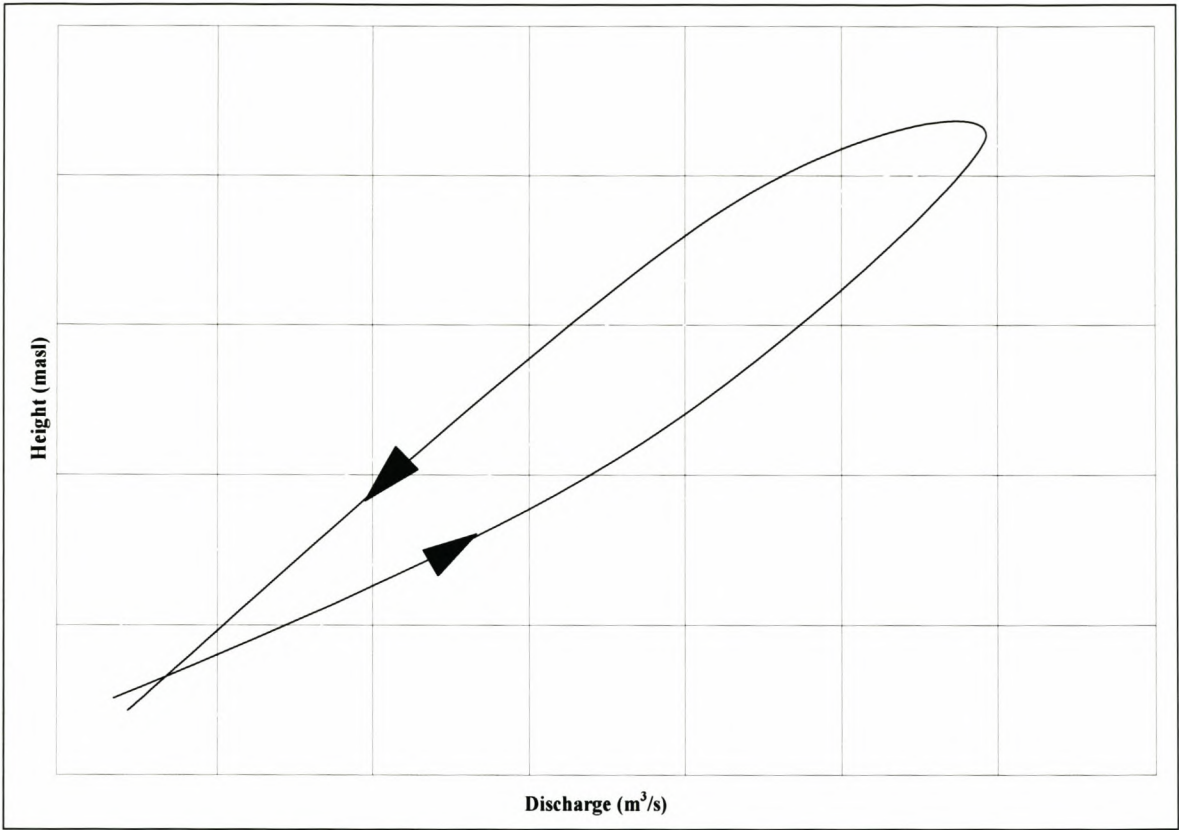


Figure 8-39 Loop effect as a hydrograph passes a specific location

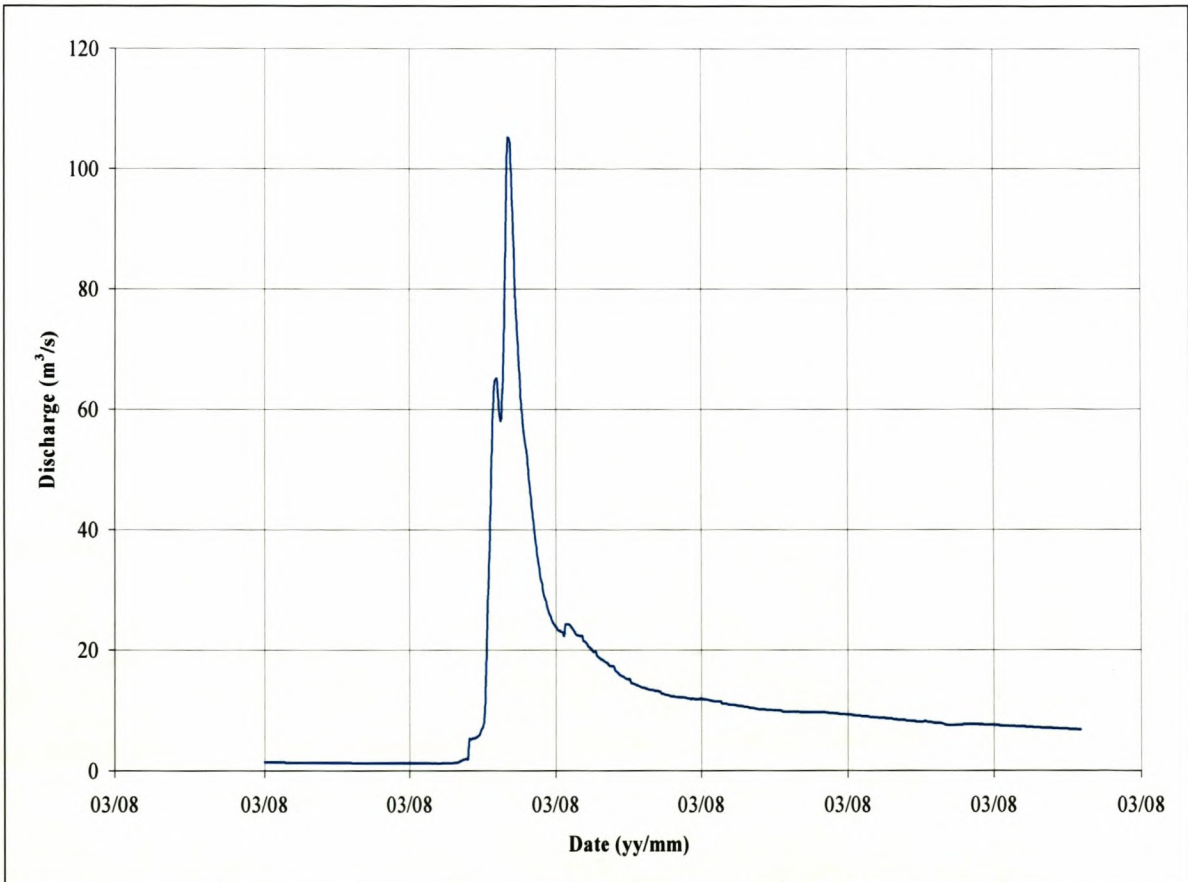


Figure 8-40 Hydrograph that was used to verify loop effect

Figure 8-41 shows the result of the simulation. From this figure it can be seen that no significant difference exists between the water depth for the same discharge on the rising and falling leg of the hydrograph. Therefore this phenomenon does not have any influence on the cork marks that were recorded during the winters of 2003 and 2004.

These water levels together with the distances as illustrated in **Figure 8-38** were used to determine a water slope for the different floods. A backwater program CFP, developed by Ninham Shand, was used to determine the n – value for each flood that corresponds with the measured water levels. A setup as illustrated in **Figure 8-42** was done for each site in order to achieve this. The bed slope and cross - sections were obtained from the biannual surveys that were carried out for the Berg River baseline monitoring study in 2003.

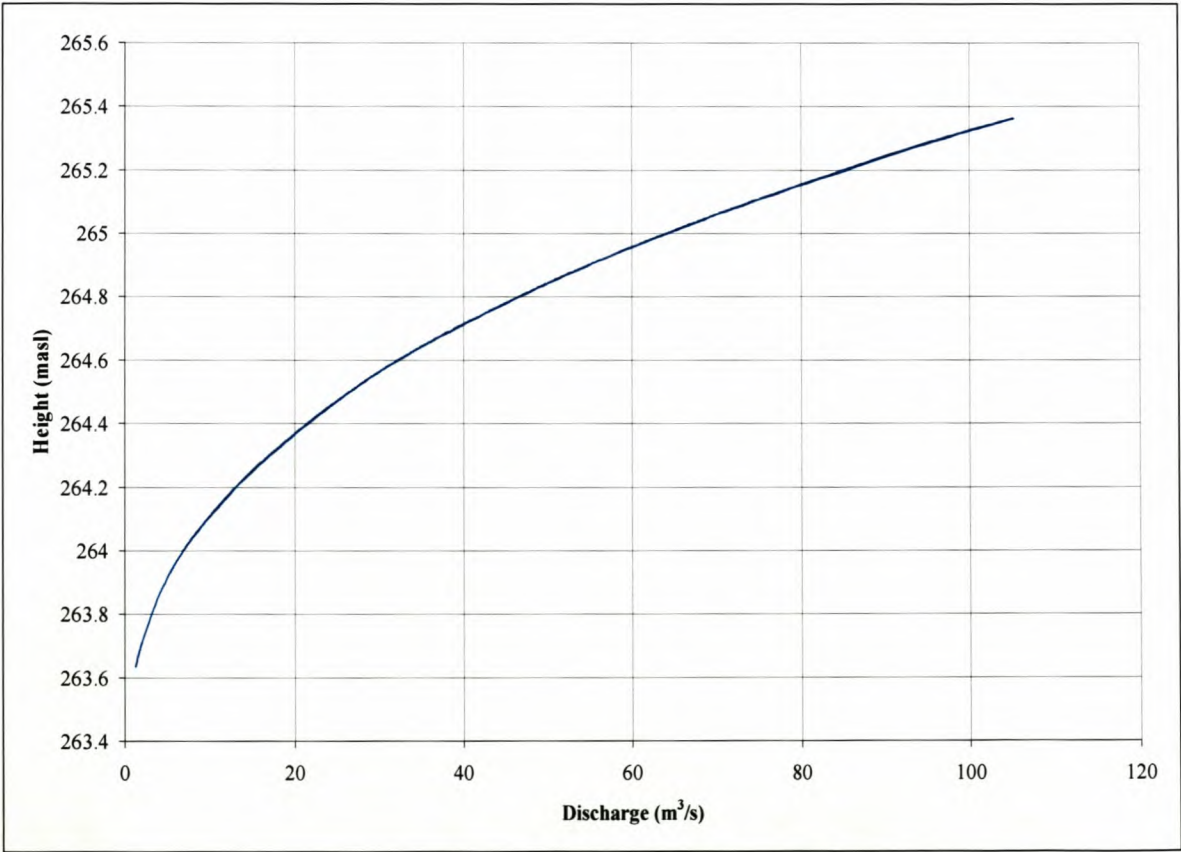


Figure 8-41 Height – discharge relationship at BRM Site 1

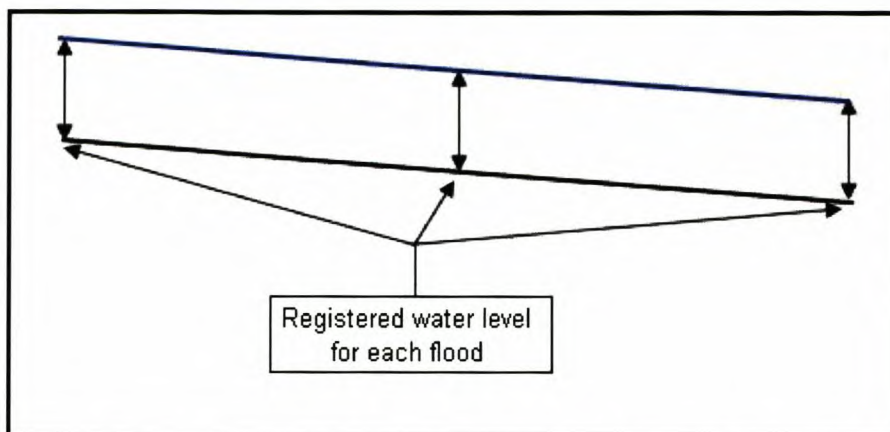


Figure 8-42 Longitudinal profile of the CFP setup for a site

The results of process that was described above is presented in **Table 8-14**

Table 8-14 Manning's n – values for the BRM sites

	Flood Peak [m^3/s]	Date	Manning's n – value
BRM Site 1	13.6	6 August 2003	0.095
	14.6	22 July 2003	0.095
	24.4	12 August 2003	0.09
	38.2	7 October 2003	0.09
	101.9	5 September 2003	0.08
	105.2	23 August 2003	0.07
BRM Site 2	17.3	6 August 2003	0.055
	19.2	22 July 2003	0.055
	28.1	12 August 2003	0.05
	179.4	5 September 2003	0.04
	184.6	23 August 2003	0.04
BRM Site 3	38.1	12 August 2003	0.03
	58.4	7 October 2003	0.035
	109.7	5 September 2003	0.045
	113.1	23 August 2003	0.045
BRM Site 4	9.7	6 August 2003	0.03
	13.5	22 July 2003	0.05
	40.3	12 August 2003	0.08
	41.3	7 October 2003	0.08
BRM Site 5	12.6	6 August 2003	0.04
	37.5	12 August 2003	0.04
	39.7	7 October 2003	0.04
	78.0	23 August 2003	0.055
	115.0	5 September 2003	0.065
BRM Site 6	12.6	6 August 2003	0.04
	37.5	12 August 2003	0.04
	39.7	7 October 2003	0.04
	78.0	23 August 2003	0.04
	115.0	5 September 2003	0.04

The discharges were obtained from the data provided by DWAF for the closest gauging weir to the BRM site. The discharge for BRM site 5 (G1H013) was also used for BRM site 6 as there is no gauging weir close to this site. The discharge data recorded by Misverstand Dam should have been used, but this data is known to be unreliable.

A new water level gauge was installed by DWAF in May 2003 at a weir, now known as G1H004 – A2, just downstream of BRM site 1. This weir together with sections upstream and downstream were surveyed in order to obtain a discharge table. This table was used to calculate the discharge at BRM site 1. All the calculations involving the generation of the discharge table as well the survey information can be seen in **APPENDIX C**

From **Table 8-14** it can be seen that the roughness values at small discharges that was obtained for BRM site 1 and 2 are higher than those that was obtained for the larger floods. In this case the water has to flow around most of the cobbles and boulders on the riverbed because the water level is lower than the exposure height of the cobbles and boulders. As the water level rises in the event of a bigger flood the resistance is reduced because the water level is high enough to flow over the cobbles and boulders. In the event of larger flows at BRM Site 4 the roughness coefficient rises more dramatically compared to the other sites (values indicated in bold). This is due to the extremely narrow main channel and dense vegetation on the flood plains. A small discharge will cause inundation of the flood plains. The dense vegetation and large trees give more resistance to flow compared to the other sites which causes the sudden increase in roughness coefficient. No difference in the resistance at BRM site 6 could be observed from a low discharge to a higher discharge (**Table 8-14**). This is due to the relatively small bed slope that causes little change in the water level slope for different discharges.

Table 8-15 Initial roughness coefficients used in the one dimensional model

		Manning’s n – value	
		Main Channel	Floodplain
Upper Section	Km 2.2 – Km 24 (cobble bed)	0.07	0.055
	Km 24 – Km 70 (sand bed)	0.045	0.055
Lower Section	Km 70 – Km 188.4	0.045	0.055

Table 8-15 shows the initial roughness coefficients that were used in the one dimensional model. The same values were used for the simulation of all the scenarios. The floodplain is defined as above the level of divide that was specified for the cross – sections. This means that a value of 0.055 was used as a roughness coefficient when, at the given section, the water level rises to a level higher than the level of the divide that was specified for that particular cross – section.

The values in **Table 8-15** were changed during the hydrodynamic calibration process. The bed roughness is one of the aspects that will determine the lag of a flood at various points along the river. The initial values were therefore changed in order to achieve the correct lag time at the gauging stations on the Berg River that were used during the hydrodynamic calibration. These values will be discussed in **CHAPTER 9**.

8.2.6 Incipient motion of coarse materials

8.2.6.1 Basic Theory

The initiation of movement of individual sediment particles is dependent on a variety of factors; both deterministic and random (**Figure 8-43**).

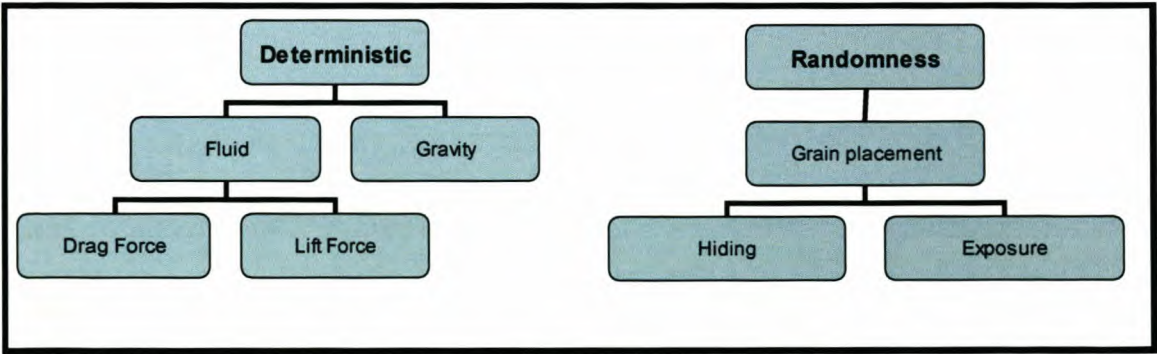


Figure 8-43 Factors influencing initiation of movement

A close inspection of an erodible bed would reveal that some particles were more exposed than others. The various forces that act on such a particle under flow conditions are shown in **Figure 8-43**.

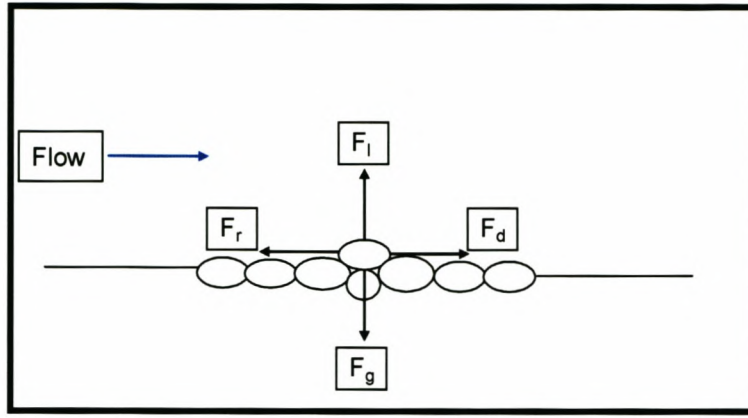


Figure 8-44 Forces acting on an exposed particle

Assuming that u_f represents the velocity, the forces may be defined as follows:

$$F_d = C_d \frac{\rho \pi D^2 u_f^2}{8} \quad \text{Equation 8-50}$$

$$F_l = C_l \frac{\rho \pi D^2 u_f^2}{8} \quad \text{Equation 8-51}$$

$$F_g = \frac{\pi g D^3 (\rho_s - \rho)}{6} \quad \text{Equation 8-52}$$

$$F_r = \mu F_n = \mu (F_g - F_l) \quad \text{Equation 8-53}$$

With:

C_d and C_l	=	Drag and lift coefficients
D	=	Particle diameter (m)
g	=	Acceleration due to gravity (m/s^2)
ρ_s	=	Sediment density (kg/m^3)
ρ	=	Fluid density (kg/m^3)
μ	=	Coulomb friction coefficient (typically in the range 0.8 – 0.9).

8.2.6.2 Shields Diagram

Just before movement of a particle occurs the drag force (F_d) will be balanced by the resistive force (F_r). Shields (1936) first proposed the general relationship based on dimensional analysis. F_d can also be expressed in terms of shear bed stress:

$$F_d \propto \frac{\tau_0 D^2}{A_p} \quad \text{Equation 8-54}$$

with:

$$A_p = \text{area of exposed particles/total area}$$

At the threshold of movement $\tau_0 = \tau_{cr}$, so

$$\tau_{cr} \frac{D^2}{A_p} \propto (\rho_s - \rho)g \frac{\pi D^3}{6} \tan \phi \quad \text{Equation 8-55}$$

with:

$$\phi = \text{the angle of repose.}$$

This can be rearranged to give a dimensional relationship:

$$\frac{\tau_{cr}}{(\rho_s - \rho)gD} \propto \frac{\pi A_p}{6} \tan \phi \quad \text{Equation 8-56}$$

Shields (1936) showed that the particle entrainment was related to some form of Reynolds' Number, based on the friction velocity, u_* . This velocity can be expressed as follows:

$$u_* = \sqrt{gSh} \quad \text{Equation 8-57}$$

and,

$$R_{e_*} = \frac{\rho u_* h}{\mu} \quad \text{Equation 8-58}$$

With:

- h = Water depth (m)
 μ = Absolute viscosity (kg/m s)
 S = Bed slope.

Shields (1936) plotted the results of his experiments and proved that there is a well defined band of results indicating the threshold of motion (**Figure 8-45**).

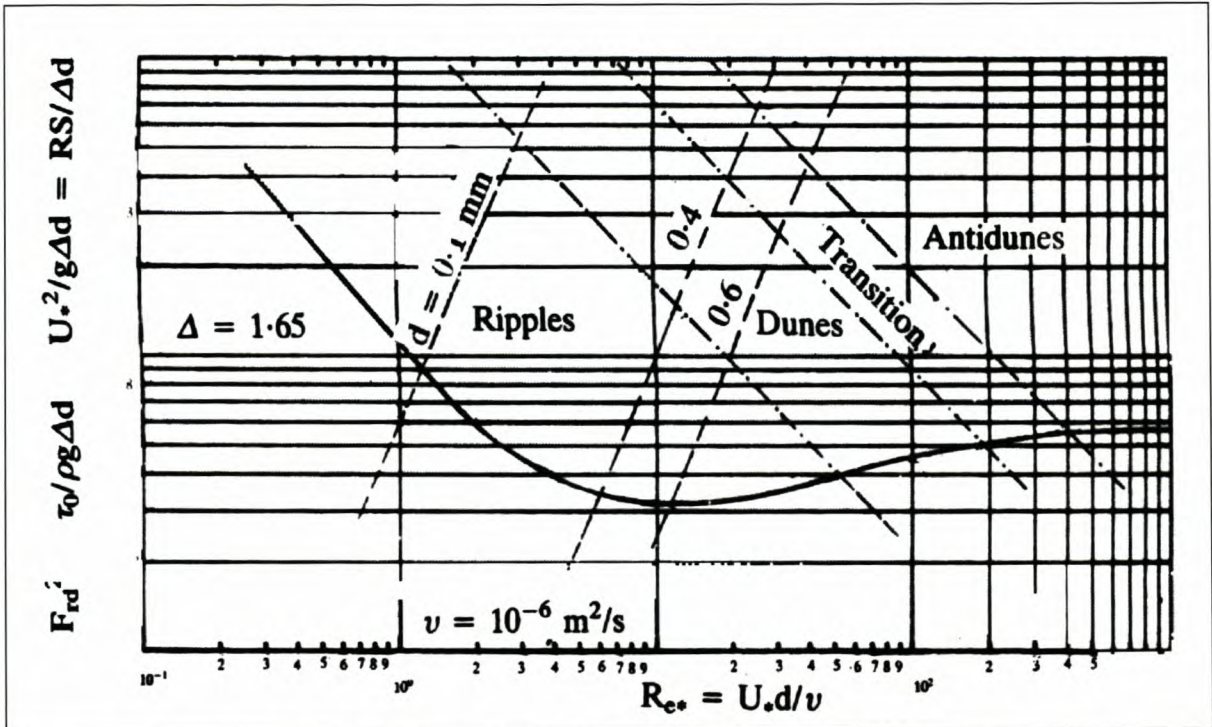


Figure 8-45 Threshold of movement (Shields, 1936)

8.2.6.3 The Liu Diagram

Results obtained by Shields (1936), however, only hold true if uniform sediment particles on relatively flat beds are investigated. No consideration is given to particles of various shapes and sizes as well as hiding and exposure. The main shortcoming is that particle grain size is neither a truly representative nor a unique measure of transportability. The settling velocity of a particle is a more significant measure in the case of non – cohesive materials.

Graf (1971) defined a relationship that describes the settling velocity.

Gravitational force = lift force.

$$\frac{\pi}{6} D^3 (\rho_s - \rho_w) g = C_d \frac{1}{2} \rho_s V_{ss}^2 \frac{\pi}{4} D^2 \quad \text{Equation 8-59}$$

with, C_d = drag coefficient.
 V_{ss} = Settling velocity (m/s).
 D = Particle Diameter (m).
 ρ_s = Sediment density (kg/m³).
 ρ = Water density (kg/m³).

From Equation 8 – 59 the following relationship for the settling velocity can be obtained:

$$V_{ss} = \sqrt{\frac{4gD}{3C_d} \Delta} \quad \text{Equation 8-60}$$

with, $\Delta = \frac{\rho_s - \rho}{\rho}$

The drag coefficient is dependent on the Reynolds number (R_e). Shiller et al. (1933) did experimental work in order to obtain a relationship between the Reynolds number and the drag coefficient. At low Reynolds numbers ($R_e < 800$) this relationship is well defined:

$$C_d = \frac{24}{R_e} (1 + 0.150 R_e^{0.687}) \quad \text{Equation 8-61}$$

At larger Reynolds numbers only qualitative indications can be given. In this range the problem gets extremely complicated because separation of the flow behind the particle starts to occur. Despite all the difficulties Dallavalle (1943) feels that the complete span of the experimental curve can be represented with a fair degree of accuracy by the expression

$$C_d = \frac{24.4}{R_e} + 0.4 \quad \text{Equation 8-62}$$

The settling velocity should also be modified to account for non – spherical particles by multiplying equation 8 – 60 with the following shape factor:

$$SF = \frac{c}{\sqrt{ab}} \quad \text{Equation 8-63}$$

with,

a, b and c = the various axial lengths of the particle under consideration.

The power approach provides us with the ability to define both the transporting capacity of a stream and the effort required to transport in directly comparable terms (Rooseboom, 1992). In rough turbulent flow the unit input stream power applied in maintaining motion along a bed consisting of particles with diameter, d, is proportional to

$$\frac{\rho g S_f h \sqrt{gh S_f}}{d}$$

with,

S_f = the energy slope.

The stream will begin entrainment when the power required to suspend particles becomes less than the power required to maintain the status quo. At this stage

$$(\rho_s - \rho)gV_{ss} \propto \rho g S_f h \frac{\sqrt{gh S_f}}{d} \quad \text{Equation 8-64}$$

Using Equation 8 – 60 for the settling velocity and assuming that C_d , the drag coefficient, is a constant, which is true for larger diameters, then from Equation 8 – 64 the condition of incipient motion under rough turbulent conditions is depicted by

$$\frac{\sqrt{gh S_f}}{V_{ss}} = \text{const.} \quad \text{Equation 8-65}$$

Figure 8-46 shows the threshold of movement that was obtained by Liu through the utilization of the settling velocity of sediment particles and the power approach. This relationship fits measured data as compiled by Yang (1973) very well with the value of the constant = 0.12, for values of

$$\frac{\sqrt{ghS_f}}{\nu} d_{50} > 13$$

With the relatively steep bed slopes in the Berg River are it fair to assume that most, if not all, flow conditions fall in the rough turbulent zone.

In order to use **Figure 8-46** to determine whether movement of a sediment distribution might occur, it is first necessary to determine the median particle size (d_{50}) within the distribution. This particle size is then used to calculate the settling velocity that is used in **Figure 8-46**. The shear velocity (V_*) in **Figure 8-46** is defined as follows:

$$V_* = \sqrt{ghS_f} \quad \text{Equation 8-66}$$

With,

- h = water depth (m)
- S_f = energy slope
- g = acceleration due to gravity (m/s^2)

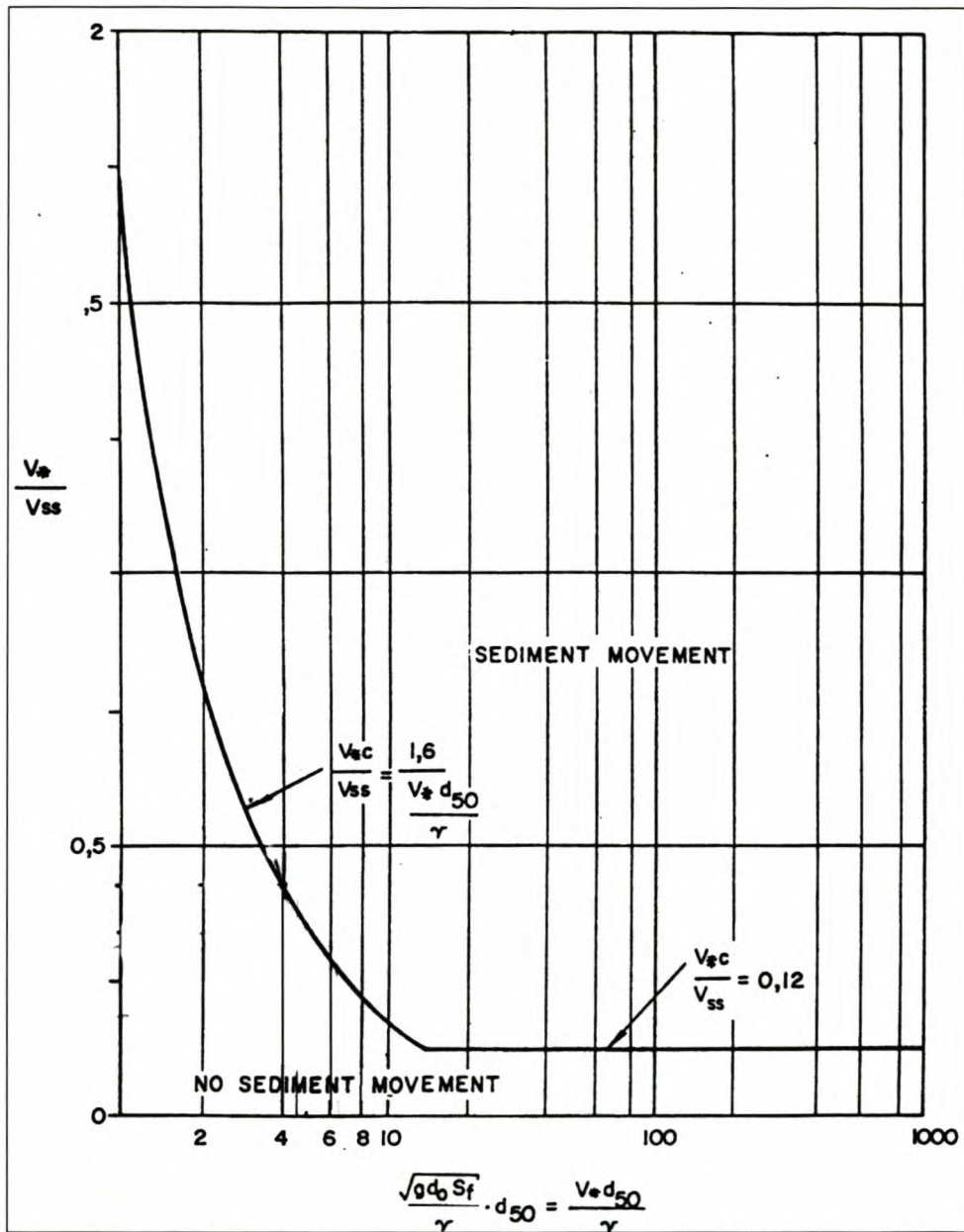


Figure 8-46 Threshold of movement (Liu, 1986)

8.2.6.4 Hiding and Exposure

Liu considered the variation in the shape and size of a sediment distribution, but no consideration was given to the interaction between sediment particles on the bed. In the process of non – uniform sediment movement, the coarse particles on the bed are easier entrained than the uniform sediment of equivalent sizes, because they have higher chance of exposure to the flow. The situation is reversed for the fine particles on the bed due to the fact that they are more likely sheltered by coarse particles. Therefore it is needed to consider the hiding and exposure effect in the modelling of non – uniform sediment transport.

The pioneering research to fractionally calculate the non – uniform bed – material load transport rate was attributed to Einstein (1950). Afterwards, Egiazaroff (1965), Ashida and Michiue (1971), Hayashi et al. (1980), Qin (1980), Parker et al. (1982) and Andrews (1983) developed several formulas to determine the incipient motion of non – uniform sediment mixtures. Until now, most of the studies on non – uniform sediment transport are based on developing some kind of correction factor to account for this hiding and exposure effect. These factors are used to modify the existing formulas of uniform sediment transport. In the method for determining the incipient motion of non – uniform sediment transport developed by Egiazaroff (1965) the correction factors were related to bed – material size by,

$$\eta_i = f_1\left(\frac{d_i}{d_m}; \text{or } \frac{d_i}{d_{50}}\right) \quad \text{Equation 8-67}$$

With,

$$\begin{aligned} d_i &= \text{diameter of the } i^{\text{th}} \text{ fraction (m)} \\ d_m &= \text{arithmetic mean of bed material (m)} \\ d_{50} &= \text{50\% sieve diameter of bed material (m)} \end{aligned}$$

MIKE11 uses an equation similar to Equation 8 – 67 in order to account for the hiding and exposure effect.

The correction factors given in Equation 8 – 67 only involve the non – dimensional grain size and can not effectively account for the influence of bed – material gradation. Wu et al. (2000) developed correction factors that are related to bed – material gradation and the hiding or exposed probabilities.

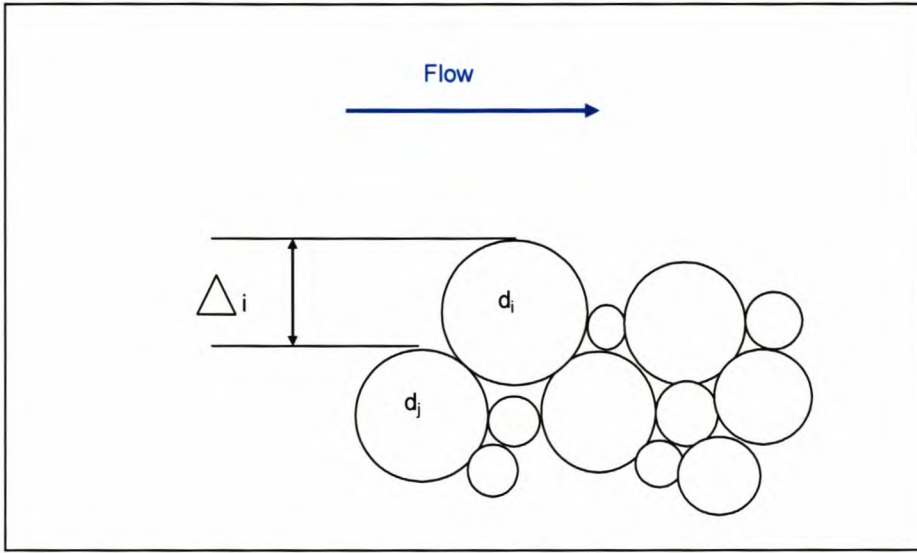


Figure 8-47 Definition of exposure height of bed material

The drag and lift forces acting on a particle staying on the bed depend on how it is situated and surrounded by others. Wu et al. (2000) defined the exposure height, Δ_i , for a particle with size d_i as the elevation difference between the apexes of this particle and its upstream particle with size d_j . If $\Delta_i > 0$, the particle is considered to be in the exposed state, and if $\Delta_i < 0$, it is in the hidden state (**Figure 8-47**). Sediment particles usually are randomly distributed on the bed, therefore it may be assumed that Δ_i is a random variable. Wu et al. (2000) assumed that the exposure height, Δ_i , follows a uniform probability distribution, f , defined as follows,

$$f = \begin{cases} \frac{1}{d_i + d_j}, & -d_j \leq \Delta_i \leq d_i \\ 0, & \text{otherwise} \end{cases} \quad \text{Equation 8-68}$$

Wu et al. (2000) proposed that the probability of particles d_j staying in the front of particles d_i can be assumed to be the percentage of particles d_j in the bed – material, p_{bj} . Therefore, the probabilities of particles d_i hidden and exposed by particles d_j can be obtained from Equation 8 – 66 as

$$p_{hi,j} = p_{bj} \frac{d_j}{d_i + d_j} \quad \text{Equation 8-69}$$

$$p_{ei,j} = p_{bj} \frac{d_i}{d_i + d_j} \quad \text{Equation 8-70}$$

The total hidden and exposed probabilities of particles d_i can be obtained by summation over all fractions, respectively,

$$p_{hi,j} = \sum_{j=1}^N p_{bj} \frac{d_j}{d_i + d_j} \quad \text{Equation 8-71}$$

$$p_{ei,j} = \sum_{j=1}^N p_{bj} \frac{d_i}{d_i + d_j} \quad \text{Equation 8-72}$$

where N is the total number of particle size fractions of the non – uniform sediment mixture. By using Equation 8 – 69 and Equation 8 – 70 Wu et al. (2000) the correction factor as

$$\eta_i = \left(\frac{p_{ei}}{p_{hi}} \right)^m \quad \text{Equation 8-73}$$

where m is an empirical parameter.

Introducing the hiding and exposure factor defined by Equation 8 – 71 to modify the criterion for sediment incipient motion proposed by Shields (1936), the following formula is obtained for determining the critical bed shear stress for incipient motion of non – uniform sediment,

$$\frac{\tau_{cr}}{(\rho_s - \rho)gD} \propto \eta_i \frac{\pi A_p}{6} \tan \phi \quad \text{Equation 8-74}$$

Wu et al. (2000) verified this relationship through laboratory test data as well as field data against various other theories and found it to have a good correlation.

8.2.6.5 Comparison between Field Data, Laboratory tests and the Theory

Field work by Maritz (2003) just upstream of the West – Portal tunnel outlet (BRM site 1) focussed on particles with diameters between 50 mm and 400 mm, marked during low flow conditions, in order to investigate the movement of these particles. These particles were not disturbed during the marking process. The x – y – z axes were also measured in order to

obtain an effective diameter for each particle by using the mean value of these three measurements. Each marked particle was plotted relative to the Perspex pipes that were installed to determine the energy slope.



Figure 8-48 Marked particle at BRM Site 1 (Maritz, 2003)

After a flood event, the marked particles that could be found were again plotted relative to the Perspex pipes. By comparing the before and after plan plots it could be determined which particles moved. For those that could be found, it was also possible to calculate the distance they had been transported.

The energy slope was determined by using the Perspex pipes, and the discharge was calculated through using the water depths at the gauging weir (G1H004 – A02) just downstream of BRM Site 1. The area and velocity during each flood event were determined by using the surveyed cross – sections that were surveyed during the Berg River Baseline Monitoring Study during February 2003. The hydraulic parameters for the various floods are indicated in **Table 8-16**.

Table 8-16 Hydraulic Parameters for 2003 floods

Date	Q (m ³ /s)	Water level (m)	S _f	Area (m ²)	V (m/s)
14 Aug 03	18.49	264.62	0.01203	24.36	0.76
21 Aug 03	92.23	265.53	0.01392	49.45	1.87
4 Sept 03	84.73	265.9	0.01299	45.71	1.85
29 Sept 03	32.07	264.88	0.01285	31.35	1.02
17 Oct 03	14.66	264.67	0.01231	25.3	0.58

The data that was obtained (APPENDIX E) was plotted on both the Shields (Figure 8-49) and the Liu (Figure 8-50) diagrams.

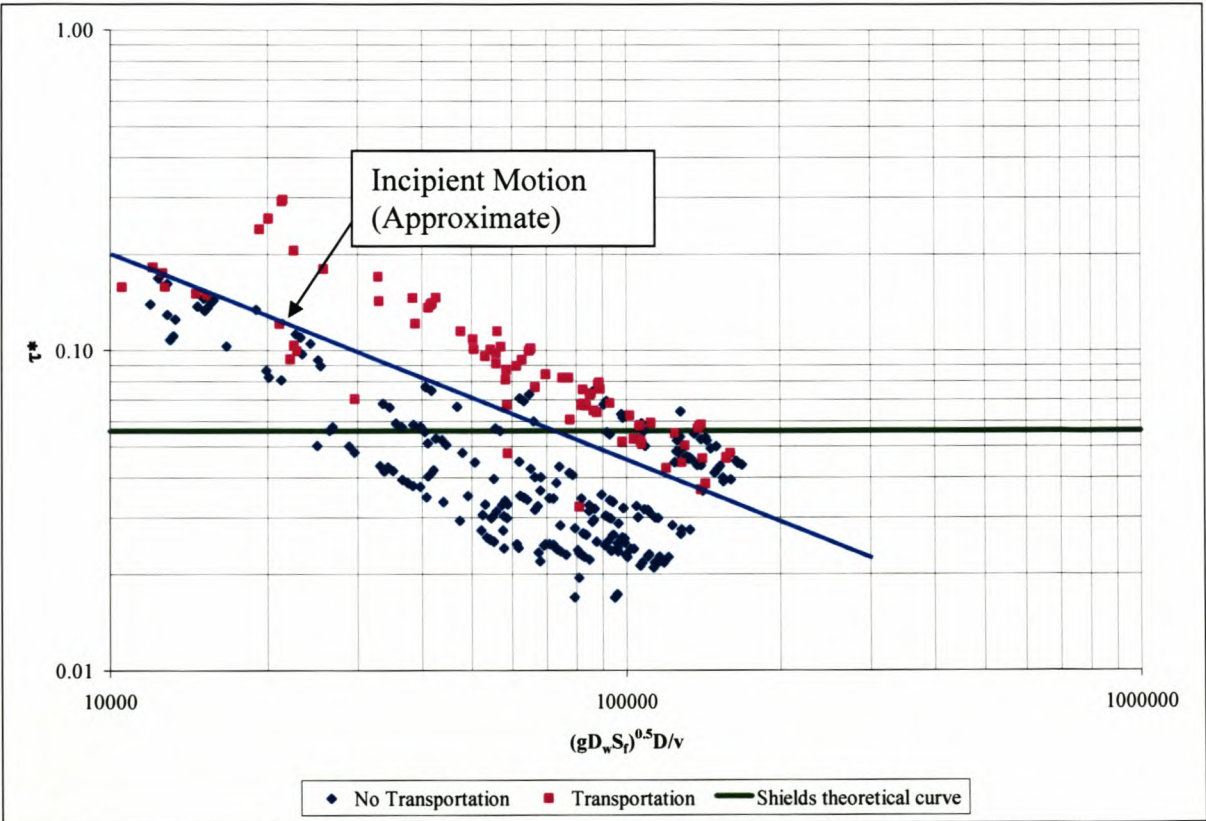


Figure 8-49 Field data plotted on the Shields Diagram

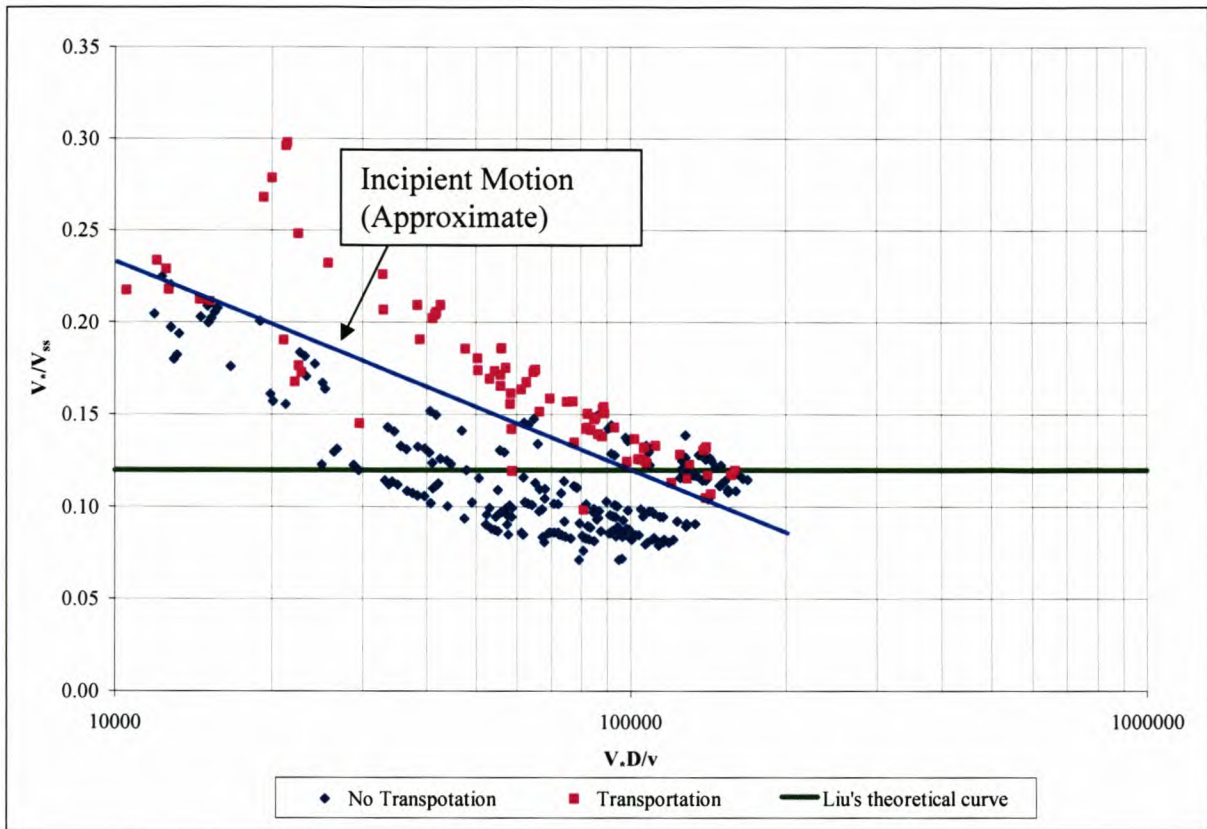


Figure 8-50 Field data plotted on the Liu Diagram

From **Figure 8-49** and **Figure 8-50** it can be seen that the field data do not completely correspond with the theories by Shields and Liu. It can also be seen that there seems to be two well defined areas on each graph, the one where transportation has occurred (above solid blue line) and where no transportation occurred (below solid blue line) with the solid blue line an indication of the estimated incipient motion condition. It can be seen that most of the data for the particles that were transported do plot above the threshold of movement as defined by both Shields and Liu. The reverse also holds true, most of the data from the particles that were not transported plotted below the threshold of movement.

Both the Liu and Shields theory are based on uniform flow in channels, whereas the field conditions are more non – uniform in nature. This could be one of the reasons that cause the discrepancy between the field data and the theoretical curves. The cross – sections in the field vary with both length and width, which cause the discharge, velocity and the energy slope to vary with both time and position. It is evident from **Figure 8-49** and **Figure 8-50** that more stream power is required to move the smaller diameters than what Shields and Liu predicted. Therefore the only conclusion that can be drawn from this is that the hiding effect must play a role in the incipient motion conditions at these sites. The fact that the smaller particles are

shielded by the larger exposed particles may be the reason that more energy is required to transport the small diameters.

Dey and Raju (2002) did some laboratory work on the incipient motion of non – uniform sediment under unidirectional steady – uniform flow conditions. Experiments were carried out in a rectangular flume, 14 m long 0.51 m wide and 0.25 m deep, with various sizes of gravel and coal samples. Before starting an experimental run, the gravel or coal bed of the test section was levelled. The downstream control valve was closed initially. Water was introduced to the setup by gradually opening an upstream valve. After the bed was completely submerged, the downstream valve was opened gradually. At the same time, the upstream valve was adjusted so that the incipient condition was reached when all fractions on the surface of the bed had moved over a period of time. The incipient condition was revealed by collecting the transported particles in a wire – net downstream. The results of the experimental data were plotted on the curve that was proposed by Shields (1936). **Figure 8-51** shows this comparison.

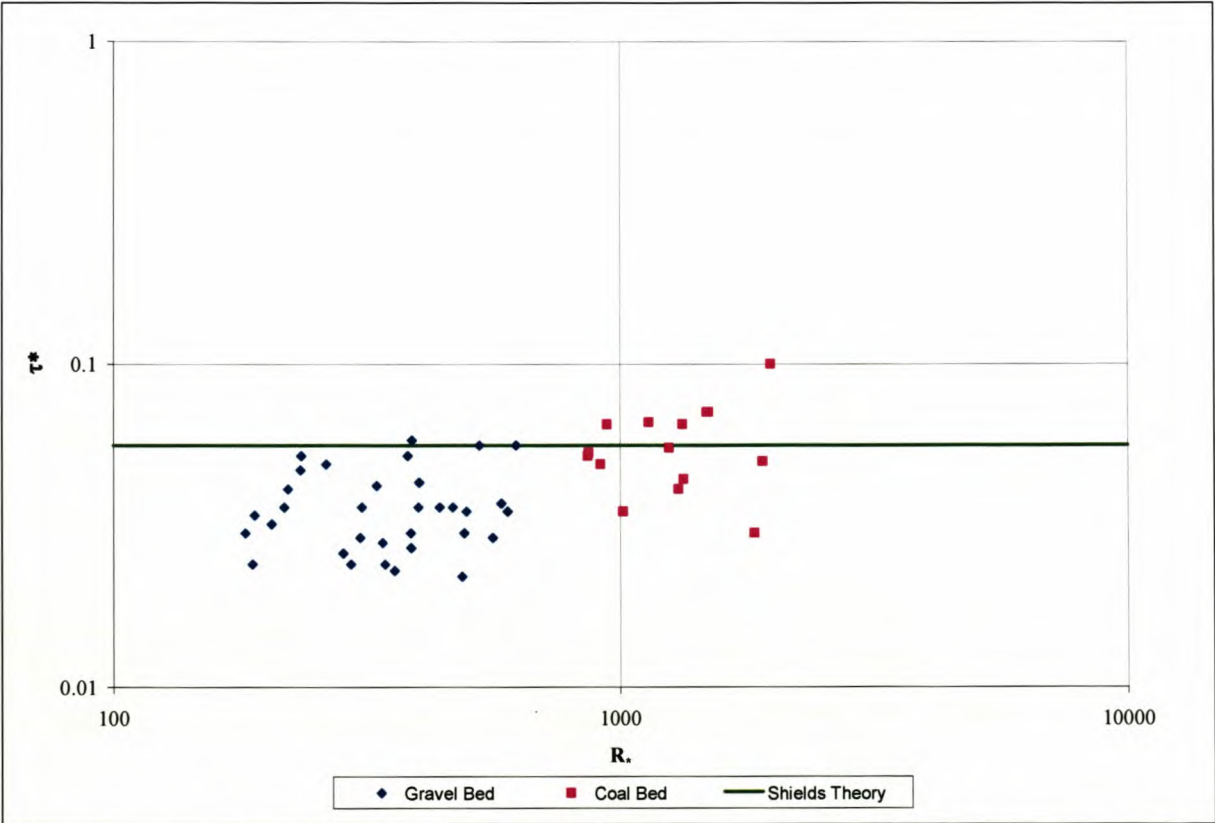


Figure 8-51 Comparison between Shields Theory and Experimental Data (Dey and Raju, 2002)

The data plotted on **Figure 8-51** represents the particles the have been transported during the experiment. From **Figure 8-51** it is evident that the data is in complete disagreement with the theory developed by Shields (1936). This disagreement is not at all uncommon for gravel beds (Andrews 1983, Kuhnle 1993).

Dey and Raju (2002) proposed a set of characteristic parameters being appropriate for the beginning of bed particle motion in functional form as,

$$\tau_b = f_1(V, d_e, h, \rho, \rho_s, k_s, g, \nu, \sigma_g) \quad \text{Equation 8-75}$$

With,

τ_b	=	Bed shear stress at incipient motion condition.
V	=	Flow velocity (m/s).
d_e	=	Effective particle diameter (m).
h	=	Water depth (m).
ρ	=	Water density (kg/m ³).
ρ_s	=	Sediment density (kg/m ³).
k_s	=	Bed roughness coefficient(m).
g	=	Acceleration due to gravity (m/s ²).
ν	=	Dynamic viscosity (kg/m.s)
σ_s	=	represents the sediment gradation on the initiation of be particle motion.

For two phase flow involving sediment – water mixture, the terms ρ and ρ_s should not appear as independent parameters. As fully developed rough – turbulent flow occurs almost always, the inclusion of ν becomes insignificant. Therefore Equation 8 – 75 becomes,

$$\tau_b = f_2(V, d_e, h, \Delta\rho, g, k_s, \sigma_g) \quad \text{Equation 8-76}$$

With,

$$\Delta\rho = \rho_s - \rho$$

Dey and Raju (2002) used the Buckingham π and selected the parameters τ_b , g and d_e as repeating variables. This analysis yielded the following,

$$\tau = f_3(F_d, \hat{d}, \hat{h}, \sigma_g) \quad \text{Equation 8-77}$$

With,

$$F_d = \frac{V}{\sqrt{gd_e}}, \text{ the particle Froude number}$$

$$\hat{d} = \frac{k_s}{d_e}$$

$$\hat{h} = \frac{d_e}{h}$$

The term σ_g represents the sediment gradation on the initiation of be particle motion. Dey and Raju (2002) assumed that this term is insignificant due to the uniformity of the gravel samples used. Thus, Equation 8 – 77 reduces to,

$$\tau = f_3(F_d, \hat{d}, \hat{h}) \quad \text{Equation 8-78}$$

The application of the above non – dimensional parametric representation was justified by Dey and Raju (2002) as follows:

- The term F_d indicates the mobility of the bed particles under stream velocity.
- The term \hat{d} refers to the role of particle size on the initiation of movement. It was reported by Dey (1999) that \hat{d} is a function of the angle of repose, ϕ .
- The term \hat{h} represents the relative submergence of the particle on the incipient motion.

A multiple – linear regression analysis was carried out, and yielded the following results for the non – dimensional critical bed shear stress or the shields parameter (indicated as τ^*),

$$\tau^* = 0.013 F_d^2 \hat{d}^{0.48} \hat{h}^{0.49}, \text{ for the gravel bed} \quad \text{Equation 8-79}$$

$$\tau^* = 0.058 F_d^2 \hat{d}^{0.62} \hat{h}^{0.63}, \text{ for the coal bed}$$

Equation 8-80

The results of the linear regressions are also graphically illustrated in **Figure 8-52** and **Figure 8-53**. Dey and Raju (2002) obtained a correlation coefficient (R^2) of 0.998 between the experimental and computed values of the critical bed shear stress (τ).

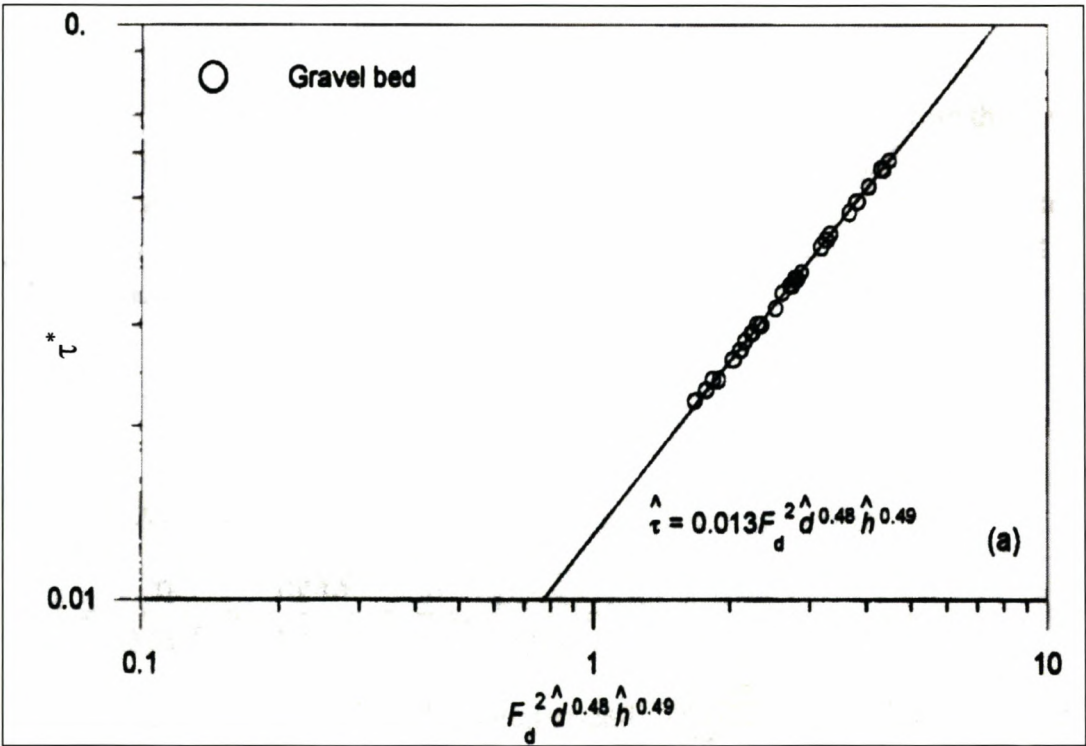


Figure 8-52 Multiple linear regression for gravel beds (Dey and Raju, 2002)

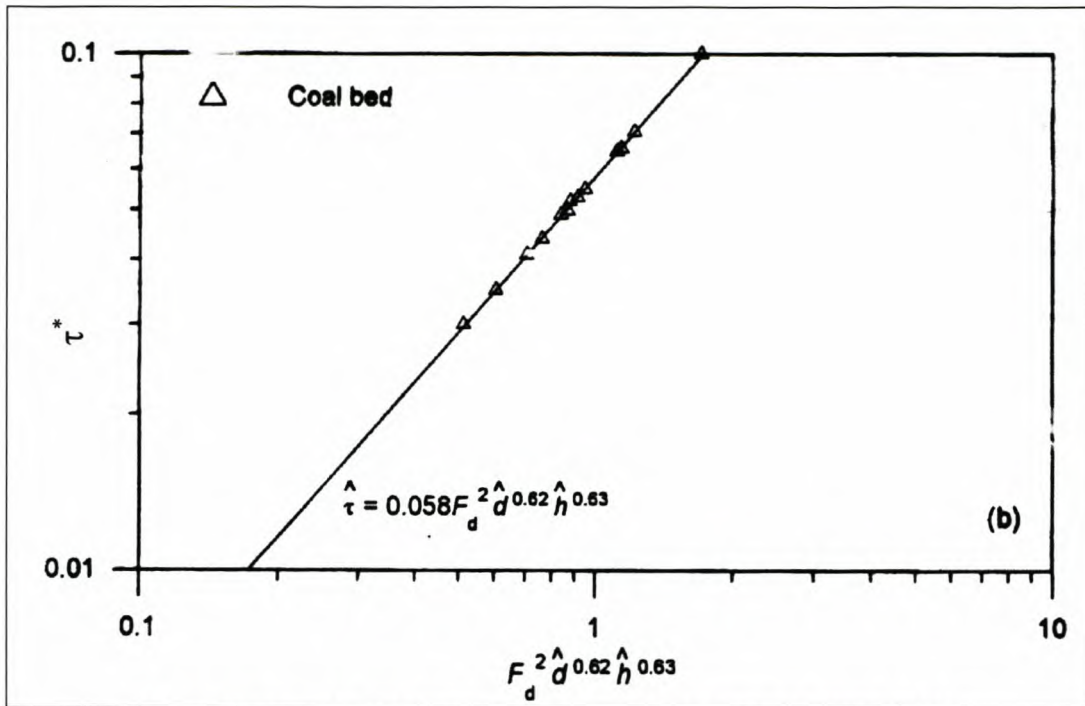


Figure 8-53 Multiple regression for coal beds (Dey and Raju, 2002)

Dey and Raju (2002) obtained good result as can be seen from **Figure 8-52** and **Figure 8-53**, and therefore they propose equations 8 – 79 and 8 – 80 be used to determine the critical bed shear stress under unidirectional steady – uniform flow conditions. The solid line on these graphs represents the threshold of movement, therefore transportation will occur above the line and no transportation will occur below the line. It should however be borne in mind that the tests were carried out under uniform flow conditions in a rectangular flume and these conditions are almost never representative of actual field flow conditions. Even though a gradation of gravel and coal was used the results might still differ from field conditions were the bed does not comprise of a uniform gradation, such as in the upper reaches of the Berg River.

In the field the following data are required as input data to calculate the critical bed shear stress (τ^*) of the bed material from the empirical equations discussed above:

- The energy slope, S , of the flood is to be determined.
- The relative density (ρ_s) and effective diameter (d_e) of the bed particles.
- The equivalent bed roughness, k_s , is to be determined through the sampling and grading of the bed material from the river site, or through calibration against measured flood levels.

In equation 8 – 79 and 8 – 80 F_d , \hat{h} and τ^* are not known. The following equations were used to calculate the various unknowns:

$$F_d = \frac{V}{\sqrt{gd_e}}$$

Equation 8-81

Also τ^* can be expressed as:

$$\tau^* = \frac{\tau_b}{\Delta\rho gd_e} = \frac{\rho ghS}{\Delta\rho gd_e} = \frac{S}{\Delta\hat{h}}$$

Equation 8-82

Equation 8 – 81 was rewritten to obtain a relationship to calculate F_d . τ^* , the non – dimensional critical bed shear stress as defined by Shields (1936), was calculated using equation 8 – 82. Theory as discussed above was used to verify the applicability of the relationship obtained by Dey and Raju (2002) on the field data for the Berg River at BRM site 1 (APPENDIX E). The results are shown graphically in **Figure 8-54**.

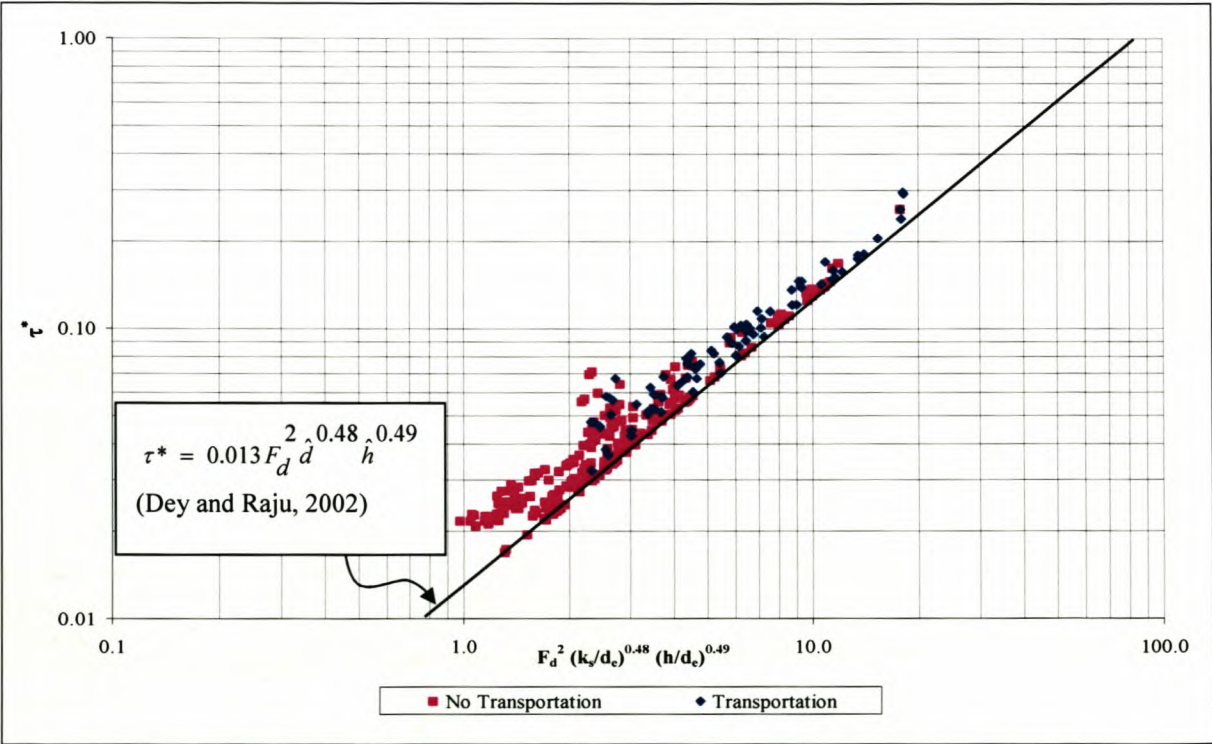


Figure 8-54 Comparison between measured and calculated critical shear stress values

From **Figure 8-54** it is clear that the field data are not in complete disagreement with the theory developed by Dey and Raju (2002), however it is evident that the critical shear stress (τ^*) that was calculated from measured values in the upper reach of the Berg River differs from the values calculated from the empirical relationship. It can be seen that the field data tends to follow the same general trend even though the exact values are not the same. If **Figure 8-54** is compare to **Figure 8-52** it can be seen that the field data has a wider spread which also indicates the possible inaccuracies of the empirical relationship. This discrepancy may be a result of the hiding and exposure phenomenon. It also has to be borne in mind that the discharge that is recorded during the field investigation represents the maximum flood and not the discharge at which each individual particle started to move. This may also contribute to the inaccuracies. The uniform gradation that was used during the laboratory tests differs from the non – uniform gradation that is present in the field. This non – uniform gradation may cause the hiding and exposure effect to be more severe than that experienced during the laboratory tests due to the fact that a much greater spread of particle size exists in the field, therefore the oversize boulders (0.3 – 0.5 m in diameter) have a greater chance of shielding finer particles (0.01 – 0.1 m in diameter). From **Figure 8-54** it can be seen that the prediction made by Dey and Raju (2002) holds true for the particles that did move but most of the particles that did not move also plot above the predicted threshold of movement.

In order to understand why the data is in disagreement with the theory developed by Dey and Raju (2002) the parameters were plotted against the critical bed shear stress (τ^*) to evaluate the correlation of each particle. The results are shown in **Figure 8-55**. As can be seen from this figure the parameter (h/d_e) has a negative correlation to the solid black line (as obtained by Dey and Raju (2002)). This relationship between the critical bed shear stress (τ^*) and the parameter h/d_e can be explained by the fact that h/d_e forms part of the relationship for the critical bed shear stress (τ^*) as defined by Dey and Raju (2002). As can be seen in Equation 8 – 83.

$$\tau^* = \frac{h}{d_e} \frac{S_f}{\rho_s - \rho_w} \quad \text{Equation 8-83}$$

Therefore it was decided to recalibrate the formula in order to obtain a closer relationship between the parameters.

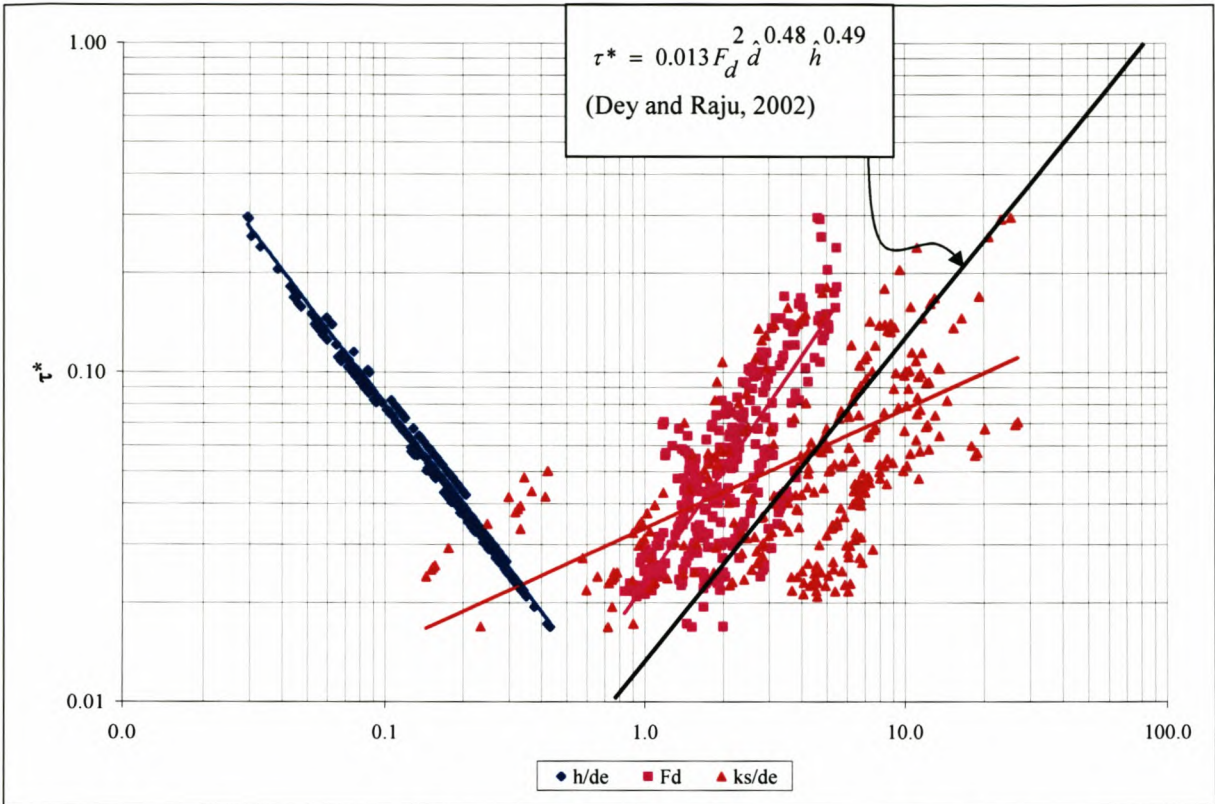


Figure 8-55 Contributing parameters plotted against the critical bed shear stress

The relationship established by Dey and Raju (2002) was recalibrated on the samples that were transported at BRM site 1 in order to find a closer relationship between the site specific parameters as measured at BRM site 1. The relationship that was found are shown in **Figure 8-56**.

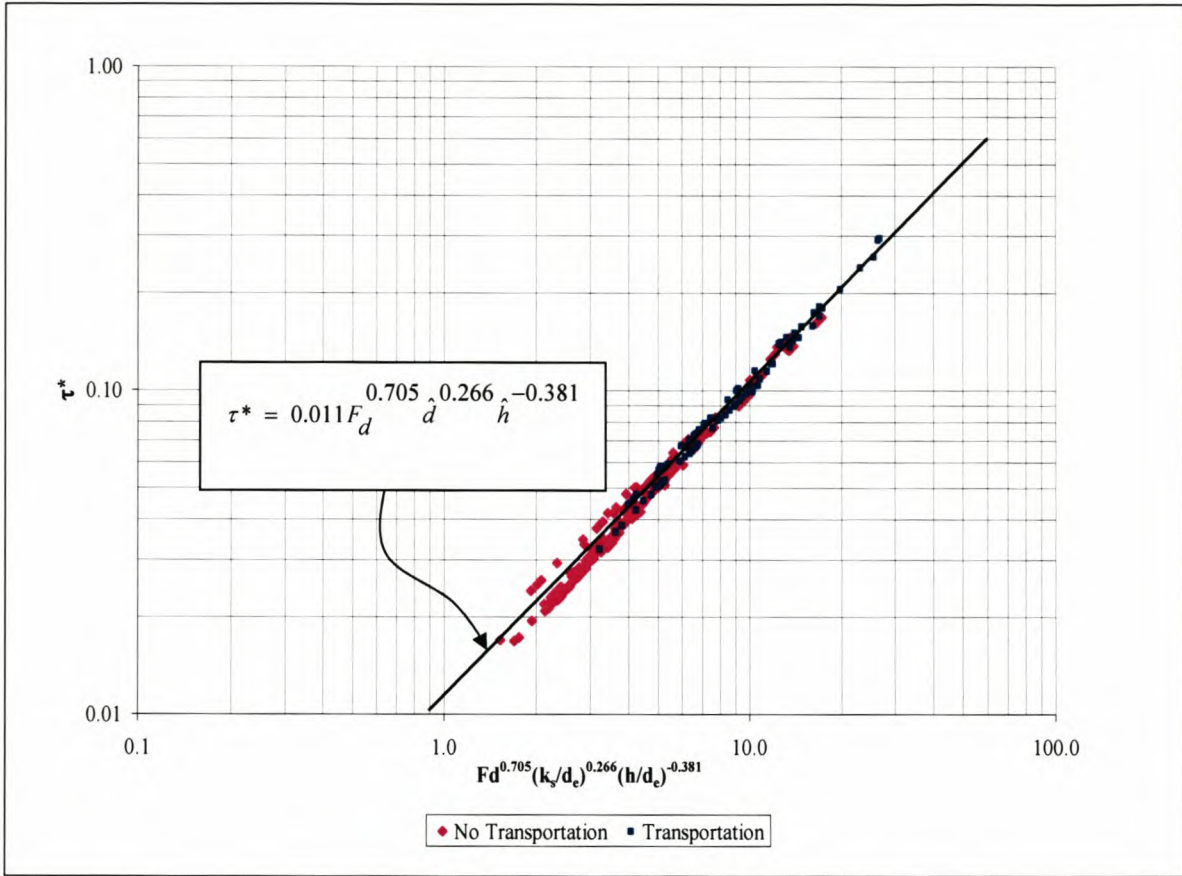


Figure 8-56 Recalibration of empirical formula

From **Figure 8-56** it can be seen that slope of the regression line is flatter compared to the relationship that was established by Dey and Raju (2002). The regression line through the Berg River data intercepts the x – axis at a lower value compared to the laboratory tests carried out by Dey and Raju (2002). The following relationship was obtained as the threshold of movement for the upper Berg River:

$$\tau^* = 0.011 F_d^{0.705} \hat{d}^{0.266} \hat{h}^{-0.381} \quad \text{Equation 8-84}$$

with a correlation coefficient (R^2) of 0.98.

Even though a relationship was found during the recalibration it is still difficult to distinguish between the particles that were transported and those that were not transported. The only conclusion that can be drawn from this is that the theory developed by Dey and Raju (2002) seems to be inaccurate in dealing with a combination of particles that were transported and not transported. This inaccuracy may also be as a result of the fact that the theory does not incorporate hiding and exposure.

In order to analysis the hiding and exposure further the theory developed by Lui (1986) was revisited.

The relative roughness that a particle experiences can be expressed as follows:

$$\text{relative roughness} = \frac{k_s}{d}$$

Equation 8-85

Hiding of smaller particles can schematically be represented as follows:

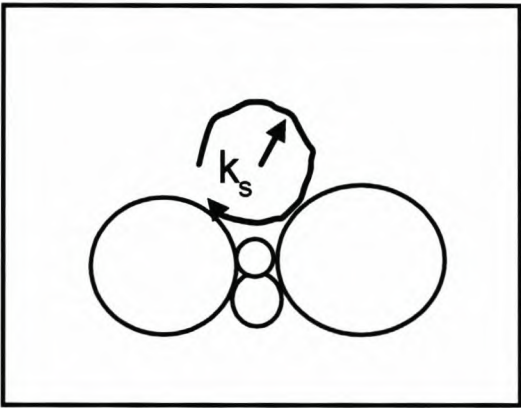


Figure 8-57 **Relative Roughness of protected paritcles**

From **Figure 8-57** it is evident that the protected particles experience a much higher relative roughness compared to a uniform bed of about the same size where the roughness coefficient is determined by the particle size.

Figure 8-58 shows the change in stream power against the change in diameter. From this figure it can be seen that the smaller particles required a higher stream power to be transported compared to that predicted by Lui (1986) (a value of 0.12 in the rough turbulent zone). The solid black line on **Figure 8-58** indicates the median particle size (d_{50}) of the specific site. The deviation from the theory as developed by Lui (1986) is the most pronounced when the particle under consideration is smaller than the median particle size (d_{50}). This is therefore an indication that these particles are protected by the bigger surrounding particles.

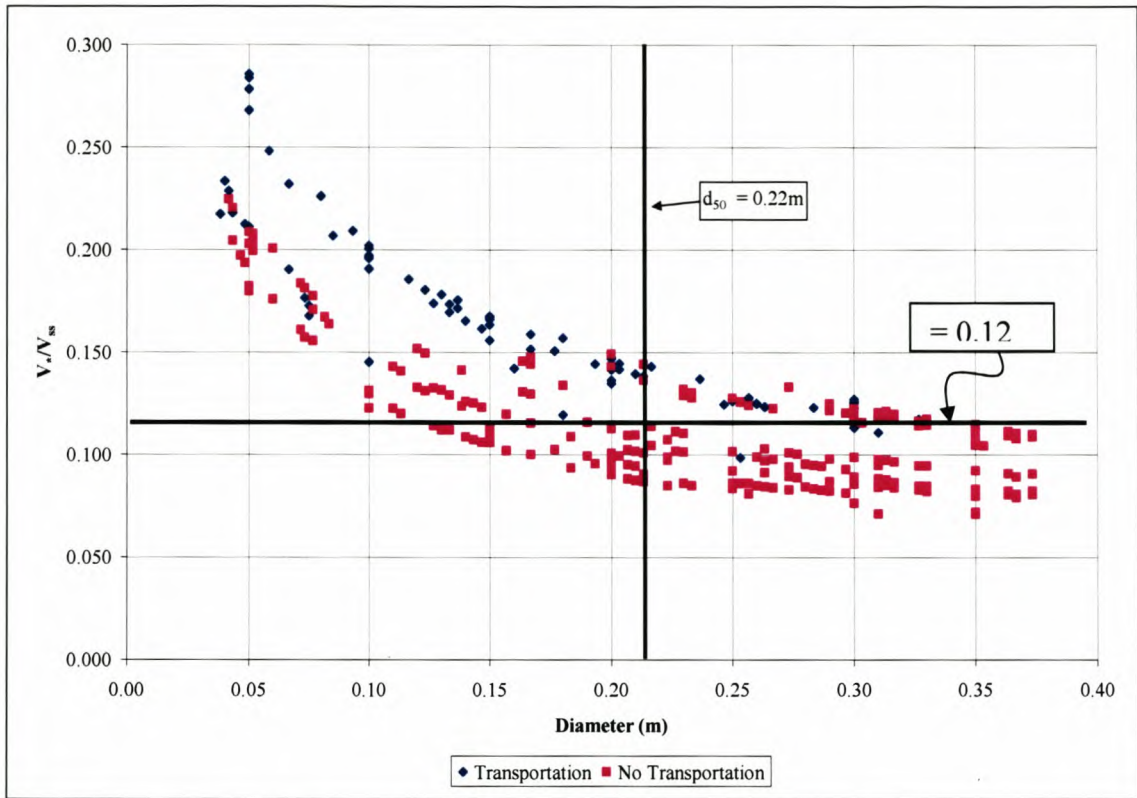


Figure 8-58 Particle diameter vs stream power

The relative roughness values (showed in **APPENDIX E**) were plotted against the particle Reynolds number (**Figure 8-59**) in order to establish whether a relationship exists between the relative roughness and the threshold of movement. The roughness values (k_s) were determined by using Chezy's formula. From **Figure 8-59** the flat part of the solid line indicates that most particles that did not move experienced a relative roughness of less than five, whereas the sloping part of the solid line indicates that the particles that did not move experienced a relative roughness of between five and nine. From **Figure 8-59** it is evident that the relative roughness may be used as an indication of incipient motion at this specific site (BRM site 1).

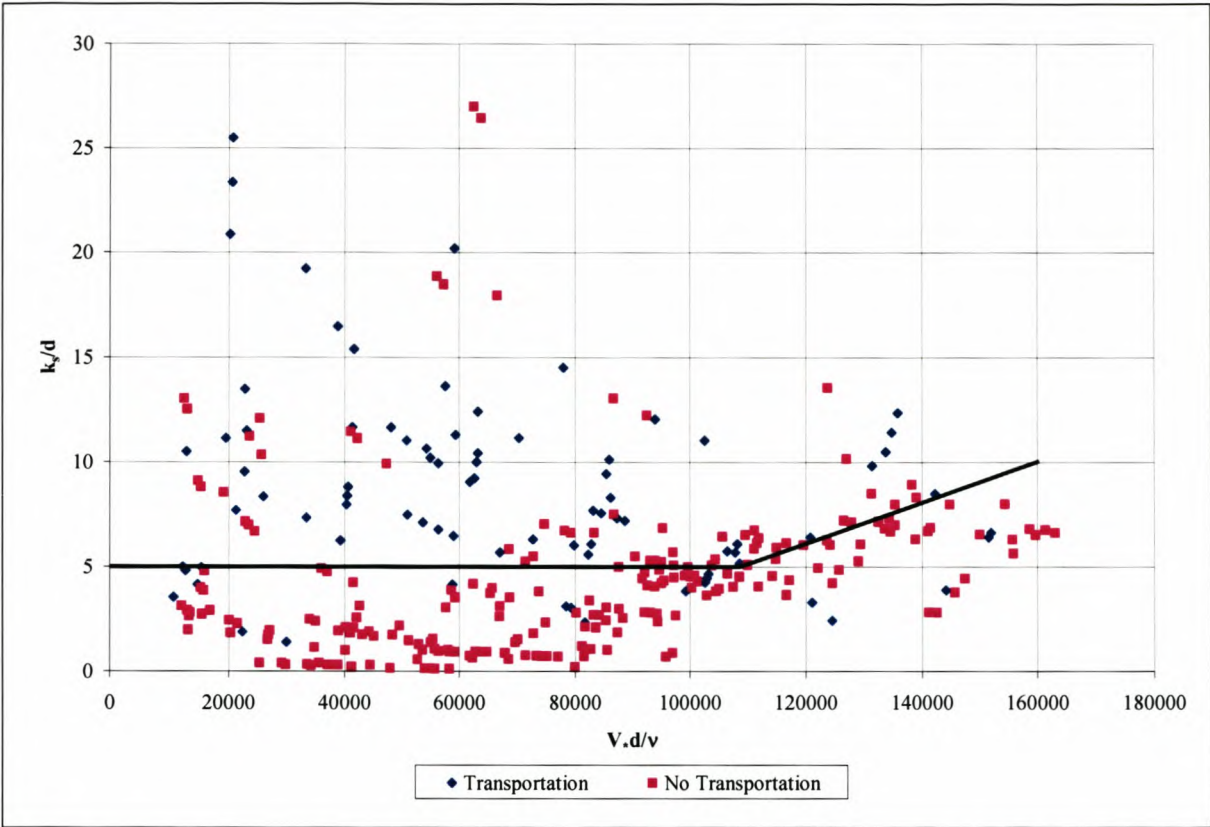


Figure 8-59 The relationship between the relative roughness and the particle Reynolds number

In order to find a graphical solution k_s/d contours were plotted on the Lui diagram (**Figure 8-60** and **Figure 8-61**). From these figures it can be seen that the trendline that stipulates the $k_s/d = 5$ contour seems to be an indication of the incipient motion condition at this site. It must be borne in mind that this will only hold true at BRM site 1 and that it can only be applied for data at that site until further calibration on a more comprehensive data is carried out. It is therefore recommended that a k_s/d value of five be used as an indication of the incipient motion condition.

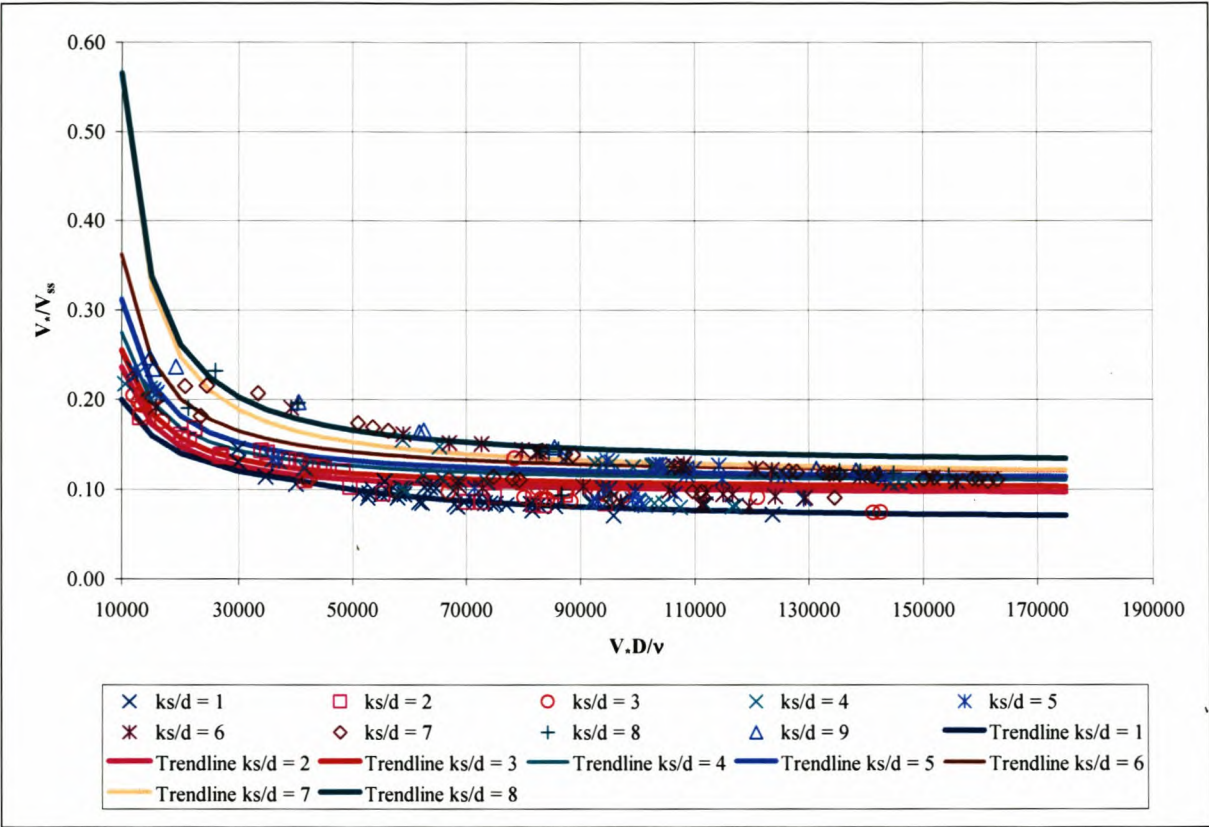


Figure 8-60 Lui diagram k_s/d contours against BRM site 1 data

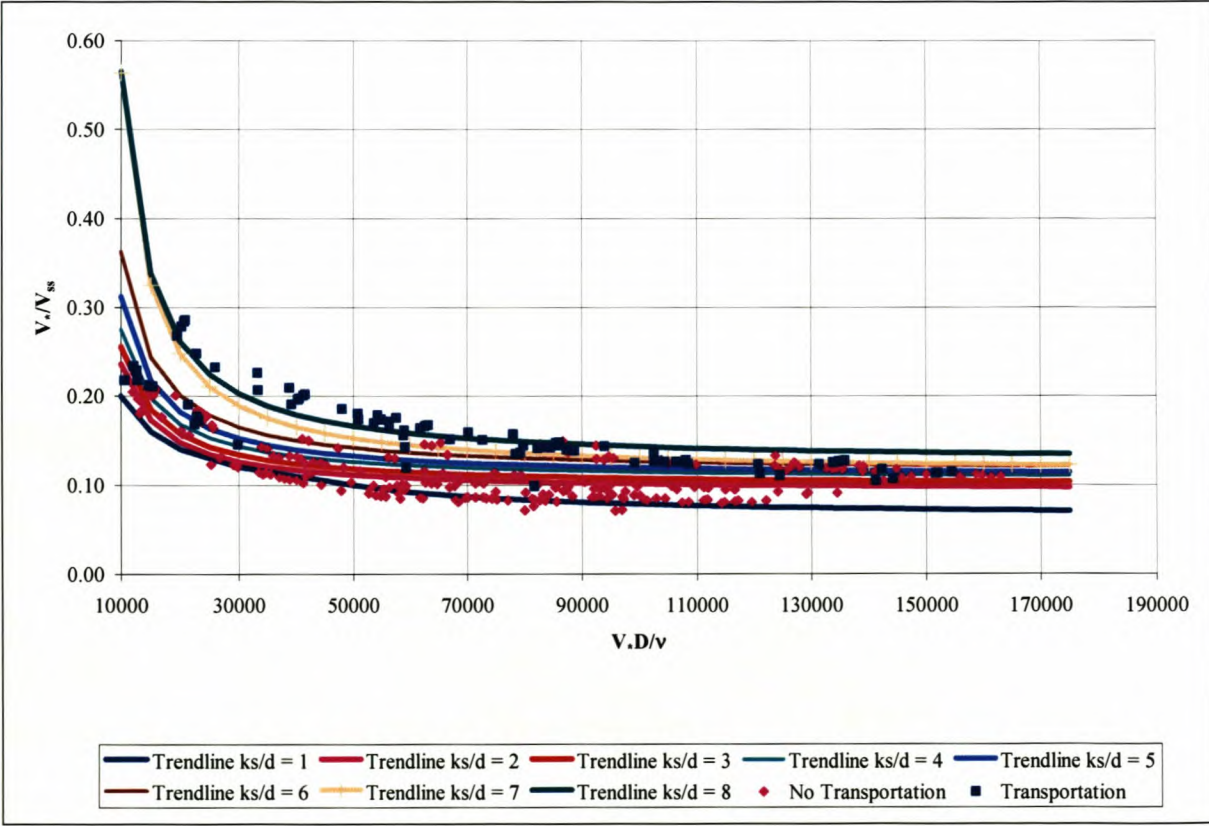


Figure 8-61 Lui Diagram k_s/d contours compared to particle movement

Figure 8-62 shows the transportation of the marked particles in relation to a relative roughness of five. It can be seen that at higher particle Reynolds numbers the trendline seems to be predicting the threshold of movement accurately. It is therefore recommended that this value be used to define the point of incipient motion at BRM site 1.

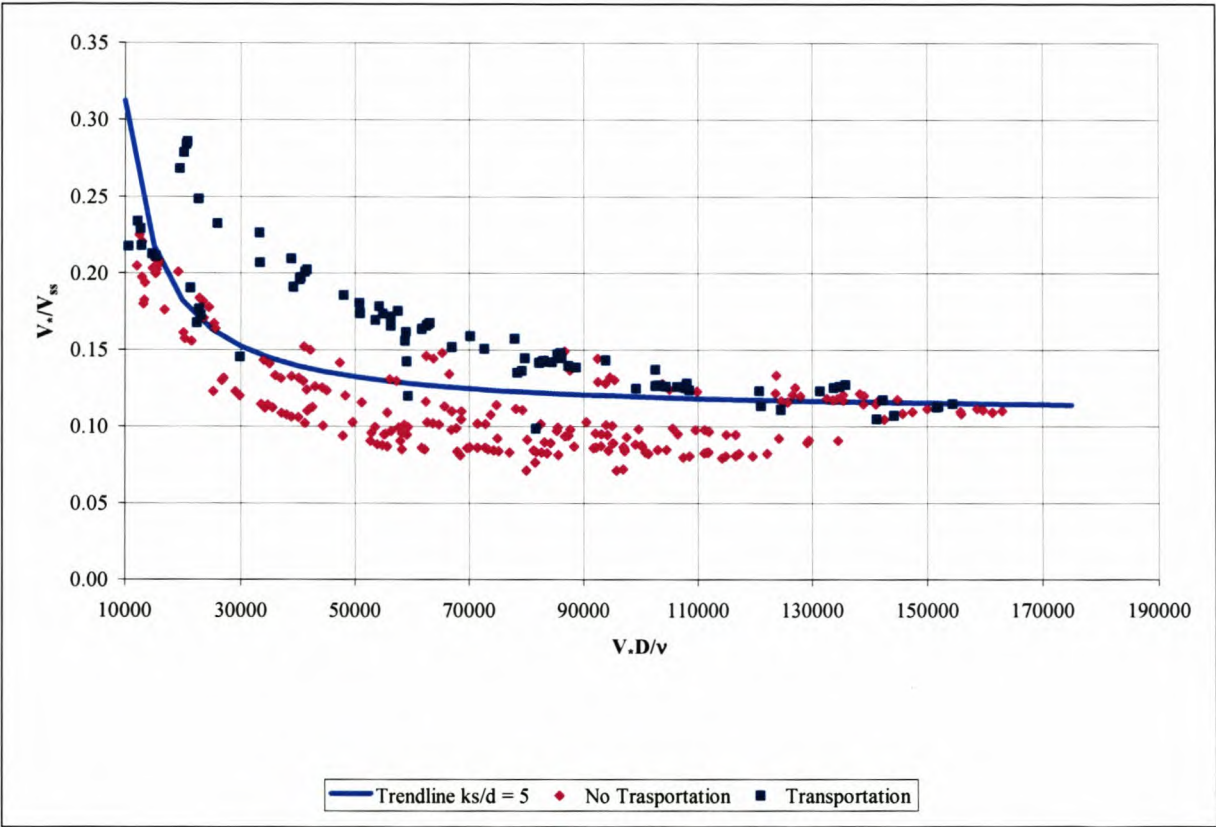


Figure 8-62 ks/d trendline compared to particle movement

Liu’s theory (1986) on incipient motion (**Figure 8-46**), the theory developed by Dey and Raju (2002) (**Figure 8-56**) as well as the theory incorporating the relative roughness (**Figure 8-62**) were used to calculate which fraction of sediment will be entrained at certain discharges at BRM site 1. The measured water levels during the 2003 winter season were used to establish a relationship between the energy slope and the discharge at the particular site. The hydraulic parameters were obtained from MIKE 11. **Table 8-17** shows the cobble diameter that will be on the verge of entrainment for each discharge. The settling velocity for the fractions of sediment was calculated by using Equation 8 -60 and Equation 8 – 62.

Table 8-17 Incipient motion at BRM site 1

Discharge (m³/s)	Sediment diameter (m)		
	Liu's Theory	Recalibrated Dey and Raju	Modified Lui
25	0.2	0.28	0.21
50	0.28	0.36	0.29
75	0.31	0.42	0.35
100	0.35	0.47	0.39
150	0.42	0.51	0.46
200	0.48	0.53	0.48

From **Table 8-17** it is evident that due to the steep bed slope at BRM site 1, large diameters will be transported. The diameters that will be transported are quite sensitive to the energy slope and water depth. It should also be noted that the recalibrated theory derived from the Dey and Raju (2002) gives larger diameters, especially at low flows compared to the theory developed by Liu (1986). The modified Lui theory gives similar value compared to the original theory developed by Lui (1986). The large particle Reynolds numbers that were obtained during the calculation caused the points to plot to the right of the X – axis where the modified Lui theory and the original theory should give the same results.

The input to the mathematical model for the three scenarios – present, post dam and the post dam with flood releases – was used to determine a duration of flood flow exceedence table (**Table 8-18**) for the various floods.

Table 8-18 Duration of flood flow exceedence

Flood (m³/s)	Duration of flood flow exceedence (hours/annum)		
	Present	Post Dam	Post Dam with Flood Releases
25	175	14	28
50	59	2	15
75	28	1	9
100	17	0	5
150	6	0	2
200	2	0	1
250	0	0	0

It can be seen from **Table 8-18** that the duration of exceedence of the $25 \text{ m}^3/\text{s}$ flood is the most affected by the dam. Under present conditions even the $25 \text{ m}^3/\text{s}$ flood will only be exceeded 175 hours/annum, while it will be exceeded only 14 hours/annum if no artificial floods are released and 28 hours/annum with the release of the prescribed floods.

From **Table 8-18** it can be seen that most of the floods have a low exceedence duration. One major weakness of this mathematical model is its inability to simulate the sediment transport of cobbles and boulders. This is due to the fact that none of the sediment transport theories are defined for those sizes. Due to this and to the fact that little movement of the cobbles and boulders will occur it was decided that this part of the sediment transport will be neglected. Even if the cobbles and boulders are transported it will most likely be only for short distances, since the flood duration is short. From **Figure 8-49** and **Figure 8-50** it can be seen that the finer particles require more input stream power to reach incipient motion than what the general theories by Shields (1936) and Liu (1986) forecast. Therefore the frequency that these particles will be transported will also be less.

CHAPTER 9 MATHEMATICAL MODEL CALIBRATION AND VERIFICATION

Even though the measured values for the gauging stations were used as input to the hydrodynamic model, the discharge scaling process that was introduced to account for the ungauged catchment area is only an estimation of the actual values. Thus, the discharge magnitude and lag time of the tributaries may not be correct as it joins the Berg River. Therefore it is necessary to calibrate and verify the calibration of the hydrodynamic model against the measured flow data for the various gauging stations along the Berg River.

The same is true for the sediment transport model. The model may transport too much or too little sediment depending on the transport capacity of the river. It unfortunately does not account for sediment availability in the catchments. Thus, this model had to be calibrated against the sediment samples that were taken during the winter of 2003.

This chapter serves as a discussion of the calibration and verification processes.

9.1 *Hydrodynamic Model*

9.1.1 Calibration

The hydrodynamic model was calibrated for a one-year period (1999) based on the measured discharges at Hermon and Drieheuwels. The calibration period covered a typical flow year. The initial flow factors that were used to account for the ungauged catchments, were revised by calibration, and are listed in **Table 9-1**.

The calibration was only carried out at Hermon and Drieheuwels as there is a problem with the data reliability at Paarl. If the tributaries between Driefontein (G1H004) and Paarl (G1H020) are scaled so that the simulated discharge match the measured values at Paarl, the simulated discharges at Hermon (G1H036) are in general much higher than the measured values, even if the three tributaries between Paarl and Hermon are neglected.

The discharge table (DT) that was used to calculate the discharge from the registered water levels at G1H004 was revised around May 2003 (Basson, 2003). As G1H036 was calibrated by DWAF through the measurement of the flow velocities by using a Dobler velocity meter it is believed that this data can also be accepted as reliable. This leaves only the gauging station at Paarl that may be faulty. The bridge just downstream of the weir may cause higher damming than anticipated. This leads to higher water levels compared to a scenario without the bridge. Thus, a higher water level will cause the calculated discharge to be higher than the actual value.

Table 9-1 **Revised calibrated adjustment factors to account for ungauged areas at tributaries**

Tributary	Initial Flow Factor	Calibrated Flow Factor
Franschhoek (G1H003)	2.59	4.28
Dwars (G1H019)	3.04	2.14
Krom (G1H037)	1.16	2.14
Doring (G1H039)	2.64	1.07
Kompanjies (G1H041)	1.64	2.57
Vis (G1H040)	1.95	1.73
Klein Berg (G1H008)	1.25	1.20
Twenty-fours River (G1H028)	1.59	0.70
Sandspruit (G1H043)	1.01	1.00
Matjies (G1H035)	1.06	1.00
Mooreesburgspruit (G1H034)	1.16	1.16

The measured and simulated discharges at Hermon and Drieheuwels for 1999 are shown in **Figure 9-1** and **Figure 9-3**, respectively.

The calibration focused on obtaining the correct flood peak magnitude and lag, as well as the correct hydrograph form. The low flows have not been calibrated accurately, since the calibration focused on floods, as the low flows are less important in sediment transport (**Figure 9-2** and **Figure 9-4**). The low flows in the field are also affected by pump station abstractions and irrigation releases, which are not simulated in the model. **Figure 9-2** and **Figure 9-4** are logarithmic plots of the calibration, which illustrate this.

The only way the flood peaks could be altered was to change the flow factor that scales the discharge of the tributary. Calibrated and observed Mean Annual Runoff (MAR) can also be used as an indication of the accuracy of the calibration. The comparisons at Hermon and Drieheuwels are shown in **Table 9-2**.

Table 9-2 Observed and calibrated MAR at Hermon (G1H036) and Drieheuwels (G1H013)

	Measured MAR ($10^6 \text{ m}^3/\text{a}$) (1997 – 2003)	Calibrated MAR ($10^6 \text{ m}^3/\text{a}$)
Hermon (G1H036)	317	339
Drieheuwels (G1H013)	457	443

As the measuring stations on the tributaries are situated at various distances from the Berg River it was also necessary, in some cases, to adjust the time at which the water level reading was registered at the gauging station on the tributary. This had to be done to account for the time it would have taken the flood to reach the confluence with Berg River. **Table 9-3** shows the tributaries at which adjustments were necessary as well as the adjustment that was made.

As shown in **Table 9-3** the time adjustment had to be made to only two tributaries. The gauging stations on these tributaries are situated relatively far away from the Berg River. It is therefore logical that adjustments at these tributaries may be necessary.

Table 9-3 Time adjustments made to the flow record at the tributaries

Tributary	Adjustment
Klein Berg River (G1H008)	12 hours later
Twenty-four Rivers (G1H028)	12 hours later

Table 9-4 shows the revised roughness coefficients that were used in order to achieve the correct lag time at the 2 gauging stations (G1H036 and G1H013). If the roughness coefficient for the main channel of the first 24 kilometres is kept as in **Table 8-15** the lag time at Hermon (G1H036) is too big, which means that the roughness coefficient needs to be decreased.

Table 9-4 Revised roughness coefficients used in the one dimensional model

		Manning's n – value	
		Main Channel	Floodplain
Upper Section	Km 2.2 – Km 24 (cobble bed)	0.07	0.055
	Km 24 – Km 70 (sand bed)	0.045	0.055
Lower Section	Km 70 – Km 188.4	0.045	0.055

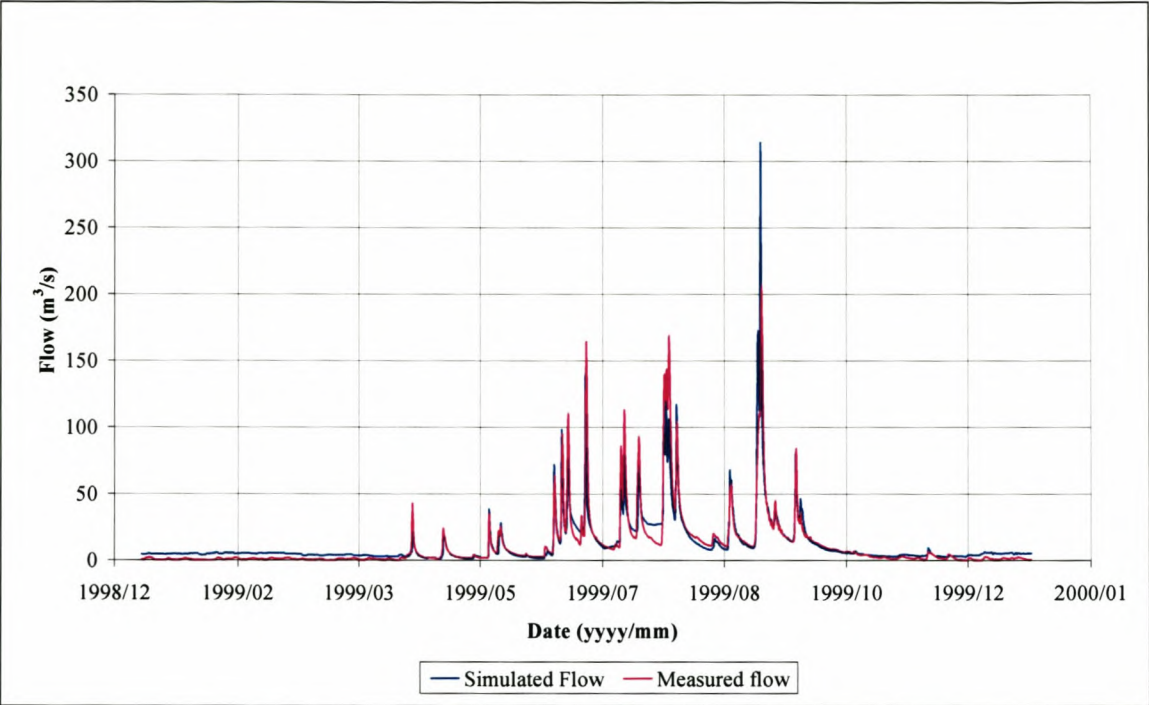


Figure 9-1 Calibration of flow at Hermon (G1H036) for 1999

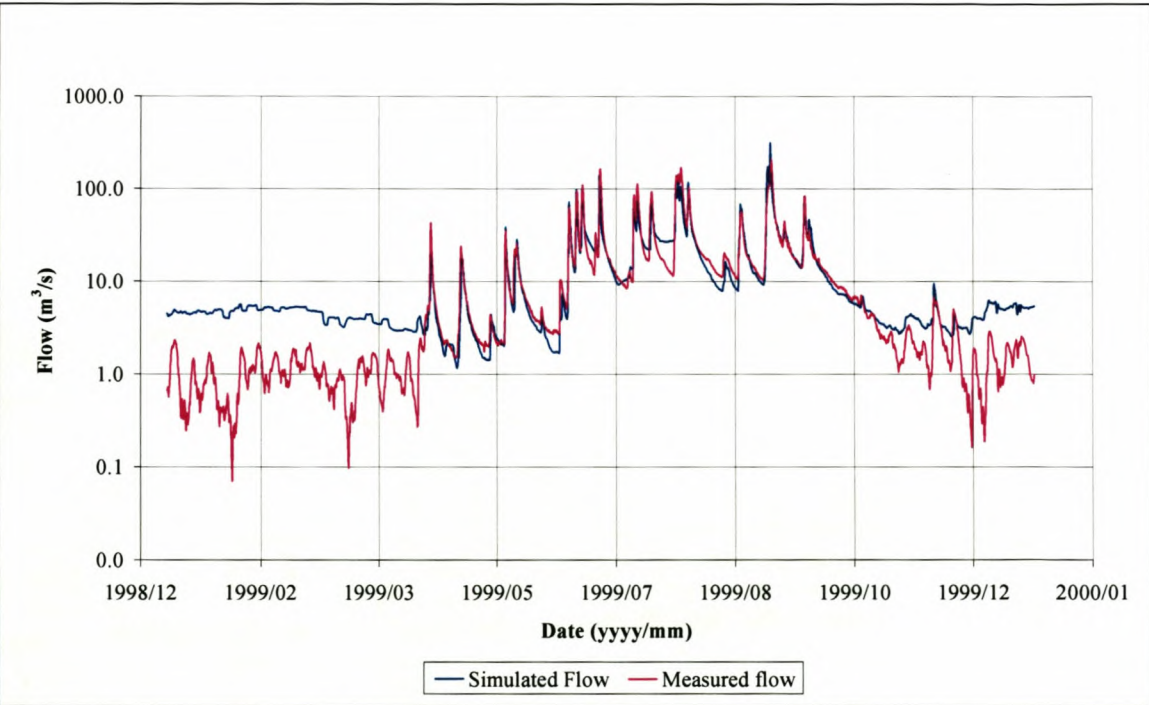


Figure 9-2 Calibration of flow at Hermon (G1H036) for 1999 (Log scale)

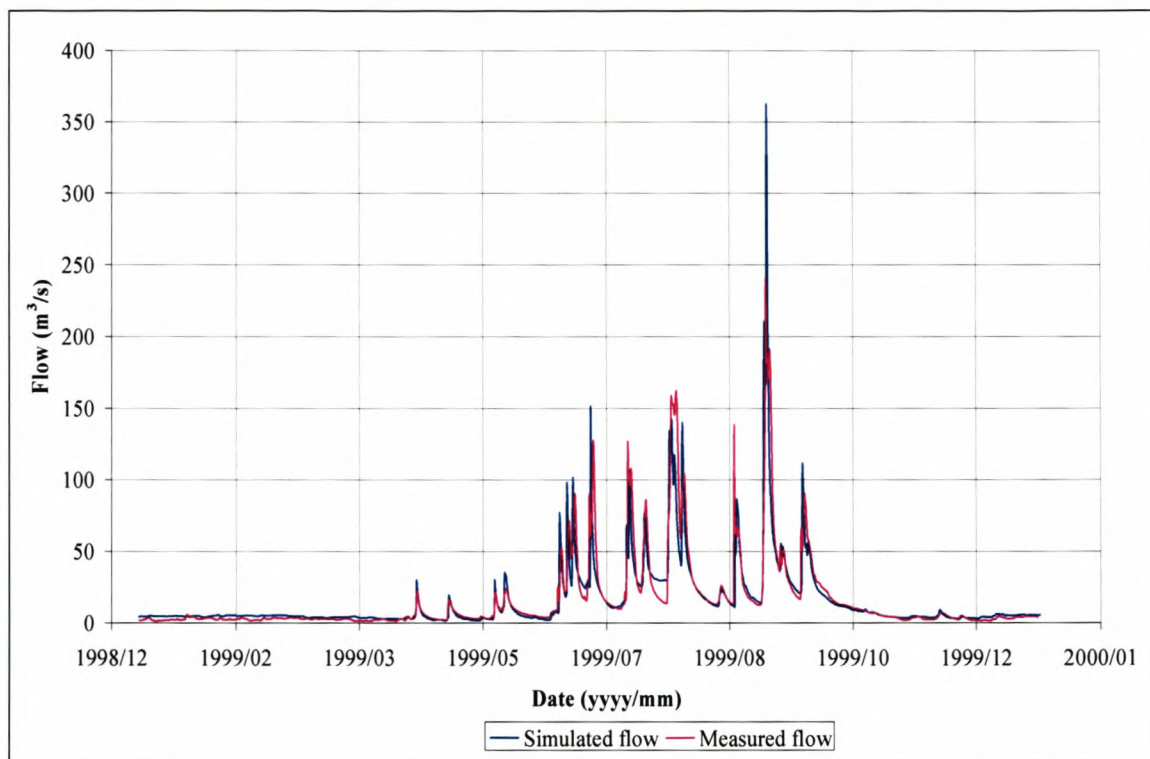


Figure 9-3 Calibration of flow at Drieheuwels (G1H013) for 1999

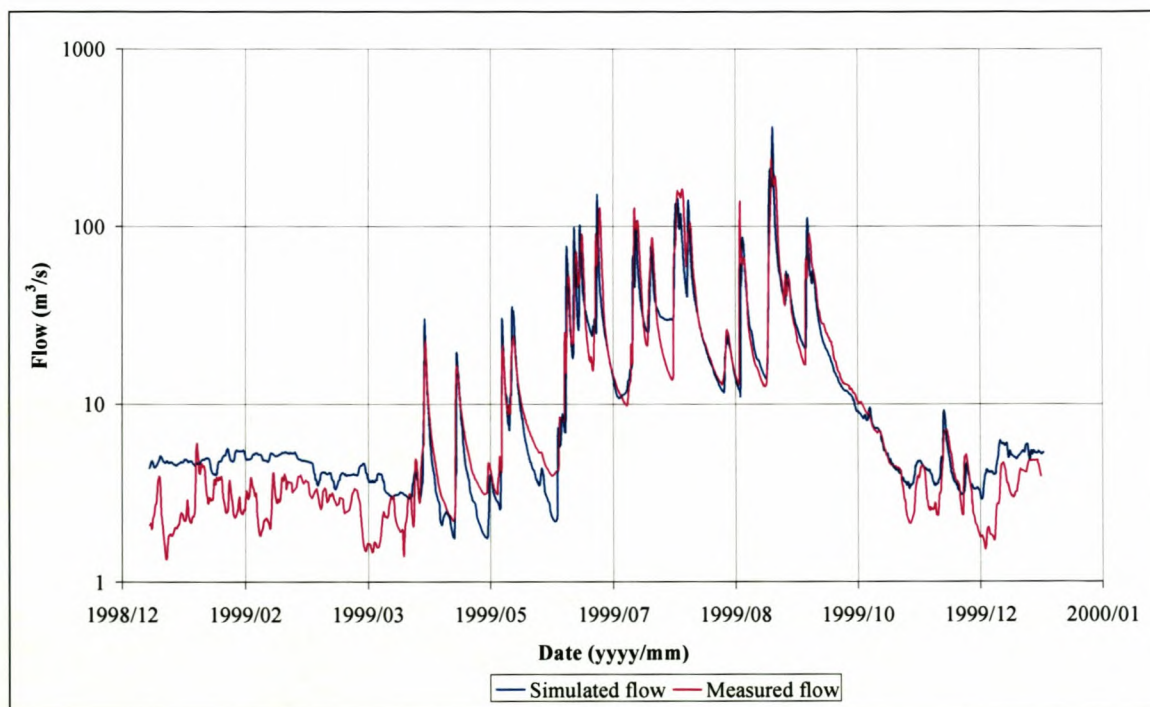


Figure 9-4 Calibration of flow at Drieheuwels (G1H013) for 1999 (Log scale)

9.1.2 Verification

The verification of the calibration was done by verifying that the factors listed in **Table 9-1** that were obtained during the calibration of the hydrodynamic model apply to the whole study period (1995 – 2003). When the discharge of the different years is compared 1999 was an average year. This means that the revised scale factors may not necessarily also apply to dry and/or wet years.

As can be seen from **Figure 9-5** the flood peaks in 1999 are not as high as in some of the other years, but there were more frequent middle size floods. These are the floods that are responsible for most of the sediment transport as they happen more often than the bigger floods. The verification was done by checking the factors for 1995 to 2001.

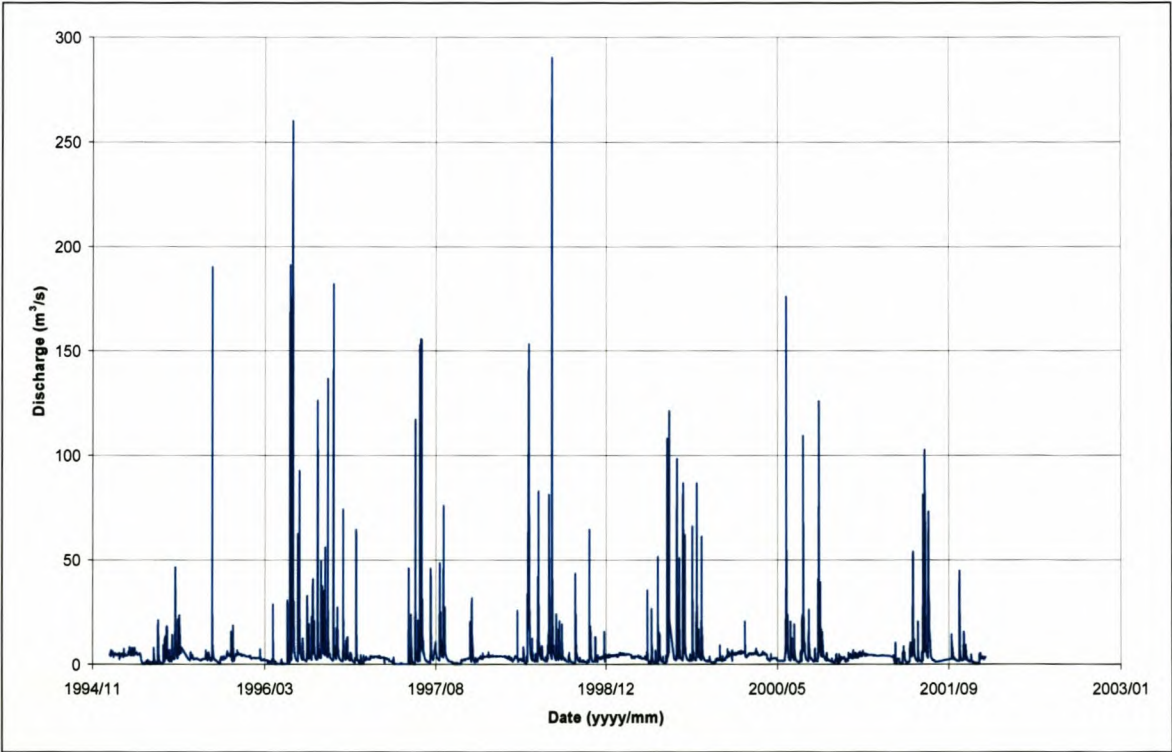


Figure 9-5 Flow record at Driefontein (G1H004)

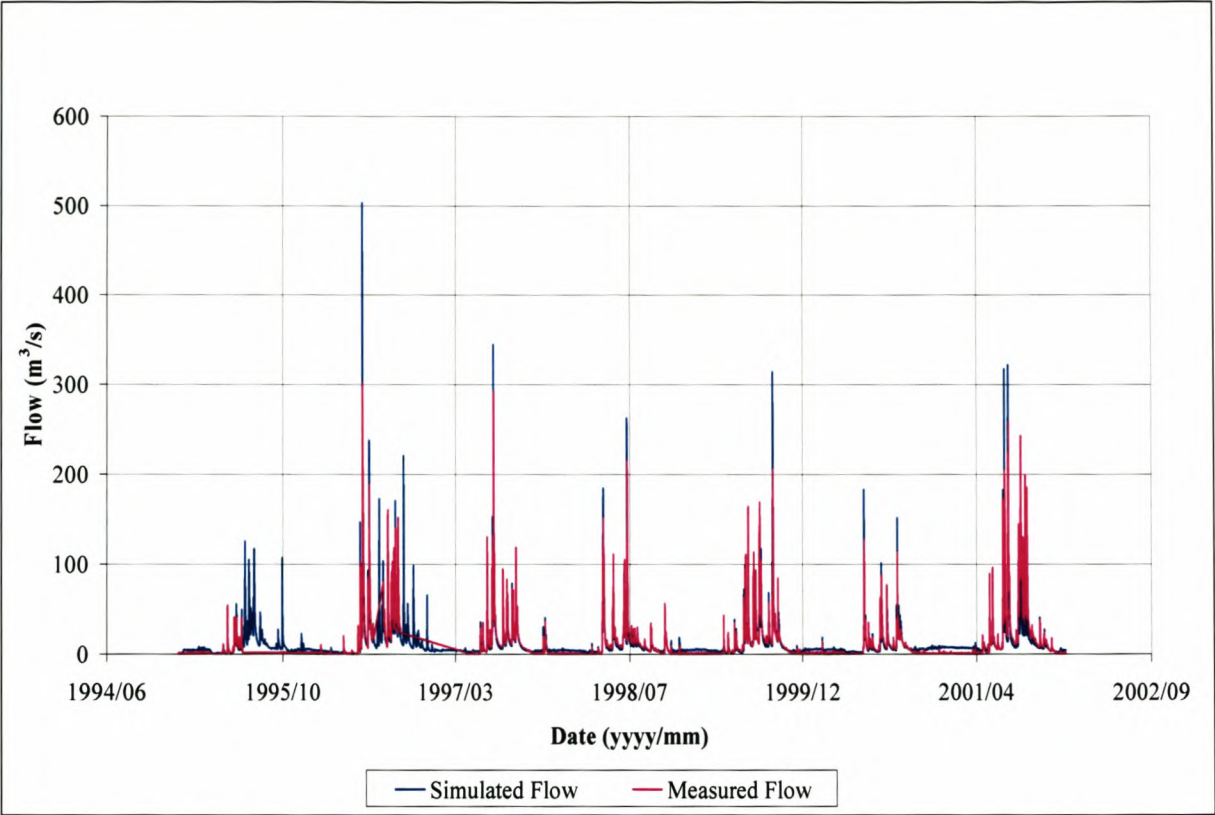


Figure 9-6 Verification of the calibration at Hermon (G1H036) for 1995 to 2001

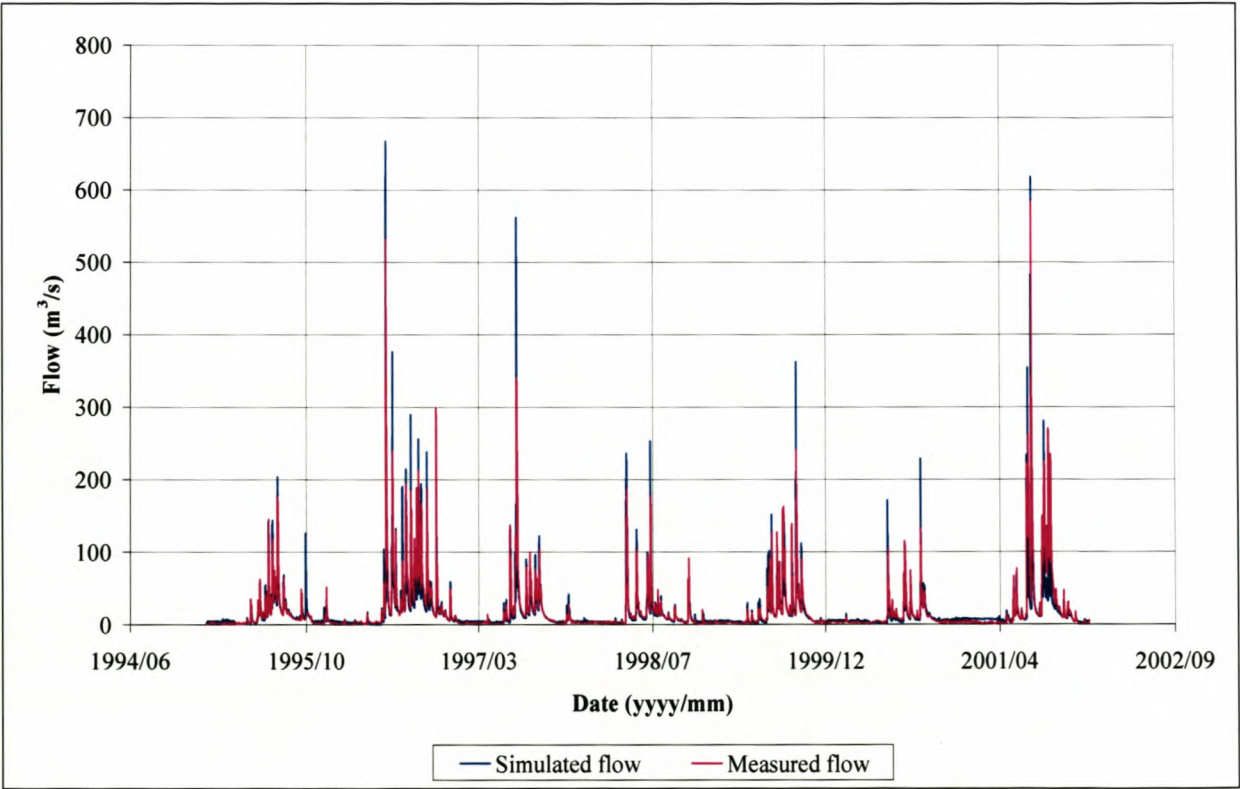


Figure 9-7 Verification of the calibration at Drieheuvels (G1H013) for 1995 to 2001

Figure 9-6 and **Figure 9-7** show the verification of the revised scaling factors that was obtained during the calibration. From these figures it can be seen that by using the revised scaling factors satisfactory results are obtained for both dryer and wetter years. No significant change in the simulated MAR was obtained.

From **Figure 9-6** it can be seen that some of the longer simulated flood peaks are noticeably higher than the measured values. The observed MAR is already larger than the simulated MAR so the scaling factors could not be revised again, as a change in these factors would cause a further decrease in the simulated MAR. The same can be said for **Figure 9-7**.

9.2 Sediment Transport Model

9.2.1 Calibration

The sediment samples that were taken at Paarl (G1H020), Hermon (G1H036) and Drieheuwels (G1H013) were used to calibrate the sediment transport. The model allows the user to change two factors in order to scale the volume of sediment that is transported by the river. One of the factors is used to scale the bed load transport while the other scales the suspended sediment transport.

The perfect scenario would have been to use sediment samples that were taken over at least 3 – 5 years to calibrate the sediment transport. As there are no such data available only the samples that were taken during 2003 was used. These samples are only representative of 2003; it was therefore used to calculate a sediment yield for only 2003. The calibration factors were adjusted so that the sediment yield that was calculated from the simulated values for 2003 matches the measured sediment yield at the above mentioned gauging stations.

Figure 9-8 and **Figure 9-9** shows the measured and simulated sediment rating curves at Hermon and Drieheuwels, respectively. These figures were used to check that the gradient of the simulated rating curves have the same order of magnitude than that of the measured rating curves. No such curve could be plotted for the Paarl (G1H020) gauging station due to the fact

that the measured discharge is incorrect. The incorrect discharge will cause the gradient of the measured values to be incorrect and incomparable to the simulated values.

From **Figure 9-8** and **Figure 9-9** it can be seen that the simulated values differ from the measured values at low discharges. As was discussed previously only two fractions of sediment were used during the simulations in MIKE11, whereas in reality there is a range of sediment that can be transported. The fine fraction (0,03mm) that was used to simulate the sediment fines does not represent the smaller particles that are available in the field for transportation; therefore, at low flows there are insufficient particles for transportation in the mathematical model.

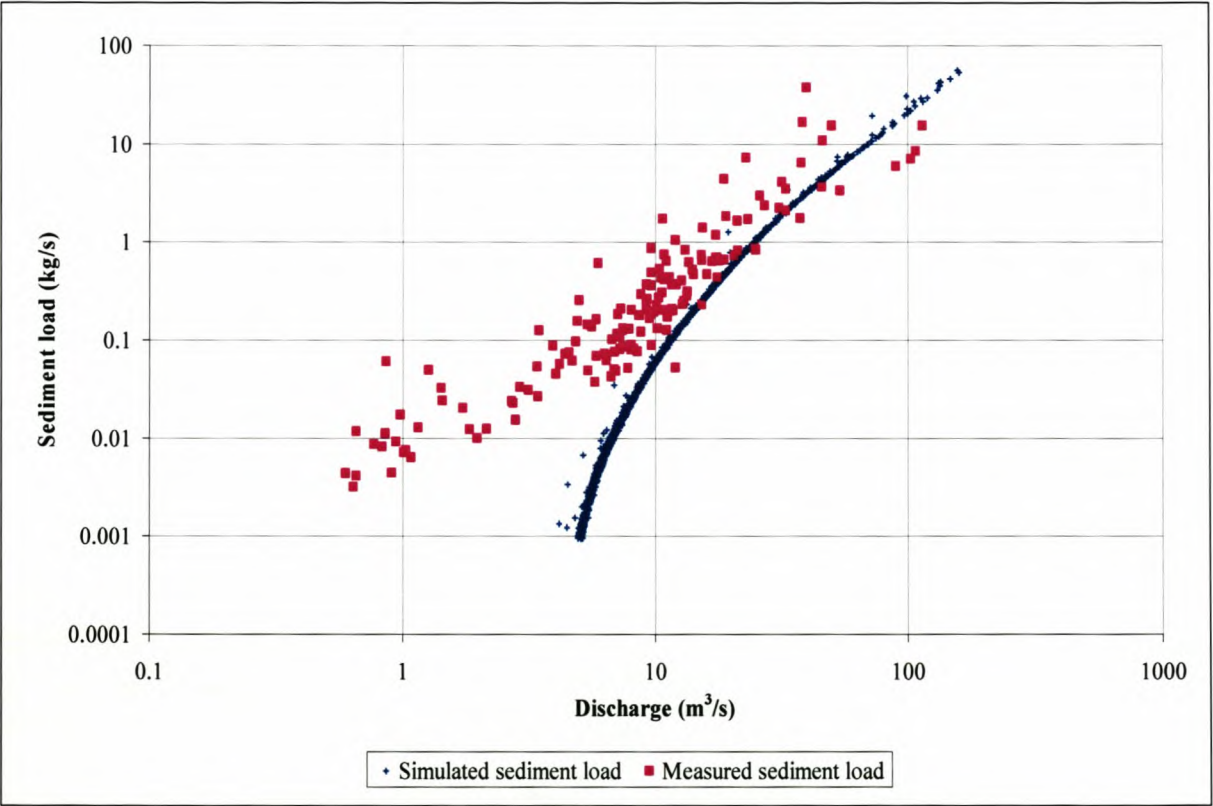


Figure 9-8 Sediment load rating curve at Hermon (G1H036)

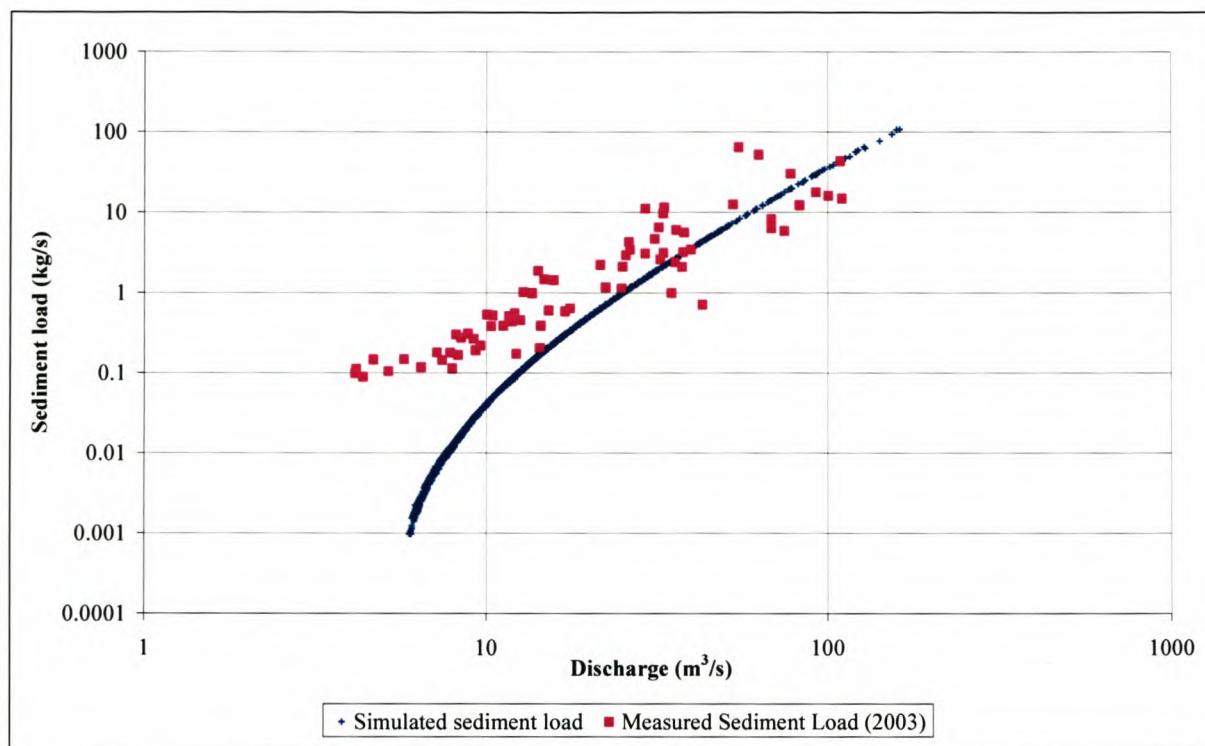


Figure 9-9 Sediment load rating curve at Drieheuvels (G1H013)

The sediment transport model takes some time to stabilize and reach a state of equilibrium. Therefore the simulations that were done for the calibration could not be carried out over only one year. It was decided to do the simulations over the whole study period, as there were also numerical instability problems that had to be solved prior to calibration.

Table 9-5 shows the factors that were used to obtain the desired sediment yield (also shown in the table) at the various locations.

Table 9-5 Factors used to calibrate the sediment transport

River Section	Calibration Factor		Sediment Yield – 2003
	Suspended load	Bed load	
Km 2.2 – Paarl	0.05	0.05	9 ton/km ² calculated at G1H020
Paarl – Hermon	0.041	0.041	5 ton/km ² calculated at G1H036
Hermon – 188.4	0.035	0.035	6 ton/km ² calculated at G1H013

The calibration factors as given in **Table 9-5** were applied to the specified river reach (Column 1) in order to obtain the measured sediment yield during 2003 at the various gauging stations (Column 4).

9.2.2 Verification

The lack of data prevented any real verification of the calibration of the sediment transport model. However the samples that were taken during the winter of 2004 were used to verify the sediment yields that were calculated from the data obtained in 2003. If samples were taken during a wet year the calculated sediment yield will differ from that of samples taken during a dry year. Therefore it should not be expected that the calculated sediment yields of the two years be the same, but it should at least be more or less in agreement, as both these years were relatively dry.

The simulated sediment rating curves for an extended period (1997 – 2003) were plotted at Hermon (G1H036) and Drieheuwels (G1H013) in order to verify that the gradients of the measured and simulated values were still of the same magnitude (**Figure 9-10** and **Figure 9-11**). These figures were also used to ensure that no abnormalities or instabilities existed in the sediment transport model.

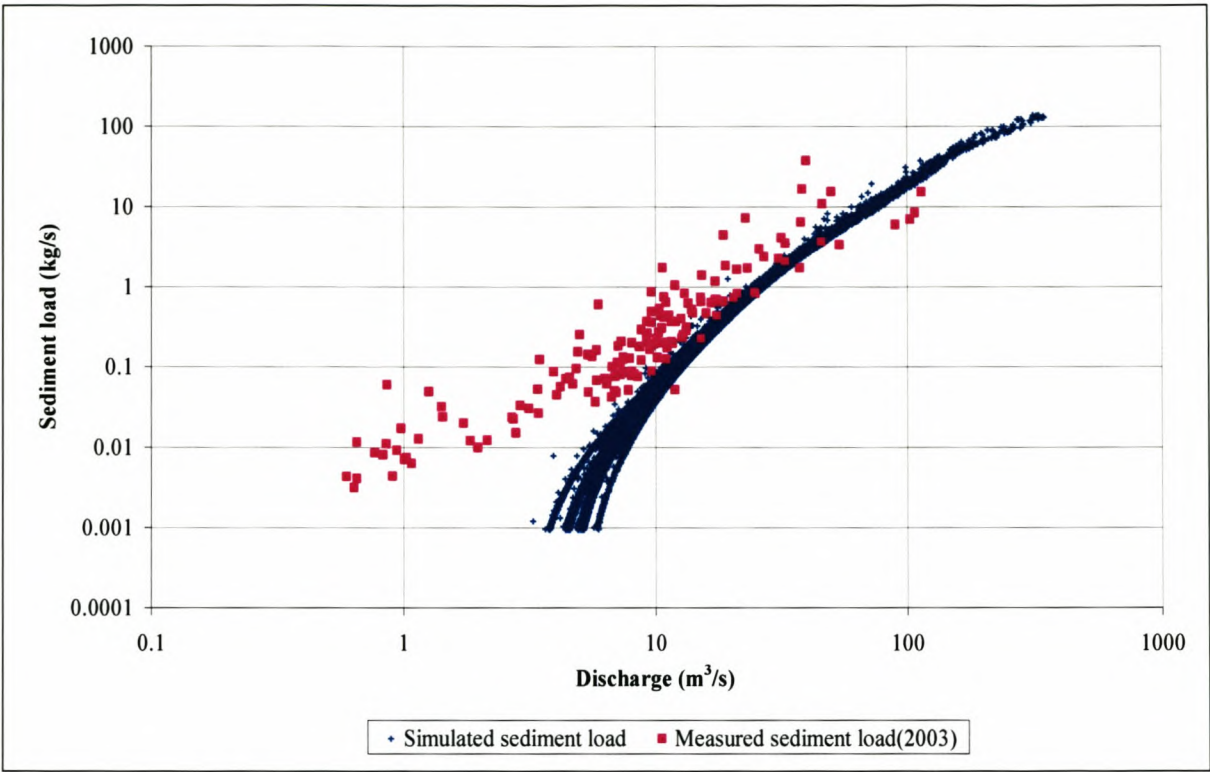


Figure 9-10 Sediment load verification at Hermon (G1H036)

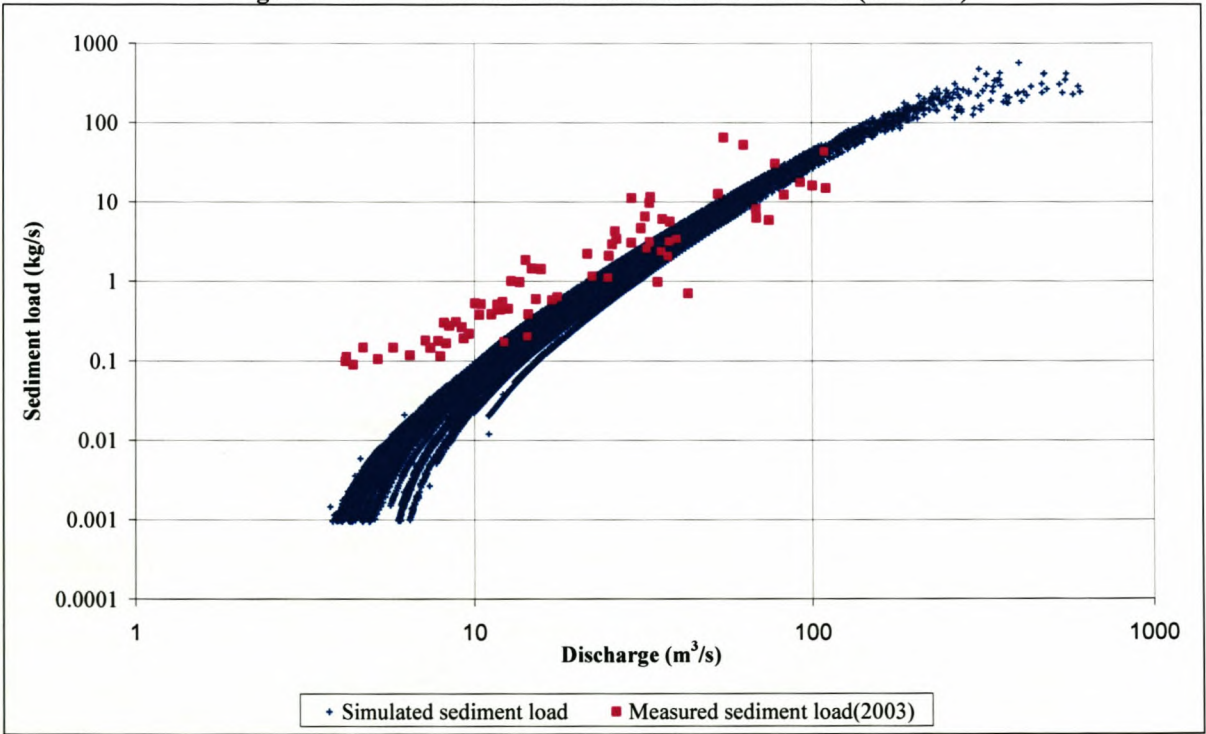


Figure 9-11 Sediment load rating curve verification at Drieheuwels (G1H013)

CHAPTER 10 SIMULATION OF SCENARIOS

10.1 Hydrodynamic Model Simulation Results

10.1.1 Return Period Floods

The floods with return periods of between 2, 10 and 20 years have been calculated for two of the three scenarios (present and post-dam), based on the 9-year simulation period with the aid of statistical methods (**Table 10-1**). These methods are based on the maximum annual flood peaks during the 9-year period. Software developed by Alexander (1991) was used to calculate the return period floods. The probability distribution providing the best fit for all the data was log-General Extreme Value (LGEV). The return period floods for the flood release scenario were not calculated because the data are not statistically independent. The return period floods thus calculated are based only on the 9-year flow sequence of 1995 to 2003, and any return period floods based on a longer period of time could of course be different to the ones listed in **Table 10-1**, however, it is only the relative differences between the two scenarios that are really important. The return period floods, as based on the long-term flow records at G1H004, G1H036 and G1H013 are listed in **Table 10-2**.

From **Table 10-1** it can be seen that for all the sites the dam has a noticeable impact on the magnitude of the larger floods (due to flood attenuation and removal of many floods as a result of the dam operation). At sites BRM 2 and BRM 3, however, the decrease in return period floods of between 2 and 20 years is significant. The post-dam 1:2-year flood peak at BRM2 is only 3% of the present flood peak, while the 1:20-year flood peak is only 41% of the flood peak at present. The differences towards BRM 5 and BRM 6 are not as pronounced, although the post-dam 1:2-year flood peak at BRM 6 is still only 83% of the flood peak at present. This is probably because the floods from the upper reaches would have made little contribution to the larger floods at BRM 5 and BRM 6 to begin with, so that when these floods are reduced the tributaries still contribute the most to the larger floods.

Table 10-1 Return period floods for two scenarios at BRM2, BRM3 BRM4, BRM5 and BRM6 (based on 9-year record)

BRM Site	Flood Recurrence Interval (years)	Present [m ³ /s]	Post Dam [m ³ /s]*
BRM 2	2	170	5
	10	265	60
	20	280	115
BRM 3	2	220	80
	10	355	175
	20	400	225
BRM 4	2	245	140
	10	435	310
	20	505	385
BRM 5	2	335	250
	10	670	550
	20	805	680
BRM 6	2	400	330
	10	920	845
	20	1150	1120

*: Without flood releases

Table 10-2 Return period floods based on total flow record at Driefontein (G1H004), Hermon (G1H036) and Drieheuwels (G1H013)

Recurrence interval (yr)	G1H004 [m ³ /s] (54-yr record)	G1H036 [m ³ /s] (25-yr record)	G1H013 [m ³ /s] (39-yr record)
2	215	230	265
10	415	460	595
20	500	555	720
50	615	690	860
100	710	805	950

10.1.2 Flood Attenuation

Flood attenuation along the Berg River for the present and post-dam scenarios was investigated by routing three flood hydrographs with different flood peaks of 100, 160 and 220 m³/s, respectively, from the dam site to the head of the estuary, without any other tributary inflows. This was done mainly to determine the significance of the artificial flood releases at the lower BRM sites. The effect of tributary floods being in phase with the released floods was determined by adding initial flows of 2, 20 or 50 m³/s to the three floods. The return periods of the three floods at BRM 2 are listed in **Table 10-3** together with the flood magnitudes at BRM 4 and BRM 6 for the same return periods. **Table 10-4** lists the attenuated flood peaks for the present

day scenario at BRM 4 and the head of the estuary (see also Figures 7.18 to 7.20). It can be seen that with a higher initial flow the attenuation is not as pronounced because the main channel does not need to be filled. This shows that it is important to ensure that the flood releases are made in phase with tributary floods, otherwise the flood attenuation is too great and the effectiveness of the artificial flood releases is reduced significantly. The annual flood peak at BRM4 is about 180 m³/s, so if the 100 m³/s flood is released in phase with a tributary flood, the resulting flood peak at BRM 4 is at least half the magnitude of the annual flood, whereas without any tributary floods, the resulting flood peak would only be about a quarter of the annual flood.

Table 10-3 Flood peaks and return periods at BRM 2, with corresponding recurrence interval flood peaks at BRM4 and BRM6

Flood Peak (m ³ /s) at BRM2	Return period (yrs)	Flood Peak (m ³ /s) at BRM4	Flood Peak (m ³ /s) at BRM6
100	1	180	220
160	2	250	400
220	4	320	600

Table 10-4 Simulated attenuated flood peaks at BRM4 (Hermon) and head of estuary with different initial flows for the present day scenario

Flood Peak (m ³ /s) at BRM2	BRM4			Head of estuary		
	2 m ³ /s initial flow	20 m ³ /s initial flow	50 m ³ /s initial flow	2 m ³ /s initial flow	20 m ³ /s initial flow	50 m ³ /s initial flow
100	49	72	86	22	46	70
160	89	114	129	37	66	93
220	132	159	172	53	87	117

From **Figure 10-1** to **Figure 10-3** it can also be seen that not only is the flood peak attenuated, but the lag is affected as well. When the flood is released in phase with tributary floods, the lag between the flood at BRM 4 and at the dam site is about 16 hours, while if it is not released in phase; the lag would be about 24 hours. At the head of the estuary the difference is even more pronounced.

For the post-dam scenario (**Table 10-5**), the flood attenuation at low initial flows is not as pronounced as it was for the present day scenario, because the cross-sections are now smaller (see 8.2.1.2). The main channel therefore fills up more quickly than it did for the present scenario, which means that the flood travels more quickly, without being attenuated to such a degree. At higher initial flows the attenuation is much the same for both scenarios because the

high initial flow ensures that the main channel is already filled when the actual flood arrives, which means that the effect of the narrowed cross-sections is limited. It can be seen from **Figure 10-4** to **Figure 10-6** that the lag is also affected by the narrower cross-sections. For example, the lag between the 100 m³/s flood peak at the dam site and BRM 4 is about 2 hours longer with the wider cross-sections.

Table 10-5 Simulated attenuated flood peaks at BRM4 (Hermon) and head of estuary with different initial flows for the post-dam scenario

Flood Peak (m ³ /s) at BRM2	BRM4			Head of estuary		
	2 m ³ /s baseflow	20 m ³ /s baseflow	50 m ³ /s baseflow	2 m ³ /s baseflow	20 m ³ /s baseflow	50 m ³ /s baseflow
100	54	74	85	23	47	70
160	96	118	130	38	67	94
220	141	163	175	54	89	119

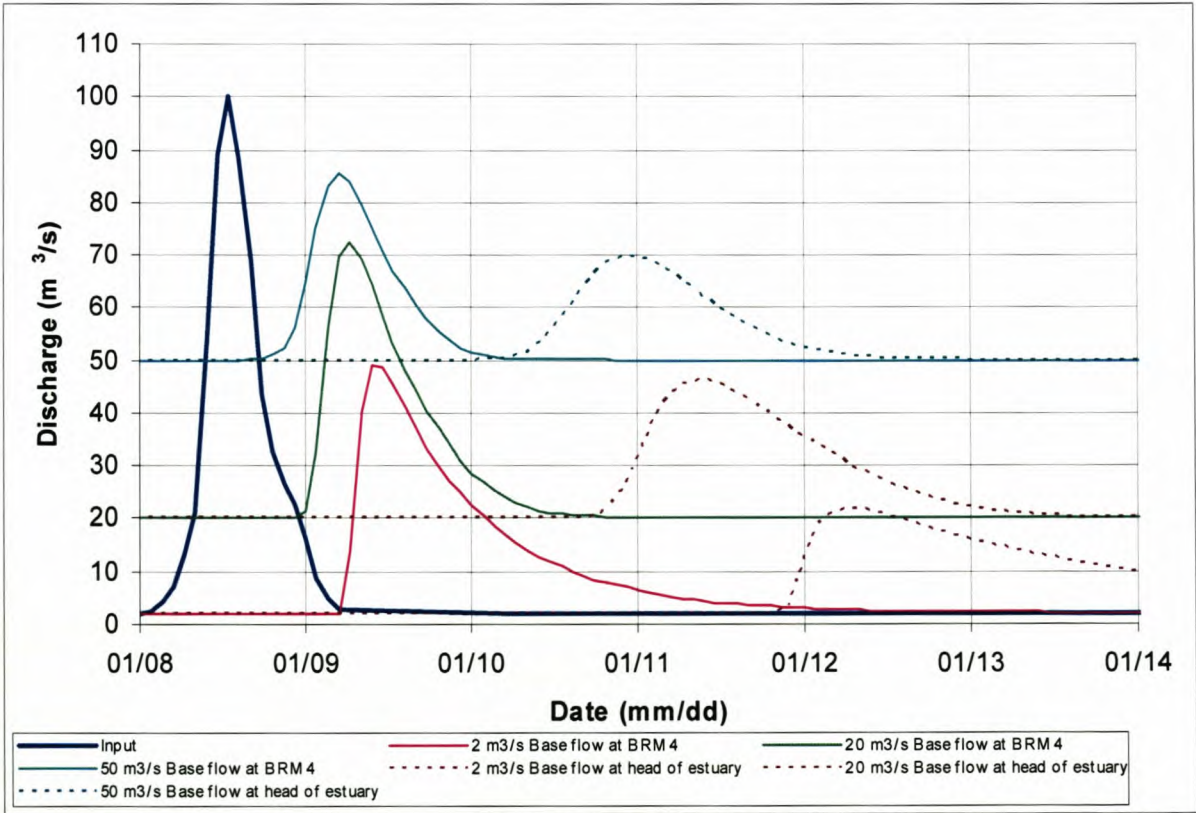


Figure 10-1 Attenuation of 100 m³/s flood peak with different initial flows at BRM4 and head of estuary for present scenario

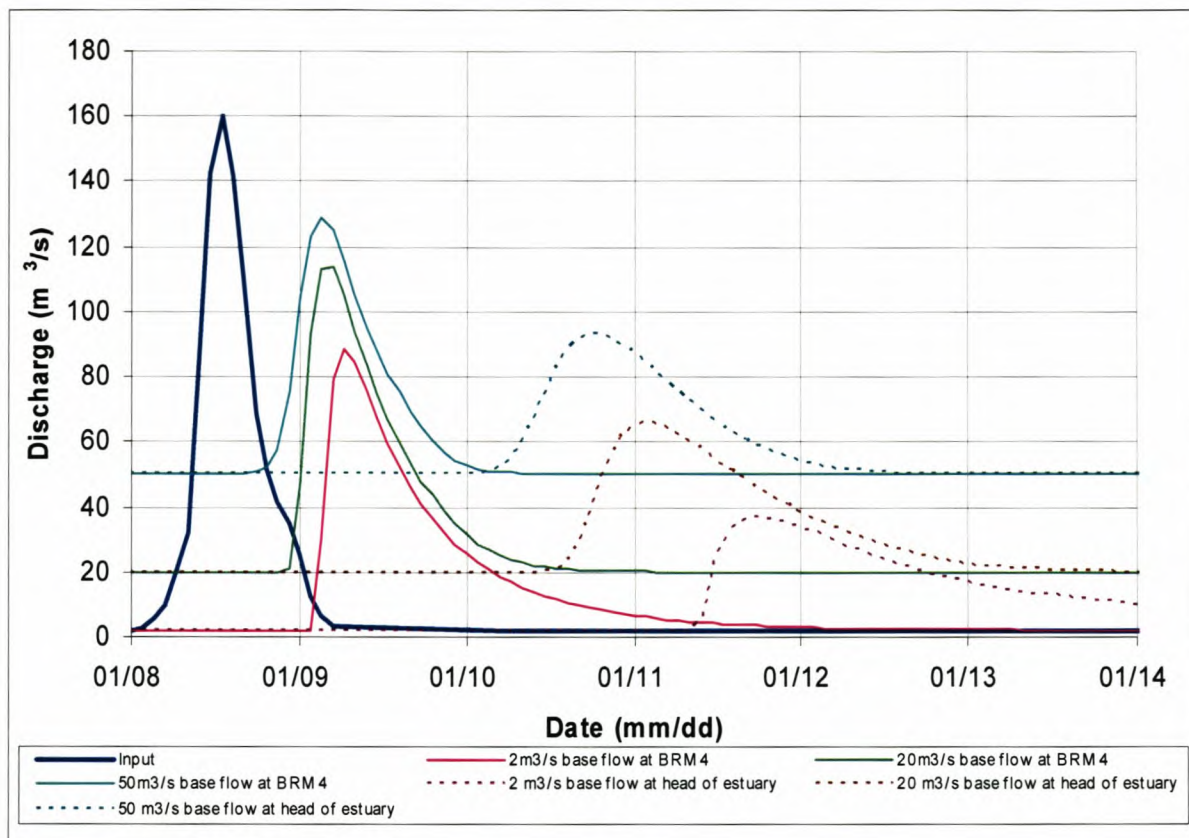


Figure 10-2 Attenuation of 160 m³/s flood peak with different initial flows at BRM4 and head of estuary for present scenario

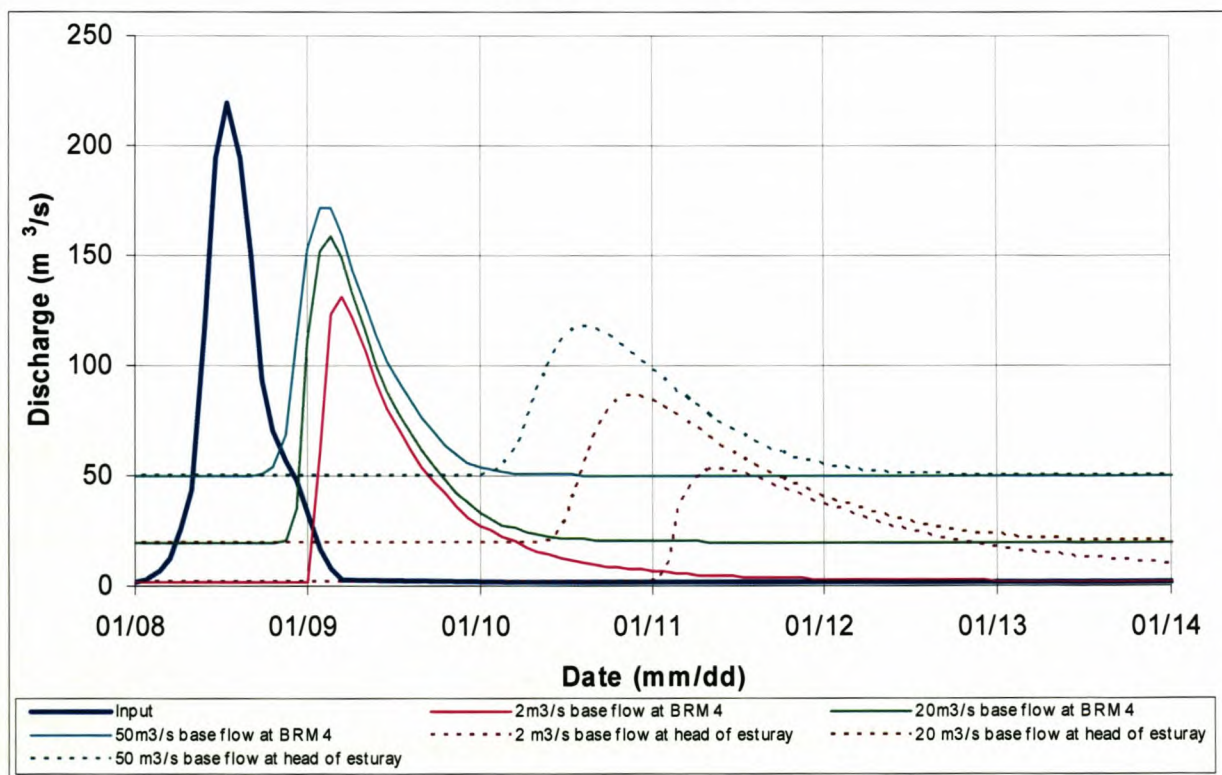


Figure 10-3 Attenuation of 220 m³/s flood peak with different initial flows at BRM4 and head of estuary for present scenario

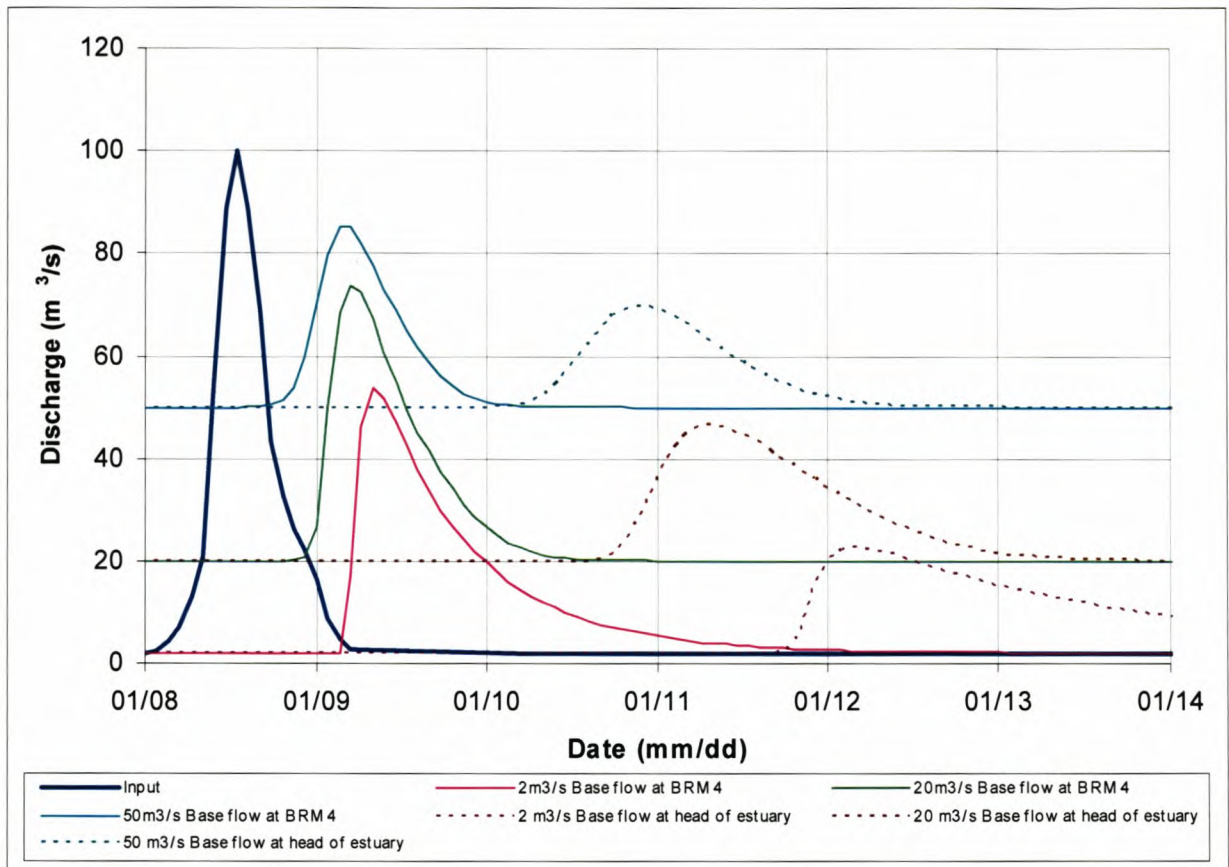


Figure 10-4 Attenuation of 100 m³/s flood peak with different initial flows at BRM4 and head of estuary for the post-dam scenario

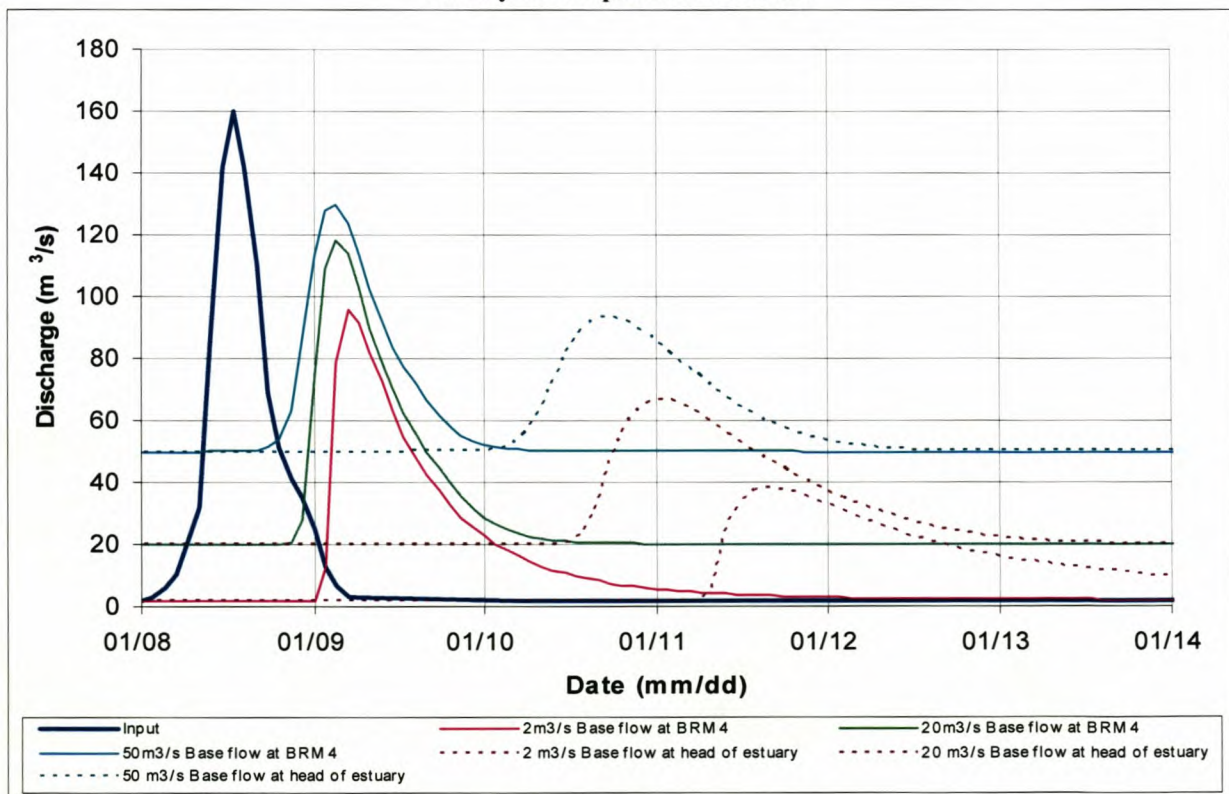


Figure 10-5 Attenuation of 160 m³/s flood peak with different initial flows at BRM4 and head of estuary for the post-dam scenario

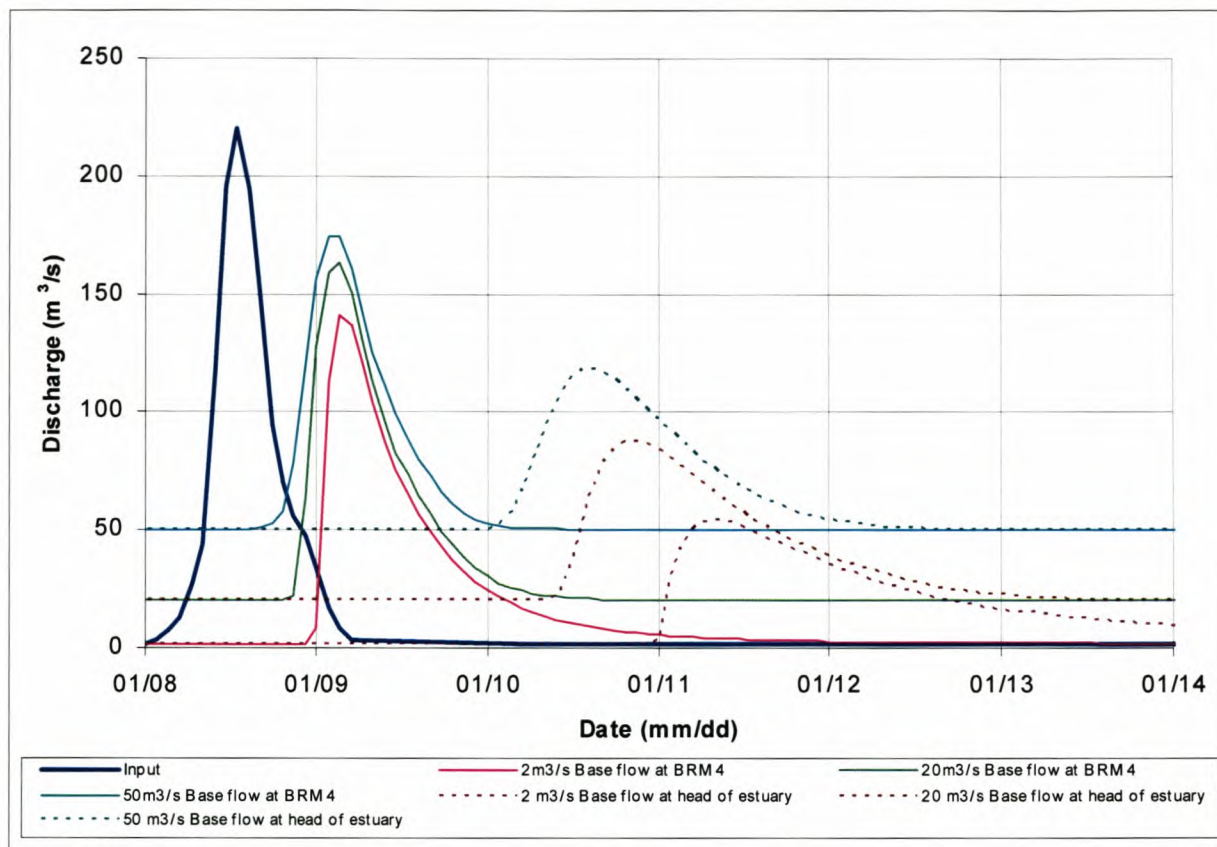


Figure 10-6 Attenuation of 220 m³/s flood peak with different initial flows at BRM4 and head of estuary for the post-dam scenario

10.1.3 Hydraulic Parameters

To illustrate the differences between the three scenarios (present, post-dam and post-dam with floods) several graphs and tables are presented for each BRM site. These include:

- simulated 9-year flow series for each scenario (based on instantaneous peak data)
- frequency curves (based on instantaneous peak data), which were generated for several hydraulic parameters (discharge, flow depth, velocity), based on the simulated data from the numerical model; these include:
 - discharge - frequency graph
 - flow depth - frequency graphs
 - flow velocity - frequency graph
- floodplain level and the bankfull discharge, shown on the flow depth – frequency graphs.
- floodplain inundation - the number of days per year during which the floodplain is inundated, calculated as a mean value of the three main transects at each site for the whole site. The floodplain level is taken as the lowest floodplain bank level at three cross-sections at each site.

10.1.3.1 Site BRM 2

Simulated 9-year flow series for each scenario are given in **Figure 10-7** to **Figure 10-12**. Because of the operating procedure adopted the dam will spill in only four of the nine years simulated without any flood releases. For very long periods only the IFR flows are present. The largest flood for the post-dam scenario is 77 m³/s compared to 288 m³/s at present. With the flood releases the largest flood is 217 m³/s. From **Figure 10-13** it can be seen that virtually all the flows are affected by the dam development. The large difference between the present and post-dam scenarios for flows of less than 10 m³/s is because at present the irrigation releases are made upstream of BRM2 (see also **Figure 10-7**), whereas for the post-dam scenarios (See **Figure 10-9**) the irrigation releases will be made at or downstream of the Wemmershoek River via a new pipeline from the Berg River abstraction scheme. The same trend can be observed for the flow depth (**Figure 10-14** to **Figure 10-16**) and velocity curves (**Figure 10-17** to **Figure 10-19**), as these two parameters are dependent on the discharge. For the post-dam scenario the flows in class 1 make up almost all the flows, with very little flows left in classes 2 and 3. With the flood releases there will again be flows in class 4 and slightly more flows in class 3 as can be seen in **Table 10-6**.

It can be seen from **Figure 10-14** to **Figure 10-16** that the floodplain (indicated by broken lines) is rarely inundated during the 9-year simulation period (see **Table 10-7**), and no inundation occurs with the dam in place. However, flood releases from the dam have increased the floodplain inundation to almost the same level as at present.

Table 10-6 Contribution of within year floods to total flow for three scenarios at BRM2

Class (DRIFT)	Discharge [m ³ /s] (Instantaneous peaks)	Present	Post-dam	Flood releases
1	0 - 16.2	96.49%	99.91%	99.69%
2	16.2 – 32.6	2.19%	0.07%	0.08%
3	32.6 – 65.3	0.97%	0.02%	0.10%
4	65.3 – 132.1	0.29%	0.0%	0.09%

Table 10-7 Floodplain inundation at BRM2

Scenario	Inundation [days/year]
Present	0.003
Post-dam	0
Flood releases	0.002

The number of large floods of say 100 m³/s and above is under present conditions about 24 (**Figure 10-7**) for the period 1995 to 2003, but there are no floods over 100 m³/s over the same period for the post-dam scenario (**Figure 10-9**). With flood releases from the dam the floods bigger than 100 m³/s at BRM2 will be five, which is still low compared to the present situation, but an improvement over the post-dam situation (see **Table 10-8**).

Table 10-8 Number of floods above 100 m ³ /s for the 9-year period at BRM2			
Discharge [m ³ /s] (Instantaneous peaks)	Present	Post-dam	Flood releases
> 100	24	0	5
> 150	11	0	3
> 200	3	0	2

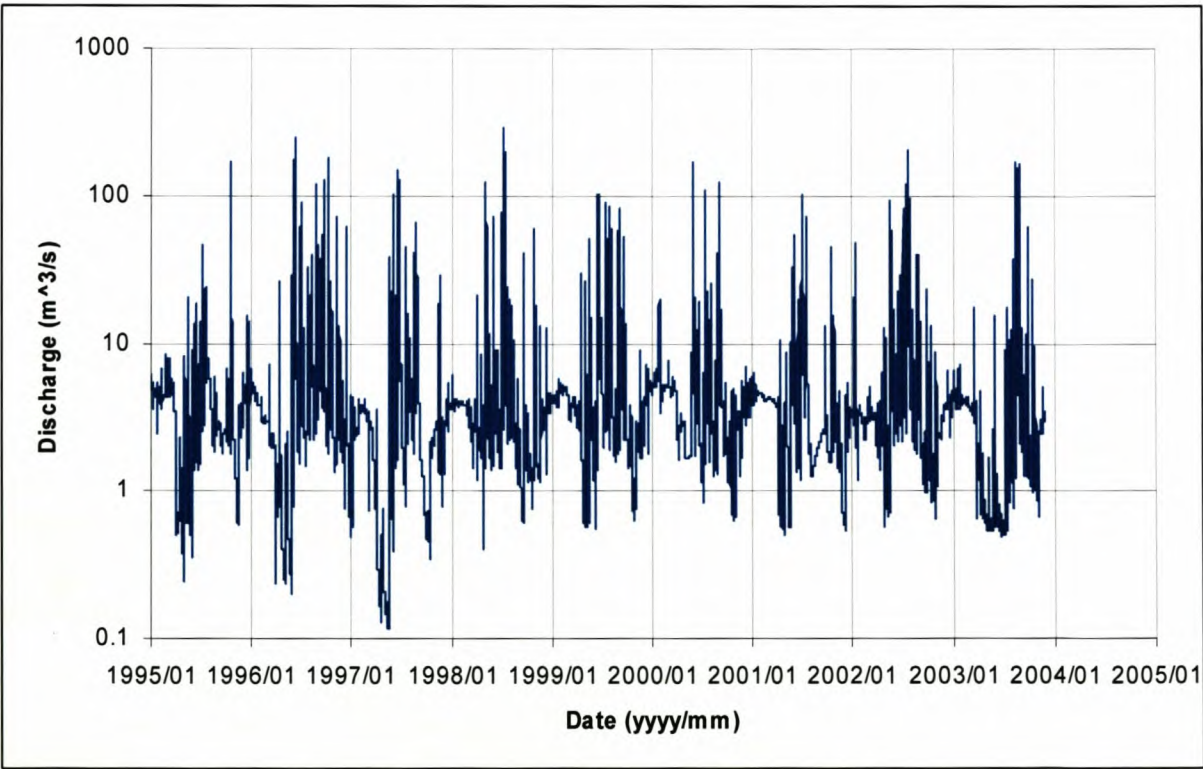


Figure 10-7 Simulated flow series (9-years) at BRM2 – present scenario (instantaneous peak data) – log scale

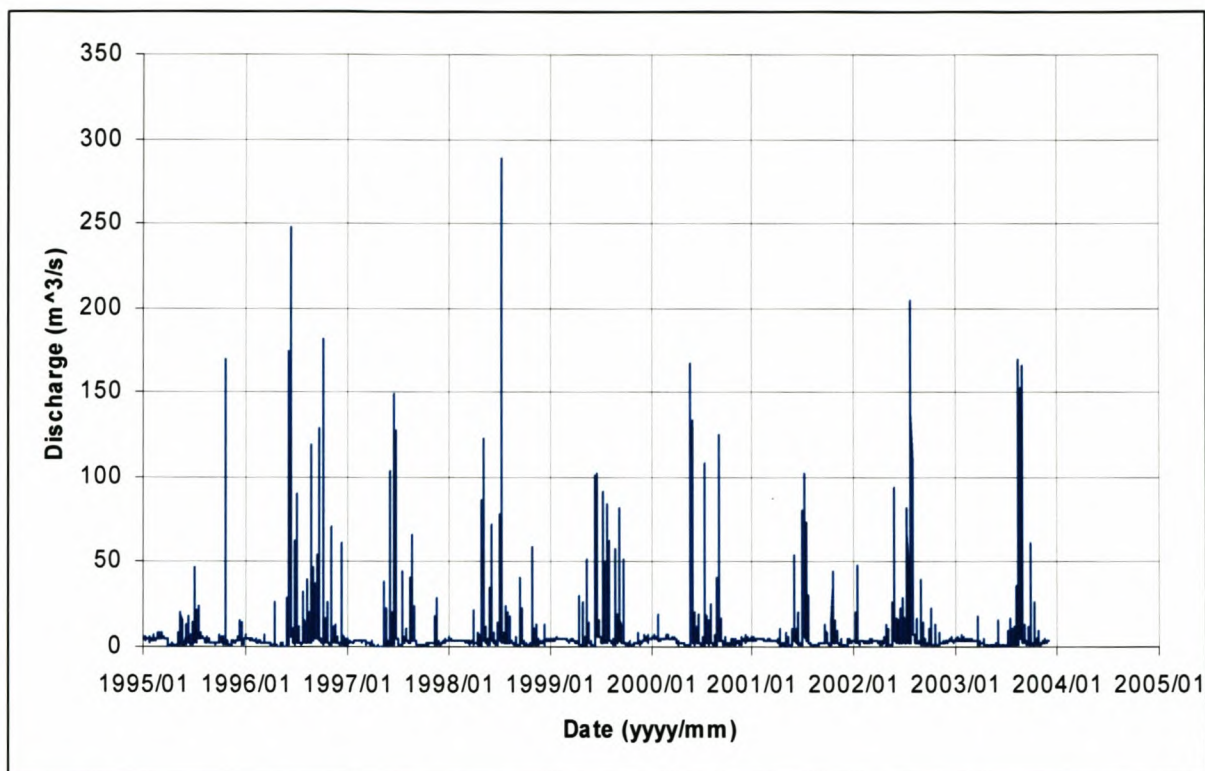


Figure 10-8 Simulated flow series (9-years) at BRM2 – present scenario (instantaneous peak data) – normal scale

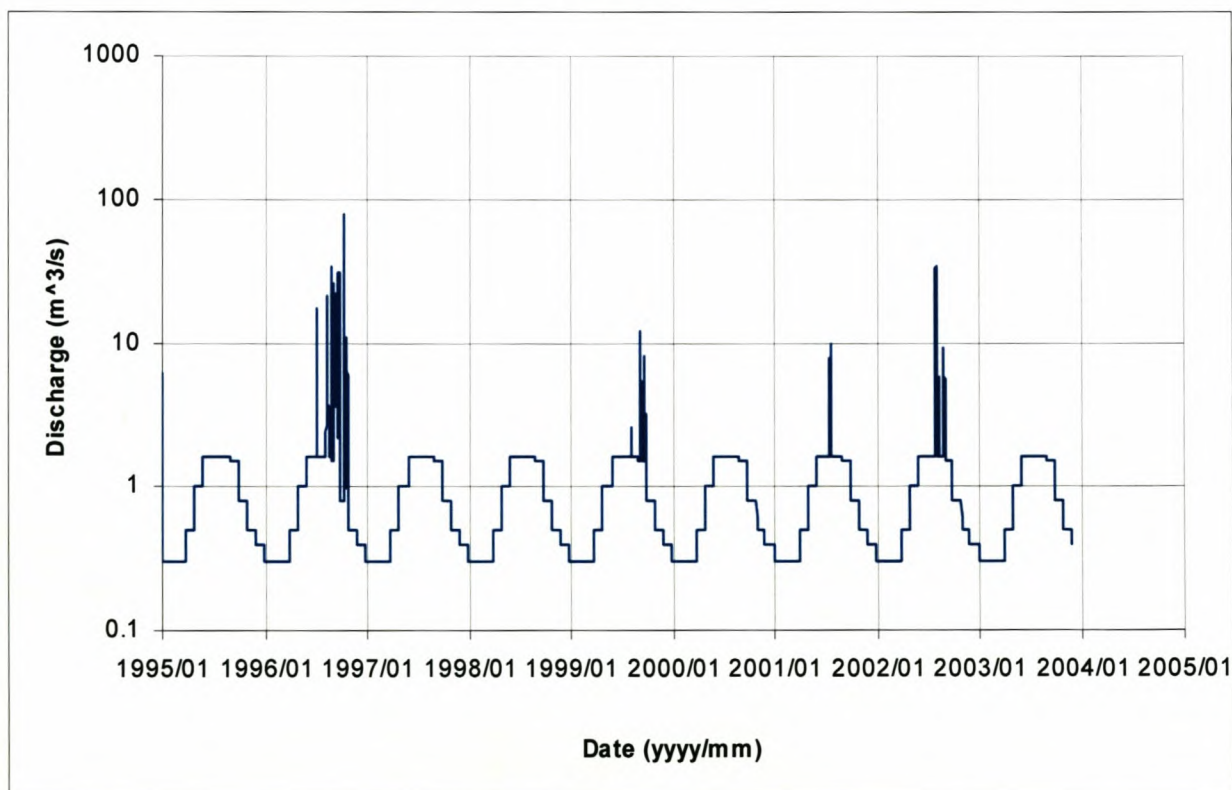


Figure 10-9 Simulated flow series (9-years) at BRM2 – post-dam scenario (instantaneous peak data) – log scale

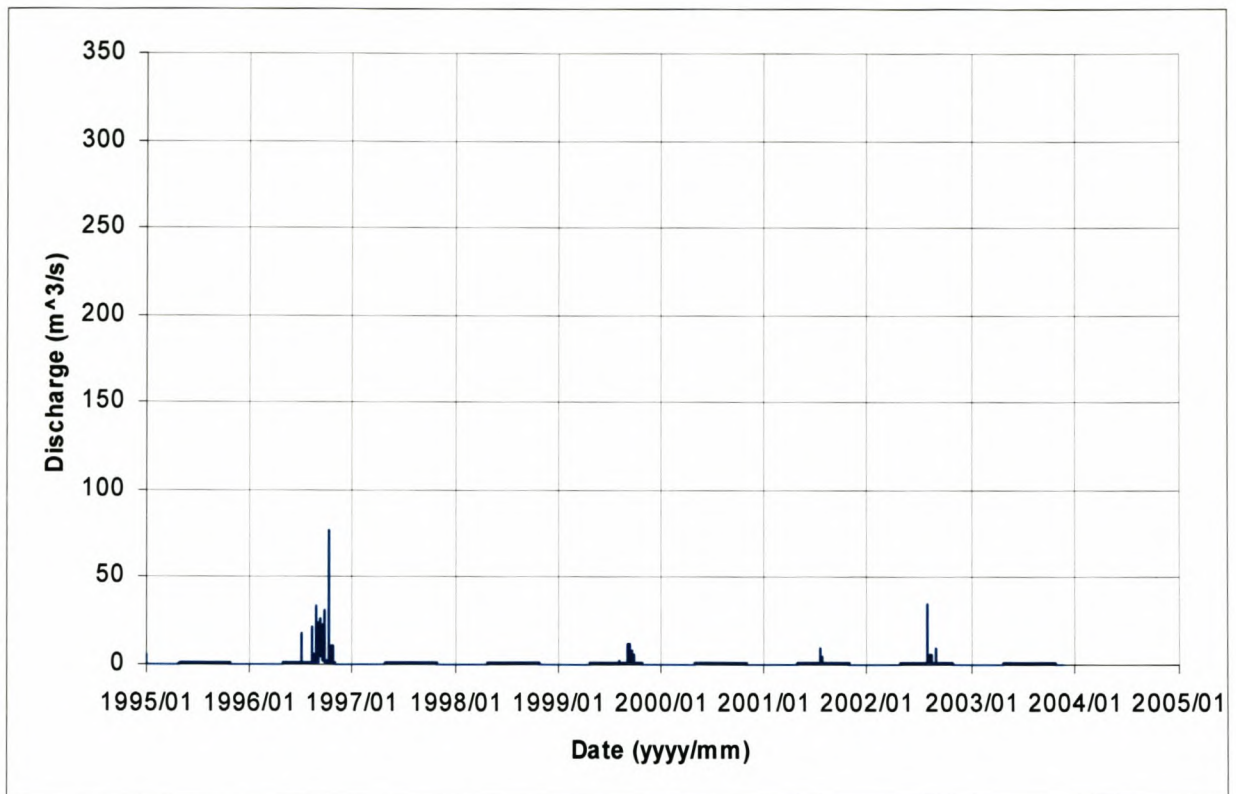


Figure 10-10 Simulated flow series (9-years) at BRM2 – post-dam scenario (instantaneous peak data) – normal scale

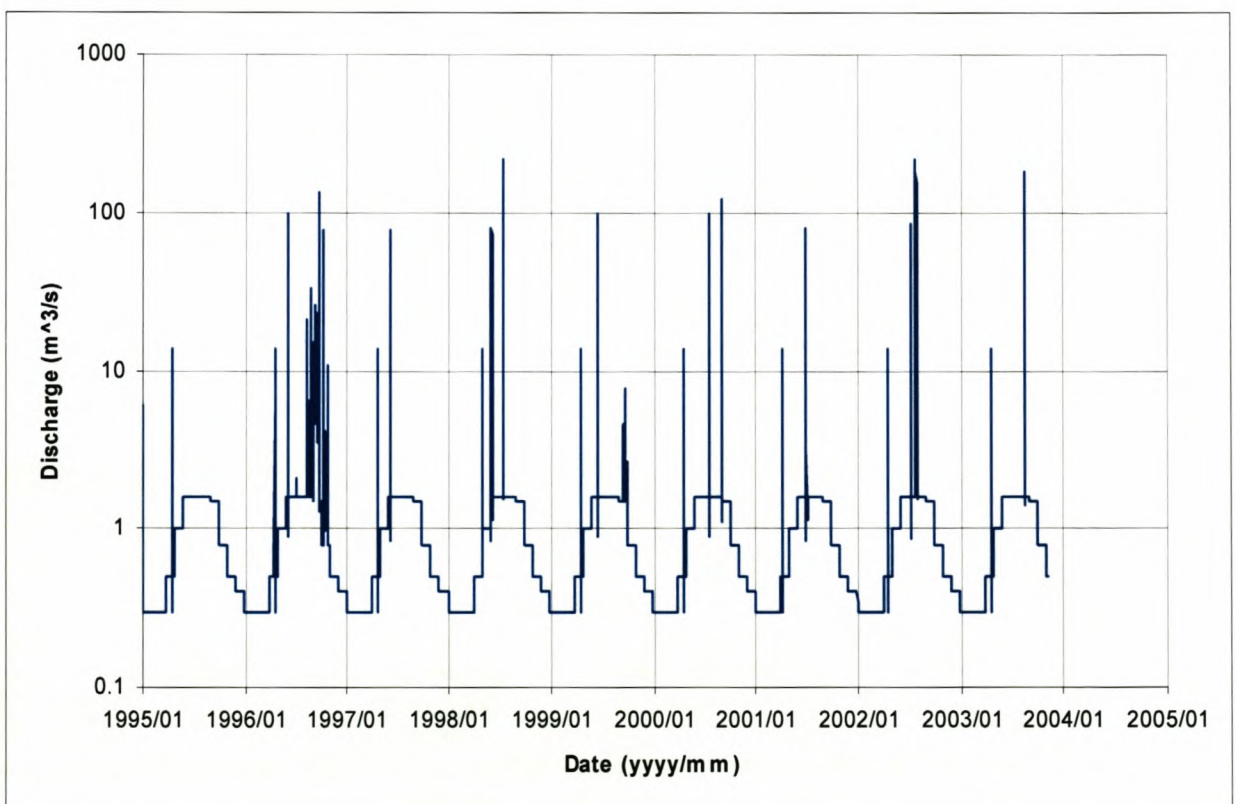


Figure 10-11 Simulated flow series (9-years) at BRM2 – Post-dam with flood releases scenario (instantaneous peak data) – log scale

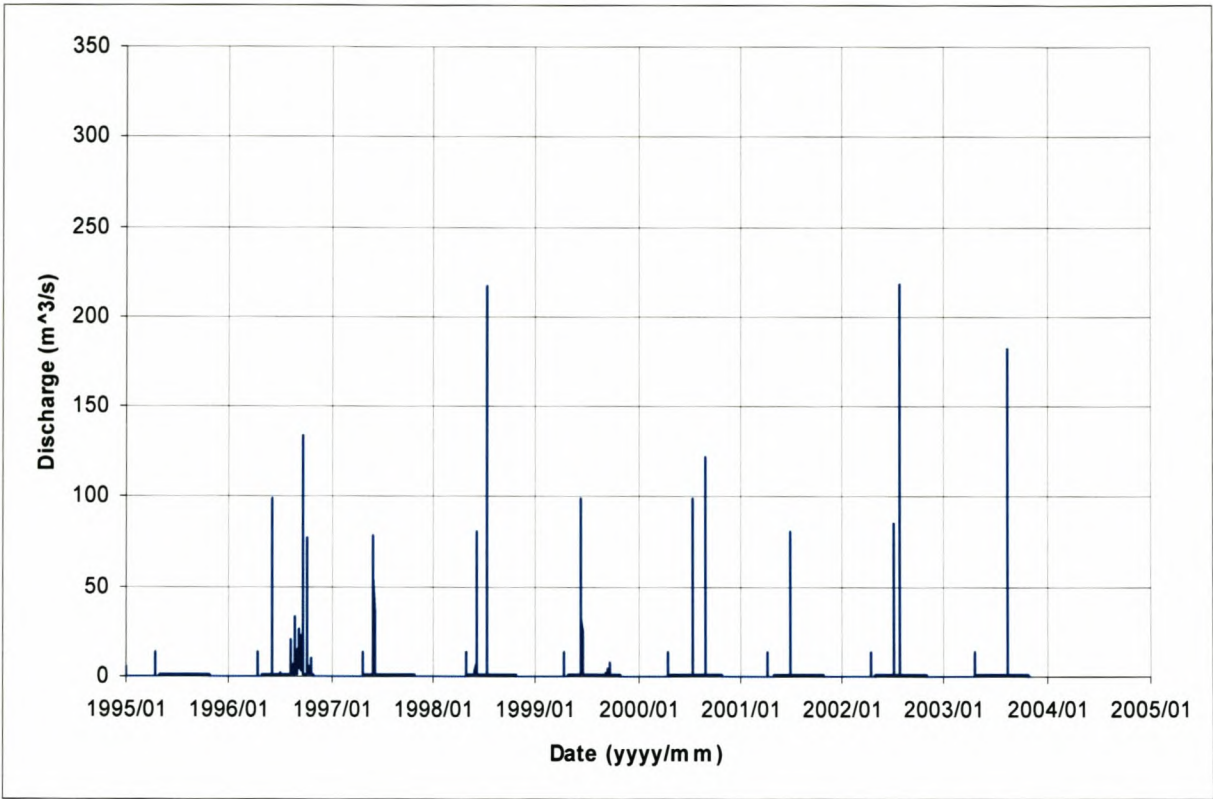


Figure 10-12 Simulated flow series (9-years) at BRM2 – Post-dam with flood releases scenario (instantaneous peak data) – normal scale

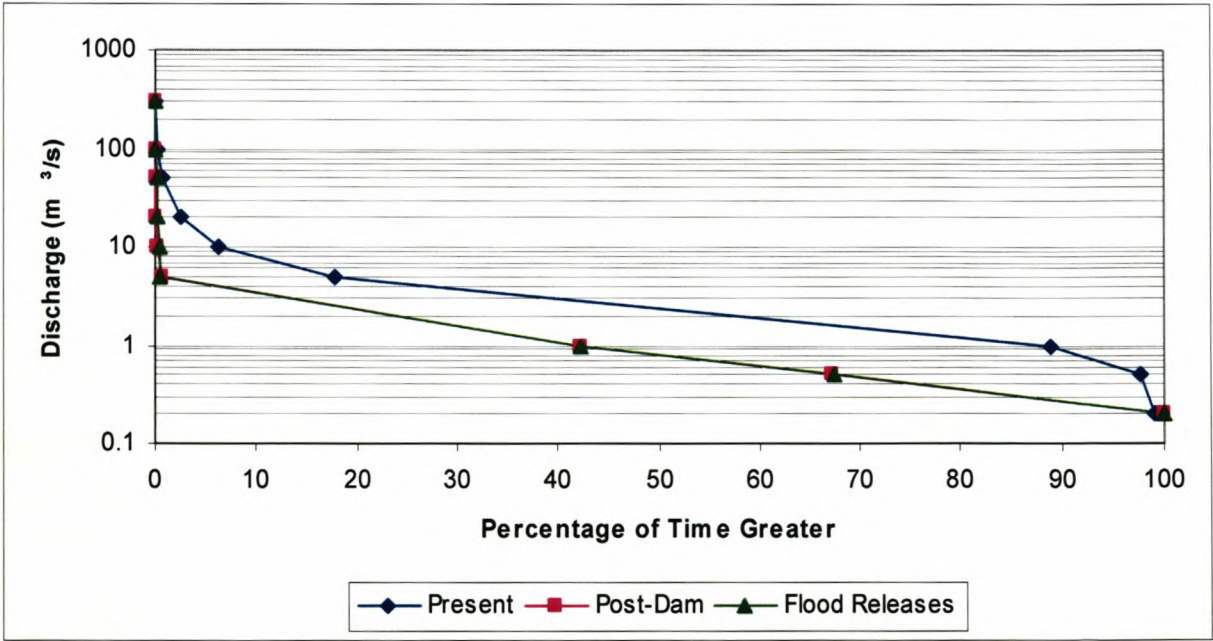


Figure 10-13 Discharge - frequency graph for BRM2

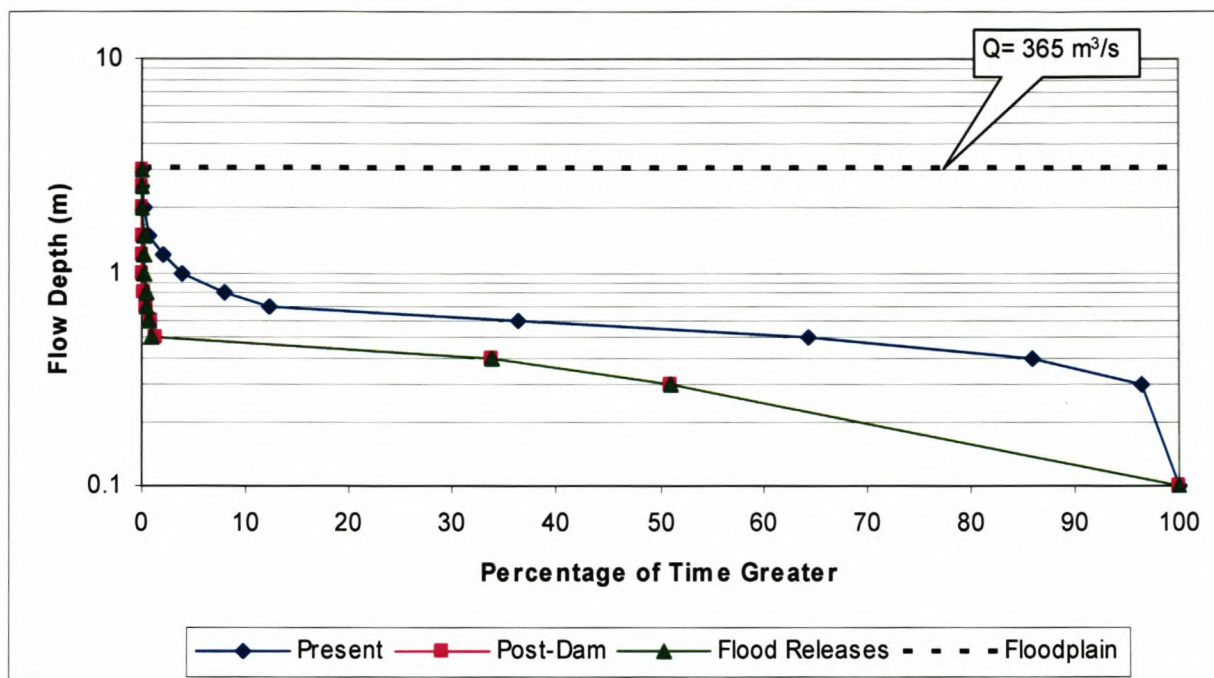


Figure 10-14 Flow depth - frequency graph for BRM2 – transect A

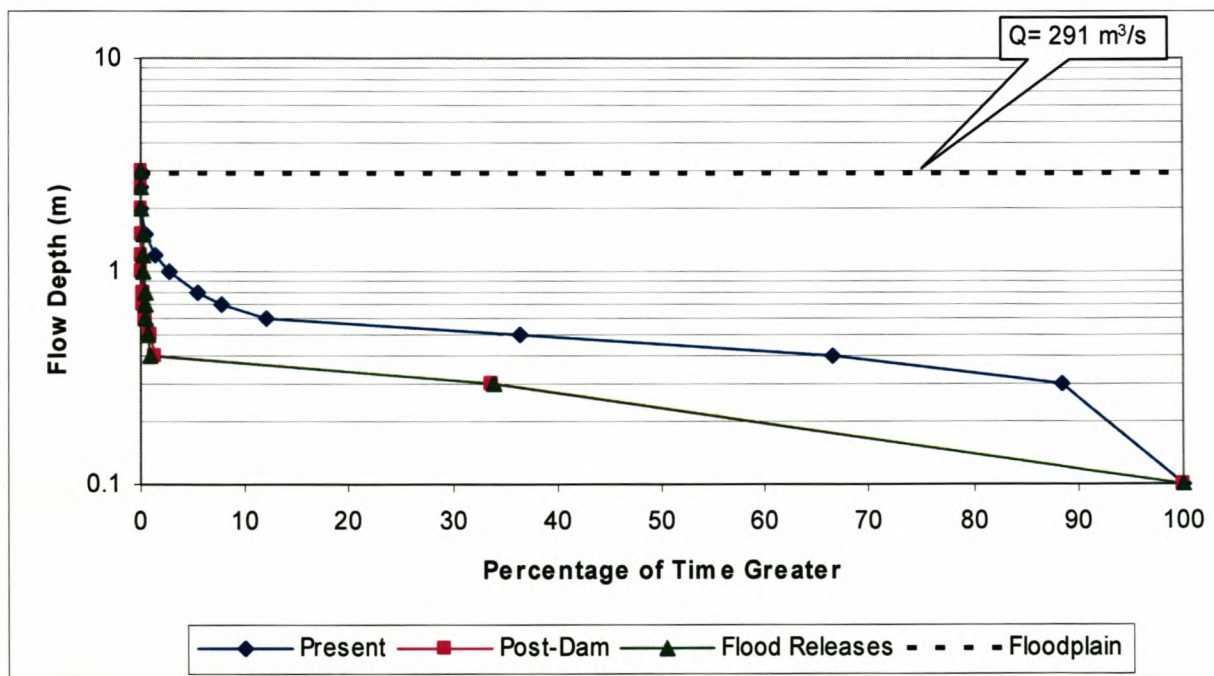


Figure 10-15 Flow depth - frequency graph for BRM2 – transect B

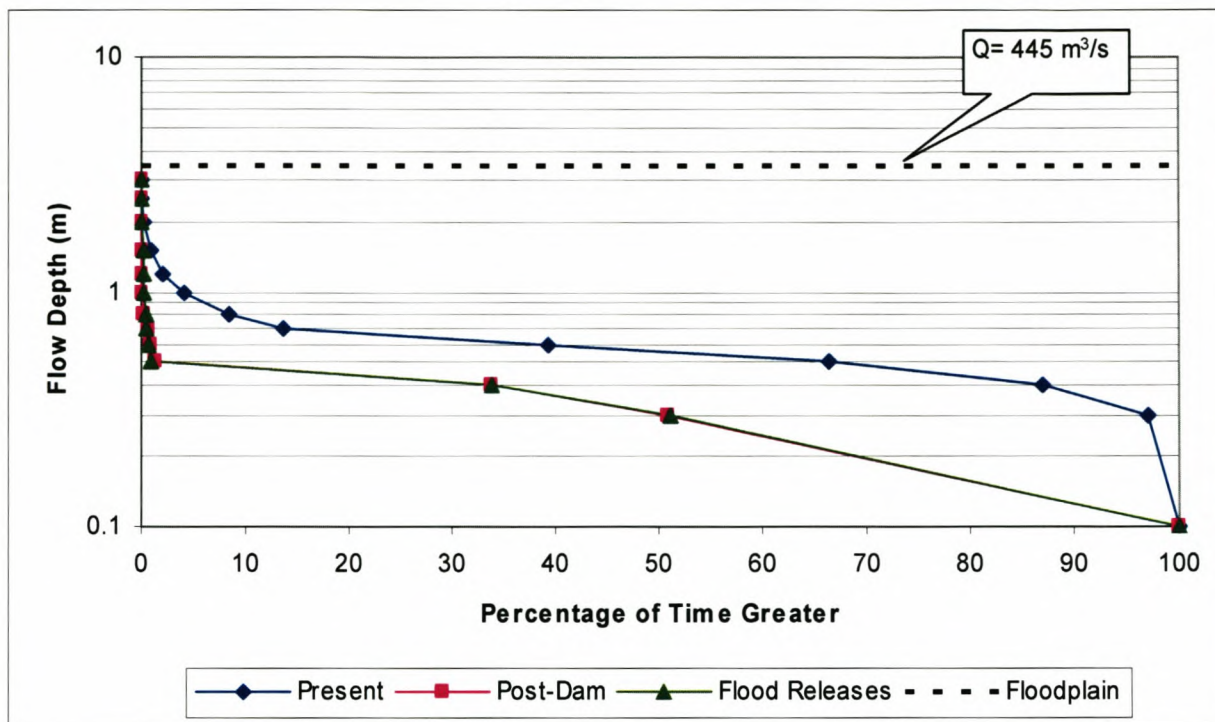


Figure 10-16 Flow depth - frequency graph for BRM2 – transect C

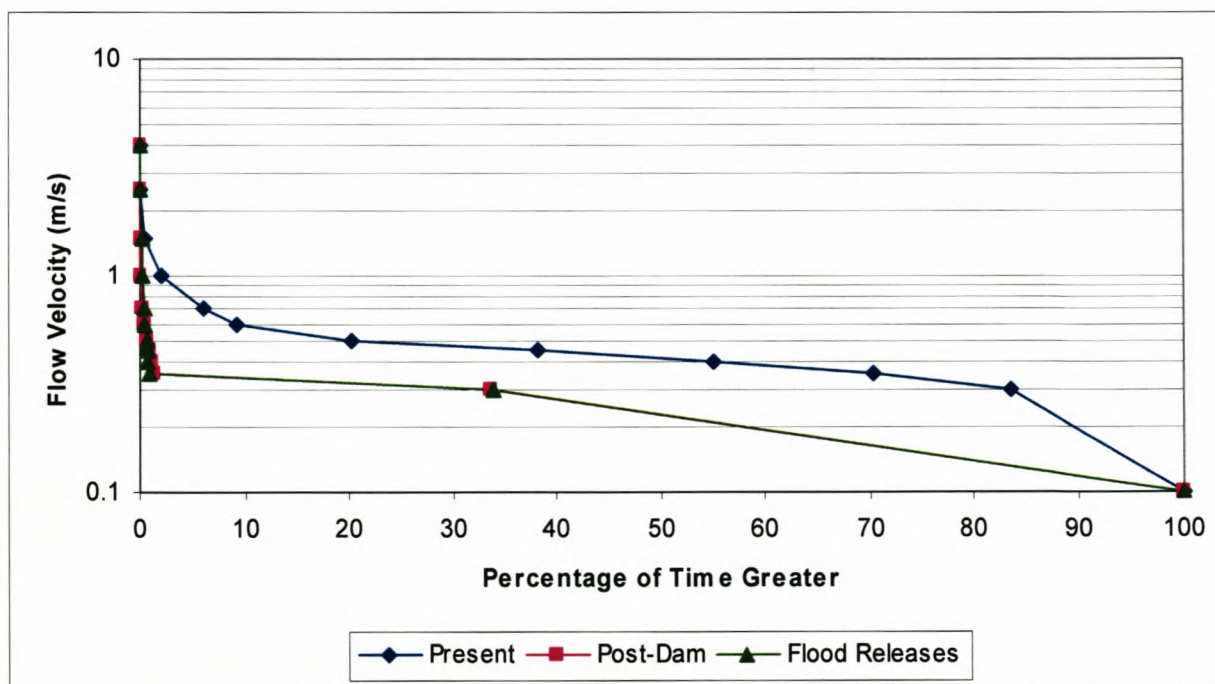


Figure 10-17 Flow velocity - frequency graph for BRM2 – transect A

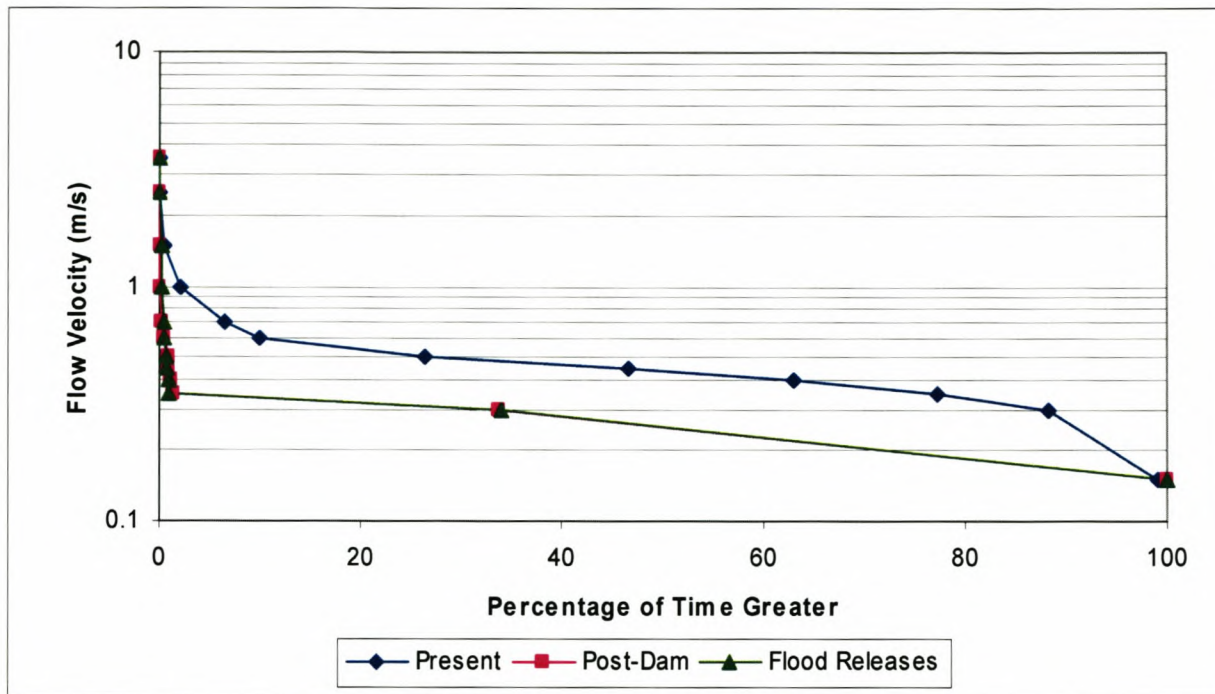


Figure 10-18 Flow velocity - frequency graph for BRM2 – transect B

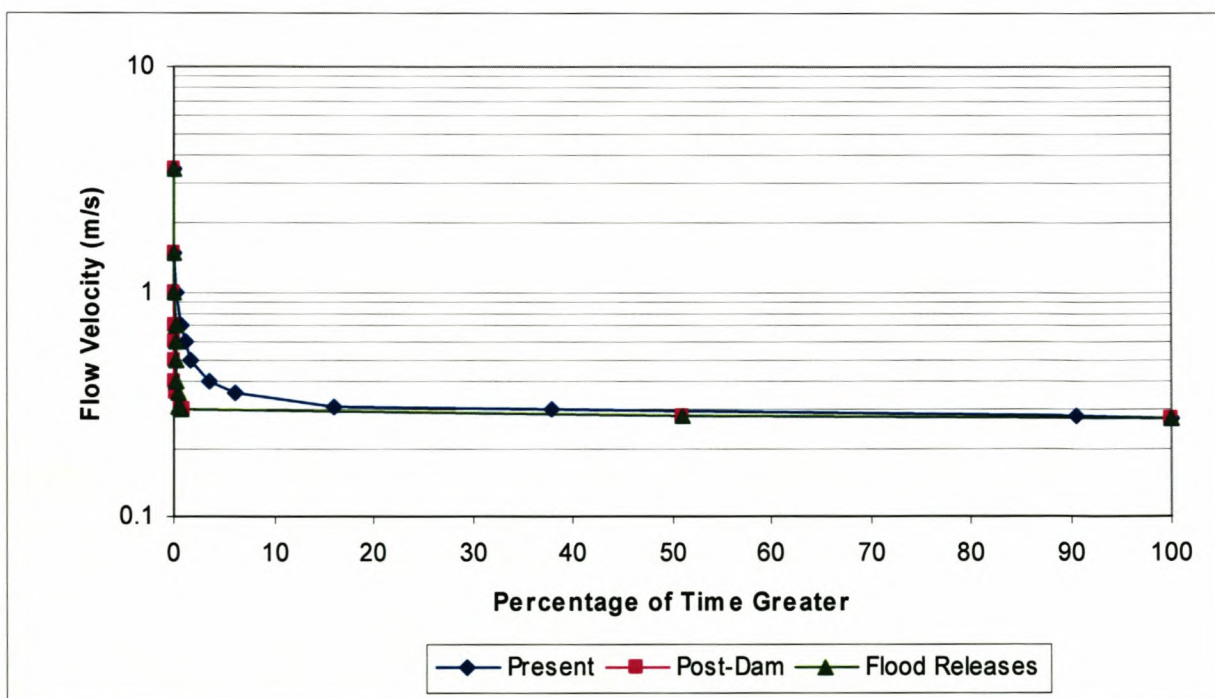


Figure 10-19 Flow velocity - frequency graph for BRM2 – transect C

10.1.3.2 Site BRM3

Simulated 9-year flow series for each scenario are given in **Figure 10-20** to **Figure 10-25**. The above normal low flows at the end of 2000, beginning of 2001, occur because there is a gap in the data from gauging station G1H003, which was used as input from the Franschhoek and Wemmershoek catchments. The gap in the data means that for the five-month period interpolated flows had to be used, which were a bit higher than the usual summer flows.

It can be seen that the number of smaller floods, which arise from the tributaries, is much higher than at BRM2, but there still are long periods of low flows between floods, although the situation is not as pronounced as it was at site BRM2. The largest flood in the nine-year period is 186 m³/s compared to the largest flood at present, which is 398 m³/s. The simulation includes IFR flows and irrigation releases, which is why the frequencies of flows between 2 and 6 m³/s are almost the same for the post-dam scenarios and the present situation (see **Figure 10-26**). The frequency of flows in classes 2 to 3 has decreased dramatically, and more than 99% of the flows fall into class 1, as can be seen in **Table 10-9**. The flood releases (falling into classes 3 and 4) have caused the contribution of classes 3 and 4 to increase above that of the post-dam scenario. The same trend can be observed on the flow depth (**Figure 10-27** to **Figure 10-29**) and velocity curves (**Figure 10-30** to **Figure 10-32**), as these two parameters are dependent on the discharge.

It can be seen from **Figure 10-27** to **Figure 10-29** that the floodplain (indicated by broken lines) is not inundated very frequently during the 9-year simulation period, and that without the flood releases the floodplain is inundated very rarely (see **Table 10-10**). The flood releases have managed to double the floodplain inundation of the post-dam scenario, but it is still only about a quarter of the inundation at present.

Table 10-9 Contribution of within year floods to total flow for three scenarios at BRM3

Class (DRIFT)	Discharge [m³/s] (Instantaneous peaks)	Present	Post-dam	Flood releases
1	0 – 37.6	97.57%	99.655%	99.49%
2	37.6 – 75.2	1.77%	0.32%	0.34%
3	75.2 – 150.4	0.55%	0.02%	0.12%
4	150.4 – 300.8	0.10%	0.005%	0.05%

Table 10-10 Floodplain inundation at BRM3

Scenario	Inundation [days/year]
Present	5.4
Post-dam	0.5
Flood releases	1.2

Similar to BRM2 simulations, the number of floods above 100 m³/s reduces considerably from present to post-dam conditions, from about 34 floods to only 4 floods, respectively. With managed flood releases, however, the post-dam BRM3 floods exceeding 100 m³/s will be about 14 (see **Table 10-11**), which is still less than half of the number of floods under present conditions, but a vast improvement over only 4 floods.

Table 10-11 Number of floods above 100 m³/s for the 9-year period at BRM3

Discharge [m³/s] (Instantaneous peaks)	Present	Post-dam	Flood releases
> 100	34	4	14
> 150	19	2	7
> 200	7	0	2

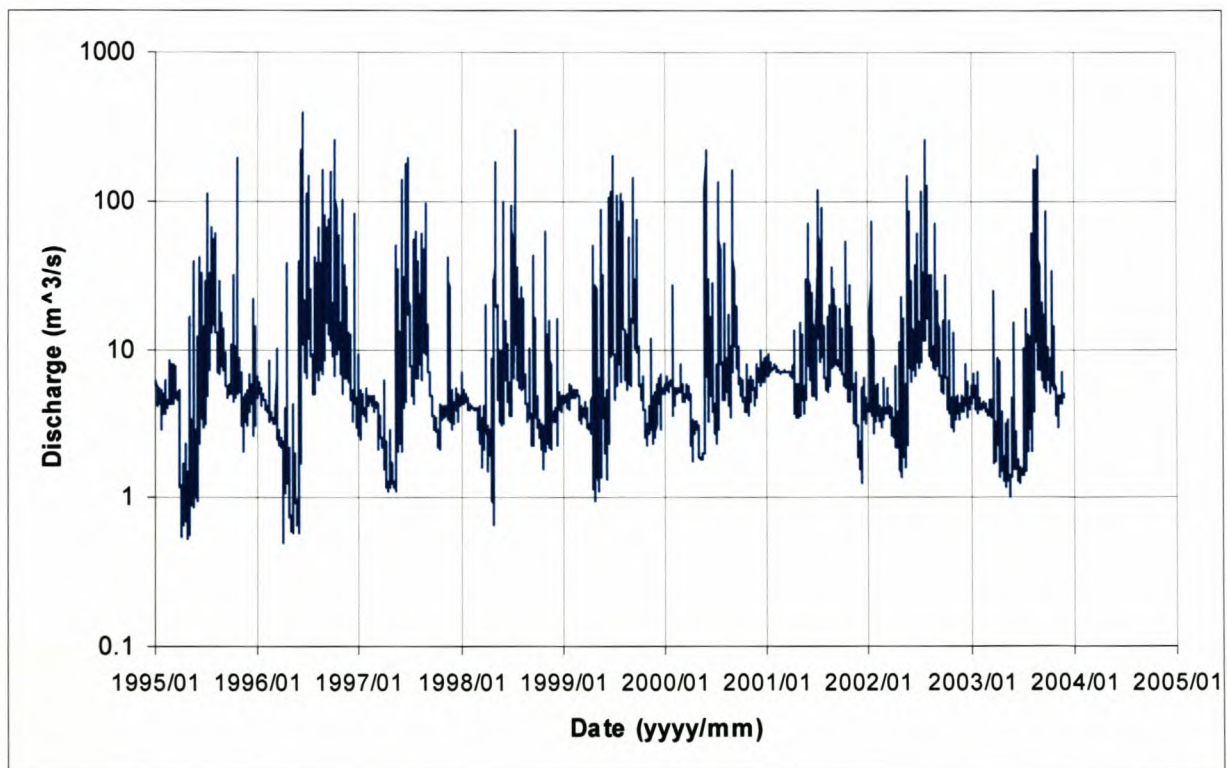


Figure 10-20 Simulated flow series (9 years) for BRM3 – present day scenario (instantaneous peak data) – log scale

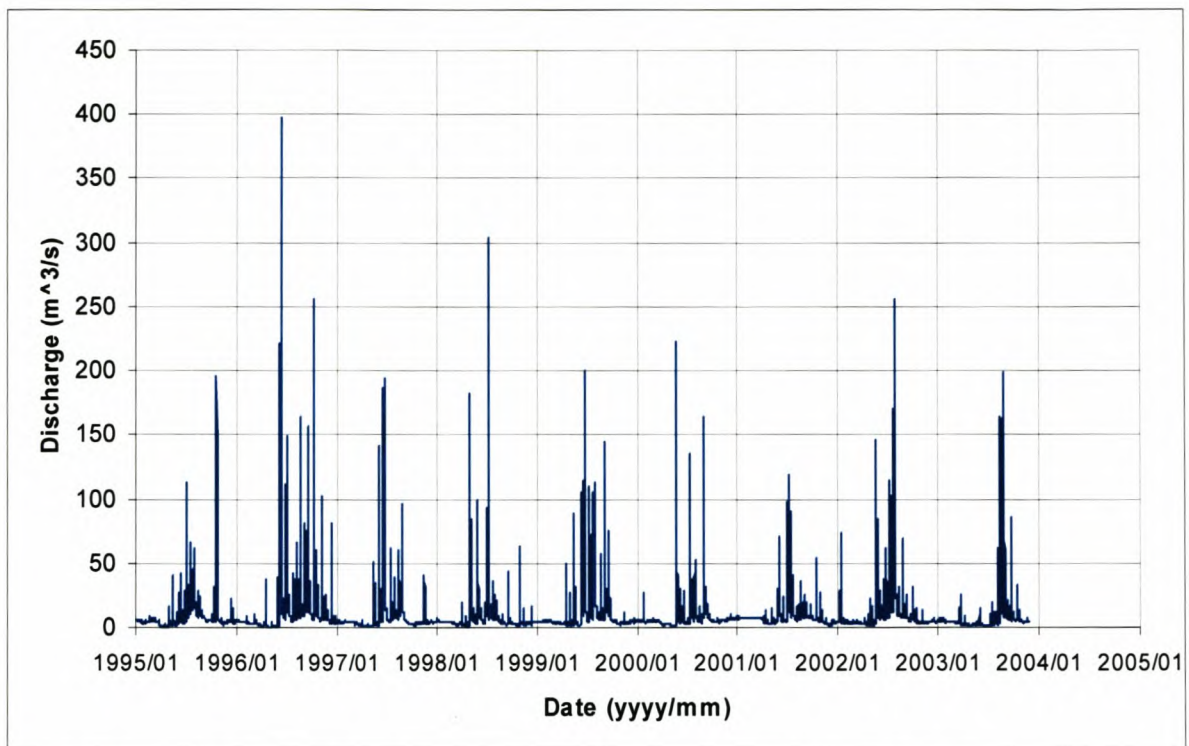


Figure 10-21 Simulated flow series (9 years) for BRM3 – present day scenario (instantaneous peak data) – normal scale

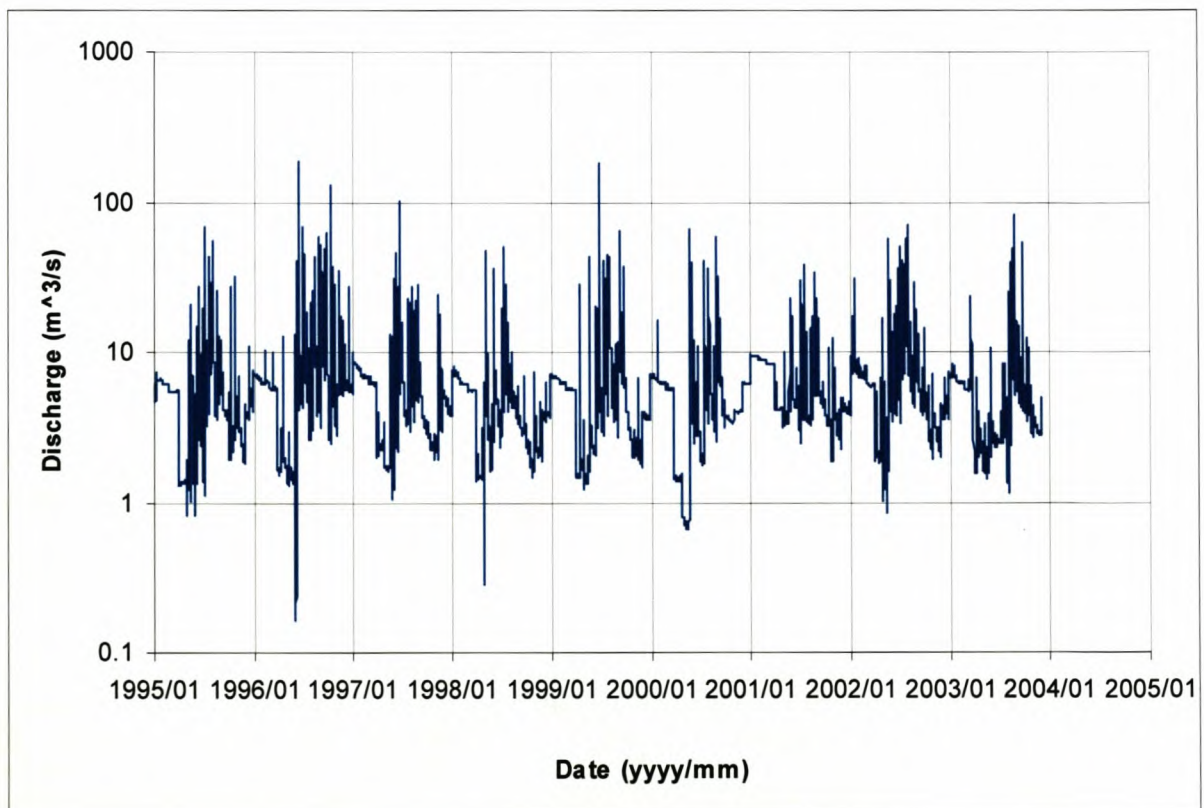


Figure 10-22 Simulated flow series (9 years) for BRM3 – post-dam scenario (instantaneous peak data) – log scale

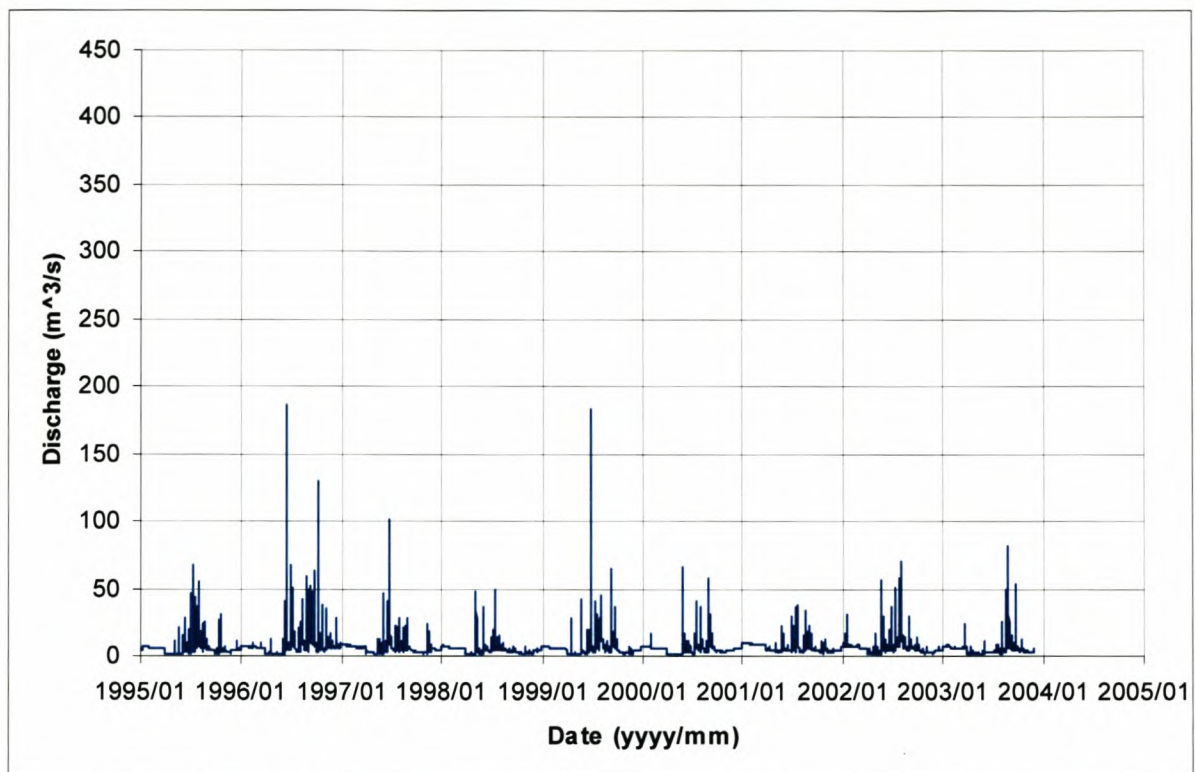


Figure 10-23 Simulated flow series (9 years) for BRM3 – post-dam scenario (instantaneous peak data) – normal scale

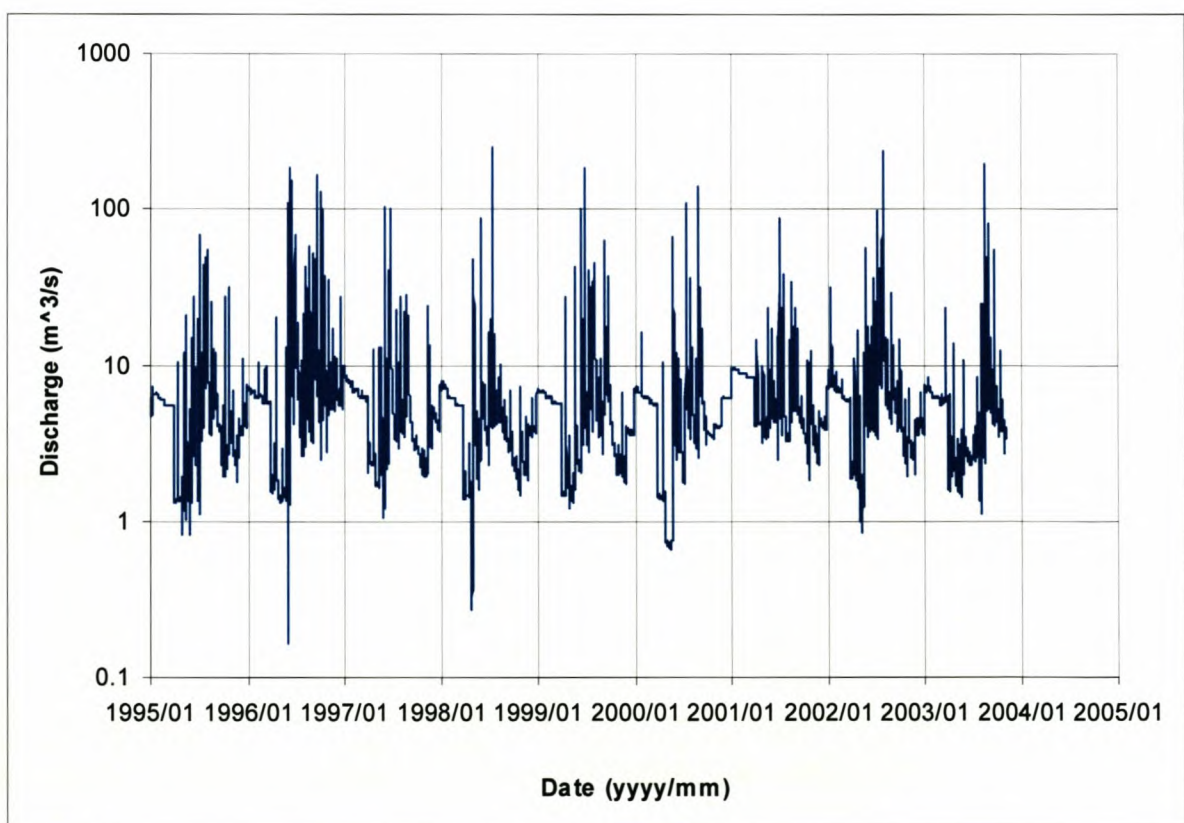


Figure 10-24 Simulated flow series (9 years) for BRM3 – post-dam with flood releases scenario (instantaneous peak data) – normal scale

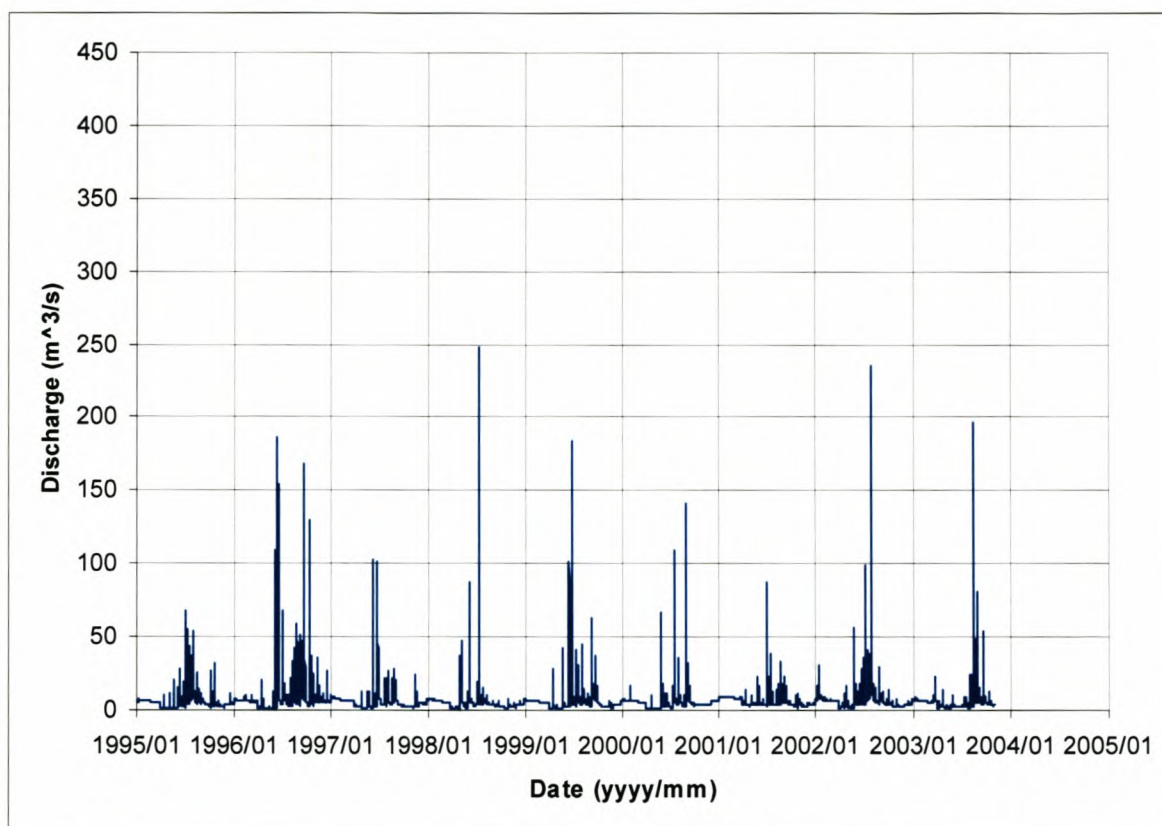


Figure 10-25 Simulated flow series (9 years) for BRM3 – post-dam with flood releases scenario (instantaneous peak data) – normal scale

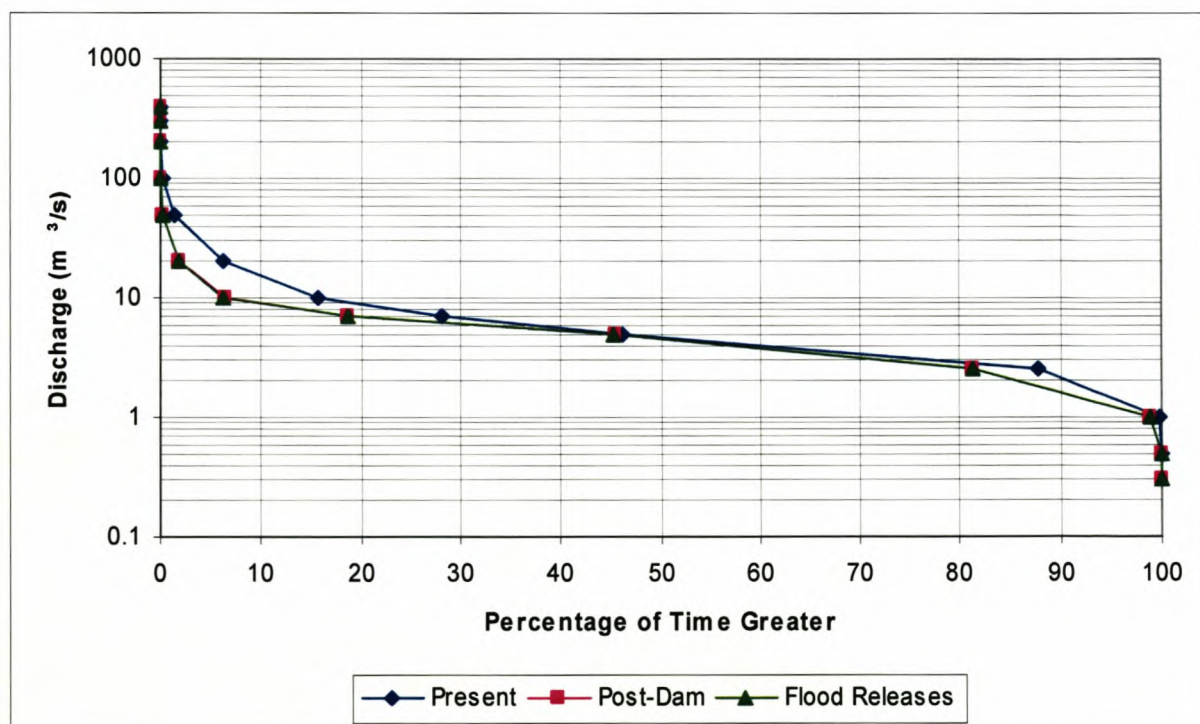


Figure 10-26 Discharge - frequency graph for BRM3

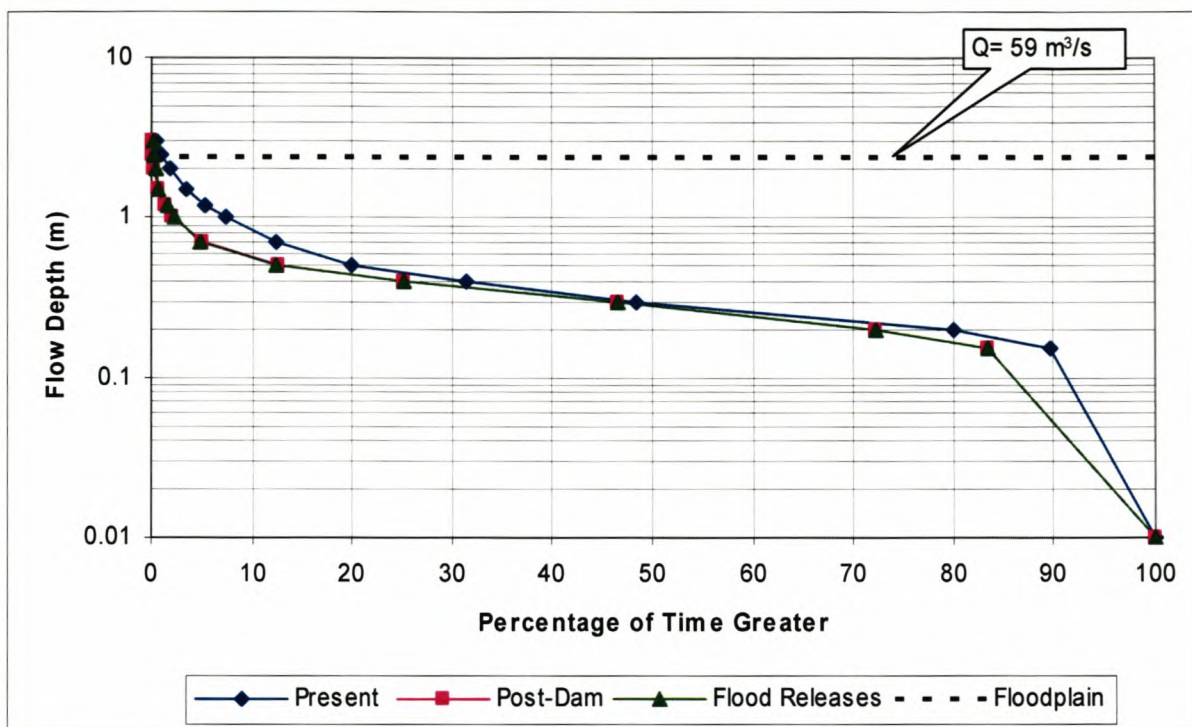


Figure 10-27 Flow depth - frequency graph for BRM3 – transect A

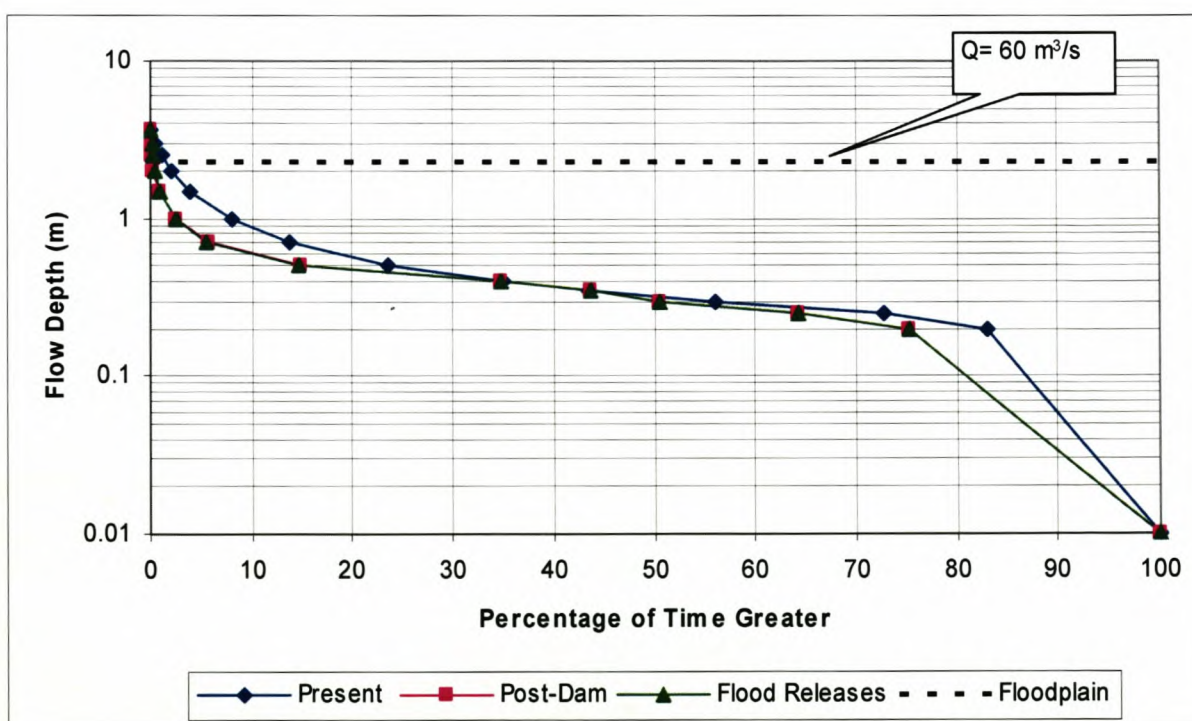


Figure 10-28 Flow depth - frequency graph for BRM3 – transect B

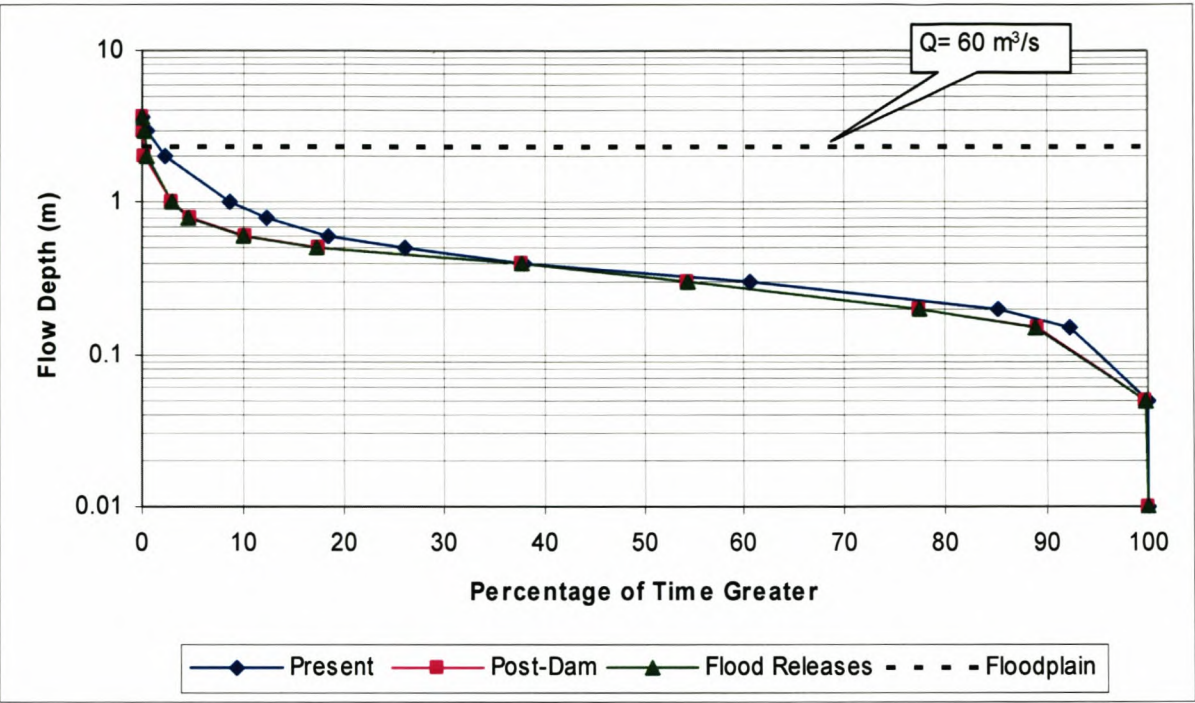


Figure 10-29 Flow depth - frequency graph for BRM3 – transect C

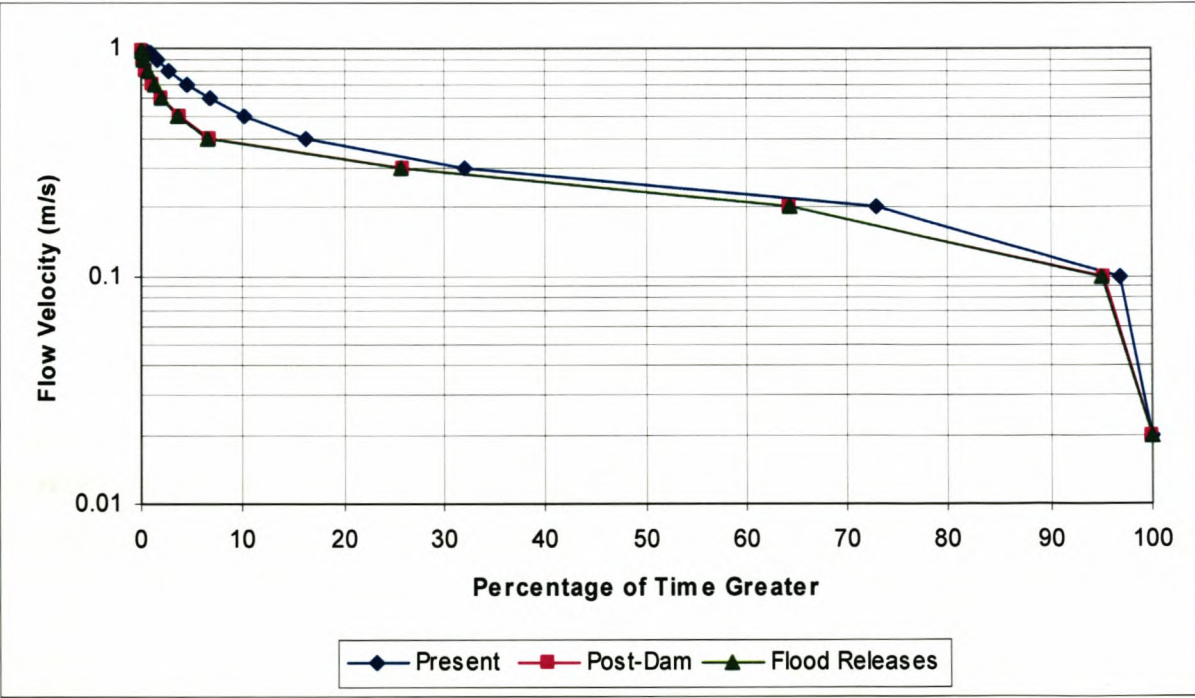


Figure 10-30 Flow velocity - frequency graph for BRM3 – transect A

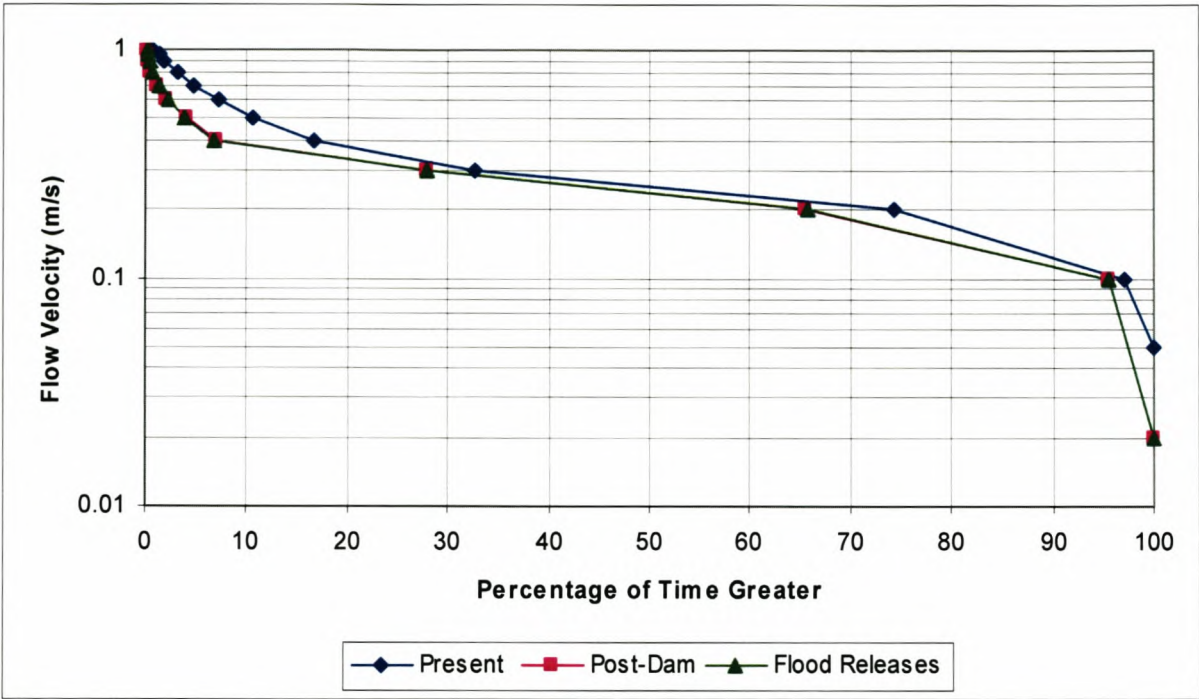


Figure 10-31 Flow velocity - frequency graph for BRM3 – transect B

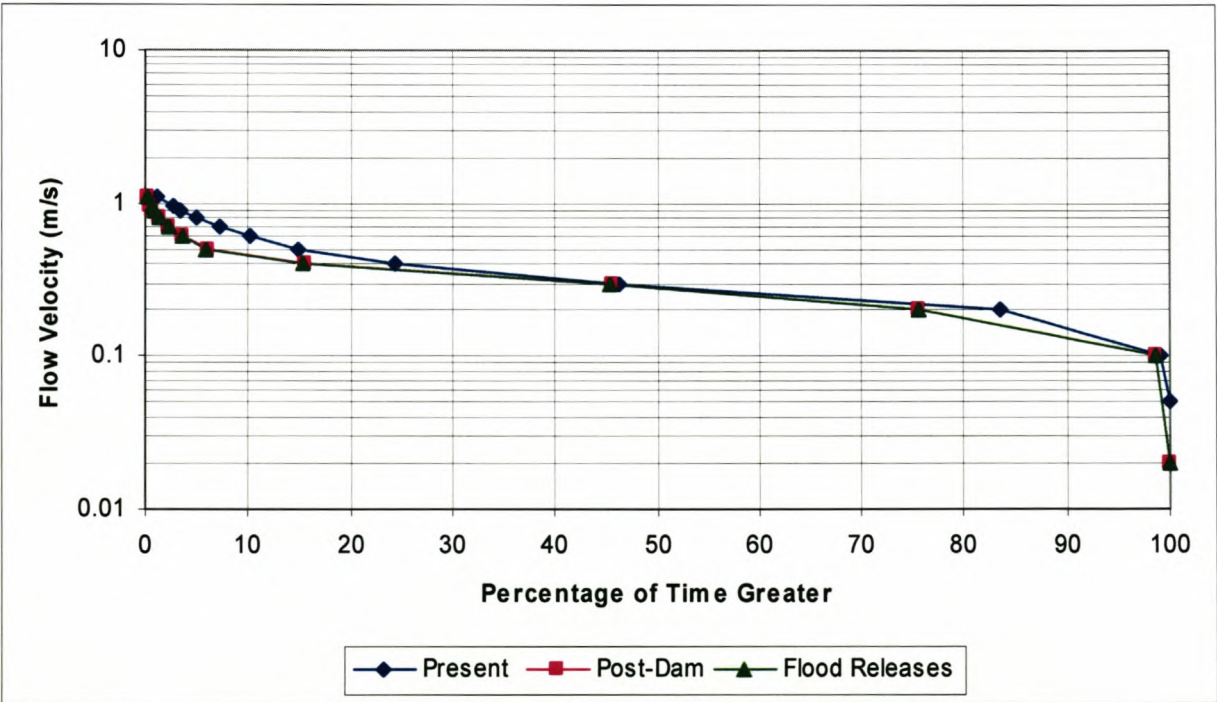


Figure 10-32 Flow velocity - frequency graph for BRM3 – transect C

10.1.3.3 Site BRM4

Simulated 9-year flow series for each scenario are given in **Figure 10-33** to **Figure 10-38**. It can be seen that number of the small and intermediate floods have increased, but the largest flood for the post-dam scenario is still only 286 m³/s compared to 498 m³/s at present. Much the same as at BRM3 it can be seen from Figure 10-39 that as a result of the IFR and irrigation releases the frequency of flows between 2 and 10 m³/s is almost the same for all three scenarios. However, floods and those flows less than 2 m³/s still occur less frequently with the dam than they did for the present scenario, although the difference is not as pronounced as it was at BRM3.

The same trend can be observed from **Table 10-12**, as the flows in class 1 have increased significantly for the post-dam scenario, while the contribution of flows in classes 3 and 4 is less than half of what it was for the present scenario. However, the flood releases have increased the flows in classes 2, 3 and 4 above that of the post-dam scenario. Flow depth - frequency graphs for each of three transects are provided in **Figure 10-40** to **Figure 10-42**. Flow velocity - frequency graph for each of three transects are provided in **Figure 10-43** to **Figure 10-45**.

It can be seen from **Figure 10-40** to **Figure 10-42** that the floodplain (indicated by broken lines) is inundated about 4% of the time during the 9-year simulation period (see **Table 10-13**), and drops to just under 2% with the dam. The floodplain inundation is slightly higher with the flood releases.

Table 10-12 Contribution of within year floods to total flow for three scenarios at BRM4

Class (DRIFT)	Discharge [m3/s] (Instantaneous peaks)	Present	Post-dam	Flood releases
1	0 – 26.9	91.99%	95.39%	95.42%
2	26.9 – 53.8	5.37%	3.55%	3.31%
3	53.8 – 107.6	1.93%	0.79%	0.91%
4	107.6 – 215.1	0.58%	0.22%	0.30%

Table 10-13 Floodplain inundation at BRM4

Scenario	Inundation [days/year]
Present	14.21
Post-dam	7.23
Flood releases	7.63

The number of floods above 100 m³/s reduces somewhat from present to post-dam conditions, from about 39 floods to only 14 floods, respectively. With managed flood releases, however, the post-dam BRM floods exceeding 100 m³/s will be about 18 (see **Table 10-14**). On the other hand the number of floods exceeding 200 m³/s will increase from 6 to 8 with the flood releases above the post-dam conditions, closer to the 10 at present.

Table 10-14 Number of floods above 100 m³/s for the 9-year period at BRM4

Discharge [m3/s] (Instantaneous peaks)	Present	Post-dam	Flood releases
> 100	39	14	18
> 150	19	8	13
> 200	10	6	8

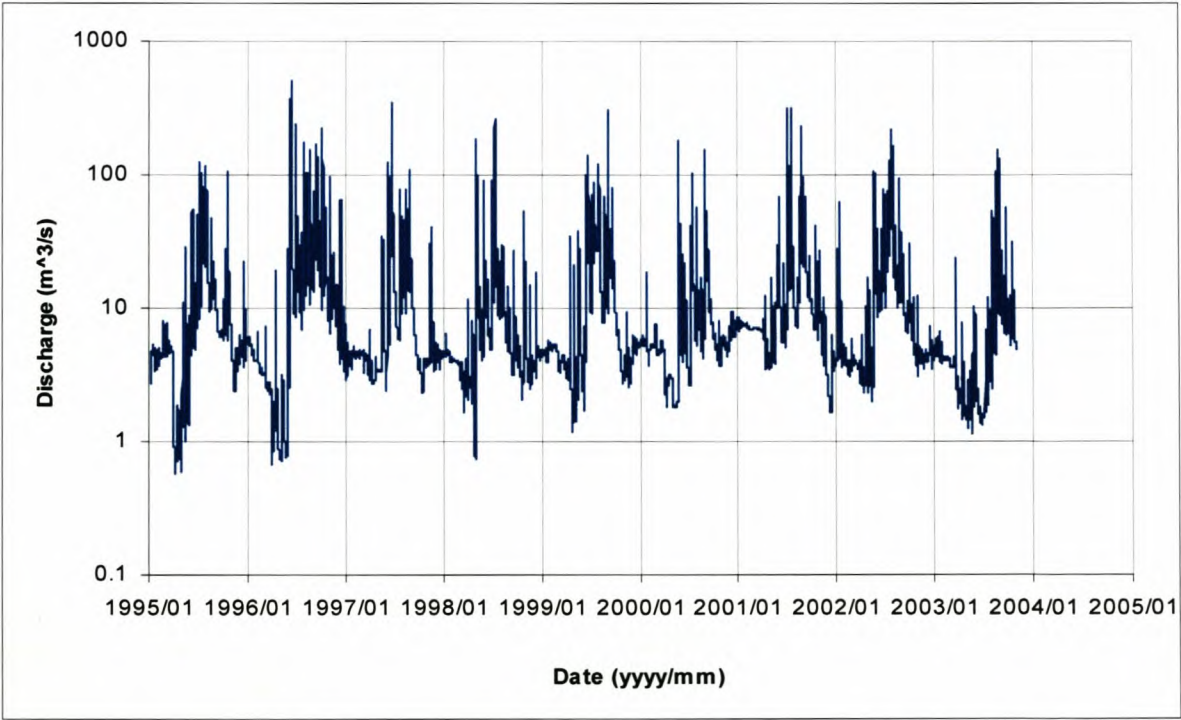


Figure 10-33 Simulated flow series (9 years) for BRM4 – present day scenario (instantaneous peak data) – log scale

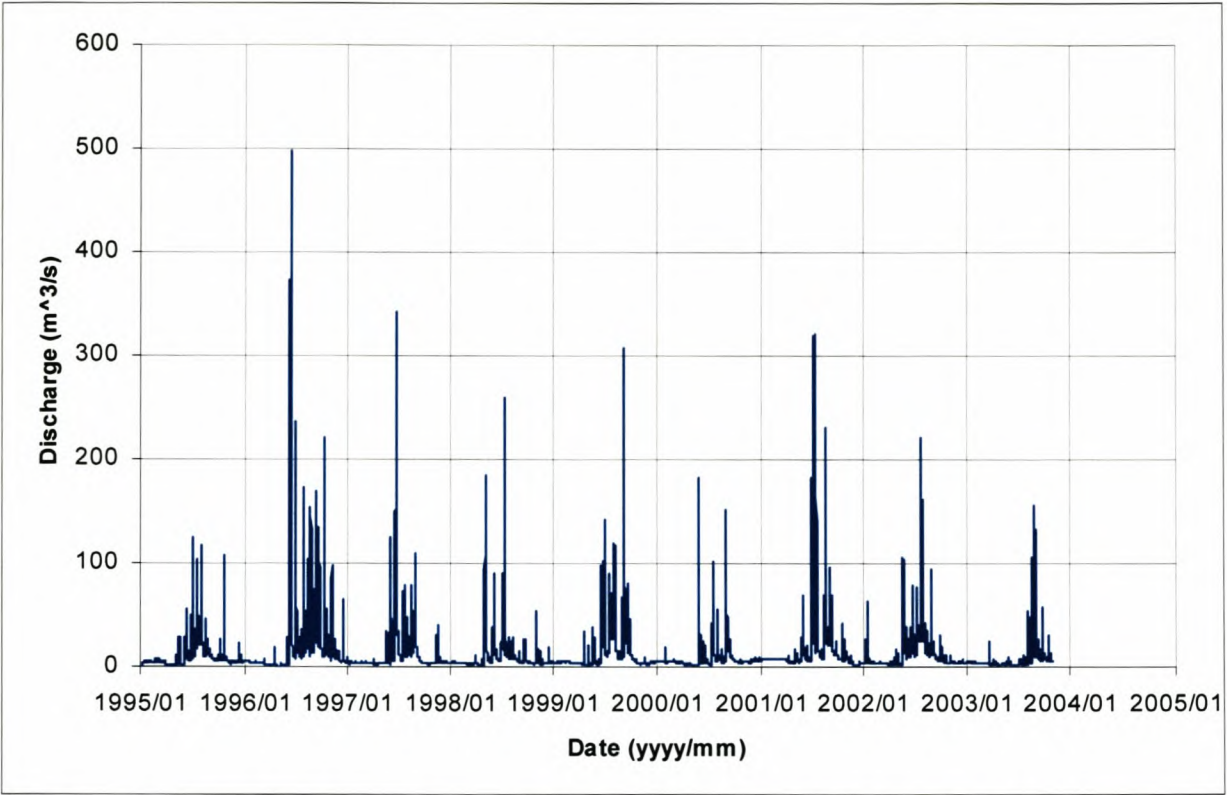


Figure 10-34 Simulated flow series (9 years) for BRM4 – present day scenario (instantaneous peak data) – normal scale

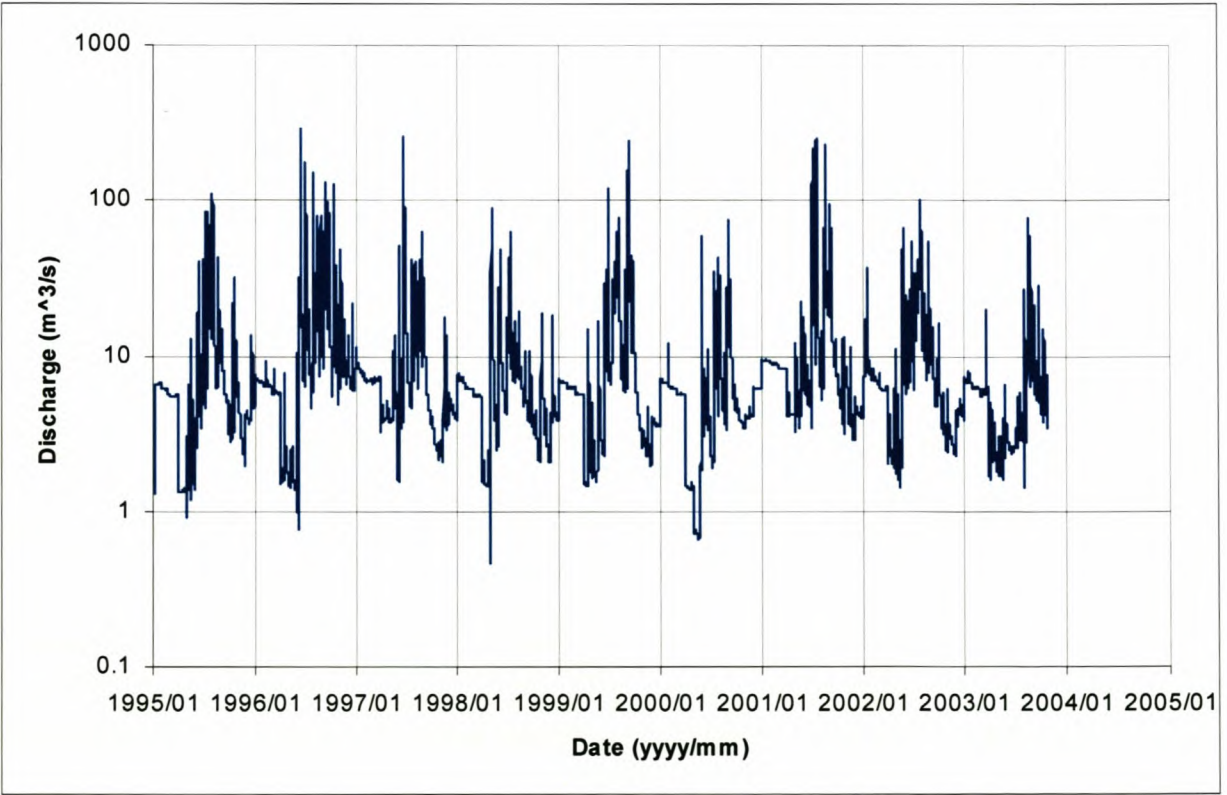


Figure 10-35 Simulated flow series (9 years) for BRM4 – post-dam scenario (instantaneous peak data) – log scale

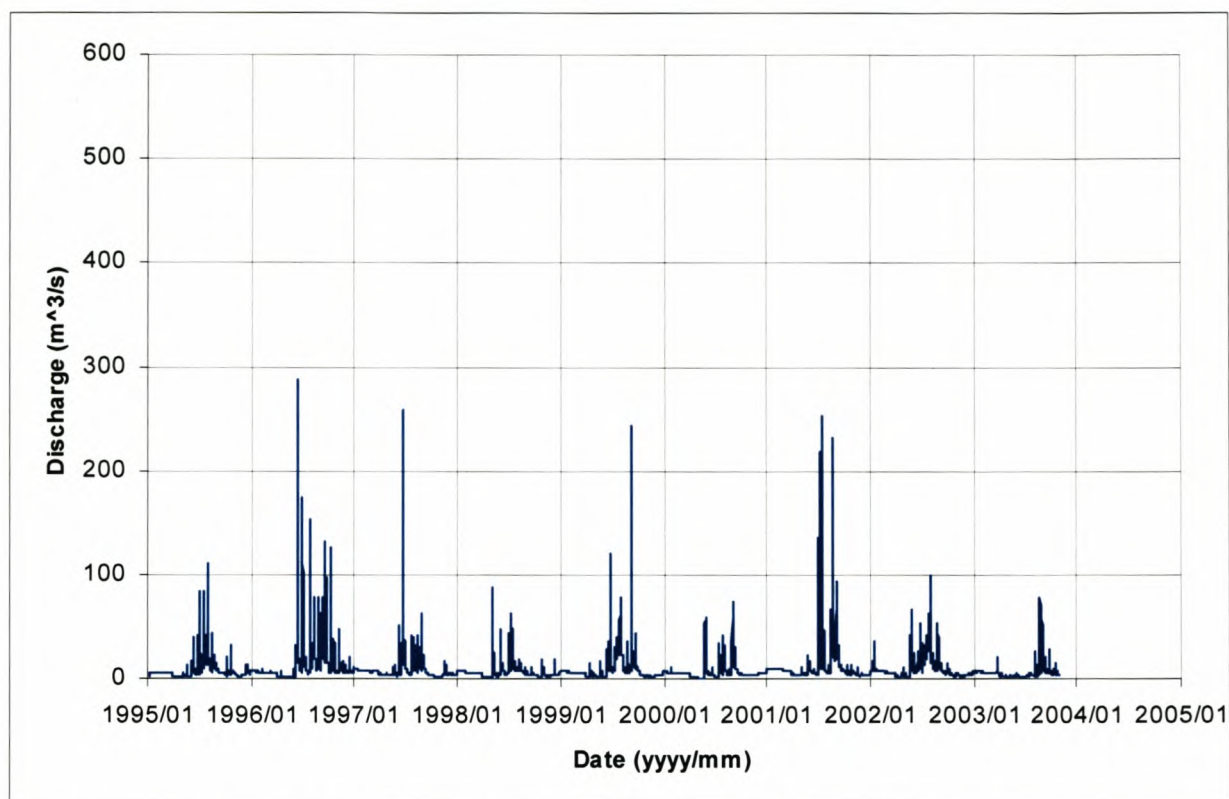


Figure 10-36 Simulated flow series (9 years) for BRM4 – post-dam scenario (instantaneous peak data) – normal scale

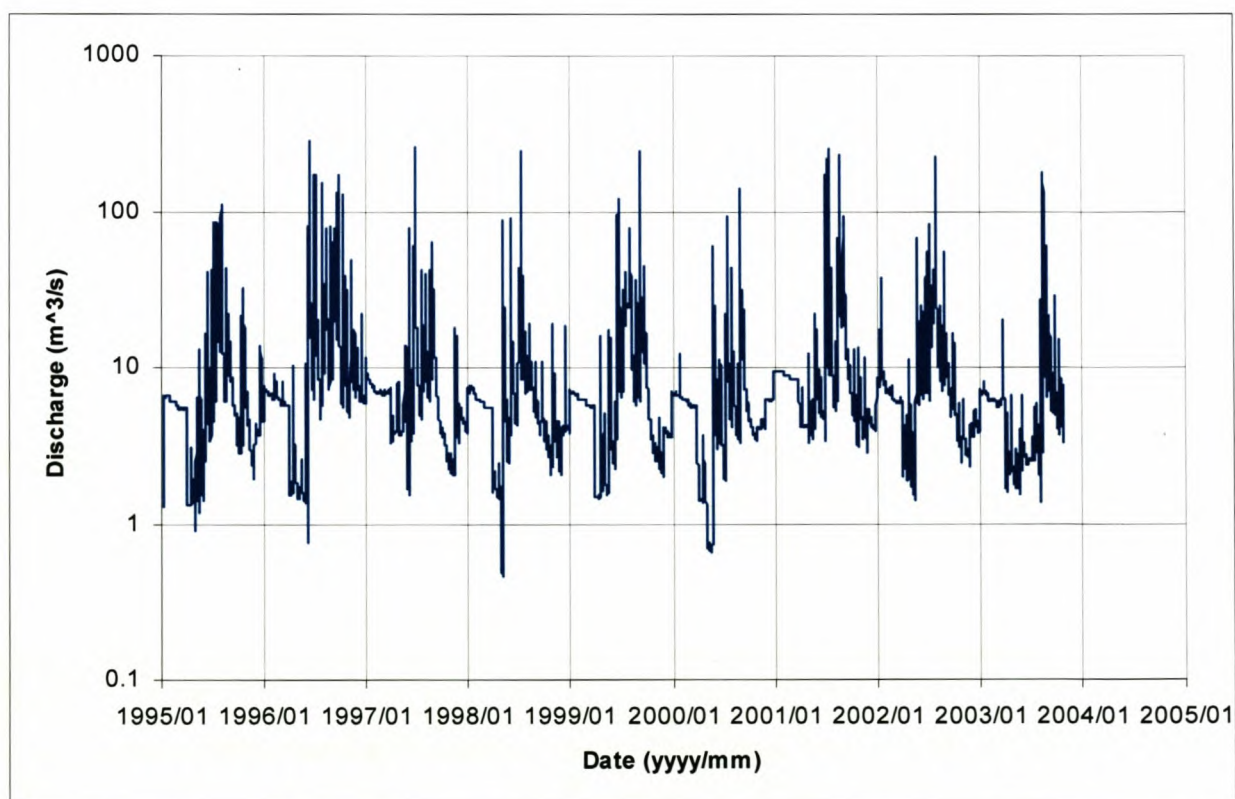


Figure 10-37 Simulated flow series (9 years) for BRM4 – post-dam with flood releases scenario (instantaneous peak data) – log scale

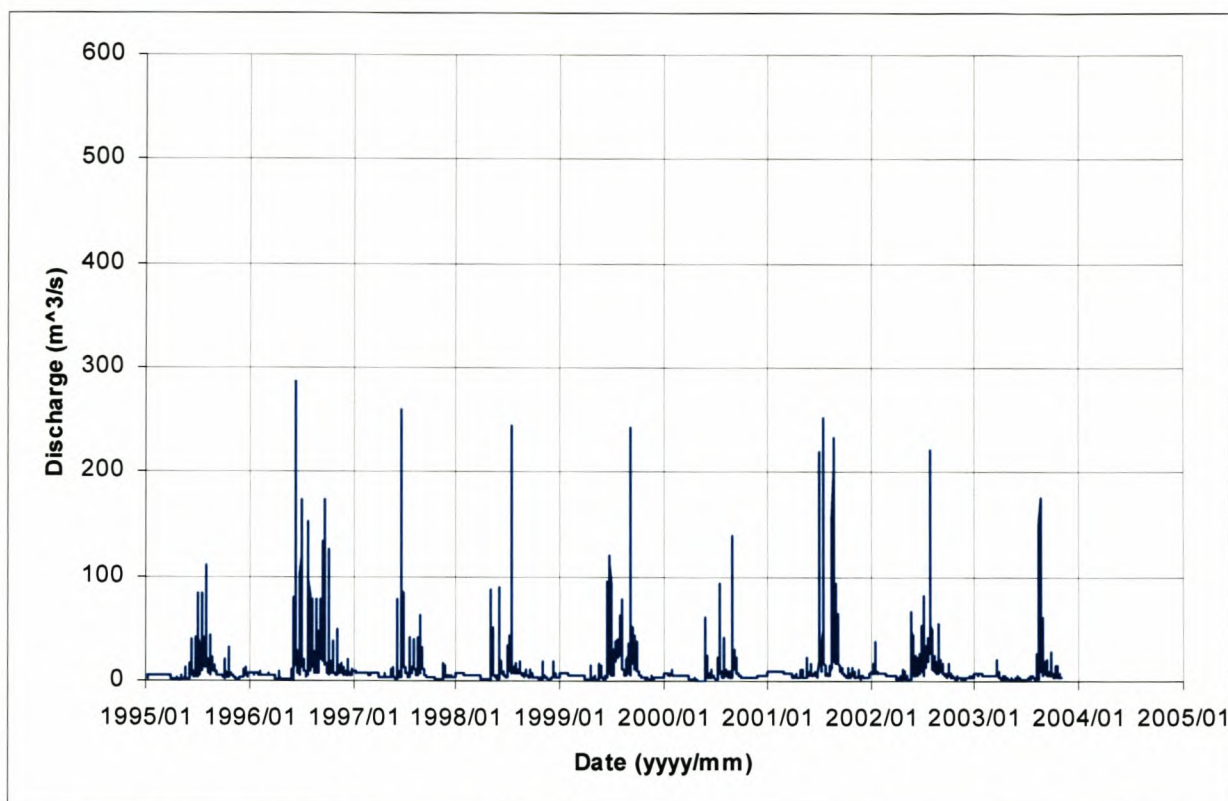


Figure 10-38 Simulated flow series (9 years) for BRM4 – post-dam with flood releases scenario (instantaneous peak data) – normal scale

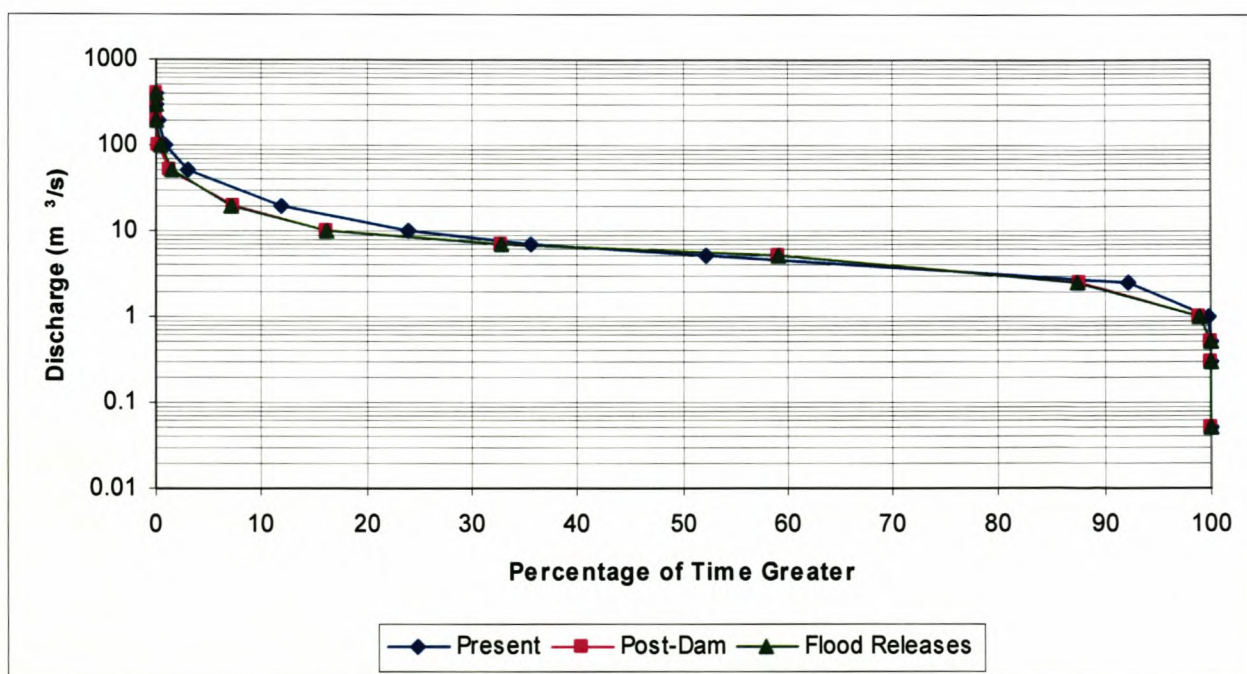


Figure 10-39 Discharge - frequency graph for BRM4

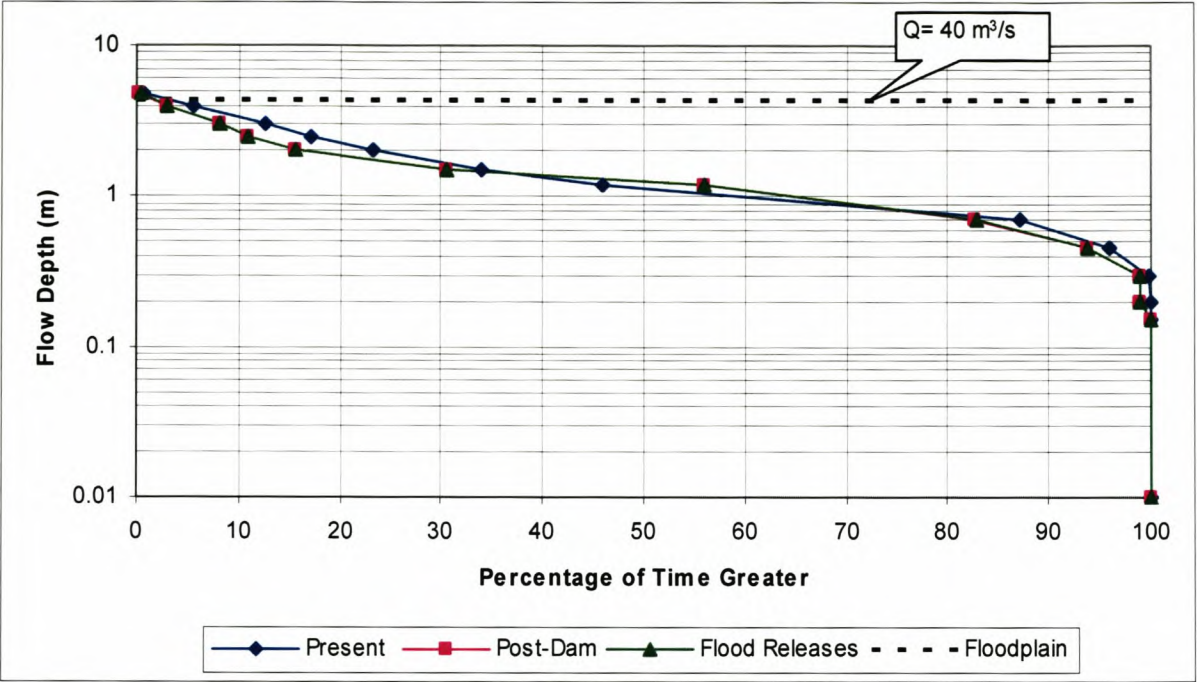


Figure 10-40 Flow depth - frequency graph for BRM4 – transect A

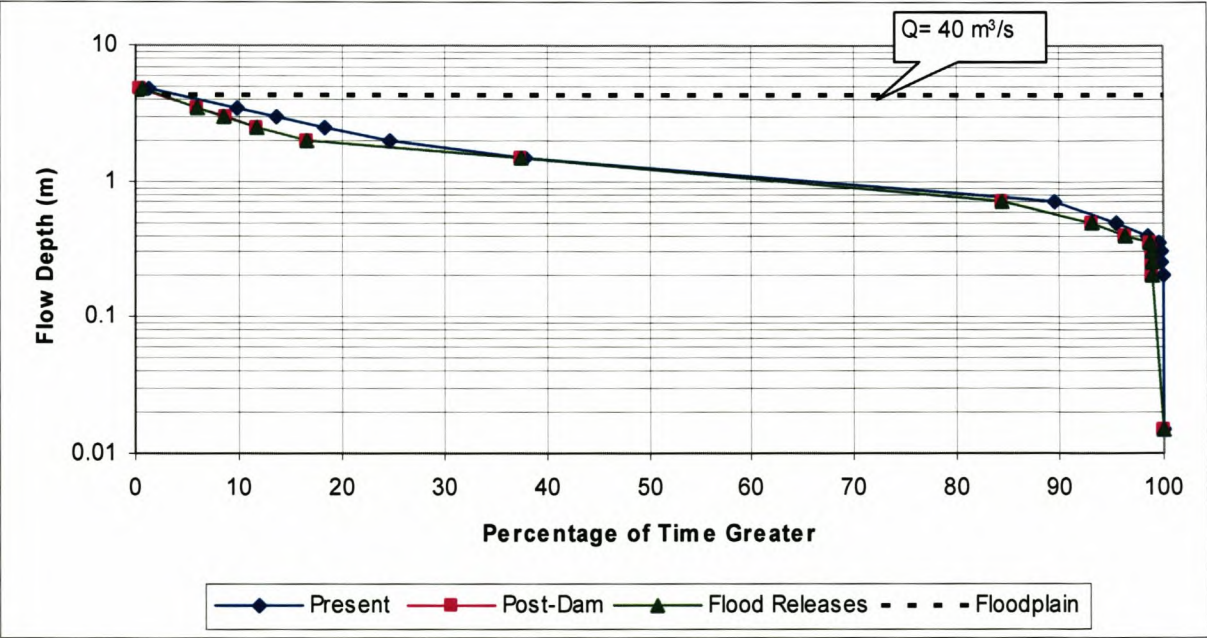


Figure 10-41 Flow depth - frequency graph for BRM4 - transect B

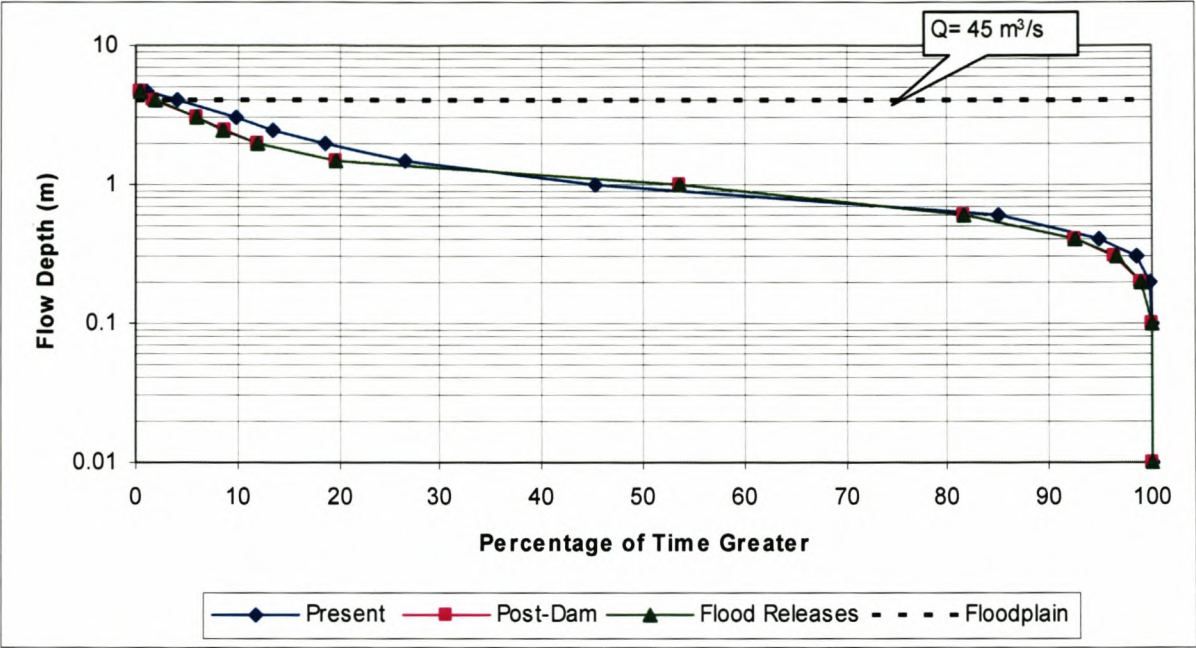


Figure 10-42 Flow depth - frequency graph for BRM4 – transect C

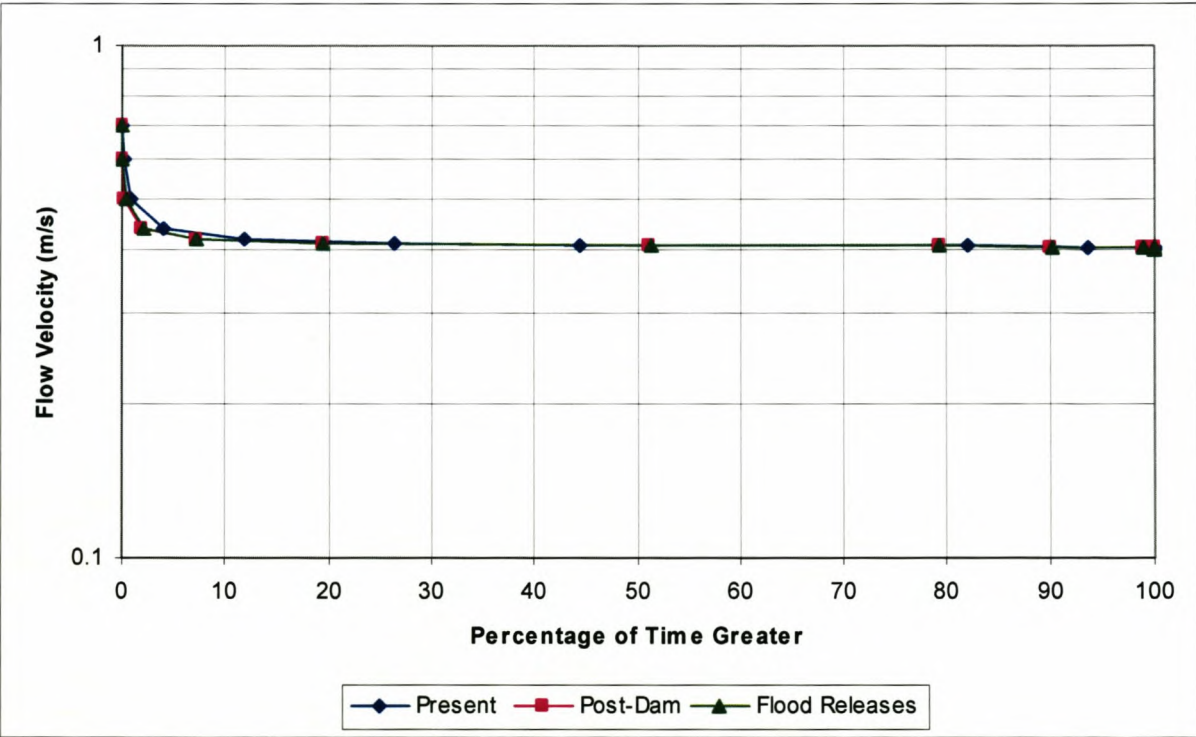


Figure 10-43 Flow velocity - frequency graph for BRM4 – transect A

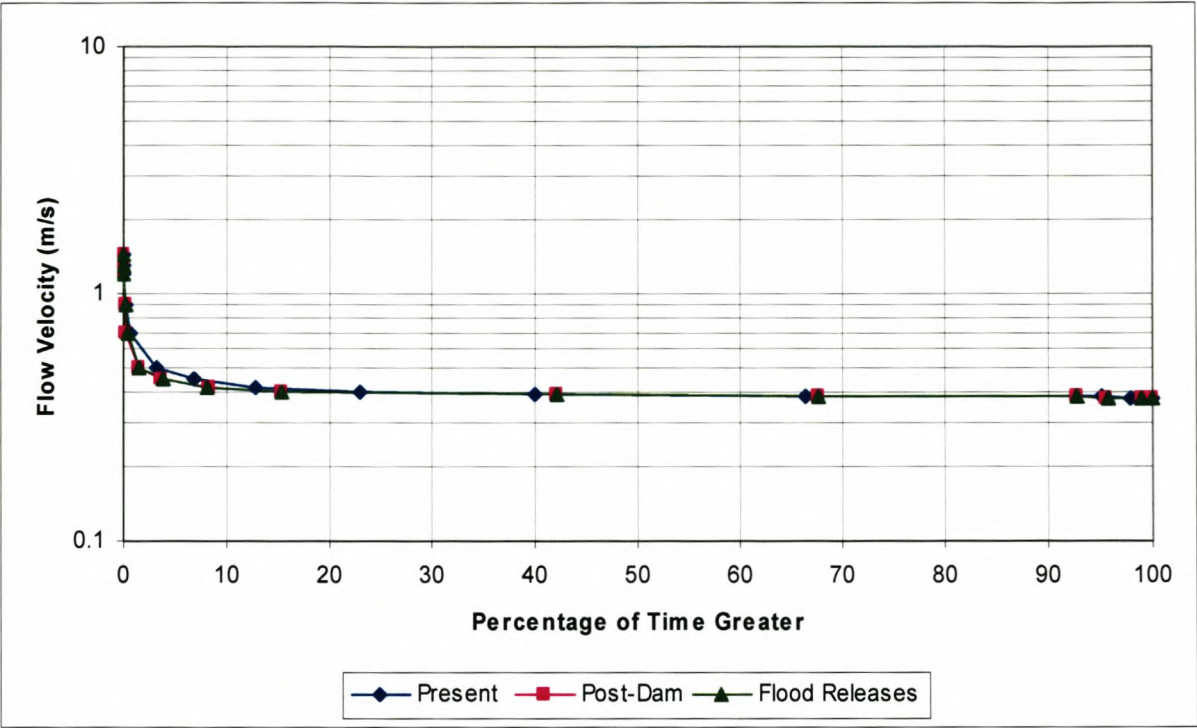


Figure 10-44 Flow velocity - frequency graph for BRM4 – transect B

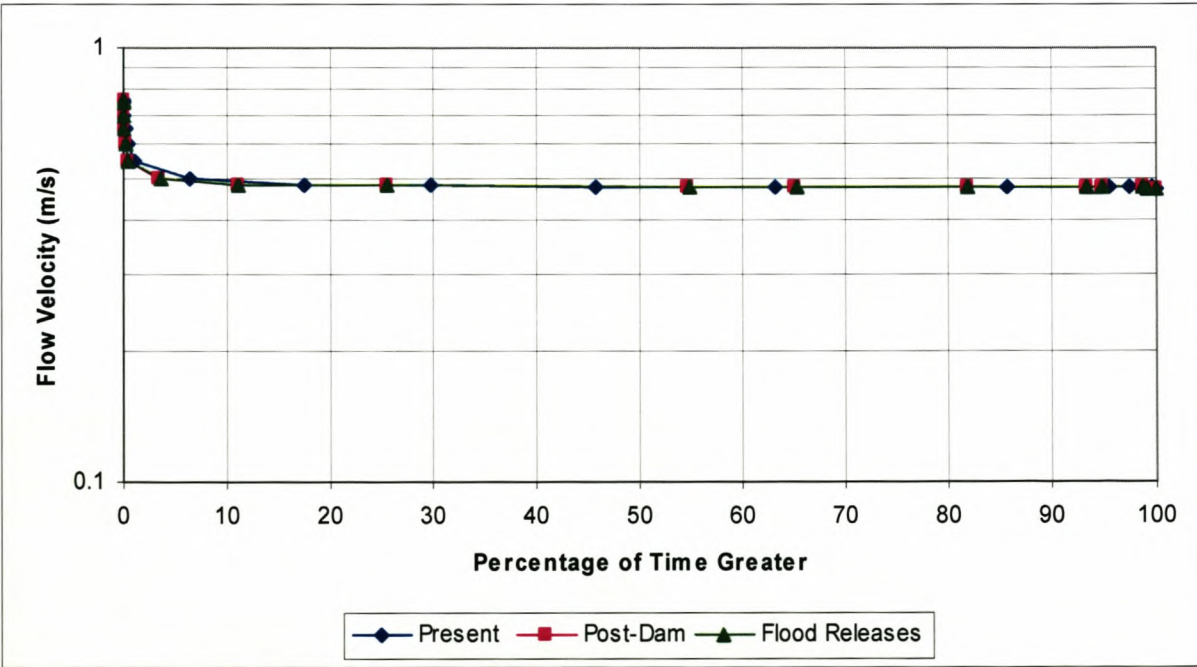


Figure 10-45 Flow velocity - frequency graph for BRM4 – transect C

10.1.3.4 Site BRM5

Simulated 9-year flow series for each scenario are given in **Figure 10-46** to **Figure 10-51**. It can be seen that the number of small and intermediate floods has increased, but the largest flood for the post-dam scenario at 554 m³/s is now closer to the 667 m³/s at present than it was at BRM4. From **Figure 10-52** it can be seen that as a result of the IFR and irrigation releases the frequency of flows between 2 and 10 m³/s is almost the same for all three scenarios, much the same as at BRM4. However, floods and those flows less than 2 m³/s still occur less frequently with the dam than they did for the present scenario, although the difference is even less pronounced than it was at BRM4.

The same trend can be observed from **Table 10-15**, as the flows in class 1 have increased significantly for the post-dam scenario, while the contribution of flows in classes 3 and 4 is less than half of what it was for the present scenario. However, the flood releases have increased the flows in classes 2, 3 and 4 above that of the post-dam scenario.

Flow depth - frequency graphs for each of three transects are provided in **Figure 10-53** to **Figure 10-55**. Flow velocity - frequency graph for each of three transects are provided in **Figure 10-56** to **Figure 10-58**.

It can be seen from **Figure 10-53** to **Figure 10-55** that the floodplain (indicated by broken lines) is inundated just under 4% of the time and drops to below 3% with the dam development (see **Table 10-16**). The flood releases increase the floodplain inundation only slightly.

Table 10-15 Contribution of within year floods to total flow for three scenarios at BRM5

Class (DRIFT)	Discharge [m³/s] (Instantaneous peaks)	Present	Post-dam	Flood releases
1	0 – 24.4	86.59%	90.33%	90.38%
2	24.4 – 48.8	8.05%	6.24%	6.12%
3	48.8 – 97.6	3.70%	2.60%	2.56%
4	97.6 – 195.2	1.29%	0.62%	0.67%

Table 10-16 Floodplain inundation for BRM5

Scenario	Inundation [days/year]
Present	14.07
Post-dam	8.84
Flood releases	9.21

The number of floods above 200 m³/s reduces slightly from present to post-dam conditions, from about 18 floods to 12 floods, respectively. With managed flood releases the post-dam BRM5 floods exceeding 200 m³/s will be about 15 (see **Table 10-17**). On the other hand the number of floods exceeding 400 m³/s will not change from present to post-dam conditions.

Table 10-17 Number of floods above 200 m³/s for the 9-year period at BRM5

Discharge [m3/s] (Instantaneous peaks)	Present	Post-dam	Flood releases
> 200	18	12	15
> 300	7	5	5
> 400	3	3	3

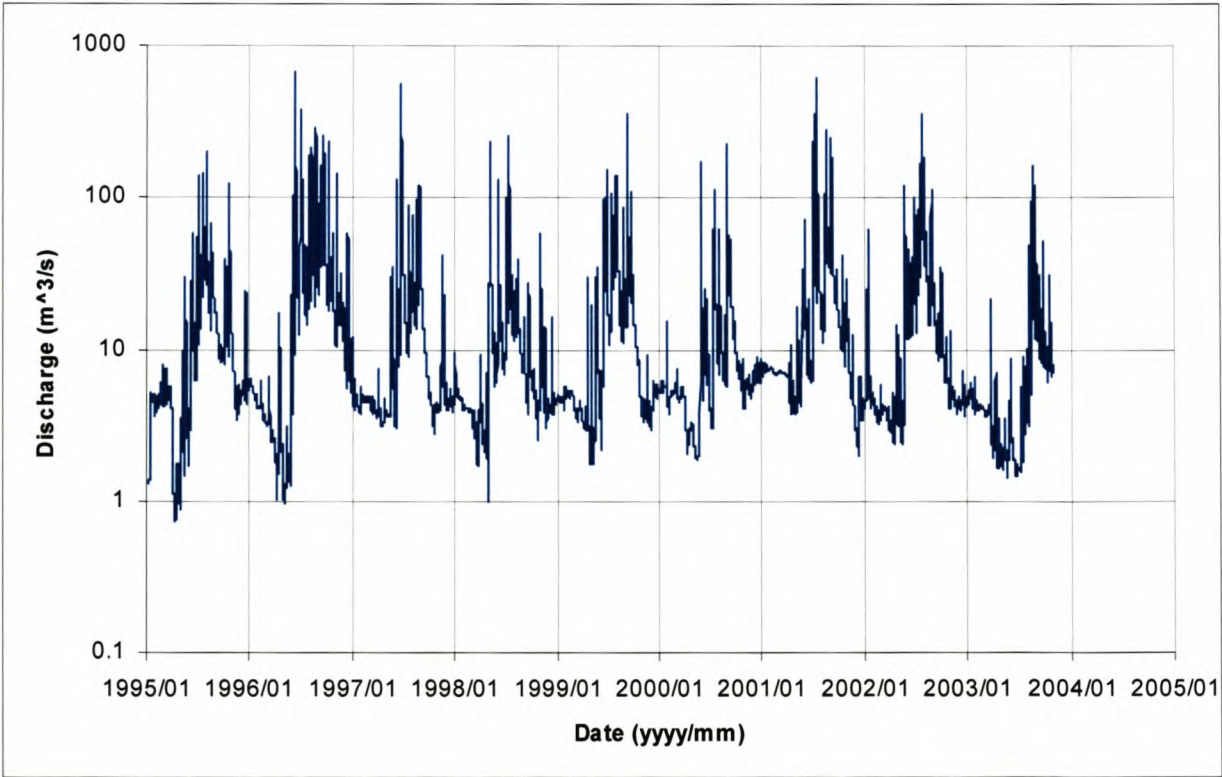


Figure 10-46 Simulated flow series (9 years) for BRM5 – present day scenario (instantaneous peak data) – log scale

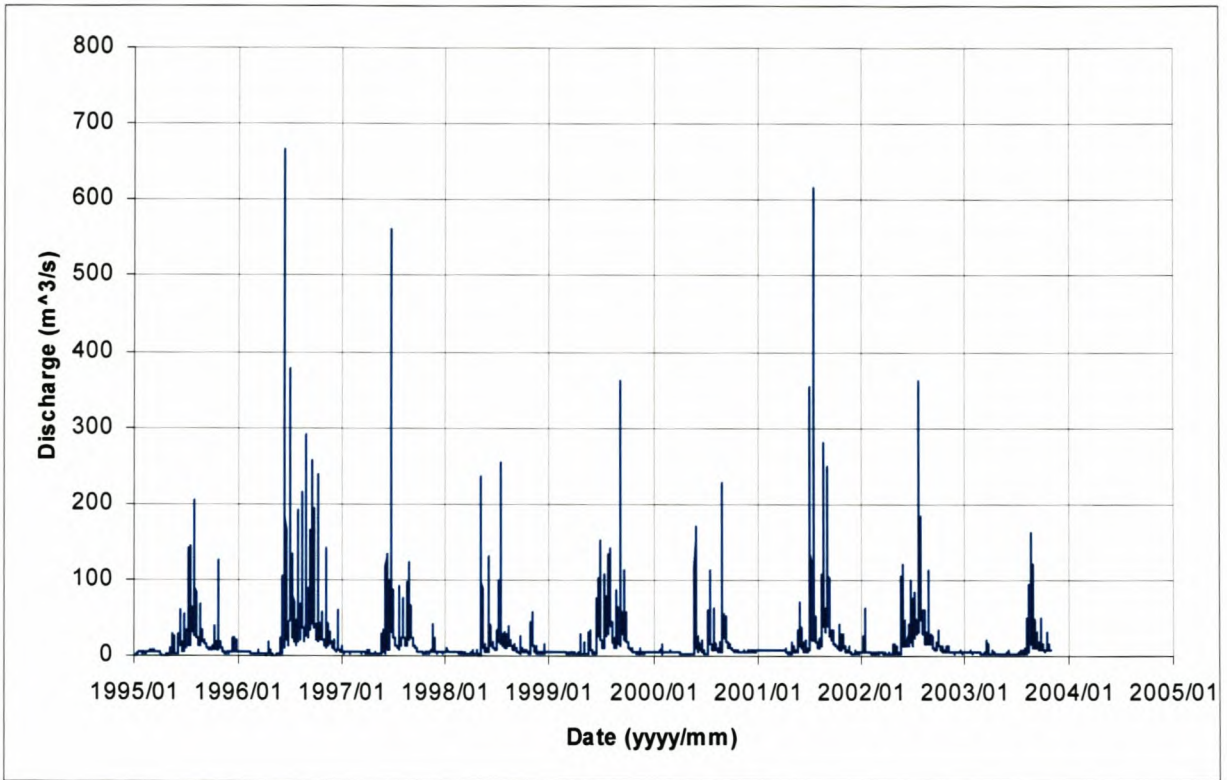


Figure 10-47 Simulated flow series (9 years) for BRM5 – present day scenario (instantaneous peak data) – normal scale

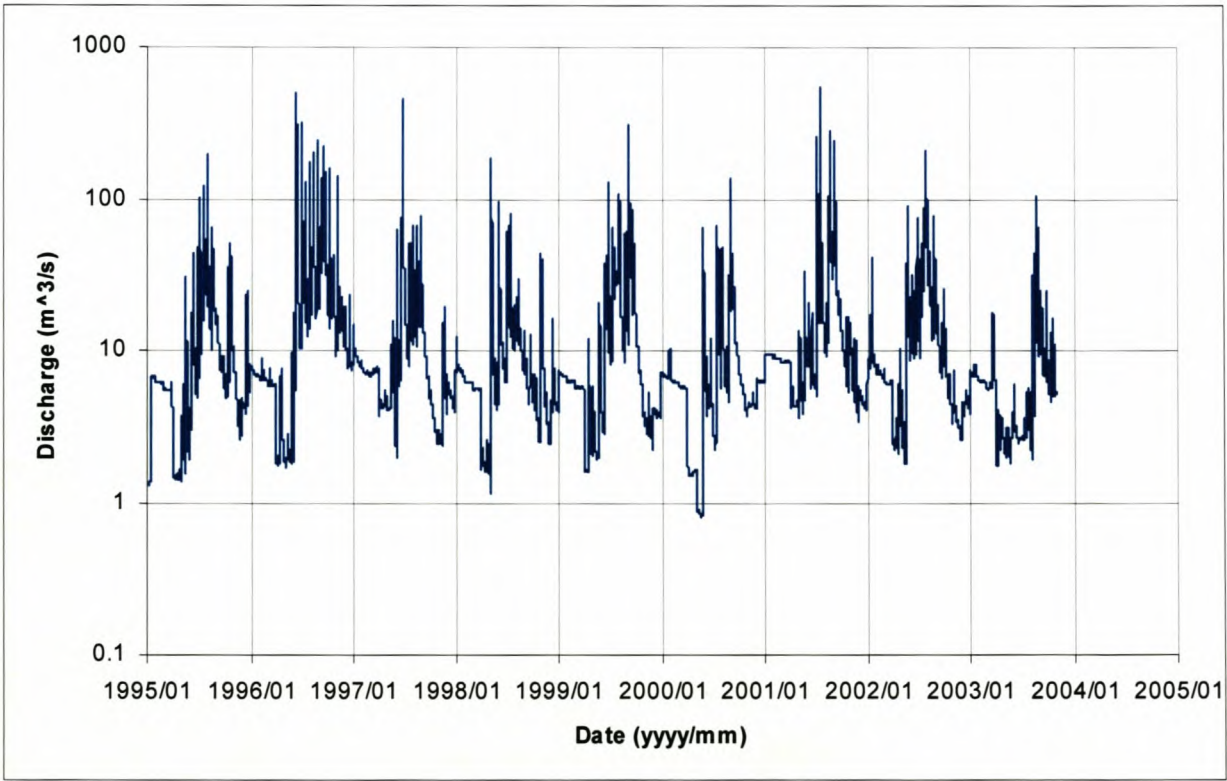


Figure 10-48 Simulated flow series (9 years) for BRM5 – post-dam scenario (instantaneous peak data) – log scale

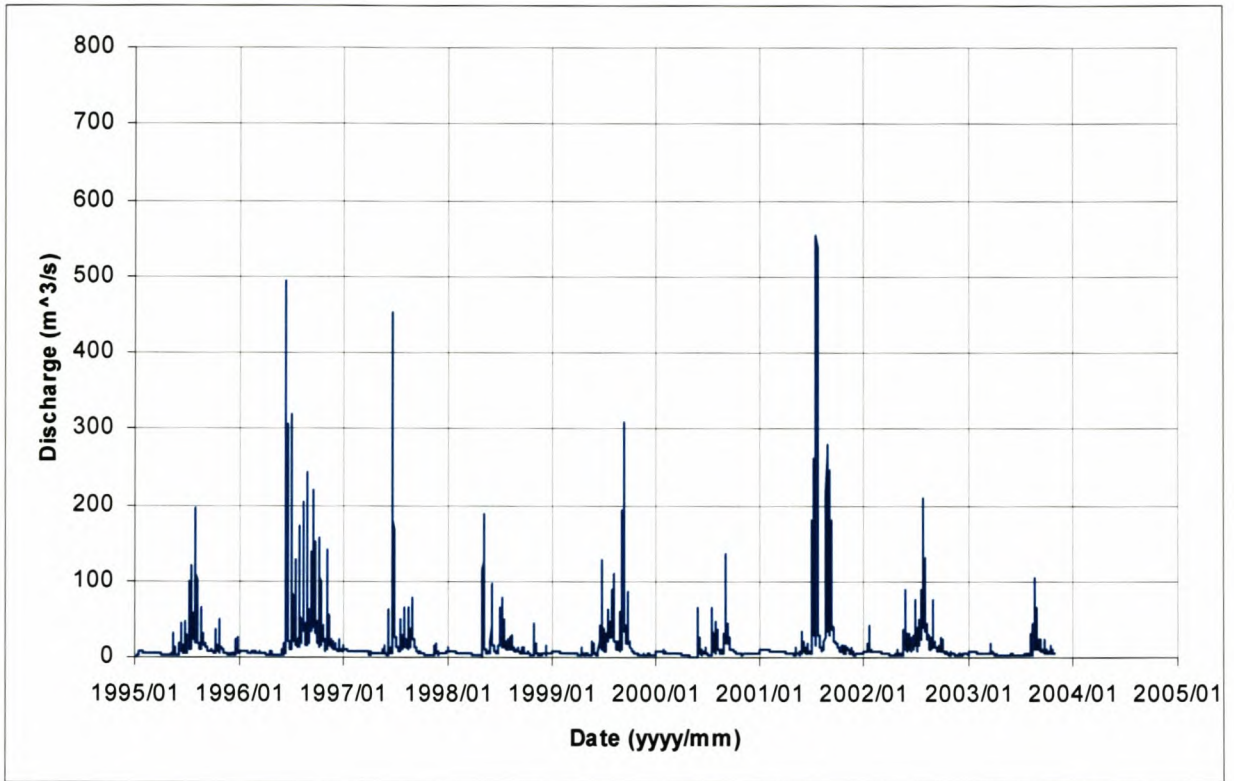


Figure 10-49 Simulated flow series (9 years) for BRM5 – post-dam scenario (instantaneous peak data) – normal scale

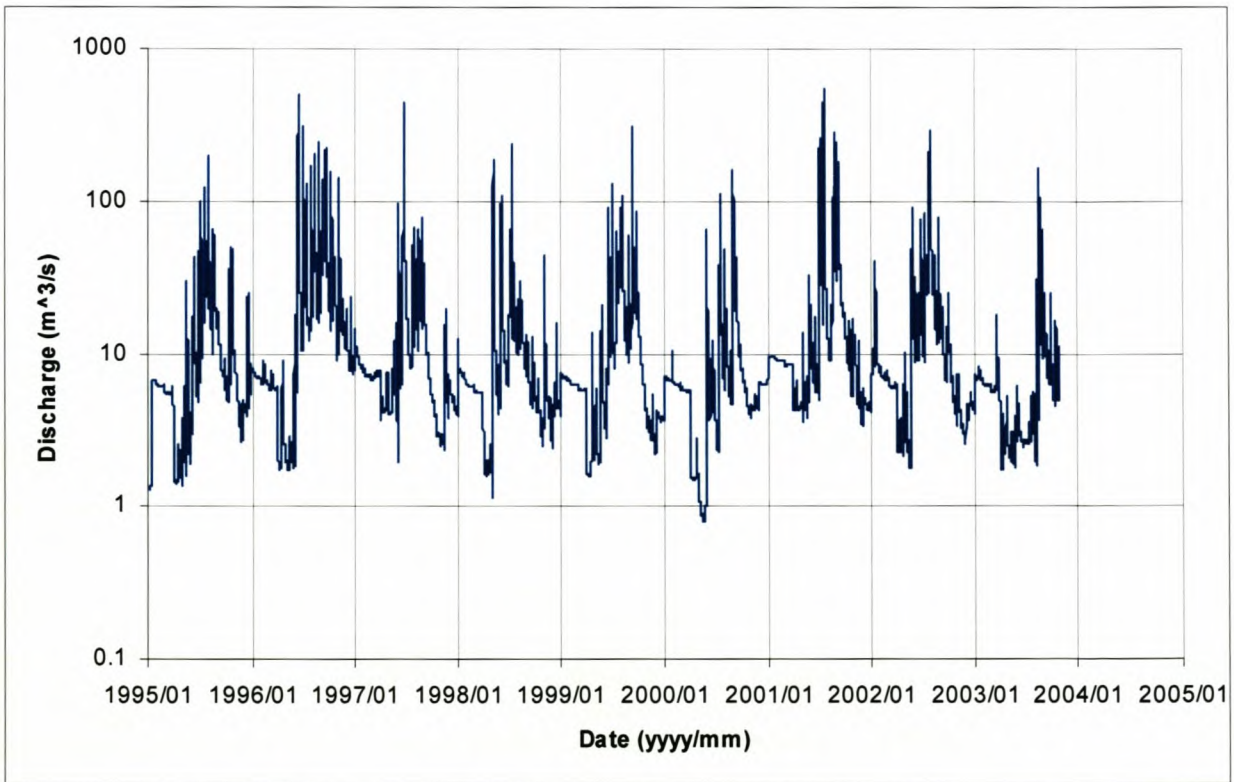


Figure 10-50 Simulated flow series (9 years) for BRM5 – post-dam with flood releases scenario (instantaneous peak data) – log scale

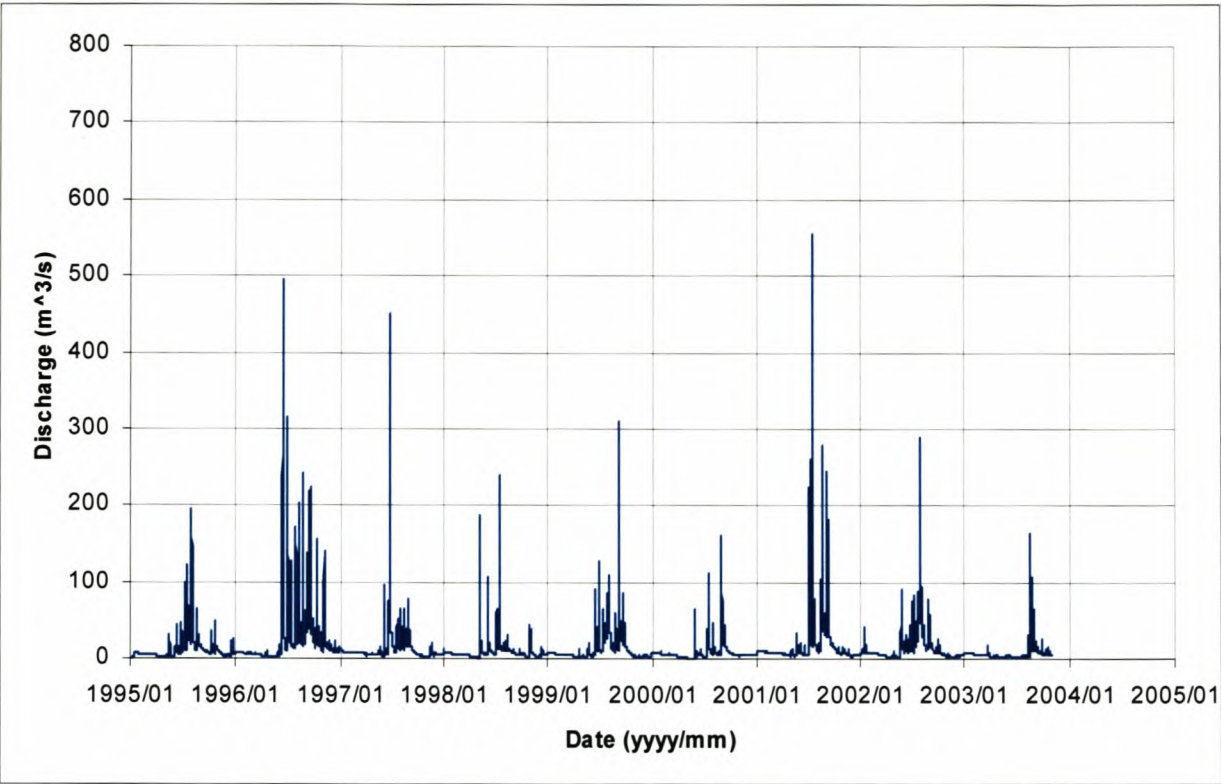


Figure 10-51 Simulated flow series (9 years) for BRM5 – post-dam with flood releases scenario (instantaneous peak data) – normal scale

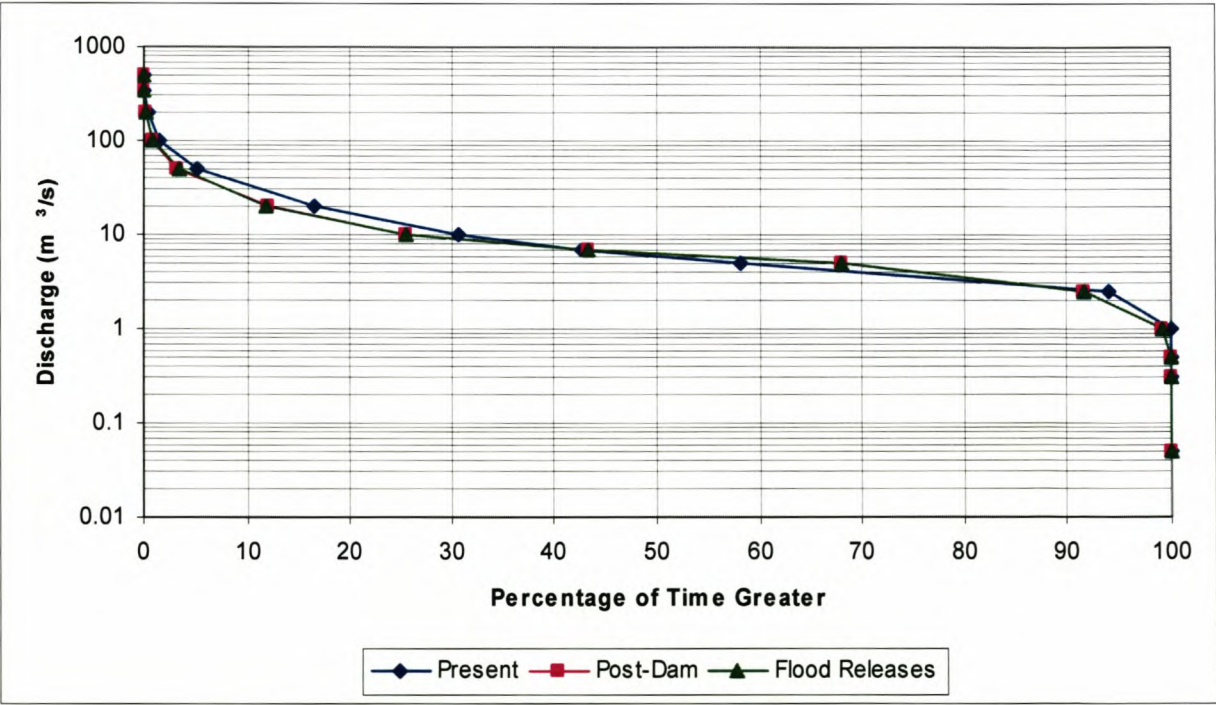


Figure 10-52 Discharge - frequency graph for BRM5

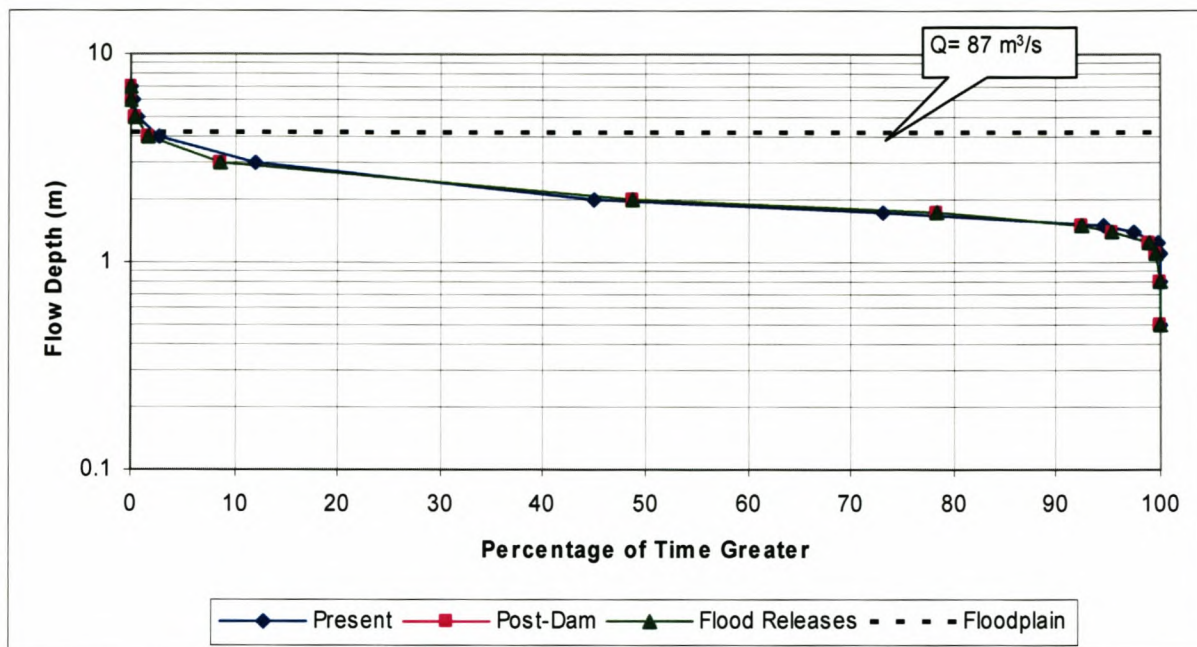


Figure 10-53 Flow depth - frequency graph for BRM5 – transect A

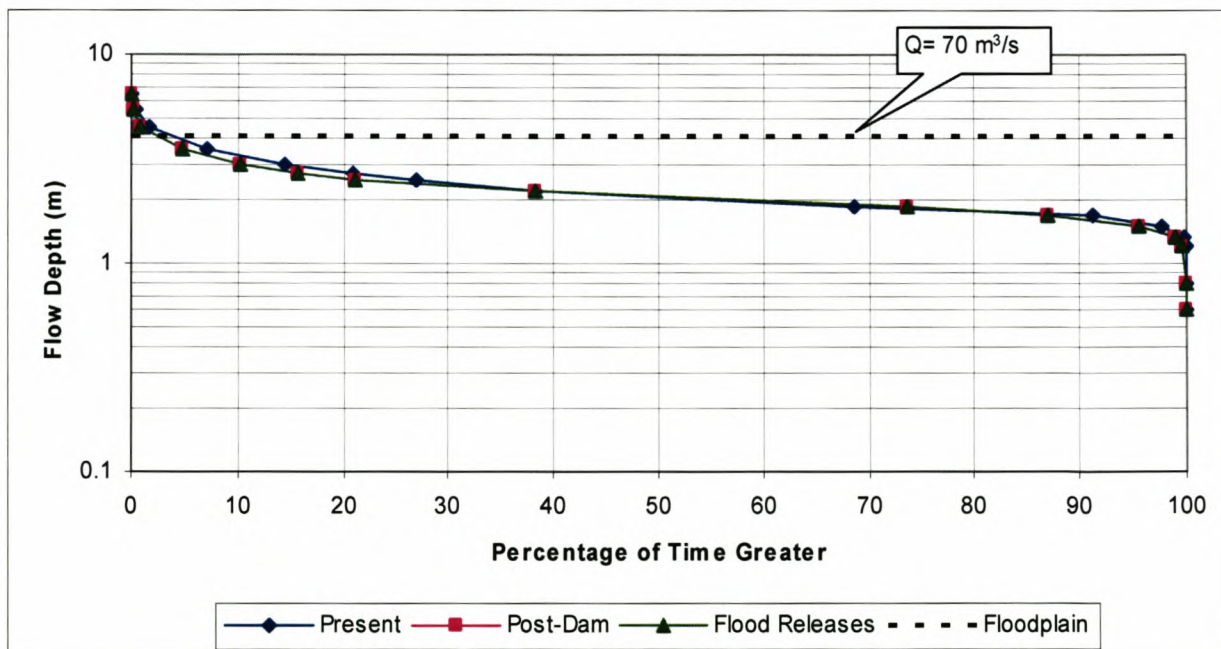


Figure 10-54 Flow depth - frequency graph for BRM5 – transect B

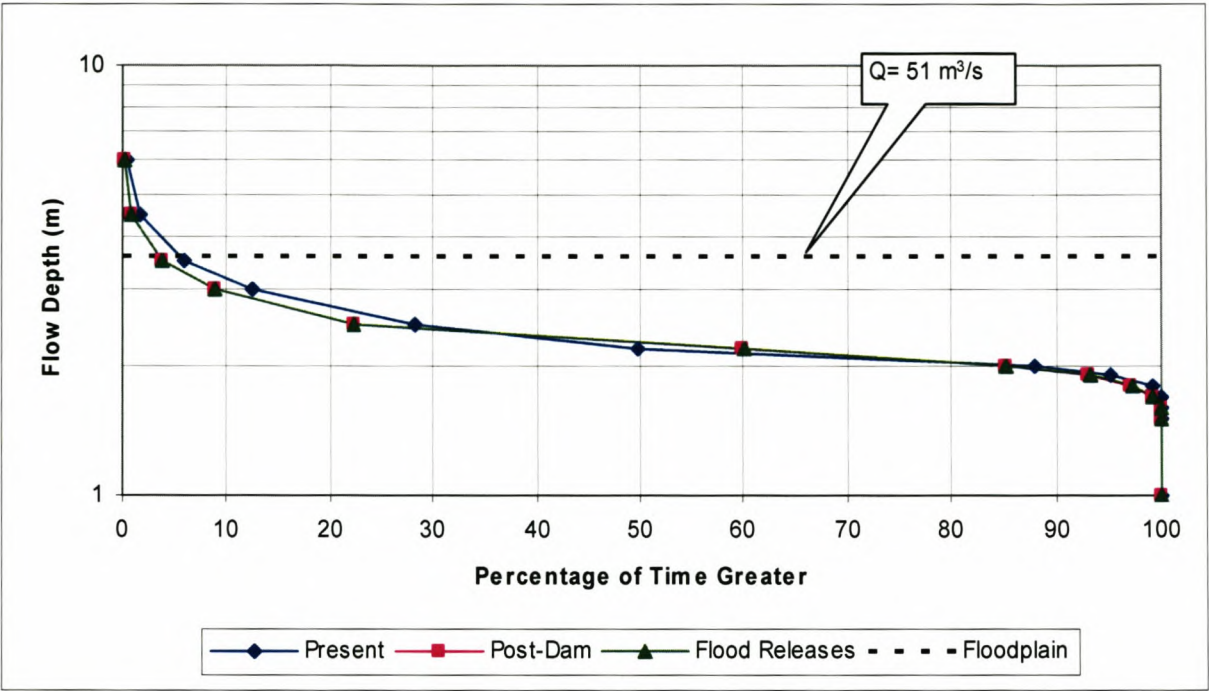


Figure 10-55 Flow depth - frequency graph for BRM5 – transect C

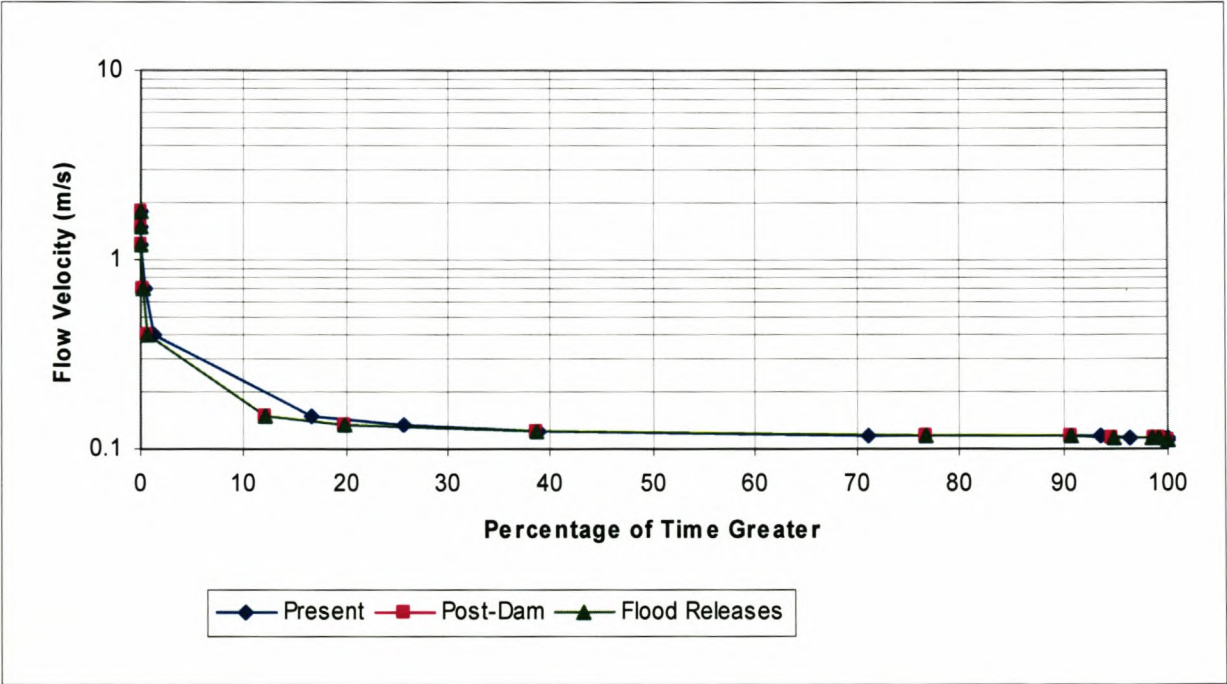


Figure 10-56 Flow velocity - frequency graph for BRM5 – transect A

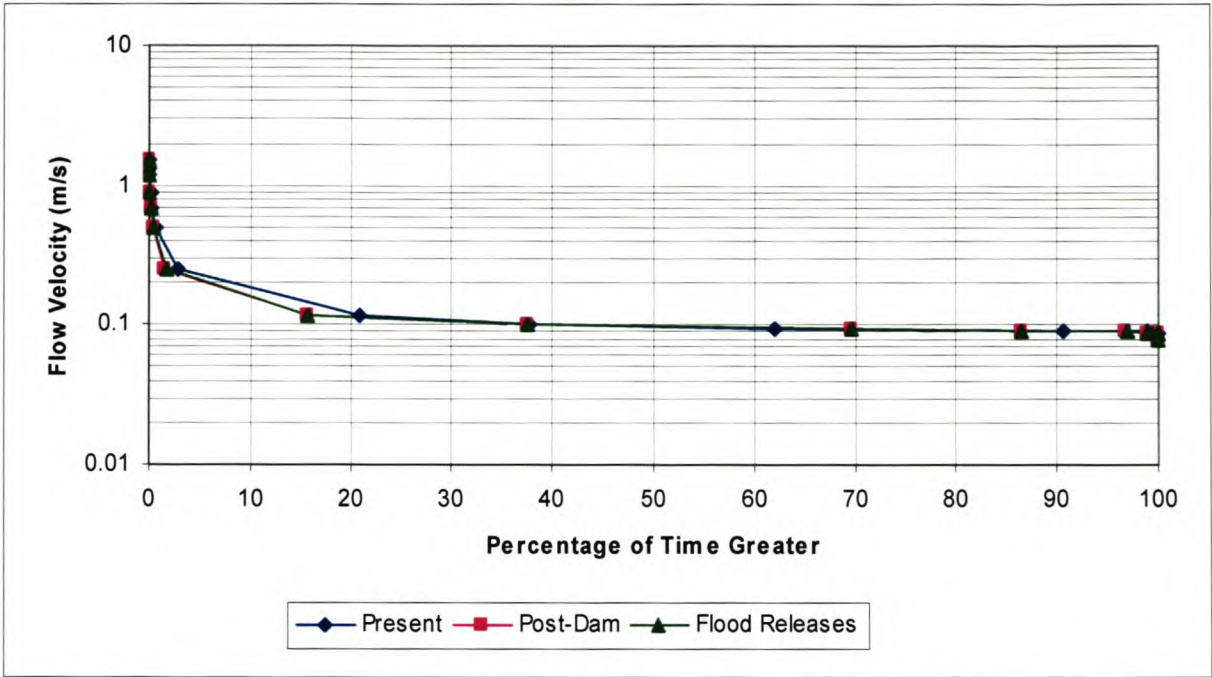


Figure 10-57 Flow velocity - frequency graph for BRM5 – transect B

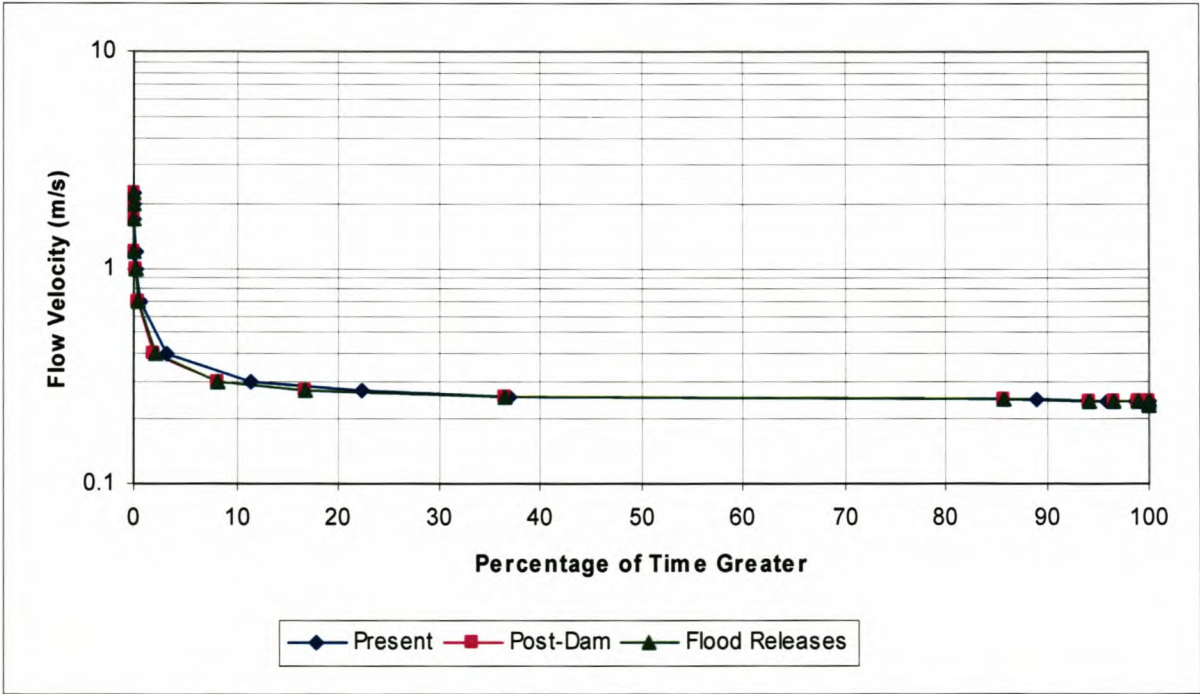


Figure 10-58 Flow velocity - frequency graph for BRM5 – transect C

10.1.3.5 Site BRM6

Simulated 9-year flow series for each scenario are given in **Figure 10-59** to **Figure 10-64**. It can be seen that number of small and intermediate floods has increased even further. However, the largest flood for the post-dam scenario at 942 m³/s is now almost the same than the 986 m³/s at present. From **Figure 10-65** it can be seen that as a result of the IFR and irrigation releases the frequency of flows between 2 and 10 m³/s is almost the same for all three scenarios as it was at

the other BRM sites as well. However, floods and those flows less than 2 m³/s occur almost as frequently with the dam than they did for the present scenario.

The same trend can be observed from **Table 10-18**, as the flows in class 1 have increased significantly for the post-dam scenario, while the contribution of flows in classes 3 and 4 is less than half of what it was for the present scenario. However, the flood releases have increased the flows in classes 2, 3 and 4 above that of the post-dam scenario. Flow depth - frequency graphs for each of three transects if provided in **Figure 10-66** to **Figure 10-68**. Flow velocity - frequency graph for each of three transects if provided in **Figure 10-69** to **Figure 10-71**.

It can be seen from **Figure 10-66** to **Figure 10-68** that the floodplain (indicated by broken lines) is inundated just over 23% of the time and drops to just below 21% with the dam development (see **Table 10-19**). The flood releases do not increase the floodplain inundation.

Table 10-18 Contribution of within year floods to total flow for three scenarios at BRM6

Class (DRIFT)	Discharge [m³/s]¹ (Instantaneous peaks)	Present	Post-dam	Flood releases
1	0 – 24.4	85.39%	89.03%	89.06%
2	24.4 – 48.8	8.02%	6.20%	6.09%
3	48.8 – 97.6	4.05%	3.11%	3.08%
4	97.6 – 195.2	1.66%	0.98%	1.04%

¹: The same ranges were taken as for BRM5 since no other gauging station data is available

Table 10-19 Floodplain inundation at BRM6

Scenario	Inundation [days/year]
Present	84.33
Post-dam	75.62
Flood releases	75.62

Much the same as at BRM5 the number of floods above 200 m³/s is under slightly reduced for the post-dam conditions from 29 at present down to 22 (see **Table 10-20**), while with the flood releases the number increases to 26. The number of floods exceeding 400 m³/s is also reduced from 11 at present to only 8 with the dam with or without the flood releases.

Table 10-20 Number of floods above 200 m³/s for the 9-year period at BRM6

Discharge [m³/s] (Instantaneous peaks)	Present	Post-dam	Flood releases
> 200	29	22	26
> 400	11	8	8
> 600	4	3	3

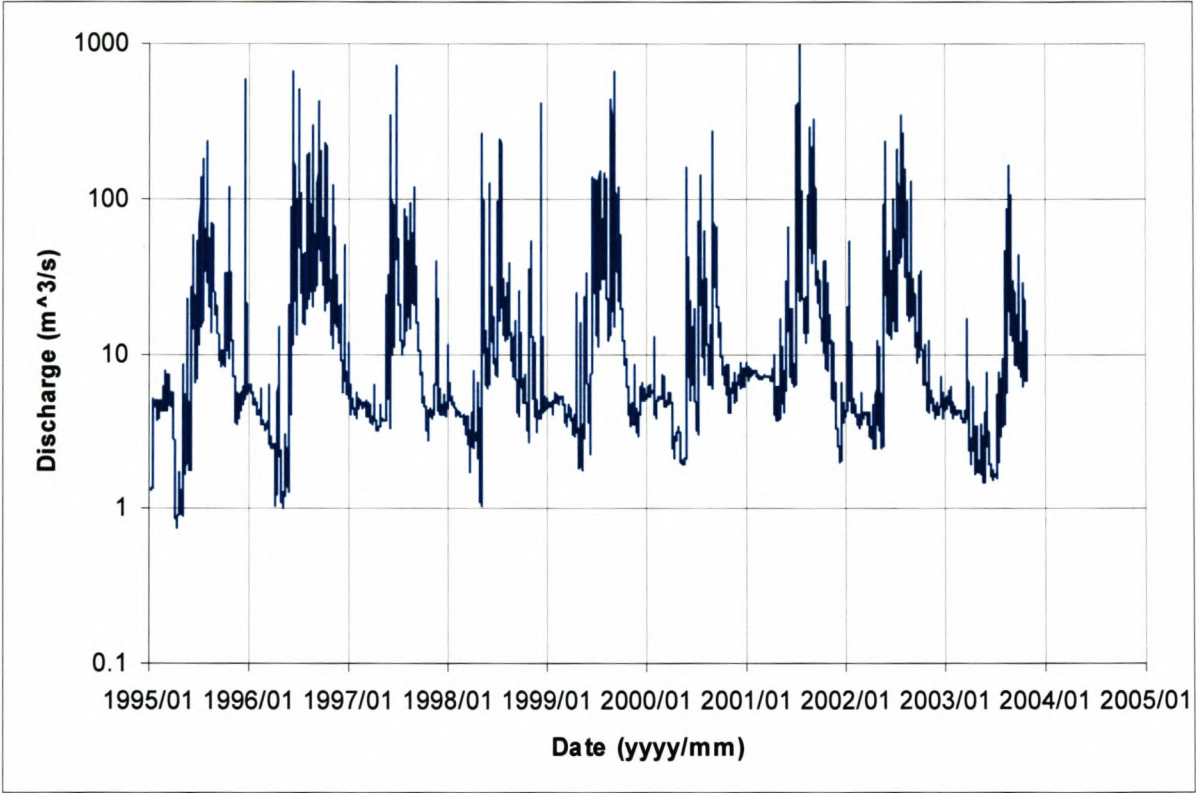


Figure 10-59 **Simulated flow series (9 years) for BRM6 – present day scenario (instantaneous peak data) – log scale**

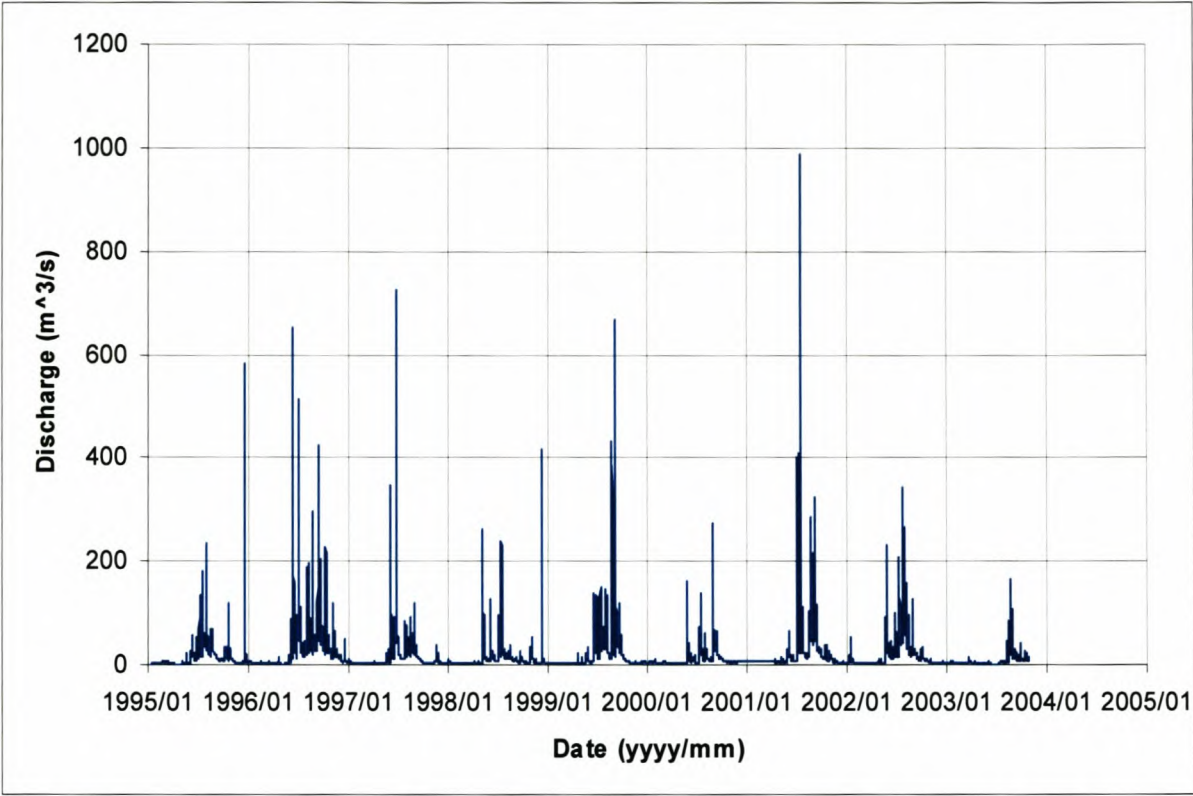


Figure 10-60 Simulated flow series (9 years) for BRM6 – present day scenario (instantaneous peak data) – normal scale

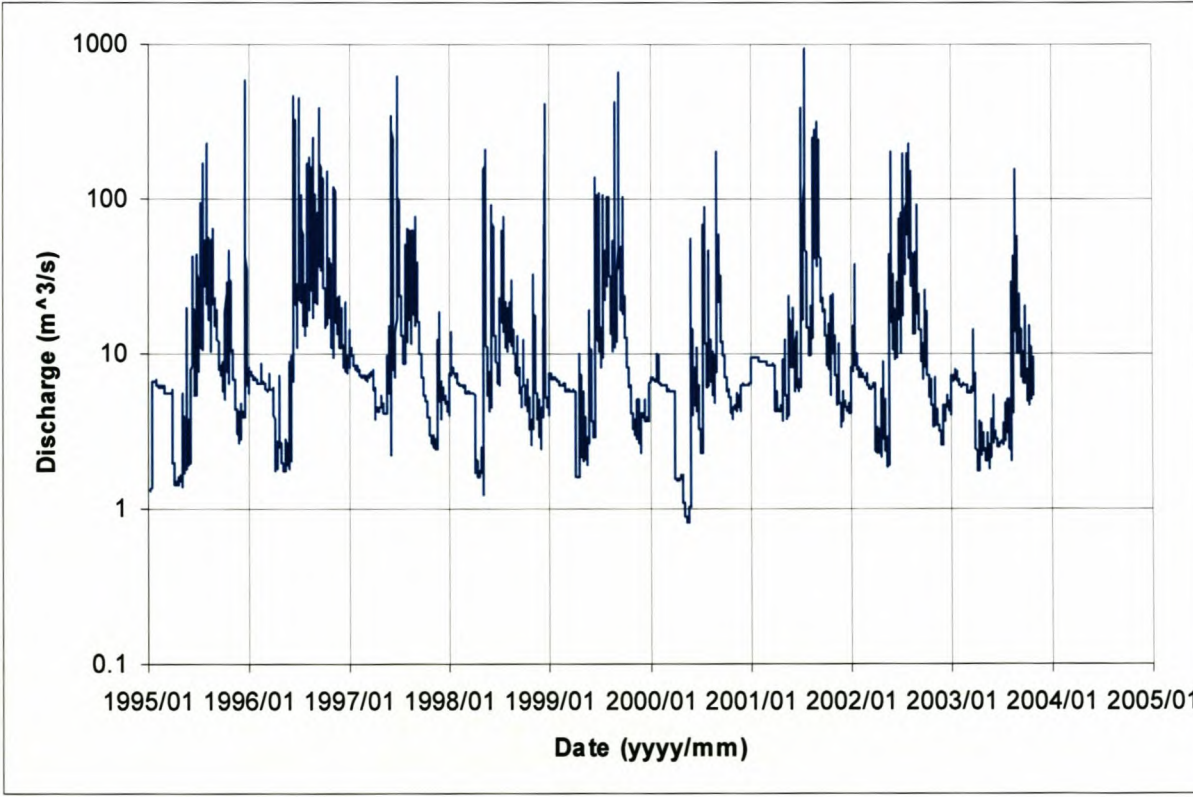


Figure 10-61 Simulated flow series (9 years) for BRM6 – post-dam scenario (instantaneous peak data) – log scale

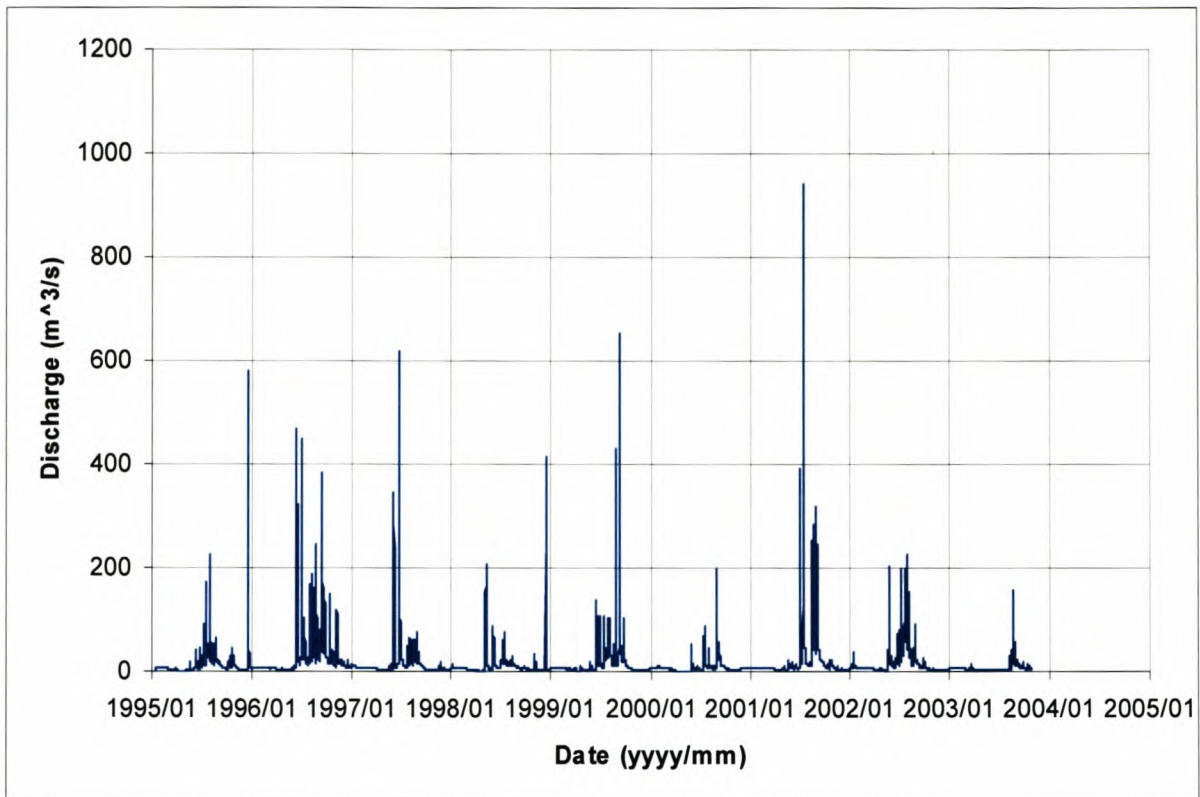


Figure 10-62 Simulated flow series (9 years) for BRM6 – post-dam scenario (instantaneous peak data) – normal scale

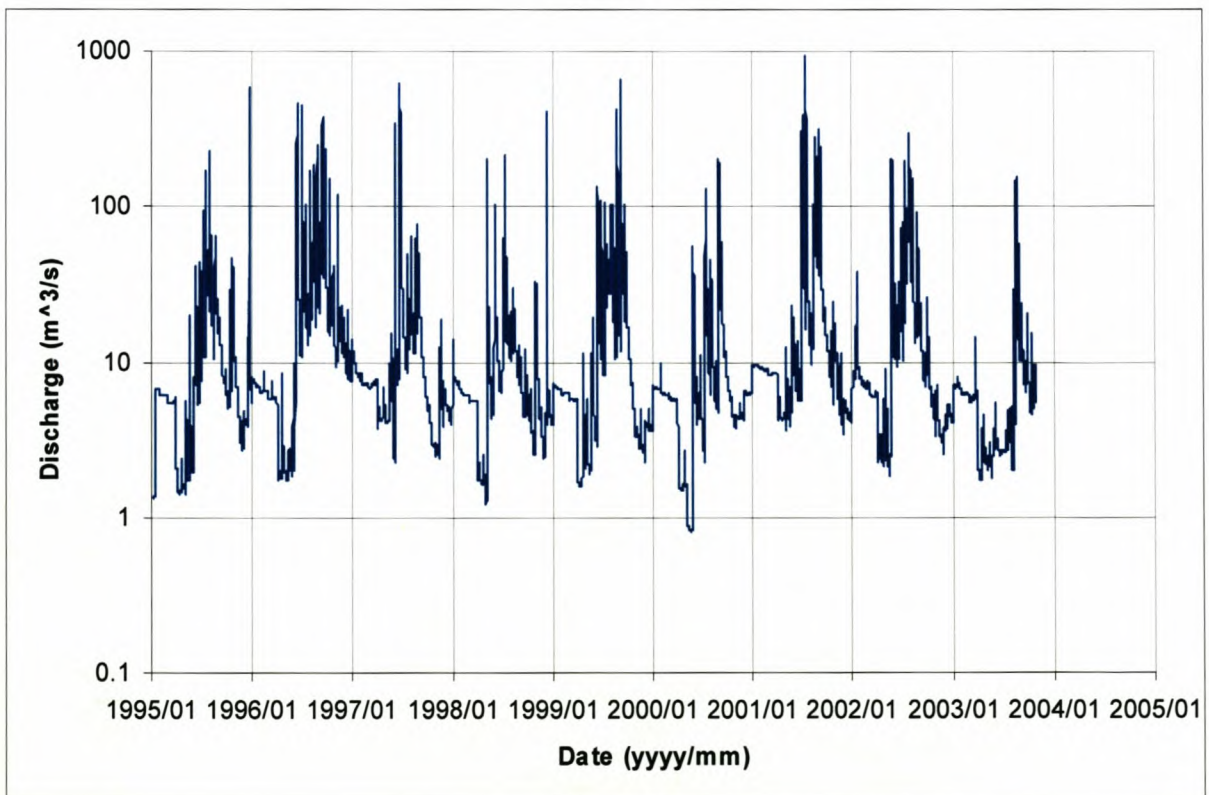


Figure 10-63 Simulated flow series (9 years) for BRM6 – post-dam with flood releases scenario (instantaneous peak data) – log scale

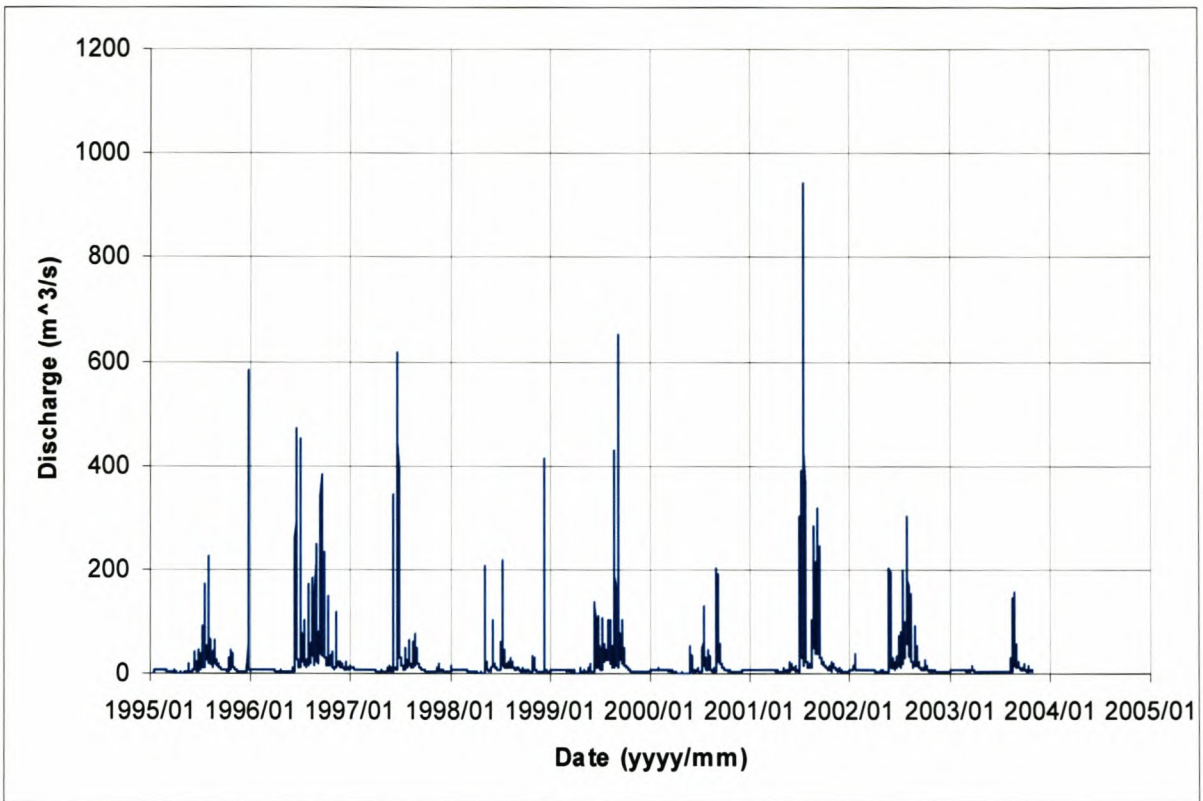


Figure 10-64 Simulated flow series (9 years) for BRM6 – post-dam with flood releases scenario (instantaneous peak data) – normal scale

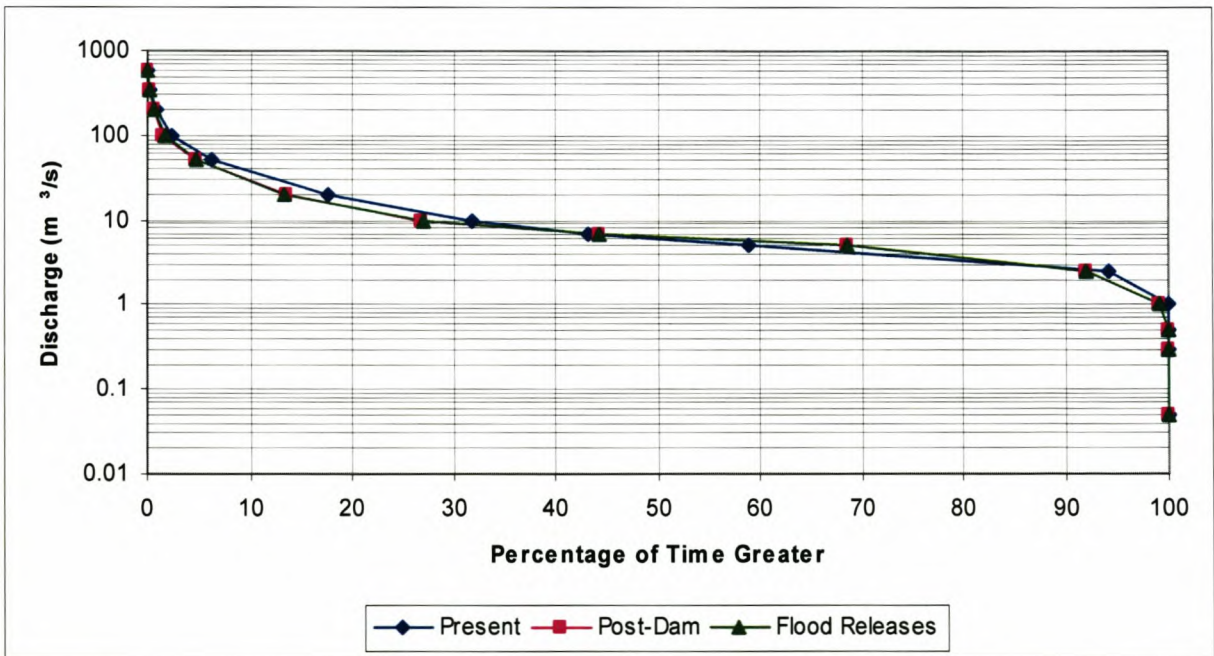


Figure 10-65 Discharge - frequency graph for BRM6

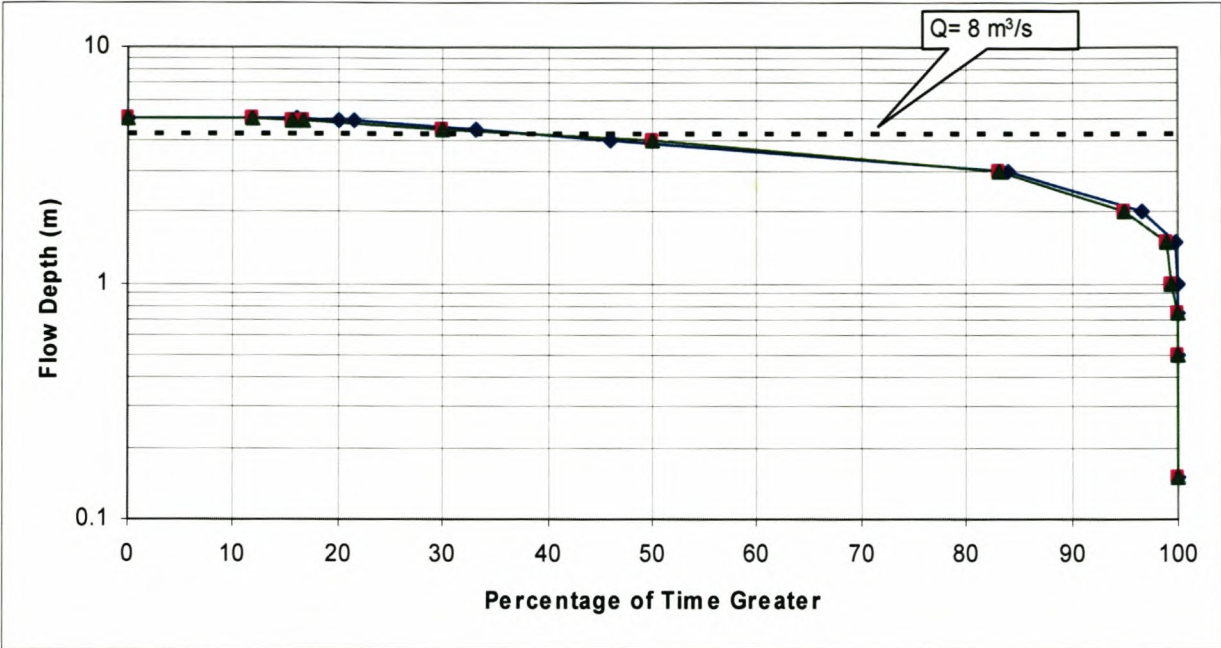


Figure 10-66 Flow depth - frequency graph for BRM6 – transect A

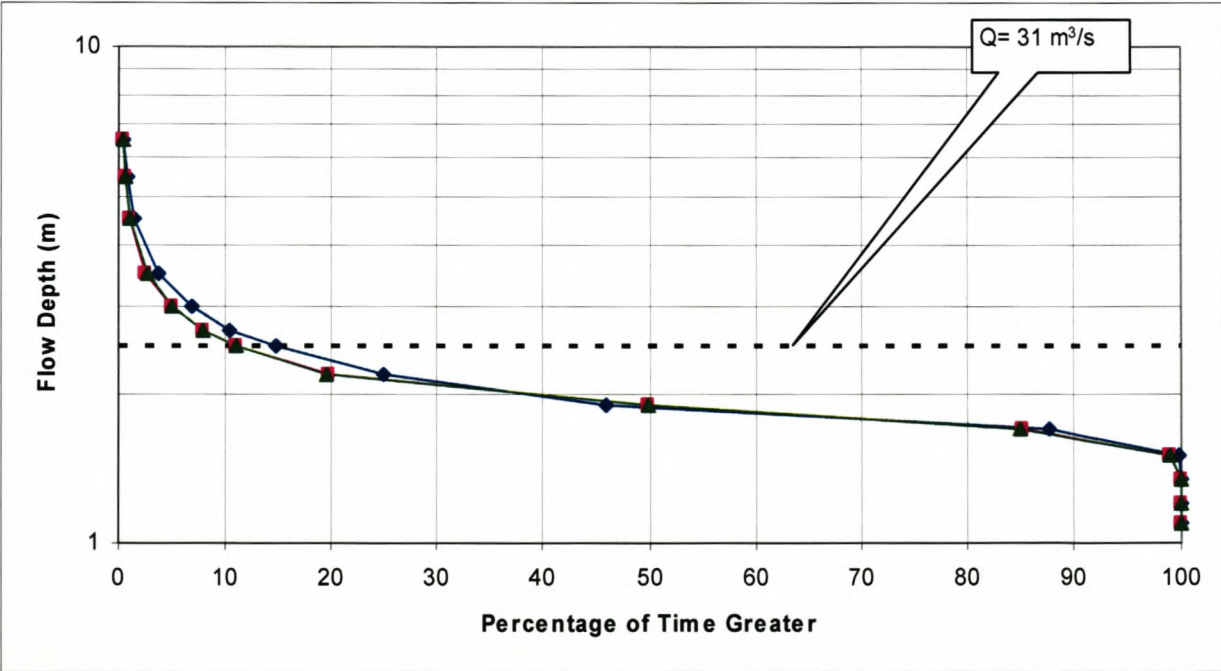


Figure 10-67 Flow depth - frequency graph for BRM6 – transect B

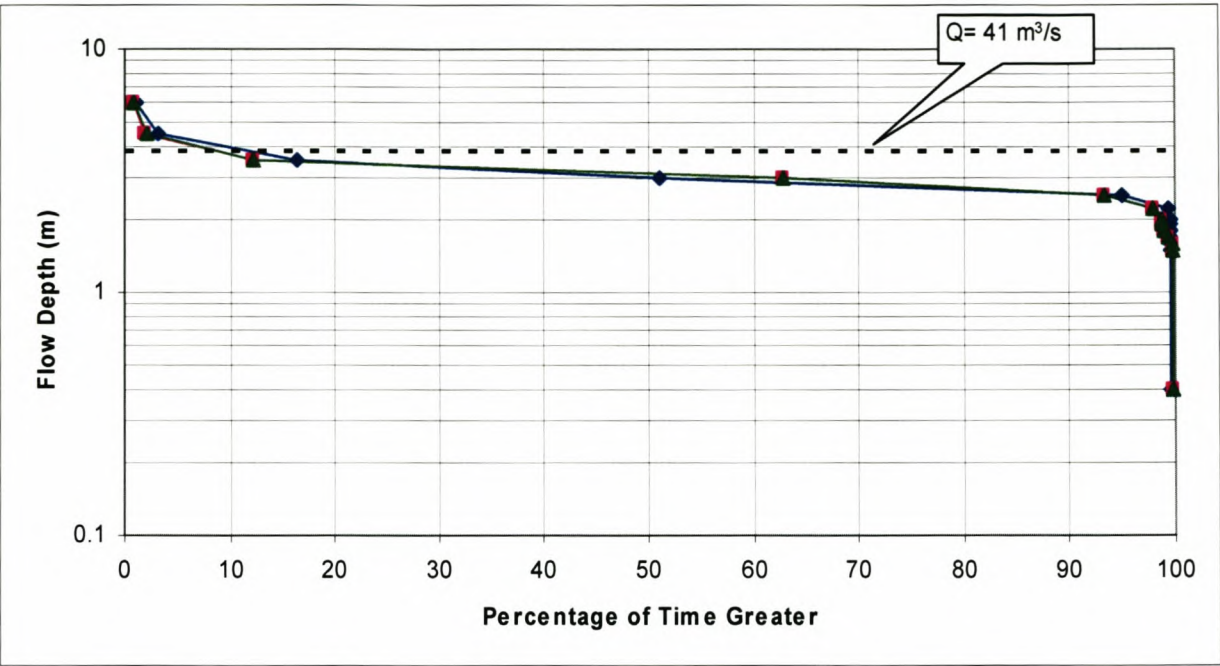


Figure 10-68 Flow depth - frequency graph for BRM6 – transect C

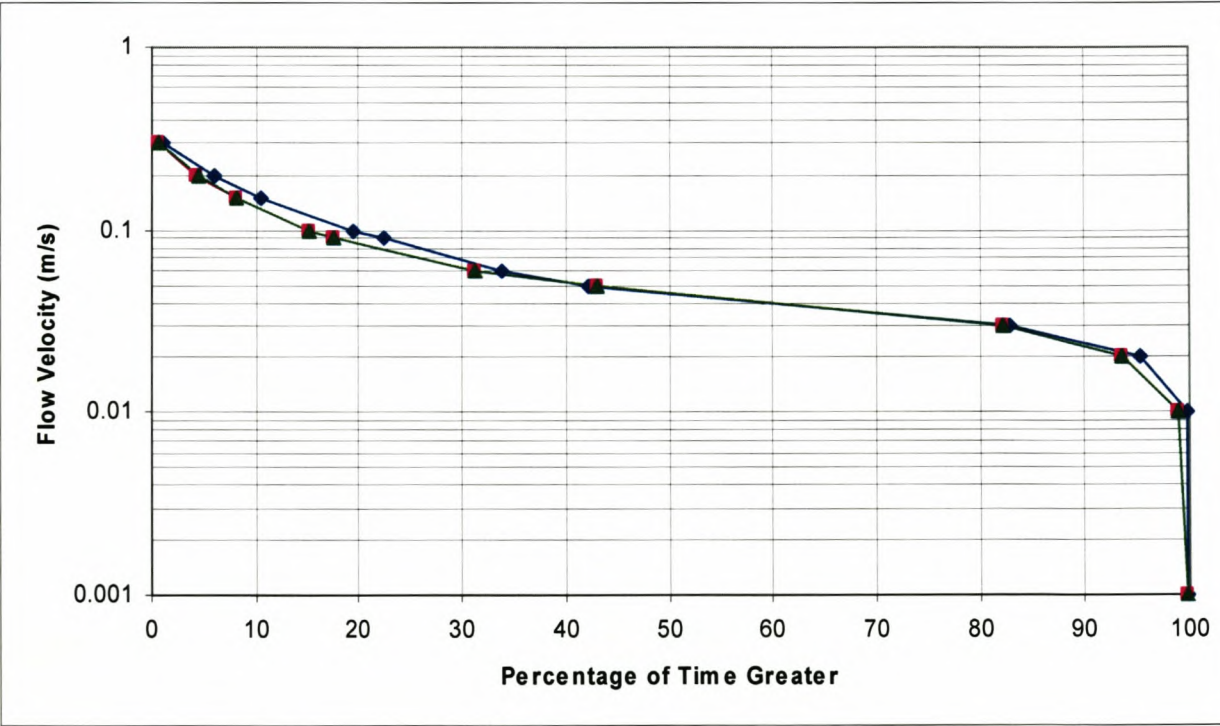


Figure 10-69 Flow velocity - frequency graph for BRM6 – transect A

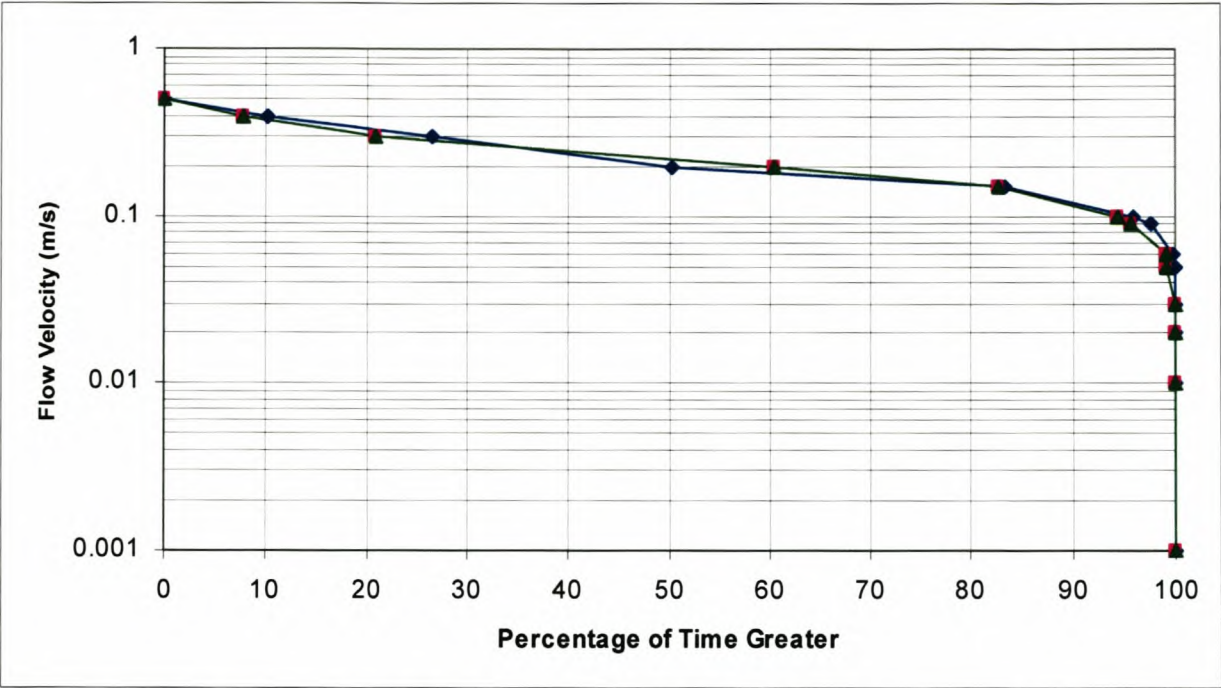


Figure 10-70 Flow velocity - frequency graph for BRM6 – transect B

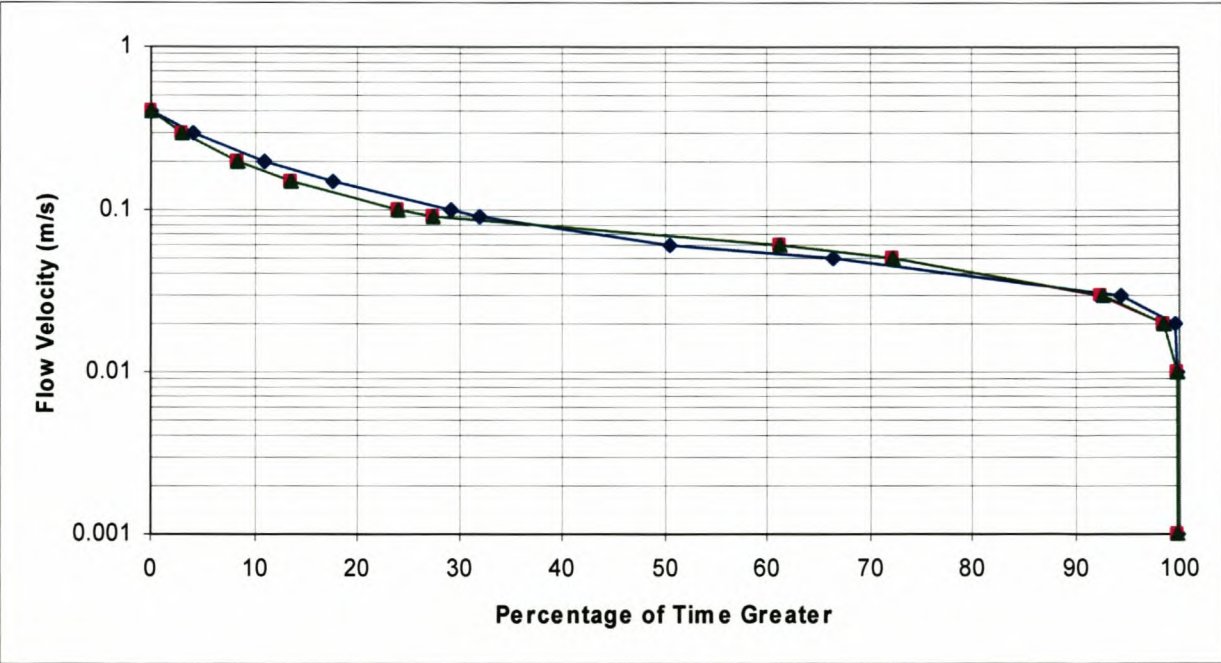


Figure 10-71 Flow velocity - frequency graph for BRM6 – transect C

10.1.4 Hydrodynamic Mass Balance

A mass balance of the volume of water at all the BRM sites, as well as tributaries and gauging stations on the Berg River is presented in **Figure 10-72** to **Figure 10-77**. Future abstractions at Drakenstein and irrigation releases at Wemmershoek are also indicated. From the graphs below it can be seen that the Berg River Dam reduces the annual volume of water in the river by about

111 million m³/a from 141 million m³/a at present. With the artificial flood releases the volume released into the river is only slightly higher at 35 million m³/a. The annual volumes are only based on the 9-year flow sequence, and will therefore differ from the volumes based on the longer period used in the hydrological analysis in this study. The relative values should, however, still be the same.

As a result of the adopted dam operating procedure only about 21% of present MAR at BRM2 will be released into the river with the dam in place. With the flood releases this increases to 25% of the MAR. At BRM3 around 70% of the present MAR will be available once the dam has been built, while with the flood releases this will be 72% of the MAR. This shows how important the tributary flows are to the total annual runoff of the Berg River. The Dwars River, for example, contributes 25 million m³/a, whereas the Wemmershoek and Franschhoek Rivers combined contribute over 80 million m³/a. Similarly for the lower Berg River the Klein Berg, Twenty-fours and Matjies River tributaries contribute much more to the total flow than the others.

At BRM4 around 78% of the present MAR will be available once the dam has been built. This indicates that the tributaries between BRM2 and BRM3 (i.e. Franschhoek, Dwars) have a much greater contribution to the total flow than those between BRM3 and BRM4 (i.e. Krom, Doring). At BRM5 more than 83% present MAR will be available once the dam has been built, while at BRM6 this percentage increases to almost 86%, while with the flood releases this percentage will be almost 87%.

Berg River Mass Balance - Present Situation - Hydrodynamics

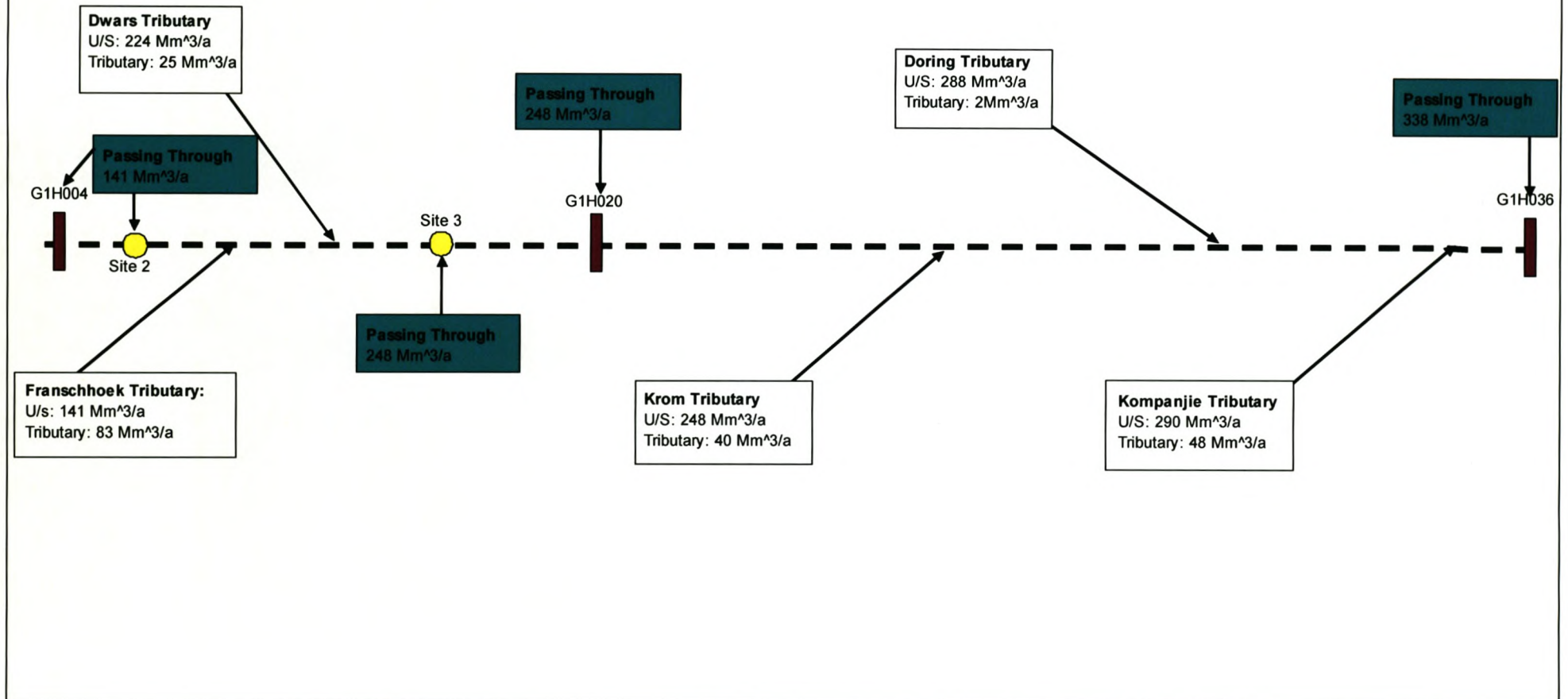


Figure 10-72 Upper Berg River mass balance – present situation (Million m³/a)

Berg River Mass Balance - Post Dam Situation - Hydrodynamics

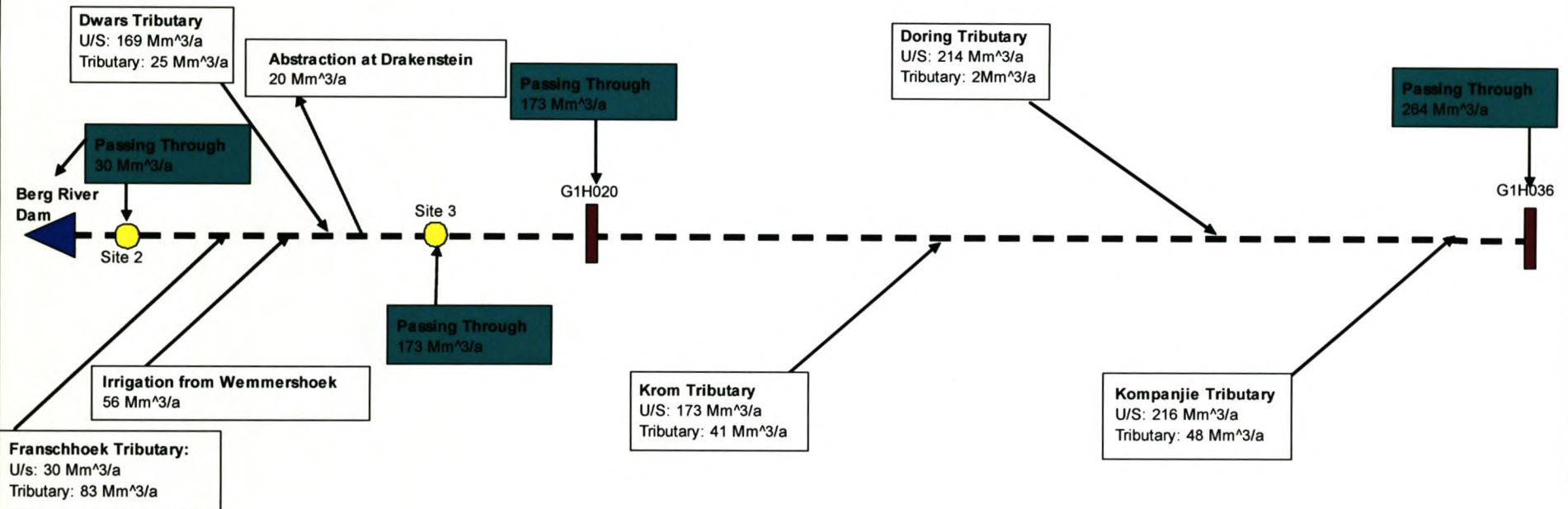


Figure 10-73 Upper Berg River mass balance – post-dam scenario (Million m³/a)

Berg River Mass Balance - Post Dam Situation & Flood Releases - Hydrodynamics

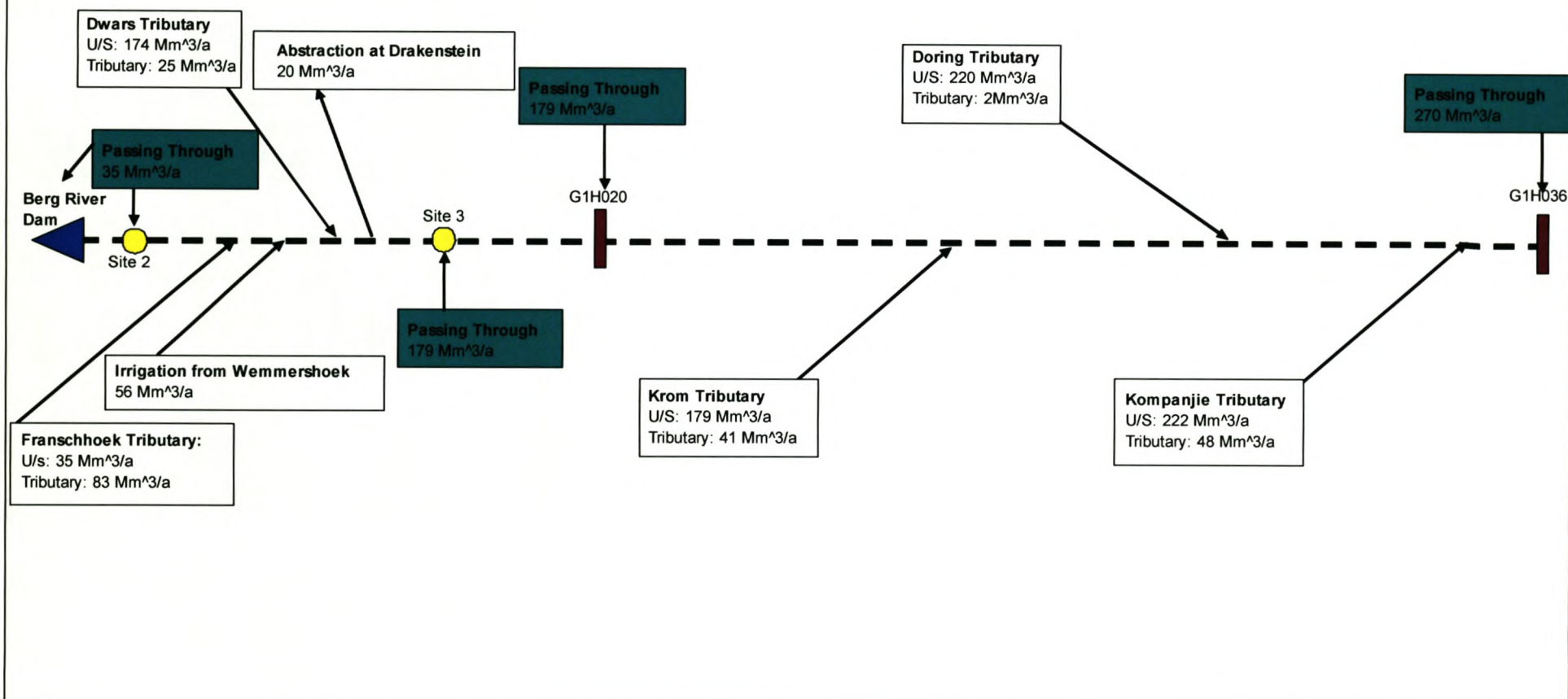


Figure 10-74 Upper Berg River mass balance – post-dam with flood releases (Million m³/a)

Berg River Mass Balance - Present Situation - Hydrodynamics

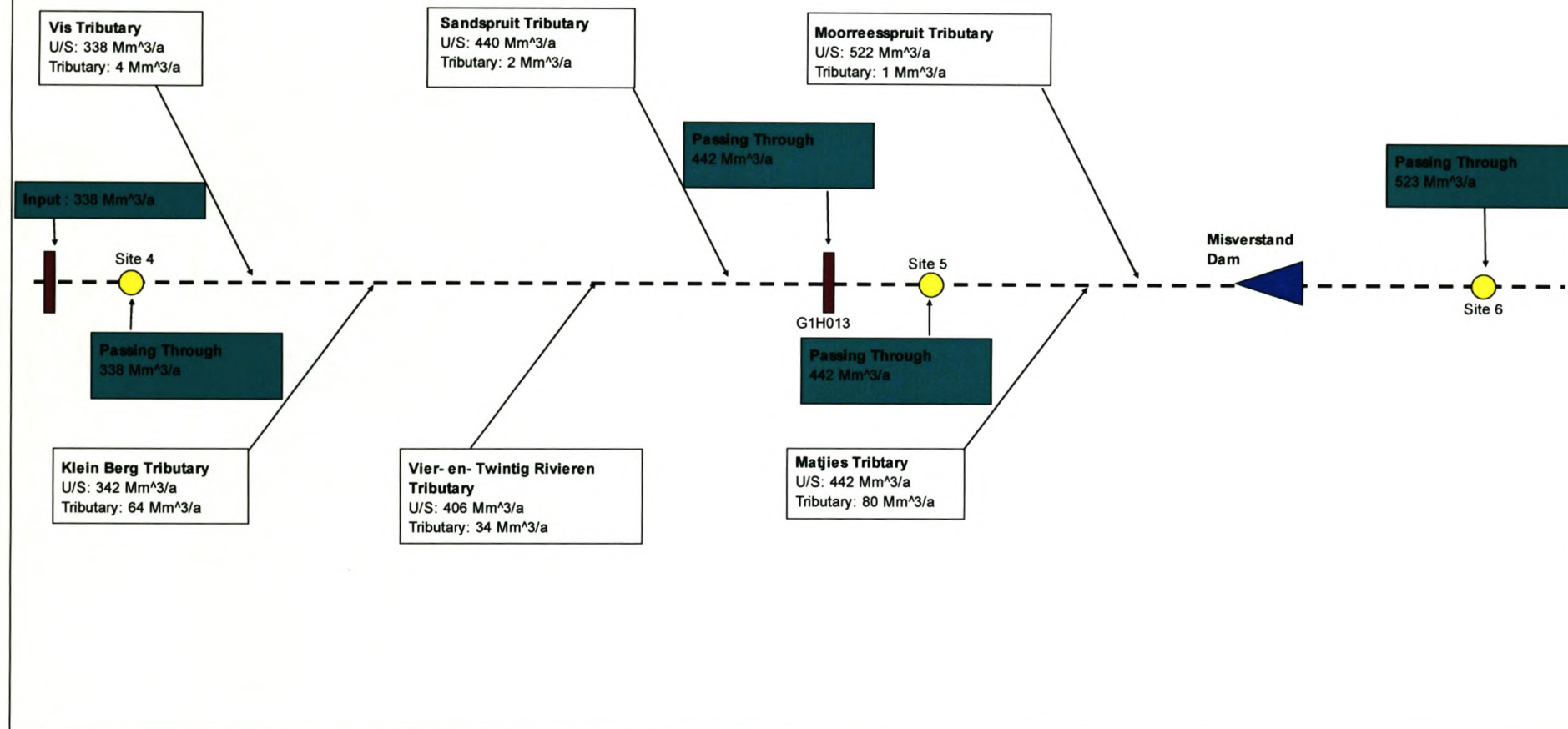


Figure 10-75 Lower Berg River hydrodynamic mass balance - present situation (Million m³/a)

Berg River Mass Balance - Post Dam Situation - Hydrodynamics

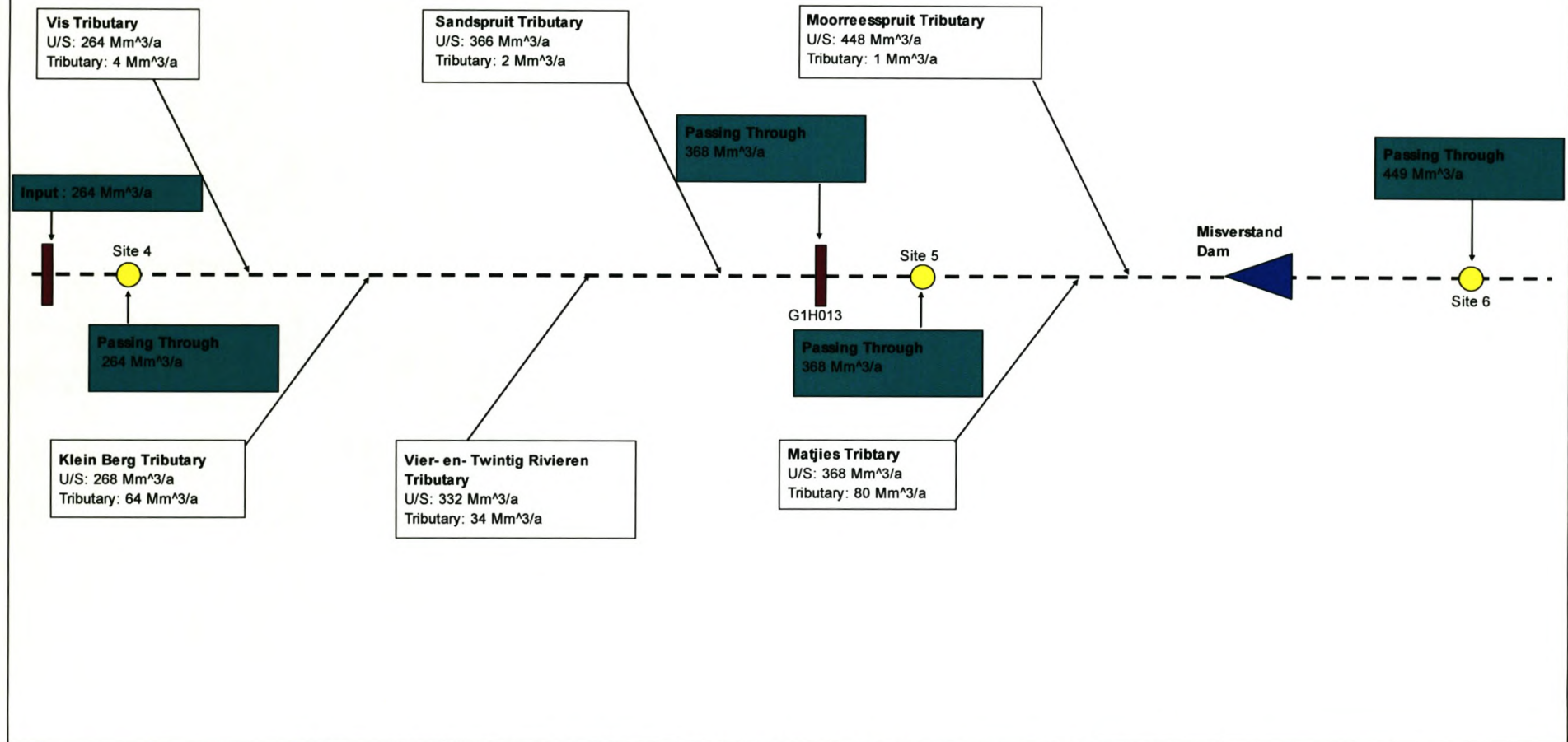


Figure 10-76 Lower Berg River hydrodynamic mass balance – post dam situation (Million m³/a)

Berg River Mass Balance - Post Dam Situation & Flood Releases - Hydrodynamics

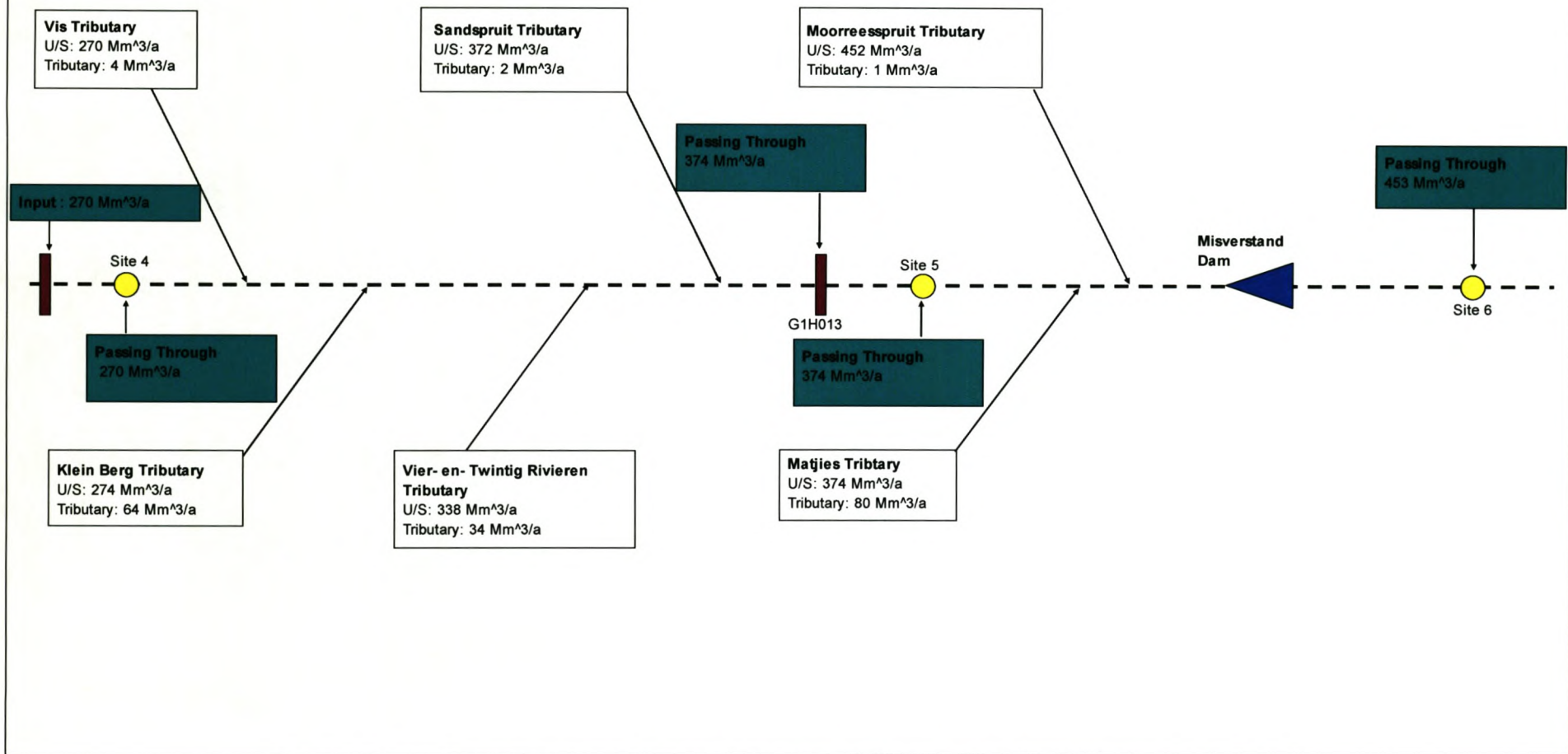


Figure 10-77 Lower Berg River hydrodynamic mass balance - post-dam with flood releases (Million m³/a)

10.2 Sediment Transport Model Results

The sediment transport module of MIKE11 was used to investigate the changes of the sediment transport in the Berg River system due to the construction of the Berg River dam as well as the changes in the sediment mass balance in the system. When the sediment transport module is used the program takes some time to reach a state of equilibrium. **Figure 10-78** to **Figure 10-82** shows the cumulative sediment discharge at the various BRM sites along the Berg River. The sediment transport is considered to be in equilibrium when no significant change in the cumulative sediment discharge occurs with time. From these figures it is evident that the sediment transport only reaches equilibrium at the beginning of 1997. Therefore when the data analysis of the results were carried out only data later than 1997 was used in order to insure that the sediment transport is in a state of equilibrium for all the scenarios that were investigated.

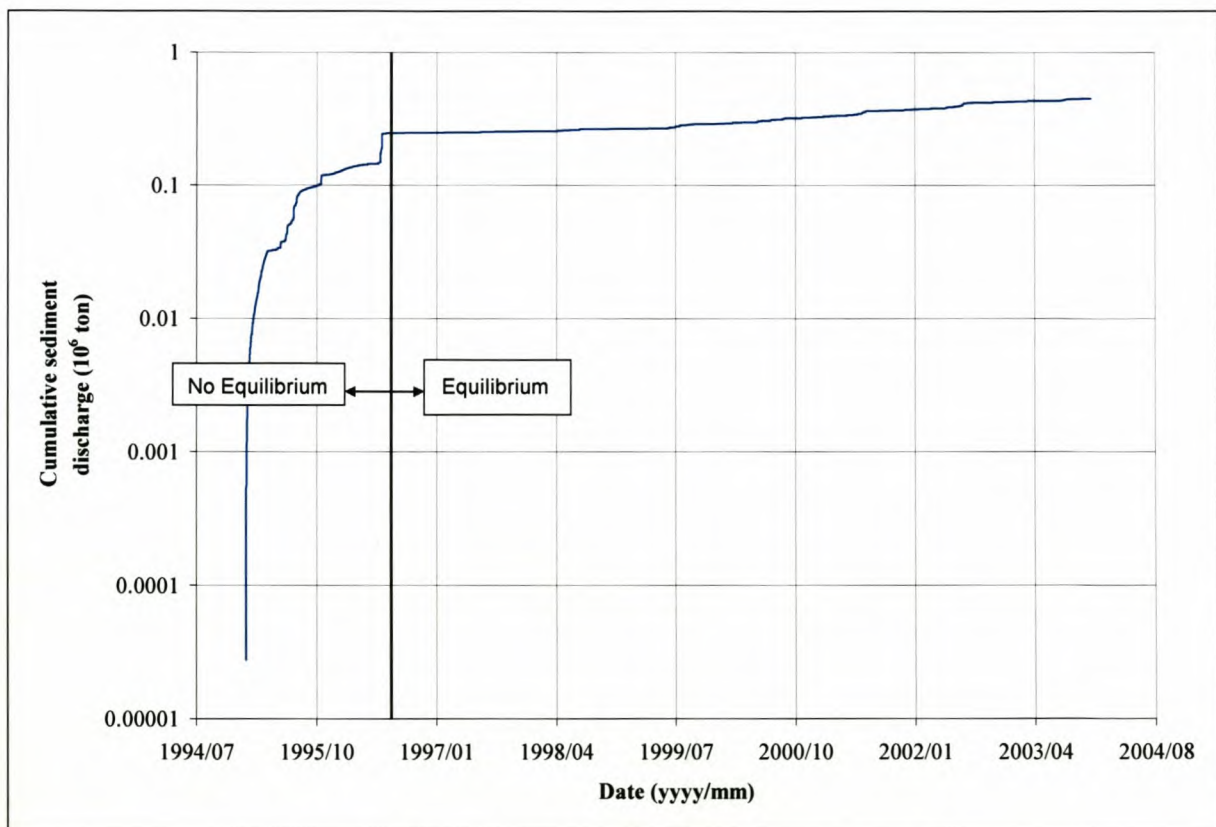


Figure 10-78 Cumulative sediment discharge at BRM2

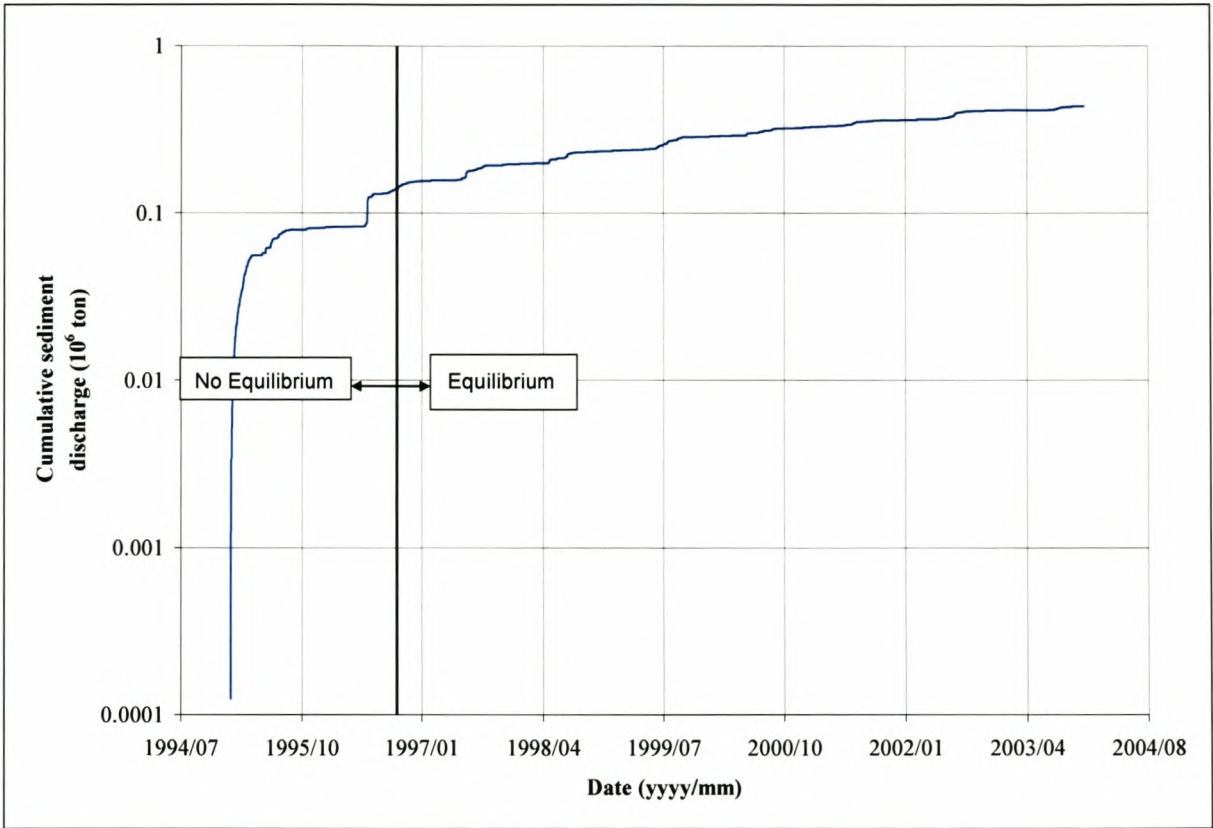


Figure 10-79 Cumulative sediment discharge at BRM3

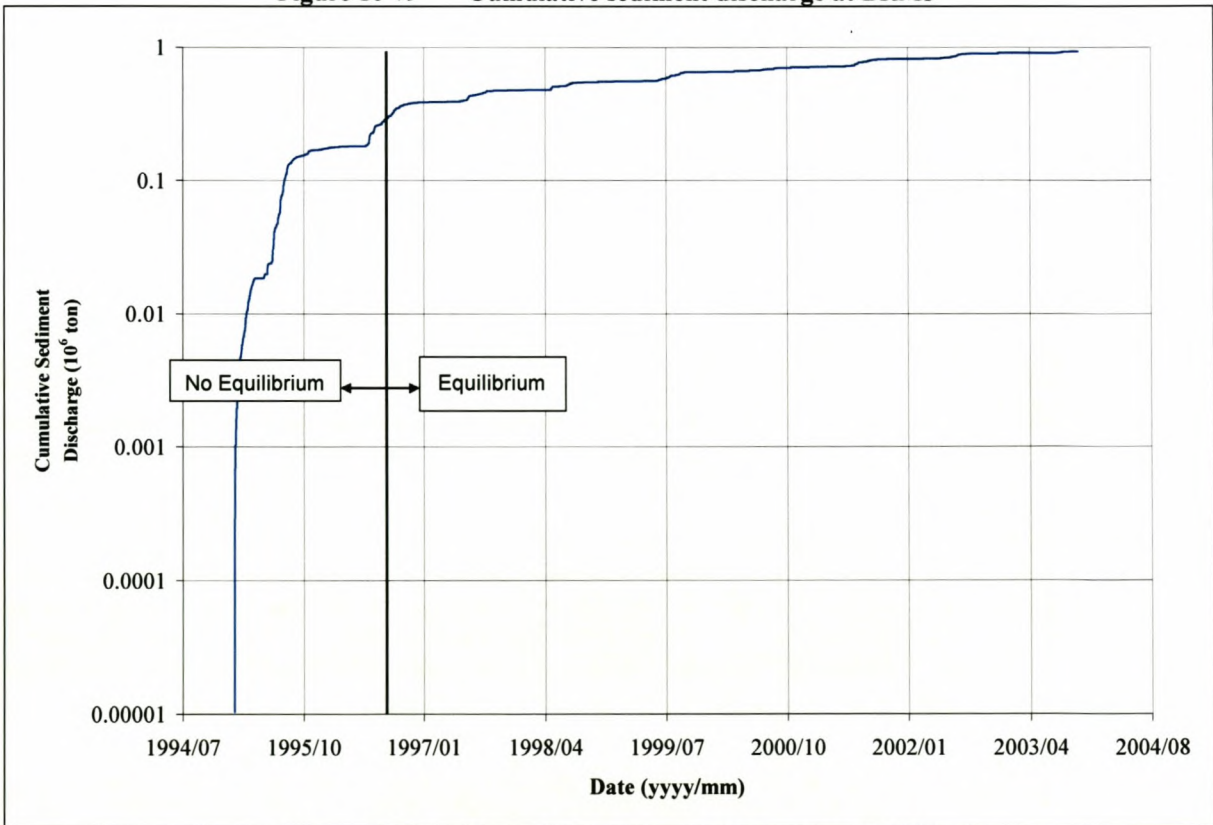


Figure 10-80 Cumulative sediment discharge at BRM4

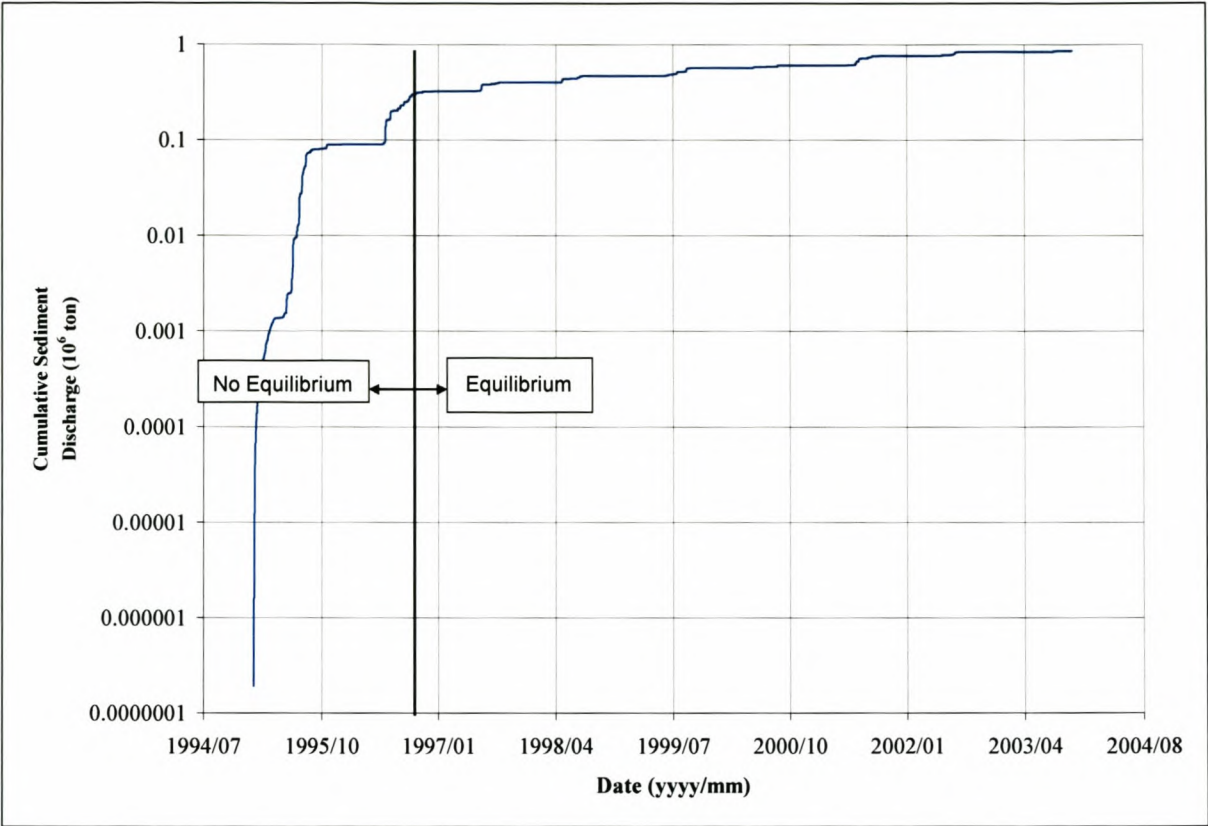


Figure 10-81 Cumulative sediment discharge at BRM5

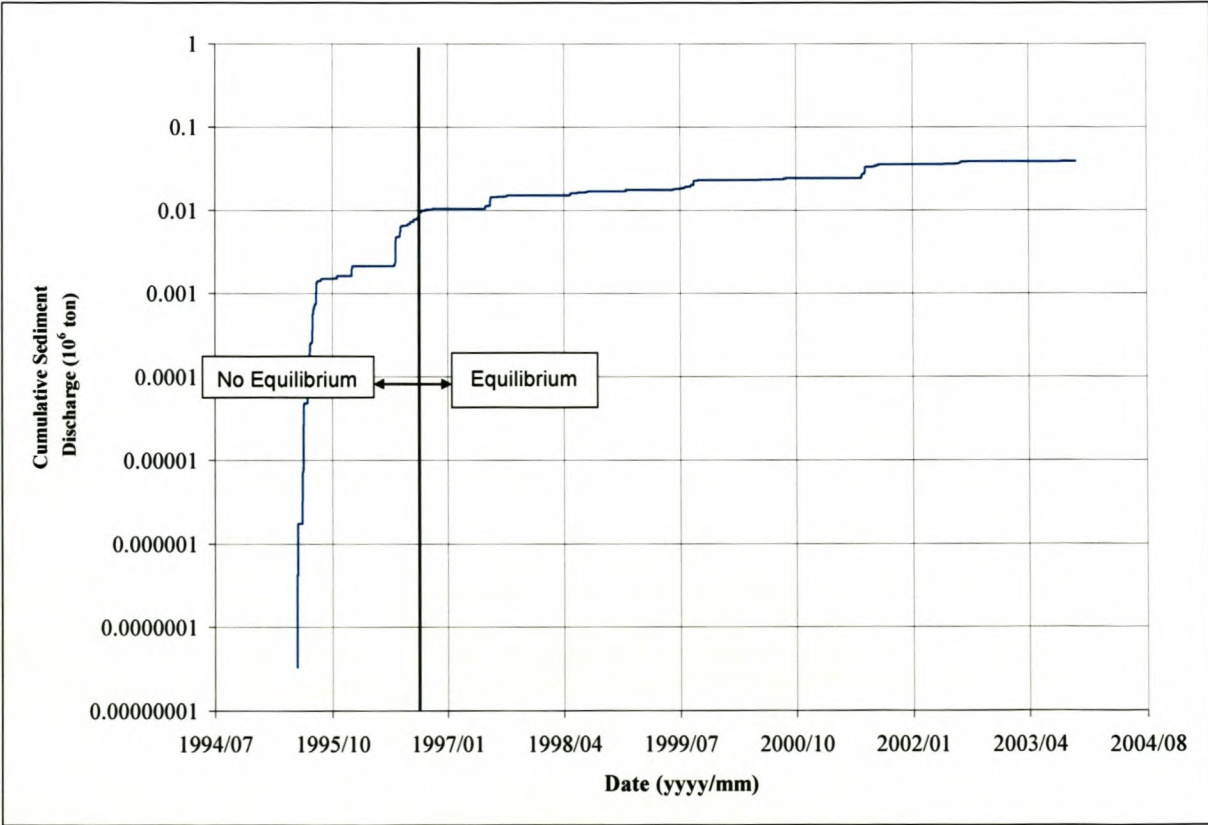


Figure 10-82 Cumulative sediment discharge at BRM6

10.2.1 Upper Berg River (Dam site to just upstream of Hermon): Effective Discharge and Sediment Mass Balance

The major downstream impacts of dams are a reduction of the magnitude and frequency of flood peaks, changes in flow duration and reduced downstream sediment supply due to the trapping of sediments in the reservoir. This, in general, will cause the river channel to narrow and increase in depth. In order to reverse some of the changes that have taken place, or prevent major changes from occurring, researchers have been attempting to define a regulated flow regime, which will have much the same effects as the natural pre-dam flow regime. The problem, however, is to define those flows that form and maintain the river channel and the floodplain. The relative importance of different flows can best be evaluated by determining the amount of sediment transported by each. The discharge that is responsible for the transportation of the greatest amount of sediment over time is termed the effective discharge. The results obtained from the simulations done in MIKE11 were used to create effective discharge tables at the various BRM sites.

The effective discharge at each of the baseline monitoring sites has been determined, based on the sediment transport data from the 7-year (1997 – 2003) simulation period.

10.2.1.1 Site BRM2

From **Table 10-21** it can be seen that the effective discharge for site 2 varies between 2.6 to 4.8 m³/s for the post dam scenario, 23.3 to 72.4 m³/s for the present scenario and 24.7 to 136.9 m³/s for the post dam with flood releases scenario. The same can be seen from **Figure 10-83**. The huge difference between the values is a result of the big influence the dam will have on the river reach just downstream of it. As more tributaries enter the Berg River this influence will decrease. It is also evident that due to the fact that the dam will only spill on major flood events it cuts off most flows between 10 and 100 m³/s if no artificial floods are released (**Figure 8-8**). This can also be seen from **Table 10-21** as, for the post dam scenario, 94.79% of this sediment are transported by a discharge smaller than 8 m³/s. Even with the artificial flood releases only the upper portion are restored to a higher value compared to the present scenario. This can be verified from **Table 10-21**, for the post dam with flood releases

scenario more than 50% of the sediment is transported by a discharge higher than 23 m³/s while for the present scenario 43.6% of the sediment is transported by a discharge higher than 23 m³/s.

Table 10-21 Site 2 - flow classes and associated sediment transport

% time equalled or exceeded	Flow class interval (%)	Present		Post-dam		Flood releases	
		Mean flow ¹ (m ³ /s)	% of total load	Mean flow (m ³ /s)	% of total load	Mean flow (m ³ /s)	% of total load
99.99							
90	9.99	0.7	0.90	0.3	0.53	0.3	0.34
80	10	1.3	1.95	0.4	0.83	0.4	0.52
70	10	1.8	2.80	0.44	0.98	0.44	0.61
60	10	2.4	3.83	0.5	1.17	0.5	0.72
50	10	3.0	4.82	0.8	2.42	0.8	1.46
40	10	3.5	5.92	1.0	3.42	1.0	2.04
30	10	4.0	6.89	1.6	6.91	1.6	4.02
20	10	4.6	8.03	2.6	14.98	2.6	8.63
10	10	5.9	10.62	3.6	24.66	3.6	13.72
5	5	10.8	10.66	4.4	16.65	4.4	9.32
1	4	23.3	20.71	4.8	15.35	4.7	8.24
0.1	0.9	72.4	17.23	7.5	6.89	24.7	21.99
0.01	0.09	203.2	5.65	27.6	5.21	136.9	28.40

¹: Mean flow over corresponding flow class

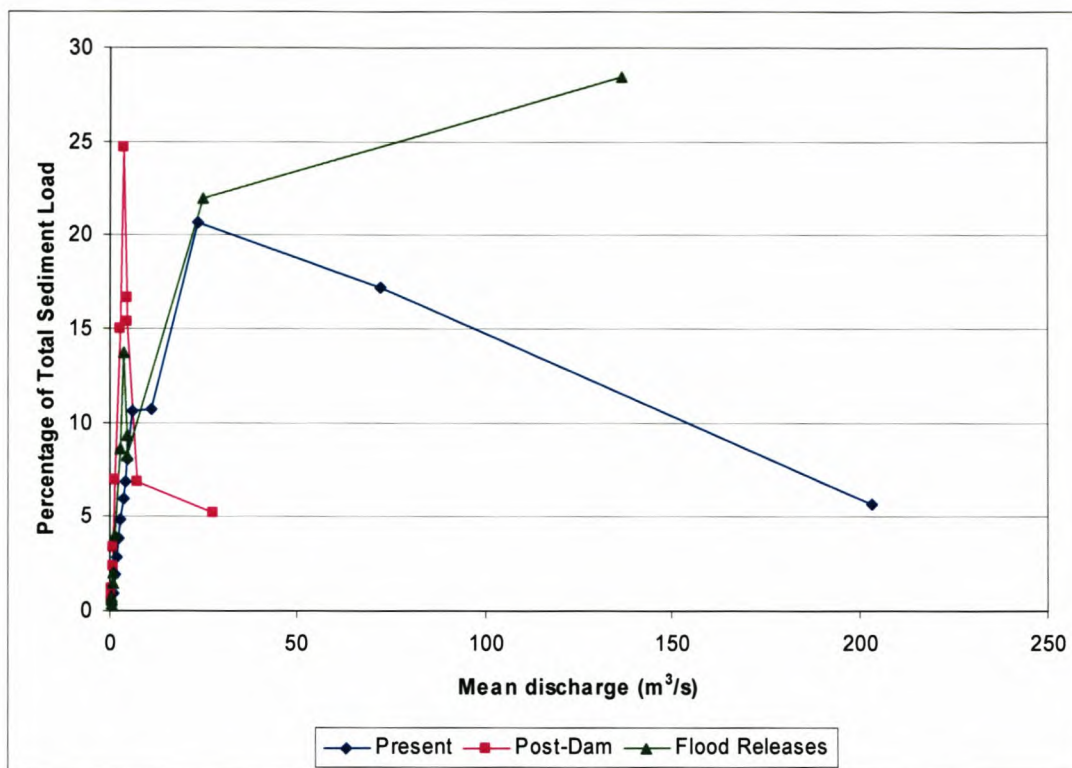


Figure 10-83 Percentage of total sediment load versus mean discharge at site 2

10.2.1.2 Site BRM3

From **Table 10-22** it can be seen that the effective discharge for BRM3 varies between 41.8 and 55.9 m³/s. The same can be seen from **Figure 10-84**.

Table 10-22 Site 3 - flow classes and associated sediment transport

% time equalled or exceeded	Flow class Interval (%)	Present		Post-dam		Flood releases	
		Mean flow1 (m3/s)	% of total load	Mean flow (m3/s)	% of total load	Mean flow (m3/s)	% of total load
99.99							
90	9.99	1.6	0.53	1.4	1.06	1.4	1.01
80	10	2.6	1.09	2.2	2.09	2.2	1.98
70	10	3.3	1.53	2.9	3.10	2.9	2.93
60	10	3.9	1.96	3.6	4.22	3.6	3.98
50	10	4.5	2.43	4.3	5.30	4.3	5.00
40	10	5.2	3.03	5.0	6.68	5.0	6.27
30	10	6.2	3.92	5.8	8.14	5.8	7.61
20	10	7.6	5.41	6.5	9.59	6.5	8.96
10	10	11.8	10.32	8.4	14.02	7.8	11.75
5	5	20.8	12.17	12.6	12.51	10.3	8.71
1	4	41.8	27.63	19.2	18.14	19.5	17.20
0.1	0.9	100.2	23.11	42.0	12.56	55.9	17.24
0.01	0.09	207.3	6.88	69.8	2.59	155.6	7.36

¹: Mean flow over corresponding flow class

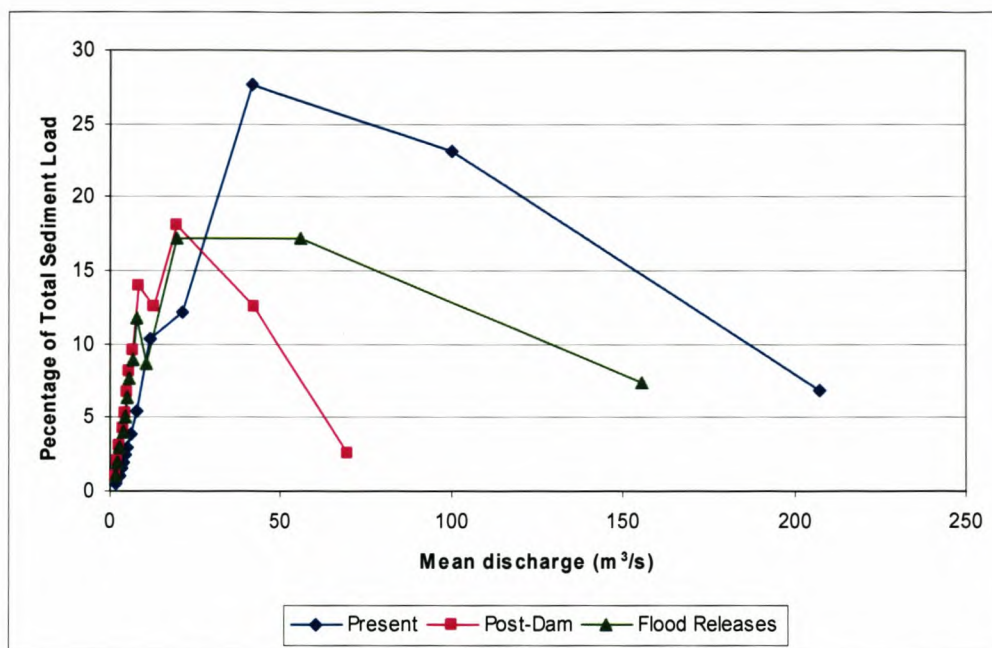


Figure 10-84 Percentage of total sediment load versus mean discharge at site 3

From **Table 10-22** and **Figure 10-84** it can be seen that the difference between the effective discharge at BRM3 for the three scenarios are already much smaller than that of BRM2. It is also evident that, for the post dam with flood releases scenario, there are two flow classes that are responsible for a large portion of the sediment transport at BRM3. It is clear from **Figure 10-84** that even though the values on the graph differ for the different scenarios it follows the same trend. This is an indication of the smaller effect the dam has on the flow regime at this point on the Berg River.

A mass balance of the sediment volumes at all the monitoring sites (BRM 2 and 3) in the upper reach of the Berg River, as well as tributaries and gauging stations on the Berg River is represented in **Figure 10-85** to **Figure 10-87**.

Berg River Mass Balance - Present Situation - Sediment Transport

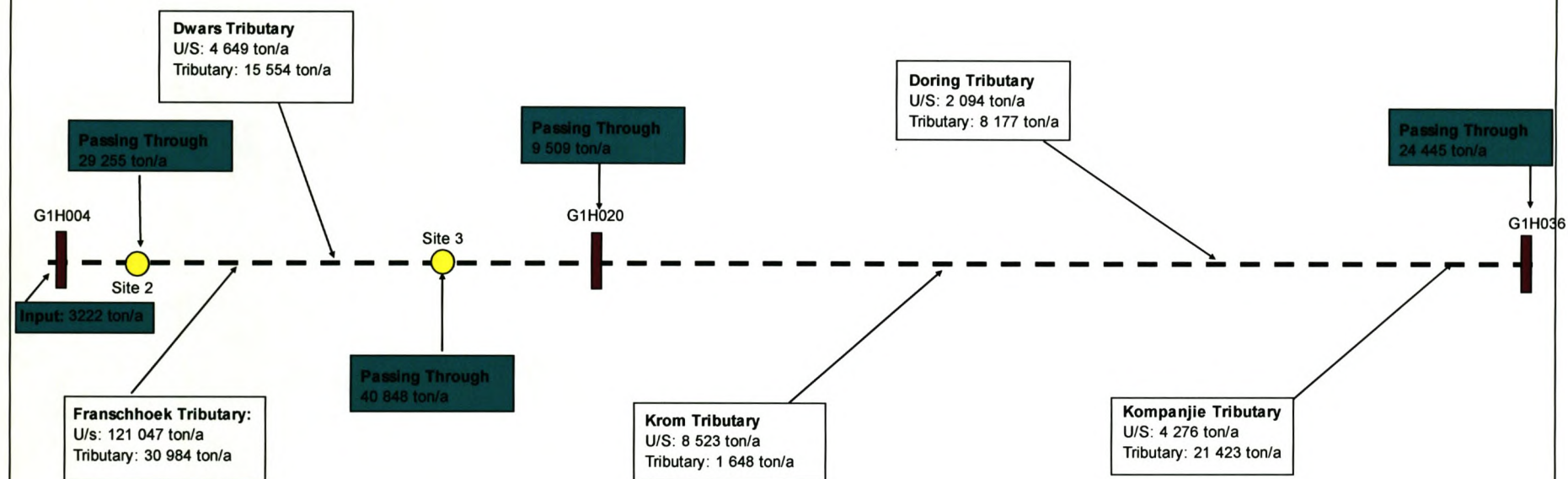


Figure 10-85 Upper Berg River mass balance – present situation

Berg River Mass Balance - Post Dam Situation - Sediment Transport

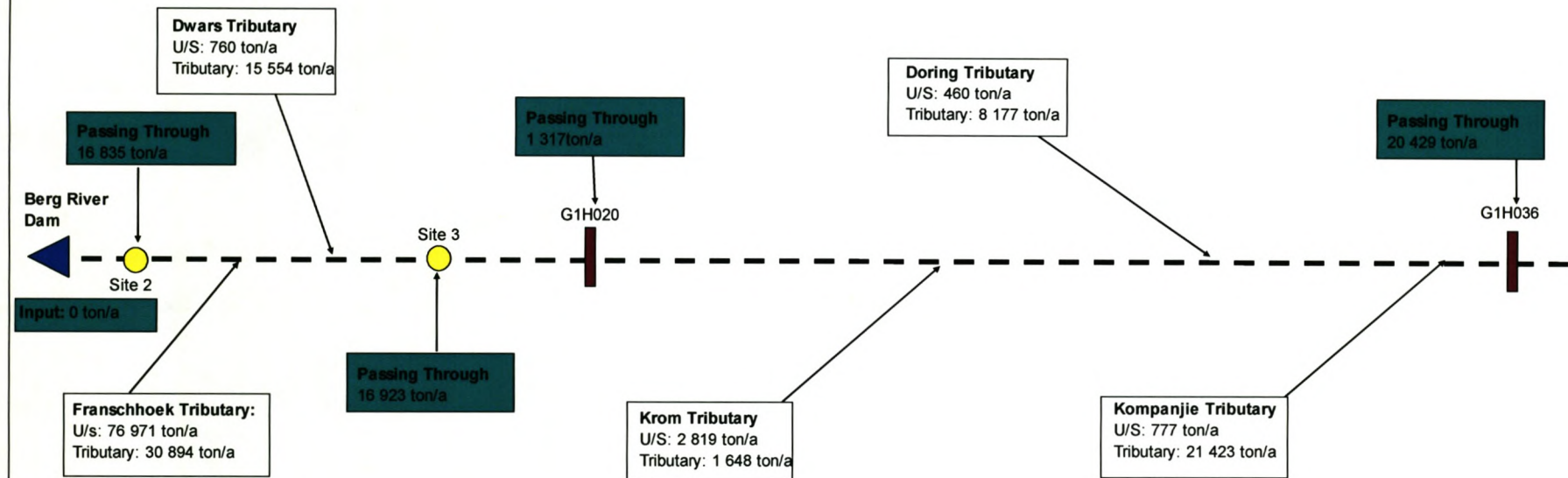


Figure 10-86 Upper Berg River mass balance – post-dam scenario

Berg River Mass Balance - Post Dam Situation & Flood Releases - Sediment Transport

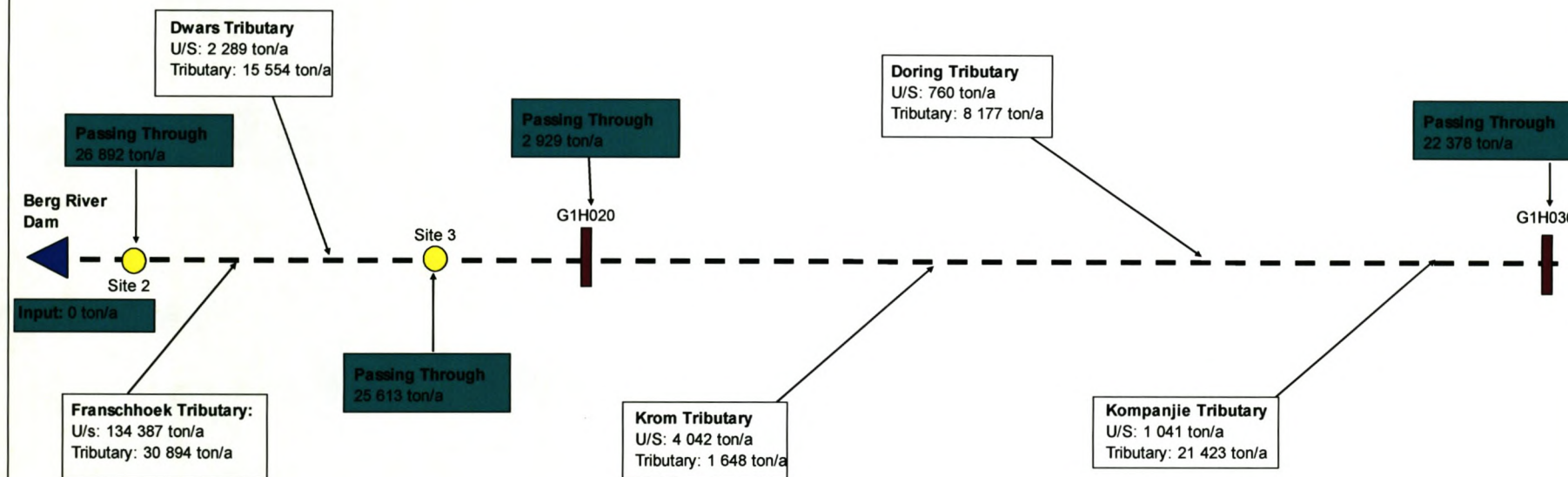


Figure 10-87 Upper Berg River mass balance – post-dam with flood releases

From **Figure 10-85** to **Figure 10-87** it can be seen that the dam will trap around 3200 ton/a, which means that less sediment will reach the river downstream of the dam, explaining why the annual sediment loads downstream will be reduced to some degree. However, the decrease in annual sediment load is in excess of 3200 ton/a, which can be explained by looking at the effective discharges in **Table 10-21**. For the present day scenario at site 2 the effective discharge is around $23.3 \text{ m}^3/\text{s}$, which accounts for 20.7% of the total load. For the post-dam scenario, however, the effective discharge is only $3.6 \text{ m}^3/\text{s}$. This lower flow has a somewhat lower sediment transport capacity, and therefore the total annual sediment loads are reduced. With the flood releases the annual sediment loads are increased to a value just below the value for the present scenario. Even though the effective discharge for the post dam with flood releases scenario is much higher ($136.9 \text{ m}^3/\text{s}$), the fact that it only occurs at most once or twice a year makes it ineffective to restore the volume of sediment to the present scenario. The smaller floods would have transported more sediment since the effective discharge in this case is about $3.6 \text{ m}^3/\text{s}$. The fact that such relatively small flows constitute the effective discharge could be as a result of the fact that the river is very steep and thus even small flows have a relatively high sediment transport capacity. This means that a lot of sediment, if it is available, is transported at low flows, and less sediment is available to be transported by the larger floods. At the other sites further downstream the effective discharge falls into a different flow class (i.e. less frequent flows), and this means that the larger floods carry more sediment, and thus the artificial flood releases are more effective.

At BRM3 the situation is very similar to that at BRM2. It can be seen that the floods that are released yet again fail to restore the sediment volume to its original state. During the present scenario 70% of the sediment is transported by floods larger than $20 \text{ m}^3/\text{s}$. The majority of these floods are being cut off by the dam, and the artificial floods that are released to replace these floods falls into a much larger flow class. The artificial floods account for a normal year flood event. Therefore those floods will be unable to restore the sediment volumes to its original state, but it definitely improves the sediment transport compared to the scenario with only the dam in place.

10.2.2 Lower Berg River (Site 4 to Head of Estuary): Effective Discharge and Sediment Mass Balance

10.2.2.1 Site BRM4

From **Table 10-23** it can be observed that the effective discharge for BRM4 varies between 42.6 and 62.0 m³/s. The same can be seen from **Figure 10-88**. It is evident from **Figure 10-88** and **Table 10-23** that the dam has a small effect on the sediment transport of the Berg River at this point. This can be seen from the smaller variation in the three graphs in **Figure 10-88** and the values in **Table 10-23**. It is evident from **Table 10-23** that the variation in magnitude of the different flow classes and their occurrences for the three scenarios is much less compared with the upstream BRM sites. This indicates that, at this point, the Berg River Dam does not have a large influence on the mass balance of sediment transport and hydrodynamics.

Table 10-23 Site 4 - flow classes and associated sediment transport

% time equalled or exceeded	Flow class interval (%)	Present		Post-dam		Flood releases	
		Mean flow ¹ (m ³ /s)	% of total load	Mean flow (m ³ /s)	% of total load	Mean flow (m ³ /s)	% of total load
99.99							
90	9.99	2.2	0.73	1.6	0.74	1.1	0.17
80	10	4.0	1.63	2.6	1.45	2.7	0.76
70	10	5.7	2.63	3.7	2.27	3.5	1.15
60	10	7.6	3.88	4.4	2.90	4.4	1.65
50	10	6.7	3.29	5.4	3.84	5.3	2.21
40	10	5.8	2.70	6.1	4.52	6.1	2.76
30	10	7.3	3.72	6.9	5.35	7.0	3.41
20	10	10.5	6.06	8.4	6.88	8.4	4.61
10	10	18.6	13.00	11.8	10.99	12.7	8.97
5	5	33.2	14.20	23.1	13.55	23.1	11.74
1	4	62.0	26.34	42.6	24.66	45.7	28.17
0.1	0.9	136.1	17.07	100.5	17.60	108.2	25.29
0.01	0.09	290.8	4.74	225.8	5.23	239.9	9.10

1: Mean flow over corresponding flow class

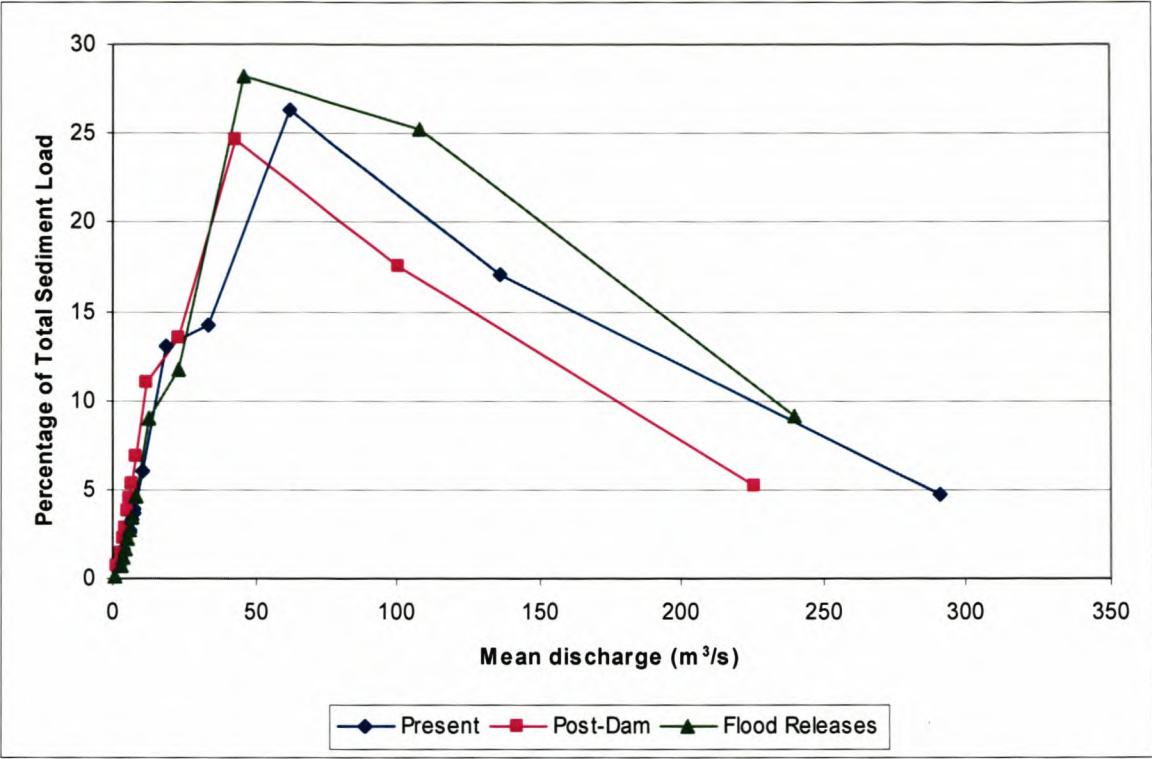


Figure 10-88 Percentage of total sediment load versus mean discharge at site 4

10.2.2.2 Site BRM5

Table 10-25 shows that the effective discharge for site 5 varies between 151.1 and 204.0 m³/s. The same can be seen from Figure 10-89. It is evident from Table 10-25 and Figure 10-89 that there is very little difference between the two scenarios: the post dam, and the post dam with flood releases. This can be explained by taking a closer look at Figure 10-6 (summarised in Table 10-24).

Table 10-24 Flood release attenuation along the Berg River

Base Flow (m³/s)	Peak Flow at BRM4 (m³/s)	Peak Flow at head of estuary (m³/s)
2	140	55
20	160	85
50	170	120

If there are no contributions from the tributaries, the flood releases are attenuated to such an extent that they becomes ineffective downstream of BRM5. From Table 10-25 it can be seen

that the effective discharge is higher than the contribution of the flood releases (Table 10-24). Therefore, the flood releases do not restore the volume of sediment to the original state.

Table 10-25 Site 5 - flow classes and associated sediment transport

% time equalled or exceeded	Flow class interval (%)	Present		Post-dam		Flood releases	
		Mean flow ¹ (m³/s)	% of total load	Mean flow (m³/s)	% of total load	Mean flow (m³/s)	% of total load
99.99							
90	9.99	2.1	0.00	2.0	0.01	2.0	0.01
80	10	3.1	0.01	3.1	0.02	3.1	0.02
70	10	3.9	0.02	4.3	0.05	4.3	0.04
60	10	4.5	0.03	5.3	0.08	5.3	0.08
50	10	5.3	0.04	6.1	0.12	6.1	0.11
40	10	6.9	0.08	7.0	0.16	7.0	0.15
30	10	8.8	0.16	8.4	0.26	8.4	0.25
20	10	13.7	0.49	11.1	0.54	11.1	0.51
10	10	25.5	2.38	19.2	2.14	19.1	2.01
5	5	44.3	4.86	34.0	4.61	34.0	4.33
1	4	80.6	17.75	61.5	16.68	62.3	16.14
0.1	0.9	204.0	42.44	151.4	37.13	157.7	38.62
0.01	0.09	449.8	31.72	378.6	38.19	386.5	37.75

1: Mean flow over corresponding flow class

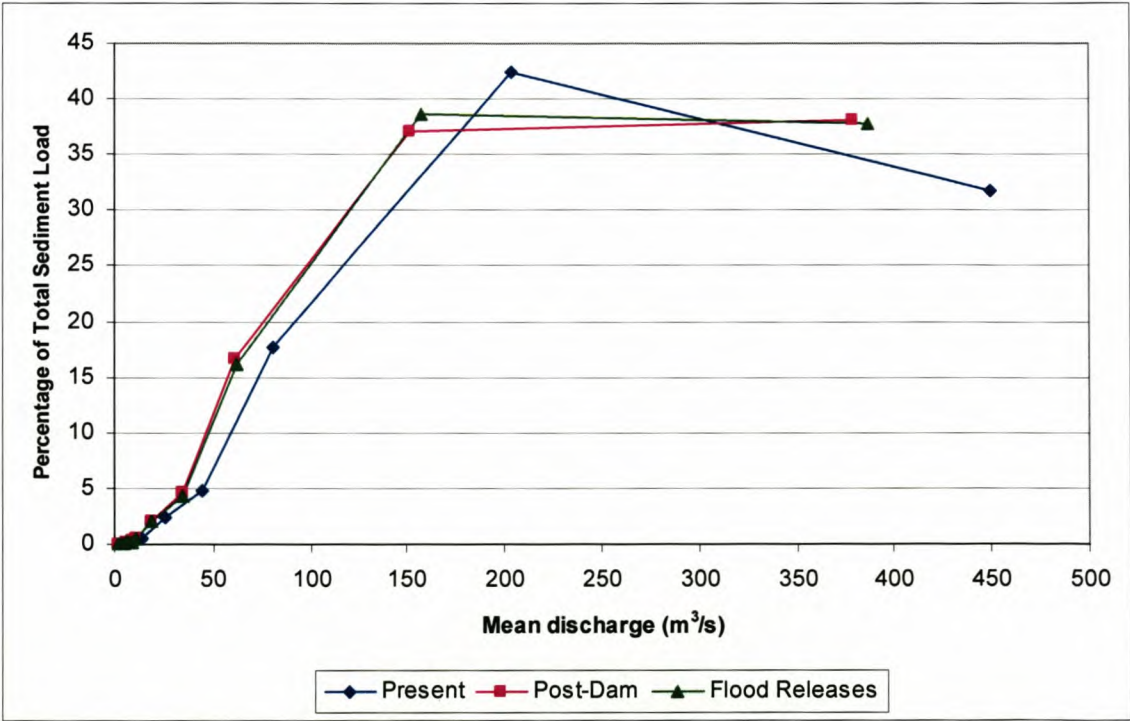


Figure 10-89 Percentage of total sediment load versus mean discharge at site 5

10.2.2.3 Site BRM6

From **Table 10-26** it can be seen that the effective discharge for site 6 varies between 257.4 and 308.6 m³/s. The same can be seen from **Figure 10-90**. It can also be seen from **Figure 10-90** that virtually no difference exists between the present scenario and that of the post dam with flood releases.

Table 10-26 Site 6 - flow classes and associated sediment transport

% time equalled or exceeded	Flow class interval (%)	Present		Post-dam		Flood releases	
		Mean flow ¹ (m ³ /s)	% of total load	Mean flow (m ³ /s)	% of total load	Mean flow (m ³ /s)	% of total load
99.99							
90	9.99	2.1	0.07	2.0	0.14	2.0	0.12
80	10	3.1	0.15	3.2	0.31	6.6	0.84
70	10	3.9	0.22	4.3	0.50	7.6	1.08
60	10	4.6	0.28	5.3	0.71	5.3	0.60
50	10	5.4	0.38	6.1	0.89	6.1	0.75
40	10	7.0	0.58	7.1	1.12	7.1	0.95
30	10	9.3	0.96	8.6	1.57	8.6	1.33
20	10	14.4	2.04	11.9	2.66	11.9	2.26
10	10	27.0	6.04	21.6	7.11	21.6	6.00
5	5	51.2	9.13	39.1	9.47	39.2	8.05
1	4	104.3	24.96	79.2	24.34	81.1	21.37
0.1	0.9	308.6	36.61	257.4	38.28	281.9	37.60
0.01	0.09	790.3	18.59	537.4	12.90	753.5	19.05

¹: Mean flow over corresponding flow class

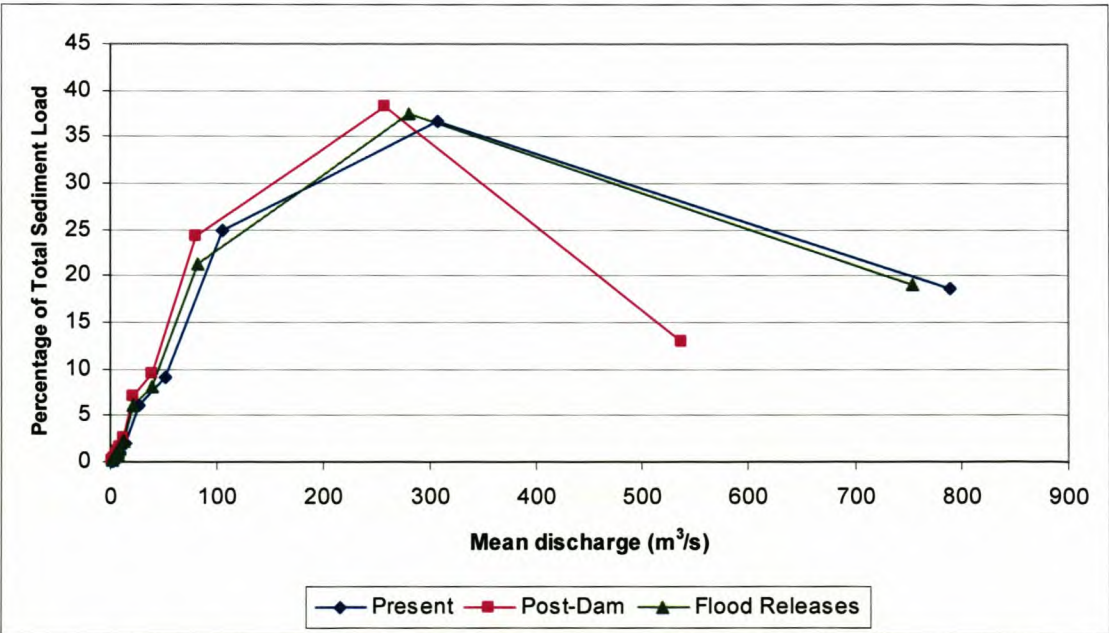


Figure 10-90 Percentage of total sediment load versus mean discharge at site 6

Mass balances of the sediment volumes at all the monitoring sites, as well as tributaries and gauging stations on the lower Berg River, are represented in **Figure 10-91** to **Figure 10-93**.

Berg River Mass Balance - Present Situation - Sediment Transport

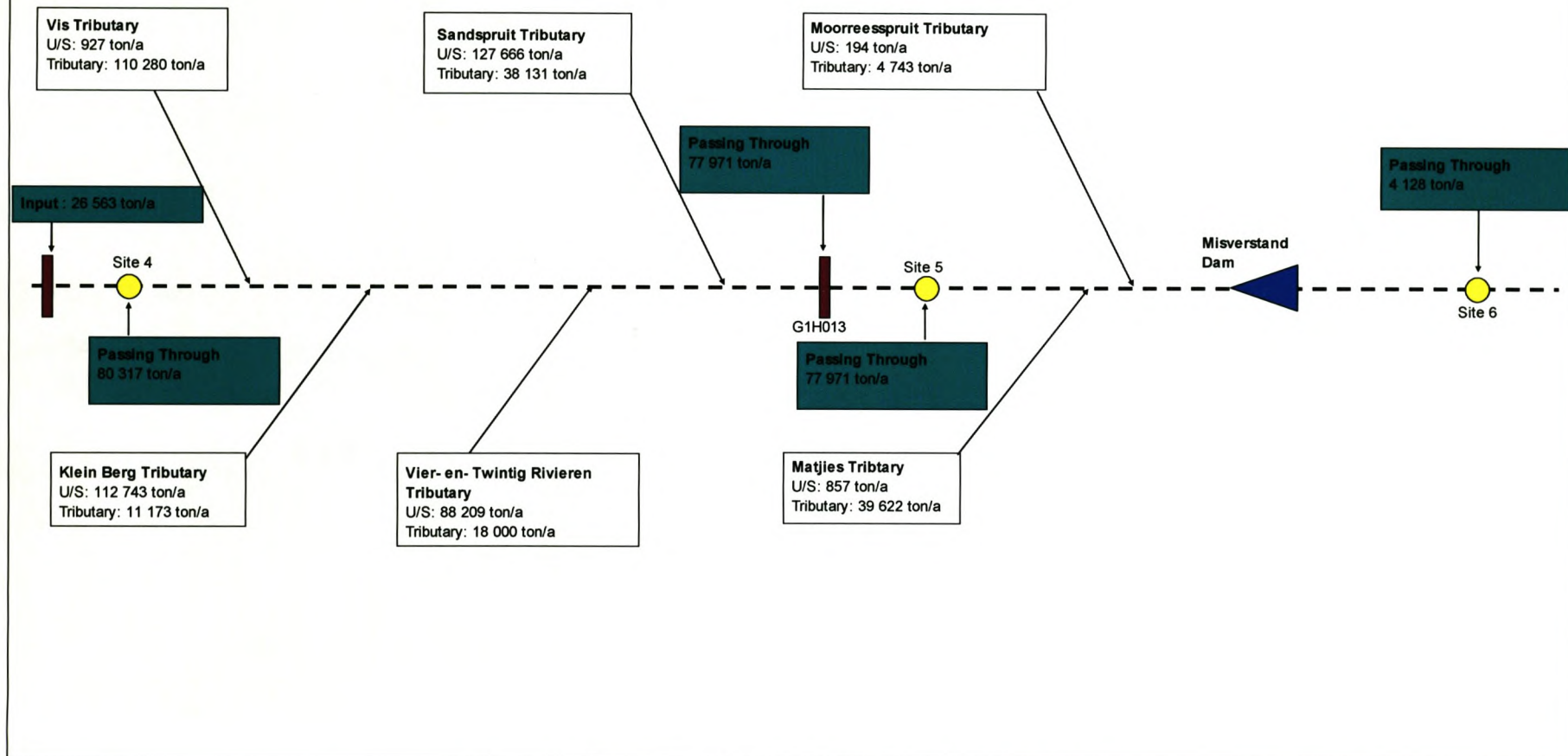


Figure 10-91 Lower Berg River mass balance – present situation

Berg River Mass Balance - Post Dam Situation - Sediment Transport

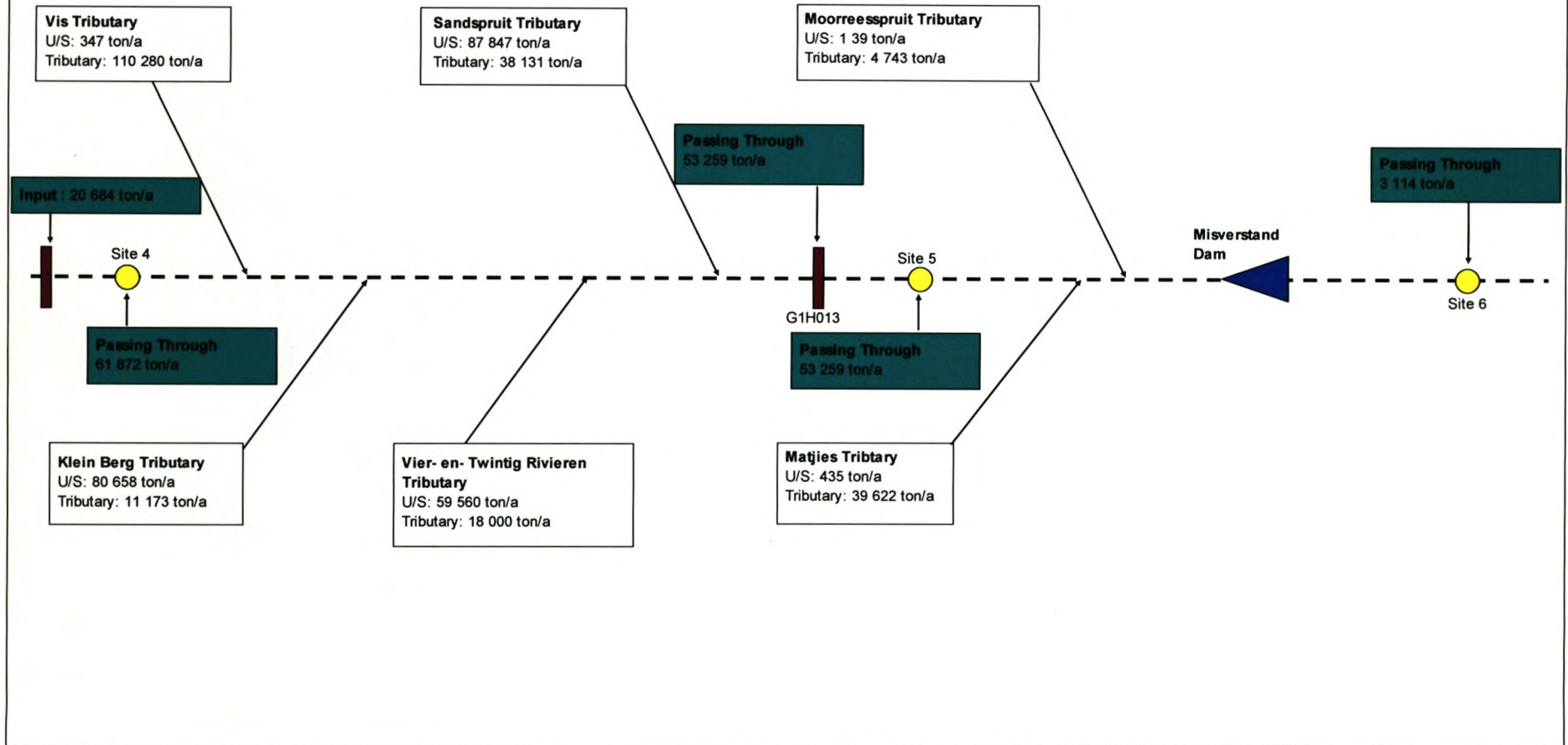


Figure 10-92 Lower Berg River mass balance – post-dam scenario

Berg River Mass Balance - Post Dam Situation & Flood Releases - Sediment Transport

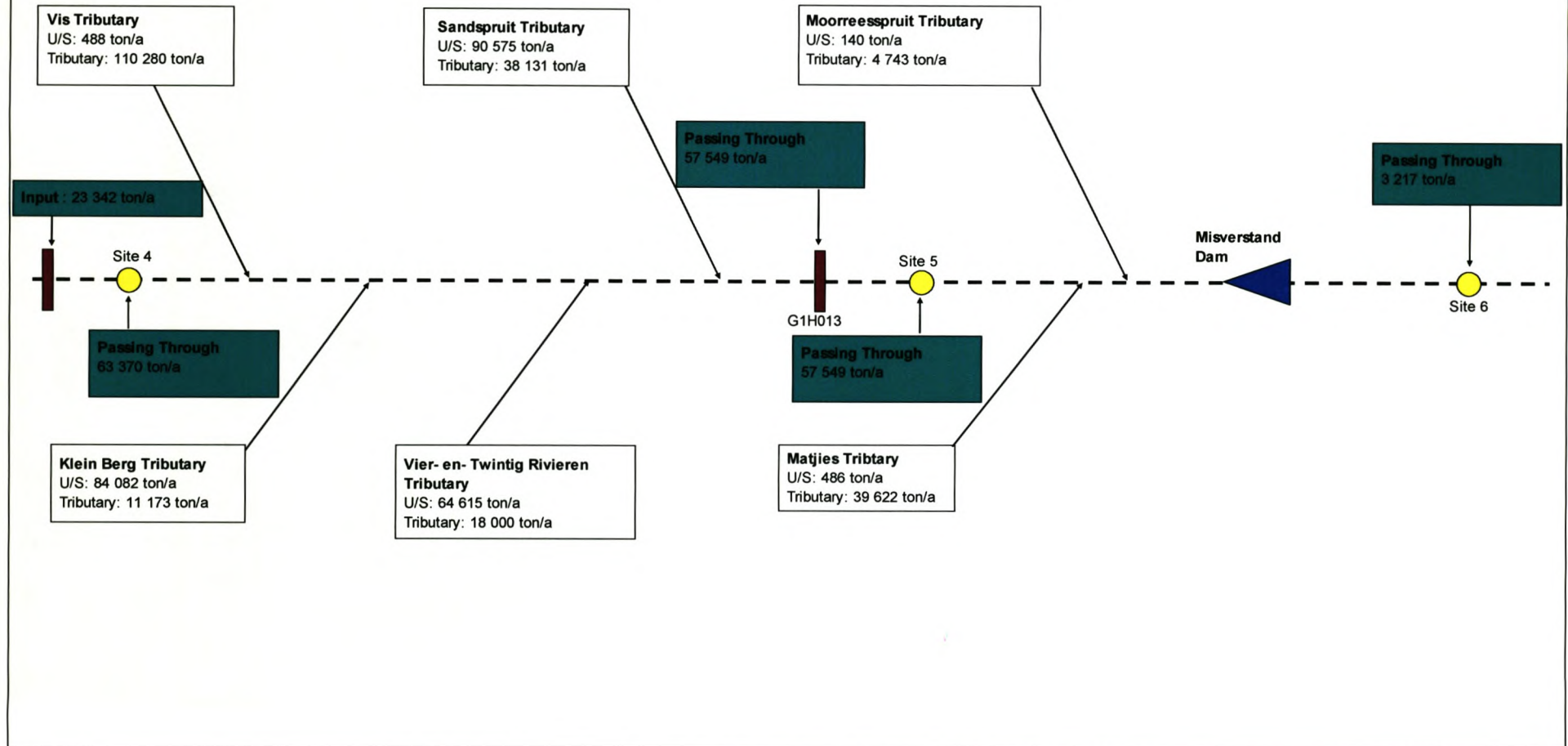


Figure 10-93 Lower Berg River mass balance – post-dam with flood releases

According to **Table 10-23** the effective discharge at BRM4 is actually made up by two flow classes, i.e. between 62 and 136.1 m³/s for the present day scenario. The same is true for the other two scenarios. However, for the post-dam scenario the effective discharge is lower (between 42.6 and 100.5 m³/s) than for the present day, and therefore less sediment transport will occur. For both these scenarios, the effective discharge is closer to the lower flow class than the upper, but for the flood release scenario the effective discharge is closer to the higher flow class, and the artificial flood releases fall into this category. This will cause the sediment transport to increase compared with the scenario of post-dam without flood releases.

For BRM5 and BRM6 the artificial flood releases have very little impact on the sediment transport in the river. This can also be seen from **Table 10-25** and **Table 10-26**, as the effective discharge are in the order of 200 m³/s for BRM5 and 300 m³/s for BRM6, with little difference among the three scenarios. This means that the effectiveness of the flood releases only lasts up to Hermon.

10.2.3 Cumulative Sediment Loads

The cumulative sediment loads were plotted for the five BRM sites against the cumulative water volumes for the nine year simulation period. These graphs are presented in **Figure 10-94** to **Figure 10-98**. These graphs clearly illustrate the influence of the Berg River Dam on both the hydrodynamics and the sediment transport in the Berg River. For instance it is clear to see that the dam has a major influence on the sediment transport of the river reach just downstream of the dam. Even if the artificial floods are being released, the sediment transport will not change back to the present state. This can be seen from **Figure 10-94**. The difference in the slope and length of the lines are a direct effect of the dam development (**Figure 10-94** and **Figure 10-95**). These figures also illustrate the major decrease in both the sediment loads and water volumes that will be transported down the Berg River. This is due to a major reduction in flood peaks that will be experienced after the construction of the Berg River Dam which will cause a reduction in the sediment transport. The simulations show that from BRM4 downstream the influence of the dam decreases to a minimum (same slope), and even though the river still experiences a drop in volumes and loads the overall trends are the same. A flat gradient represents a dry period while a steeper gradient represents wetter periods with more sediment transport (**Figure 10-97**).

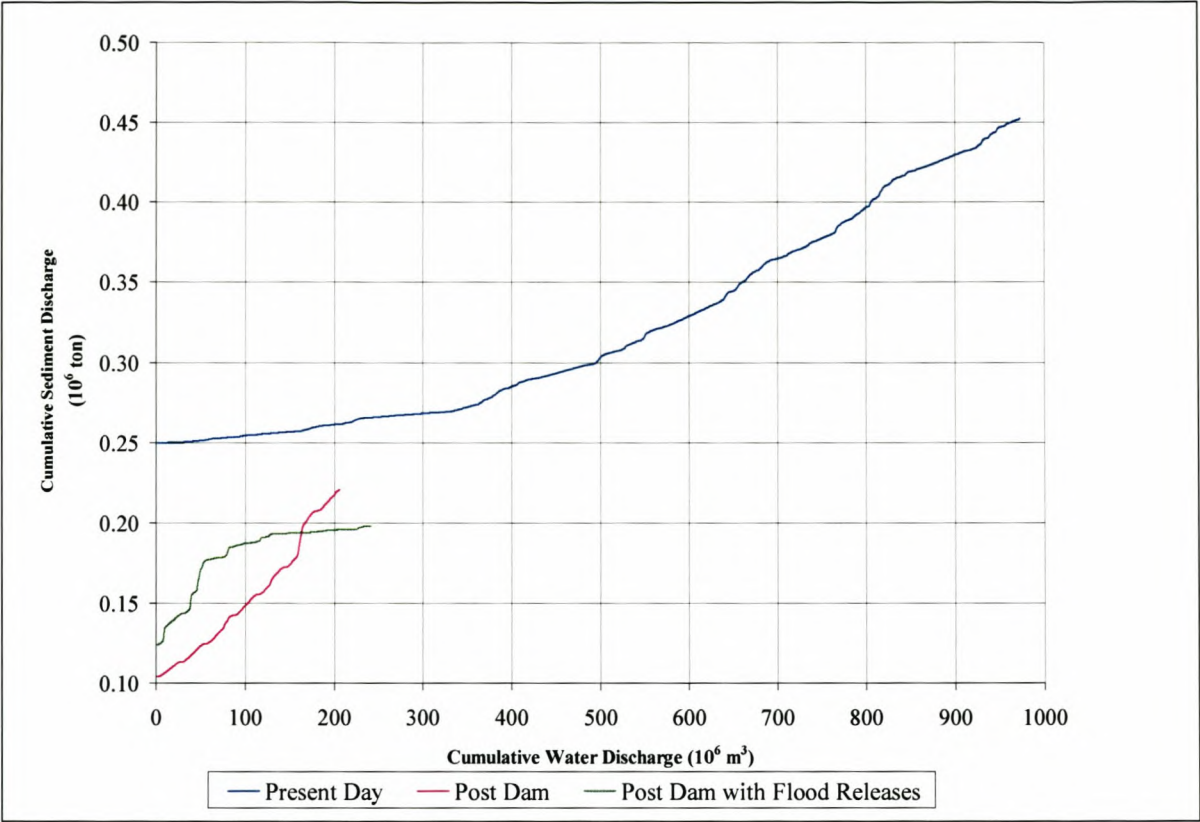


Figure 10-94 Cumulative sediment load and water discharge at BRM2(97 - 03)

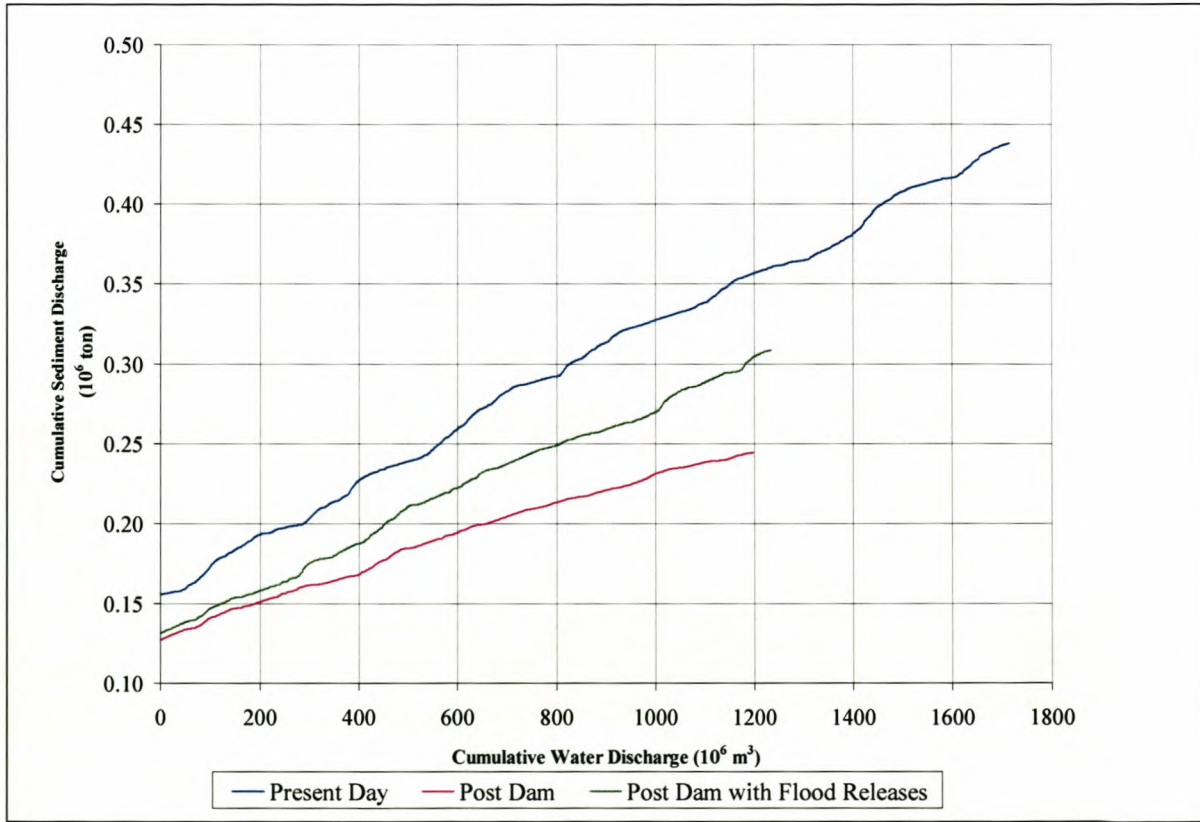


Figure 10-95 Cumulative sediment load and water discharge at BRM3(97 - 03)

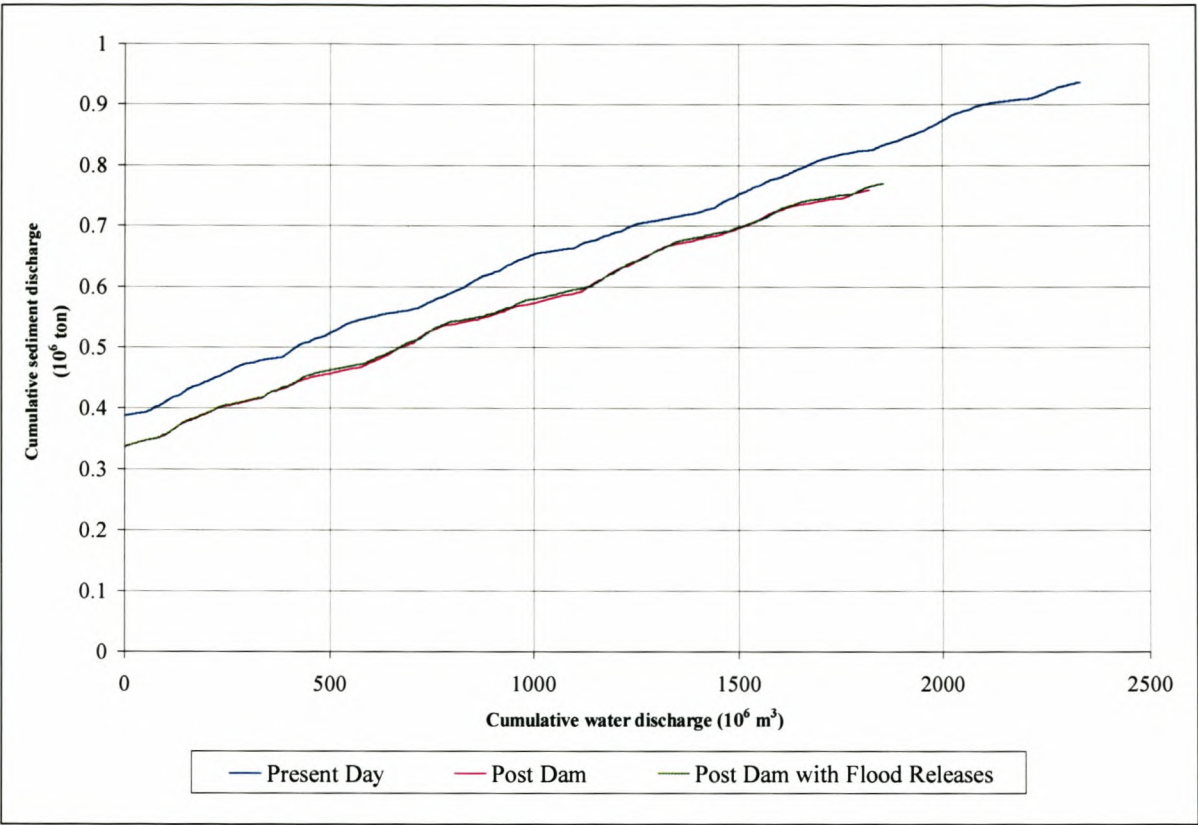


Figure 10-96 Cumulative sediment load and water discharge at BRM4 (97 – 03)

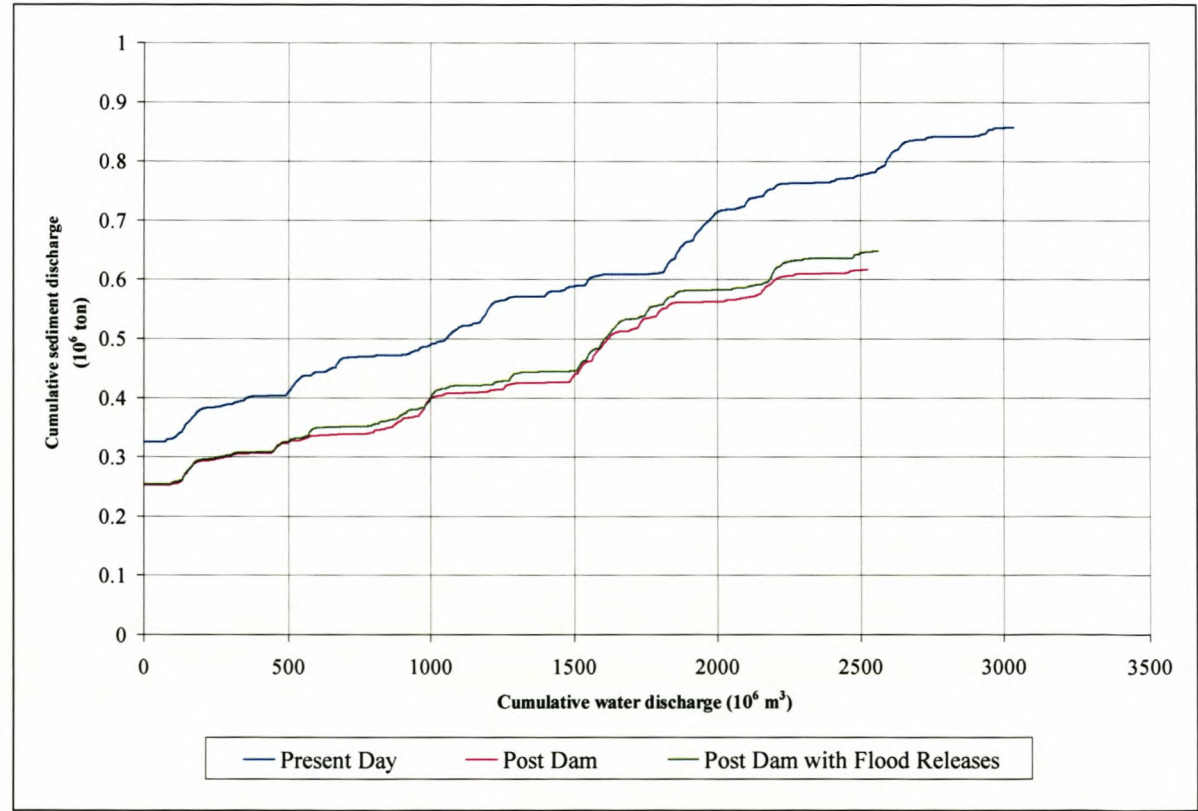


Figure 10-97 Cumulative sediment load and water discharge at BRM5 (97 - 03)

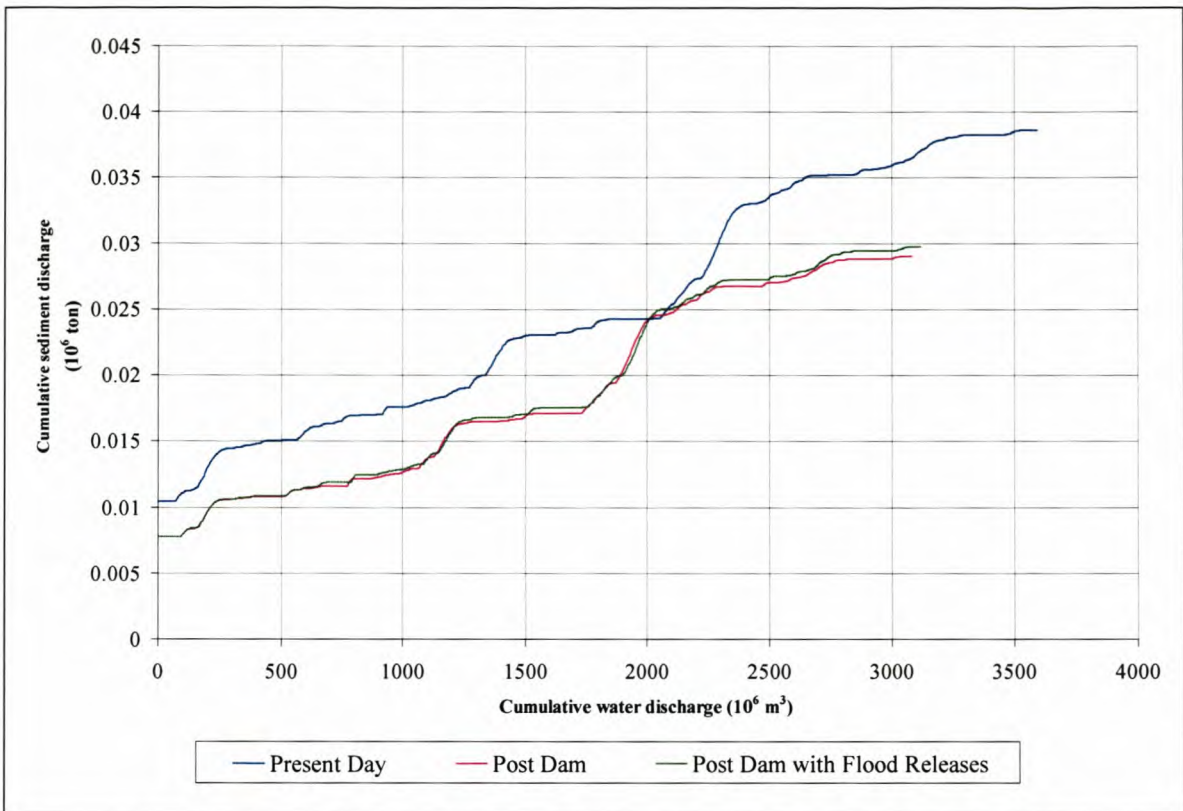


Figure 10-98 Cumulative sediment load and water discharge at BRM6 (97 - 03)

10.2.4 Sediment Rating Curves

Beck and Basson (2003) illustrated the effect of the proposed Berg River Dam with and without the flood releases by comparing the simulated sediment load – discharge rating curves at various locations along the Berg River. The same method was used with the data obtained from the simulations, **Figure 10-99** to **Figure 10-103** show these rating curves at the various BRM sites. In **Figure 10-99** it can be seen that the rating curve for the proposed Berg River Dam plots above that of the current scenario. This is because of the reduced flood peaks with more material available to be transported at lower flows. With the artificial flood releases the transport capacity at higher flows are increased, leaving less sediment available to be transported by the lower discharges. From the sediment mass balance presented in **Figure 10-85** to **Figure 10-87** it can be seen that even with the higher transport capacity at BRM2 of the post dam scenario the total sediment that will be transported is lower compared to the current scenario. This is due to the lower frequency of the floods that will be able to transport the large volumes of sediment that are available. This can also be seen from **Figure 8-8** which shows the reservoir water levels over the simulation period. If no artificial flows are released, the dam will only spill twice over a nine year period.

At BRM3 (**Figure 10-100**) the situation is quite different compared to the one depicted in **Figure 10-99**, indicating a slightly reduced sediment transport capacity after the Berg River Dam has been built. As more water and sediment enters the Berg River via the tributaries the effect of the dam will diminish. Beck and Basson (2003) found that a flood release of $160 \text{ m}^3/\text{s}$ had insufficient restoring capacity, since in the research that was carried out the sediment rating curve did not recover to its original position. In this instance, however, a flood release of $220 \text{ m}^3/\text{s}$ overcompensates slightly at BRM3. From the sediment mass balance presented in **Figure 10-85** to **Figure 10-87** it can again be seen that due to the lower frequency of occurrence of the flood releases the total sediment volume will be slightly less compared to the current scenario.

At BRM4 (**Figure 10-101**) it is almost impossible to note the difference between the scenario with no flood releases and the one with the artificial releases. This is mainly because of the attenuation of the released flood as it progresses down the river. From **Figure 10-3** it is evident that a $220 \text{ m}^3/\text{s}$ flood, with a baseflow of $2 \text{ m}^3/\text{s}$, will reduce to $130 \text{ m}^3/\text{s}$ when it reaches BRM4. The same can be seen at BRM5 (**Figure 10-102**) and BRM6 (**Figure 10-103**), the $220 \text{ m}^3/\text{s}$ flood will reduce further to about $60 \text{ m}^3/\text{s}$ as it progresses past BRM6. This reduction in flood peak causes a reduction in the sediment transport capacity which in turn causes a reduction in the efficiency of the flood releases. Another issue that needs consideration is the timing of the releases. If these floods are not released in such a way that they coincide precisely with the natural floods in the sub – catchments they will have an even more insignificant effect on the reinstatement of the sediment mass balance in the lower reaches of the Berg River (BRM4, 5 and 6). From **Figure 10-103** it is evident that the dam has virtually no influence on the sediment transport capacity of the Berg River at BRM6.

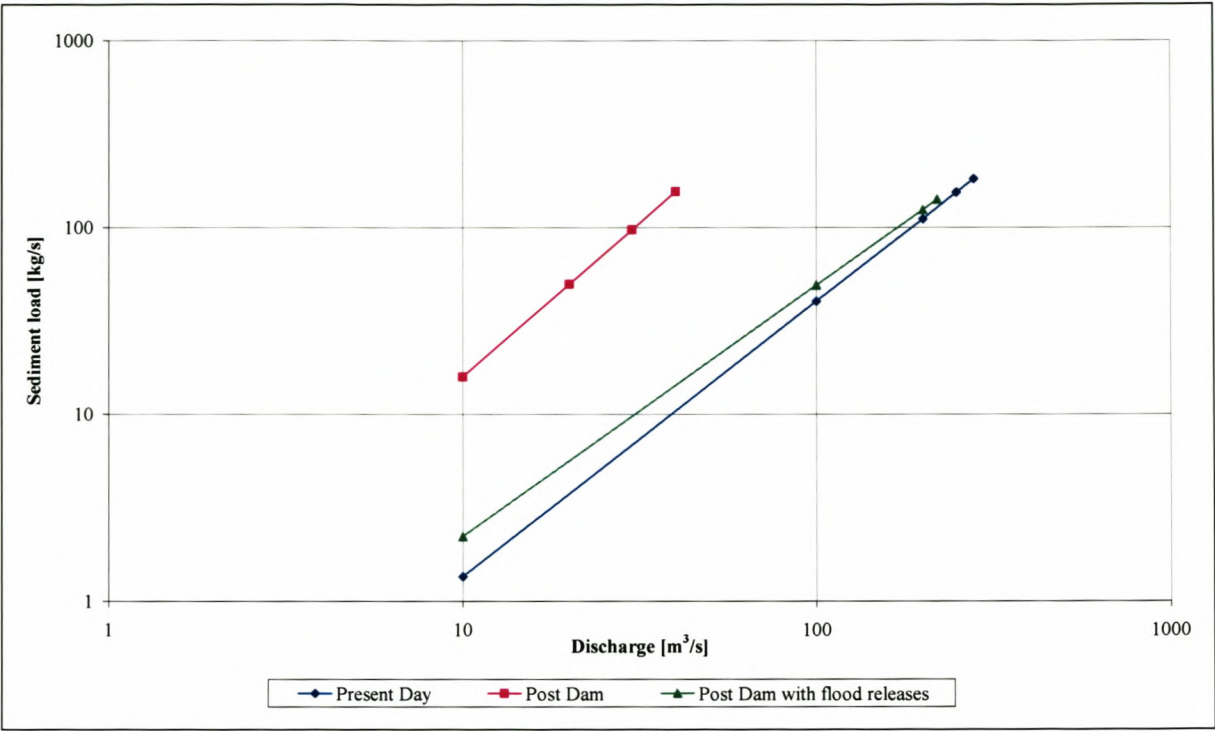


Figure 10-99 Sediment rating curves at BRM2

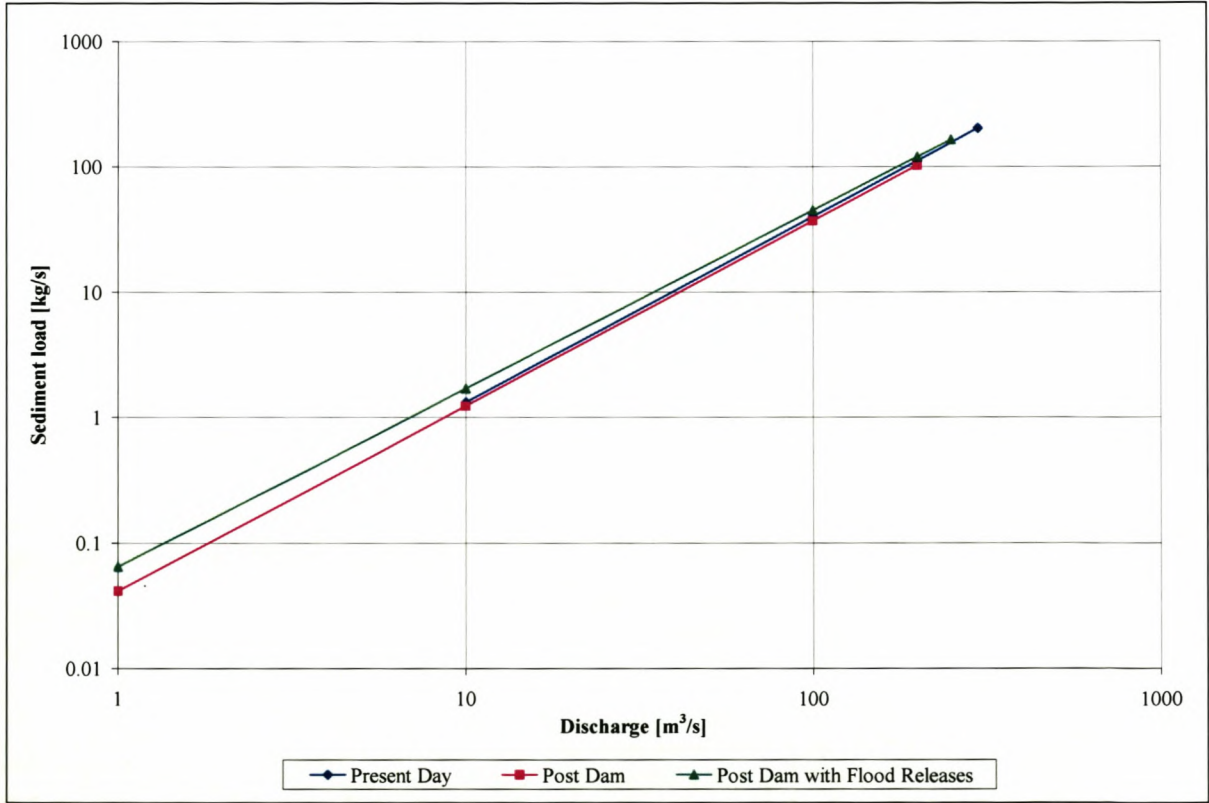


Figure 10-100 Sediment rating curves at BRM3

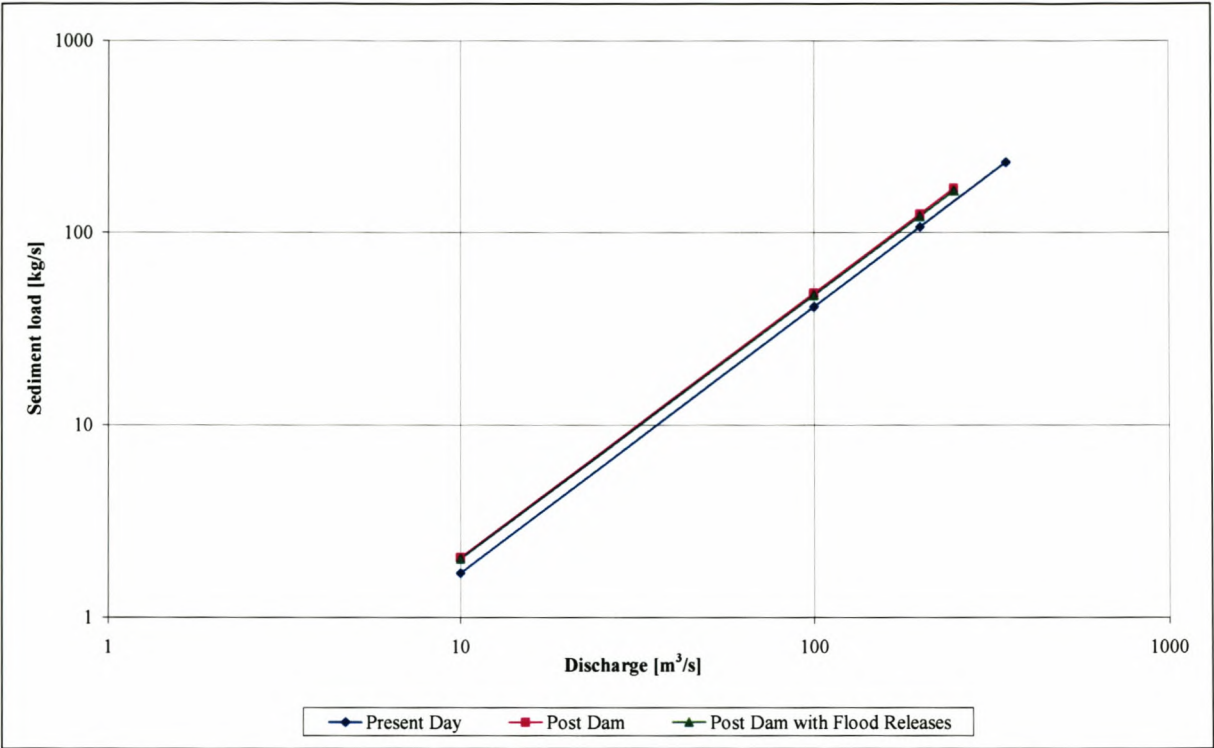


Figure 10-101 Sediment rating curves at BRM4

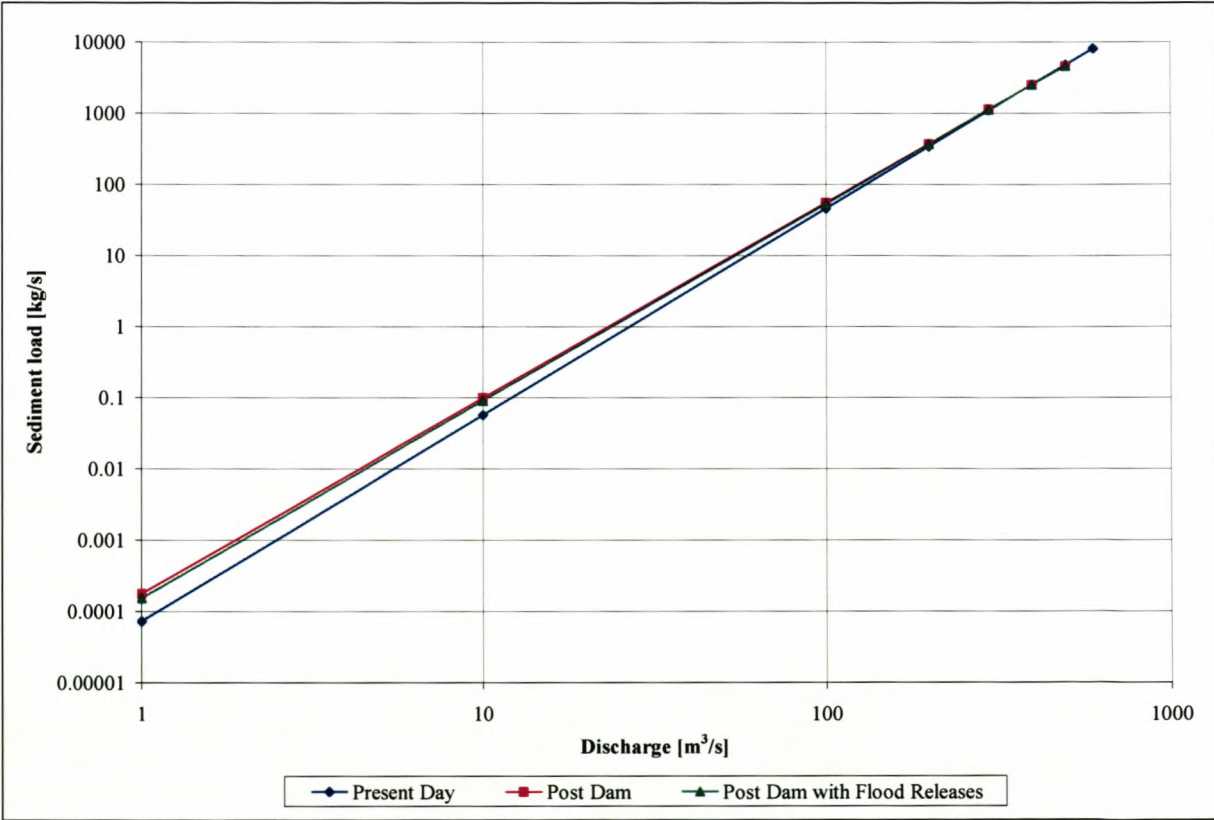


Figure 10-102 Sediment rating curves at BRM5

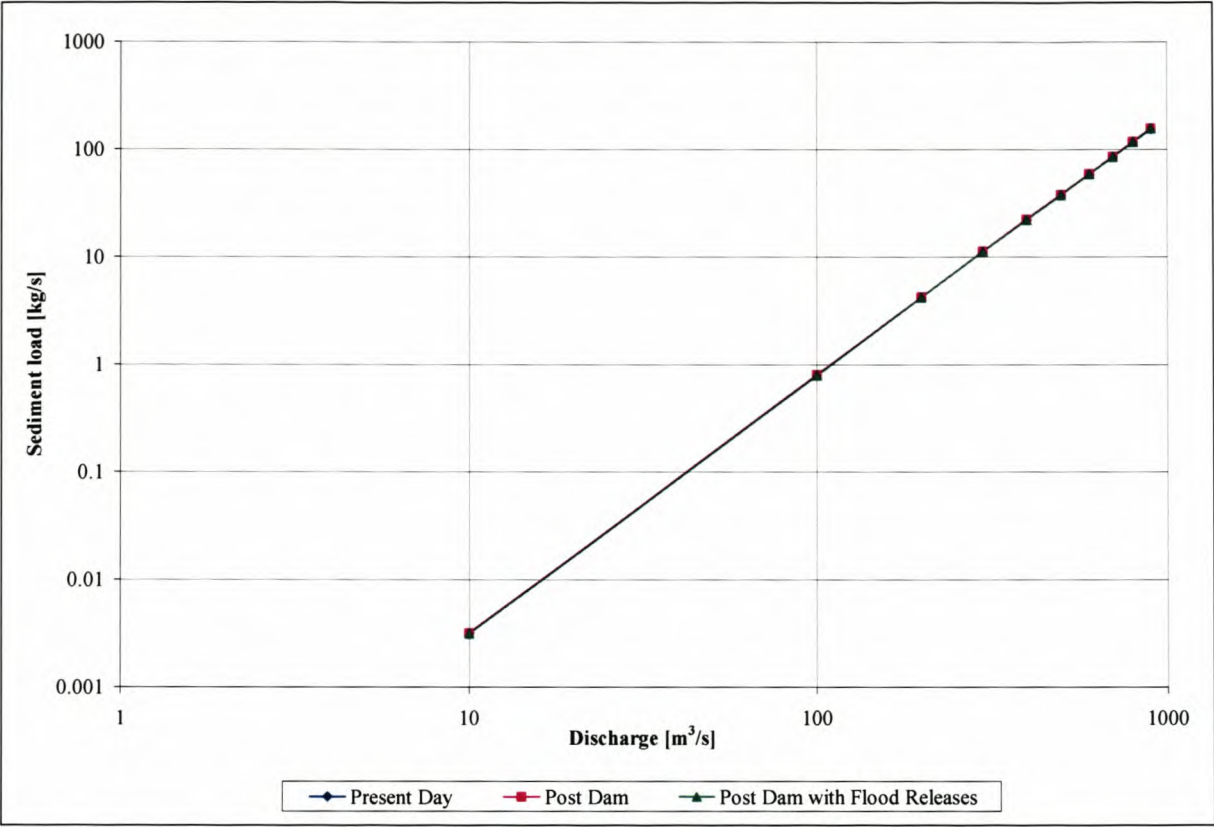


Figure 10-103 Sediment rating curves at BRM6

10.3 Discussion

The cumulative plots and the sediment – discharge rating curves indicate the same impacts of the Berg River Dam development on the hydrodynamics and the sediment transport of the Berg River. The two methods give a graphical presentation of the effect of the dam development on the downstream river reach with their respective disadvantages and advantages. The method used by Beck and Basson (2003) is based on a log scale in both axes of the graph; differences in slopes of the lines give an indication of the influence of the dam, the log scale may cause the difference in the slopes to appear less dramatic. This method will be more suited when an investigation of low discharge and sediment transport is carried out. The differences in the slopes of cumulative plots also give an indication of the severity of the effect of the dam development. In this case the seasonal influence complicates the graph, which makes it difficult to assess the degree of parallelism that exists between the various lines (Figure 10-97). Even though the trend stays the same, the dry seasons (flat parts of the graph) during the post – dam scenarios are presented closer to the origin due to the decrease in both the water volumes and sediment loads.

The Berg River Dam will have a much larger effect on the water volumes released than most other dams in South Africa. This is mainly due to the pump station that will abstract water from the reservoir when the water level in the reservoir reaches a certain height. The short spillway length (40m) will cause major flood attenuation and the abstraction work downstream of the Franschhoek and Dwars Rivers' confluence with the Berg River will decrease the flow even more by abstracting the water of these two tributaries to supplement water storage of the Berg River Dam. This reduced water volume due to the dam can clearly be seen from the hydrodynamic mass balance that was constructed from the simulated data (**Figure 10-72 to Figure 10-77**).

As can be seen from the sediment mass balance (**Figure 10-85 to Figure 10-87 and Figure 10-91 to Figure 10-93**) the Berg River dam will have a significant effect on the river reach just downstream of the dam (BRM site 2 to Paarl). Further downstream the flood releases seem to have a significant reversing effect on the sediment transport with regards to the reinstatement of the effect of the dam compared to the scenario with no managed flood releases. It has to be borne in mind that the river reach between the Berg River Dam and the confluence with the Franschhoek River relies solely on the IFR, as well as managed flood releases to supply the river with water. Therefore the effect of the dam will be the worst on this part of the Berg River. As soon as tributaries contribute to the discharge, the effect of the Berg River Dam becomes less dramatic.

CHAPTER 11 CONCLUSIONS

The objective of this thesis was to investigate the impact of the proposed Berg River Dam on the downstream river morphology and sediment transport of the Berg River. The following conclusions can be drawn:

- The Berg River Dam will have a larger impact on downstream flows than many other dams in South Africa for the following reasons:
 - A pump-station abstracts water at $6 \text{ m}^3/\text{s}$ (first phase $3 \text{ m}^3/\text{s}$) when the reservoir storage reaches a certain level and the water is pumped to a new water treatment plant, and to Theewaterskloof Dam through the tunnel. This operating rule has been set in the simulations in this research to allow spillage by the Berg River Dam on average 1 out of 4 years (with flood releases), but with the larger pump capacity it is possible to operate the dam so that it never spills.
 - The spillway length is only 40 m which creates damming in the reservoir and large flood attenuation which has an impact on small and medium floods. For example the Probable Maximum Flood (PMF) which is equal to about $1300 \text{ m}^3/\text{s}$ is reduced to $740 \text{ m}^3/\text{s}$ when it spills at the dam.
 - The benefit of winter flows and floods from tributaries downstream of the dam is reduced by the supplement scheme to be located downstream of the Dwars River. This pump-station will pump water at a rate of $5 \text{ m}^3/\text{s}$ to the Berg River Dam, abstracting about 21 million m^3 per year from the river during winter.
- With the above operation the MAR in the post-dam scenario with managed flood releases downstream at BRM site 2 (upstream of Franschhoek River), will decrease from the present 141 million m^3 to only 35 million m^3 . The managed flood releases are therefore extremely important for the river channel maintenance and ecology. The dam will however have an effect longitudinally up to the estuary.
- The adopted dam operating rule ensures that the dam spills only in four of the nine years simulated (without managed flood releases), which means that the largest flood peak spilling into the river will be only $77 \text{ m}^3/\text{s}$ as compared to an incoming flood peak of 240

m³/s. With the managed flood releases the dam spills only in two of the nine years, but between one and three managed flood releases are made each year in addition to the spillage from the dam. In between the managed flood releases and natural spillage, the IFR and irrigation releases make up the only flow in the upper river reaches, until contributions from the tributaries augment these flows. The proposed operating rule with regard to the managed flood releases ensures that the flood release pattern has a more natural variability.

- MIKE 11, a one – dimensional model, was calibrated and validated on 9 years of flow records, from 1995 to 2003. Hydrodynamic routing by mathematical modelling with MIKE 11 of the pre- and post Berg River Dam and tributary inflows through the river system indicated that for all the sites the dam has a significant impact on all the flows in the river, but especially at BRM site 2 as this site relies solely on the releases from the dam. At the other sites the dam releases are augmented by the tributary flows. The further away from the dam the sites are located the closer the post-dam flow patterns are to the present situation. At BRM Site 2 the decrease in mean annual runoff is almost 79%, while at BRM6 the reduction is only 14%.
- The IFR and irrigation releases ensure that the frequency of the flows between 2 and 10 m³/s is almost the same for the post-dam and present scenarios.
- The aerial photograph analysis that was carried out on the catchment showed that the river morphology is constantly changing. This is evident from the change in main channel width, the sinuosity of the river as well as the movement of sandbars over the years. The change in main channel morphology will be more pronounced after construction of the Berg River Dam due to the change in flow regime. Therefore it was decided to manually change the cross sectional width of the main channel for the simulation of the post dam and post dam with managed flood releases scenarios. Between the dam and Hermon the river will become narrower in the post dam scenario between 15 to 25 %.
- Flood attenuation along the Berg River for the present and post-dam scenarios was investigated and it was found that if the managed floods are released in phase with tributary floods, the attenuation is not as pronounced because the main channel does not

need to be filled. This shows that it is important to ensure that the flood releases are made in phase with tributary floods as it would occur naturally during a storm. For the post-dam scenario the flood attenuation at low initial flows are not as pronounced as it were for the present day scenario, because of the smaller cross-sections. The main channel fills up more quickly than it does for the present scenario, which means that the flood travels more quickly, without being attenuated to such a degree.

- The operating rule decided on for this research to meet the IFR requirements seems realistic and practical without releasing larger floods than the inflow into the Berg River Reservoir. The rules also provide variability from year to year. These flood operating rules were optimised, based on the fluvial morphology and sediment balance of the river.
- In this research only the IFR requirements of the upper Berg River were considered in the dam operation. The IFR required at Hermon is however significantly higher and, based on frequency graphs for each month of the year, a decision will have to be made whether the lower Berg IFR should be supplemented from the Berg River Dam or Voëlvlei Dam.
- Even though the managed flood releases (with operating rules as discussed earlier) cannot undo the impact of the Berg River Dam at BRM site 2, it gives the best results further downstream. Therefore these releases are the best in terms of magnitude and duration without compromising the yield of the proposed Berg River Dam.
- MIKE 11 was also set up to simulate the sediment transport in the Berg River. Only two fractions of sediment were used during the sediment modelling, 0.5mm and 0.03mm. The larger of the two fractions represents the sand part of the available sediment while the smaller fraction represents the silt and clay part of the available sediment. The movement of the cobbles and boulders were investigated during the study of the incipient motion conditions. It was concluded that the frequency of movement of the larger particles (cobbles and boulders) maybe negligible; therefore the chosen fractions are a reasonable representation of the available sediment for transport.
- From the incipient motion studies that were conducted it is evident that hiding and exposure are prominent at BRM site 1 and site 2 due to the cobbles and boulders found at

these sites. The theory developed by Dey and Raju (2002) is not applicable to data collected from BRM1 but after recalibration gives an improved indication on the threshold of movement. The following equation based on the Shields parameter was obtained after recalibration:

$$\tau^* = 0.011 F_d^{0.705} \hat{d}^{0.266} \hat{h}^{-0.381}$$

- It is recommended that the relative roughness contour, $k_s/d = 5$, drawn on the Lui diagram, be used for prediction of the initiation of movement at BRM site 1. This method considers the effect of hiding of smaller particles. The value of relative roughness is only applicable at BRM site 1 and further research should be conducted in order to establish similar relationships at other locations along the river to verify the applicability of this value.
- The suspended and bedload sediment samples that were taken during the winter of 2003 and 2004 were used to calibrate the sediment transport model provisionally. The mathematical model was calibrated at the gauging weirs at Hermon (G1H036) and Drieheuwels (G1H013). It has to be borne in mind that more samples are required to assist in properly calibrating the model. Continuous sampling of more than 3 years will give reliable results that include the seasonal effects on sediment transport.
- The sediment samples were also used to calculate the sediment yield of the various catchments. The simulated sediment yield of each catchment over the simulated period was scaled so that the yield of 2003 equals the measured yield from the samples taken. Sediment yield time series were used at the model boundaries (tributaries).
- A mass balance of both the hydrodynamics and the simulated transported sediment volumes were done. The hydrodynamic mass balance was used to determine the reduction in the water volume as a result of the dam while the sediment mass balance was used to investigate sediment deposition and erosion areas along the river. The effect of the dam was evaluated by comparing the change in these areas between the three scenarios.

- Sediment rating curves, cumulative plots of the sediment volumes as well as effective discharge tables were drawn up in order to evaluate the effect of the dam on the sediment transport. The cumulative plots and the sediment – discharge rating curves both illustrate the impact of the dam development on the hydrodynamics and the sediment transport of the Berg River. Both methods only give a graphical representation of the effect of the dam development on the downstream river reach with their respective disadvantages and advantages. The method used by Beck and Basson (2003) uses a log scale on both axes of the graph; a difference in slopes of the lines gives an indication of the influence of the dam, the log scale may however cause the difference in the slopes to appear less dramatic. This method will be more suited when an investigation of low discharge and sediment transport is carried out. The difference in the slope of cumulative plots also gives an indication of the severity of the effect of the dam development. In this case the seasonal influence complicates the graph which makes it difficult to assess the degree of parallelism that exists between the various lines. Even though the trend stays the same, the dry seasons (flat parts presented on the graph) during the post – dam scenarios are present closer to the origin due to the decrease in both the water and sediment volumes.
- The effect of the Berg River Dam will be most pronounced up to Paarl, it will also have a significant effect on the sediment and water volumes between Paarl and Hermon. As the water contribution from the tributaries increase further downstream the effect will decrease to a minimum at Misverstand Dam.
- This research showed that a fully hydrodynamic model, in this case 1D, can be calibrated and validated for both hydrodynamics and sediment transport in a large river system such as the Berg River. It can therefore be used for environmental impact assessments, mitigation measures to limit the impact of the dam and dam operation to assess flow and fluvial morphological changes in the river.

CHAPTER 12 RECOMMENDATIONS

The following recommendations are being made:

- It is recommended that a rainfall-runoff model of the Berg River Dam catchment and downstream tributary catchments including Franschhoek, Dwars and Wemmershoek Rivers, be calibrated and verified so that managed flood operation can start during the first winter when filling of the reservoir commences. A real time flood warning and operation approach is required to ensure:
 - that the flood released is not too small for the IFR
 - that the flood is in phase with the downstream tributaries and not attenuated by the dam
 - that the flood peak released is not larger than the reservoir inflow
 - that the flood hydrograph shape and volume is correct
 - that the outlet tower can be filled with water prior to the flood release.
- At least the field data of 2003, 2004 and 2005 should be used for calibration and verification purposes.
- Studies such as those done in the United States (Williams and Wolman, 1984) and in China (Chien, 1985) should be done in South Africa to determine the nature and extent of the effects that dams will have on rivers, in the form of repeated surveys downstream of dams, and to compare these findings to international experience. The programme launched by the Department of Water Affairs and Forestry, the Berg River Baseline Monitoring Programme, seems to be a step in the above mentioned direction.
- The sediment transport of cohesive – non-cohesive mixtures and fine sediment other than those studied in this research should be investigated to obtain more data for proper calibration of the sediment transport model. One should also consider investigating different particle sizes in the transport model. Due to the steepness of the upper Berg River the transport model tends to become mathematically unstable once a smaller

fraction is used to describe the fine portion that will be transported. Therefore it is recommended that a different type of model be used for this simulation.

- Attention should, in future research, be given to the movement of cobbles and boulders and the incorporation thereof into the mathematical model.
- Further suspended and bedload sediment sampling should be done especially during floods in order to improve the calibration of the sediment transport model. Sampling should also be done during low (summer) flows to obtain representative samples of this flow regime that could assist to improve calibration at low flows.

CHAPTER 13 REFERENCES

- Aberle, J. Dittrich, A and Nestmann, F. (1999). *Discussion of Estimation of Gravel – Bed River Flow Resistance by H. Afzalimehr and F Anctil*. Journal of Hydraulic Engineering. ASCE, 125, pp 1315 – 1317.
- Ackers, P. and White, R. (1973). *Sediment Transport: New Approach and Analysis*. Journal of the Hydraulics Division. ASCE.99, HY11. pp. 2041 – 2060.
- Alexander, W.J.R. (1991). *Flood Hydrology for Southern Africa*. SANCOLD. South Africa.
- Andrews, E.D. 1983. *Entrainment of Gravel from Sorted Riverbed Material*. Geological Society of America Bulletin. Vol. 94, pp 1225 – 1231.
- Ashida, K and Michiue, M. (1971). *An Investigation of River Bed Degradation Downstream of a Dam*. Proc. 14th Congress of the IAHR.
- Bath, A.J. (1989). Phosphate Transport in the Berg River, Western Cape Technical Report of the Department of Water Affairs and Forestry, TR 143. Pretoria.
- Birkhead, A.L., Heritage, C.S., Rogers, K.H. and van Niekerk, A.W. (1998) *Geomorphological change models for the Sabie River in the Kruger National Park*. WRC Report No. 782/1/98. Water Research Commission, Pretoria.
- Beck, J.S., Basson, G.R. (2003). *The Hydraulics of the Impacts of Dam Developments on the River Morphology*. WRC Report No. 1102/1/03. Water Research Commission, Pretoria.
- Bagnold, R.A. (1966). *An Approach to the Sediment Transport Problem form General Physics*. Geological survey. Professional paper 422-I. Washington D.C.
- Basson, G.R. (2004). *Review of the State – of – the – Art Research on Erosion and Sediment Dynamics from Catchment to Coast – A Southern Perspective*. UNSECO report.
- Bishop, A.A., Simons, D.B., and Richardson, E.V. (1965). *Total Bed – Material Transport*. Proc. Am. Soc. Civil Engineers., Vol 91, no. HY2.
- BRC and TCTA. (2003). *Berg River Project – Berg River Dam – Flood Line Hydrology*.
- BRC. 2004. *Preliminary Design of Supplement Scheme*.
- Chadwick, A. and Morfett, J. (1998). *Hydraulics in Civil and Environmental Engineering*. Third Edition. E & FN SPON. London and New York
- Chien, N. (1985). *Changes in River Regime after the Construction of Upstream Reservoirs*. Earth Surface Processes and Landforms, No. 10. pp. 143 – 159.
- Colby, B.R.(1964). *Practical Computations of Bed – Material Discharge*. Proc. Am. Soc. Civil Engineers., Vol 90, no. HY2.

- Churchill, M.A.(1948). *Analysis and Use of Reservoir Sedimentation Data*. Discussion by L.C. Gottschalk. Proc. Federal Interagency Sedimentation Conference, Washington DC, Jan 1948, pp. 139-140.
- Dallavalle, J. (1943). *Micrometrics*. Pitman. New York.
- Department of Water Affairs and Forestry, South Africa. (1993). Quibell, G. Water Quality in the Berg River: A Situation Analysis. Department of Water Affairs and Forestry.
- Department of Water Affairs and Forestry, South Africa. (1994). Western Cape System Analysis – Summary Report. Department of Water Affairs and Forestry.
- Department of Water Affairs and Forestry, South Africa. (1996). *Skuifraam Dam Feasibility Study Berg River IFR Refinement Workshop Proceedings*. Compiled and Consulting cc for Ninham Shand Consulting Engineers. Report No. PG100/00/1296.
- Department of Water Affairs and Forestry, South Africa. (2003). *Preliminary Determination of the Reserve and Resource Class: Berg River – Quaternary Catchment G10A – Berg River Dam (Skuifraam Dam)*. Department of Water Affairs and Forestry. Pretoria.
- Department of Water Affairs and Forestry, South Africa. (2004). *Berg River Baseline monitoring – Annual Report April 2004* . Department of Water Affairs and Forestry. Pretoria.
- Dey, S. (1999). *Sediment Threshold*. Appl. Math. Modelling 23. pp. 399 – 417.
- Dey, S and Raju, U.V. (2002). *Incipient Motion of Gravel and Coal Beds*. Sadhana, Vol 27. Part 5, pp. 559 – 568. India.
- DHI of Water and Environment. (1992). *MIKE11: Microcomputer Based Modelling System for Rivers and Channels, Reference Manual*. Danish Hydraulic Institute of Water and Environment software. Denmark.
- Egiazaroff, I.V. (1965). *Calculation of Non – Uniform Sediment Concentration*. Journal of the Hydraulics Division. ASCE No. HY4.
- Engelund, F. and Hansen, E. (1967). *A monograph on Sediment Transport*. Tecknish Forlag, Copenhagen, Denmark.
- Einstein, H.A. (1950). *The Bed Load Function for Sediment Transportation in Open Channel Flow*. United States Department of Agriculture. Washington D.C.
- Graf, H.W., (1971). *Hydraulics of Sediment Transport*. McGraw Hill.
- Greyling, A.H. (2001). *Optimisering van Besproeiings Loslatings in die Bo – Berg Rivier*. B.Eng(Civil) Thesis, Department of Civil Engineering. University of Stellenbosch.

- Guy, H.P., Simons, D.B. and Middleton, B.J. (1966). *Summary of Alluvial Channel Data from Flume Experiments (1956 – 61)*. Geological Survey. Professional Paper 462-I. Washington D.C.
- Hadley, R.F. and Emmett, W.W. (1988). *Channel Changes Downstream of a Dam*. Journal of the American Water Resources Association. Vol 34(4). pp. 629 – 637.
- Hayashi, T.S., Ozaki and Ichibashi, T. (1980). *Study on Bed – Load Transport of Sediment Mixture*. Proc. 24th Japanese Conference on Hydraulics.
- Kersandt, U. and Marais, G. v. R. (1973). *A Mathematical Model for the Hydro – Salinity Flow Systems of the Upper Berg River Basin*. University of Cape Town, Department of Civil Engineering. Research Report No. W6.
- Kuhnle, R.A. (1993). *Incipient Motion of Sand – Gravel Sediment Mixtures*. Journal of Hydraulic Engineering. Am. Soc. Civil Eng. Vol. 119. pp. 1400 – 1415.
- Liu, X.L. (1986). *Non – uniform Bed – Load Transport Rate and Coarsening Stabilization*. Thesis for Master Degree of Chengdu University of Technology. (In Chinese).
- Meyer – Peter, E. and Muller, R. (1948). Formulas for Bed Load Transport. Proceedings, Second meeting of IAHR, Stockholm, Sweden.
- Maddock, T.Jr. (1976). *Hydraulic Relations for Sand Bedded Streams*. Sediment symposium to honour Prof. H.A. Einstein and H.W. Shen. pp. 15-1 – 15-22.
- Maritz, G.S. (2003). *Kritiese Toestand van Beweging van Spoelklip in die Bergrivier*. Finale year thesis as part of BEng (Civil). University of Stellenbosch. South Africa.
- Ninham Shand. (2001/2004). *Personal Communication*.
- Nitsche, N.C. (2000). *Assessment of a Hydrodynamic Water Quality Model, Duflow, for a Winter Rainfall River*. MSc Thesis. University of Stellenbosch. Stellenbosch, South Africa.
- Parker, G., Kilingeman, P.C. and McLean, D.G. (1982). *Bed – Load and Size Distribution in Paved Gravel – Bed Streams*. Journal of the Hydraulics Division, ASCE. Vol. 108, No. 4, pp. 544 – 571.
- Qin, Y.Y. (1980). *Incipient Motion of Non – uniform Sediment*. Journal of Sediment Research, No. 1 (Resume Publication). (In Chinese).
- Rooseboom, A.R. (1992). *Sediment Transport in Rivers and Reservoirs – A Southern Perspective*. WRC Report No. 297/1/92. Water Research Commission, Pretoria.
- Rowntree, K.M. and McGregor, G.K. (1996). *Geomorphology of the Berg River and the Potential Impacts of Impoundments*. Department of Geography, Rhodes University. (Unpublished)

- Rutherford, I. (2000). *Some Human Impacts on Australian Stream Channel Morphology*. In: Brizga, S. and Finlayson, B. (eds.). *River Management: The Australian Experience*. John Wiley and Sons. Chichester, United Kingdom. pp. 11 – 49.
- Ryan, S.E. and Troendle, C.A. (1997). *Measuring Bed – Load in Coarse Grained Mountain Channels: Procedures, Problems, and Recommendations*. In *Water Resources Education, Training and Practice: Opportunities for the Next Century*. AWRA Symposium. Jun 29 – Jul 3, pp 949 – 958. Keystone. CO.
- Schiller, L. and Naumann, A. (1933). *Über die Grundlegenden Berechnungen Bei der Schwerkraftaufbereitung*. Z. VDI, Vol 77.
- Shields, A. (1936). *Anwendungen der Ähnlichkeitsmechanik und Turbulenzforschung auf die Geschiebebewegung*. Mitteilungen der Preussischen Versuchsanstalt für Wasser und Schiffsbau, Berlin, No. 26.
- Stein, R.A. (1973). *Laboratory Studies of Total and Apparent Bed Load*. Journal of Geophysical Research. Vol 70. No. 8.
- Toffaletti, F.B. (1968). *A Procedure for Computation of the Total River Sand Discharge and Detailed Distribution, Bed to Surface*. Technical Report No. 5. US Army Corps of Engineers. Vicksburg.
- Van Rijn, L.C. (1981). *Computation of Bed – Load Concentration and Bed – Load Transport*. Delft Hydraulics Laboratory Research Report S487 – I, Delft. The Netherlands.
- Van Rijn, L.C. (1984). *Sediment Transport Part I: Bed Load Transport*. Journal of Hydraulic Engineering. ASCE Vol. No. HY10. pp. 1431 – 1456.
- Williams, G.P. and Wolman, M.G. (1984). *Downstream effects of Dams on Alluvial Rivers*. Geological Survey. Professional Paper 1286. Washington D.C.
- WCD. (2000). *Orange River Development Project, South Africa*. Case Study prepared as Input to the World Commission on Dams, Cape Town. www.dams.org.
- Wu, W.S., Wang, S.Y. and Yafeijia. (2000). *Non – uniform Sediment Transport in Alluvial Rivers*. Journal of Hydraulic Research, Vol. 38. No. 6, pp. 427 – 434.
- Yang, C.T. (1973). *Incipient Motion and Sediment Transport*. Journal of the Hydraulics Division. ASCE.99(10). pp. 1679 - 1704.
- Yang, C.T. (1979). *Unit Stream Power Equations*. Journal of the Hydrology, 40. pp. 123 - 138.
- Yang, C.T. and Molinas, A. (1982). *Sediment Transport and Unit Stream Power Function*. Journal of the Hydraulics Division. ASCE.100(6). pp. 774 – 793.

APPENDIX A MIKE 11 CROSS SECTIONS

The cross sections that were used in the simulation for the current scenario are presented in tabular format below.

Legend:

River Name	
Chainage	
Profile	
Distance from the Left bank in metres	Level in metres

Berg	
2200	
Profile	
-200	215.01
0	210.01
32.77	201.95
40.14	197.35
49	194.41
55.27	194.88
62.91	195.01
73.11	195.34
80.78	197.53
87.38	198.08
112.69	197.59
312.69	212.59

Berg	
2500	
Profile	
-200	200.99
0	195.99
31.68	195.28
35.87	194.76
40.09	194.35
49.97	194.63
65.56	194.19
80.11	193.84
103.05	195.5
104.4	195.84
107.57	195.59
307.57	200.59

Berg	
2800	
Profile	
-200	198.4
0	193.4
9.37	193.38
15.17	192.27
23.46	189.21
34.15	188.46
38.08	190.17
43.46	191.99
56.13	193.16
57.25	193.07
257.25	198.07

Berg	
3100	
Profile	
-200	195.95
0	190.95
3.92	191.01
14.57	190.97
16.7	188.98
18.82	190.97
20.63	188.12
28.16	188.4
39.84	189.22
49.79	190.06
58.07	189.9
69.78	189.49
71.87	189.02
74.9	189.37
77.82	189.31
80.33	189.35
84.92	190.56
87.2	191.12
95.52	190.87
295.52	195.87

Berg	
3400	
Profile	
-200	193.94
0	188.94
6.87	186.41
7.44	187.2
9.49	187.28
14.66	187.78
18.14	189.29
28.97	188.8
38.15	189.66
45.31	188.9
47.16	188.9
49.8	187.8
54.26	188.9
60.41	187.92
68.1	187.49
74.35	186.8
81.86	186.36
92.52	186.91
96.25	188.21
98.78	189.02
101.32	188.21
301.32	193.21

Berg	
3700	
Profile	
-200	191.89
0	186.89
40.51	186.87
44.53	185.43
45.49	184.27
51	183.81
60.01	184.55
65.79	184.38
71.9	184.17
77.46	184.78
81.66	187.1
85.43	187.35
122.41	187.47
322.41	192.47

Berg	
4000	
Profile	
-200	189.27
0	184.27
49.9	184.58
53.77	183.77
56.55	181.78
66.38	181.37
72.5	181.5
77.62	181.78
81.05	182.28
86.03	184.71
89.3	184.63
96.08	184.4
103.79	183.96
104.49	183.34
107.75	182.65
109.01	183.01
110.22	184.42
111.77	183.96
120.33	184.8
320.33	189.8

Berg	
4300	
Profile	
-200	187.63
0	182.63
9.02	182.78
11.43	182.61
14.65	180.52
25.09	179.97
38.06	180.55
56.21	180.57
61.4	181.78
64.43	182.65
81.62	182.5
104.49	183.02
304.49	188.02

Berg	
4600	
Profile	
-200	185.1
0	180.1
15.42	181.34
18.3	179.66
49.69	178.71
94.59	177.59
109.79	176.56
117.89	177.8
121.68	180.52
123.5	180.9
137.47	180.82
143.79	178.56
166.78	178.02
172.48	180.7
196.04	180.66
396.04	185.66

Berg	
4900	
Profile	
-200	183.77
0	178.77
19.73	179.36
34.45	177.78
42.13	177.78
44.73	177.78
48.78	175.84
58.58	176.55
66.12	175.93
79.75	175.48
105.82	175.76
112.15	175.72
115.17	175.21
117.06	175.06
119.58	175.26
122.24	177.21
132.88	177.78
156.17	177.98
176.84	177.88
376.84	182.88

Berg	
5200	
Profile	
-200	179.12
0	174.12
27.86	174.25
33.2	173.77
33.7	173.31
60.16	173.74
85.3	173.3
91.17	172.48
97.4	171.19
106.02	172.4
112.41	174.02
125.49	173.27
325.49	178.27

Berg	
5400	
Profile	
-200	177.87
0	172.87
27.71	173.56
32.85	171.53
39.36	171.12
68.47	171.5
70.84	172.55
86.98	172.67
112.29	171.54
117.39	171.25
125.77	171.94
147.95	170.86
158.57	171.96
179.95	170.33
212.22	170.64
217.12	169.63
220.97	170.08
226.9	172.17
229.34	172.79
258.53	172.88
458.53	177.88

Berg	
5700	
Profile	
-200	175.78
0	170.78
11.89	171.16
14.26	170.66
16.03	169.08
19.03	168.63
23.45	168.99
24.87	169.56
32.65	169.98
43.16	169.87
46.23	169.29
53.79	169.04
59.97	169.13
61.85	170.63
65.64	170.84
82.32	170.88
282.32	175.88

Berg	
6000	
Profile	
-200	173.79
0	168.79
3.72	167.14
10.6	166.44
14.07	166.98
15.46	167.57
20.55	169.06
25.26	168.18
30.52	166.09
37.88	166.59
46.43	166.92
59.33	167.37
64.79	168.41
83.94	166.89
101.94	167.04
129.56	166.37
131.13	165.72
135.72	165.62
139.83	165.9
144.49	166.93
151.84	168.07
158.56	169.78

Berg	
6300	
Profile	
-200	171.01
0	166.01
12.18	166.28
16.44	166.1
18.52	164.34
27.16	163.66
37.56	164.05
47.11	164.36
55.7	165.6
71.36	166.58
79.48	167.54
82.49	167.34
85.12	165.93
95.58	165.89
295.58	170.89

164.47	170.32
171.2	170.17
371.2	175.17

Berg	
6600	
Profile	
-200	172.24
0	167.24
6.52	164.46
10.88	163.62
16.63	163.16
20.35	163.38
25.12	163.86
30.68	162.83
41.36	163.57
49	163.38
51.43	162.92
53.75	162.73
56.17	163.02
57.26	163.29
59.95	163.34
61.92	162.97
69.38	163.26
71.67	162.99
75.77	162.02
83.05	162.91
88.18	165.74
94.28	168.53
106	167.33
306	172.33

Berg	
6900	
Profile	
0	165
14	164
24	163
32	162
44	161
66	160
70	159
82	159
88	160
94	161
112	162
176	163
192	164
328	165

Berg	
7670	
Profile	
0	161
94	160
120	159
178	158
184	157
184.6	156.4
203	156.4
204	157
220	157
238	158
250	159
262	160
270	161

Berg	
8190	
Profile	
0	160
0	160
84	159
178	158
220	157
298	156
302	155
302.4	154.6
325.6	154.6
326	156
366	157
374	157
388	157
416	157
502	157
584	157

Berg	
8680	
Profile	
0	160
2	155
4	154
8	153
8.6	152.4
27.4	152.4
28	153
44	153
84	154
88	155
92	156
100	156
164	156
186	156
386	155
406	155

Berg	
9240	
Profile	
0	155
4	154
12	153
13	152
14	151
16	150
16.2	150
34.8	150
35	150
40	151
82	152
88	153
234	153
274	153
284	155

690	157
695	160

412	156
422	157

Berg	
9710	
Profile	
0	155
8	154
12	153
14	152
18	151
19	150
20	149.2
51	149.2
52	150
58	151
62	152
160	153
170	155

Berg	
10200	
Profile	
0	152
126	151
180	150
188	150
230	150
236	149
236	148
243	147
243	147
265	146.8
266	147
282	148
289	149
289	149
289	149
302	150
322	150
594	151
746	152

Berg	
10720	
Profile	
0	150
100	149
188	149
366	148
424	147
440	146
446	146
446.8	145.2
489	145.2
490	146
494	147
500	148
568	148
602	148
738	148
746	149
766	149
794	148
802	148
820	149
826	150

Berg	
11280	
Profile	
0	148
66	147
180	146
196	145
206	144
234	144
236	145
322	145
326	144
327	143.4
347	143.4
348	144
354	144
388	144
397	144
400	144
428	145
452	146
496	147
550	148

Berg	
11800	
Profile	
0	146
88	145
198	144
204	143
205	142
206	141.1
252.1	141
253	142
276	143
410	143
426	143
444	144
460	145
470	146

Berg	
12480	
Profile	
0	144
84	143
104	143
112	143
116	142
124	141
134	140
138	139
139	138.5
173.5	138.5
174	139
178	140
180	141
220	142
402	143
482	144

Berg	
12950	
Profile	
0	142
132	141
182	140
334	140
388	140
396	139
404	138
405	137
479	137
480	138
482	139
486	140
494	140
586	140
598	140
658	140
705	141
710	141
717	141
722	142

Berg	
13500	
Profile	
-500	140
0	135
3	132
5	132
8	131.5
42	131.5
45	132
47	132
50	135
750	140

Berg	
14000	
Profile	
-900	140
0	134.5
2.5	132
10	132
13	131.5
37	131.5
40	132
47	132
50	135
900	140

Berg	
14500	
Profile	
-1270	140
0	135
2	133
15	133
18	132.5
47	132.5
50	133
63.5	133
65	134.5
100	140

Berg	
15000	
Profile	
-450	135
0	130
2	128
10	128
13	127.5
42	127.5
45	128
53	128
55	130
670	135

Berg	
15500	
Profile	
-750	135
0	130
3	127
30	127
33	126.5
52	126.5
55	127
67	127
70	130
500	135

Berg	
16000	
Profile	
-750	135
0	129.5
2.5	127
10	127
13	126.5
27	126.5
30	127
77.5	127
80	129.5
1500	135

Berg	
16500	
Profile	
-800	130
0	125
2	123
20	123
23	122.5
52	122.5
55	123
58	123
60	125
450	130

Berg	
17000	
Profile	
-500	130
0	125
3	122
10	122
13	121.5
47	121.5
50	122
57	122
60	125
900	127

Berg	
17500	
Profile	
-500	130
0	123
2	121
50	121
53	120.5
77	120.5
80	121
88	121
90	123
300	125

Berg	
18000	
Profile	
-300	125
0	121
3	118
20	118
23	117.5
37	117.5
40	118
98	118
100	120
750	125

Berg	
18500	
Profile	
-250	125
0	120
3	117
10	117
13	116.5
47	116.5
50	117
57	117
60	120
670	125

Berg	
19000	
Profile	
-300	125
0	119
2	117
20	117
23	116.5
47	116.5
50	117
68	117
70	119
750	125

Berg	
19500	
Profile	
-400	120
0	115
2	113
10	113
13	112.5
37	112.5
40	113
48	113
50	115
500	120

Berg	
20000	
Profile	
-200	120
0	115.86
9.04	115.3
11.81	114.2
18.09	113.8
34.15	113.9
48.18	113.8
60.88	113.9
68	114.5
71.54	115.3
76.58	116.3
80.12	118
280.12	120

Berg	
20700	
Profile	
-200	120
0	115.2
3.27	115
5.31	113.5
9.5	111.8
11.32	111
17.41	110.5
23.46	110.4
28.82	110.3
33.67	110.4
37.95	110.7
40.18	111.6
41.45	113.3
44.77	113.2
54.17	116.2
254.17	120

Berg	
21000	
Profile	
-1150	120
0	115
2	113
30	113
33	112.5
57	112.5
60	113
68.5	113
70	114.5
480	120

Berg	
21500	
Profile	
-1130	120
0	115
2.5	112.5
25	112.5
28	112
47	112
50	112.5
78	112.5
80	114.5
940	120

Berg	
22000	
Profile	
-300	115
0	110
2	108
10	108
13	107.5
42	107.5
45	108
48	108
50	110
430	115

Berg	
22500	
Profile	
-920	115
0	109.5
1.5	108
20	108
23	107.5
57	107.5
60	108
88	108
90	110
350	115

Berg	
23000	
Profile	
-600	115
0	110
3	107
15	107
18	106.5
27	106.5
30	107
107	107
110	110
600	115

Berg	
23500	
Profile	
-400	115
0	108
1	107
30	107
33	106.5
72	106.5
75	107
97	107
100	110
600	115

Berg	
24000	
Profile	
-150	110
0	105
2	103
30	103
33	102.5
57	102.5
60	103
78	103
80	105
300	110

Berg	
24500	
Profile	
-90	110
0	105
3	102
5	102
8	101.5
47	101.5
50	102
57	102
60	105
570	110

Berg	
25000	
Profile	
-320	110
0	104
3	101
40	101
43	100.5
87	100.5
90	101
96	101
100	105
730	110

Berg	
25500	
Profile	
-180	110
0	103
3	100
10	100
13	99.5
47	99.5
50	100
55	100
60	105
400	106

Berg	
26000	
Profile	
-60	105
0	100
2	98
20	98
23	97.5
87	97.5
90	98
97	98
100	101
900	105

Berg	
26500	
Profile	
-70	105
0	100
3	97
10	97
13	96.5
47	96.5
50	97
77	97
80	100
850	105

Berg	
27000	
Profile	
-200	105
0	100
3	97
10	97
13	96.5
52	96.5
55	97
72	97
75	100
790	105

Berg	
27500	
Profile	
-370	105
0	100
3	97
20	97
23	96.5
77	96.5
80	97
97	97
100	100
610	105

Berg	
28000	
Profile	
-210	105
0	100
3	97
10	97
13	96.5
47	96.5
50	97
77	97
80	100
650	105

Berg	
28500	
Profile	
-420	105
0	100
3	97
10	97
13	96.5
47	96.5
50	97
67	97
70	100
600	105

Berg	
29000	
Profile	
-270	105
0	99
3	96
20	96
23	95.5
37	95.5
40	96
57	96
60	99
720	105

Berg	
29500	
Profile	
-90	100
0	95
3	92
10	92
13	91.5
42	91.5
45	92
52	92
55	95
530	100

Berg	
30000	
Profile	
-170	100
0	95
3	92
5	92
8	91.5
47	91.5
50	92
67	92
70	95
650	100

Berg	
30500	
Profile	
-270	100
0	95
4	91
20	91
23	90.5
57	90.5
60	91
76	91
80	95
540	100

Berg	
31000	
Profile	
-250	100
0	96
5	91
10	91
13	90.5
57	90.5
60	91
76	91
80	95
450	100

Berg	
31500	
Profile	
-260	100
0	93
2	91
20	91
23	90.5
47	90.5
50	91
76	91
80	95
530	100

Berg	
32000	
Profile	
-500	100
0	94
3	91
20	91
23	90.5
37	90.5
40	91
57	91
60	94
1050	100

Berg	
32500	
Profile	
-380	100
0	92
2	90
20	90
23	89.5
47	89.5
50	90
95	90
100	95
1270	100

Berg	
33000	
Profile	
-200	100
0	91
2	89
20	89
23	88.5
47	88.5
50	89
67	89
70	92
1130	100

Berg	
33500	
Profile	
-30	100
0	95
7	88
10	88
13	87.5
27	87.5
30	88
48	88
50	90
1300	100

Berg	
34000	
Profile	
-200	95
0	91
4	87
10	87
13	86.5
32	86.5
35	87
36	87
40	91
1250	100

Berg	
34500	
Profile	
-250	100
0	91
4	87
5	87
8	86.5
27	86.5
30	87
36	87
40	91
700	95

Berg	
35000	
Profile	
-120	95
0	90.5
2.5	88
10	88
13	87.5
27	87.5
30	88
37.5	88
40	90.5
550	95

Berg	
35500	
Profile	
-450	93
0	90
3	87
10	87
13	86.5
27	86.5
30	87
37	87
40	90
400	95

Berg	
36000	
Profile	
-480	95
0	90
4	86
10	86
13	85.5
37	85.5
40	86
46	86
50	90
150	95

Berg	
36500	
Profile	
-230	95
0	90
4	86
25	86
28	85.5
72	85.5
75	86
86	86
90	90
160	95

Berg	
37000	
Profile	
-230	95
0	90
3	87
10	87
13	86.5
37	86.5
40	87
49	87
50	88
300	95

Berg	
37500	
Profile	
-200	95
0	88
3	85
20	85
23	84.5
57	84.5
60	85
76	85
80	89
480	95

Berg	
38000	
Profile	
-430	95
0	90
3	87
20	87
23	86.5
52	86.5
55	87
67	87
70	90
900	100

Berg	
38500	
Profile	
-300	95
0	90
3	87
5	87
8	86.5
37	86.5
40	87
47	87
50	90
1350	100

Berg	
39000	
Profile	
-320	95
0	90
3	87
20	87
23	86.5
47	86.5
50	87
57	87
60	90
370	95

Berg	
39500	
Profile	
-830	90
0	88
2	86
10	86
13	85.5
32	85.5
35	86
43	86
45	88
200	90

Berg	
40000	
Profile	
-150	95
0	88
3	85
10	85
13	84.5
57	84.5
60	85
77	85
80	88
560	95

Berg	
40500	
Profile	
-340	95
0	88
3	85
30	85
33	84.5
62	84.5
65	85
67	85
70	88
370	90

Berg	
41000	
Profile	
-1	95
0	90
6	84
35	84
38	83.5
52	83.5
55	84
67	84
70	87
650	95

Berg	
41500	
Profile	
-500	90
0	87
4	83
15	83
18	82.5
57	82.5
60	83
66	83
70	87
250	95

Berg	
42000	
Profile	
-340	90
0	86
4	82
20	82
23	81.5
37	81.5
40	82
46	82
50	86
550	90

Berg	
42500	
Profile	
-170	90
0	85
3	82
10	82
13	81.5
47	81.5
50	82
57	82
60	85
160	90

Berg	
43000	
Profile	
-100	90
0	84
2	82
10	82
13	81.5
37	81.5
40	82
47	82
50	85
200	90

Berg	
43500	
Profile	
-50	90
0	85
3	82
10	82
13	81.5
37	81.5
40	82
57	82
60	85
750	90

Berg	
44000	
Profile	
-200	90
0	84.5
2.5	82
10	82
13	81.5
27	81.5
30	82
47	82
50	85
450	90

Berg	
44500	
Profile	
-70	90
0	84.5
3.5	81
30	81
33	80.5
47	80.5
50	81
66.5	81
70	84.5
350	90

Berg	
45000	
Profile	
-150	90
0	84
3	81
20	81
23	80.5
42	80.5
45	81
57	81
60	84
600	90

Berg	
45500	
Profile	
-130	90
0	83.5
3.5	80
20	80
23	79.5
37	79.5
40	80
46.5	80
50	83.5
730	90

Berg	
46000	
Profile	
-100	90
0	83.5
3.5	80
10	80
13	79.5
37	79.5
40	80
46.5	80
50	83.5
770	90

Berg	
46500	
Profile	
-430	85
0	83
3	80
20	80
23	79.5
47	79.5
50	80
57	80
60	83
640	85

Berg	
47000	
Profile	
-880	85
0	82
3	79
30	79
33	78.5
57	78.5
60	79
97	79
100	82
450	85

Berg	
47500	
Profile	
-500	90
0	81
2	79
20	79
23	78.5
67	78.5
70	79
85	79
90	84
140	90

Berg	
48000	
Profile	
-1050	85
0	80
2	78
20	78
23	77.5
47	77.5
50	78
58	78
60	80
170	85

Berg	
48500	
Profile	
-470	85
0	80
3	77
30	77
33	76.5
57	76.5
60	77
77	77
80	80
140	85

Berg	
49650	
Profile	
0	80.1
2.56	79.5
5.38	77.5
7.19	76.5
10.51	75.5
20.77	75.5
31.12	76
39.26	76
47.49	75.8
49.83	77
50.87	77.5
55.86	78.2
58.44	79.6
64.23	80.2
69.63	83.5

Berg	
50000	
Profile	
-70	85
0	80
4	76
170	76
173	75.5
207	75.5
210	76
211	76
215	80
800	85

Berg	
50500	
Profile	
-20	85
0	80
4	76
180	76
183	75.5
187	75.5
190	76
196	76
200	80
500	82

Berg	
51000	
Profile	
-200	85
0	79
4	75
100	75
103	74.5
207	74.5
210	75
216	75
220	79
350	85

Berg	
51500	
Profile	
-150	85
0	79
4	75
230	75
233	74.5
267	74.5
270	75
296	75
300	79
350	85

Berg	
52000	
Profile	
-100	85
0	80
6	74
250	74
253	73.5
327	73.5
330	74
334	74
340	80
400	85

Berg	
52500	
Profile	
-150	85
0	79
4	75
280	75
283	74.5
307	74.5
310	75
316	75
320	79
430	85

Berg	
53000	
Profile	
-60	80
0	75
2	73
150	73
153	72.5
187	72.5
190	73
198	73
200	75
300	80

Berg	
53500	
Profile	
-180	80
0	75
3	72
110	72
113	71.5
147	71.5
150	72
157	72
160	75
190	80

Berg	
54000	
Profile	
-10	80
0	75
3	72
40	72
43	71.5
197	71.5
200	72
297	72
300	75
410	80

Berg	
54500	
Profile	
-40	80
0	74
3	71
150	71
153	70.5
167	70.5
170	71
197	71
200	74
350	80

Berg	
55000	
Profile	
-200	80
0	74
3	71
70	71
73	70.5
87	70.5
90	71
97	71
100	74
170	80

Berg	
55500	
Profile	
-80	80
0	74
3	71
130	71
133	70.5
167	70.5
170	71
197	71
200	74
270	80

Berg	
56000	
Profile	
-90	80
0	74
3	71
100	71
103	70.5
147	70.5
150	71
196	71
200	75
300	80

Berg	
56500	
Profile	
-230	80
0	74
3	71
150	71
153	70.5
177	70.5
180	71
197	71
200	74
320	80

Berg	
57000	
Profile	
-70	80
0	75
4	71
10	71
13	70.5
187	70.5
190	71
196	71
200	75
300	80

Berg	
57500	
Profile	
-100	80
0	75
4	71
20	71
23	70.5
67	70.5
70	71
196	71
200	75
270	80

Berg	
58000	
Profile	
-10	80
0	75
4	71
20	71
23	70.5
57	70.5
60	71
97	71
100	74
600	80

Berg	
58500	
Profile	
-10	80
0	75
4	71
20	71
23	70.5
57	70.5
60	71
97	71
100	74
600	80

Berg	
59000	
Profile	
-60	80
0	75
6	69
50	69
53	68.5
297	68.5
300	69
344	69
350	75
500	80

Berg	
59500	
Profile	
-100	80
0	73
5	68
10	68
13	67.5
147	67.5
150	68
165	68
170	73
300	80

Berg	
60000	
Profile	
-110	80
0	73
5	68
50	68
53	67.5
197	67.5
200	68
225	68
230	73
270	80

Berg	
60500	
Profile	
-100	75
0	67
3	64
20	64
23	63.5
147	63.5
150	64
157	64
160	67
220	75

Berg	
61000	
Profile	
-30	75
0	67
3	64
50	64
53	63.5
147	63.5
150	64
197	64
200	67
270	75

Berg	
61500	
Profile	
-50	75
0	67
3	64
50	64
53	63.5
147	63.5
150	64
247	64
250	67
350	75

Berg	
62000	
Profile	
-40	70
0	65
5	60
30	60
33	59.5
107	59.5
110	60
135	60
140	65
210	70

Berg	
62500	
Profile	
-20	70
0	65
5	60
30	60
33	59.5
117	59.5
120	60
165	60
170	65
250	70

Berg	
63000	
Profile	
-180	70
0	65
5	60
20	60
23	59.5
77	59.5
80	60
95	60
100	65
220	70

Berg	
63500	
Profile	
-160	70
0	65
5	60
40	60
43	59.5
147	59.5
150	60
195	60
200	65
350	70

Berg	
64000	
Profile	
-30	70
0	64
4	60
30	60
33	59.5
97	59.5
100	60
125	60
130	65
220	70

Berg	
64500	
Profile	
-130	70
0	63
4	59
30	59
33	58.5
147	58.5
150	59
196	59
200	63
220	70

Berg	
65000	
Profile	
-150	70
0	63
3	60
30	60
33	59.5
67	59.5
70	60
127	60
130	63
150	70

Berg	
65500	
Profile	
-130	65
0	60
2	58
20	58
23	57.5
87	57.5
90	58
98	58
100	60
140	65

Berg	
66000	
Profile	
-50	65
0	60
2	58
50	58
53	57.5
97	57.5
100	58
118	58
120	60
300	65

Berg	
66500	
Profile	
-300	62
0	60
2	58
10	58
13	57.5
37	57.5
40	58
48	58
50	60
300	65

Berg	
67000	
Profile	
-550	65
0	60
2	58
10	58
13	57.5
57	57.5
60	58
68	58
70	60
140	65

Berg	
67500	
Profile	
-280	65
0	60
2	58
5	58
8	57.5
32	57.5
35	58
38	58
40	60
350	65

Berg	
68000	
Profile	
-320	65
0	60
2	58
5	58
8	57.5
22	57.5
25	58
28	58
30	60
550	65

Berg	
68500	
Profile	
-320	65
0	60
2	58
10	58
13	57.5
47	57.5
50	58
58	58
60	60
550	65

Berg	
69000	
Profile	
-400	65
0	60
2	58
20	58
23	57.5
67	57.5
70	58
98	58
100	60
500	65

Berg	
69500	
Profile	
-600	65
0	60
3	57
30	57
33	56.5
97	56.5
100	57
118	57
120	59
700	65

Berg	
70000	
Profile	
-820	65
0	58
1	57
10	57
13	56.5
57	56.5
60	57
67	57
70	60
250	65

Berg	
70500	
Profile	
-480	65
0	59
2	57
5	57
8	56.5
37	56.5
40	57
48	57
50	59
560	65

Berg	
71000	
Profile	
-230	65
0	59
2	57
10	57
13	56.5
87	56.5
90	57
98	57
100	59
850	65

Berg	
71500	
Profile	
-110	65
0	59
2	57
20	57
23	56.5
77	56.5
80	57
98	57
100	59
400	62

Berg	
72000	
Profile	
-80	65
0	58
1	57
30	57
33	56.5
87	56.5
90	57
137	57
140	60
300	65

Berg	
72500	
Profile	
-260	65
0	58
1	57
30	57
33	56.5
97	56.5
100	57
119	57
120	58
750	65

Berg	
73000	
Profile	
-90	65
0	60
4	56
30	56
33	55.5
87	55.5
90	56
106	56
110	60
650	75

Berg	
73500	
Profile	
-500	65
0	60
4	56
20	56
23	55.5
67	55.5
70	56
96	56
100	60
700	65

Berg	
73750	
Profile	
-33.3	59.5
-27.37	55.3
-22.47	54.2
-11.13	54
-4.39	55.3
0	58.67
13.58	59

Berg	
74000	
Profile	
-500	65
0	60
6	54
30	54
33	53.5
97	53.5
100	54
124	54
130	60
650	65

Berg	
74500	
Profile	
-950	65
0	60
6	54
10	54
13	53.5
37	53.5
40	54
46	54
50	58
300	65

Berg	
75000	
Profile	
-100	65
0	58
5	53
20	53
23	52.5
47	52.5
50	53
65	53
70	58
500	65

Berg	
75500	
Profile	
-380	65
0	58
5	53
20	53
23	52.5
57	52.5
60	53
65	53
70	58
250	65

Berg	
76000	
Profile	
-650	65
0	58
5	53
10	53
13	52.5
47	52.5
50	53
57	53
60	58
600	62

Berg	
76500	
Profile	
-250	65
0	60
7	53
10	53
13	52.5
47	52.5
50	53
56	53
60	57
550	60

Berg	
77000	
Profile	
-220	65
0	58
5	53
20	53
23	52.5
67	52.5
70	53
85	53
90	58
270	61

Berg	
77500	
Profile	
-280	65
0	58
5	53
20	53
23	52.5
57	52.5
60	53
75	53
80	58
250	61

Berg	
78000	
Profile	
-320	65
0	57
4	53
10	53
13	52.5
47	52.5
50	53
56	53
60	57
200	60

Berg	
78500	
Profile	
-400	65
0	57
4	53
20	53
23	52.5
47	52.5
50	53
56	53
60	57
100	60

Berg	
79000	
Profile	
-300	62
0	59
6	53
20	53
23	52.5
67	52.5
70	53
74	53
80	59
100	62

Berg	
79500	
Profile	
-70	60
0	58
5	53
50	53
53	52.5
97	52.5
100	53
105	53
110	58
150	60

Berg	
80000	
Profile	
-250	60
0	58
5	53
10	53
13	52.5
47	52.5
50	53
53	53
60	60

Berg	
80500	
Profile	
-120	60
0	55
3	52
20	52
23	51.5
97	51.5
100	52
117	52
120	55
170	60

Berg	
81000	
Profile	
-120	60
0	55
3	52
10	52
13	51.5
57	51.5
60	52
67	52
70	55
350	60

Berg	
81250	
Profile	
0	54.6
7.33	52.7
17.37	52.7
18.56	51
23.37	49.02
35	48.5
38.92	49.5
42.32	52.9
46.85	52.5
52.82	50.9
58.66	52.7
61.51	54.7
74.26	56.11

Berg	
81500	
Profile	
-70	60
0	54
2	52
20	52
23	51.5
77	51.5
80	52
88	52
90	54
180	60

Berg	
82000	
Profile	
-90	60
0	55
4	51
20	51
23	50.5
57	50.5
60	51
67	51
70	54
330	56

Berg	
82500	
Profile	
-50	60
0	55
4	51
20	51
23	50.5
57	50.5
60	51
66	51
70	55
150	59

Berg	
83000	
Profile	
-40	60
0	55
4	51
30	51
33	50.5
67	50.5
70	51
96	51
100	55
450	60

Berg	
83500	
Profile	
-100	60
0	55
4	51
20	51
23	50.5
47	50.5
50	51
126	51
130	55
400	60

Berg	
84000	
Profile	
-250	60
0	55
4	51
30	51
33	50.5
77	50.5
80	51
146	51
150	55
350	60

Berg	
84500	
Profile	
-250	60
0	55
4	51
30	51
33	50.5
67	50.5
70	51
76	51
80	55
460	60

Berg	
85000	
Profile	
0	60
250	55
251.724	53.276
334.5	53.276
335	52.776
345	52.776
345.5	53.276
428.276	53.276
430	55
530	60
690	65
700	70

Berg	
85500	
Profile	
0	50
370	55
371.965	53.035
544.5	53.035
545	52.535
555	52.535
555.5	53.035
728.035	53.035
730	55
1010	60
1160	65

Berg	
86000	
Profile	
0	65
200	60
530	55
532.206	52.794
594.5	52.794
595	52.294
605	52.294
605.5	52.794
667.794	52.794
670	55
920	60
1080	65

Berg	
86500	
Profile	
0	65
180	60
410	55
412.447	52.553
469.5	52.553
470	52.053
480	52.053
480.5	52.553
537.553	52.553
540	55
970	60
1050	65

Berg	
87000	
Profile	
0	65
310	60
550	55
552.687	52.313
639.5	52.313
640	51.813
650	51.813
650.5	52.313
737.313	52.313
740	55
1200	60
1280	65

Berg	
87500	
Profile	
0	65
320	60
470	55
472.928	52.072
524.5	52.072
525	51.572
535	51.572
535.5	52.072
587.072	52.072
590	55
700	60
750	65

Berg	
88000	
Profile	
0	65
110	60
200	55
260	55
263.169	51.831
299.5	51.831
300	51.331
310	51.331
310.5	51.831
346.831	51.831
350	55
810	60
1080	65

Berg	
88500	
Profile	
0	65
90	60
140	55
143.409	51.591
204.5	51.591
205	51.091
215	51.091
215.5	51.591
276.591	51.591
280	55
670	60
1020	65

Berg	
89000	
Profile	
0	65
120	60
380	55
383.65	51.35
444.5	51.35
445	50.85
455	50.85
455.5	51.35
516.35	51.35
520	55
1200	60
1360	65

Berg	
89500	
Profile	
0	65
310	60
480	55
483.891	51.109
574.5	51.109
575	50.609
585	50.609
585.5	51.109
676.109	51.109
680	55
1370	60
1620	65

Berg	
90000	
Profile	
0	65
130	60
190	55
193.891	51.109
234.5	51.109
235	50.609
265	50.609
265.5	51.109
306.109	51.109
310	55
1050	60
1290	65

Berg	
90500	
Profile	
0	65
140	60
220	55
224.372	50.628
254.5	50.628
255	50.128
285	50.128
285.5	50.628
315.628	50.628
320	55
960	60
1130	65

Berg	
91000	
Profile	
0	65
280	60
400	55
530	55
660	55
664.613	50.387
729.5	50.387
730	49.887
770	49.887
770.5	50.387
835.387	50.387
840	55
1420	60
1520	65

Berg	
91500	
Profile	
0	60
60	55
64.854	50.146
114.5	50.146
115	49.646
175	49.646
175.5	50.146
225.146	50.146
230	55
440	55

Berg	
92000	
Profile	
0	60
120	55
170	55
220	55
340	50
340.095	49.905
349.5	49.905
350	49.405
360	49.405
360.5	49.905
369.905	49.905
370	50
660	55
840	65

Berg	
92500	
Profile	
0	65
170	60
230	55
330	50
330.335	49.665
359.5	49.665
360	49.165
370	49.165
370.5	49.665
399.665	49.665
400	50
960	55
1160	60

Berg	
93000	
Profile	
0	65
140	60
470	55
500	50
500.576	49.424
559.5	49.424
560	48.924
570	48.924
570.5	49.424
629.424	49.424
630	50
1160	55
1240	60

Berg	
93500	
Profile	
0	65
110	60
200	55
340	50
340.817	49.183
379.5	49.183
380	48.683
420	48.683
420.5	49.183
459.183	49.183
460	50
510	55
790	55
1110	55
1190	60

Berg	
94000	
Profile	
0	60
360	55
660	50
661.058	48.942
664.5	48.942
665	48.442
715	48.442
715.5	48.942
718.942	48.942
720	50
900	55
1030	60

Berg	
94500	
Profile	
0	60
840	55
860	50
861.298	48.702
924.5	48.702
925	48.202
935	48.202
935.5	48.702
998.702	48.702
1000	50
1100	55
1220	60
1270	65

Berg	
95000	
Profile	
0	60
160	55
600	50
601.539	48.461
699.5	48.461
700	47.961
750	47.961
750.5	48.461
848.461	48.461
850	50
1040	55
1310	60

Berg	
95500	
Profile	
0	60
520	55
760	50
761.78	48.22
799.5	48.22
800	47.72
830	47.72
830.5	48.22
868.22	48.22
870	50
1200	55
1530	60

Berg	
96000	
Profile	
0	60
270	55
400	50
402.02	47.98
439.5	47.98
440	47.48
480	47.48
480.5	47.98
517.98	47.98
520	50
580	55
700	60
930	65

Berg	
96600	
Profile	
0	60
160	55
370	50
372.309	47.691
434.5	47.691
435	47.191
495	47.191
495.5	47.691
557.691	47.691
560	50
810	55
960	60

Berg	
97100	
Profile	
0	60
150	55
350	50
352.55	47.45
409.5	47.45
410	46.95
440	46.95
440.5	47.45
497.45	47.45
500	50
660	55
770	60

Berg	
97600	
Profile	
0	60
110	55
190	50
192.791	47.209
249.5	47.209
250	46.709
290	46.709
290.5	47.209
347.209	47.209
350	50
600	55
900	60

Berg	
98200	
Profile	
0	60
220	55
380	50
383.08	46.92
424.5	46.92
425	46.42
435	46.42
435.5	46.92
476.92	46.92
480	50
600	55
630	60

Berg	
98700	
Profile	
0	60
200	55
370	50
373.32	46.68
454.5	46.68
455	46.18
465	46.18
465.5	46.68
546.68	46.68
550	50
570	55
660	60

Berg	
99200	
Profile	
0	60
290	55
620	50
623.561	46.439
669.5	46.439
670	45.939
710	45.939
710.5	46.439
756.439	46.439
760	50
1150	55
1330	60

Berg	
99700	
Profile	
0	60
160	55
210	50
213.802	46.198
249.5	46.198
250	45.698
290	45.698
290.5	46.198
326.198	46.198
330	50
600	55
750	60

Berg	
100200	
Profile	
0	60
110	55
380	50
384.043	45.957
424.5	45.957
425	45.457
455	45.457
455.5	45.957
495.957	45.957
500	50
600	55
670	60

Berg	
100700	
Profile	
0	55
170	50
174.283	45.717
329.5	45.717
330	45.217
370	45.217
370.5	45.717
525.717	45.717
530	50
580	55
990	55

Berg	
101200	
Profile	
0	60
80	55
170	50
190	45
189.562	45.438
199.5	45.438
200	44.938
240	44.938
240.5	45.438
250.438	45.438
250	45
400	50
610	55
1040	60

Berg	
101700	
Profile	
0	60
130	55
180	50
270	45
270.186	44.814
289.5	44.814
290	44.314
320	44.314
320.5	44.814
339.814	44.814
340	45
430	50

Berg	
102200	
Profile	
0	60
160	55
270	50
350	45
350.809	44.191
379.5	44.191
380	43.691
430	43.691
430.5	44.191
459.191	44.191
460	45
510	50
1250	55
1460	60

Berg	
102700	
Profile	
0	60
30	55
40	50
90	45
91.433	43.567
109.5	43.567
110	43.067
130	43.067
130.5	43.567
148.567	43.567
150	45
800	50
950	55
1160	60

Berg	
103200	
Profile	
0	60
550	55
700	50
730	45
732.056	42.944
774.5	42.944
775	42.444
805	42.444
805.5	42.944
847.944	42.944
850	45
1580	50
1730	55
1940	60

Berg	
103700	
Profile	
0	60
70	55
120	50
210	45
212.68	42.32
234.5	42.32
235	41.82
285	41.82
285.5	42.32
307.32	42.32
310	45
550	50
800	55
1190	60

Berg	
104200	
Profile	
0	60
110	55
220	50
500	45
503.303	41.697
534.5	41.697
535	41.197
555	41.197
555.5	41.697
586.697	41.697
590	45
790	50
920	50
1100	50
1290	55

Berg	
104700	
Profile	
0	60
210	55
290	50
360	50
420	50
640	45
643.926	41.074
654.5	41.074
655	40.574
675	40.574
675.5	41.074
686.074	41.074
690	45
750	50
920	55
1230	60

Berg	
105200	
Profile	
0	60
160	55
250	50
280	45
340	40
339.524	40.476
344.5	40.476
345	39.976
355	39.976
355.5	40.476
360.476	40.476
360	40
440	45
550	50
710	55
900	60

Berg	
105700	
Profile	
0	60
80	55
120	50
210	45
330	40
329.818	40.182
334.5	40.182
335	39.682
365	39.682
365.5	40.182
370.182	40.182
370	40
420	45
590	50
830	55
1000	60

Berg	
106200	
Profile	
0	60
40	55
60	50
70	45
80	40
80.112	39.888
89.5	39.888
90	39.388
100	39.388
100.5	39.888
109.888	39.888
110	40
270	45
630	50
1030	55
1190	60

Berg	
106700	
Profile	
0	60
40	55
190	50
330	45
410	40
410.407	39.593
414.5	39.593
415	39.093
465	39.093
465.5	39.593
469.593	39.593
470	40
490	45
1130	50
1220	55
1420	60

Berg	
107200	
Profile	
0	60
30	55
80	50
150	45
310	40
310.72	39.28
319.5	39.28
320	38.78
360	38.78
360.5	39.28
369.28	39.28
370	40
580	45
1060	50
1160	55
1290	60

Berg	
107700	
Profile	
0	60
160	55
860	50
910	45
960	40
960.996	39.004
979.5	39.004
980	38.504
1040	38.504
1040.5	39.004
1059.004	39.004
1060	40
1330	45
1470	50
1580	55
1690	60

Berg	
108200	
Profile	
0	60
160	55
810	50
980	45
990	40
1010	40
1080	40
1081.29	38.71
1124.5	38.71
1125	38.21
1135	38.21
1135.5	38.71
1178.71	38.71
1180	40
1360	45
1430	50
1480	55

Berg	
108700	
Profile	
0	50
140	45
300	40
301.585	38.415
314.5	38.415
315	37.915
355	37.915
355.5	38.415
368.415	38.415
370	40
380	45
390	50
440	55
460	60

Berg	
109200	
Profile	
0	55
220	50
390	45
460	40
461.879	38.121
479.5	38.121
480	37.621
540	37.621
540.5	38.121
558.121	38.121
560	40
610	45
740	50
870	55

Berg	
109700	
Profile	
0	55
80	50
140	45
180	40
182.174	37.826
239.5	37.826
240	37.326
270	37.326
270.5	37.826
327.826	37.826
330	40
430	45
530	50
690	55

Berg	
110200	
Profile	
0	60
150	55
230	50
350	45
380	40
382.468	37.532
449.5	37.532
450	37.032
490	37.032
490.5	37.532
557.532	37.532
560	40
590	45
620	50
670	55
740	60

Berg	
110800	
Profile	
0	60
80	55
140	50
190	45
260	40
262.822	37.178
354.5	37.178
355	36.678
365	36.678
365.5	37.178
457.178	37.178
460	40
680	45
1740	50

Berg	
111300	
Profile	
0	55
130	50
170	45
190	40
193.116	36.884
639.5	36.884
640	36.384
1060	36.384
1060.5	36.884
1506.884	36.884
1510	40
1690	45
1700	50
1720	55
1740	60

Berg	
111800	
Profile	
0	60
80	55
110	50
120	45
130	40
133.41	36.59
139.5	36.59
140	36.09
240	36.09
240.5	36.59
246.59	36.59
250	40
490	45
800	45
1430	45
1440	50
1460	55
1490	60

Berg	
112300	
Profile	
0	60
60	55
130	50
190	45
240	40
243.705	36.295
319.5	36.295
320	35.795
330	35.795
330.5	36.295
406.295	36.295
410	40
1440	45
1460	50
1490	55
1510	60

Berg	
112800	
Profile	
0	60
120	55
250	550
320	45
330	40
333.999	36.001
369.5	36.001
370	35.501
410	35.501
410.5	36.001
446.001	36.001
450	40
480	40
520	40
1000	45
1020	50
1140	55
1210	60

Berg	
113300	
Profile	
0	60
90	55
220	50
310	45
500	40
504.294	35.706
579.5	35.706
580	35.206
590	35.206
590.5	35.706
665.706	35.706
670	40
680	45
685	50
700	55
730	60

Berg	
113800	
Profile	
0	60
20	55
50	50
90	45
180	40
210	35
209.753	35.247
254.5	35.247
255	34.747
295	34.747
295.5	35.247
340.247	35.247
340	35
360	40
470	45
510	50
570	55
720	60

Berg	
114300	
Profile	
0	60
140	55
220	50
390	45
430	40
450	35
450.598	34.402
494.5	34.402
495	33.902
525	33.902
525.5	34.402
569.402	34.402
570	35
600	40
670	45
770	50
900	55

Berg	
114800	
Profile	
0	60
20	55
70	50
90	45
130	40
170	35
171.443	33.557
204.5	33.557
205	33.057
245	33.057
245.5	33.557
278.557	33.557
280	35
310	40
380	45
430	50
460	55
490	60

Berg	
115300	
Profile	
0	60
70	55
120	50
230	45
380	40
400	35
402.287	32.713
409.5	32.713
410	32.213
550	32.213
550.5	32.713
557.713	32.713
560	35
570	40
580	45
590	50
600	55
610	60

Berg	
115800	
Profile	
0	60
20	55
60	50
90	45
130	40
170	35
173.132	31.868
184.5	31.868
185	31.368
315	31.368
315.5	31.868
326.868	31.868
330	35
340	40
350	45
360	50
370	55
390	60

Berg	
116300	
Profile	
0	60
40	55
90	50
140	45
150	40
180	35
183.976	31.024
219.5	31.024
220	30.524
380	30.524
380.5	31.024
416.024	31.024
420	35
480	40
550	45
600	50

Berg	
116800	
Profile	
0	40
100	35
130	35
140	40
260	40
290	35
360	30
359.611	30.389
374.5	30.389
375	29.889
385	29.889
385.5	30.389
400.389	30.389
400	30
560	35
600	40
680	45
720	50

Berg	
117300	
Profile	
0	40
120	35
160	35
210	40
320	45
470	45
490	40
530	35
580	30
579.904	30.096
609.5	30.096
610	29.596
620	29.596
620.5	30.096
650.096	30.096
650	30
770	35
820	40
850	45
920	50
990	55
1100	60

Berg	
117800	
Profile	
0	60
60	55
90	50
120	45
150	40
160	35
180	30
180.198	29.802
224.5	29.802
225	29.302
235	29.302
235.5	29.802
279.802	29.802
280	30
520	35
590	40
620	45
710	50
830	55
960	60

Berg	
118300	
Profile	
0	55
30	50
60	45
100	40
140	35
160	30
160.491	29.509
169.5	29.509
170	29.009
220	29.009
220.5	29.509
229.509	29.509
230	30
260	35
430	40
460	45
490	50
520	55
700	60

Berg	
118800	
Profile	
0	50
90	45
170	40
250	35
290	30
290.784	29.216
299.5	29.216
300	28.716
340	28.716
340.5	29.216
349.216	29.216
350	30
370	35
630	40
700	45
740	50
760	55
780	60

Berg	
119300	
Profile	
0	50
60	45
140	40
210	35
370	30
371.077	28.923
414.5	28.923
415	28.423
425	28.423
425.5	28.923
468.923	28.923
470	30
480	35
510	40
560	45
640	50
770	55

Berg	
119800	
Profile	
0	50
40	45
80	40
110	35
130	30
131.37	28.63
134.5	28.63
135	28.13
185	28.13
185.5	28.63
188.63	28.63
190	30
230	35
480	40
540	45
590	50
650	55
750	60

Berg	
120300	
Profile	
0	60
70	55
130	50
270	45
360	40
380	35
390	30
391.663	28.337
399.5	28.337
400	27.837
430	27.837
430.5	28.337
438.337	28.337
440	30
660	35
910	40
930	45
980	50
1020	55
1130	60

Berg	
120800	
Profile	
0	60
60	55
100	50
230	45
360	40
760	35
950	30
990	30
1010	30
1011.956	28.044
1034.5	28.044
1035	27.544
1045	27.544
1045.5	28.044
1068.044	28.044
1070	30
1130	35
1150	40
1170	45
1210	50
1330	55
1440	60

Berg	
121300	
Profile	
0	55
30	50
50	45
70	40
190	35
320	30
322.249	27.751
364.5	27.751
365	27.251
405	27.251
405.5	27.751
447.751	27.751
450	30
590	35
750	40
820	45
880	50
960	55
1020	60

Berg	
121800	
Profile	
0	50
70	45
150	40
280	35
300	30
302.542	27.458
309.5	27.458
310	26.958
360	26.958
360.5	27.458
367.458	27.458
370	30
400	30
430	30
530	35
720	40
730	45
780	50
870	55
910	60

Berg	
122300	
Profile	
0	45
220	40
300	35
330	30
332.835	27.165
394.5	27.165
395	26.665
435	26.665
435.5	27.165
497.165	27.165
500	30
590	35
600	40
630	45
650	50
740	55
850	60

Berg	
122800	
Profile	
0	60
60	55
130	50
440	45
540	40
590	35
670	30
673.128	26.872
779.5	26.872
780	26.372
800	26.372
800.5	26.872
906.872	26.872
910	30
960	35
990	40
1110	45
1180	50
1300	55
1470	60

Berg	
123300	
Profile	
0	60
20	55
50	50
80	45
130	40
260	40
330	40
350	35
360	30
363.421	26.579
479.5	26.579
480	26.079
500	26.079
500.5	26.579
616.579	26.579
620	30
680	35
760	40

Berg	
123800	
Profile	
0	50
60	45
80	40
190	35
310	30
313.715	26.285
369.5	26.285
370	25.785
410	25.785
410.5	26.285
466.285	26.285
470	30
490	35
500	40
530	45
580	50

Berg	
124400	
Profile	
0	60
10	55
20	50
50	45
90	40
110	35
190	30
194.066	25.934
234.5	25.934
235	25.434
275	25.434
275.5	25.934
315.934	25.934
320	30
510	35
830	40
980	45
1030	50

Berg	
124900	
Profile	
0	50
10	45
30	40
40	35
60	30
64.359	25.641
74.5	25.641
75	25.141
135	25.141
135.5	25.641
145.641	25.641
150	30
170	30
180	30
190	30
210	30
550	35
840	40
970	45
1030	50

Berg	
125400	
Profile	
0	60
30	55
60	50
100	45
140	40
240	35
250	30
260	25
259.582	25.418
265.5	25.418
266	24.918
316	24.918
316.5	25.418
322.418	25.418
322	25
340	30
370	30
400	30
640	35
910	40
1140	45
1180	50

Berg	
125900	
Profile	
0	50
110	45
190	40
240	35
290	30
330	30
610	30
620	25
619.74	25.26
629.5	25.26
630	24.76
660	24.76
660.5	25.26
670.26	25.26
670	25
700	30
710	30
730	35
1070	40
1330	55
1630	50

Berg	
126400	
Profile	
0	50
20	45
30	40
90	35
310	30
390	25
389.898	25.102
389.5	25.102
390	24.602
420	24.602
420.5	25.102
420.102	25.102
420	25
460	30
520	35
670	40
720	45
780	50

Berg	
126900	
Profile	
0	55
140	50
180	45
290	40
330	35
460	30
540	25
540.057	24.943
549.5	24.943
550	24.443
560	24.443
560.5	24.943
569.943	24.943
570	25
600	30
610	35
620	40
640	45
750	50

Berg	
127400	
Profile	
0	60
90	55
120	50
160	45
190	40
195	35
200	30
260	25
260.531	24.469
324.5	24.469
325	23.969
335	23.969
335.5	24.469
394.469	24.469
400	30
420	35
550	40
610	45
740	50

Berg	
127900	
Profile	
0	50
30	45
70	40
100	35
110	30
120	25
120.373	24.627
154.5	24.627
155	24.127
165	24.127
165.5	24.627
199.627	24.627
200	25
250	30
320	35
440	40
490	45
570	50

Berg	
128400	
Profile	
0	45
40	40
190	35
260	30
390	25
390.531	24.469
394.5	24.469
395	23.969
425	23.969
425.5	24.469
429.469	24.469
430	25
470	30
520	35
570	40
600	45
630	50

Berg	
128900	
Profile	
0	45
120	40
180	35
220	30
270	30
310	30
490	30
510	25
510.689	24.311
514.5	24.311
515	23.811
555	23.811
555.5	24.311
559.311	24.311
560	25
640	30
720	35
770	40
810	45
890	50

Berg	
129400	
Profile	
0	50
330	45
370	40
380	35
390	30
400	25
400.847	24.153
409.5	24.153
410	23.653
420	23.653
420.5	24.153
429.153	24.153
430	25
520	30
690	35
770	40

Berg	
129900	
Profile	
0	45
190	40
230	35
350	30
360	25
361.005	23.995
364.5	23.995
365	23.495
395	23.495
395.5	23.995
398.995	23.995
400	25
500	30
590	35
680	40
750	45

Berg	
130400	
Profile	
0	45
560	40
620	35
790	30
830	25
831.48	23.52
839.5	23.52
840	23.02
860	23.02
860.5	23.52
868.52	23.52
870	25
920	30
1060	35
1180	40
1230	45

Berg	
130900	
Profile	
0	45
420	40
490	35
530	30
550	25
551.638	23.362
604.5	23.362
605	22.862
630	22.862
630.5	23.362
678.362	23.362
680	25
690	30
700	35
720	40
740	45
840	50

Berg	
131400	
Profile	
0	55
70	50
110	45
120	40
130	35
140	30
150	25
151.796	23.204
164.5	23.204
165	22.704
205	22.704
205.5	23.204
218.204	23.204
220	25
270	30
310	35
400	40
520	45
680	50

Berg	
131900	
Profile	
0	50
160	45
270	40
340	35
370	30
390	25
391.954	23.046
419.5	23.046
420	22.546
470	22.546
470.5	23.046
498.046	23.046
500	25
510	30
520	35
550	40
570	45
600	50
660	55

Sim River	
Berg	
132400	
Profile	
0	55
100	50
250	45
310	40
360	35
470	30
490	25
492.112	22.888
499.5	22.888
500	22.388
560	22.388
560.5	22.888
567.888	22.888
570	25
590	30
740	35
780	40
810	45
970	50
1350	55

Berg	
132900	
Profile	
0	60
90	55
150	50
200	45
250	40
300	35
360	30
400	25
402.27	22.73
409.5	22.73
410	22.23
490	22.23
490.5	22.73
497.73	22.73
500	25
510	30
520	35
530	40
560	45
630	50

Berg	
133400	
Profile	
0	60
30	55
90	50
140	45
190	40
230	35
330	30
340	25
342.429	22.571
389.5	22.571
390	22.071
420	22.071
420.5	22.571
467.571	22.571
470	25
480	30
490	35
510	40
530	45
560	50
590	55

Berg	
133900	
Profile	
0	55
60	50
100	45
150	40
190	35
230	30
240	25
242.587	22.413
289.5	22.413
290	21.913
320	21.913
320.5	22.413
367.413	22.413
370	25
390	30
450	35
480	40
510	45
620	50
810	55
880	60

Berg	
134400	
Profile	
0	45
20	40
50	35
90	30
110	25
112.745	22.255
119.5	22.255
120	21.755
220	21.755
220.5	22.255
227.255	22.255
230	25
260	30
400	35
510	40
600	45

Berg	
134900	
Profile	
0	55
100	50
160	45
220	40
240	35
270	30
280	25
282.903	22.097
299.5	22.097
300	21.597
430	21.597
430.5	22.097
447.097	22.097
450	25
470	30
550	35
590	40
630	45
690	50

Berg	
135400	
Profile	
0	45
120	40
200	35
250	30
330	25
333.061	21.939
344.5	21.939
345	21.439
435	21.439
435.5	21.939
446.939	21.939
450	25
470	30
490	35
500	40
530	45
540	50
600	55
720	60

Berg	
135900	
Profile	
0	60
70	55
100	50
110	45
130	40
160	35
190	30
200	25
203.219	21.781
244.5	21.781
245	21.281
275	21.281
275.5	21.781
316.781	21.781
320	25
360	30
430	35
510	40
550	45
660	50
820	55

Berg	
136400	
Profile	
0	55
70	50
130	45
190	40
205	35
210	30
230	25
233.377	21.623
244.5	21.623
245	21.123
365	21.123
365.5	21.623
376.623	21.623
380	25
430	30
480	35
540	40
590	45
670	50
740	55
800	60

Berg	
136900	
Profile	
0	50
40	45
90	40
190	35
230	30
280	25
283.535	21.465
314.5	21.465
315	20.965
375	20.965
375.5	21.465
406.465	21.465
410	25
450	30
500	35
540	40
590	45
640	50
690	55

Berg	
137400	
Profile	
0	55
100	50
130	45
190	40
220	35
240	30
260	25
263.694	21.306
269.5	21.306
270	20.806
330	20.806
330.5	21.306
336.306	21.306
340	25
370	30
400	35
440	40
490	45

Berg	
137900	
Profile	
0	55
90	50
160	45
190	40
220	35
230	30
240	25
243.852	21.148
249.5	21.148
250	20.648
340	20.648
340.5	21.148
346.148	21.148
350	25
380	30
410	35
440	40
490	45
630	50

Berg	
138400	
Profile	
0	55
100	50
220	45
260	40
280	35
300	30
330	25
334.01	20.99
394.5	20.99
395	20.49
475	20.49
475.5	20.99
535.99	20.99
540	25
560	30
580	35
610	40
630	45
650	50
690	55

Berg	
138900	
Profile	
0	55
40	50
60	45
100	40
110	35
120	30
130	25
134.168	20.832
204.5	20.832
205	20.332
295	20.332
295.5	20.832
365.832	20.832
370	25
400	30
440	35
480	40
510	45
540	50

Berg	
139400	
Profile	
0	45
30	40
50	35
70	30
80	25
84.326	20.674
134.5	20.674
135	20.174
255	20.174
255.5	20.674
305.674	20.674
310	25
350	30
360	35
380	40
390	45
400	50

Berg	
140000	
Profile	
0	50
30	45
60	40
80	35
120	30
140	25
190	20
189.54	20.46
199.5	20.46
200	19.96
230	19.96
230.5	20.46
240.46	20.46
240	20
250	25
260	30
280	35
310	40
330	45
390	50
460	55
510	60

Berg	
140500	
Profile	
0	50
50	45
90	40
110	35
140	30
160	25
200	20
199.94	20.06
209.5	20.06
210	19.56
250	19.56
250.5	20.06
260.06	20.06
260	20
280	25
290	30
320	35
330	40
360	45
380	50
440	55

Berg	
141000	
Profile	
0	45
30	40
60	35
90	30
100	25
120	20
120.34	19.66
219.5	19.66
220	19.16
240	19.16
240.5	19.66
339.66	19.66
340	20
350	25
370	30
390	35
400	40
440	45
470	50
570	55

Berg	
141500	
Profile	
0	45
70	40
100	35
110	30
130	25
150	20
150.74	19.26
189.5	19.26
190	18.76
270	18.76
270.5	19.26
309.26	19.26
310	20
330	25
380	30
430	35
470	40
510	45

Berg	
142000	
Profile	
0	50
40	45
80	40
120	35
140	30
150	25
190	20
191.14	18.86
244.5	18.86
245	18.36
255	18.36
255.5	18.86
308.86	18.86
310	20
330	25
380	30
400	35
430	40
460	45
480	50

Berg	
142500	
Profile	
0	45
30	40
70	35
110	30
160	25
200	20
201.54	18.46
214.5	18.46
215	17.96
265	17.96
265.5	18.46
278.46	18.46
280	20
290	25
300	30
320	35
340	40
360	45
390	50
420	55

Berg	
143000	
Profile	
0	40
40	35
70	30
80	25
100	20
101.94	18.06
149.5	18.06
150	17.56
230	17.56
230.5	18.06
278.06	18.06
280	20
310	25
340	30
380	35
420	40

Berg	
143500	
Profile	
0	35
70	30
90	25
110	20
112.34	17.66
129.5	17.66
130	17.16
200	17.16
200.5	17.66
217.66	17.66
220	20
250	25
280	30
310	35

Berg	
144000	
Profile	
0	40
25	35
50	30
70	25
100	20
102.74	17.26
144.5	17.26
145	16.76
155	16.76
155.5	17.26
197.26	17.26
200	20
260	25
300	30
320	35
350	40

Berg	
144500	
Profile	
0	35
50	30
100	25
120	20
123.14	16.86
169.5	16.86
170	16.36
190	16.36
190.5	16.86
236.86	16.86
240	20
260	25
264	30
270	35
280	40

Berg	
145000	
Profile	
0	30
90	25
120	20
123.54	16.46
139.5	16.46
140	15.96
180	15.96
180.5	16.46
196.46	16.46
200	20
220	25
230	30
240	35
250	40

Berg	
145500	
Profile	
0	35
30	30
60	25
80	30
93.94	16.06
134.5	16.06
135	15.56
165	15.56
165.5	16.06
216.06	16.06
220	20
240	25
270	30
320	35

Berg	
146000	
Profile	
0	30
50	25
90	20
94.34	15.66
149.5	15.66
150	15.16
180	15.16
180.5	15.66
235.66	15.66
240	20
250	25
270	30
310	35

Berg	
146500	
Profile	
0	30
90	25
125	20
180	15
179.633	15.367
214.5	15.367
215	14.867
225	14.867
225.5	15.367
260.367	15.367
260	15
290	20
320	25
360	30
370	35
400	40

Berg	
147000	
Profile	
0	25
20	20
90	15
89.854	15.146
104.5	15.146
105	14.646
135	14.646
135.5	15.146
150.146	15.146
150	15
160	20
190	25
210	30

Berg	
147500	
Profile	
0	30
20	25
50	20
60	15
60.075	14.925
74.5	14.925
75	14.425
135	14.425
135.5	14.925
149.925	14.925
150	15
160	20
170	25
210	30
240	35

Berg	
148000	
Profile	
0	30
40	25
80	20
110	15
110.296	14.704
159.5	14.704
160	14.204
180	14.204
180.5	14.704
229.704	14.704
230	15
240	20
280	25
330	30

Berg	
148500	
Profile	
0	30
30	25
80	20
110	15
110.518	14.482
114.5	14.482
115	13.982
185	13.982
185.5	14.482
189.482	14.482
190	15
200	20
230	25
250	30

Berg	
149000	
Profile	
0	30
20	25
40	20
80	15
80.739	14.261
144.5	14.261
145	13.761
155	13.761
155.5	14.261
219.261	14.261
220	15
240	20
260	25
290	30

Berg	
149500	
Profile	
0	30
30	25
80	20
110	15
110.96	14.04
174.5	14.04
175	13.54
185	13.54
185.5	14.04
249.04	14.04
250	15
370	20
410	25

Berg	
150000	
Profile	
0	30
30	25
50	20
90	15
91.181	13.819
154.5	13.819
155	13.319
165	13.319
165.5	13.819
228.819	13.819
230	15
250	20
270	25
280	30

Berg	
150500	
Profile	
0	30
30	25
60	20
80	15
81.403	13.597
109.5	13.597
110	13.097
150	13.097
150.5	13.597
178.597	13.597
180	15
250	20

Berg	
151000	
Profile	
0	30
10	25
30	20
50	15
51.624	13.376
129.5	13.376
130	12.876
160	12.876
160.5	13.376
238.376	13.376
240	15
290	20

Berg	
151500	
Profile	
0	25
30	20
50	15
51.845	13.155
144.5	13.155
145	12.655
155	12.655
155.5	13.155
243.155	13.155
250	20
310	30
390	40

Berg	
152000	
Profile	
0	25
80	20
120	15
122.066	12.934
159.5	12.934
160	12.434
190	12.434
190.5	12.934
227.934	12.934
230	15
400	20
550	30

Berg	
152500	
Profile	
0	45
120	40
200	30
320	20
327.288	12.712
444.5	12.712
445	12.212
495	12.212
495.5	12.712
612.712	12.712
620	20
700	30

Berg	
153000	
Profile	
0	40
70	30
150	20
157.509	12.491
249.5	12.491
250	11.991
270	11.991
270.5	12.491
362.491	12.491
370	20
470	30

Berg	
153500	
Profile	
0	45
40	40
70	35
90	30
130	25
160	20
170	15
172.73	12.27
214.5	12.27
215	11.77
305	11.77
305.5	12.27
347.27	12.27
350	15
420	20
690	25

Berg	
154000	
Profile	
0	30
30	25
50	20
70	15
72.951	12.049
109.5	12.049
110	11.549
150	11.549
150.5	12.049
187.049	12.049
190	15
380	20
670	25

Berg	
154500	
Profile	
0	25
30	20
40	15
43.173	11.827
54.5	11.827
55	11.327
105	11.327
105.5	11.827
116.827	11.827
120	15
270	20

Berg	
155000	
Profile	
0	25
100	20
170	15
173.394	11.606
194.5	11.606
195	11.106
235	11.106
235.5	11.606
256.606	11.606
260	15
270	20
290	25
300	30

Berg	
155500	
Profile	
0	30
40	25
70	20
100	15
103.615	11.385
144.5	11.385
145	10.885
165	10.885
165.5	11.385
206.385	11.385
210	15
290	20
420	25
500	30

Berg	
156000	
Profile	
0	30
60	25
100	25
140	25
170	20
190	15
193.836	11.164
264.5	11.164
265	10.664
295	10.664
295.5	11.164
366.164	11.164
370	15
440	20
490	25
560	30
650	35

Berg	
156500	
Profile	
0	30
160	25
370	20
400	15
404.058	10.942
459.5	10.942
460	10.442
500	10.442
500.5	10.942
555.942	10.942
560	15
580	20
590	25
600	30
680	35

Berg	
157000	
Profile	
0	30
40	25
90	20
150	15
310	15
314.279	10.721
339.5	10.721
340	10.221
390	10.221
390.5	10.721
415.721	10.721
420	15
440	20
460	25
530	30
740	35

Berg	
157500	
Profile	
0	35
30	30
50	25
60	20
70	15
74.5	10.5
124.5	10.5
125	10
165	10
165.5	10.5
215.5	10.5
220	15
290	20
330	25
380	30
440	35

Berg	
158000	
Profile	
0	35
430	30
510	25
610	20
640	15
780	10
779.761	10.239
784.5	10.239
785	9.739
815	9.739
815.5	10.239
820.239	10.239
820	10
850	15
860	20
880	25
890	30
895	35
900	40
910	45
930	50

Berg	
158500	
Profile	
0	35
60	30
100	25
130	20
150	15
190	10
190.021	9.979
194.5	9.979
195	9.479
215	9.479
215.5	9.979
219.979	9.979
220	10
360	15
390	20
500	25
560	30
610	35

Berg	
159000	
Profile	
0	35
130	30
170	25
200	20
260	15
310	10
310.282	9.718
324.5	9.718
325	9.218
355	9.218
355.5	9.718
369.718	9.718
370	10
440	15
480	20
510	25
540	30

Berg	
159300	
Profile	
0	35
190	30
250	25
320	20
370	15
460	10
460.543	9.457
474.5	9.457
475	8.957
485	8.957
485.5	9.457
499.457	9.457
500	10
520	15
530	20
580	25

Berg	
160000	
Profile	
0	35
100	30
180	25
220	20
260	15
270	10
270.803	9.197
279.5	9.197
280	8.697
290	8.697
290.5	9.197
299.197	9.197
300	10
420	15
450	20
600	25

Berg	
160500	
Profile	
0	35
90	30
140	25
220	20
260	15
280	10
281.064	8.936
284.5	8.936
285	8.436
295	8.436
295.5	8.936
298.936	8.936
300	10
370	15
380	20
400	25
410	30
490	35
560	40

Berg	
161000	
Profile	
0	30
70	25
90	20
110	15
190	10
191.325	8.675
199.5	8.675
200	8.175
210	8.175
210.5	8.675
218.675	8.675
220	10
290	15
380	20
410	25
440	30
480	35
510	40
530	45
600	50

Berg	
161500	
Profile	
0	30
130	25
190	20
230	15
250	10
251.586	8.414
254.5	8.414
255	7.914
275	7.914
275.5	8.414
278.414	8.414
280	10
400	15
470	20
500	25
530	30
560	35
590	40
630	45
690	50

Berg	
162000	
Profile	
0	25
100	20
180	15
230	10
231.846	8.154
234.5	8.154
235	7.654
255	7.654
255.5	8.154
258.154	8.154
260	10
340	15
360	20
370	25
390	30
420	35
440	40

Berg	
162500	
Profile	
0	25
100	20
190	15
250	10
252.107	7.893
252	7.893
252.5	7.393
292.5	7.393
293	7.893
292.893	7.893
295	10
370	15
380	20
410	25
440	30
480	35

Berg	
163000	
Profile	
0	20
170	15
190	10
192.368	7.632
194.5	7.632
195	7.132
215	7.132
215.5	7.632
217.632	7.632
220	10
360	15
430	20
480	25
550	30
620	35

Berg	
163500	
Profile	
0	30
50	25
80	20
120	15
170	10
172.628	7.372
189.5	7.372
190	6.872
210	6.872
210.5	7.372
227.372	7.372
230	10
360	15
460	20
590	25
660	30
740	35

Berg	
164000	
Profile	
0	25
150	20
220	15
290	10
292.889	7.111
299.5	7.111
300	6.611
330	6.611
330.5	7.111
337.111	7.111
340	10
480	15
550	20
600	25
650	30
710	35

Berg	
164500	
Profile	
0	15
100	10
103.15	6.85
109.5	6.85
110	6.35
140	6.35
140.5	6.85
146.85	6.85
150	10
210	15
240	20
270	25
330	30

Berg	
165000	
Profile	
0	30
130	25
220	20
250	15
270	10
273.41	6.59
359.5	6.59
360	6.09
380	6.09
380.5	6.59
466.59	6.59
470	10
550	15
580	20
630	25
680	30

Berg	
165500	
Profile	
0	25
100	20
200	15
380	10
383.671	6.329
389.5	6.329
390	5.829
410	5.829
410.5	6.329
416.329	6.329
420	10
480	15
510	20
550	25
590	30

Berg	
166100	
Profile	
0	20
40	15
250	10
253.984	6.016
264.5	6.016
265	5.516
275	5.516
275.5	6.016
286.016	6.016
290	10
320	15
350	20
370	25
380	30
400	35
520	40

Berg	
166400	
Profile	
0	20
170	15
210	10
214.14	5.86
244.5	5.86
245	5.36
255	5.36
255.5	5.86
285.86	5.86
290	10
320	15
350	20
370	25
380	30
400	35
520	40

Berg	
167000	
Profile	
0	20
160	15
280	10
284.453	5.547
294.5	5.547
295	5.047
325	5.047
325.5	5.547
335.547	5.547
340	10
470	15
510	20

Berg	
167500	
Profile	
0	20
160	15
280	10
284.453	5.547
294.5	5.547
295	5.047
325	5.047
325.5	5.547
335.547	5.547
340	10
470	15
510	20

Berg	
168000	
Profile	
0	20
130	15
320	10
330	5
329.894	5.106
334.5	5.106
335	4.606
375	4.606
375.5	5.106
380.106	5.106
380	5
520	10

Berg	
168500	
Profile	
0	20
130	15
320	10
330	5
329.894	5.106
334.5	5.106
335	4.606
375	4.606
375.5	5.106
380.106	5.106
380	5
520	10

Berg	
169000	
Profile	
0	15
320	10
340	5
340.034	4.966
344.5	4.966
345	4.466
375	4.466
375.5	4.966
379.966	4.966
380	5
500	10

Berg	
169500	
Profile	
0	15
250	10
290	5
290.174	4.826
294.5	4.826
295	4.326
325	4.326
325.5	4.826
329.826	4.826
330	5
390	10
400	15
410	20
415	25
420	30
430	35
440	40

Berg	
170000	
Profile	
0	15
120	10
140	5
140.314	4.686
144.5	4.686
145	4.186
165	4.186
165.5	4.686
169.686	4.686
170	5
220	10
280	15
310	20
330	25
340	30
380	35

Berg	
170500	
Profile	
0	15
400	10
410	5
410.454	4.546
414.5	4.546
415	4.046
445	4.046
445.5	4.546
449.546	4.546
450	5
480	10
600	15
670	20
710	25

Berg	
171000	
Profile	
0	25
80	20
190	15
240	10
250	5
250.593	4.407
259.5	4.407
260	3.907
290	3.907
290.5	4.407
299.407	4.407
300	5
330	10
440	15
480	20

Berg	
171500	
Profile	
0	25
80	20
270	15
310	10
340	5
340.733	4.267
359.5	4.267
360	3.767
370	3.767
370.5	4.267
389.267	4.267
390	5
430	10
460	15
500	20
540	25
580	30

Berg	
172000	
Profile	
0	30
160	25
190	20
210	15
230	10
240	5
240.873	4.127
244.5	4.127
245	3.627
265	3.627
265.5	4.127
269.127	4.127
270	5
390	10
440	15
500	20
560	25
600	30

Berg	
172500	
Profile	
0	25
50	20
80	15
130	10
140	5
141.013	3.987
149.5	3.987
150	3.487
170	3.487
170.5	3.987
178.987	3.987
180	5
250	10
350	15
400	20
480	25
540	30

Berg	
172900	
Profile	
0	25
60	20
130	15
200	10
370	5
371.125	3.875
384.5	3.875
385	3.375
405	3.375
405.5	3.875
418.875	3.875
420	5
430	10
490	15
510	20
610	25
690	30
720	35

Berg	
173400	
Profile	
0	20
120	15
170	10
270	5
271.265	3.735
274.5	3.735
275	3.235
295	3.235
295.5	3.735
298.735	3.735
300	5
350	10
390	15
470	20

Berg	
173900	
Profile	
0	20
30	15
140	10
170	5
171.404	3.596
179.5	3.596
180	3.096
200	3.096
200.5	3.596
208.596	3.596
210	5
340	10
390	15
460	20

Berg	
174400	
Profile	
0	15
70	10
100	10
130	10
160	5
161.544	3.456
164.5	3.456
165	2.956
185	2.956
185.5	3.456
188.456	3.456
190	5
470	10
550	15
610	20

Berg	
174900	
Profile	
0	20
50	15
120	10
250	5
251.684	3.316
259.5	3.316
260	2.816
270	2.816
270.5	3.316
278.316	3.316
280	5
570	10
600	15
640	20

Berg	
175400	
Profile	
0	20
30	15
80	10
200	5
201.824	3.176
209.5	3.176
210	2.676
240	2.676
240.5	3.176
248.176	3.176
250	5
440	10
490	15
620	20

Berg	
175900	
Profile	
0	20
50	15
80	10
140	5
141.964	3.036
154.5	3.036
155	2.536
185	2.536
185.5	3.036
198.036	3.036
200	5
420	10
480	15
540	20

Berg	
176400	
Profile	
0	20
60	15
130	10
280	5
282.103	2.897
299.5	2.897
300	2.397
320	2.397
320.5	2.897
337.897	2.897
340	5

Berg	
176900	
Profile	
0	20
60	15
130	10
290	5
292.243	2.757
304.5	2.757
305	2.257
325	2.257
325.5	2.757
337.757	2.757
340	5

Berg	
177400	
Profile	
0	20
70	15
210	10
400	5
402.383	2.617
409.5	2.617
410	2.117
430	2.117
430.5	2.617
437.617	2.617
440	5

540	10
Berg	
177900	
Profile	
0	20
50	15
200	10
290	5
292.523	2.477
324.5	2.477
325	1.977
335	1.977
335.5	2.477
367.477	2.477
370	5
460	10
490	15
510	20
Berg	
179400	
Profile	
0	20
110	15
280	10
420	5
422.942	2.058
429.5	2.058
430	1.558
450	1.558
450.5	2.058
457.058	2.058
460	5
470	10
490	15
500	20
Berg	
180900	
Profile	
0	15
230	10
280	5
283.362	1.638
329.5	1.638
330	1.138
370	1.138
370.5	1.638
416.638	1.638
420	5
570	10
630	15

480	10
Berg	
178400	
Profile	
0	20
50	15
100	10
170	5
172.663	2.337
184.5	2.337
185	1.837
215	1.837
215.5	2.337
227.337	2.337
230	5
400	10
450	15
500	20
Berg	
179900	
Profile	
0	15
50	10
170	5
173.082	1.918
184.5	1.918
185	1.418
215	1.418
215.5	1.918
226.918	1.918
230	5
400	10
490	15
570	20
Berg	
181400	
Profile	
0	15
260	10
390	5
393.502	1.498
409.5	1.498
410	0.998
460	0.998
460.5	1.498
476.498	1.498
480	5
610	10
670	15

500	10
Berg	
178900	
Profile	
0	20
80	15
160	10
230	5
232.803	2.197
237	2.197
237.5	1.697
272.5	1.697
273	2.197
277.197	2.197
280	5
460	10
500	15
630	20
Berg	
180400	
Profile	
0	20
40	15
80	10
200	5
203.222	1.778
229.5	1.778
230	1.278
250	1.278
250.5	1.778
276.778	1.778
280	5
480	10
710	15
820	20
Berg	
181900	
Profile	
0	20
130	15
360	10
430	5
433.641	1.359
454.5	1.359
455	0.859
505	0.859
505.5	1.359
526.359	1.359
530	5
620	10

Berg	
182400	
Profile	
0	20
110	15
180	10
190	5
193.781	1.219
204.5	1.219
205	0.719
255	0.719
255.5	1.219
266.219	1.219
270	5
400	10
540	10
570	10
700	15
Berg	
183900	
Profile	
0	20
100	15
240	10
280	5
284.201	0.799
289.5	0.799
290	0.299
320	0.299
320.5	0.799
325.799	0.799
330	5
520	10
530	15
Berg	
185400	
Profile	
0	20
170	15
290	10
640	5
644.62	0.38
644.5	0.38
645	-0.12
675	-0.12
675.5	0.38
675.38	0.38
680	5
800	10

720	20
Berg	
182900	
Profile	
0	20
80	15
140	10
260	5
263.921	1.079
274.5	1.079
275	0.579
365	0.579
365.5	1.079
376.079	1.079
380	5
400	10
430	15
450	20
Berg	
184400	
Profile	
0	20
100	15
270	10
480	5
484.341	0.659
489.5	0.659
490	0.159
520	0.159
520.5	0.659
525.659	0.659
530	5
590	10
610	15
Berg	
185900	
Profile	
0	20
30	15
40	10
120	5
124.76	0.24
144.5	0.24
145	-0.26
205	-0.26
205.5	0.24
225.24	0.24
230	5
630	10

920	15
Berg	
183400	
Profile	
0	20
40	15
70	10
150	5
154.061	0.939
169.5	0.939
170	0.439
180	0.439
180.5	0.939
195.939	0.939
200	5
390	10
420	15
480	20
Berg	
184900	
Profile	
0	20
40	15
190	10
410	5
414.48	0.52
419.5	0.52
420	0.02
430	0.02
430.5	0.52
435.52	0.52
440	5
590	10
610	15
Berg	
186400	
Profile	
0	20
70	15
90	10
120	5
124.9	0.1
139.5	0.1
140	-0.4
150	-0.4
150.5	0.1
165.1	0.1
170	5
490	5

APPENDIX B CROSS SECTION COORDINATES

X-Coordinate (m)	Y- Coordinate (m)	Chainage (m)
3753190	-5210	2200
3752900	-5150	2500
3752620	-5050	2800
3752340	-4950	3100
3752070	-4840	3400
3751780	-4765	3700
3751520	-4655	4000
3751250	-4545	4300
3750975	-4425	4600
3750805	-4215	4900
3750555	-4065	5200
3750395	-3955	5400
3750185	-3735	5700
3750035	-3505	6000
3749855	-3245	6300
3749735	-2995	6600
3749715	-2715	6900
3749660	-1960	7670
3749565	-1460	8190
3749420	-1000	8680
3749140	-650	9240
3748905	-210	9710
3749425	-80	10200
3747920	-5	10720
3747440	200	11280
3747040	440	11800
3746530	660	12480
3746120	820	12950
3745510	1600	13500
3745240	2000	14000
3744860	2300	14500
3744530	2640	15000
3744090	2785	15500
3743895	3190	16000
3745430	3360	16500
3743190	3690	17000
3742820	4030	17500
3742330	4130	18000
3741850	4070	18500
3740270	4045	19000
3741090	3560	19500
3740814	3308	20000
3740240	2892	20700
3739950	2800	21000
3739460	2850	21500

3739110	2535	22000
3738660	2380	22500
3738160	2330	23000
3737725	2130	23500
3737300	2280	24000
3736810	2400	24500
3736380	2360	25000
3736100	2750	25500
3735350	2880	26000
3735175	2970	26500
3734680	2850	27000
3734240	2700	27500
3733720	2550	28000
3733300	2330	28500
3732830	2250	29000
3732350	2350	29500
3731875	2540	30000
3731340	2640	30500
3730860	2300	31000
3730450	2030	31500
3730000	1800	32000
3729560	1970	32500
3729115	2120	33000
3728660	2350	33500
3728190	2160	34000
3727750	2220	34500
3727350	1970	35000
3727090	1590	35500
3726740	1455	36000
3726470	1760	36500
3726430	2260	37000
3726360	2750	37500
3725950	3020	38000
3725470	3170	38500
3725000	3050	39000
3724450	2900	39500
3724060	2810	40000
3723730	2400	40500
3723620	1940	41000
3723770	1500	41500
3723320	1470	42000
3722970	1770	42500
3722610	2080	43000
3722100	2150	43500
3721620	2350	44000
3721180	2520	44500
3720680	2540	45000
3720180	2440	45500
3719710	2490	46000
3719230	2390	46500
3718730	2500	47000
3718390	2770	47500

3717880	2840	48000
3717950	3780	48500
3717886	4431	49650
3717670	4900	50000
3717080	5100	50500
3716650	4870	51000
3716160	4650	51500
3715750	4480	52000
3715400	4480	52500
3714930	4770	53000
3714758	5170	53500
3714640	5800	54000
3714040	5680	54500
3713460	5410	55000
3713220	5600	55500
3712760	5960	56000
3712180	6000	56500
3711690	6110	57000
3711200	6150	57500
3710750	6350	58000
3710296	6135	58500
3710150	5785	59000
3709800	5600	59500
3709300	5780	60000
3708820	5870	60500
3708250	5780	61000
3707930	5600	61500
3707560	5780	62000
3707900	6080	62500
3706570	5930	63000
3706130	5840	63500
3705630	5780	64000
3705130	5820	64500
3704620	5700	65000
3704130	5530	65500
3703950	5060	66000
3703860	4560	66500
3703620	4240	67000
3703310	4580	67500
3702860	4720	68000
3702440	4520	68500
3702650	4070	69000
3701630	3850	69500
3701170	3830	70000
3700700	4030	70500
3700150	4100	71000
3699890	3630	71500
3700100	3200	72000
3699780	2820	72500
3699300	3040	73000
3698850	2780	73500
3698683	2634	73750

3698420	2520	74000
3698000	2310	74500
3697620	1980	75000
3697450	1620	75500
3697000	2000	76000
3696640	1720	76500
3696510	1240	77000
3696370	770	77500
3695970	750	78000
3695530	1000	78500
3695100	750	79000
3694780	740	79500
3694680	1210	80000
3694250	1300	80500
3693860	970	81000
3693400	830	81500
3692980	550	82000
3692800	970	82500
3692420	1270	83000
3692030	920	83500
3691640	800	84000
3691180	1020	84500
3690820	1380	85000
3690520	1790	85500
3690060	1760	86000
3689750	1370	86500
3689380	1020	87000
3688990	1080	87500
3688910	1560	88000
3688530	1860	88500
3687960	1950	89000
3687490	1830	89500
3687150	1460	90000
3687200	970	90500
3687220	480	91000
3686800	310	91500
3686380	510	92000
3686260	1010	92500
3685800	790	93000
3685500	1170	93500
3685050	1650	94000
3684550	1670	94500
3684310	2140	95000
3683870	2330	95500
3683380	2140	96000
3682820	2350	96600
3682680	2850	97100
3682280	3130	97600
3681750	3380	98200
3681710	3890	98700
3681730	4410	99200
3681260	4270	99700

3680790	4210	100200
3680400	4510	100700
3680330	4950	101200
3679890	4780	101700
3679470	4540	102200
3679000	4730	102700
3678570	4730	103200
3678250	4360	103700
3677920	3970	104200
3677420	4020	104700
3676940	3960	105200
3676470	4120	105700
3676170	4550	106200
3675720	4840	106700
3675350	5180	107200
3674930	4980	107700
3674450	5120	108200
3674470	5640	108700
3674620	6140	109200
3674270	6260	109700
3673980	5810	110200
3673520	6110	110800
3673320	6550	111300
3673070	6980	111800
3672760	7420	112300
3672220	7400	112800
3671730	7560	113300
3671030	7750	113800
3670590	8030	114300
3670300	8450	114800
3669680	8330	115300
3669630	8930	115800
3669710	9430	116300
3669780	9920	116800
3669760	10420	117300
3669510	11000	117800
3668970	11040	118300
3668550	11340	118800
3668500	11820	119300
3668560	12380	119800
3668270	12830	120300
3667670	12810	120800
3667250	13110	121300
3666730	12920	121800
3666620	13440	122300
3666330	13840	122800
3665840	13790	123300
3665270	13730	123800
3665300	14280	124400
3664990	14680	124900
3664520	14850	125400
3664000	14920	125900

3663530	14850	126400
3663010	14940	126900
3662860	15460	127400
3662380	15510	127900
3661880	15410	128400
3661460	15790	128900
3661000	16050	129400
3660500	15980	129900
3660000	15870	130400
3659930	16290	130900
3659890	16810	131400
3659380	16670	131900
3658880	16760	132400
3658390	16920	132900
3657950	17220	133400
3657950	17720	133900
3657740	18140	134400
3657300	18000	134900
3656850	17760	135400
3656320	17780	135900
3655950	17350	136400
3655480	17530	136900
3655430	18050	137400
3655090	18400	137900
3654770	18790	138400
3655180	19140	138900
3655300	19610	139400
3654780	19830	140000
3654280	19960	140500
3653790	20120	141000
3653290	20230	141500
3652790	20410	142000
3652270	20450	142500
3651850	20720	143000
3651500	21080	143500
3651110	21410	144000
3650590	21490	144500
3650350	21940	145000
3650220	22460	145500
3649870	22820	146000
3649390	22950	146500
3649100	23280	147000
3649040	23750	147500
3648660	24080	148000
3648350	24470	148500
3647950	24780	149000
3647460	24920	149500
3647080	25260	150000
3646760	25640	150500
3646620	26050	151000
3646450	26550	151500
3646580	27040	152000

3646260	27460	152500
3646020	27910	153000
3645950	28410	153500
3645930	28920	154000
3645570	29110	154500
3645440	29550	155000
3645720	29990	155500
3645280	30080	156000
3644810	30100	156500
3644400	30370	157000
3643930	30530	157500
3643260	30340	158000
3643340	30990	158500
3643140	31460	159000
3643090	31780	159300
3642760	32370	160000
3642560	32780	160500
3642510	33290	161000
3642390	33800	161500
3642270	34270	162000
3642520	34700	162500
3642810	35120	163000
3642810	35690	163500
3642470	36070	164000
3642550	36540	164500
3642950	37020	165000
3642420	37270	165500
3641860	37500	166100
3641610	37650	166400
3641120	37900	167000
3640800	38270	167500
3640810	38770	168000
3640930	39270	168500
3640990	39770	169000
3641200	40220	169500
3641680	40260	170000
3642180	40310	170500
3642150	40760	171000
3642220	41190	171500
3642690	41450	172000
3642780	41950	172500
3642670	42340	172900
3643110	42630	173400
3643550	42480	173900
3643900	42180	174400
3644400	42180	174900
3644850	42390	175400
3645250	42670	175900
3645470	43120	176400
3645400	43610	176900
3645280	44100	177400
3645660	44480	177900

3645760	44960	178400
3645670	45430	178900
3645700	45890	179400
3646110	46170	179900
3646250	46650	180400
3646000	47080	180900
3646180	47540	181400
3646650	47710	181900
3646870	48130	182400
3646670	48600	182900
3646510	49060	183400
3646140	49380	183900
3645900	49830	184400
3646210	50230	184900
3646510	50630	185400
3646980	51210	185900
3647650	51330	186400
3647150	51260	186900
3646660	51260	187400
3646660	51750	187900
3646550	52280	188400

APPENDIX C WEIR CALIBRATION

C.1. Surveyed Cross Sections

Upstream Section		Weir		Downstream Section	
Distance From Left Bank (m)	Height (m)	Distance From Left Bank (m)	Height (m)	Distance From Left Bank (m)	Height (m)
0.000	102.868	0.000	102.345	0.000	102.537
0.896	102.436	4.189	101.933	15.452	100.942
1.975	101.297	8.867	101.425	17.212	100.51
4.171	101.405	13.339	100.955	20.318	100.197
5.185	101.317	16.934	100.284	23.057	99.961
6.033	100.912	18.942	100.468	26.031	99.769
7.534	100.756	23.872	100.422	28.011	99.56
8.909	100.75	30.702	100.344	32.031	99.438
11.083	100.827	34.983	100.308	35.161	99.331
12.850	100.703	35.035	100.001	37.486	99.355
14.497	100.738	38.133	100	39.675	99.459
15.994	100.457	40.947	99.978	41.811	99.473
17.270	99.931	41.101	100.312	44.179	99.593
20.039	99.707	47.790	100.302	45.640	99.762
22.241	99.674	51.901	100.476	47.998	99.375
24.514	99.698	53.610	100.808	49.734	99.458
26.768	99.608	55.915	100.559	50.982	99.355
28.211	99.507	57.847	100.609	52.254	99.56
29.802	99.906	59.209	100.828	53.292	99.943
31.372	99.569	62.064	100.977	54.711	100.052
33.155	99.574	63.911	101.102	56.437	99.991
35.057	99.769	65.726	101.331	57.885	100.189
36.340	99.992	68.035	101.694	59.371	100.544
37.616	99.968	69.676	102.078	60.724	100.971
39.178	99.91	72.061	102.587	65.922	101.625
40.598	100.049			69.096	102.057
41.651	100.492			72.213	102.558
42.464	100.398				
43.779	100.548				
45.399	100.386				
46.993	100.558				
49.120	100.608				
51.922	100.815				
54.118	100.886				
56.016	101.234				
57.798	101.611				
59.228	101.843				

60.672	101.732
61.667	101.608
62.633	101.659
63.662	102.034
66.149	102.23
68.879	102.566
71.048	102.716
72.810	103.157

C.2 Discharge Table

	0	0.01	0.02	0.03	0.04	0.05	0.06	0.07	0.08	0.09
0	0	0	0.02	0.04	0.07	0.1	0.14	0.18	0.23	0.28
0.1	0.33	0.38	0.44	0.5	0.5	0.56	0.62	0.68	0.74	0.8
0.2	0.86	0.93	0.99	1.06	1.13	1.2	1.27	1.34	1.42	1.49
0.3	1.57	1.64	1.72	2.05	2.14	2.25	2.36	2.49	2.62	2.78
0.4	2.94	3.12	3.32	3.53	3.77	4.02	4.29	4.58	4.9	5.23
0.5	5.59	5.96	6.35	6.76	7.18	7.61	8.06	8.52	8.99	9.48
0.6	9.98	10.5	11.04	11.58	12.43	12.98	13.54	14.12	14.71	15.32
0.7	15.95	16.61	17.28	17.96	18.66	19.37	20.09	20.82	21.57	22.33
0.8	23.1	23.88	24.68	25.5	27.34	28.1	28.87	29.65	30.42	31.21
0.9	31.99	32.78	33.58	34.37	35.18	35.98	36.79	37.61	38.42	39.25
1	40.07	40.91	41.74	42.59	43.44	44.29	45.15	46.01	46.87	47.74
1.1	48.61	49.56	50.53	51.5	52.48	53.47	54.46	55.46	56.47	57.49
1.2	58.51	59.55	60.59	61.64	62.69	63.76	64.83	65.91	67	68.09
1.3	69.19	70.32	71.44	72.57	73.71	74.85	76.01	76.97	77.77	78.57
1.4	79.35	80.13	80.88	81.61	82.34	83.05	83.75	84.44	85.11	85.76
1.5	86.39	87.01	87.6	88.16	88.7	89.21	89.7	90.17	90.61	91.02
1.6	91.41	91.76	92.08	92.36	92.6	92.8	92.95	93.04	93.1	

APPENDIX D SEDIMENT SAMPLES

D.1 Portal (G1H004 – A02)

Date	Time	Q[m ³ /s]	Qs[kg/s]	Concentration [mg/l]
2003/07/12	14:20	1.858	0.0141	7.6
2003/07/15	13:40	0.703	0.0036	5.1
2003/07/18	09:28	12.602	0.1235	9.8
2003/07/22	09:45	1.378	0.0303	22
2003/07/22	15:30	1.245	0.0063	5.1
2003/07/23	08:50	1.111	0.1240	111.6
2003/07/23	14:56	0.995	0.0056	5.6
2003/07/24	09:12	0.911	0.0135	14.8
2003/07/24	14:38	0.853	0.0879	103
2003/07/25	09:50	7.795	0.0553	7.1
2003/07/28	13:45	7.24	0.0471	6.5
2003/07/29	09:15	5.469	0.0405	7.4
2003/07/30	15:41	5.335	0.0763	14.3
2003/07/31	10:30	6.29	0.0862	13.7
2003/07/31	17:00	5.799	0.0464	8
2003/08/01	09:15	5.335	0.0758	14.2
2003/08/04	09:30	1.773	0.0140	7.9
2003/08/05	09:50	1.361	0.0084	6.2
2003/08/06	07:30	1.089	0.0089	8.2
2003/08/06	15:30	1.013	0.0064	6.3
2003/08/07	08:45	0.911	0.0077	8.5
2003/08/07	14:45	0.824	0.0049	5.9
2003/08/08	09:00	1.361	0.0103	7.6
2003/08/08	14:30	23.59	0.2854	12.1
2003/08/11	08:50	6.859	0.0597	8.7
2003/08/11	15:25	6.384	0.0370	5.8
2003/08/12	08:40	5.903	0.0738	12.5
2003/08/12	15:00	5.732	0.0665	11.6
2003/08/13	08:15	5.469	0.0394	7.2
2003/08/18	08:50	1.803	0.0088	4.9
2003/08/18	16:25	105.008	10.7213	102.1
2003/08/25	10:15	65.929	1.8526	28.1
2003/09/01	14:50	78.612	4.7324	60.2
2003/09/02	14:45	9.174	2.6054	284
2003/09/03	09:18	5.851	1.6868	288.3

D.2 Driefontein Weir (G1H004)

Date	Time	Q[m ³ /s]	Qs[kg/s]	Concentration [mg/l]
2003/07/08	10:40	0.517	0.0114	22.0
2003/07/08	15:40	0.517	0.0088	17.0
2003/07/09	09:35	0.507	0.0061	12.0
2003/07/09	15:00	0.507	0.0243	48.0
2003/07/10	09:35	6.380	0.3190	50.0
2003/07/10	15:25	4.308	0.0388	9.0
2003/07/11	09:15	3.889	0.1711	44.0
2003/07/12	10:50	2.037	0.0163	8.0
2003/07/12	14:40	1.848	0.0942	51.0
2003/07/13	15:45	1.168	0.0164	14.0
2003/07/14	10:05	0.931	0.0130	14.0
2003/07/15	09:00	0.747	0.0052	7.0
2003/07/15	13:55	0.705	0.0169	24.0
2003/07/17	09:06	0.579	0.0047	8.2
2003/07/17	15:28	0.550	0.0072	13.0
2003/07/18	09:43	14.137	0.2121	15.0
2003/07/18	14:15	8.043	0.0651	8.1
2003/07/21	09:20	2.037	0.0285	14.0
2003/07/21	14:35	1.773	0.0922	52.0
2003/07/22	10:31	1.374	0.0673	49.0
2003/07/22	15:10	1.250	0.0588	47.0
2003/07/23	09:05	1.110	0.0144	13.0
2003/07/23	15:15	0.992	0.0436	44.0
2003/07/24	09:30	0.911	0.0046	5.0
2003/07/25	10:15	6.445	0.0773	12.0
2003/07/25	15:05	3.320	0.0398	12.0
2003/07/28	14:08	5.605	0.1121	20.0
2003/07/29	10:00	2.393	0.0144	6.0
2003/07/30	10:45	1.438	0.0086	6.0
2003/07/30	16:05	3.842	0.1806	47.0
2003/07/31	17:00	3.066	0.0583	19.0
2003/08/01	08:30	2.219	0.0533	24.0
2003/08/01	15:58	10.199	0.1938	19.0
2003/08/04	10:00	1.758	0.0105	6.0
2003/08/04	17:10	1.700	0.0272	16.0
2003/08/05	10:01	1.361	0.0299	22.0
2003/08/05	16:08	1.274	0.0153	12.0
2003/08/06	08:30	1.089	0.0131	12.0
2003/08/06	14:30	1.024	0.0164	16.0
2003/08/07	09:30	0.911	0.0128	14.0
2003/08/08	09:30	1.594	0.0163	10.2
2003/08/18	09:30	1.973	0.0138	7.0
2003/08/18	15:30	122.191	28.5927	234.0
2003/08/19	09:15	24.113	0.1206	5.0
2003/08/25	09:50	71.092	2.8437	40.0
2003/08/25	16:20	59.436	0.3566	6.0
2004/07/01	10:45	1.622	0.351	216.3

2004/07/02	09:30	1.448	0.004	2.6
2004/07/05	10:15	3.631	0.307	84.5
2004/07/05	15:50	3.335	0.424	127.0
2004/07/06	09:10	2.786	0.255	91.5
2004/07/06	16:10	2.55	0.776	304.5
2004/07/07	08:10	2.258	0.617	273.4
2004/07/07	15:20	2.08	0.536	257.6
2004/07/08	09:40	1.91	0.024	12.7
2004/07/08	16:10	1.792	0.533	297.6
2004/07/09	09:10	1.636	0.082	50.0
2004/07/09	15:45	1.594	0.012	7.7
2004/07/12	10:10	1.335	0.006	4.8
2004/07/12	15:40	1.205	0.004	3.2
2004/07/13	09:45	1.112	0.010	9.0
2004/07/23	08:55	3.653	0.546	149.6
2004/07/23	15:20	71.665	3.074	42.9
2004/07/26	16:40	4.214	0.009	2.1
2004/07/27	10:07	3.481	1.164	334.4
2004/07/27	15:49	3.274	0.010	3.0
2004/07/28	16:15	2.621	0.046	17.7
2004/07/29	10:15	2.376	0.011	4.5
2004/07/29	17:00	2.258	0.028	12.2
2004/07/30	09:00	39.979	0.176	4.4
2004/07/30	16:15	17.094	0.026	1.5
2004/08/02	09:15	5.706	0.036	6.3
2004/08/02	17:30	4.727	1.132	239.4
2004/08/03	17:20	3.545	0.009	2.4
2004/08/04	08:30	3.153	0.030	9.5
2004/08/04	17:10	2.976	0.457	153.4
2004/08/05	10:45	62.933	3.241	51.5
2004/08/05	16:40	70.714	7.361	104.1
2004/08/06	14:55	10.802	1.441	133.4
2004/08/12	09:00	5.27	0.019	3.7

D.3 Franschhoek River (G1H003)

Date	Time	Q[m ³ /s]	Q _s [kg/s]	Concentration [mg/l]
2003/07/08	10:35	0.187	0.0016	8.7
2003/07/08	15:50	0.178	0.0038	21.6
2003/07/10	09:50	0.275	0.0084	30.4
2003/07/10	15:40	0.222	0.0019	8.5
2003/07/11	09:35	0.299	0.0025	8.3
2003/07/11	15:15	0.196	0.0013	6.6
2003/07/12	15:10	0.163	0.0009	5.6
2003/07/13	10:23	0.159	0.0034	21.3
2003/07/14	10:21	0.164	0.0035	21.5
2003/07/16	15:00	0.173	0.0059	34.3

2003/07/18	09:56	0.648	0.4120	635.8
2003/07/18	14:37	0.361	0.0665	184.3
2003/07/21	09:40	0.186	0.0010	5.4
2003/07/21	14:17	0.189	0.0015	8.2
2003/07/22	10:45	0.185	0.0016	8.8
2003/07/23	09:20	0.178	0.0012	6.9
2003/07/23	15:27	0.183	0.0039	21.3
2003/07/24	09:48	0.18	0.0017	9.3
2003/07/24	15:00	0.183	0.0009	5
2003/07/25	10:30	0.285	0.0176	61.7
2003/07/25	15:15	0.258	0.0099	38.5
2003/07/28	14:15	0.507	0.0214	42.2
2003/07/29	10:30	0.257	0.0021	8
2003/07/30	10:30	0.22	0.0064	28.9
2003/07/30	16:30	0.219	0.0015	6.8
2003/07/31	11:15	0.287	0.0072	25
2003/08/01	16:50	0.626	0.1034	165.1
2003/08/04	10:15	0.265	0.0025	9.3
2003/08/05	16:45	0.232	0.0018	7.6
2003/08/06	17:19	0.236	0.0030	12.8
2003/08/07	10:00	0.236	0.0029	12.1
2003/08/08	09:50	0.251	0.0024	9.6
2003/08/08	15:48	2.9	0.1299	44.8
2003/08/11	08:07	1.13	0.0331	29.3
2003/08/11	15:50	0.947	0.0300	31.7
2003/08/12	10:30	0.813	0.0307	37.8
2003/08/12	15:40	0.775	0.0216	27.9
2003/08/13	08:40	0.71	0.0160	22.5
2003/08/13	16:56	0.633	0.0093	14.7
2003/08/14	11:50	0.601	0.0094	15.6
2003/08/14	16:50	0.582	0.0123	21.1
2003/08/15	10:15	0.567	0.0069	12.1
2003/08/15	16:30	0.544	0.0112	20.5
2003/08/18	09:45	0.468	0.0055	11.7
2003/08/18	15:02	1.163	0.1760	151.3
2003/08/19	09:40	3.79	0.5564	146.8
2003/08/19	16:35	2.38	0.3979	167.2
2003/08/21	08:15	2.643	0.1308	49.5
2003/08/21	18:30	1.955	0.1349	69
2003/08/22	07:50	1.8	0.0598	33.2
2003/08/22	14:30	1.581	0.0557	35.2
2003/08/25	09:20	4.835	2.3575	487.6
2003/08/25	16:45	3.714	1.4347	386.3
2003/08/26	09:40	2.268	0.3164	139.5
2003/08/26	16:30	2	0.2084	104.2
2003/08/27	09:52	1.546	0.1211	78.3
2003/08/27	17:09	1.478	0.0436	29.5
2003/08/28	09:58	1.207	0.0410	34
2003/08/28	17:10	1.23	0.0584	47.5
2003/08/29	10:15	1.029	0.0288	28
2003/08/29	16:50	1.002	0.0487	48.6
2003/09/01	09:49	0.956	0.0303	31.7

2003/09/01	16:20	14.25	73.2279	5138.8
2003/09/02	09:50	3.265	0.1665	51
2003/09/02	15:10	2.838	0.1984	69.9
2003/09/03	10:59	2.098	0.0932	44.4
2003/09/03	16:10	1.995	0.0712	35.7
2004/07/01	10:50	0.18	0.012	66.9
2004/07/01	16:50	0.185	0.024	131.3
2004/07/05	15:40	0.328	0.004	10.8
2004/07/07	08:00	0.287	0.004	15
2004/07/07	15:40	0.273	0.005	18.7
2004/07/08	16:25	0.244	0.003	11.3
2004/07/09	15:35	0.221	0.004	17.4
2004/07/12	10:25	0.212	0.012	55.8
2004/07/12	15:50	0.219	0.015	67.5
2004/07/13	09:45	0.218	0.002	10.8
2004/07/13	15:35	0.216	0.001	3.6
2004/08/02	08:54	1.607	0.031819	19.8
2004/08/03	17:45	1.607	0.116	72
2004/08/04	07:46	1.607	0.033104	20.6
2004/08/04	16:59	1.598	0.02429	15.2
2004/08/05	10:30	3.12	2.810	900.8
2004/08/05	16:30	7.1	3.442	484.8
2004/08/06	07:20	2.35	0.241	102.4
2004/08/08	07:30	7.121	0.378	53.1
2004/08/10	15:10	3.054	0.242	79.4
2004/08/11	17:10	2.171	0.108	49.7
2004/09/16	15:25	0.291	0.003	8.6
2004/09/20	07:30	0.426	0.008	18.9
2004/09/20	17:35	0.376	0.007	17.5
2004/09/21	15:50	0.349	0.003	10
2004/09/22	08:30	0.351	0.004	10
2004/09/23	07:56	0.357	0.004	12.2
2004/10/04	07:25	0.251	0.006	23.3
2004/10/05	19:45	0.234	0.001	5.6
2004/10/06	07:45	0.271	0.003	10.6
2004/10/07	08:45	6.638	0.562	84.7
2004/10/08	07:30	0.855	0.024	28
2004/10/08	08:00	8.49	0.369	43.5
2004/10/10	09:45	0.601	0.005	8.7
2004/10/11	07:00	0.525	0.012	22.9
2004/10/07	15:19	1.643	0.144	87.4

D.4 Paarl Weir (G1H020)

Date	Time	Q[m ³ /s]	Qs[kg/s]	Concentration [mg/l]
2003/07/02	11:20	1.610	0.016	10.2
2003/07/08	07:45	1.115	0.007	6.2
2003/07/08	17:08	1.115	0.009	7.9
2003/07/09	09:30	1.057	0.006	5.4
2003/07/09	17:00	1.057	0.045	43
2003/07/10	09:00	2.080	0.022	10.4
2003/07/10	09:30	1.932	0.021	11.1
2003/07/10	17:00	8.445	0.160	18.9
2003/07/11	09:30	6.100	0.141	23.1
2003/07/11	15:50	5.247	0.048	9.1
2003/07/14	09:35	3.574	0.049	13.8
2003/07/15	09:45	2.522	0.016	6.4
2003/07/15	17:13	2.206	0.044	19.9
2003/07/16	09:50	2.080	0.020	9.8
2003/07/17	10:15	1.316	0.012	9.1
2003/07/17	17:10	1.255	0.013	10
2003/07/18	09:45	3.669	0.165	44.9
2003/07/18	15:45	16.121	3.735	231.7
2003/07/22	09:45	3.959	0.030	7.5
2003/07/23	17:16	3.000	0.148	49.3
2003/07/24	07:34	2.884	0.042	14.6
2003/07/25	07:45	4.157	0.048	11.6
2003/07/25	16:01	12.631	0.240	19
2003/07/28	09:50	5.210	0.215	41.3
2003/07/28	16:50	5.137	0.043	8.3
2003/07/28	16:50	5.137	0.026	5
2003/07/30	09:35	4.636	0.037	8
2003/07/30	11:00	4.532	0.084	18.6
2003/07/30	15:00	4.601	0.084	18.2
2003/07/30	17:00	7.608	0.062	8.2
2003/07/31	09:30	11.636	0.387	33.3
2003/07/31	16:50	8.901	0.190	21.3
2003/08/01	09:30	5.967	0.030	5
2003/08/01	16:00	9.842	0.202	20.5
2003/08/04	09:30	5.284	0.027	5.2
2003/08/04	17:00	4.956	0.034	6.9
2003/08/05	17:00	4.292	0.039	9.1
2003/08/06	09:00	3.892	0.025	6.3
2003/08/08	09:20	3.237	0.030	9.2
2003/08/11	09:30	15.013	0.131	8.7
2003/08/11	17:00	12.792	0.333	26
2003/08/12	09:30	10.035	0.119	11.9
2003/08/12	16:45	9.413	0.090	9.6
2003/08/13	16:55	7.608	0.110	14.4
2003/08/14	09:30	7.522	0.099	13.1
2003/08/14	17:00	6.931	0.096	13.9
2003/08/15	09:30	6.931	0.321	46.3

2003/08/15	15:45	6.766	0.075	11.1
2003/08/18	09:30	7.178	0.115	16
2003/08/18	17:00	15.244	1.855	121.7
2003/08/19	09:30	62.723	14.571	232.3
2003/08/19	16:45	39.566	4.776	120.7
2003/08/19	17:00	38.973	1.738	44.6
2003/08/20	09:30	27.680	0.626	22.6
2003/08/20	17:00	23.932	0.404	16.9
2003/08/21	17:00	16.777	1.606	95.7
2003/08/22	09:30	14.775	0.205	13.9
2003/08/22	15:55	13.443	0.104	7.7
2003/08/25	08:00	33.969	9.094	267.7
2003/08/25	17:00	111.333	32.999	296.4
2003/08/26	09:30	47.550	8.537	179.54
2003/08/26	17:00	35.522	0.320	9
2003/09/01	09:25	8.717	0.620	71.1
2003/09/01	09:35	8.717	0.694	79.6
2003/09/01	16:50	11.124	0.283	25.4
2003/09/02	17:00	30.023	0.952	31.7
2003/09/03	09:35	18.685	0.579	31
2003/09/03	17:05	16.637	0.466	28
2004/06/24	12:10	8.266	0.148	17.9
2004/06/24	17:05	6.973	0.054	7.8
2004/06/25	09:45	5.395	0.058	10.7
2004/06/25	16:00	5.028	0.027	5.4
2004/06/28	09:25	6.163	0.029	4.7
2004/06/28	17:10	5.395	0.005	1
2004/06/29	09:25	5.028	0.319	63.5
2004/06/30	09:30	4.326	0.032	7.4
2004/06/30	17:00	4.326	0.046	10.7
2004/07/01	09:15	3.992	0.096	24
2004/07/02	15:45	3.992	0.139	34.7
2004/07/07	09:45	5.028	0.003	0.6
2004/07/23	09:25	5.774	0.076	13.2
2004/07/23	14:30	13.773	1.894	137.5
2004/07/23	15:50	94.426	38.328	405.9
2004/07/26	17:00	10.623	0.151	14.2
2004/07/26	09:30	12.155	0.089	7.3
2004/07/27	16:50	8.266	0.028	3.4
2004/07/28	09:30	7.393	0.060	8.1
2004/07/29	09:50	6.163	0.052	8.5
2004/07/29	17:10	6.163	0.025	4.1
2004/07/30	10:35	17.261	1.174	68
2004/07/30	15:00	55.182	9.083	164.6
2004/07/30	15:45	50.31	5.987	119
2004/08/02	11:00	13.224	0.077	5.8
2004/08/02	17:00	12.155	0.078	6.4
2004/08/03	09:10	10.132	0.045	4.4
2004/08/03	17:10	9.179	0.070	7.6
2004/08/04	09:35	8.266	0.028	3.4
2004/08/05	10:00	17.628	1.000	56.7
2004/08/05	14:00	31.263	1.416	45.3

2004/08/05	16:45	200.434	43.214	215.6
2004/08/06	09:30	32.287	0.730	22.6
2004/08/06	14:35	28.653	1.066	37.2
2004/08/06	15:50	26.357	2.483	94.2
2004/08/10	09:20	37.695	0.479	12.7
2004/08/10	17:10	30.641	0.457	14.9
2004/08/11	09:20	22.689	0.204	9
2004/08/12	16:45	15.944	0.193	12.1
2004/08/13	09:24	14.163	0.065	4.6
2004/08/13	15:19	13.662	0.097	7.1
2004/08/16	16:24	64.637	4.434	68.6
2004/08/17	10:05	69.628	1.225	17.6
2004/08/19	16:40	18.842	0.925	49.1

D.5 Hermon Weir (G1H036)

Date	Time	Q[m ³ /s]	Qs[kg/s]	Concentration [mg/l]
2003/07/02	16:53	0.770	0.009	11.2
2003/07/03	08:10	1.150	0.013	11.1
2003/07/04	07:10	1.010	0.007	7.1
2003/07/04	17:45	0.830	0.008	9.8
2003/07/05	17:30	0.855	0.011	13
2003/07/06	07:45	1.028	0.008	7.3
2003/07/06	17:35	0.980	0.017	17.7
2003/07/07	07:10	1.077	0.006	5.9
2003/07/07	17:35	0.942	0.009	9.8
2003/07/08	07:10	0.905	0.004	4.9
2003/07/08	17:40	0.636	0.003	5
2003/07/09	07:15	0.652	0.012	17.9
2003/07/09	17:45	0.591	0.004	7.4
2003/07/10	07:10	0.860	0.061	70.6
2003/07/10	17:45	0.652	0.004	6.3
2003/07/11	07:15	1.833	0.012	6.7
2003/07/11	17:45	5.586	0.137	24.6
2003/07/12	07:15	5.364	0.144	26.9
2003/07/12	18:40	5.813	0.164	28.2
2003/07/13	07:20	4.828	0.097	20
2003/07/13	18:15	4.028	0.046	11.3
2003/07/14	07:35	3.422	0.027	7.8
2003/07/15	07:15	2.785	0.015	5.5
2003/07/15	17:15	2.722	0.023	8.4
2003/07/16	08:10	2.142	0.012	5.8
2003/07/16	17:35	1.964	0.010	5.1
2003/07/17	07:30	1.725	0.020	11.8
2003/07/17	17:35	1.430	0.024	16.8
2003/07/18	07:15	1.419	0.032	22.9
2003/07/18	17:45	1.264	0.050	39.3

2003/07/19	07:15	3.458	0.126	36.4
2003/07/19	17:40	9.280	0.264	28.5
2003/07/21	07:15	6.715	0.102	15.2
2003/07/21	17:40	5.915	0.612	103.4
2003/07/29	17:40	8.601	0.181	21.1
2003/07/30	07:15	6.399	0.072	11.2
2003/07/30	17:35	5.386	0.049	9.1
2003/07/31	07:15	4.379	0.073	16.6
2003/07/31	17:45	11.028	0.646	58.6
2003/08/01	17:45	7.089	0.184	25.9
2003/08/02	09:55	10.840	0.749	69.1
2003/08/02	17:30	13.544	0.627	46.3
2003/08/03	07:45	9.600	0.494	51.5
2003/08/03	17:30	8.027	0.203	25.3
2003/08/04	07:15	6.375	0.062	9.8
2003/08/04	17:45	5.813	0.069	11.9
2003/08/05	07:15	4.891	0.157	32.2
2003/08/05	17:40	4.540	0.075	16.5
2003/08/06	07:15	4.163	0.057	13.7
2003/08/06	17:35	3.914	0.088	22.5
2003/08/07	07:10	3.387	0.054	15.8
2003/08/07	17:45	3.129	0.031	9.9
2003/08/08	07:10	2.898	0.033	11.5
2003/08/08	17:40	2.690	0.024	8.9
2003/08/09	07:40	22.813	7.271	318.7
2003/08/09	17:30	39.772	37.887	952.6
2003/08/10	07:30	27.031	2.384	88.2
2003/08/10	17:30	32.850	3.502	106.6
2003/08/14	17:45	7.421	0.133	17.9
2003/08/11	18:00	17.310	0.703	40.6
2003/08/12	07:10	13.095	0.838	64
2003/08/12	17:35	11.345	0.442	39
2003/08/13	07:10	9.600	0.872	90.8
2003/08/13	17:40	8.768	0.295	33.7
2003/08/14	07:10	7.867	0.131	16.6
2003/08/15	17:35	7.039	0.116	16.5
2003/08/15	07:10	7.241	0.109	15
2003/08/16	17:45	6.280	0.073	11.6
2003/08/16	07:30	6.666	0.043	6.4
2003/08/17	07:40	5.745	0.037	6.5
2003/08/18	07:10	4.975	0.256	51.5
2003/08/18	17:40	4.662	0.062	13.3
2003/08/19	07:10	38.300	16.706	436.2
2003/08/19	17:35	89.653	5.998	66.9
2003/08/20	07:10	53.868	3.361	62.4
2003/08/20	17:30	32.884	2.105	64
2003/08/21	07:10	25.026	0.838	33.5
2003/08/21	17:50	21.155	0.825	39
2003/08/22	07:10	17.823	0.651	36.5
2003/08/22	17:35	16.736	0.636	38
2003/08/23	08:50	13.964	0.522	37.4
2003/08/24	17:30	13.303	0.287	21.6

2003/08/25	17:35	37.911	6.494	171.3
2003/08/27	07:10	45.747	3.692	80.7
2003/08/28	07:10	24.728	0.868	35.1
2003/08/28	17:35	20.513	0.732	35.7
2003/08/29	07:10	17.550	0.439	25
2003/08/29	07:30	17.518	0.701	40
2003/08/29	17:30	15.973	0.471	29.5
2003/08/31	07:40	11.958	1.051	87.9
2003/08/31	17:30	11.377	0.200	17.6
2003/09/01	07:10	10.593	0.308	29.1
2003/09/01	17:35	10.378	0.533	51.4
2003/09/02	07:10	50.072	15.512	309.8
2003/09/02	17:35	107.536	8.495	79
2003/09/03	07:10	37.525	1.752	46.7
2003/09/03	17:35	23.250	1.730	74.4
2003/09/04	07:10	18.661	0.662	35.5
2003/09/04	17:35	17.326	1.185	68.4
2003/09/05	07:10	15.227	0.231	15.2
2003/08/24	07:50	12.056	0.371	30.8
2003/08/25	07:14	31.676	4.115	129.9
2003/08/26	07:10	114.408	15.434	134.9
2003/08/26	17:45	102.732	7.058	68.7
2003/08/27	17:35	30.874	2.245	72.7
2003/09/05	17:35	14.141	0.475	33.6
2003/09/06	07:30	12.688	0.406	32
2003/09/06	17:30	11.958	0.053	4.4
2003/09/07	07:10	11.154	0.174	15.6
2003/09/07	17:35	10.685	0.203	19
2003/09/08	17:35	9.483	0.169	17.8
2003/09/09	07:10	9.223	0.252	27.3
2003/09/09	17:30	9.223	0.371	40.2
2003/09/10	07:10	9.866	0.196	19.9
2003/09/10	17:30	21.086	1.662	78.8
2003/09/11	07:10	18.694	4.430	237
2003/09/11	17:35	15.338	1.408	91.8
2003/09/12	07:10	12.925	0.252	19.5
2003/09/12	17:35	11.698	0.201	17.2
2003/09/13	07:00	10.840	0.421	38.8
2003/09/13	17:35	10.106	0.227	22.5
2003/09/14	07:35	9.571	0.184	19.2
2003/09/14	18:00	9.194	0.204	22.2
2003/09/15	07:10	8.768	0.123	14
2003/09/15	17:35	8.462	0.077	9.1
2003/09/16	07:10	8.027	0.090	11.2
2003/09/16	17:35	7.787	0.052	6.7
2003/09/17	07:10	7.421	0.086	11.6
2003/09/17	17:35	7.241	0.081	11.2
2003/09/18	07:10	6.864	0.051	7.4
2003/09/19	07:10	6.399	0.068	10.7
2003/09/19	17:35	8.000	0.080	10
2003/09/20	07:30	10.286	0.273	26.5
2003/09/20	17:50	9.659	0.090	9.3

2003/09/21	07:30	10.196	0.133	13
2003/09/21	17:50	11.601	0.209	18
2003/09/22	07:10	15.153	0.741	48.9
2003/09/22	17:35	12.756	0.233	18.3
2003/09/23	07:10	10.685	1.737	162.6
2003/09/23	17:35	9.600	0.363	37.8
2003/09/24	07:10	8.656	0.180	20.8
2003/09/24	17:35	8.216	0.082	10
2003/09/25	07:10	7.421	0.127	17.1
2003/09/25	17:35	7.292	0.209	28.7
2003/09/26	07:10	6.963	0.049	7
2003/09/26	17:40	6.888	0.076	11.1
2003/09/28	17:30	46.040	10.944	237.7
2003/09/29	07:10	25.894	2.993	115.6
2003/09/29	17:35	19.013	1.850	97.3
2003/09/30	07:10	15.227	0.659	43.3
2003/09/30	17:45	13.336	0.315	23.6
2003/10/01	07:10	11.601	0.372	32.1
2003/10/01	17:45	11.060	0.127	11.5
2003/10/02	07:10	10.500	0.438	41.7
2004/06/24	07:15	5.762	0.133	23.1
2004/06/24	17:45	10.287	0.447	43.5
2004/06/25	07:15	8.545	0.562	65.8
2004/06/25	17:45	7.216	0.667	92.5
2004/06/26	07:30	6.232	0.110	17.7
2004/06/26	17:45	5.998	0.071	11.8
2004/06/27	07:45	9.689	0.204	21.1
2004/06/27	17:45	12.857	0.747	58.1
2004/06/28	07:45	9.986	1.611	161.3
2004/06/28	17:45	8.545	0.127	14.9
2004/06/29	07:15	7.216	0.067	9.3
2004/06/29	17:45	6.715	0.097	14.4
2004/06/30	07:15	5.767	0.095	16.5
2004/06/30	17:50	5.542	0.129	23.2
2004/07/01	07:15	5.103	0.278	54.5
2004/07/02	07:15	4.479	0.047	10.5
2004/07/02	17:45	4.280	0.080	18.7
2004/07/03	07:15	4.086	0.126	30.9
2004/07/03	17:00	10.593	0.556	52.5
2004/07/04	07:40	16.852	1.323	78.5
2004/07/04	17:15	13.544	1.144	84.5
2004/07/05	07:15	11.537	0.198	17.2
2004/07/05	17:45	10.287	0.194	18.9
2004/07/06	17:45	7.734	0.080	10.3
2004/07/07	07:15	6.963	0.055	7.9
2004/07/07	17:45	6.472	0.098	15.2
2004/07/08	07:15	5.767	0.255	44.2
2004/07/08	17:45	5.542	0.168	30.4
2004/07/10	07:30	4.280	0.043	10
2004/07/10	17:40	4.086	0.007	1.8
2004/07/11	07:00	3.710	0.049	13.1
2004/07/11	17:00	3.529	0.045	12.8

2004/07/15	07:15	2.536	0.078	30.9
2004/07/15	17:45	2.536	0.023	9
2004/07/20	17:45	1.706	0.263	154.2
2004/07/23	17:45	1.833	0.158	86.3
2004/07/24	07:15	33.201	3.416	102.9
2004/07/24	17:45	50.350	3.751	74.5
2004/07/25	07:15	26.120	1.403	53.7
2004/07/25	17:45	21.481	1.340	62.4
2004/07/26	07:15	18.199	0.471	25.9
2004/07/26	17:45	14.970	0.493	32.9
2004/07/27	17:45	10.903	0.584	53.6
2004/07/27	07:15	12.188	0.594	48.7
2004/07/28	17:45	8.545	0.086	10.1
2004/07/28	07:15	9.396	0.140	14.9
2004/07/29	07:15	7.473	0.084	11.2
2004/07/29	17:45	7.216	0.113	15.7
2004/07/31	07:15	37.655	0.471	12.5
2004/07/31	17:45	24.314	1.544	63.5
2004/08/01	07:15	18.035	0.157	8.7
2004/08/01	17:45	17.550	0.953	54.3
2004/08/02	07:15	19.030	0.466	24.5
2004/08/02	17:45	16.467	0.538	32.7
2004/08/03	07:15	13.198	0.211	16
2004/08/03	17:45	11.537	0.143	12.4
2004/08/05	07:15	8.796	0.140	15.9
2004/08/06	07:15	50.196	7.278	145
2004/08/06	17:45	75.744	4.196	55.4
2004/08/07	07:15	27.686	1.836	66.3
2004/08/07	17:45	21.727	1.734	79.8
2004/08/08	07:15	30.355	1.733	57.1
2004/08/08	17:45	61.915	2.941	47.5
2004/08/09	17:45	100.503	5.699	56.7
2004/08/10	07:15	100.220	2.345	23.4
2004/08/10	17:45	63.892	5.054	79.1
2004/08/11	07:15	34.867	1.416	40.6
2004/08/11	17:45	27.199	1.920	70.6
2004/08/12	07:15	22.271	1.303	58.5
2004/08/12	17:45	19.781	0.552	27.9
2004/08/13	07:15	17.840	0.530	29.7
2004/08/13	17:45	16.582	0.496	29.9
2004/08/14	07:15	14.715	1.173	79.7
2004/08/14	17:45	13.894	1.395	100.4
2004/08/15	07:15	47.985	5.077	105.8
2004/08/15	17:45	56.541	6.480	114.6
2004/08/16	07:45	30.108	2.731	90.7
2004/08/17	07:30	51.590	2.187	42.4
2004/08/18	17:30	40.307	1.943	48.2
2004/08/18	07:00	66.200	2.410	36.4
2004/08/19	07:00	28.134	0.810	28.8
2004/08/20	07:50	20.023	0.897	44.8
2004/08/20	17:05	18.562	0.767	41.3
2004/08/23	07:45	13.027	0.276	21.2

2004/09/29	17:45	7.318	0.071	9.7
2004/10/04	07:15	2.032	0.029	14.4
2004/10/05	07:15	2.046	0.034	16.5
2004/10/06	17:45	1.232	0.111	90.3
2004/10/07	17:45	9.807	0.802	81.8
2004/10/07	07:15	1.430	0.203	142.2
2004/10/10	17:45	10.046	0.140	13.9
2004/10/11	07:15	8.243	0.245	29.7
2004/10/11	17:45	7.318	0.340	46.5
2004/10/13	17:45	4.163	0.076	18.2

D.6 Drieheuwels Weir (G1H013)

Date	Time	Q[m ³ /s]	Qs[kg/s]	Concentration [mg/l]
2003/08/06	18:00	5.76	0.1486	25.8
2003/08/07	08:20	5.19	0.1054	20.3
2003/08/07	18:05	4.69	0.1473	31.4
2003/08/08	08:45	4.37	0.0896	20.5
2003/08/08	17:30	4.17	0.1122	26.9
2003/08/09	08:15	4.14	0.0989	23.9
2003/08/11	08:05	35.73	2.4118	67.5
2003/08/11	18:22	37.45	2.1047	56.2
2003/08/12	08:00	33.21	11.6003	349.3
2003/08/12	17:25	24.83	1.1223	45.2
2003/08/13	08:00	16.98	0.5858	34.5
2003/08/13	17:30	14.19	1.8802	132.5
2003/08/14	07:55	11.68	0.5116	43.8
2003/08/14	18:00	10.34	0.3836	37.1
2003/08/15	07:30	9.2	0.2650	28.8
2003/08/15	17:40	8.45	0.2755	32.6
2003/08/16	08:10	7.96	0.1146	14.4
2003/08/16	16:15	7.85	0.1790	22.8
2003/08/17	08:00	7.44	0.1458	19.6
2003/08/17	17:10	7.18	0.1809	25.2
2003/08/18	17:15	6.46	0.1182	18.3
2003/08/19	07:50	39.72	3.4556	87
2003/08/19	17:40	12.25	0.1740	14.2
2003/08/20	07:55	34.85	0.9932	28.5
2003/08/20	18:15	68.43	8.2595	120.7
2003/08/21	07:55	74.7	5.9312	79.4
2003/08/21	17:35	54.85	65.1289	1187.4
2003/08/22	07:50	37.74	3.2041	84.9
2003/08/22	18:00	32.32	2.6115	80.8
2003/08/23	07:30	25	2.1175	84.7
2003/08/25	07:40	29.16	11.2674	386.4
2003/08/25	17:45	31.99	6.5420	204.5
2003/08/26	08:25	108.95	43.8742	402.7

2003/08/26	17:50	82.72	12.3501	149.3
2003/08/27	07:50	100.45	16.1524	160.8
2003/08/27	18:10	110.09	15.0053	136.3
2003/08/28	07:50	77.93	30.4706	391
2003/08/28	17:45	52.84	12.6393	239.2
2003/08/29	08:00	37.97	5.6651	149.2
2003/08/29	18:00	32.99	9.7980	297
2003/08/30	07:40	26.08	4.2980	164.8
2003/09/01	17:40	14.77	1.4652	99.2
2003/09/01	07:35	15.75	1.4380	91.3
2003/09/02	18:10	33.04	3.1388	95
2003/09/02	07:45	36.02	6.0982	169.3
2003/09/03	18:15	92.41	17.8629	193.3
2003/09/03	08:00	62.84	52.5531	836.3
2003/09/04	17:50	42.99	0.7093	16.5
2003/09/04	07:45	68.46	6.3668	93
2003/09/05	07:30	31.1	4.6837	150.6
2003/09/05	18:10	25.57	2.9354	114.8
2003/09/06	07:45	21.56	2.2358	103.7
2003/09/08	07:30	14.35	0.2052	14.3
2003/09/08	17:30	13.63	0.9854	72.3
2003/09/09	07:45	12.85	1.0216	79.5
2003/09/09	17:35	12.11	0.5534	45.7
2003/09/10	07:40	12.6	0.4574	36.3
2003/09/10	18:00	14.44	0.3870	26.8
2003/09/11	07:15	15.2	0.6019	39.6
2003/09/11	17:30	26.31	3.4387	130.7
2003/09/12	07:15	29.13	3.0907	106.1
2003/09/12	17:40	22.31	1.1624	52.1
2003/09/13	07:15	17.55	0.6371	36.3
2003/09/15	07:30	11.89	0.4423	37.2
2003/09/15	17:40	11.22	0.3871	34.5
2003/09/16	07:45	10.45	0.5194	49.7
2003/09/16	17:55	10.06	0.5352	53.2
2003/09/17	07:20	9.63	0.2205	22.9
2003/09/17	17:35	9.32	0.1920	20.6
2003/09/18	07:20	8.85	0.3089	34.9
2003/09/18	17:45	8.28	0.1673	20.2
2003/09/19	07:30	8.17	0.3023	37
2004/06/25	17:45	6.193	0.206	33.2
2004/06/25	09:13	5.346	0.094	17.6
2004/06/26	08:20	9.938	0.187	18.8
2004/06/26	17:20	8.735	0.212	24.3
2004/06/27	09:10	8.175	0.194	23.7
2004/06/27	17:00	7.134	0.163	22.9
2004/06/28	09:20	8.735	0.717	82.1
2004/06/28	17:45	11.963	0.307	25.7
2004/06/29	08:25	12.7	0.638	50.2
2004/06/29	17:15	10.583	0.785	74.2
2004/06/30	08:45	9.322	0.209	22.4
2004/06/30	17:45	8.175	0.382	46.7
2004/07/01	08:35	7.641	0.154	20.2

2004/07/01	17:50	7.134	0.462	64.7
2004/07/02	08:45	6.193	0.469	75.8
2004/07/02	17:45	6.193	0.810	130.8
2004/07/03	08:20	6.193	0.280	45.2
2004/07/03	17:20	5.758	0.101	17.6
2004/07/04	07:30	6.651	0.198	29.7
2004/07/04	18:15	7.134	1.337	187.4
2004/07/05	08:20	18.821	0.384	20.4
2004/07/05	17:30	16.891	1.079	63.9
2004/07/06	08:15	14.273	0.579	40.6
2004/07/06	17:15	11.963	1.738	145.3
2004/07/07	08:45	10.583	1.338	126.4
2004/07/07	17:40	9.322	1.518	162.8
2004/07/08	07:50	8.735	0.739	84.6
2004/07/08	17:45	7.641	1.417	185.5
2004/07/09	08:25	7.134	0.088	12.3
2004/07/09	17:40	6.193	0.944	152.5
2004/07/10	08:46	6.193	0.639	103.2
2004/07/10	17:00	5.758	0.656	113.9
2004/07/11	09:20	5.346	0.078	14.5
2004/07/11	16:20	4.586	0.208663	45.5
2004/07/12	07:45	5.346	0.114404	21.4
2004/07/12	17:45	4.955	0.203155	41
2004/07/13	08:30	4.586	0.318268	69.4
2004/07/13	17:44	4.237	0.108891	25.7
2004/07/14	08:13	4.237	0.10762	25.4
2004/07/14	17:55	3.908	0.075815	19.4
2004/07/15	08:30	3.908	0.080114	20.5
2004/07/15	17:52	3.598	0.083114	23.1
2004/07/17	17:15	2.535	0.044	17.4
2004/07/18	08:30	2.775	0.050	17.9
2004/07/18	17:10	2.346	0.047	20
2004/07/19	07:45	2.775	0.061	22.1
2004/07/19	17:40	2.266	0.050	21.9
2004/07/20	08:20	2.347	0.035	15.1
2004/07/20	18:00	2.266	0.031	13.5
2004/07/21	17:40	2.031	0.021	10.5
2004/07/22	07:30	2.108	0.101	47.7
2004/07/22	17:30	1.955	0.118	60.3
2004/07/23	08:20	1.955	0.098	50.2
2004/07/23	17:30	1.955	0.088	44.9
2004/07/24	08:35	3.033	0.164	54.1
2004/07/24	17:40	4.955	0.352	71
2004/07/25	08:25	29.542	1.232	41.7
2004/07/25	17:20	49.716	2.332	46.9
2004/07/26	08:30	38.782	1.734	44.7
2004/07/26	17:20	33.097	2.525	76.3
2004/07/27	08:25	26.851	2.610	97.2
2004/07/27	18:12	20.906	0.711	34
2004/07/28	08:20	15.983	0.302	18.9
2004/07/28	17:40	13.47	1.400	103.9
2004/07/29	08:25	12.7	2.342	184.4

2004/07/29	17:40	10.583	0.443	41.9
2004/07/30	08:15	9.938	0.349	35.1
2004/07/30	17:35	9.938	0.341	34.3
2004/07/31	08:20	15.11	0.346	22.9
2004/07/31	17:15	17.837	0.482	27
2004/08/01	08:30	41.731	1.448	34.7
2004/08/01	17:10	37.622	1.381	36.7
2004/08/02	08:25	26.851	0.502	18.7
2004/08/02	17:20	20.906	0.477	22.8
2004/08/03	07:55	25.574	1.051	41.1
2004/08/03	17:45	20.906	0.408	19.5
2004/08/04	08:25	16.981	0.428	25.2
2004/08/04	17:29	14.273	0.337	23.6
2004/08/05	08:45	11.963	0.443	37
2004/08/05	17:33	11.963	0.535	44.7
2004/08/06	08:15	11.963	0.44622	37.3
2004/08/06	17:25	12.7	0.356	28
2004/08/07	08:30	53.227	5.067	95.2
2004/08/07	16:30	70.469	5.814	82.5
2004/08/08	09:15	44.749	3.347	74.8
2004/08/08	17:30	38.201	3.614	94.6
2004/08/09	08:25	74.746	5.957	79.7
2004/08/09	17:35	90.336	6.911	76.5
2004/08/10	08:15	145.068	10.590	73
2004/08/10	16:25	136.253	10.410	76.4
2004/08/11	08:02	115.838	4.830	41.7
2004/08/11	17:25	95.74	9.344	97.6
2004/08/12	08:25	54.197	361.088	6662.5
2004/08/12	17:35	41.136	1.469	35.7
2004/08/13	08:20	32.544	161.789	4971.4
2004/08/13	17:25	28.173	3.553	126.1
2004/08/14	08:35	23.155	3.098	133.8
2004/08/14	17:15	20.906	1.551	74.2
2004/08/15	08:40	37.046	2.623	70.8
2004/08/15	17:10	32.544	1.744	53.6
2004/08/16	08:20	63.523	3.970	62.5
2004/08/16	17:44	69.061	3.764	54.5
2004/08/17	08:35	60.81	4.117	67.7
2004/08/17	17:49	52.904	2.899	54.8
2004/08/18	08:10	71.176	6.804	95.6
2004/08/18	17:30	87.294	14.997	171.8
2004/08/19	07:50	82.794	4.263891	51.5
2004/08/19	17:40	62.162	2.853236	45.9
2004/08/20	07:40	41.136	1.608418	39.1

APPENDIX E INCIPIENT MOTION FIELD DATA

Depth (m)	Discharge (m ³ /s)	Velocity (m/s)	τ	F_d	d^{\wedge}	h^{\wedge}	k_s (m)	Energy Slope	Status
0.76	24.386	3.157	0.1108	4.5083	2.67	0.0658	0.13	0.01203	N
0.76	24.386	3.157	0.1108	4.5083	2.67	0.0658	0.13	0.01203	N
0.76	24.386	3.157	0.1108	4.5083	2.67	0.0658	0.13	0.01203	N
0.76	24.386	3.157	0.1108	4.5083	2.67	0.0658	0.13	0.01203	N
0.76	24.386	3.157	0.1108	4.5083	2.67	0.0658	0.13	0.01203	N
0.74	24.386	3.312	0.1079	4.7295	1.99	0.0676	0.10	0.01203	N
0.74	24.386	3.312	0.1079	4.7295	1.99	0.0676	0.10	0.01203	N
0.74	24.386	3.312	0.1079	4.7295	1.99	0.0676	0.10	0.01203	N
0.74	24.386	3.312	0.1079	4.7295	1.99	0.0676	0.10	0.01203	N
0.74	24.386	3.312	0.1079	4.7295	1.99	0.0676	0.10	0.01203	N
0.74	24.386	3.312	0.1079	4.7295	1.99	0.0676	0.10	0.01203	N
0.79	24.386	2.945	0.0576	2.9737	1.99	0.1266	0.20	0.01203	N
0.79	24.386	2.945	0.0576	2.9737	1.99	0.1266	0.20	0.01203	N
0.78	24.386	3.013	0.0569	3.0425	1.75	0.1282	0.17	0.01203	N
0.78	24.386	3.013	0.0569	3.0425	1.75	0.1282	0.17	0.01203	N
0.77	24.386	3.084	0.0561	3.1138	1.53	0.1299	0.15	0.01203	N
0.69	24.386	3.756	0.0503	3.7922	0.42	0.1449	0.04	0.01203	N
0.69	24.386	3.756	0.0503	3.7922	0.42	0.1449	0.04	0.01203	N
0.69	24.386	3.756	0.0503	3.7922	0.42	0.1449	0.04	0.01203	N
0.69	24.386	3.756	0.0503	3.7922	0.42	0.1449	0.04	0.01203	N
0.69	24.386	3.756	0.0503	3.7922	0.42	0.1449	0.04	0.01203	N
0.69	24.386	3.756	0.0503	3.7922	0.42	0.1449	0.04	0.01203	N
0.77	24.386	3.084	0.0432	2.7310	1.18	0.1688	0.15	0.01203	N
0.77	24.386	3.084	0.0374	2.5424	1.02	0.1948	0.15	0.01203	N
0.77	24.386	3.084	0.0374	2.5424	1.02	0.1948	0.15	0.01203	N
0.87	24.386	2.477	0.0423	2.0421	3.14	0.1724	0.47	0.01203	N
0.85	24.386	2.583	0.0413	2.1291	2.59	0.1765	0.39	0.01203	N
0.83	24.386	2.695	0.0403	2.2220	2.11	0.1807	0.32	0.01203	N
0.83	24.386	2.695	0.0403	2.2220	2.11	0.1807	0.32	0.01203	N
0.83	24.386	2.695	0.0403	2.2220	2.11	0.1807	0.32	0.01203	N
0.83	24.386	2.695	0.0403	2.2220	2.11	0.1807	0.32	0.01203	N
0.83	24.386	2.695	0.0403	2.2220	2.11	0.1807	0.32	0.01203	N
0.93	24.386	2.198	0.0339	1.5693	3.91	0.2151	0.78	0.01203	N
0.93	24.386	2.198	0.0339	1.5693	3.91	0.2151	0.78	0.01203	N
0.93	24.386	2.198	0.0339	1.5693	3.91	0.2151	0.78	0.01203	N
0.93	24.386	2.198	0.0339	1.5693	3.91	0.2151	0.78	0.01203	N
0.93	24.386	2.198	0.0339	1.5693	3.91	0.2151	0.78	0.01203	N
0.93	24.386	2.198	0.0339	1.5693	3.91	0.2151	0.78	0.01203	N
0.83	24.386	2.695	0.0303	1.9243	1.58	0.2410	0.32	0.01203	N
0.82	24.386	2.755	0.0299	1.9666	1.42	0.2439	0.28	0.01203	N
0.92	24.386	2.241	0.0330	1.5868	3.56	0.2210	0.72	0.01203	N
0.84	24.386	2.638	0.0245	1.6846	1.40	0.2976	0.35	0.01203	N
0.81	24.386	2.816	0.0305	2.0448	1.31	0.2387	0.25	0.01203	N
0.80	24.386	2.880	0.0233	1.8387	0.90	0.3125	0.22	0.01203	N
0.80	24.386	2.880	0.0273	1.9905	1.05	0.2667	0.22	0.01203	N

0.80	24.386	2.880	0.0233	1.8387	0.90	0.3125	0.22	0.01203	N
0.75	24.386	3.233	0.0273	2.3084	0.58	0.2667	0.12	0.01203	N
0.85	24.386	2.583	0.0248	1.6492	1.56	0.2941	0.39	0.01203	N
0.85	24.386	2.583	0.0248	1.6492	1.56	0.2941	0.39	0.01203	N
0.85	24.386	2.583	0.0351	1.9618	2.20	0.2078	0.39	0.01203	N
0.90	24.386	2.331	0.0328	1.6642	3.07	0.2222	0.61	0.01203	N
0.72	24.386	3.479	0.0169	1.9953	0.23	0.4306	0.07	0.01203	N
0.78	24.386	3.013	0.0247	2.0062	0.76	0.2949	0.17	0.01203	N
0.77	24.386	3.084	0.0241	2.0385	0.66	0.3030	0.15	0.01203	N
0.77	24.386	3.084	0.0219	1.9436	0.60	0.3333	0.15	0.01203	N
0.87	24.386	2.477	0.0247	1.5611	1.84	0.2950	0.47	0.01203	N
1.04	24.386	1.800	0.0253	1.0490	5.31	0.2885	1.59	0.01203	N
1.01	24.386	1.896	0.0245	1.1054	4.47	0.2970	1.34	0.01203	N
1.09	24.386	1.655	0.0265	0.9647	6.86	0.2752	2.06	0.01203	N
1.09	24.386	1.655	0.0291	1.0106	7.53	0.2508	2.06	0.01203	N
1.09	24.386	1.655	0.0265	0.9647	6.86	0.2752	2.06	0.01203	N
0.83	24.386	2.695	0.0173	1.4546	0.90	0.4217	0.32	0.01203	N
0.81	24.386	2.816	0.0169	1.5197	0.72	0.4321	0.25	0.01203	N
0.80	24.386	2.880	0.0194	1.6785	0.75	0.3750	0.22	0.01203	N
0.90	24.386	2.331	0.0232	1.3982	2.17	0.3148	0.61	0.01203	N
0.90	24.386	2.331	0.0226	1.3820	2.12	0.3222	0.61	0.01203	N
1.02	24.386	1.863	0.0212	1.0055	4.07	0.3431	1.42	0.01203	N
1.02	24.386	1.863	0.0212	1.0055	4.07	0.3431	1.42	0.01203	N
1.10	24.386	1.628	0.0229	0.8787	6.17	0.3182	2.16	0.01203	N
1.10	24.386	1.628	0.0229	0.8787	6.17	0.3182	2.16	0.01203	N
1.09	24.386	1.655	0.0227	0.8931	5.88	0.3211	2.06	0.01203	N
1.04	24.386	1.800	0.0242	1.0265	5.09	0.3013	1.59	0.01203	N
1.04	24.386	1.800	0.0217	0.9712	4.55	0.3365	1.59	0.01203	N
1.02	24.386	1.863	0.0235	1.0571	4.50	0.3105	1.42	0.01203	N
1.02	24.386	1.863	0.0225	1.0355	4.31	0.3235	1.42	0.01203	N
1.02	24.386	1.863	0.0248	1.0861	4.74	0.2941	1.42	0.01203	N
1.11	24.386	1.602	0.0217	0.8372	6.06	0.3363	2.26	0.01203	N
1.08	24.386	1.682	0.0217	0.8911	5.40	0.3364	1.96	0.01203	N
1.06	24.386	1.739	0.0249	0.9975	5.72	0.2925	1.77	0.01203	N
1.05	24.386	1.769	0.0209	0.9328	4.59	0.3492	1.68	0.01203	N
1.03	24.386	1.831	0.0230	1.0228	4.61	0.3172	1.51	0.01203	N
1.64	101.937	3.351	0.2584	4.7851	20.89	0.0305	1.04	0.013	Y
1.64	101.937	3.351	0.2584	4.7851	20.89	0.0305	1.04	0.013	Y
1.64	101.937	3.351	0.2584	4.7851	20.89	0.0305	1.04	0.013	Y
1.64	101.937	3.351	0.2584	4.7851	20.89	0.0305	1.04	0.013	Y
1.64	101.937	3.351	0.2584	4.7851	20.89	0.0305	1.04	0.013	Y
1.52	101.937	3.833	0.2395	5.4724	11.15	0.0329	0.56	0.013	Y
1.52	101.937	3.833	0.2053	5.0664	9.56	0.0384	0.56	0.013	Y
1.52	101.937	3.833	0.1796	4.7392	8.36	0.0439	0.56	0.013	Y
1.52	101.937	3.833	0.2395	5.4724	11.15	0.0329	0.56	0.013	Y
1.52	101.937	3.833	0.2395	5.4724	11.15	0.0329	0.56	0.013	Y
1.73	101.937	3.050	0.1363	3.0793	15.40	0.0578	1.54	0.013	Y
1.73	101.937	3.050	0.1704	3.4428	19.24	0.0462	1.54	0.013	Y
1.73	101.937	3.050	0.1460	3.1874	16.49	0.0539	1.54	0.013	Y
1.73	101.937	3.050	0.1363	3.0793	15.40	0.0578	1.54	0.013	Y
1.73	101.937	3.050	0.1363	3.0793	15.40	0.0578	1.54	0.013	Y
1.54	101.937	3.745	0.1213	3.7812	6.25	0.0649	0.63	0.013	Y

1.54	101.937	3.745	0.1427	4.1013	7.36	0.0552	0.63	0.013	Y
1.54	101.937	3.745	0.1213	3.7812	6.25	0.0649	0.63	0.013	Y
1.54	101.937	3.745	0.1213	3.7812	6.25	0.0649	0.63	0.013	Y
1.54	101.937	3.745	0.1213	3.7812	6.25	0.0649	0.63	0.013	Y
1.70	101.937	3.145	0.0893	2.5930	9.08	0.0882	1.36	0.013	Y
1.70	101.937	3.145	0.1086	2.8596	11.04	0.0725	1.36	0.013	Y
1.70	101.937	3.145	0.0980	2.7166	9.97	0.0804	1.36	0.013	Y
1.70	101.937	3.145	0.1148	2.9402	11.67	0.0686	1.36	0.013	Y
1.70	101.937	3.145	0.1005	2.7503	10.21	0.0784	1.36	0.013	Y
1.78	101.937	2.900	0.0935	2.3910	12.42	0.0843	1.86	0.013	Y
1.78	101.937	2.900	0.0935	2.3910	12.42	0.0843	1.86	0.013	Y
1.78	101.937	2.900	0.0841	2.2683	11.18	0.0936	1.86	0.013	Y
1.78	101.937	2.900	0.1026	2.5050	13.63	0.0768	1.86	0.013	Y
1.78	101.937	2.900	0.0935	2.3910	12.42	0.0843	1.86	0.013	Y
1.54	101.937	3.745	0.0607	2.6737	3.13	0.1299	0.63	0.013	Y
1.54	101.937	3.745	0.0607	2.6737	3.13	0.1299	0.63	0.013	Y
1.54	101.937	3.745	0.0607	2.6737	3.13	0.1299	0.63	0.013	Y
1.54	101.937	3.745	0.0728	2.9289	3.75	0.1082	0.63	0.013	N
1.54	101.937	3.745	0.0809	3.0873	4.17	0.0974	0.63	0.013	Y
1.62	101.937	3.425	0.0957	2.9944	7.12	0.0823	0.95	0.013	Y
1.62	101.937	3.425	0.0766	2.6783	5.70	0.1029	0.95	0.013	Y
1.62	101.937	3.425	0.0870	2.8551	6.48	0.0905	0.95	0.013	Y
1.62	101.937	3.425	0.1008	3.0722	7.50	0.0782	0.95	0.013	Y
1.62	101.937	3.425	0.0912	2.9223	6.78	0.0864	0.95	0.013	Y
1.73	101.937	3.050	0.0682	2.1774	7.70	0.1156	1.54	0.013	Y
1.73	101.937	3.050	0.0649	2.1249	7.33	0.1214	1.54	0.013	Y
1.73	101.937	3.050	0.0670	2.1595	7.57	0.1175	1.54	0.013	Y
1.73	101.937	3.050	0.0639	2.1082	7.22	0.1233	1.54	0.013	Y
1.73	101.937	3.050	0.0639	2.1082	7.22	0.1233	1.54	0.013	Y
1.88	101.937	2.634	0.0823	1.9822	14.52	0.0957	2.61	0.013	Y
1.88	101.937	2.634	0.0684	1.8067	12.06	0.1152	2.61	0.013	Y
1.88	101.937	2.634	0.0626	1.7287	11.04	0.1259	2.61	0.013	Y
1.88	101.937	2.634	0.0694	1.8208	12.25	0.1135	2.61	0.013	N
1.88	101.937	2.634	0.0741	1.8805	13.07	0.1064	2.61	0.013	N
1.82	101.937	2.789	0.0458	1.5908	6.85	0.1722	2.15	0.013	N
1.72	101.937	3.081	0.0447	1.7862	4.88	0.1764	1.48	0.013	N
1.92	101.937	2.538	0.0522	1.5048	10.18	0.1510	2.95	0.013	N
1.92	101.937	2.538	0.0504	1.4795	9.84	0.1562	2.95	0.013	Y
1.82	101.937	2.789	0.0483	1.6349	7.24	0.1630	2.15	0.013	N
1.62	101.937	3.425	0.0555	2.2799	4.13	0.1420	0.95	0.013	N
1.62	101.937	3.425	0.0547	2.2636	4.07	0.1440	0.95	0.013	N
1.72	101.937	3.081	0.0528	1.9418	5.76	0.1492	1.48	0.013	Y
1.72	101.937	3.081	0.0521	1.9293	5.69	0.1512	1.48	0.013	Y
1.62	101.937	3.425	0.0517	2.2016	3.85	0.1523	0.95	0.013	Y
1.70	101.937	3.145	0.0383	1.6975	3.89	0.2059	1.36	0.013	Y
1.70	101.937	3.145	0.0502	1.9448	5.11	0.1569	1.36	0.013	N
1.70	101.937	3.145	0.0529	1.9953	5.38	0.1490	1.36	0.013	N
1.70	101.937	3.145	0.0509	1.9570	5.17	0.1549	1.36	0.013	Y
1.70	101.937	3.145	0.0529	1.9953	5.38	0.1490	1.36	0.013	Y
1.90	101.937	2.585	0.0458	1.4442	8.51	0.1719	2.78	0.013	Y
1.63	101.937	3.388	0.0363	1.8196	2.82	0.2168	1.00	0.013	N
1.63	101.937	3.388	0.0367	1.8282	2.85	0.2147	1.00	0.013	Y

1.63	101.937	3.388	0.0367	1.8282	2.85	0.2147	1.00	0.013	N
1.63	101.937	3.388	0.0428	1.9747	3.32	0.1840	1.00	0.013	Y
1.84	101.937	2.736	0.0463	1.5605	7.33	0.1703	2.30	0.013	N
1.84	101.937	2.736	0.0414	1.4765	6.56	0.1902	2.30	0.013	N
1.83	101.937	2.762	0.0455	1.5672	7.02	0.1730	2.22	0.013	N
1.83	101.937	2.762	0.0437	1.5352	6.73	0.1803	2.22	0.013	N
1.82	101.937	2.789	0.0478	1.6258	7.16	0.1648	2.15	0.013	N
1.87	101.937	2.659	0.0395	1.3894	6.78	0.1996	2.53	0.013	N
1.84	101.937	2.736	0.0399	1.4491	6.32	0.1975	2.30	0.013	N
1.83	101.937	2.762	0.0465	1.5840	7.17	0.1694	2.22	0.013	N
1.81	101.937	2.816	0.0389	1.4849	5.66	0.2026	2.07	0.013	N
1.81	101.937	2.816	0.0437	1.5732	6.35	0.1805	2.07	0.013	N
0.93	38.167	3.440	0.150433	4.9961	4.15	0.0520	0.20	0.013	Y
0.93	38.167	3.440	0.181773	5.4919	5.02	0.0430	0.20	0.013	Y
0.93	38.167	3.440	0.140727	4.8323	3.89	0.0556	0.20	0.013	N
0.93	38.167	3.440	0.145418	4.9121	4.02	0.0538	0.20	0.013	N
0.93	38.167	3.440	0.174502	5.3810	4.82	0.0448	0.20	0.013	Y
0.95	38.167	3.312	0.148545	4.7285	4.97	0.0526	0.25	0.013	Y
0.95	38.167	3.312	0.148545	4.7285	4.97	0.0526	0.25	0.013	Y
0.95	38.167	3.312	0.143754	4.6516	4.81	0.0544	0.25	0.013	N
0.95	38.167	3.312	0.148545	4.7285	4.97	0.0526	0.25	0.013	Y
0.95	38.167	3.312	0.148545	4.7285	4.97	0.0526	0.25	0.013	Y
1.03	38.167	2.866	0.105036	3.3044	6.70	0.0744	0.51	0.013	N
1.03	38.167	2.866	0.112364	3.4177	7.17	0.0696	0.51	0.013	N
1.03	38.167	2.866	0.134212	3.7353	8.56	0.0583	0.51	0.013	N
1.03	38.167	2.866	0.120791	3.5436	7.71	0.0647	0.51	0.013	Y
1.03	38.167	2.866	0.10981	3.3787	7.01	0.0712	0.51	0.013	N
0.9	38.167	3.648	0.070364	3.6836	1.42	0.1111	0.14	0.013	Y
0.9	38.167	3.648	0.070364	3.6836	1.42	0.1111	0.14	0.013	Y
0.9	38.167	3.648	0.070364	3.6836	1.42	0.1111	0.14	0.013	Y
0.9	38.167	3.648	0.136188	5.1247	2.75	0.0574	0.14	0.013	N
0.9	38.167	3.648	0.093818	4.2534	1.89	0.0833	0.14	0.013	Y
0.96	38.167	3.250	0.052364	2.7409	1.92	0.1493	0.27	0.013	N
0.96	38.167	3.250	0.068231	3.1287	2.50	0.1146	0.27	0.013	N
0.96	38.167	3.250	0.057734	2.8780	2.11	0.1354	0.27	0.013	N
0.96	38.167	3.250	0.047907	2.6217	1.75	0.1632	0.27	0.013	N
0.96	38.167	3.250	0.066225	3.0824	2.42	0.1181	0.27	0.013	N
1.18	38.167	2.249	0.076879	2.0724	11.47	0.1017	1.38	0.013	N
1.18	38.167	2.249	0.076879	2.0724	11.47	0.1017	1.38	0.013	N
1.18	38.167	2.249	0.074801	2.0442	11.16	0.1045	1.38	0.013	N
1.18	38.167	2.249	0.076879	2.0724	11.47	0.1017	1.38	0.013	N
1.18	38.167	2.249	0.06669	1.9302	9.95	0.1172	1.38	0.013	N
1.38	38.167	1.703	0.059939	1.2813	17.98	0.1304	3.24	0.013	N
1.38	38.167	1.703	0.067432	1.3590	20.23	0.1159	3.24	0.013	Y
1.48	38.167	1.504	0.069425	1.1764	26.47	0.1126	4.41	0.013	N
1.48	38.167	1.504	0.070842	1.1884	27.01	0.1104	4.41	0.013	N
1.48	38.167	1.504	0.069425	1.1764	26.47	0.1126	4.41	0.013	N
0.95	38.167	3.312	0.044564	2.5899	1.49	0.1754	0.25	0.013	N
0.95	38.167	3.312	0.055705	2.8956	1.86	0.1404	0.25	0.013	N
0.95	38.167	3.312	0.053052	2.8258	1.77	0.1474	0.25	0.013	N
0.95	38.167	3.312	0.058636	2.9708	1.96	0.1333	0.25	0.013	N
0.95	38.167	3.312	0.05064	2.7608	1.69	0.1544	0.25	0.013	N

1.09	38.167	2.590	0.042609	1.8491	4.00	0.1835	0.80	0.013	N
1.09	38.167	2.590	0.044852	1.8972	4.21	0.1743	0.80	0.013	N
1.06	38.167	2.722	0.0401	1.9120	3.13	0.1950	0.65	0.013	N
1.08	38.167	2.633	0.040208	1.8345	3.56	0.1944	0.75	0.013	N
1.08	38.167	2.633	0.040208	1.8345	3.56	0.1944	0.75	0.013	N
1.2	38.167	2.182	0.040791	1.4528	6.64	0.1917	1.53	0.013	N
1.2	38.167	2.182	0.043301	1.4969	7.05	0.1806	1.53	0.013	N
1.2	38.167	2.182	0.04139	1.4635	6.74	0.1889	1.53	0.013	N
1.1	38.167	2.548	0.0344	1.6272	3.42	0.2273	0.86	0.013	N
1.1	38.167	2.548	0.038507	1.7216	3.83	0.2030	0.86	0.013	N
1.09	38.167	2.590	0.032776	1.6218	3.08	0.2385	0.80	0.013	N
1.09	38.167	2.590	0.031957	1.6014	3.00	0.2446	0.80	0.013	N
1.06	38.167	2.722	0.031471	1.6938	2.46	0.2484	0.65	0.013	N
1.05	38.167	2.769	0.032404	1.7564	2.37	0.2413	0.60	0.013	Y
1.03	38.167	2.866	0.029461	1.7501	1.88	0.2654	0.51	0.013	N
0.93	38.167	3.440	0.03966	2.5653	1.10	0.1971	0.20	0.013	N
0.93	38.167	3.440	0.035182	2.4161	0.97	0.2222	0.20	0.013	N
0.93	38.167	3.440	0.034082	2.3781	0.94	0.2294	0.20	0.013	N
0.93	38.167	3.440	0.032556	2.3242	0.90	0.2401	0.20	0.013	N
0.93	38.167	3.440	0.034623	2.3969	0.96	0.2258	0.20	0.013	N
1.09	38.167	2.590	0.030435	1.5628	2.86	0.2569	0.80	0.013	N
1.09	38.167	2.590	0.028725	1.5183	2.70	0.2722	0.80	0.013	N
1.09	38.167	2.590	0.030077	1.5536	2.82	0.2599	0.80	0.013	N
1.09	38.167	2.590	0.028725	1.5183	2.70	0.2722	0.80	0.013	N
1.09	38.167	2.590	0.029727	1.5445	2.79	0.2630	0.80	0.013	N
1.19	38.167	2.215	0.033628	1.3445	5.24	0.2325	1.45	0.013	N
1.19	38.167	2.215	0.032082	1.3133	5.00	0.2437	1.45	0.013	N
1.19	38.167	2.215	0.03533	1.3781	5.51	0.2213	1.45	0.013	N
1.19	38.167	2.215	0.030012	1.2702	4.68	0.2605	1.45	0.013	N
1.19	38.167	2.215	0.034038	1.3527	5.31	0.2297	1.45	0.013	N
1.27	38.167	1.973	0.031689	1.1254	6.77	0.2467	2.12	0.013	N
1.27	38.167	1.973	0.028369	1.0648	6.06	0.2756	2.12	0.013	N
1.26	38.167	2.001	0.031108	1.1353	6.41	0.2513	2.03	0.013	N
1.26	38.167	2.001	0.029851	1.1121	6.15	0.2619	2.03	0.013	N
1.25	38.167	2.029	0.032576	1.1830	6.47	0.2400	1.94	0.013	N
1.31	38.167	1.867	0.027433	0.9757	6.70	0.2850	2.50	0.013	N
1.28	38.167	1.946	0.027543	1.0306	6.09	0.2839	2.21	0.013	N
1.26	38.167	2.001	0.031777	1.1474	6.55	0.2460	2.03	0.013	N
1.25	38.167	2.029	0.026653	1.0701	5.30	0.2933	1.94	0.013	N
1.25	38.167	2.029	0.029917	1.1337	5.94	0.2613	1.94	0.013	N
0.94	28.840	2.550	0.16828	3.9889	13.04	0.0443	0.54	0.0123	N
0.94	28.840	2.550	0.161807	3.9114	12.54	0.0461	0.54	0.0123	N
0.92	28.840	2.650	0.158365	4.0650	10.53	0.0471	0.46	0.0123	Y
0.92	28.840	2.650	0.132822	3.7228	8.83	0.0562	0.46	0.0123	N
0.92	28.840	2.650	0.137249	3.7843	9.13	0.0543	0.46	0.0123	N
0.81	28.840	3.330	0.157616	5.4309	3.56	0.0473	0.14	0.0123	Y
0.81	28.840	3.330	0.13943	5.1080	3.15	0.0535	0.14	0.0123	N
0.81	28.840	3.330	0.125006	4.8365	2.82	0.0597	0.14	0.0123	N
0.81	28.840	3.330	0.125006	4.8365	2.82	0.0597	0.14	0.0123	N
0.81	28.840	3.330	0.129471	4.9221	2.92	0.0576	0.14	0.0123	N
0.83	28.840	3.188	0.080754	3.6757	2.30	0.0924	0.18	0.0123	N
0.83	28.840	3.188	0.086388	3.8018	2.46	0.0863	0.18	0.0123	N

0.83	28.840	3.188	0.103186	4.1550	2.94	0.0723	0.18	0.0123	N
0.81	28.840	3.330	0.08239	3.9265	1.86	0.0905	0.14	0.0123	N
1	28.840	2.283	0.097294	2.6324	11.26	0.0767	0.86	0.0123	N
1	28.840	2.283	0.099456	2.6615	11.51	0.0750	0.86	0.0123	Y
1	28.840	2.283	0.08951	2.5249	10.36	0.0833	0.86	0.0123	N
1.02	28.840	2.203	0.103751	2.5979	13.49	0.0719	0.99	0.0123	Y
1.02	28.840	2.203	0.093164	2.4618	12.11	0.0801	0.99	0.0123	N
0.74	28.840	3.917	0.03851	3.3036	0.32	0.1937	0.05	0.0123	N
0.74	28.840	3.917	0.05018	3.7710	0.42	0.1486	0.05	0.0123	N
0.73	28.840	4.014	0.041886	3.5547	0.30	0.1781	0.04	0.0123	N
0.73	28.840	4.014	0.034757	3.2380	0.25	0.2146	0.04	0.0123	N
0.73	28.840	4.014	0.048046	3.8071	0.34	0.1553	0.04	0.0123	N
0.95	28.840	2.502	0.059052	2.3063	4.92	0.1263	0.59	0.0123	N
0.95	28.840	2.502	0.059052	2.3063	4.92	0.1263	0.59	0.0123	N
0.95	28.840	2.502	0.057456	2.2750	4.79	0.1298	0.59	0.0123	N
0.95	28.840	2.502	0.059052	2.3063	4.92	0.1263	0.59	0.0123	N
0.95	28.840	2.502	0.051226	2.1481	4.27	0.1456	0.59	0.0123	N
1.15	28.840	1.779	0.047656	1.3386	11.32	0.1565	2.04	0.0123	Y
1.25	28.840	1.534	0.055944	1.1993	18.51	0.1333	3.08	0.0123	N
1.25	28.840	1.534	0.057086	1.2115	18.89	0.1307	3.08	0.0123	N
1.25	28.840	1.534	0.055944	1.1993	18.51	0.1333	3.08	0.0123	N
0.75	28.840	3.824	0.033566	2.9906	0.33	0.2222	0.06	0.0123	N
0.75	28.840	3.824	0.041958	3.3436	0.42	0.1778	0.06	0.0123	N
0.74	28.840	3.917	0.039427	3.3426	0.33	0.1892	0.05	0.0123	N
0.74	28.840	3.917	0.043577	3.5142	0.37	0.1712	0.05	0.0123	N
0.74	28.840	3.917	0.037635	3.2658	0.32	0.1982	0.05	0.0123	N
0.84	28.840	3.120	0.031329	2.2274	0.99	0.2381	0.20	0.0123	N
0.84	28.840	3.120	0.032978	2.2853	1.05	0.2262	0.20	0.0123	N
0.84	28.840	3.120	0.030318	2.1912	0.96	0.2460	0.20	0.0123	N
0.84	28.840	3.120	0.029837	2.1737	0.95	0.2500	0.20	0.0123	N
0.84	28.840	3.120	0.029837	2.1737	0.95	0.2500	0.20	0.0123	N
1.06	28.840	2.057	0.034377	1.3695	5.52	0.2170	1.27	0.0123	N
1.06	28.840	2.057	0.036493	1.4110	5.86	0.2044	1.27	0.0123	N
1.05	28.840	2.092	0.034554	1.4031	5.28	0.2159	1.20	0.0123	N
0.95	28.840	2.502	0.028345	1.5979	2.36	0.2632	0.59	0.0123	N
0.95	28.840	2.502	0.031729	1.6906	2.64	0.2351	0.59	0.0123	N
0.84	28.840	3.120	0.024099	1.9536	0.77	0.3095	0.20	0.0123	N
0.84	28.840	3.120	0.023497	1.9290	0.75	0.3175	0.20	0.0123	N
0.84	28.840	3.120	0.023794	1.9411	0.76	0.3135	0.20	0.0123	N
0.84	28.840	3.120	0.024733	1.9791	0.79	0.3016	0.20	0.0123	N
0.84	28.840	3.120	0.022923	1.9053	0.73	0.3254	0.20	0.0123	N
0.72	28.840	4.115	0.029294	3.0684	0.18	0.2546	0.03	0.0123	N
0.72	28.840	4.115	0.025987	2.8900	0.16	0.2870	0.03	0.0123	N
0.72	28.840	4.115	0.025175	2.8445	0.15	0.2963	0.03	0.0123	N
0.72	28.840	4.115	0.024048	2.7801	0.14	0.3102	0.03	0.0123	N
0.72	28.840	4.115	0.025574	2.8670	0.15	0.2917	0.03	0.0123	N
0.89	28.840	2.813	0.02371	1.6971	1.23	0.3146	0.34	0.0123	N
0.88	28.840	2.870	0.022126	1.6824	1.05	0.3371	0.31	0.0123	N
0.88	28.840	2.870	0.023167	1.7216	1.09	0.3220	0.31	0.0123	N
0.88	28.840	2.870	0.022126	1.6824	1.05	0.3371	0.31	0.0123	N
0.88	28.840	2.870	0.022898	1.7115	1.08	0.3258	0.31	0.0123	N
0.98	28.840	2.367	0.026422	1.4367	2.70	0.2823	0.75	0.0123	N

0.98	28.840	2.367	0.025207	1.4033	2.57	0.2959	0.75	0.0123	N
0.98	28.840	2.367	0.02776	1.4726	2.84	0.2687	0.75	0.0123	N
0.98	28.840	2.367	0.023581	1.3573	2.41	0.3163	0.75	0.0123	N
0.98	28.840	2.367	0.026744	1.4454	2.73	0.2789	0.75	0.0123	N
1.08	28.840	1.990	0.02571	1.1348	4.55	0.2901	1.43	0.0123	N
1.08	28.840	1.990	0.023017	1.0738	4.07	0.3241	1.43	0.0123	N
1.06	28.840	2.057	0.024969	1.1672	4.01	0.2987	1.27	0.0123	N
1.06	28.840	2.057	0.02396	1.1433	3.85	0.3113	1.27	0.0123	N
1.06	28.840	2.057	0.026356	1.1991	4.23	0.2830	1.27	0.0123	N
1.13	28.840	1.835	0.022577	0.9590	4.96	0.3304	1.85	0.0123	N
1.1	28.840	1.926	0.022583	1.0199	4.37	0.3303	1.59	0.0123	N
1.08	28.840	1.990	0.025987	1.1409	4.60	0.2870	1.43	0.0123	N
1.07	28.840	2.023	0.021767	1.0666	3.67	0.3427	1.35	0.0123	N
1.05	28.840	2.092	0.023976	1.1688	3.66	0.3111	1.20	0.0123	N
1.70	105.221	3.247	0.2957	4.6359	25.50	0.0294	1.27	0.01320	Y
1.70	105.221	3.247	0.2957	4.6359	25.50	0.0294	1.27	0.01320	Y
1.70	105.221	3.247	0.2957	4.6359	25.50	0.0294	1.27	0.01320	Y
1.70	105.221	3.247	0.2957	4.6359	25.50	0.0294	1.27	0.01320	Y
1.70	105.221	3.247	0.2957	4.6359	25.50	0.0294	1.27	0.01320	Y
1.68	105.221	3.315	0.2922	4.7337	23.37	0.0298	1.17	0.01320	Y
1.68	105.221	3.315	0.2922	4.7337	23.37	0.0298	1.17	0.01320	Y
1.68	105.221	3.315	0.2922	4.7337	23.37	0.0298	1.17	0.01320	Y
1.68	105.221	3.315	0.2922	4.7337	23.37	0.0298	1.17	0.01320	Y
1.68	105.221	3.315	0.1461	3.3472	11.69	0.0595	1.17	0.01320	Y
1.68	105.221	3.315	0.1461	3.3472	11.69	0.0595	1.17	0.01320	Y
1.68	105.221	3.315	0.1461	3.3472	11.69	0.0595	1.17	0.01320	Y
1.68	105.221	3.315	0.1461	3.3472	11.69	0.0595	1.17	0.01320	Y
1.68	105.221	3.315	0.1461	3.3472	11.69	0.0595	1.17	0.01320	Y
1.68	105.221	3.315	0.1461	3.3472	11.69	0.0595	1.17	0.01320	Y
1.62	105.221	3.535	0.1409	3.5691	8.82	0.0617	0.88	0.01320	Y
1.61	105.221	3.574	0.1400	3.6083	8.40	0.0621	0.84	0.01320	Y
1.60	105.221	3.613	0.1392	3.6482	7.98	0.0625	0.80	0.01320	Y
1.60	105.221	3.613	0.1392	3.6482	7.98	0.0625	0.80	0.01320	Y
1.60	105.221	3.613	0.1392	3.6482	7.98	0.0625	0.80	0.01320	Y
1.72	105.221	3.181	0.1151	2.8164	10.67	0.0756	1.39	0.01320	Y
1.72	105.221	3.181	0.0997	2.6219	9.25	0.0872	1.39	0.01320	Y
1.72	105.221	3.181	0.0997	2.6219	9.25	0.0872	1.39	0.01320	Y
1.75	105.221	3.085	0.1015	2.5432	10.43	0.0857	1.57	0.01320	Y
1.75	105.221	3.085	0.1015	2.5432	10.43	0.0857	1.57	0.01320	Y
1.74	105.221	3.116	0.1009	2.5690	10.03	0.0862	1.50	0.01320	Y
1.72	105.221	3.181	0.0997	2.6219	9.25	0.0872	1.39	0.01320	Y
1.72	105.221	3.181	0.0997	2.6219	9.25	0.0872	1.39	0.01320	Y
1.72	105.221	3.181	0.0997	2.6219	9.25	0.0872	1.39	0.01320	Y
1.72	105.221	3.181	0.0997	2.6219	9.25	0.0872	1.39	0.01320	Y
1.80	105.221	2.936	0.0783	2.0957	9.45	0.1111	1.89	0.01320	Y
1.80	105.221	2.936	0.0783	2.0957	9.45	0.1111	1.89	0.01320	Y
1.80	105.221	2.936	0.0783	2.0957	9.45	0.1111	1.89	0.01320	Y
1.80	105.221	2.936	0.0783	2.0957	9.45	0.1111	1.89	0.01320	Y
1.82	105.221	2.879	0.0792	2.0553	10.15	0.1099	2.03	0.01320	Y
1.82	105.221	2.879	0.0792	2.0553	10.15	0.1099	2.03	0.01320	Y
1.69	105.221	3.281	0.0735	2.3422	6.11	0.1183	1.22	0.01320	Y

1.67	105.221	3.350	0.0726	2.3919	5.59	0.1198	1.12	0.01320	Y
1.77	105.221	3.024	0.0757	2.1410	8.32	0.1149	1.69	0.01320	Y
1.70	105.221	3.247	0.0591	2.0732	5.10	0.1471	1.27	0.01320	N
1.68	105.221	3.315	0.0756	2.4073	6.04	0.1151	1.17	0.01320	Y
1.68	105.221	3.315	0.0584	2.1170	4.67	0.1488	1.17	0.01320	Y
1.66	105.221	3.386	0.0677	2.3406	5.01	0.1285	1.07	0.01320	N
1.66	105.221	3.386	0.0578	2.1622	4.27	0.1506	1.07	0.01320	Y
1.55	105.221	3.822	0.0674	2.7285	3.05	0.1290	0.61	0.01320	Y
1.67	105.221	3.350	0.0581	2.1394	4.47	0.1497	1.12	0.01320	Y
1.67	105.221	3.350	0.0581	2.1394	4.47	0.1497	1.12	0.01320	Y
1.67	105.221	3.350	0.0822	2.5450	6.33	0.1058	1.12	0.01320	Y
1.71	105.221	3.213	0.0744	2.2941	6.65	0.1170	1.33	0.01320	N
1.59	105.221	3.654	0.0446	2.0951	2.44	0.1950	0.76	0.01320	Y
1.67	105.221	3.350	0.0632	2.2305	4.86	0.1377	1.12	0.01320	N
1.65	105.221	3.422	0.0615	2.2621	4.37	0.1414	1.02	0.01320	N
1.65	105.221	3.422	0.0559	2.1568	3.97	0.1556	1.02	0.01320	N
1.75	105.221	3.085	0.0593	1.9442	6.10	0.1467	1.57	0.01320	Y
1.99	105.221	2.460	0.0577	1.4337	11.42	0.1508	3.43	0.01320	Y
1.96	105.221	2.526	0.0568	1.4726	10.51	0.1531	3.15	0.01320	Y
2.02	105.221	2.395	0.0586	1.3963	12.37	0.1485	3.71	0.01320	Y
2.02	105.221	2.395	0.0643	1.4629	13.58	0.1353	3.71	0.01320	N
2.02	105.221	2.395	0.0586	1.3963	12.37	0.1485	3.71	0.01320	Y
1.75	105.221	3.085	0.0435	1.6649	4.47	0.2000	1.57	0.01320	N
1.71	105.221	3.213	0.0425	1.7342	3.80	0.2047	1.33	0.01320	N
1.70	105.221	3.247	0.0493	1.8926	4.25	0.1765	1.27	0.01320	N
1.79	105.221	2.964	0.0550	1.7781	6.43	0.1583	1.82	0.01320	Y
1.79	105.221	2.964	0.0537	1.7576	6.28	0.1620	1.82	0.01320	N
1.86	105.221	2.771	0.0462	1.4952	6.64	0.1882	2.32	0.01320	Y
1.85	105.221	2.797	0.0460	1.5095	6.43	0.1892	2.25	0.01320	Y
1.92	105.221	2.620	0.0477	1.4139	8.02	0.1823	2.81	0.01320	N
1.92	105.221	2.620	0.0477	1.4139	8.02	0.1823	2.81	0.01320	N
1.92	105.221	2.620	0.0477	1.4139	8.02	0.1823	2.81	0.01320	Y
1.92	105.221	2.620	0.0533	1.4943	8.96	0.1632	2.81	0.01320	N
1.92	105.221	2.620	0.0477	1.4139	8.02	0.1823	2.81	0.01320	N
1.90	105.221	2.669	0.0522	1.5141	8.34	0.1667	2.64	0.01320	N
1.90	105.221	2.669	0.0501	1.4832	8.00	0.1737	2.64	0.01320	N
1.89	105.221	2.694	0.0548	1.5701	8.53	0.1587	2.56	0.01320	N
1.88	105.221	2.719	0.0438	1.4207	6.64	0.1986	2.48	0.01320	N
1.88	105.221	2.719	0.0450	1.4401	6.83	0.1933	2.48	0.01320	N
1.88	105.221	2.719	0.0527	1.5591	8.00	0.1649	2.48	0.01320	N
1.87	105.221	2.745	0.0444	1.4471	6.55	0.1961	2.40	0.01320	N
1.85	105.221	2.797	0.0493	1.5625	6.88	0.1766	2.25	0.01320	N